

# **Synthesis and biological characterization of esterified lipid mediators**

**Dissertation**

**zur Erlangung des Doktorgrades der Naturwissenschaften  
(Dr. rer. nat.)**

**vorgelegt beim Fachbereich Biochemie, Chemie und Pharmazie (14)  
der Johann Wolfgang Goethe-Universität  
in Frankfurt am Main**

**von**

**Bjarne Goebel  
aus Göttingen**

**Frankfurt am Main**

**2023**

**(D 30)**



Vom Fachbereich Biochemie, Chemie und Pharmazie (14) der Johann Wolfgang Goethe-Universität als Dissertation angenommen.

Dekan: Prof. Dr. Clemens Glaubitz

Gutachter: Prof. Dr. Dieter Steinhilber

Prof. Dr. Eugen Proschak

Datum der Disputation:

## Table of Contents

List of figures .....	IX
List of tables.....	XII
Abbreviations .....	XIV
1 Abstract .....	1
2 Introduction .....	2
2.1 Biological membranes .....	2
2.2 <i>De novo</i> synthesis – The Kennedy pathway .....	2
2.3 Lipid remodeling – The Lands’ cycle.....	4
2.4 Acyl-CoA synthetases .....	5
2.4.1 Acyl-CoA synthetase long-chain family member 4.....	7
2.5 Lysophosphatidylcholine acyltransferases .....	8
2.5.1 Lysophosphatidylcholine acyltransferase 2 .....	9
2.6 Ferroptosis .....	10
2.7 Lipoxygenases .....	12
2.7.1 5-Lipoxygenase.....	14
2.7.2 15-Lipoxygenase 1.....	15
2.7.3 15-Lipoxygenase 2.....	16
2.8 Oxylipins.....	18
2.8.1 Esterified oxylipins .....	18
2.9 Lipid mediators in inflammation .....	19
2.9.1 Leukotrienes .....	20
2.9.2 Lipoxins, D-series, and E-series resolvins.....	22
3 Aim of thesis .....	25
4 Materials and methods.....	26
4.1 Materials.....	26
4.1.1 Cell culture.....	26
4.1.2 Chemicals and reagents .....	27
4.1.3 Antibodies .....	32
4.1.4 Buffers and stock solutions .....	34
4.1.5 Bacterial strains and cultivation.....	35
4.1.6 Devices and equipment.....	36



---

4.1.7 Software and web tools.....	38
4.2 Cloning work .....	39
4.2.1 Standard techniques for DNA preparation.....	39
4.2.2 Plasmid preparation .....	40
4.2.3 Transformation in <i>E. coli</i> .....	45
4.2.4 Selection.....	45
4.2.5 Amplification and isolation of vector DNA.....	46
4.2.6 DNA sequencing.....	46
4.3 Protein expression and purification of ACSL4.....	46
4.3.1 Pre-culture .....	46
4.3.2 Large-scale expression .....	47
4.3.3 Cell lysis and disruption by sonification .....	47
4.3.4 Ultracentrifugation.....	47
4.3.5 Ni-affinity chromatography .....	47
4.3.6 Desalting and buffer exchange.....	47
4.3.7 Ion exchange chromatography (IEX).....	48
4.3.8 Size exclusion chromatography (SEC).....	48
4.4 Protein expression and purification of PALOX .....	48
4.5 Analysis of recombinant proteins.....	48
4.5.1 Determination of protein concentration.....	48
4.5.2 Concentration of proteins .....	49
4.5.3 Storage of purified proteins .....	49
4.5.4 Sodium dodecylsulfate polyacrylamide gel electrophoresis (SDS-PAGE) .....	49
4.5.5 Western blotting.....	50
4.6 Human cell culture.....	50
4.6.1 Cultivation .....	50
4.6.2 Cell harvest and cell count .....	50
4.6.3 Storage of cells .....	51
4.6.4 Thawing of cells .....	51
4.7 Cell culture experiments .....	51
4.7.1 Transient transfection of HEK293T cells .....	51
4.7.2 Transfection efficiency .....	51

---

4.7.3 Stable transfection of HEK293T cells using the sleeping beauty system .....	52
4.7.4 Cell lysis.....	53
4.7.5 Bicinchoninic acid assay (BCA).....	53
4.7.6 Doxycycline treatment.....	54
4.7.7 Sample preparation for membrane composition analysis .....	54
4.7.8 Cell viability assay.....	55
4.7.9 Slide preparation for laser scanning confocal microscopy .....	55
4.7.10 Laser scanning confocal microscopy.....	56
4.8 Activity assays .....	56
4.8.1 ACSL4 activity assay .....	56
4.8.2 LPCAT2 activity assay .....	59
4.8.3 Lipoxygenase activity assay.....	60
4.8.4 PA-LOX activity assay.....	61
4.9 Thermal shift experiments .....	61
4.9.1 Buffer and salt screen .....	61
4.9.2 Compound screen.....	62
4.9.3 Fatty acid library screen .....	62
4.9.4 Prestwick drug fragment library screen .....	62
4.9.5 Prestwick approved drug library screen.....	63
4.10 Statistics.....	63
5 Results.....	64
5.1 Investigation of a biosynthetic approach for the formation of esterified lipid mediators using recombinant enzymes .....	64
5.1.1 Expression and purification of human ACSL4 from <i>E. coli</i> .....	64
5.1.2 Optimization of ACSL4_His6x purification and yield .....	66
5.1.3 Stability studies on purified recombinant ACSL4_His6x protein.....	72
5.1.4 Activity investigations of ACSL4_His6x .....	76
5.1.5 A recombinant 15S-lipoxygenating enzyme from <i>pseudomonas aeruginosa</i> (PA-LOX) .....	79
5.1.6 Stability and activity investigations of purified PA-LOX.....	80
5.1.7 Expression and purification of human LPCAT2 .....	84
5.2 Cell-based overexpression system for the formation of esterified lipid mediators .....	88
5.2.1 Stably transfected HEK293T cells express ACSL4 and/or LPCAT2 .....	88

---

5.2.2 ACSL4 and LPCAT2 overexpression effects on the oxylipin composition .....	89
5.2.3 Transient transfection of 5-LO, 15-LO1 and 15-LO2 .....	92
5.2.4 Determination of transient transfection efficiencies .....	93
5.2.5 Doxycycline-dependent expression of 5-LO, 15-LO1 and 15-LO2.....	94
5.2.6 Laser scanning confocal microscopy investigation of ACSL4 and LPCAT2 localization.....	96
5.3 Biological characterization of esterified lipid mediators formed in stably transfected HEK293T cells .....	98
5.3.1 Investigation of free and total oxylipins in stably transfected HEK293T cells .....	98
5.3.2 Cell viability investigation using ferroptosis-inducing agents .....	100
5.3.3 Investigation of LO and LPCAT2 localization following treatment with ferroptosis-inducing agents.....	101
5.3.4 Investigation of the influence of ferroptosis-inducing agent RSL3 on the oxylipin composition of HEK293T_LPCAT2_15LO1 cells .....	105
6 Discussion .....	107
6.1 A recombinant approach for the formation of esterified lipid mediators utilizing PA-LOX, human ACSL4, and human LPCAT2.....	107
6.2 Establishing a cell-based model system for the formation of esterified lipid mediators .....	110
6.3 Cell viability of LPCAT2 overexpressing cell lines is reduced following ferroptosis induction.....	112
6.4 LPCAT2 overexpression alters 15-LO1 localization in stably transfected HEK293T cells .....	112
6.5 Investigation of the cellular oxylipin profile.....	115
6.6 Conclusion and perspective.....	117
7 Zusammenfassung .....	118
8 References .....	123
9 Appendix.....	145
9.1 Primer .....	145
9.2 Plasmid maps.....	148
9.3 ÄKTA methods for protein purification .....	152
9.3.1 Ni-affinity chromatography – HisTrap™ HP, CV = 5 mL.....	152
9.3.2 Buffer exchange – HiTrapDesalting, CV = 15 mL (3x5 mL).....	153
9.3.3 Cation exchange chromatography – Resource S, CV = 1 mL .....	153

9.3.4 Size exclusion chromatography – HiLoad™ 16/60 Superdex™ 200 pg, CV = 120 mL .....	157
9.4 Laser scanning confocal microscopy images .....	158
9.5 Complete oxylipin analysis .....	161
9.6 Oxylipin analysis of RSL3/Ferrostation samples .....	167
9.7 Compound libraries .....	169
Danksagung.....	<b>Fehler! Textmarke nicht definiert.</b>
Declaration of Contribution.....	215
Curriculum Vitae .....	<b>Fehler! Textmarke nicht definiert.</b>

## List of figures

Figure 2.1: Two branches of the Kennedy pathway. ....	3
Figure 2.2: Schematic overview of the lipid remodeling process. ....	5
Figure 2.3: Fatty acid activation is a two-step reaction that is catalyzed by the acyl-CoA synthetase family. ....	5
Figure 2.4: Enzymatic dioxygenation mechanism of a (1Z,4Z)-1,4-pentadiene unit by lipoxygenase enzymes. ....	13
Figure 2.5: Schematic overview of leukotriene biosynthesis and signaling. ....	21
Figure 2.6: Biosynthesis routes of LXs, D-series, and E-series resolvins. ....	22
Figure 5.1: Initial expression and purification experiments of different ACSL4 constructs. ...	65
Figure 5.2: Protein expression and purification of ACSL4_His6x using different conditions. ...	68
Figure 5.3: Representative chromatograms of His6x-tagged ACSL4 purification using a 5 mL HisTrap™ HP column (A) and three consecutive 5 mL HiTrapDesalting columns (B). ....	69
Figure 5.4: ACSL4_His6x purification by Ni-affinity chromatography and SEC. ....	70
Figure 5.5: Effect of different Triton X-100 concentrations on the purification of ACSL4_His6x by SEC. ....	71
Figure 5.6: ACSL4_His6x purification by cation exchange chromatography. ....	71
Figure 5.7: Thermal shift analysis of ACSL4_His6x protein purified by Ni-affinity chromatography or Ni-affinity chromatography with subsequent SEC. ....	73
Figure 5.8: Heatmap of ACSL4_His6x unfolding temperatures. ....	74
Figure 5.9: Schematic overview of the ACSL4 activity assay setup. ....	76
Figure 5.10: Evaluation of ACSL4_His6x activity. ....	77
Figure 5.11: Adaptation of ACSL4 assay setup for the determination of enzyme kinetics. ...	78
Figure 5.12: Turnover kinetics of EPA by purified ACSL4_His6x protein. ....	79
Figure 5.13: SDS-PAGE analysis of the purification of PA-LOX. ....	80
Figure 5.14: Stability analysis of the recombinant PA-LOX protein. ....	81
Figure 5.15: Activity verification of purified PA-LOX. ....	82
Figure 5.16: Expression test of His6x-tagged LPCAT2 in <i>E. coli</i> BL21(De3) cells. ....	85
Figure 5.17: Western blot analysis of His6x-tagged LPCAT2 to determine protein integrity. ...	86
Figure 5.18: N-terminal amino acid sequence of human LPCAT2. ....	86
Figure 5.19: Purification analysis of two shortened LPCAT2 constructs. ....	87
Figure 5.20: Purification of the MBP_s1LPCAT2 construct. ....	88
Figure 5.21: Western blot analysis of stably transfected HEK293T cells. ....	89

---

Figure 5.22: Overview of the total oxylipin formation in different stably transfected HEK293T cell lines.....	90
Figure 5.23: Overview of the free oxylipin formation in different stably transfected HEK293T cell lines.....	91
Figure 5.24: Time series of 15-LO1 expression.....	92
Figure 5.25: Time series of 5-LO and 15-LO2 expression after transient transfection. ....	92
Figure 5.26: Transfection efficiency determination. ....	93
Figure 5.27: Western blot analysis of 5-LO, 15-LO1, and 15-LO2 expression in transiently transfected HEK293T_LPCAT2 cells. ....	94
Figure 5.28: Doxycycline-dependent expression of 5-LO, 15-LO1 and 15-LO2.....	95
Figure 5.29: LO product formation in transfected HEK293T cells. ....	96
Figure 5.30: Localization of ACSL4 and LPCAT2 in HEK293T_VC and HEK293T_LPCAT2 cells. ....	97
Figure 5.31: Localization of ACSL4 and LPCAT2 in stably transfected HEK293T_A+L cells. ....	98
Figure 5.32: Oxylipin formation in HEK293T_VC_LO, HEK293T_LPCAT2_LO, and HEK293T_A+L_LO cells. ....	99
Figure 5.33: Effects of RSL3 and erastin treatment on the cell viability of stably transfected HEK293T cells. ....	101
Figure 5.34: Effect of ferroptosis inducers on the localization of lipoxygenases in stably transfected HEK293T cells.....	102
Figure 5.35: Effect of ferroptosis inducers on the localization of lipoxygenases in stably transfected HEK293T cells.....	103
Figure 5.36: Localization of LOs in stably transfected HEK293T_LPCAT2 cells.....	104
Figure 5.37: RSL3 treatment increases the oxylipin formation after 4 h in HEK293T_LPCAT2_15LO1 cells. ....	105
Figure 9.1: Recombinant expression plasmid of ACSL4 with C-terminal His6x-tag. ....	148
Figure 9.2: Sleeping beauty transfection plasmid with empty MCS. ....	148
Figure 9.3: Sleeping beauty transfection plasmid for constitutive expression of ACSL4. ....	149
Figure 9.4: Sleeping beauty transfection plasmid for constitutive expression of LPCAT2... ..	149
Figure 9.5: Sleeping beauty transfection plasmid for constitutive expression of the genes ACSL4 and LPCAT2 separated by a P2A linker sequence. ....	150
Figure 9.6: Sleeping beauty transfection plasmid for inducible expression of 5-LO. ....	150
Figure 9.7: Sleeping beauty transfection plasmid for inducible expression of 15-LO1. ....	151
Figure 9.8: Sleeping beauty transfection plasmid for inducible expression of 15-LO2. ....	151

Figure 9.9: Method: Result\Bjarne\220913HisTrap5mlACSL4His6x001.res ..... 152

Figure 9.10 Method: Result\Bjarne\220913HitrapACSL4His6x(3x5ml)001.res ..... 153

Figure 9.11: Method: Result\Bjarne\190724 CationIEX 1mL ACSL4001.res ..... 156

Figure 9.12: Method: Result\Bjarne\211206BJACSL4SE001.res ..... 157

Figure 9.13: Effect of ferroptosis inducers on the localization of 5-lipoxygenase in stably transfected HEK293T cells..... 158

Figure 9.14: Effect of ferroptosis inducers on the localization of 15-lipoxygenase 1 in stably transfected HEK293T cells..... 159

Figure 9.15: Effect of ferroptosis inducers on the localization of 15-lipoxygenase 2 in stably transfected HEK293T cells..... 160

## List of tables

Table 4.1: Buffers and chemicals for cell culture use. ....	26
Table 4.2: Fetal bovine serum batches with suppliers and lot numbers, respectively. ....	26
Table 4.3: Sterile cell culture items. ....	27
Table 4.4: Common chemicals and reagents. ....	27
Table 4.5: Fatty acids and lipids. ....	30
Table 4.6: Enzymes, kits, and reagents. ....	31
Table 4.7: Primary antibodies, their manufacturers, and species of origin. ....	32
Table 4.8: Primary antibodies and their incubation conditions. ....	33
Table 4.9 Secondary antibodies and their incubation conditions. ....	33
Table 4.10: Common buffer stocks. ....	34
Table 4.11: Stock solutions. ....	34
Table 4.12: Bacterial strains. ....	35
Table 4.13: Medium for bacterial growth. ....	35
Table 4.14: Cultivation items for bacterial growth. ....	35
Table 4.15: Devices and equipment used in this work with the respective manufacturers. ....	36
Table 4.16: Software that was used to gather and analyze experimental data. ....	38
Table 4.17: Online tools and web services used. ....	38
Table 4.18: Standard protocol for the amplification of DNA. ....	39
Table 4.19: Concentration of agarose used for the separation of DNA fragments. ....	40
Table 4.20: Commercially available plasmids. ....	41
Table 4.21: Plasmids for recombinant protein expression in <i>E. coli</i> . ....	41
Table 4.22: Plasmids for transient transfection of HEK293T cells. ....	42
Table 4.23: Plasmids used for stable transfection and constitutive protein expression. ....	45
Table 4.24: Plasmids for stable transfection and inducible protein expression. ....	45
Table 4.25: Buffers used for purification of recombinant ACSL4. ....	46
Table 4.26: Buffers used for purification of recombinant PALOX. ....	48
Table 4.27: Stable cell lines with constitutive protein expression. ....	52
Table 4.28: Stable cell lines with inducible lipoxygenase expression. ....	53
Table 4.29: Primary antibodies and their dilution for confocal staining. ....	55
Table 4.30: Initial setup for the verification of ACSL4 activity. ....	56
Table 4.31: Stock solutions for ACSL4 activity analysis. ....	57



---

Table 4.32: Substrate mixes for ACSL4 activity analysis.....	58
Table 4.33: Assay conditions for ACSL4 activity analysis. ....	58
Table 4.34: HEK293T_LPCAT2 buffers. ....	59
Table 4.35: Separation program for LPCAT2 product analysis. The mobile phase consisted of: A: ultra-pure water, B: acetonitrile, D: methanol, D: 1 % aqueous acetic acid. ....	60
Table 4.36: Solutions used to determine lipoxygenase activity.....	60
Table 4.37: Separation program for lipoxygenase product analysis. The mobile phase consisted of A: ultra-pure water, B: acetonitrile, C: methanol, D: 1 % aqueous acetic acid. .	61
Table 5.1: Specifications of recombinant ACSL4 expression constructs. ....	65
Table 5.2: Matrices and buffer compositions of initial ACSL4 purification attempts. ....	66
Table 5.3: Buffer conditions tested for optimization of ACSL4_His6x purification. ....	67
Table 5.4: Approved drug library hits that increased the unfolding temperature of ACSL4 by more than 1 °C compared to DMSO controls. 5 µM protein was incubated with 20 µM compound.....	75
Table 5.5: Determined melting temperatures ( $T_m$ ) for the ACSL4_His6x interaction with mitoxantrone dihydrochloride and triclabendazole. ....	75
Table 5.6: Comparison of recombinantly expressed PA-LOX yields.....	80
Table 5.7: Results of the FAL screen with the PA-LOX protein. ....	83
Table 5.8: Drug fragment library hits with the strongest effects on $\Delta T$ . Values display mean $\pm$ SD of duplicates.....	84
Table 5.9: Overview of LO containing HEK293T cell lines. ....	95
Table 9.1: Cloning primer.....	145
Table 9.2: Primers for preparation of plasmids for transient transfection in HEK293T cells.	146
Table 9.3: Primers for preparation of plasmids for stable transfection of HEK293T cells. ....	147
Table 9.4: Complete total oxylipin analysis in $1 \times 10^7$ HEK293T cells.....	161
Table 9.5: Complete non-esterified oxylipin analysis in $1 \times 10^7$ HEK293T cells.....	164
Table 9.6: Total oxylipins in $1 \times 10^7$ HEK293T cells. ....	167
Table 9.7: Non-esterified oxylipins in $1 \times 10^7$ HEK293T cells. ....	168
Table 9.8: Fatty acid library.....	169
Table 9.9: Prestwick drug fragment library. ....	172
Table 9.10: Prestwick approved drug library. ....	182

## Abbreviations

<b>12-HHT</b>	12S-hydroxyheptadecatrienoic acid
<b>AAG</b>	alkyl-acylglycerol
<b>ACS</b>	Acyl-CoA synthetases
<b>ACSL</b>	ACS long chain
<b>ACSL4V1/2</b>	ACSL4 version 1/2
<b>ADP</b>	adenosine diphosphate
<b>AGPAT</b>	acylglycerophosphate acyltransferase
<b>AGPAT11</b>	1-acylglycerol-3-phosphate O-acyltransferase 11
<b>ALX</b>	lipoxin A <sub>4</sub> receptor
<b>AML</b>	acute myeloid leukemia
<b>APS</b>	Ammonium peroxydisulfate
<b>ARA</b>	arachidonic acid
<b>ARA-CoA</b>	arachidonoyl-CoA
<b>AT</b>	aspirin-triggered
<b>ATP</b>	adenosine triphosphate
<b>AYTL1</b>	acyltransferase-like 1
<b>BCA</b>	Bicinchoninic acid assay
<b>BLT<sub>1/2</sub></b>	B leukotriene receptor 1/2
<b>BSA</b>	Bovine serum albumin
<b>cAMP</b>	Cyclic adenosine monophosphate
<b>CCT</b>	CTP:phosphocholine cytidyltransferase
<b>CDP</b>	cytidine diphosphate
<b>CK</b>	choline kinase
<b>CMP</b>	cytidine monophosphate
<b>CoA</b>	coenzyme A
<b>COX1 or 2</b>	Cyclooxygenase 1 or 2
<b>cPLA<sub>2</sub></b>	cytosolic phospholipase A <sub>2</sub>
<b>CPT</b>	choline phosphotransferase
<b>CRISPR</b>	clustered regularly interspaced short palindromic repeats
<b>CTP</b>	cytidyl triphosphate
<b>CV</b>	column volumes
<b>cys-LTs</b>	cysteinyl LTs

---

<b>DAG</b>	diacylglycerol
<b>DAPI</b>	4',6-Diamidino-2-phenylindol
<b>DGLA</b>	dihomo-gamma-linolenic acid
<b>DHA</b>	docosahexaenoic acid
<b>DMEM</b>	Dulbecco's Modified Eagle Medium
<b>DMSO</b>	Dimethyl sulfoxide
<b>DNA</b>	Deoxyribonucleic acid
<b>DPPC</b>	dipalmitoyl PC
<b>DSMZ</b>	Deutsche Sammlung von Mikroorganismen und Zellkulturen, Braunschweig, Germany
<b>DTT</b>	Dithiothreitol
<b>ECT</b>	CTP:phosphoethanolamine cytidyltransferase
<b>EDTA</b>	Titriplex® III ethylenedinitrilotetraacetic acid
<b>EETs</b>	epoxyeicosatetraenoic acids
<b>EK</b>	ethanolamine kinase
<b>eLO3</b>	epidermis-type LO 3
<b>EMA</b>	European Medicines Agency
<b>EPA</b>	eicosapentaenoic acid
<b>EPT</b>	ethanolamine phosphotransferase
<b>ER</b>	endoplasmic reticulum
<b>ESI</b>	Electrospray ionization
<b>EtOH</b>	Ethanol
<b>FAL</b>	Fatty acid library
<b>FBS</b>	Fetal bovine serum
<b>FDA</b>	Food and Drug Administration
<b>FLAP</b>	5-LO activating protein
<b>GFP</b>	Green fluorescent protein
<b>GPCRs</b>	G-protein-coupled receptors
<b>GPX4</b>	glutathione peroxidase 4
<b>GSH</b>	Glutathione
<b>HCV</b>	hepatitis C virus
<b>HEK</b>	Human embryonal kidney
<b>HEPES</b>	4-(2-hydroxyethyl)-1-piperazineethane sulfonic acid
<b>HETEs</b>	hydroxyeicosatetraenoic acids

<b>HpDHA</b>	hydroperoxydocosahexaenoic acid
<b>HpEPE</b>	hydroperoxyeicosapentaenoic acid
<b>HpETE</b>	hydroperoxyeicosatetraenoic acid
<b>HpODE</b>	hydroperoxyoctadecadienoic acid
<b>IEX</b>	Ion exchange chromatography
<b>IL-13</b>	interleukin 13
<b>IL-4</b>	interleukin 4
<b>IPTG</b>	Isopropyl- $\beta$ -D-thiogalactopyranosid
<b>IR</b>	ionizing radiation
<b>LA</b>	Linoleic acid
<b>LB</b>	Luria Broth Base
<b>LC-MS</b>	Liquid chromatography - mass spectrometry
<b>LDL</b>	low-density lipoprotein
<b>LDs</b>	lipid droplets
<b>L-LDH</b>	L-Lactate Dehydrogenase
<b>LLOQ</b>	Lower limit of quantification
<b>LOs</b>	lipoxygenases
<b>LPCATs</b>	lysophosphatidylcholine acyltransferases
<b>LPLATs</b>	lysophospholipid acyltransferases
<b>LPS</b>	Lipopolysaccharides
<b>LT</b>	leukotriene
<b>LTA<sub>4</sub></b>	leukotriene A <sub>4</sub>
<b>LTA<sub>4</sub>H</b>	LTA <sub>4</sub> hydrolase
<b>LTB<sub>4</sub></b>	leukotriene B <sub>4</sub>
<b>LTC<sub>4</sub>S</b>	LTC <sub>4</sub> synthase
<b>LxA<sub>4</sub></b>	lipoxin A <sub>4</sub>
<b>LxB<sub>4</sub></b>	lipoxin B <sub>4</sub>
<b>LXs</b>	lipoxins (lipoxygenase reaction products)
<b>LysoPAFAT</b>	lyso-platelet-activating factor acyltransferase
<b>MAPK</b>	mitogen-activated protein kinase
<b>MBOAT</b>	membrane-bound O-acyltransferase
<b>MeOH</b>	Methanol
<b>mRNA</b>	messenger ribonucleic acid
<b>MW</b>	molecular weight

---

<b>n-3</b>	omega-3
<b>n-6</b>	omega-6
<b>NADH</b>	$\beta$ -Nicotinamide adenine dinucleotide, reduced disodium salt hydrate
<b>NaP<sub>i</sub></b>	Sodium phosphate
<b>NO</b>	nitric oxide
<b>PA</b>	phosphatic acid
<b>PAF</b>	platelet-activating factor
<b>PA-LOX</b>	15S-lipoxygenating enzyme from <i>pseudomonas aeruginosa</i>
<b>PBS</b>	Dulbecco's Phosphate-Buffered Saline
<b>PC</b>	phosphatidylcholine
<b>PCRs</b>	Polymerase chain reactions
<b>PE</b>	phosphatidylethanolamine
<b>PEBP1</b>	phosphatidylethanolamine binding protein 1
<b>PEI</b>	Polyethylenimine
<b>PEP-K</b>	Phosphoenolpyruvate mono potassium salt
<b>PG</b>	phosphatidylglycerol
<b>PGB<sub>1</sub></b>	Prostaglandin B1
<b>PGE2</b>	prostaglandin E2
<b>PI</b>	phosphatidylinositol
<b>PLA<sub>2</sub></b>	phospholipase A <sub>2</sub>
<b>PLAT</b>	Polycystin-1, Lipoxygenase, Alpha-Toxin
<b>PMNL</b>	polymorphonuclear leukocytes
<b>PMSF</b>	Phenylmethanesulfonyl fluoride
<b>PPAR<math>\gamma</math></b>	peroxisome proliferator-activated receptor- $\gamma$
<b>PP<sub>i</sub></b>	pyrophosphate
<b>PS</b>	phosphatidylserine
<b>PSS1/2</b>	phosphatidylserine synthase-1 and -2
<b>PUFAs</b>	polyunsaturated fatty acids
<b>ROS</b>	reactive oxygen species
<b>RSL3</b>	1S,3R-RSL 3
<b>RT</b>	room temperature
<b>RvD1-6</b>	resolvins D1-6
<b>RvE1-4</b>	resolvin E1-4
<b>SD</b>	standard deviation

<b>SDS</b>	Sodium dodecyl sulfate
<b>SDS-PAGE</b>	Sodium dodecylsulfate polyacrylamide gel electrophoresis
<b>SEC</b>	size exclusion chromatography
<b>SIR</b>	selected ion recording
<b>siRNA</b>	Small interfering RNA
<b>SMCs</b>	smooth muscle cells
<b>SO</b>	SYPRO™ Orange
<b>SPE</b>	Solid phase extraction
<b>SPMs</b>	specialized pro-resolving lipid mediators
<b>STI</b>	Trypsin inhibitor from <i>Glycin max</i>
<b>TAG</b>	triacylglycerol
<b>TCEP</b>	Tris-(2-carboxyethyl)-phosphine Hydrochloride
<b>TE</b>	Trypsin-EDTA
<b>TEMED</b>	N,N,N',N'-Tetramethylethylenediamine
<b>TEV</b>	tobacco etch virus
<b>T<sub>m</sub></b>	melting temperatures
<b>Tris</b>	Tris-(hydroxymethyl)-aminomethane
<b>TSA</b>	thermal shift analysis
<b>TX-100</b>	Triton® X-100
<b>ULOQ</b>	upper limit of quantification
<b>WB</b>	Western blot

## 1 Abstract

This work focused on the biosynthesis and characterization of esterified lipid mediators. Lipid mediators were generally thought to exert their effects as free molecules, and their esterification was regarded as a storage mechanism. However, more recent studies indicate that esterified lipid mediators are a distinct class of mediators. When this thesis started back in 2017, the idea of esterified lipids as a new class of mediators was relatively new so that respective compounds were either quite expensive or not commercially available at all. Therefore, a biosynthetic approach had to be established first to enable the study of the new lipid mediator class. Within the cell, esterified lipids are produced by activation and subsequent incorporation of polyunsaturated fatty acids. These steps are enzymatically catalyzed by members of the acyl-CoA synthetase family and the lysophosphatidylcholine acyltransferase family, respectively. Therefore, the enzymes acyl-CoA synthetase long-chain family member 4 (ACSL4) and lysophosphatidylcholine acyltransferase 2 (LPCAT2) were selected for a biosynthetic approach due to their broad substrate acceptance.

In a first attempt, recombinant protein expression in *E. coli* was studied. While the expression and purification of C-terminally His6x-tagged ACSL4 resulted in a pure and active protein, the expression of LPCAT2 turned out quite troublesome. Although several expression and purification parameters were varied, including purification tags, buffer compositions, and chromatography strategies, successful purification of LPCAT2 was not achieved.

Instead, a second approach was studied. This time, stably transfected cells overexpressing ACSL4 and/or LPCAT2 were generated from the human embryonal kidney (HEK) 293T cell line. Stably transfected cell lines were characterized on protein level and regarding their oxylipin profile. After confirming the overexpression and functionality of the enzymes, lipoxygenases (LOs) were co-expressed in a doxycycline-inducible manner to prevent premature cell death due to increased oxidative stress. As a result, LO product formation was enhanced and enabled the investigation of specific oxylipins. Since increased lipid peroxidation is also a key component of the ferroptosis cell death mechanisms, cell lines were investigated towards their cell viability. Indeed, expression of ACSL4 and/or LPCAT2 promoted cell death when treated with the ferroptosis inducers erastin or RSL3, even in the absence of LO expression. Furthermore, analysis by laser scanning confocal microscopy revealed that the localization of 15-LO1 was altered in the presence of LPCAT2, similar to treatment with RSL3 in vector control cells.

In conclusion, a stable overexpression system of ACSL4 and/or LPCAT2 was successfully established in HEK293T cells, which enabled the synthesis and characterization of esterified oxylipins. Interestingly, characterization of the cell lines revealed a correlation with the cell death mechanism ferroptosis. Although the expression of ACSL4 has already been reported as a biomarker for ferroptosis, this is the first time that a potential connection of LPCAT2 with ferroptosis was demonstrated. As a result, this may provide new therapeutic options for ferroptosis-related pathologies such as neurodegeneration, autoimmune diseases, or tumorigenesis.

## 2 Introduction

### 2.1 Biological membranes

Cellular membranes consist of lipids, proteins, and carbohydrates, as described by Singer and Nicolson back in 1972 [1]. They first reported the 'fluid mosaic hypothesis', which is still the consensus model today. Here, the main component of membranes are phospholipids which contain both hydrophilic headgroups and hydrophobic acyl chains. In biological systems, this results in the spontaneous formation of lipid droplets or bilayers with hydrophobic core regions and a hydrophilic surface. While the term mosaic refers to the presence of multiple components in distinct amounts, the ability of integral proteins and lipids to undergo lateral diffusion within the membrane led to a fluid characteristic. Although proteins and lipids are found on both sides of the membrane bilayer, lipid movement from the inner side to the outer surface or *vice versa* is, in general, prevented by the polar headgroup. However, this transfer can be enabled through membrane proteins known as flippases [2,3]. This restriction causes distinct compositions on each of the two monolayers forming the membrane, which is known as the asymmetry of membranes [4].

Lipids exist in structurally diverse forms, such as glycerophospholipids, sphingolipids, and sterols [5]. Sterols represent the group of non-polar lipids with cholesterol as the single most occurring member in eukaryotic membranes [6]. In addition, the group of polar lipids is represented by glycerophospholipids and sphingolipids. Glycerophospholipids of eukaryotic membranes include mainly phosphatidylcholine (PC) and phosphatidylethanolamine (PE) but also less-common members such as phosphatidylserine (PS), phosphatidylinositol (PI), phosphatic acid (PA) and phosphatidylglycerol (PG) [7,8]. Besides their hydrophilic head groups, these lipids contain a diacylglycerol unit which, in general, consists of one saturated as well as one *cis*-unsaturated fatty acyl chain at the *sn*-1 or *sn*-2 position, respectively [8]. Sphingolipids are a structurally distinct class of membrane lipids. These lipids have a ceramide backbone and occur mainly as sphingomyelin or glycosphingolipids. The latter contain sugar moieties like mono-, di- or oligosaccharides. Sphingolipids contain saturated fatty acids, but in contrast to glycerophospholipids, they may also attach *trans*-unsaturated acyl chains [7].

### 2.2 *De novo* synthesis – The Kennedy pathway

PC and PE, the most abundant phospholipids in mammals, can be synthesized *de novo* in the Kennedy pathway (Figure 2.1) [9] or by a remodeling mechanism known as Lands' Cycle [10]. The biosynthesis of PC and PE follows the same route and only differs in the respective enzymes necessary to convert either choline or ethanolamine and their intermediates (Figure 2.1). The first step in the formation of PC and PE is the adenosine triphosphate (ATP) dependent phosphorylation of choline and ethanolamine to their intermediates, phosphocholine, and phosphoethanolamine, respectively. This reaction is catalyzed by choline and ethanolamine kinases. Although it was initially highly discussed whether the phosphorylation is mediated by an enzyme with dual activity, Brophy and colleagues in 1977 provided evidence for two enzymes with separate activity [11]. Next, cytidyl triphosphate (CTP) is coupled to phosphocholine and phosphoethanolamine either by a CTP:phosphocholine



cytidyltransferase (CCT) or a CTP:phosphoethanolamine cytidyltransferase (ECT), which has been proven to be the rate-limiting step in the Kennedy pathway [12].

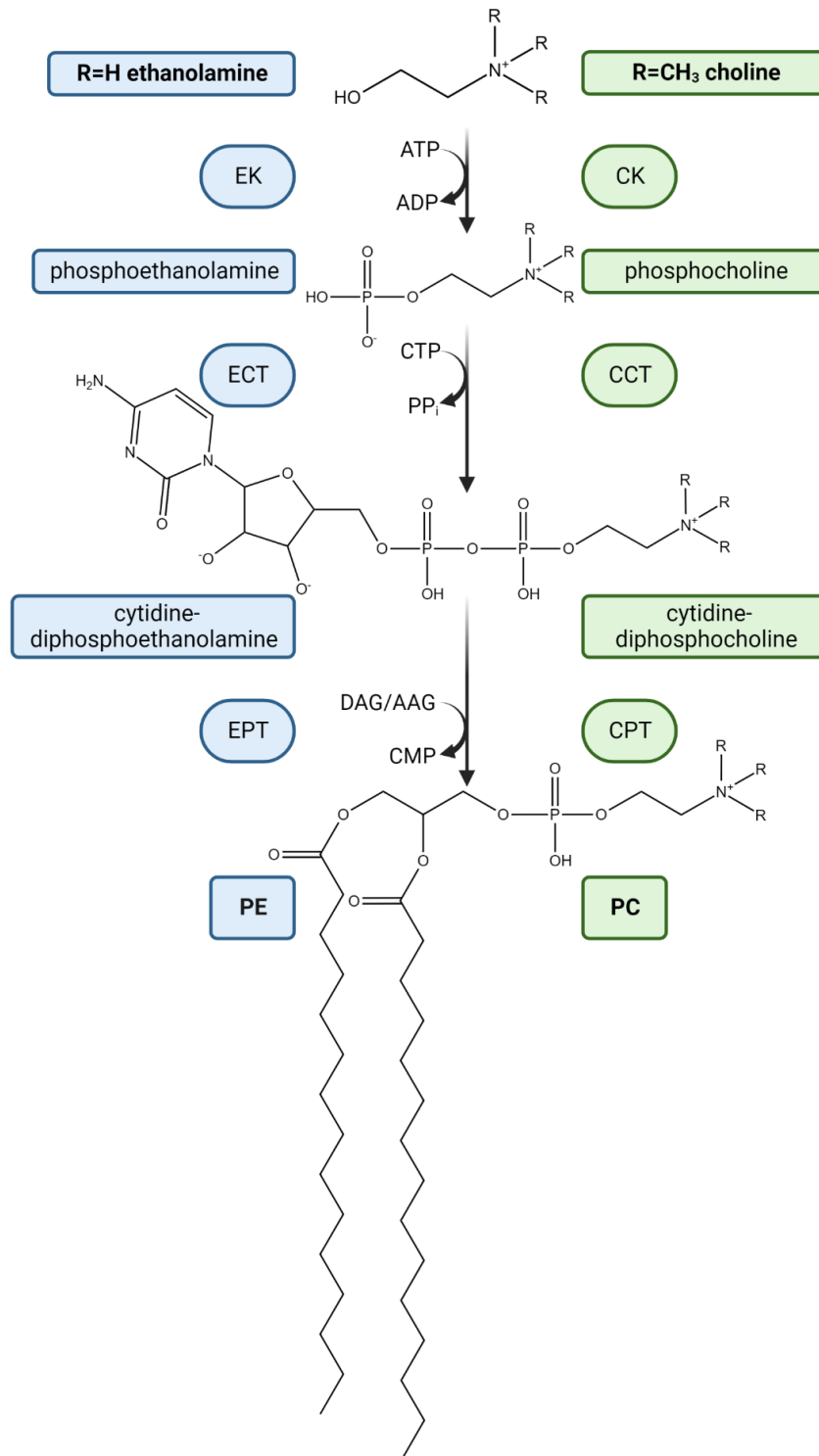


**Figure 2.1: Two branches of the Kennedy pathway.**

Figure adapted from [13]. CK: choline kinase; AAG: alkyl-acylglycerol; ADP: adenosine diphosphate; ATP: adenosine triphosphate; CCT: CTP:phosphocholine cytidyltransferase; CPT: choline phosphotransferase; CMP: cytidine monophosphate; CTP: cytidyl triphosphate; DAG: diacylglycerol; EK: ethanolamine kinase; ECT: CTP:phosphoethanolamine cytidyltransferase; EPT: ethanolamine phosphotransferase; PC: phosphatidylcholine; PE: phosphatidylethanolamine; PP<sub>i</sub>: pyrophosphate.

The final phospholipid is then produced by the reaction of the previous intermediate with either alkyl-acylglycerol (AAG) or diacylglycerol (DAG). The PE derivative is obtained through an ethanolamine phosphotransferase (EPT), while the PC version is catalyzed by a choline phosphotransferase (CPT). Other phospholipids, however, require different biosynthetic approaches. While PA is produced *de novo* from glycerol-3-phosphate through two consecutive acylation reactions with lysophosphatic acid as an intermediate (reviewed in more detail recently in [14]), PI is synthesized from PA. In contrast to the Kennedy pathway, PA is not converted to DAG but is used as a substrate in the CDP (cytidine diphosphate) -DAG pathway. From here, PI synthase combines inositol and CDP-DAP to PI (reviewed in more detail in [15]). While it has to be mentioned that PS can, in principle, be produced from CDP-DAP, this is only the case in fungi and prokaryotes. In eukaryotes, PS is gained from enzymatic base exchange of the polar headgroup from either PC or PE instead. This reaction is catalyzed by phosphatidylserine synthase-1 and -2 (PSS1/2), where PSS2 is highly specific for PE while the PSS1 specificity is still under discussion (reviewed in more detail in [16]).

The acyl and alkyl chain composition of these phospholipids is highly tissue and cell type dependent and thus is adjusted later-on in a lipid remodeling process.

### 2.3 Lipid remodeling – The Lands’ cycle

The diversity of phospholipids with various acyl and alkyl chains and also several different headgroups results in enormous molecule numbers. While this is definitely true for some phospholipids, the entirety of phospholipid diversity cannot be fully explained solely by *de novo* biosynthesis [17]. It was not until 1958 that William E. Lands [10] described the rapid turnover at the *sn*-2 position, where polyunsaturated fatty acids (PUFAs) are preferentially incorporated, in a remodeling pathway, which has since been referred to as Lands’ cycle. Figure 2.2 summarizes the enzymes required for this mechanism. Although stage 1 is not exactly part of the Lands’ cycle, the activation of PUFAs by an acyl-CoA synthetase (ACS, described in more detail in 2.4) produces acyl-CoAs that function as acyl-chain-donors. The remodeling pathway itself relies on phospholipase A<sub>2</sub> (PLA<sub>2</sub>) enzymes and lysophospholipid acyltransferases (LPLATs). While PLA<sub>2</sub>s release PUFAs from the *sn*-2 position by hydrolysis resulting in lysophospholipids lacking one acyl chain (as reviewed in detail in [18]), the family of LPLATs is responsible for their re-acylation [19,20]. The class of LPLATs was studied by several groups, which resulted in a plethora of names. Allegedly new LPLATs were characterized and named according to activity or sequence homology. As a consequence, LPLAT9 is also known as lysophosphatidylcholine acyltransferase 2 (LPCAT2), 1-acylglycerol-3-phosphate O-acyltransferase 11 (AGPAT11), lyso-platelet-activating factor acyltransferase (LysoPAFAT) and acyltransferase-like 1 (AYTL1) protein [21–23]. Since all of these acyltransferase families have multiple members, it is very easy to lose the thread. Multiple reviews sorted this comprehensive field and presented helpful overviews [8,24,25]. Hereafter, this work will focus on the family of lysophosphatidylcholine acyltransferases (LPCATs), as these are necessary for the remodeling of PC, which is the most abundant phospholipid in mammals.

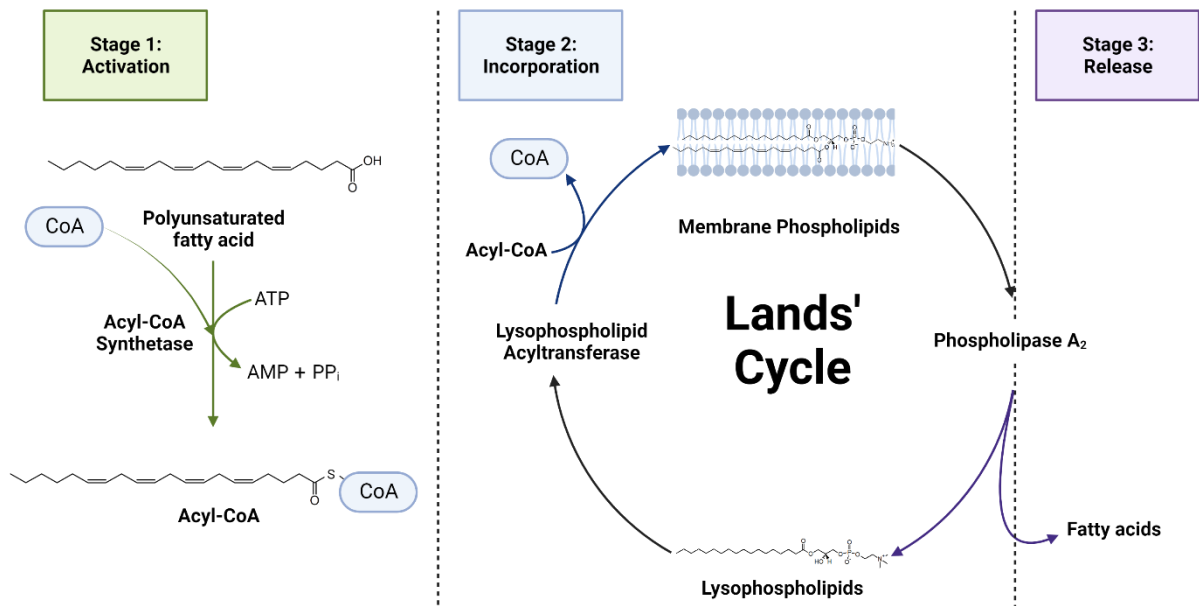


Figure 2.2: Schematic overview of the lipid remodeling process.

## 2.4 Acyl-CoA synthetases

ACs are an important class of enzymes required for lipid metabolism. They catalyze the activation of fatty acids, thereby enabling their use in anabolic or catabolic pathways [26]. The ATP-dependent activation is a two-step reaction (Figure 2.3) in which the fatty acid is coupled to coenzyme A (CoA).

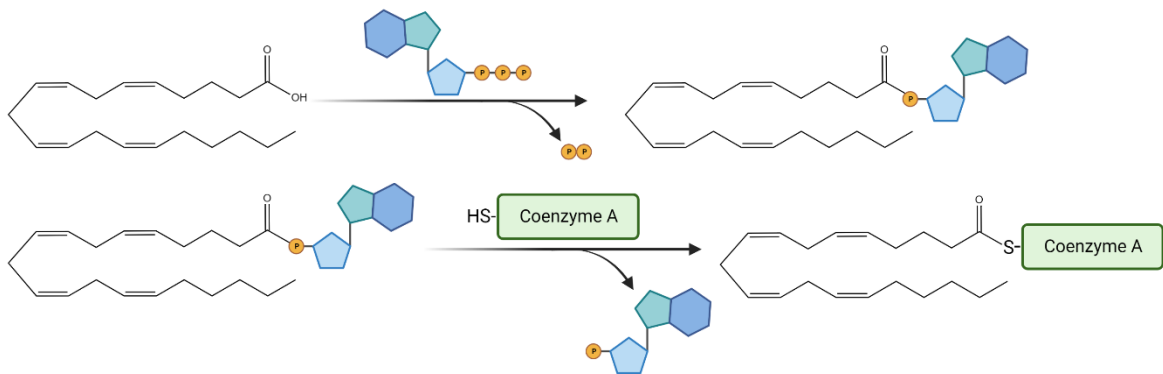


Figure 2.3: Fatty acid activation is a two-step reaction that is catalyzed by the acyl-CoA synthetase family.

Arachidonic acid first reacts with ATP to form the intermediate acyl-AMP under release of pyrophosphate. In the second step, the AMP moiety is replaced by coenzyme A (CoA) to form the final acyl-CoA thioester.

The varying fatty acid chain lengths require different substrate specificities covered by five separate subfamilies within the ACS family. These subfamilies differ in their preference for short (C2-C4), medium (C4-C12), long (C12-C22), bubblegum (C14-C24), and very long acyl chains (C18-C26). The ability to activate C20 fatty acids like arachidonic acid (ARA) and eicosapentaenoic acid (EPA), important precursors of bioactive lipid mediators (covered in more detail in 2.9), highlights especially the ACS long chain (ACSL) family when it comes to therapeutic use. The ACSL family contains five isoenzymes (ACSL1, ACSL3, ACSL4, ACSL5, and ACSL6) that were identified and characterized in the laboratory of Yamamoto and colleagues [27–29]. While ACSL1 preferentially converts oleic acid and linoleic acid (LA) [30],

ACSL3 uses myristic acid, lauric acid, ARA, and EPA as substrates [29]. ACSL4 has a preference for ARA, while ACSL5 accepts palmitic acid, palmitoleic acid, oleic acid, and LA [31]. Meanwhile, ACSL6 does not favor a specific substrate and does not even distinguish between saturated and unsaturated fatty acids as long as the chain has a length of 16-20 carbon atoms [32]. On a side note, it should be mentioned that an earlier nomenclature, which was prone to confusion, was renamed in 2004 [33]. Since FACL1 and FACL2, the former equivalents of ACSL1 and the alleged 'ACSL2', were found to be identical, ACSL1 is the new title of FACL1/FACL2 while 'ACSL2' is not assigned anymore [33].

ACSLs do not only have distinct substrate preferences but also vary in tissue distribution and cellular localization. ACSL1 is found in the liver, heart, as well as in white and brown adipose tissue and skeletal muscle cells [34]. Knockout studies imply that the enzyme is involved in different pathways depending on the tissue. Li *et al.* reported a 50 % decrease in total ACSL activity upon knockout of *ACSL1* in the liver and therefore assumed that the enzyme either does not favor between synthetic and degradative pathways or that its occurrence in mitochondria and ER results in support of both pathways [35]. In the heart as well as in brown and white adipose tissue,  $\beta$ -oxidation seems to be the main metabolic route for acyl-CoAs [36,37]. In addition, it has been shown that the knockout of *ACSL1* in brown adipose tissue resulted in impaired thermogenesis [37]. ACSL3 is expressed in the brain [29] but is also found in adipocytes [38], epithelial cells [39], and hepatocytes [40]. The enzyme is located in lipid droplets and the endoplasmic reticulum (ER) membrane [38,41], where its products or downstream metabolites are involved in the regulation of hepatic lipogenesis [42]. ACSL4 is mainly expressed in the adrenal gland, ovary, testis, and brain [27], where it is associated with endosomes [43], peroxisomes [44], the plasma membrane [45], the ER as well as mitochondrial membranes [44] and in the secretory pathway [46]. With its ability to preferentially activate ARA but also EPA, as shown *in vitro* by Kang *et al.* [27], ACSL4 is linked to the eicosanoid metabolism, as shown, for example, in smooth muscle cells (SMCs) [47]. Here, ARA-CoA formation was highly increased upon overexpression of ACSL4 in SMCs. The authors concluded that the enzyme supports the incorporation of ARA into triacylglycerol (TAG) while it does not significantly affect  $\beta$ -oxidation. Furthermore, persistent overexpression of ACSL4 caused a decrease in prostaglandin E2 (PGE2) levels as an effect of the increased ARA conversion and, thus, diminished availability of free substrate for competing enzymes like cyclooxygenase (COX) 1 or 2 [47]. In mice, ACSL5 is most prominent in intestinal mucosa but also found in the lung, liver, adrenal gland, kidney, and brown adipose tissue [28,48]. *Acs/5* mRNA levels were increased by insulin and SREBP-1c treatment in the liver, indicating that the enzyme is also involved in TAG synthesis [49,50]. This finding was further reinforced by a siRNA-mediated knockdown of *Acs/5* in primary rat hepatocytes which negatively affected lipid accumulation, TAG content, and the conversion of long-chain fatty acids into phospholipids and cholesterol esters [51]. Lastly, ACSL6 is most prominent in the brain [52], while its subcellular localization was not demonstrated yet. ACSL6 was shown to be a main regulator of the docosahexaenoic acid (DHA) metabolism in brain tissue of mice, where a decrease in ACSL6 negatively affected, among other factors, the spatial memory and early-onset neuroinflammation [53].

### 2.4.1 Acyl-CoA synthetase long-chain family member 4

The human *ACSL4* gene is located at the Xq23 chromosome region [54] and displays a higher resemblance to *Acs14* (98 %) and *Acs13* (72.8 %) of rats than to other human *ACSLs* [55]. Alternative splicing results in the formation of two isoforms, *ACSL4V1* (*ACSL4* version 1) and *ACSL4V2* (*ACSL4* version 2) [54,55]. While *ACSL4V1* is the most abundant form and encodes for a 74,436 Da (UniProt entry: O60488-2) enzyme, *ACSL4V2* carries an additional 41-amino acid peptide at the N-terminus resulting in an increased molecular weight of 79,188 Da (UniProt entry: O60488-1) [54]. Although it was assumed that the N-terminal part might play a role in substrate specificity, kinetic studies of both *ACSL4* versions, recombinantly expressed in *Spodoptera frugiperda* 9 (His-tagged), revealed comparable affinities for ARA, EPA, and DHA (order of preference: ARA>EPA>DHA) [56]. Comparison of rat *ACSL4V1* (FLAG-tagged) activity in *Escherichia coli* (*E. coli*) and human COS7 cells revealed the ability to activate epoxyeicosatetraenoic acids (EETs) and hydroxyeicosatetraenoic acids (HETEs) [31]. The study also included the remaining isoenzymes of the *ACSL* family, with *ACSL4* being the most effective in EET activation, while HETEs were preferentially converted by *ACSL1*.

With its ability to influence lipid metabolism by activation of important lipid mediator precursors and also oxidized PUFAs, it is not surprising that *ACSL4* is involved in the immune response, cell death mechanisms, and especially cancer. Activation of ARA promotes the formation of eicosanoids such as prostaglandins, thromboxanes, and leukotrienes which are important regulators of inflammation. Recent studies on CD8<sup>+</sup>T cells indicate that the specific immune response is dependent on *ACSL4* [57], while Drijvers *et al.* demonstrated that *ACSL4* deficiency prevents the induction of ferroptosis in these cells [58]. Ferroptosis is a cell death mechanism that was first reported by Dixon *et al.* in 2012 (covered in more detail in chapter 2.6) [59]. Here, cell death is mediated by iron accumulation and lipid peroxidation, and thus, an increase in *ACSL4* expression is correlated with the promotion of ferroptosis [60]. In-line with these findings, it has been shown that a decrease in *ACSL4*, either by inhibition or genetic manipulation, resulted in increased resistance against ferroptotic induction [61]. In 2016, Yuan *et al.* reported that *ACSL4* expression might even be used as a biomarker of ferroptosis since its expression levels correlated with the amount of ferroptosis in cancer cells [60]. This was accompanied by a bioinformatic analysis that reported increased *ACSL4* expression in several cancer types, including liver, colorectal, kidney, head, and neck [62]. The correlation of *ACSL4* expression with ferroptosis induction in cancer was also reported during ionizing radiation (IR) of cancer cells [63]. The IR treatment induced lipid peroxidation, reactive oxygen species (ROS) formation, and *ACSL4* expression, resulting in ferroptotic cell death. However, the connection between radiotherapy and elevated protein level remains elusive. Despite these quite clear indications on the effects of *ACSL4* in ferroptosis and cancer, it needs to be mentioned that there are also types of cancer with decreased *ACSL4* levels [62]. Furthermore, the authors state that the role of *ACSLs* and especially *ACSL4* varies between different types of cancers and future therapeutic approaches should consider both inhibitors and activators since their findings also support a suppressive role.

## 2.5 Lysophosphatidylcholine acyltransferases

LPLATs are essential for the re-acylation of membrane lysophospholipids. Although the remodeling process was described back in 1958 [10], LPLATs were not identified until 1997 [64], and the first LPCAT was cloned in 2006 by two independent groups [65,66]. The report of *Lpcat1* was soon followed by the discovery of *Lpcat2* in 2007 [23], and the final two mammalian enzymes, LPCAT3 and LPCAT4, were identified in 2008 [67–69]. The four LPCATs can be divided into two sub-groups based on their amino acid sequence, with LPCAT1 and LPCAT2 being members of the acylglycerophosphate acyltransferase (AGPAT) family. The enzymes, also called AGPAT9 and AGPAT11, respectively, contain four lyso-PA acyltransferase motifs [21,70] as well as an ER localization sequence [71]. In contrast, LPCAT3 and LPCAT4 are members of the membrane-bound O-acyltransferase (MBOAT) family. The enzymes, also known as MBOAT5 and MBOAT2, respectively, also localize to the ER membrane but lack the lyso-PA motifs [67] and instead contain several MBOAT motifs [72]. As was seen for the ACSL family, the members of the LPCAT family differ in substrate specificity and tissue distribution. While LPCAT1 expression is prominent in lung alveolar type II cells [65,66], a strong LPCAT2 expression is found in inflammatory cells, especially in resident macrophages and casein-induced neutrophils, but also in skin, colon, spleen, and brain tissue [23]. LPCAT3 is found in the testis, kidney, and several metabolic tissues like the liver and adipose tissue [67,68,73], while LPCAT4 is present in the epididymis, brain, testis, and ovary [67]. Moreover, they also vary in their enzymatic activity and substrate preference. According to their name, all LPCATs are able to incorporate fatty acids into lyso-PC. In addition, LPCAT1 and LPCAT2 have an acetyl activity, which results in the formation of the platelet-activating factor (PAF) from lyso-PAF [74]. Furthermore, LPCAT1 is able to use lyso-PG and lyso-PA [66], while LPCAT3 and LPCAT4 show activity towards lyso-PE, with LPCAT3 also being able to transfer acyl chains to lyso-PS [67]. Besides their different acyl-acceptor abilities, LPCATs also vary in their acyl-CoA preferences. Palmitoyl-CoA is the preferred saturated substrate of LPCAT1 [65,66], but linoleoyl-CoA and linolenoyl-CoA are favored when it comes to unsaturated substrates [65]. LPCAT2 prefers arachidonoyl-CoA as substrate under normal conditions, but the substrate preference is shifted towards acetyl-CoA under inflammatory conditions [23]. LPCAT3 and LPCAT4 also prefer unsaturated fatty acid CoA thioesters such as linoleoyl-CoA and arachidonoyl-CoA (LPCAT3), and oleoyl-CoA (LPCAT4) [67,73].

Due to their ability to affect lipid metabolism, LPCATs are involved in several physiological and pathophysiological processes. Lipid droplets (LDs) are depots of neutral lipids that are used as substrates for membrane synthesis and lipid signaling [75]. In agreement with the lipid composition of eukaryotic membranes, PC is the main phospholipid present in LDs [76]. The lipids form droplets with a hydrophobic inner core region and a hydrophilic outer surface. In addition to the presence of phospholipids, proteins are found in or associated with the lipid monolayer of LDs. Both LPCAT1 and LPCAT2 were reported to translocate to LDs in several mammalian cells [77,78]. Therefore, it is not surprising that LDs display an acyltransferase activity towards lyso-PC [78]. Furthermore, it has been shown that the presence of LPCAT1/2 affects the size of LDs. Knockout experiments not only revealed larger sizes in the absence of LPCAT1/2 but also showed that the morphology of LDs is altered [79]. Although LDs are important for many biological processes, including lipid storage, lipid signaling, and activation

of transcription factors, only few information is available on the correlation with LPCAT1/2-mediated lipid remodeling [75]. However, at least for LPCAT2, it has been shown that the enzyme regulates autophagy in an LD-dependent manner [80]. Furthermore, a correlation between LPCAT2 expression and LD formation in colorectal cancer has been demonstrated, resulting in resistance to chemotherapy if the enzyme is overexpressed [81]. LPCAT1 plays an important role in hepatitis C virus (HCV) infections, where lipid metabolism in host cells is altered (reviewed in detail in [82]). It has been shown that LDs are highly involved here and that LPCAT1 expression was inhibited after HCV infection of primary human hepatocytes. These findings were confirmed by shRNA-mediated knockdown of LPCAT1 in Huh-7.5.1 cells, which resulted in elevated levels of HCV particles [83]. Aside from LD formation, *Lpcat1* is also responsible for the formation of dipalmitoyl PC (DPPC) and, therefore, the maintenance of pulmonary surfactant homeostasis in the lung [84]. Approx. 55-75 % of the DPPC content in the lung is obtained by lipid remodeling [85], which underlines the importance of *Lpcat1* protein in the rat, especially since pulmonary diseases like the acute respiratory distress syndrome are correlated with a defect in surfactant production [86].

*Lpcat3* was first related to lipid metabolism in mice when its gene was described as a transcriptional target of the two lipid-activated nuclear receptors LXR [73,87] and PPAR (alpha and gamma) [68,88] that are necessary for lipid homeostasis. The enzyme has been shown to affect hepatic SREBP-1 processing after LXR activation [89] and also plays an important role in regulating lipid metabolism in the small intestine in mice [90]. Here, a knockout of *Lpcat3* resulted in mice that were not affected at birth but died soon after due to hypoglycemia [90,91]. Furthermore, LPCAT3 is assumed to play a role in atherosclerosis due to its ability to produce oxidized phospholipids and modulate the polarization of macrophages [92]. In addition, it has been shown that LPCAT3 levels were decreased in late atherosclerosis, resulting in lower AA-PC and higher lyso-PC formation [93].

Compared to the first three members of the LPCAT family, only few information is available on LPCAT4. Nevertheless, it has been demonstrated that LPCAT4 is overexpressed in colorectal cancer cells. Here, siRNA-mediated knockdown of LPCAT2 was linked to reduced 16:0-16:1-PC levels and impaired cell growth in HCT116 and DLD1 cells [94]. Interestingly, LPCAT4 is not the only LPCAT member involved in cancer. LPCAT1 expression is also upregulated in several tumor types, including, among others, clear renal cell carcinoma, gastric, breast, colorectal, and prostate cancers [95–100]. Overexpression of LPCAT1 has been shown to go hand in hand with increased tumor cell proliferation, migration, and metastasis [95,96] and is therefore linked to poor prognosis and patient survival [95,97,99,100]. As already mentioned above, LPCAT2 expression has been proven to alter chemoresistance in colorectal cancer in an LD-dependent manner [81]. Furthermore, LPCAT2 is also overexpressed in cervical and breast cancers [22]. Similar to LPCAT1, LPCAT3 is overexpressed in several types of cancer and linked to poor prognosis, especially in acute myeloid leukemia (AML), lower-grade glioma, ovarian cancer, and uveal melanoma [101].

### 2.5.1 Lysophosphatidylcholine acyltransferase 2

The human *LPCAT2* gene encodes for a 544 amino acids protein with a size of 60,208 Da (UniProt entry: Q7L5N7-1) and a shorter version produced by alternative splicing, which lacks

the first 270 amino acids (UniProt entry: Q7L5N7-2). Since the EGTC and the HXXXXD motif, which is essential for acyltransferase activity, are missing in the shorter version, the long version is considered the canonical one. Furthermore, LPCAT2 consists of two predicted EF-hand-like motifs as well as a C-terminal retention motif (KKXX) and is located in LDs, ER membrane, Golgi apparatus membrane, and the cellular membrane [22,78].

LPCAT2 stands out in the LPCAT family due to its ability to incorporate not only long-chain PUFAs from CoA thioesters into lyso-PC but also acetyl moieties. Even though LPCAT1 is able to convert acetyl-CoA as well, only the acetyltransferase activity of LPCAT2 is enhanced under inflammatory conditions. The transfer of an acetyl moiety results in the formation of PAF, which is an important pro-inflammatory mediator promoting several inflammation-related diseases [23]. As recently reviewed by Upton *et al.*, PAF is involved in anaphylaxis, cardiovascular disease, and ocular disease, and even a link to Covid-19 is proposed [102]. In mouse peritoneal macrophages and RAW264.7 cells, LPCAT2 activation was mediated by phosphorylation at Ser34, presumably by MAPK-activated protein kinase 2 [103]. Interestingly, not only acetyltransferase activity but also acyltransferase activity was enhanced after LPS stimulation in RAW264.7 cells. Consequently, the authors suggested phosphorylated LPCAT2 as a potentially new therapeutic target. Indeed, Tarui and colleagues screened a large compound library and discovered an inhibitor of LPCAT2 that subsequently led to reduced PAF production in macrophages [104]. Although the connection of PAF with several diseases is well documented, the development of therapeutic strategies based on PAF did not lead to satisfying results in clinical phase 3 trials [102]. This emphasizes that the therapeutic focus on PAF is still relevant today.

## 2.6 Ferroptosis

The field of cell death research was commonly divided into three different mechanisms. First the programmed cell death, apoptosis, which is responsible for the maintenance of homeostasis. Apoptosis results in the clearance of so-called apoptotic bodies without damaging the surrounding tissue and is correlated to changes in the cell morphology, including chromosome shrinkage, chromatin condensation, and cytoplasmic fragmentation [105]. Besides controlled cell death, there is also uncontrolled cell death, known as necrosis. Necrosis occurs as the result of a critical injury like hypoxia or inflammation. In contrast to apoptosis, cellular insides are released into the surrounding tissue, which leads to further cell death in neighboring areas [106]. Furthermore, there is a recycling mechanism known as autophagy, which is mainly triggered by nutrient deprivation or during cellular differentiation. Here, cellular components such as proteins or up to whole organelles undergo lysosomal degradation in order to allow the formation of new cellular structures. Alternatively, degradation continues and yields small units that can be used as a source of energy [107]. Despite its role in the renovation of cells, autophagy can lead to cell death, especially when it comes to senescent cells or neoplastic lesions [108].

Since 2005, the field of cell death mechanisms has been broadened by newly discovered forms such as necroptosis, pyroptosis, NETosis, and ferroptosis. Although some of these novel forms are actually subcategories of the old mechanisms, they differ unequivocally. While necroptosis differs from necrosis in its tightly controlled behavior [109], pyroptosis, unlike apoptosis, causes



inflammation in surrounding tissue [110]. While NETosis can be divided into a suicidal and a vital form, the former is the classic one and is categorized as another member of programmed cell death [111]. The most recent member, ferroptosis, was first described in 2012 by Dixon *et al.* and is characterized by oxidative stress and iron accumulation [59].

Ferroptosis was discovered as a form of non-apoptotic cell death that is also distinct from necrosis and necroptosis. Although the mechanism was not termed before 2012, the first investigations started back in 2003 when treatment with the small molecule erastin caused an unknown form of cell death [112]. Further analysis by Yang *et al.* in 2008 revealed RSL3 (1*S*,3*R*-RSL 3), another small molecule, that also caused cell death in an iron-dependent manner [113]. At the same time, Seiler *et al.* [114] and Banjac *et al.* [115] published their work on lipid peroxidation regarding glutathione peroxidase 4 (GPX4) and system Xc-, a cystine/glutamate transporter, respectively. They observed that inactivation of GPX4 also resulted in non-apoptotic cell death, while overexpression of the light chain system Xc- prevented cells from dying. These findings were eventually brought in accordance with the previous small molecule studies when ferroptosis inducer erastin was shown to inhibit system Xc- and RSL3 was found to target GPX4 [116,117]. Lipid peroxidation can occur through non-enzymatic Fenton reaction [118] or via iron-containing enzymes such as lipoxygenases (LOs) [119–122] and cytochrome P450 oxidoreductases [123,124]. Taken together, the iron-mediated oxidation of lipids and especially the accumulation of these as a result of impaired glutathione (GSH) metabolism either by inhibition of GPX4 or by blocking the substrate supply is very likely to cause ferroptosis. Interestingly, several publications have shown that the oxidation of PUFAs alone is not enough to trigger ferroptosis. In fact, these oxylipins need to be present within phospholipids in order to mediate ferroptotic conditions [125]. As already described before, the incorporation of such PUFAs requires an initial activation step catalyzed by a member of the ACSL family as well as subsequent transfer mediated by a member of the LPCAT family (see chapters 2.4 and 2.5).

Analysis of cell lines resistant to ferroptosis, a CRISPR screen as well as an insertional mutagenesis approach revealed ACSL4 as a key player in ferroptosis [61,126]. On the one hand, the absence of ACSL4 or inactivation prevented the cells from ferroptosis after treatment with RSL3, while overexpression, on the other hand, promoted ferroptotic cell death. Consequently, the correlation between ACSL4 and ferroptosis was highly investigated. Yuan *et al.* could show that ACSL4 is not only involved in the beginning of ferroptosis but also during its progression [60]. Furthermore, they demonstrated that ACSL4 upregulation was the driving force of enzymatic ARA oxidation by LOs or COXs in HepG2 and HL60 cells. This is in accordance with previous findings of Maloberti *et al.*, who also described the regulation of LO and COX metabolism by ACSL4 in breast cancer cells [127]. These findings led to the assumption that ACSL4 favors the development and progression of ferroptosis and can therefore be seen as a biomarker of ferroptosis [60].

In addition to ACSL4, the insertional mutagenesis approach of Dixon *et al.* also indicated a connection between LPCAT3 and ferroptosis [126]. *LPCAT3* expression in different types of human cancer was analyzed, and a poor survival prognosis was linked to an excess of LPCAT3. When they further analyzed this correlation, they figured out that the *LPCAT3*

expression affected cancer immunity, ferroptosis, and lipid metabolism. Interestingly, they also observed these effects in AML and therefore suggest focusing especially on ferroptosis and lipid metabolism as potential therapeutic targets [101].

Despite being a cell death mechanism, ferroptosis is also involved in physiological processes, including immune functions and aging. p53, an important tumor suppressor, was shown to mediate part of its actions through induction of ferroptosis by inhibition of system Xc- [128] on the one hand and enhanced lipid peroxidation through *ALOX12* activation on the other hand [129]. In 2016, a mutated form of p53 was described, which lacked anti-tumor activity in mice [130]. Interestingly, the mutated version was able to prevent malaria infections instead, which could also explain its existence in areas with high malaria risk [131]. Aside from immune functions, ferroptosis has been demonstrated to be involved in embryonic erythropoiesis in rats [132]. This connection to the issue of aging has also been shown by Jenkins *et al.* in 2020 [133]. It was demonstrated that iron accumulation and dysregulation of GSH get enhanced with aging, leading to the induction of ferroptosis eventually. However, it has to be stated that this experiment was carried out in *Caenorhabditis elegans*, and thus, further studies are required.

In addition to its role in physiology, ferroptosis is involved in several pathophysiological processes. Since ferroptosis is characterized by iron accumulation, the connection with so-called iron-overload diseases is not surprising. In 2017, Wang *et al.* provided evidence that hereditary hemochromatosis in mice causes liver damage and displays characteristic markers of ferroptosis [134]. In addition, ferroptosis is involved in infections. Of particular interest are *Mycobacterium tuberculosis* and *Pseudomonas aeruginosa* infections which are promoted by ferroptosis [135,136]. Although ferroptosis is involved in immune response and correlated with anti-tumor properties, it is also correlated with autoimmune diseases such as asthma. 15-LO1 mediated ferroptosis in human airway epithelial cells led to enhanced asthma, as described recently [137]. The pathophysiology of ferroptosis contains even more processes, including organ injury, retinal degeneration, neurodegeneration, and tumorigenesis, which are summarized by Brent R. Stockwell in his review of a decade in ferroptosis research [125].

## 2.7 Lipoxygenases

LOs are responsible for the oxygenation of PUFAs. Today, an ensemble of six different LO genes is known in humans, namely *ALOX5*, *ALOX12*, *ALOX12B*, *ALOX15*, *ALOX15B*, and *ALOXE3* [138]. These genes encode for 5-LO, 12-LO, 12R-LO, 15-LO1, which is sometimes also referred to as 12/15-LO due to its dual activity, 15-LO2 and epidermis-type LO 3 (eLO3), respectively. The enzymes were named according to their site of oxygenation based on the C20 chain of ARA [139]. While LOs are also capable of oxygenating other substrates such as LA, EPA, and DHA, the regioselectivity is altered with varying chain lengths. This might lead to confusion, since the 15-LO1 enzyme produces 15S-HpETE (15S-hydroperoxy-5Z,8Z,11Z,13E-eicosatetraenoic acid) from ARA but 13S-HpODE (13S-hydroperoxy-9Z,11E-octadecadienoic acid) and 17S-HpDHA (17S-hydroperoxy-4Z,7Z,10Z,13Z,15E,19Z-docosahexaenoic acid) from LA and DHA, respectively. Since the majority of LOs produce the S enantiomer during oxygenation, the stereoselectivity is in general not mentioned within the name. However, 12R-LO stands out with its ability to produce the R enantiomer predominantly

[140] and, thus, carries an additional letter to prevent confusion. Human *ALOX5* is located on chromosome 10, while the remaining LO genes are clustered on chromosome 17 [138].

All mammalian LOs display a similar structure. They consist of two separate domains that are formed by a single polypeptide chain. The N-terminal domain is formed by  $\beta$ -sheets and is associated with lipid-binding, while the C-terminal domain predominantly consists of  $\alpha$ -helices and contains a non-heme iron at the catalytic center [140]. Thus, the N-terminal domain has a regulatory function, whereas the C-terminal domain is responsible for the catalytic activity [140].

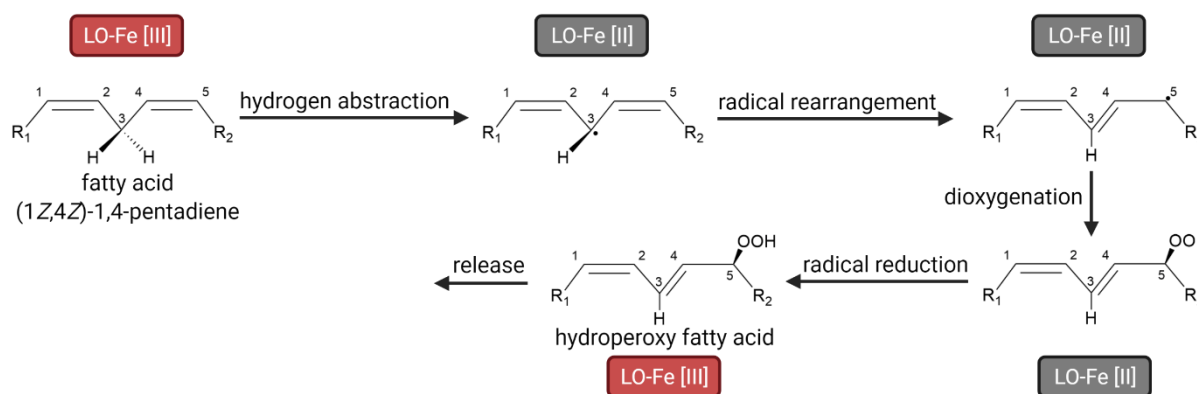


**Figure 2.4: Enzymatic dioxygenation mechanism of a (1Z,4Z)-1,4-pentadiene unit by lipoxigenase enzymes.**

Figure adapted from [141].

The iron within the catalytic center is required for the incorporation of oxygen into the respective substrate. However, in order to facilitate oxygenation, the iron has to be present in its ferric form ( $\text{Fe}^{3+}$ ). Otherwise, ferrous iron ( $\text{Fe}^{2+}$ ) leads to a catalytic inactive LO and needs to be oxidized in advance [139]. Thus, it is not surprising that LOs are regulated by the cellular redox state. The underlying mechanism requires PUFAs with at least two double bonds separated by a methylene unit forming a (1Z,4Z)-1,4-pentadiene motif. In the first step, one of the hydrogen atoms of the central carbon atom (C3) is removed, while the ferric iron accepts an electron-yielding ferrous iron and a pentadiene radical (Figure 2.4). Then, the molecule rearranges, resulting in a conjugated (1Z,3E)-system with the radical on carbon atom C5. Here, an oxygen molecule is inserted stereospecifically, forming a peroxy radical. The ferrous iron then transfers the electron back, yielding the active ferric iron species again and a peroxy anion which subsequently is protonated and released from the enzyme [140,142]. Segraves and Holman had a closer look at the catalytic cycle of human 12-LO and 15-LO1 and determined the initial hydrogen abstraction as the rate-limiting step [143].

12-LO was the first LO discovered in human platelets back in 1974 by Hamberg and Samuelsson [144]. Consequently, the enzyme is also referred to as platelet-type 12-LO. In addition, 12-LO was found to a lesser extent in skin tissue [145], together with 12*R*-LO and eLO3, which are necessary for epidermal development and water homeostasis [146,147]. Since 5-LO, 15-LO1, and 15-LO2 are of particular interest for this work, they will be covered in detail below.

### 2.7.1 5-Lipoxygenase

The human *ALOX5* gene encodes for a 674 amino acids protein which is 77,983 Da in size (UniProt entry: P09917-1) [148]. *ALOX5* consists of 14 exons and 13 introns, which can undergo alternative splicing resulting in several putative isoforms. Although these protein-isoforms do not show enzymatic activity, they are believed to regulate 5-LO activity through other mechanisms [149–151].

As already described above, the protein structure of 5-LO can be divided into two domains. The smaller N-terminal domain which is able to bind phosphatidylcholines, the coactosin-like protein [152,153], Dicer [154], and  $Ca^{2+}$ , which leads to a translocation to the nuclear membrane [155]. Thus, the regulatory domain is also referred to as PLAT (Polycystin-1, Lipoxygenase, Alpha-Toxin) or C2-like domain due to its membrane-binding ability. The C-terminal domain contains the non-heme iron and is responsible for catalytic activity [156,157]. Although both domains contain an ATP-binding site, ATP is bound at an equimolar ratio. Furthermore, it has been shown that ATP-binding stabilizes the enzyme, but hydrolysis is not required for enzymatic activity [158,159]. However, it has to be mentioned that the current crystal structure solved by Gilbert *et al.* is based on a stable mutant of the 5-LO [156]. Here, several destabilizing amino acids were removed or mutated, including a sequence at the C-terminal end of the protein, which is involved in iron binding.

As an important member of the innate immune response, 5-LO is predominantly expressed in immune cells, including B lymphocytes, granulocytes, mast cells, and macrophages [160]. Within the cell, 5-LO can be found in the soluble part of both cytosol and nucleus, depending on the cell type and its phosphorylation state. While phosphorylation of Ser523 by protein kinase A causes cytosolic localization [161], phosphorylation at Ser271 by MAPK-activated protein kinase 2 prevents nuclear export and thus leads to accumulation in the nuclear compartment [162]. In addition, Ser663 was also described as a potential phosphorylation site. However, the phosphorylation could neither be detected in *in vitro* kinase assays nor in immunoprecipitation experiments with MonoMac6 cells [163]. Activation of 5-LO by increased intracellular calcium levels triggers its translocation to the nuclear membrane, where it colocalizes with the 5-LO activating protein (FLAP) [164,165]. This is an essential step since cytosolic phospholipase A<sub>2</sub> (cPLA<sub>2</sub>) releases ARA from the nuclear membrane, which is then transferred by FLAP into the active site of 5-LO [166,167]. In fact, previous studies have shown that even 5-LO overexpression in HEK293 cells did not lead to product formation in the absence of FLAP until exogenous substrates were added [168]. Several stimuli that result in an increased calcium influx and, therefore, 5-LO activation are known today, including *N*-formylmethionyl-leucyl-phenylalanine, PAF, and calcium ionophore A23187 [169]. In addition, treatment with sphingosine-1-phosphate (S1P) also increases intracellular calcium levels through the S1P4 receptor and thereby causes 5-LO translocation to the cellular membrane [170]. However, its effect on 5-LO is highly dependent on the substrate availability. If S1P treatment is combined with the addition of substrates or stimuli such as LPS, 5-LO product formation is strongly increased, whereas insufficient substrate availability leads to an irreversible inactivation of 5-LO in PMNL [170].

5-LO is the key component in the leukotriene (LT) cascade, where it catalyzes the two-step conversion of ARA to leukotriene A<sub>4</sub> (LTA<sub>4</sub>) through a 5S-HpETE intermediate [139,171]. Then, LTA<sub>4</sub> is processed to leukotriene B<sub>4</sub> (LTB<sub>4</sub>) by LTA<sub>4</sub> hydrolase (LTA<sub>4</sub>H) or to cysteinyl LTs (cys-LTs) by LTC<sub>4</sub> synthase (LTC<sub>4</sub>S). Interestingly, the localization of 5-LO has an effect on the downstream products formed. While LTB<sub>4</sub> is preferentially formed if 5-LO resides at the inside of the nuclear envelope [172], cys-LTs are favored if 5-LO is located at the membrane side facing the cytosol. In fact, this behavior is not caused solely by 5-LO but by LTA<sub>4</sub>H and LTC<sub>4</sub>S. While LTA<sub>4</sub>H is able to move between nucleus and cytosol, LTC<sub>4</sub>S is found exclusively in the cytosolic compartment explaining the product pattern [173–175].

In addition to LT synthesis, 5-LO is also involved in the formation of so-called specialized pro-resolving lipid mediators (SPMs) such as lipoxins (lipoxygenase reaction products, LXs) and resolvins, which will be described in detail in chapter 2.9.

### 2.7.2 15-Lipoxygenase 1

The human *ALOX15* gene encodes for a 662 amino acid protein with a size of 74,804 Da (UniProt entry: P16050-1). In accordance with its enzymatic oxygenation of ARA to 15-HpETE, the enzyme was termed 15-LO [176]. Later on, a second 15-LO enzyme was discovered, which led to the clarified terms 15-LO1 and 15-LO2, respectively. Although 15-LO1 predominantly produces 15S-HpETE, it is also able to produce minor amounts (10 %) of 12S-HpETE (12S-hydroperoxy-5Z,8Z,10E,14Z-eicosatetraenoic acid) and is therefore sometimes referred to as 12/15-LO. This dual product formation is also seen for other substrates like DHA, where 14S-HpDHA (14S-hydroperoxy-4Z,7Z,10Z,12E,16Z,19Z-docosahexaenoic acid) accounts for more than 40 % of the total product formation [177]. However, the ability to produce 12-LO metabolites is much more distinct in lower mammals than it is in higher mammals like humans [176]. Interestingly, 15-LO1 is able to convert esterified substrates in addition to their free counterparts. This includes PUFAs incorporated in phospholipids, as well as lipoprotein and cholesterol-bound fatty acids [141,178]. This is a significant difference to 5-LO, which is limited to unbound PUFAs. The substrate specificity can be further manipulated by the phosphatidylethanolamine binding protein 1 (PEBP1). Similar to 5-LO, 15-LO1 translocates to the nuclear envelope when Ca<sup>2+</sup> levels are increased [179]. Here, 15-LO1 can interact with PEBP1, which causes a shift in the substrate preference from the favored free substrate to the esterified one. This effect is further enhanced upon treatment with interleukin 13 (IL-13) or LPS [121,180].

Just like 5-LO, 15-LO1 consists of a single polypeptide chain that forms two different domains. A smaller N-terminal domain is responsible for membrane binding and therefore referred to as the regulatory domain as well as a larger C-terminal domain which is in charge of the catalytic activity, including binding of the non-heme iron [181,182].

15-LO1 is expressed in macrophages, reticulocytes, eosinophils, and airway epithelium [183,184]. Furthermore, 15-LO1 expression is increased upon treatment with interleukin 4 (IL-4), IL-13, or by LPS stimulation [185]. Within the cell, 15-LO1 resides in the cytosol but translocates to the nuclear membrane as a result of elevated Ca<sup>2+</sup> levels. This leads to enhanced activity and may also affect substrate specificity by PEBP1 binding, as described

before. 15-LO1 is involved in several physiological processes, including cholesterol homeostasis in macrophages, procoagulant phospholipid formation in eosinophils, differentiation of erythrocytes, and in the formation of SPMs [178,186–188]. Although 15-LO1 is involved in the biosynthesis of more complex lipid mediators like SPMs (covered in 2.9.2), already the primary products are biologically relevant. In fact, the direct peroxide products 15S-HpETE and 12S-HpETE are quite unstable and consequently are reduced first either enzymatically by GPXs or in a spontaneous fashion to 15S-HETE and 12S-HETE, respectively. In macrophages, 15S-HETE and 13S-HODE, the 15-LO1 product of LA, are believed to have regulating effects on peroxisome proliferator-activated receptor- $\gamma$  (PPAR $\gamma$ ). Furthermore, the authors propose that the IL-4-dependent upregulation of 15-LO1 and PPAR $\gamma$  might be used for the activation of transcription in a tissue-specific manner [189]. Unlike their free counterparts, esterified PUFAs are not secreted and instead remain in the membrane [190]. Therefore, it is assumed that they mediate their effects by altering the membrane composition affecting fluidity and protein-membrane interactions. Phospholipid products of 15-LO1 were shown to block the maturation of dendritic cells upon LPS stimulation [191]. Furthermore, specifically, HETE-PC and HETE-PE are involved in PS-dependent thrombin generation and, thereby, regulation of hemostasis [190].

Besides their physiological functions, 15-LO1 products are also involved in a variety of pathophysiological processes. 15-LO1 is, in general, considered a proinflammatory enzyme and therefore involved, among others, in atherosclerosis, diabetes, hypertension, and arthritis. While it has been shown in several mouse models that 15-LO1 can contribute to airway epithelial injury and that it is involved in the formation of atherosclerotic lesions, also several studies in human monocytes, bronchial epithelial cells, and eosinophils were conducted [190]. In IL-4-treated macrophages, the formation of 15-HETE was enhanced, with 15-HETE-PE being the predominant product [192]. This was in accordance with a mouse model of lung allergy, which showed increased 15-LO1 expression and product formation related to type 2 inflammation [193]. Furthermore, 15-HETE levels were also highly elevated in bronchial epithelial cells and infiltrating macrophages and eosinophils [187,192]. Thus, it is not surprising that both enzyme and product levels are enriched during the resolution phase of inflammation, together with the occurrence of eosinophils and, alternatively, activated macrophages. Furthermore, 15-LO1 and its products were shown to affect cell death mechanisms such as ferroptosis and apoptosis and, thereby, diseases such as arthritis, diabetes, and cardiovascular disease, indicating a key role in immunoregulation [190].

### 2.7.3 15-Lipoxygenase 2

The *ALOX15* gene was discovered by Schewe *et al.* back in 1975 [178], while a second gene, *ALOX15B*, was not discovered until 1997 [194]. Here, Brash and colleagues reported the cloning of a LO gene that shared roughly 40 % sequence homology with the already-known 5-, 12- and 15-LOs [194]. The *ALOX15B* gene encodes for a 676 amino acid protein with a size of 75,857 Da (UniProt entry: O15296-1) [194]. Expression experiments in HEK293 cells and consecutive activity studies revealed the formation of 15S-HpETE as the main product of ARA, terming the enzyme 15-LO2. Although both 15-LO enzymes are similar in size and structure, they only show 38 % sequence homology. This might also explain the distinct

product patterns. While 15-LO1 produces roughly 10 % of 12S-HpETE as a side product, 15-LO2 forms 15S-HpETE exclusively. This is also the case for other substrates like DHA, which leads to the formation of around 40 % 14S-HpDHA, while 15-LO2 only yields 4 % of the side product [177]. Furthermore, the two 15-LO enzymes differ in their substrate acceptance of LA. While LA is only a poor substrate for 15-LO2, it is readily accepted by 15-LO1 [194]. Despite these differences, both enzymes share several properties, including the conversion of multiple PUFAs as well as esterified substrates, activation by increased  $\text{Ca}^{2+}$  levels, and interaction with PEBP1 (see 2.7.2).

The 15-LO2 protein structure is quite similar to other LOs, forming a two-domain structure separated by their regulatory and catalytic function. Interestingly, 15-LO2 differs from other human LOs at the iron-binding site. Here, one of the five putative iron ligands, which is commonly a histidine or asparagine, was found to be a serine (Ser558) instead [194].

15-LO2 is mainly expressed in epithelial cells of the prostate and esophagus but was also found in macrophages, skin, lung, and cornea [194,195]. In contrast to 15-LO1, 15-LO2 is constitutively expressed in macrophages with increased protein expression upon treatment with LPS or other 15-LO1-inducing agents such as cytokines IL-4 and IL-13. Furthermore, elevated 15-LO2 levels were found under hypoxia conditions [195]. 15-LO2 is not only localized within the cytosol but also found at the cell-cell border and within the nucleus. Although the nuclear import and export of 5-LO are well investigated today, it is unclear how 15-LO2 is imported. A putative nuclear localization sequence of 15-LO2 was investigated, but a mutagenesis approach was not able to fully prevent nuclear import. Therefore, the respective N-terminal sequence is only partially involved in the nuclear import, and the exact mechanism remains elusive [196].

Due to the very similar product spectrum, 15-LO2 shares several physiological properties with 15-LO1. Surprisingly, knock-down experiments with 15-LO1 and 15-LO2 revealed that only the absence of 15-LO1 affected SPM formation [186]. Thus, 15-LO2, despite its ability to form hydroperoxide products at the C15 position, is not involved in the formation of more complex lipid mediator structures such as LXs and resolvins. However, 15-LO2 has been shown to be correlated with cell cycle arrest in normal human prostate epithelial cells. Expression studies not only revealed that 15-LO2 is a negative regulator of the cell cycle [140,197] but also indicated that the expression inhibits the proliferation of prostate cancer cells [196,197]. The effect of cell growth inhibition was also investigated a few years later by Schweiger and colleagues [198]. They analyzed 15-LO2 as well as the respective murine variant: 8-LO. The enzymes vary in their product spectrum, with 8-HpETE and 9-HpODE being the products of ARA and LA from 8-LO, respectively. Nevertheless, both enzymes were described to affect DNA synthesis and, thus, cell growth [198]. In addition to the enzymatic activity of 15-LO2, another unknown pathway leading to cell cycle arrest was proposed by Bhatia *et al.* [196]. They described 15-LO2 as well as other splice variants that were able to affect the cell cycle, although the splice variants were unable to enter the nucleus. Moreover, 15-LO2 is involved in the pathophysiological process of atherosclerosis. Here, the enzyme is responsible for the oxidation of low-density lipoprotein (LDL), which subsequently is picked up by macrophages [199]. As a result, macrophages become foam cells and cause atherosclerotic plaques [200].

In fact, 15-LO1 is also able to catalyze LDL oxidation. However, the expression levels of 15-LO1 are much lower, indicating that the majority of LDL is processed by 15-LO2 [201].

## 2.8 Oxylipins

Oxidized lipids, also referred to as oxylipins, display an important family of signaling lipid mediators derived from PUFAs. As already mentioned above, lipid peroxidation may occur both non-enzymatically or enzymatically through a variety of over 50 cell-specific enzymes [202]. The major biosynthetic routes for the conversion of PUFAs to oxylipins include COX, LO, and cytochrome P450 oxidoreductase pathways [203]. While free oxylipins are well investigated, especially eicosanoids and eicosanoid-like lipid mediators, which will be described in detail in chapter 2.9, the majority of oxylipins in human plasma is bound in lipids and lipoproteins [204]. These esterified lipid mediators were originally believed to have a storage character, whereas more recent studies investigated their signaling function. Indeed, it has been shown that esterified oxylipins mediate effects that do not necessarily mimic their free counterparts. In fact, esterified lipid mediators caused distinct or, in some cases, more potent responses [205] as will be described in more detail below (chapter 2.8.1).

### 2.8.1 Esterified oxylipins

First studies on esterified oxylipins focused on the incorporation of exogenous substrates such as radio-labeled HETEs [205]. Subsequently, several cell types were characterized regarding their preferred phospholipid for the incorporation of different HETE positional isomers [205]. For example, these studies reported that the incorporation of 5-HETE in PC and PE is favoured in kidney epithelial cells [206], whereas immune cells preferentially form the respective PC or triglycerides [207]. In addition, the incorporation of several other HETEs, such as 12- or 15-HETE, was investigated as reviewed in [205]. However, as these studies usually include high compound concentrations and sometimes use cell lines that do not express LOs under basal conditions, these findings might not represent the *in vivo* behaviour [205].

Although the analysis of endogenous, and therefore unlabeled, oxylipins is quite challenging, improved LC-MS techniques have enabled the investigation of comprehensive oxylipins sets today [203,204,208–212]. As this offered new possibilities for the analysis of esterified oxylipins, researchers started to get insights into their biological roles. For example, it could be shown that the bleeding disorder known as ‘Scotts syndrome’ is associated with an impaired externalization of PS and 12-HETE-PE [213]. In human monocytes, treatment with 18:0a/15-HETE-PE showed no effect under basal conditions but mediated anti-inflammatory effects in LPS-stimulated cells [193]. The authors reported that 18:0a/15-HETE-PE inhibited the formation of tumor necrosis factor- $\alpha$  (TNF- $\alpha$ ) and granulocyte colony-stimulating factor whereas the respective ARA-containing phospholipid had no effect. Phospholipid-bound HETEs are also assumed to form during murine and human infections and, therefore, are associated with neutrophil influx [214]. Interestingly, Clark *et al.* reported that 5-HETE-PE led to an increase in interleukin 8 (IL-8) but not TNF- $\alpha$  levels in neutrophils, whereas free 5-HETE completely abrogated both IL-8 and TNF- $\alpha$  formation [214]. As they also found that both 5-HETE species increased superoxide formation, esterified mediators may mediate both similar and distinct actions compared to their free counterparts. Furthermore, 15-HETE-PE is



assumed to promote asthmatic conditions in human epithelial cells [215]. More recently, a phospholipidomics study revealed that the PE hydroperoxide SAPE-OOH (1-stearoyl-2-15-HpETE-*sn*-glycero-3-phosphatidylethanolamine) is the major signal for phagocytic clearance of ferroptotic cells [216]. The study also investigated the mechanism of the signaling and found that the interaction of SAPE-OOH with toll-like receptor 2 triggered the clearance by THP-1-derived macrophages in an *in vitro* 4T1 mammary carcinoma cell model. Another report on the involvement of esterified oxylipins in infections was published by Dar *et al.* [136]. Here, they demonstrated that a 15-lipoxygenating enzyme from the Gram-negative bacterial pathogen *Pseudomonas aeruginosa* produces 15-HpETE-AA-PE and thereby triggers ferroptotic cell death in bronchial epithelial cells.

## 2.9 Lipid mediators in inflammation

Lipid mediators are often referred to as eicosanoids which were originally used as an umbrella term for mediators derived from C20 fatty acids [217]. Among the ARA-derived eicosanoids, the most important ones in terms of biological relevance are prostanoids, LTs, and LXs. Although not included in the original scope of eicosanoids, lipid mediators derived from substrates with different chain lengths, such as DHA, are often also referred to as eicosanoids or eicosanoid-like mediators. Other important eicosanoids or eicosanoid-like mediators are the DHA-derived classes of D-series resolvins, protectins, and maresins, and also the EPA-derived E-series resolvins. Prostaglandins, a subgroup of the prostanoids, and LTs play an important role in both the initiation and acute inflammation and are therefore considered pro-inflammatory mediators [218]. Initially, the resolution phase was believed to be a passive mechanism driven simply by consumption and dilution [219]. Whereas nowadays, it is considered an active process that is accompanied by a lipid mediator class switch. Prostaglandins, resolvins, protectins, and maresins are reported to be involved in the active resolution of inflammation, leading to the summarized term of specialized pro-resolving mediators [219,220]. However, recent reviews raised the question of whether the vanishingly low SPM levels are sufficient to cause relevant biological effects [212,221]. In addition, they pointed out that there are discrepancies in the methodology of detection and evaluation of SPM signals between different laboratories. Thus, the field of SPM research is shaken up right now and needs careful evaluation.

Inflammation is the organism's response to tissue damage which can have multiple causes, including injury by physical or chemical forces as well as microbial infections. Due to this variety of inflammatory triggers, the immune response needs to cover a large array of defense mechanisms. Thus, an effective interplay of multiple mediators and cell types is utilized in a tightly controlled manner in order to prevent autoimmune disorders, neurodegenerative disease, and cancer [222]. At first, inflammatory triggers are recognized by tissue-specific immune cells like resting macrophages and mast cells which release pro-inflammatory molecules, including chemokines, cytokines, and eicosanoids [223]. As a consequence, leukocytes, especially neutrophils, are recruited to the site of inflammation, where they get activated. In order to tackle microbial pathogens, they release several noxious substances, among these are reactive oxygen and nitrogen species [224]. Once the invading pathogens are defeated, the resolution phase of inflammation takes place. This phase is accompanied by

a switch in the lipid mediator formation from pro-inflammatory to pro-resolving [223]. Thus, instead of prostaglandins and LTs, LXs are produced, which leads to reduced neutrophil but increased macrophage recruitment [225]. The recruited macrophages further support the process of resolution by clearance of apoptotic debris on one hand and formation of pro-resolving mediators such as resolvins and protectins as well as TGF- $\beta$  and other growth factors on the other hand [225,226]. In the following chapters, the biosynthesis and effects of selected pro-inflammatory as well as pro-resolving mediators will be covered in more detail.

### 2.9.1 Leukotrienes

LTB<sub>4</sub>, as well as the cys-LTs, are pro-inflammatory mediators derived from ARA (Figure 2.5) [227]. Although enzymatic conversion of ARA is mediated by 5-LO and subsequently by LTA<sub>4</sub>H or LTC<sub>4</sub>S, cPLA<sub>2</sub>, and FLAP also play an important role [228,229]. cPLA<sub>2</sub> releases ARA from the membrane, while FLAP colocalizes with 5-LO at the nuclear envelope and enhances the substrate interaction. Once the substrate is placed in the binding pocket of 5-LO, two subsequent conversions take place. At first, oxygenation of ARA leads to 5-HpETE formation, which is then converted to the highly unstable LTA<sub>4</sub>. Next, the unstable epoxide undergoes one of two possible reactions: hydrolysis or conjugation with glutathione [230]. As a result, the LTA<sub>4</sub>H-mediated hydrolysis yields LTB<sub>4</sub>, while conversion by LTC<sub>4</sub>S leads to the enzymatic conjugation with reduced glutathione to form LTC<sub>4</sub> [166,230,231]. LTB<sub>4</sub> and LTC<sub>4</sub> are then released from the cell, and the latter can be converted further to LTD<sub>4</sub> and LTE<sub>4</sub> extracellularly [227]. Once LTs are released from the cell, they mediate their effects through G-protein-coupled receptors (GPCRs) [202,227] that are located in the outer plasma membrane of inflammatory cells [227]. LTB<sub>4</sub> is a potent ligand of the B leukotriene receptor 1 (BLT<sub>1</sub>), which binds with sub-nanomolar affinity [232]. In addition, a second B leukotriene receptor (BLT<sub>2</sub>) is expressed in several tissues and was described to bind LTB<sub>4</sub> as well, but with much lower affinity [232,233]. Nowadays, BLT<sub>2</sub> is considered a promiscuous receptor that also binds other oxylipins such as 12S-hydroxyheptadecatrienoic acid (12-HHT), 12S-HETE, 12S-HEPE and 15S-HETE [234]. Interestingly, Okuno *et al.* reported that especially 12-HHT had been shown to bind BLT<sub>2</sub> with higher affinity than LTB<sub>4</sub> [235]. Accordingly, BLT<sub>2</sub> has been shown to be involved in wound healing correlated with 12-HHT levels [234]. BLT<sub>1</sub> binding leads to elevated intracellular Ca<sup>2+</sup> and reduced cAMP levels and, thus, causes several cellular actions mainly mediated through activated kinase pathways. Ultimately, this leads to enhanced neutrophil secretion [227]. Another set of GPCRs are the cysteinyl leukotriene receptors, CysLT<sub>1</sub> and CysLT<sub>2</sub>, which can bind LTC<sub>4</sub> and LTD<sub>4</sub> [236,237]. While CysLT<sub>1</sub> is expressed in airway SMCs [236] and vascular endothelial cells [238], it is not surprising that cys-LTs cause bronchoconstriction and mucus secretion in the lung. The correlation between CysLT<sub>1</sub> and airway inflammation was further underlined when treatment with CysLT<sub>1</sub> antagonists inhibited these asthma-promoting effects [227]. Interestingly, CysLT<sub>2</sub> was found in spleen, heart, and adrenal gland tissue, promoting inflammation and fibrosis but not bronchoconstriction.

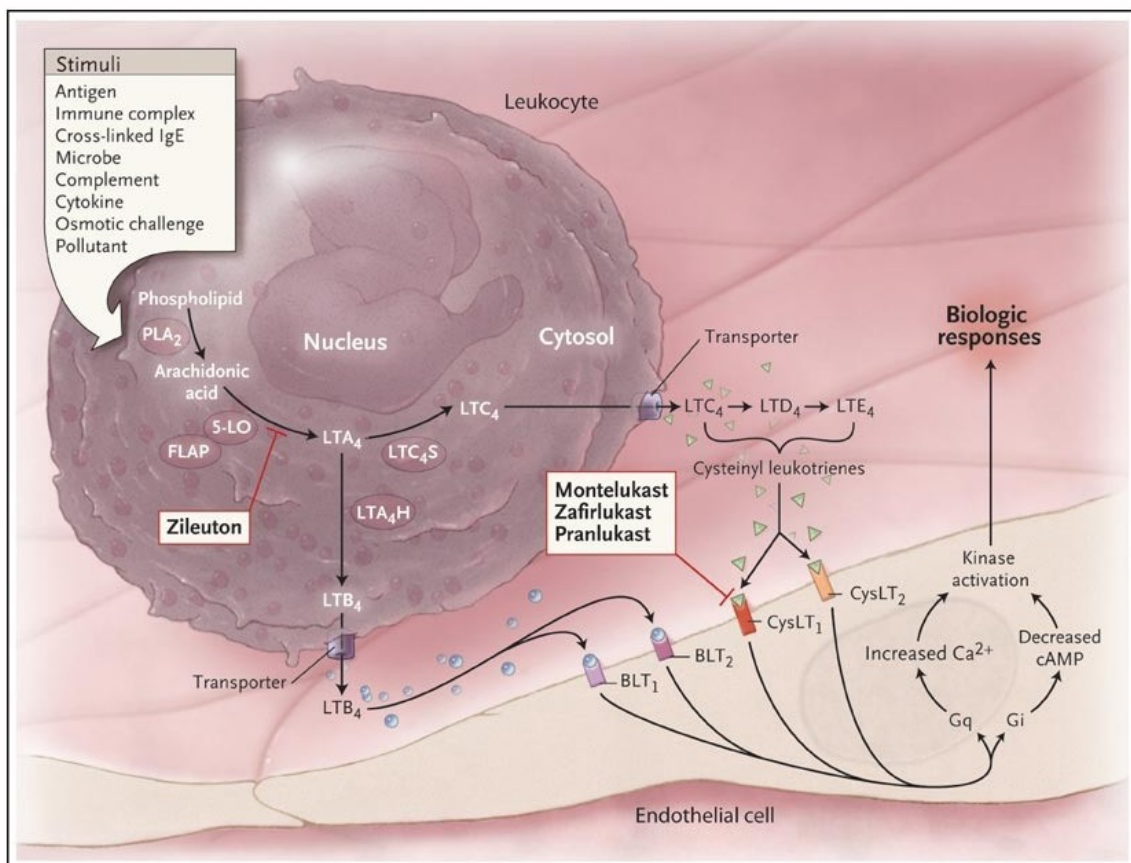


**Figure 2.5: Schematic overview of leukotriene biosynthesis and signaling.**

Figure taken from [227].

Even overexpression of CysLT<sub>2</sub> in the lung of mice was not able to change that [239]. When it comes to therapeutic use, two potential targets exist to interfere with biosynthesis and the signaling cascade. Today, there is only one drug approved by the Food and Drug Administration, zileuton, a direct 5-LO inhibitor [240] and, therefore, targets the biosynthetic route. In contrast, there are three LT antagonists, namely montelukast, zafirlukast, and pranlukast, which inhibit the interaction with the CysLT<sub>1</sub> receptor [227]. Although 5-LO inhibition is an effective way of preventing the formation of both LTB<sub>4</sub> and cys-LTs, zileuton has its drawbacks being hepatotoxic. Furthermore, the drug requires a frequent administration of four times a day, which limits its clinical use. However, it has to be mentioned that the hepatotoxicity is not an effect of 5-LO inhibition but instead is caused by the drug itself. Therefore, focusing on 5-LO remains a promising target in the LT cascade. Summed up, these LT modifiers, as they are sometimes referred to, have their legitimation in the treatment of asthma. However, the use of LT modifiers is often only considered once the preferred treatment of inhaled corticosteroids fails or is not applicable [241].

Interestingly, LT formation is not restricted to cells that express 5-LO. LTA<sub>4</sub>, the precursor of LTB<sub>4</sub> and the cys-LTs, is exported from 5-LO-containing cells and then used for the LT formation in 5-LO deficient cells such as platelets, endothelial cells, and smooth muscle cells [242].

## 2.9.2 Lipoxins, D-series, and E-series resolvins

Among all eicosanoids, SPMs are the ones suggested to be responsible for the resolution of inflammation. Here, LXs, D-series, and E-series resolvins (Figure 2.6) will be described exemplarily displaying ARA, DHA, and EPA-derived mediators, respectively.

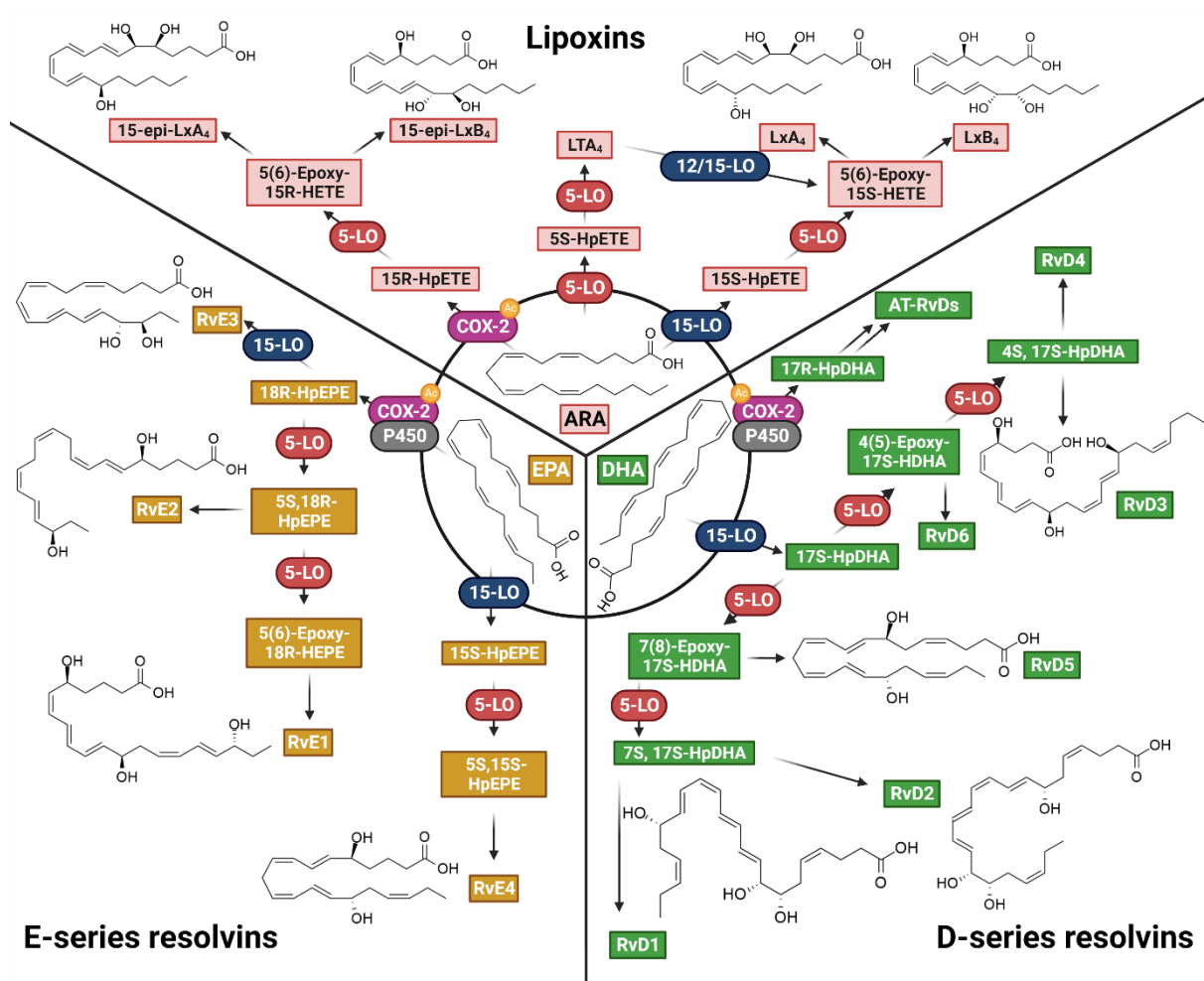


**Figure 2.6: Biosynthesis routes of LXs, D-series, and E-series resolvins.**

Not all pathways shown are equally efficient or active under physiological conditions.

Back in 1984, a new class of ARA-derived mediators was discovered in human leukocytes and described to contain four conjugated double bonds and three hydroxyl groups [243]. At that time, neither the stereochemistry nor their biological actions were known. Today, these mediators are known as LXs [244]. Biosynthesis starts with ARA, which is converted by 5-LO or 15-LO1/2 to 5S-HETE or 15S-HETE, respectively (Figure 2.6) [221]. In addition, acetylated COX-2 can lead to the formation of 15R-HETE and 15R-prostaglandins in general [245]. However, as this requires treatment with acetylsalicylic acid to introduce the acetylation at Ser530 [245], the COX-2 pathway does not play a role under physiological conditions and will therefore not be described in detail here. Instead, the 12/15-LO:5-LO pathway is usually considered responsible for the SPM formation [212,221]. As shown in Figure 2.6, the 12/15-LO pathway results in the formation of lipoxin A<sub>4</sub> (LxA<sub>4</sub>) and lipoxin B<sub>4</sub> (LxB<sub>4</sub>) but also converts DHA to D-series resolvins and EPA to resolvin E<sub>4</sub> (RvE<sub>4</sub>) [219,246,247]. However, the 5-LO:12/15-LO pathway is also capable of converting ARA to LxA<sub>4</sub> and LxB<sub>4</sub> [212,221]. Following

the initial oxygenation step of the LX pathway, 5S-HETE and 15S-HETE are converted by 5-LO to LTA<sub>4</sub>, and 5(6)-epoxy-15S-HETE, respectively. The unstable LTA<sub>4</sub> is then converted by 12-LO or 15-LO1 and also yields 5(6)-epoxy-15S-HETE. Finally, the epoxy intermediate undergoes enzymatic hydrolysis yielding LxA<sub>4</sub> and LxB<sub>4</sub> [244,248]. Similar to the biosynthesis of LTs, it is very likely that the LX formation is a multicellular process [249]. Although it was shown that the complete formation of LXs can occur within a single cell, several studies could also prove a cell-cell interaction (as reviewed in [248]). One of the best-studied cell-cell interactions in terms of LX biosynthesis is the interplay of platelets with polymorphonuclear leukocytes (PMNL). Platelets incubated with stimulated PMNL were able to produce LXs even without the addition of exogenous ARA. Interestingly, platelets can interact with the LX pathway in different steps. While platelets release ARA as a substrate for 5- and 15-LO of PMNL in order to facilitate LX formation, the LTA<sub>4</sub> intermediate is released by PMNL and subsequently converted by 12-LO of platelets [248].

As already mentioned above, the 12/15-LO:5-LO pathway is also responsible for the formation of RvE4 from EPA. Here, EPA is oxygenated first by 15-LO1/2 to 15S-HpEPE (15S-hydroperoxy-5Z,8Z,11Z,13E,17Z-eicosapentaenoic acid) and subsequent conversion by 5-LO is followed by an enzymatic reduction to form the final RvE4 [250]. As shown in Figure 2.6 E-series resolvins also include RvE1-3, which require the formation of 18R-HpEPE (18R-hydroperoxy-5Z,8Z,11Z,14Z,16E-eicosapentaenoic acid) in a first step. As the formation of 18-HEPE by 15-LO1/2 is very inefficient and the *S/R*-ratio of the product is below 3:1 [251], the intermediate has to originate from another source. As shown by Isobe *et al.* CYP450 enzymes are capable of converting EPA to 18R-HEPE [252], however, a physiological relevance has not been demonstrated yet. Alternatively, acetylated COX-2 was assumed to cause 18R-HEPE formation as demonstrated by aspirin-treated human endothelial cells [253]. In contrast, Oh *et al.* later investigated the product formation of human recombinant COX-2 and reported that aspirin treatment increased the formation of 18S-HEPE [254]. These findings were recently summarized in comprehensive review articles and the authors state that the origin of the 18R-HEPE intermediate under physiological conditions remains highly speculative [212,221]. Regardless of its origin, 18R-HEPE is converted by two subsequent 5-LO reactions and enzymatic hydrolysis to RvE1. Alternatively, the intermediate of 18R-HEPE converted only once by 5-LO can be reduced by peroxidases to yield RvE2 [255]. In addition, 18R-HEPE can be converted by 15-LO1/2 instead of 5-LO to yield RvE3 [256].

Finally, D-series resolvins are also formed by the 12/15-LO:5-LO pathway under physiological conditions. At first, DHA is oxygenated by 15-LO1/2 to 17S-HpHDA (17S-hydroperoxy-4Z,7Z,10Z,13Z,15E,19Z-docosahexaenoic acid). Alternatively, 17R-HpHDA can be formed by CYP450 enzymes or acetylated COX-2, however, as mentioned before these pathways are not physiologically relevant. 17S-HpHDA is oxygenated again, this time by 5-LO, to form one of two epoxide structures. Both epoxides can then be further converted by subsequent reaction of 5-LO and an enzymatic reduction to resolvins D1 (RvD1) and D2 (RvD2) or resolvins D3 (RvD3) and D4 (RvD4) from the 7(8)-epoxide or the 4(5)-epoxide, respectively (Figure 2.6). Alternatively, the 7(8)-epoxide can undergo enzymatic hydrolysis to form resolvin D5 (RvD5) while hydrolysis of the 4(5)-epoxide yields resolvin D6 (RvD6). The catalytic pathway is followed analogously if 17R-HpHDA is present within the cells. The respective final products

show the opposite stereochemistry at C17 and are referred to as aspirin-triggered (AT) resolvins, e.g., AT-RvD1 [257].

While RvE4 and RvD5 are produced in similar amounts as LTs [258,259], trihydroxylated SPMs such as RvE1, RvD1, RvD2, LxA<sub>4</sub> and LxB<sub>4</sub> are only formed in vanishingly low amounts in human leukocytes [221]. In fact, their amounts are mostly below the detection limit [212,260]. In general, dihydroxylated SPMs are formed to a higher extent than the trihydroxylated ones but their levels are still remarkably lower compared to monohydroxylated products such as HETEs, HEPes and HDHAs [221].

RvE2 has been shown to alter the shape and chemotactic velocity of human PMNL and stimulate IL-10 production and nonphlogistic phagocytosis in macrophages [261]. Furthermore, RvE2 is associated with a pain reduction in rheumatoid arthritis patients [262]. RvE4 was reported to promote efferocytosis of PMNL and red blood cells [247,250] whereas RvD5 stimulates phagocytosis of *E. coli* through M1 and M2 macrophages as well as PMNL [263–265]. These and other effects were summarized recently in a comprehensive review article [221].

Depending on the respective type of SPM, a variety of GPCRs was originally proposed to mediate their anti-inflammatory and pro-resolving effects. However, as reviewed in detail, the results of later studies were inconsistent with the initial reports [212]. For example, LxA<sub>4</sub> was reported to bind to formyl peptide receptor 2 (FPR2, also referred to as ALX) and thereby cause its cell type specific response [266–269], whereas two independent studies demonstrated that LxA<sub>4</sub> had no effect in HL60 cells transfected with FPR2 and in human neutrophils which express the receptor endogenously [270,271]. Furthermore, RvD2 was reported to mediate its anti-inflammatory effects through the G-protein coupled receptor (GPR) 18 [219,272]. However, these findings were not confirmed yet by an independent laboratory but an attempt to reproduce the results of the initial  $\beta$ -arrestin assay used to identify the RvD2 interaction was unsuccessful [273]. Another receptor potentially involved in SPM signaling is GPR32 which was initially reported to interact with RvD1 [274,275] and later on extended to RvD3 and RvD5 [264,276]. But again, all reports on the agonism of D-series resolvins on GPR32 originate from one laboratory and these results could not be confirmed by independent studies [277,278]. There are even more SPM receptors proposed such as chemerin receptor 23 (ChemR23), BLT1 and others but due to the lack of sufficient controls and inconsistent reports, endogenous SPM receptors remain to be validated [212].

As described above, recent reviews critically questioned the available data on SPMs and state that a final proof for their biological relevance in humans remains to be provided [212,221].

### 3 Aim of thesis

Eicosanoids mediate important biological functions due to their pro- and anti-inflammatory effects. As described before, they are formed through various pathways by enzymatic conversion of LOs, COXs, and cytochrome P450. Commonly believed to mediate their effects as free fatty acids, their esterified counterparts were assumed to have a storage character. However, at that time, several studies on the esterification and release of HETEs were performed using exogenous substrates without careful consideration of regio- and stereoselectivity. As a result, cells were treated with eicosanoids that typically originate from different cell types or are formed under specific conditions, e.g., inflammation. Later on, especially with the help of improved LC-MS analysis, a new understanding started to arise. Investigations presented evidence that esterified eicosanoids were not used for storage reasons but instead were formed by primary immune cells as a response to acute inflammation. Interestingly, the formed esterified mediators did not mimic the effects or their free counterparts but rather led to distinct or, in some cases, more potent responses [205].

These findings started to support the acceptance of esterified lipid mediators as a new class of lipid mediators that has to be seen separately from their free fatty acids. However, with this change in perspective, new challenges became apparent. When this thesis started in 2017, esterified compounds were either quite expensive or not commercially available at all. Thus, this work focused on the development of a biosynthetic approach to produce oxidized esterified lipids, also referred to as esterified oxylipins. For this purpose, the biosynthetic approach should be focused on enzymes involved in the lipid remodeling process known as Lands' cycle. Based on publications on long-chain acyl-CoA synthetases and their substrate specificity [31] as well as on the enormous field of acyltransferases [8,24,25], two enzymes were selected: Acyl-CoA synthetase long-chain family member 4 (ACSL4) and lysophosphatidylcholine acyltransferase 2 (LPCAT2). The two enzymes were chosen due to their broad substrate acceptance, which, in theory, should allow the generation of several esterified lipids without the need of a myriad of enzymes.

## 4 Materials and methods

### 4.1 Materials

#### 4.1.1 Cell culture

Human embryonal kidney (HEK) 293T cells were used for cell culture experiments. HEK293T cells (ACC 635) were obtained from DSMZ (Deutsche Sammlung von Mikroorganismen und Zellkulturen, Braunschweig, Germany) and cultured at 37 °C in a humidified atmosphere with 5 % CO<sub>2</sub>.

All buffers and chemicals listed in Table 4.1 were either purchased from Thermo Fisher Scientific™ (Waltham, Massachusetts, USA) or their associated company Life Technologies™ (Carlsbad, California, USA).

**Table 4.1: Buffers and chemicals for cell culture use.**

Chemicals for cell culture use				Specifications
Dulbecco's Modified Eagle Medium (DMEM), high glucose				L-glutamine, phenol red
Dulbecco's Modified Eagle Medium (DMEM), high glucose				L-glutamine, no phenol red
Dulbecco's Phosphate-Buffered (PBS)		Saline		without CaCl <sub>2</sub> , without MgCl <sub>2</sub>
Hygromycin B				50 mg/mL
Opti-MEM™ I Reduced Serum Medium				L-glutamine, no phenol red
Pen Strep				10,000 U/mL Penicillin, 10,000 µg/mL Streptomycin
Puromycin Dihydrochloride				10 mg/mL
Sodium Pyruvate				100 mM
Trypan Blue Solution				0.4 %
Trypsin-EDTA (TE)				0.5 %, 10x diluted in 1x PBS (1:10) before use
UltraPure™ Distilled Water				DNase/RNase-Free

**Table 4.2: Fetal bovine serum batches with suppliers and lot numbers, respectively.**

Fetal bovine serum (FBS) suppliers	LOT
Capricorn Scientific GmbH, Ebsdorfergrund, Germany	CP16-1537 and CP19-2834
Gibco, Life Technologies™, Carlsbad, California, USA	42Q4467K



Table 4.3: Sterile cell culture items.

Cell culture items	Specifications	Distributor
CELLSTAR® Cell culture dishes	10 cm, 56.7 cm <sup>2</sup>	Greiner Bio-One International GmbH, Kremsmünster, Austria
CELLSTAR® Cell culture dishes	15 cm, 145 cm <sup>2</sup>	Greiner Bio-One International GmbH, Kremsmünster, Austria
CELLSTAR® Cell culture flasks	650 mL, 175 cm <sup>2</sup>	Greiner Bio-One International GmbH, Kremsmünster, Austria
CELLSTAR® Cell culture flasks	250 mL, 75 cm <sup>2</sup>	Greiner Bio-One International GmbH, Kremsmünster, Austria
CELLSTAR® Cell culture flasks	50 mL, 25 cm <sup>2</sup>	Greiner Bio-One International GmbH, Kremsmünster, Austria
CELLSTAR® Conical Bottom Tubes	15 mL, 50 mL	Greiner Bio-One International GmbH, Kremsmünster, Austria
CELLSTAR® Multiwell plates	6-well, 96-well	Greiner Bio-One International GmbH, Kremsmünster, Austria
Corning® Cell Lifter	19 mm	Corning Incorporated, New York, USA
Cryo.s™ vials	2 mL, 12.5x48 mm	Greiner Bio-One International GmbH, Kremsmünster, Austria
Menzel coverslips	24x55 mm (0.13-0.16 mm)	Thermo Fisher Scientific™
Nunc™ Lab-Tek™    CC2™ chamber slides	8-well	Thermo Fisher Scientific™

#### 4.1.2 Chemicals and reagents

Table 4.4: Common chemicals and reagents.

Chemicals and reagents	Manufacturers
1S,3R-RSL 3	Sigma-Aldrich, St. Louis Missouri, USA
2-Mercaptoethanol	Sigma-Aldrich, St. Louis Missouri, USA
2-Propanol	VWR International, Radnor, Pennsylvania, USA
4-(2-hydroxyethyl)-1-piperazineethane sulfonic acid (HEPES) for buffer solutions	PanReac AppliChem ITW Reagents, Darmstadt, Germany
4',6-Diamidino-2-phenylindol (DAPI)	Sigma-Aldrich, St. Louis Missouri, USA
Acetic acid	PanReac AppliChem ITW Reagents, Darmstadt, Germany

<b>Chemicals and reagents</b>	<b>Manufacturers</b>
Acrylamide 4K solution, (30 %) Mix 37.5:1	PanReac AppliChem ITW Reagents, Darmstadt, Germany
Adenosine triphosphate (ATP)	Invitrogen™ by life technologies™, Thermo Fisher Scientific Waltham Massachusetts, USA
Agar-Agar, Kobe I	Carl Roth®, Karlsruhe, Germany
Albumin from human serum, fatty acid-free	Sigma-Aldrich, St. Louis Missouri, USA
Ammonium peroxydisulfate (APS)	Carl Roth®, Karlsruhe, Germany
Ampicillin Sodium Salt	PanReac AppliChem ITW Reagents, Darmstadt, Germany
Amylose resin	Sigma-Aldrich, St. Louis Missouri, USA
ATP-Agarose	Sigma-Aldrich, St. Louis Missouri, USA
Bromophenol blue	Merck KGaA, Darmstadt, Germany
Ca <sup>2+</sup> Ionophore (A23187)	Sigma-Aldrich, St. Louis Missouri, USA
Calcium chloride (CaCl <sub>2</sub> ) Dihydrate	Carl Roth®, Karlsruhe, Germany
Chloramphenicol	Carl Roth®, Karlsruhe, Germany
Chloroform	PanReac AppliChem ITW Reagents, Darmstadt, Germany
cOmplete™ Mini, EDTA-free Protease Inhibitor Cocktail	Roche Diagnostics GmbH, Mannheim, Germany
Coomassie® Brilliant Blue G-250	PanReac AppliChem ITW Reagents, Darmstadt, Germany
D-(+)-Glucose anhydrous	Carl Roth®, Karlsruhe, Germany
Dimethyl sulfoxide (DMSO)	PanReac AppliChem ITW Reagents, Darmstadt, Germany
di-Sodium hydrogen phosphate anhydrous (Na <sub>2</sub> HPO <sub>4</sub> )	VWR International, Radnor, Pennsylvania, USA
Dithiothreitol (DTT)	PanReac AppliChem ITW Reagents, Darmstadt, Germany
Doxycycline hydrochloride	Sigma-Aldrich, St. Louis Missouri, USA
Erastin	CAYMAN Chemical Company, Ann Arbor, Michigan, USA
Ethanol (EtOH) ROTIPURAN®	Carl Roth®, Karlsruhe, Germany
Ethidium bromide (solution 10mg/mL)	Carl Roth®, Karlsruhe, Germany
Ferrostatin-1 (Fer-1)	Sigma-Aldrich, St. Louis Missouri, USA

<b>Chemicals and reagents</b>	<b>Manufacturers</b>
Glycerol 87 %	PanReac AppliChem ITW Reagents, Darmstadt, Germany
Glycerol anhydrous	PanReac AppliChem ITW Reagents, Darmstadt, Germany
Glycine	Carl Roth®, Karlsruhe, Germany
Hydrochloric acid (HCl), 37 %	VWR International, Radnor, Pennsylvania, USA
Imidazole	Carl Roth®, Karlsruhe, Germany
Isopropyl-β-D-thiogalactopyranosid (IPTG)	Carl Roth®, Karlsruhe, Germany
Kanamycin sulfate	Carl Roth®, Karlsruhe, Germany
Luria Broth Base (LB)	Invitrogen™ by life technologies™, Thermo Fisher Scientific Waltham Massachusetts, USA
Magnesium chloride (MgCl <sub>2</sub> ) hexahydrate	Merck KGaA, Darmstadt, Germany
Methanol (MeOH) for HPLC	VWR International, Radnor, Pennsylvania, USA
Methanol (MeOH) ROTISOLV®	Carl Roth®, Karlsruhe, Germany
N,N,N',N'-Tetramethylethylenediamine (TEMED)	PanReac AppliChem ITW Reagents, Darmstadt, Germany
Nickel(II) sulfate (NiSO <sub>4</sub> ) hexahydrate	Sigma-Aldrich, St. Louis Missouri, USA
Nonident NP-40	Sigma-Aldrich, St. Louis Missouri, USA
Peptone from Casein	Carl Roth®, Karlsruhe, Germany
Phenylmethanesulfonyl fluoride (PMSF)	Honeywell International Inc., Charlotte North Carolina, USA
Phosphoenolpyruvate mono potassium salt (PEP-K)	Sigma-Aldrich, St. Louis Missouri, USA
PhosSTOP, Phosphatase Inhibitor Cocktail	Roche Diagnostics GmbH, Mannheim, Germany
Polyethylenimine (PEI) branched	Sigma-Aldrich, St. Louis Missouri, USA
Potassium chloride (KCl)	PanReac AppliChem ITW Reagents, Darmstadt, Germany
Sodium chloride (NaCl)	Carl Roth®, Karlsruhe, Germany
Sodium di-hydrogen Phosphate 1-hydrate (NaH <sub>2</sub> PO <sub>4</sub> * H <sub>2</sub> O)	PanReac AppliChem ITW Reagents, Darmstadt, Germany
Sodium dodecyl sulfate (SDS)	PanReac AppliChem ITW Reagents, Darmstadt, Germany
Sodium hydroxide (NaOH) pellets	VWR International, Radnor, Pennsylvania, USA

<b>Chemicals and reagents</b>	<b>Manufacturers</b>
Titriplex® III ethylenedinitrilotetraacetic acid (EDTA) disodium salt dihydrate	Merck, Darmstadt, Germany
Tris-(2-carboxyethyl)-phosphine Hydrochloride, 5 g, >98 % (TCEP)	Carl Roth®, Karlsruhe, Germany
Tris-(hydroxymethyl)-aminomethane (Tris)	PanReac AppliChem ITW Reagents, Darmstadt, Germany
Triton® X-100 (TX-100) for molecular biology	PanReac AppliChem ITW Reagents, Darmstadt, Germany
Trypsin inhibitor from <i>Glycin max</i> (STI)	Sigma-Aldrich, St. Louis Missouri, USA
Tween® 20 for molecular biology	PanReac AppliChem ITW Reagents, Darmstadt, Germany
UltraPure™ Agarose	Invitrogen™ by life technologies™, Thermo Fisher Scientific, Waltham Massachusetts, USA
Yeast extract	Carl Roth®, Karlsruhe, Germany
β-Nicotinamide adenine dinucleotide, reduced disodium salt hydrate (NADH)	Sigma-Aldrich, St. Louis Missouri, USA

**Table 4.5: Fatty acids and lipids.**

<b>Fatty acids and lipids</b>	<b>Manufacturers</b>
Arachidonic Acid (ARA) peroxide free	CAYMAN Chemical Company, Ann Arbor, Michigan, USA
Arachidonoyl-CoA (ARA-CoA)	Sigma-Aldrich, St. Louis Missouri, USA
Coenzyme A, lithium salt (CoA)	Sigma-Aldrich, St. Louis Missouri, USA
Docosahexanoic Acid (DHA)	CAYMAN Chemical Company, Ann Arbor, Michigan, USA
Eicosapentaenoic Acid (EPA)	CAYMAN Chemical Company, Ann Arbor, Michigan, USA
Prostaglandin B1 (PGB1)	CAYMAN Chemical Company, Ann Arbor, Michigan, USA
Lyso-PAF C-16	CAYMAN Chemical Company, Ann Arbor, Michigan, USA
Platelet Activating Factor C-16 (PAF)	CAYMAN Chemical Company, Ann Arbor, Michigan, USA
5(S)-HETE	CAYMAN Chemical Company, Ann Arbor, Michigan, USA
Acetyl-CoA, sodium salt	CAYMAN Chemical Company, Ann Arbor, Michigan, USA

<b>Fatty acids and lipids</b>	<b>Manufacturers</b>
20:5 Coenzyme A (EPA-CoA)	Sigma-Aldrich, St. Louis Missouri, USA

Table 4.6: Enzymes, kits, and reagents.

<b>Kits, reagents, and enzymes</b>	<b>Manufacturer</b>
1 kb DNA Gene Ruler	Thermo Fisher Scientific™, Waltham Massachusetts, USA
100 bp DNA Gene Ruler	Thermo Fisher Scientific™, Waltham Massachusetts, USA
Albumin Standard (BSA)	Thermo Fisher Scientific™, Waltham Massachusetts, USA
Cell proliferation reagent WST-1	Sigma-Aldrich, St. Louis Missouri, USA
dNTP Mix	Invitrogen™ by life technologies™, Thermo Fisher Scientific, Waltham Massachusetts, USA
EveryBlot blocking buffer	BIO-RAD, Hercules, California, USA
Gel Loading Dye, Purple (6x)	New England Biolabs, Inc. Ipswich Massachusetts, USA
GeneJET Gel Extraction Kit	Thermo Fisher Scientific™, Waltham Massachusetts, USA
GeneJET PCR Purification Kit	Thermo Fisher Scientific™, Waltham Massachusetts, USA
GeneJET Plasmid Miniprep Kit	Thermo Fisher Scientific™, Waltham Massachusetts, USA
L-Lactate Dehydrogenase (L-LDH)	Sigma-Aldrich, St. Louis Missouri, USA
Lysozyme from chicken egg white	Sigma-Aldrich, St. Louis Missouri, USA
Myokinase from rabbit muscle	Sigma-Aldrich, St. Louis Missouri, USA
NEBuilder® HiFi DNA Assembly Master Mix	New England Biolabs, Inc. Ipswich Massachusetts, USA
NucleoBond® Xtra Maxi	MACHEREY-NAGEL GmbH & Co. KG, Düren, Germany
Odyssey®Blocking-Puffer	LI-COR Biosciences, Lincoln, Nebraska, USA
PhosSTOP™ Phosphatase Inhibitor Cocktail	Roche Diagnostics GmbH, Mannheim, Germany
Phusion® High-Fidelity DNA Polymerase	New England Biolabs, Inc. Ipswich Massachusetts, USA
Pierce™ BCA Protein Assay Kit	Thermo Fisher Scientific™, Waltham Massachusetts, USA

<b>Kits, reagents, and enzymes</b>	<b>Manufacturer</b>
Precision Plus Protein™ All Blue Prestained Protein Standards	BIO-RAD, Hercules, California, USA
Pyruvate Kinase from rabbit muscle	Sigma-Aldrich, St. Louis Missouri, USA
Q5® High-Fidelity DNA Polymerase	New England Biolabs, Inc. Ipswich Massachusetts, USA
Restriction enzymes	New England Biolabs, Inc. Ipswich Massachusetts, USA
SYPRO™ Orange protein gel stain	Invitrogen™ by life technologies™, Thermo Fisher Scientific, Waltham Massachusetts, USA
T4 DNA Ligase	New England Biolabs, Inc. Ipswich Massachusetts, USA

### 4.1.3 Antibodies

All antibodies listed below (Table 4.7, Table 4.8, and Table 4.9) were diluted in full-strength EveryBlot blocking buffer without further supplements for western blot analysis. For antibody usage in laser scanning confocal microscopy experiments, see chapter 4.7.9.

**Table 4.7: Primary antibodies, their manufacturers, and species of origin.**

<b>Primary antibody</b>	<b>Manufacturer</b>	<b>Species</b>
15-LO-2 (D-9): sc-271290	Santa Cruz Biotechnology, Dallas, Texas, USA	mouse, monoclonal
5-LO (D-3): sc-515821	Santa Cruz Biotechnology, Dallas, Texas, USA	mouse, monoclonal
5-LO 10021-1-Ig	Proteintech, Rosemont, Illinois, USA	rabbit, polyclonal
5-LO (66326-1-Ig)	Proteintech, Rosemont, Illinois, USA	mouse, monoclonal
ACSL4 (F-4): sc-365230	Santa Cruz Biotechnology, Dallas, Texas, USA	mouse, monoclonal
Anti-15-LO-1 (ab119774)	Abcam, Cambridge, United Kingdom	mouse, monoclonal
ANTI-FLAG® M2 (F1804)	Sigma-Aldrich, St. Louis Missouri, USA	mouse, monoclonal
Anti-FLAP (ab85227)	Abcam, Cambridge, United Kingdom	goat, monoclonal
Anti-β-Actin (ab8229)	Abcam, Cambridge, United Kingdom	goat, polyclonal
His-Tag Polyclonal Antibody (#2365)	Cell Signaling Technology, Inc., Danvers, Massachusetts, USA	rabbit, polyclonal
LPCAT2 (H-7): sc-514354	Santa Cruz Biotechnology, Dallas, Texas, USA	mouse, monoclonal
LPCAT2 (PA5-39008)	Thermo Fisher Scientific™, Waltham Massachusetts, USA	rabbit, polyclonal

Primary antibody	Manufacturer	Species
$\beta$ -Actin (I-19): sc-1616	Santa Cruz Biotechnology, Dallas, Texas, USA	goat, polyclonal

For western blot analysis, primary antibody solutions were prepared, and incubation was performed according to Table 4.8.

**Table 4.8: Primary antibodies and their incubation conditions.**

Primary antibody	Dilution	Incubation
15-LO-2 (D-9): sc-271290	1:500	4 °C, ON
5-LO (D-3): sc-515821	1:500	1 h, RT or 4 °C, ON
ACSL4 (F-4): sc-365230	1:100	2 h, RT or 4 °C, ON
Anti-15-LO-1 (ab119774)	1:2,000	4 °C, ON
ANTI-FLAG® M2 (F1804)	1:1,000	1 h, RT or 4 °C, ON
Anti-FLAP (ab85227)	1:1,000	1 h, RT or 4 °C, ON
Anti- $\beta$ -Actin (ab8229)	1:1,000	1 h, RT or 4 °C, ON
His-Tag Polyclonal Antibody (#2365)	1:1,000	4 °C, ON
LPCAT2 (H-7): sc-514354	1:100	1 h, RT or 4 °C, ON
LPCAT2 (PA5-39008)	1:500-1:1000	1 h, RT or 4 °C, ON
$\beta$ -Actin (I-19): sc-1616	1:5,000	1 h, RT or 4 °C, ON

To visualize protein bands, secondary antibodies coupled to IR dyes were used (Table 4.9). All secondary antibodies were purchased from LI-COR Biosciences, Lincoln, Nebraska, USA, and the species of origin was donkey.

**Table 4.9 Secondary antibodies and their incubation conditions.**

Secondary antibody	Dilution	Incubation
IRDye® 680RD Anti-Goat IgG	1:20,000	1 h, RT
IRDye® 680RD Anti-Mouse IgG	1:20,000	1 h, RT
IRDye® 680RD Anti-Rabbit IgG	1:20,000	1 h, RT
IRDye® 800CW Anti-Goat IgG	1:15,000	1 h, RT
IRDye® 800CW Anti-Mouse IgG	1:15,000	1 h, RT
IRDye® 800CW Anti-Rabbit IgG	1:15,000	1 h, RT

#### 4.1.4 Buffers and stock solutions

Buffers used on a regular basis were prepared as stock solutions (Table 4.10) and diluted prior to use. 100 mL of 10× running buffer, 100 mL of 10× TBS, and 200 mL of 50× TAE buffer were diluted with ultra-pure water to a final volume of 1 L, 1 L, and 10 L, respectively. 80 mL of 12.5× transfer buffer was first diluted with 720 mL ultra-pure water and then filled up to 1 L with methanol.

**Table 4.10: Common buffer stocks.**

Buffers	Composition
10× Running buffer	0.25 M Tris, 1.92 M glycine, 35 mM SDS
10× Tris-buffered saline (TBS)	0.5 M Tris, pH 7.4, 1 M NaCl
12.5× Transfer buffer	0.31 M Tris, 2.4 M glycine
50× TAE buffer for agarose gels	2 M Tris, 1 M acetic acid, 50 mM EDTA

If not stated otherwise, all stock solutions listed in Table 4.11 were prepared in ultra-pure water.

**Table 4.11: Stock solutions.**

Stock solutions	Specification
1,000× Ampicillin	100 mg/mL, stored at -20 °C
1,000× Chloramphenicol	34 mg/mL, stored at -20 °C
10 % (w/v) APS	100 mg/mL, stored at -20 °C
Doxycycline	2 mg/mL (stored in black or brown tubes for light protection), stored at -20 °C
1000× Kanamycin	50 mg/mL, stored at 4 °C
5× SDS Loading Dye	250 mM Tris, 5 mM EDTA, 50 % (v/v) glycerol, 10 % (w/v) SDS, 0.05 % (w/v) bromophenol blue, adjusted with HCl to pH 6.8 10 % (v/v) β-mercaptoethanol added before use, stored at RT
CaCl <sub>2</sub>	0.4 M, stored at RT
Coomassie brilliant blue stain solution	70 mg coomassie brilliant blue G250, dissolved in 3 mL HCl and filled up to 1 L with ultra-pure water, stored at RT
IPTG	1 M, stored at -20 °C
PEI	1 mg/mL
PMSF	100 mg/mL in ethanol, stored at 4 °C
STI	60 mg/mL, stored at -20 °C
α-D-Glucose	20 mg/mL, stored at -20 °C



#### 4.1.5 Bacterial strains and cultivation

*E. coli* strains (Table 4.12) were either used for DNA amplification (DH5 $\alpha$ ) or protein expression (BL21(De3)).

**Table 4.12: Bacterial strains.**

Organism	Supplier
DH5 $\alpha$ competent <i>E. coli</i>	Invitrogen™ by life technologies™, Thermo Fisher Scientific, Waltham Massachusetts, USA
BL21(De3) competent <i>E. coli</i>	New England Biolabs, Inc. Ipswich Massachusetts, USA

Medium for *E. coli* growth was prepared as described in Table 4.13. LB-Medium was prepared in 1 L Erlenmeyer flasks sealed with tinfoil. After the sterilization process, the medium was stored at RT. Autoclaved LB-Agar was allowed to cool down to approx. 50 °C, mixed with the selection antibiotic of choice, and filled in culture dishes. LB-Agar plates were stored at 4 °C for up to one month. Sterile-filtered SOC-Medium was stored at -20 °C in 1 mL aliquots.

**Table 4.13: Medium for bacterial growth.**

Medium	Specifications
LB-Medium	12.5 g Lauria Broth-Medium dissolved in 500 mL ultra-pure water and autoclaved
LB-Agar	10 g Lauria Broth-Medium, 6 g Agar-Agar Kobe I dissolved in 400 mL ultra-pure water and autoclaved
SOC-Medium	20 g Tryptone, 5 g yeast extract, 4.5 g MgSO <sub>4</sub> , 0.5 g NaCl, 186 mg KCl dissolved in 1 L ultra-pure water. The solution was autoclaved, 4.36 g glucose was added, and the final medium was sterile filtered.

Petri dishes and cultivation tubes listed in Table 4.14 were purchased from Greiner Bio-One International GmbH, Kremsmünster, Austria.

**Table 4.14: Cultivation items for bacterial growth.**

Cultivation items	Specifications
Petri Dish	94×16 mm, without vents, with logo, light version
Tube, 14 mL	PP, 18/95 mm, round bottom, two-position vent stopper, sterile

##### 4.1.5.1 Cultivation of *E. coli*

Cultivation of *E. coli* both in liquid culture and on LB-Agar plates was carried out under sterile conditions. Selection of *E. coli* cultures was achieved by the addition of either ampicillin (100  $\mu$ g/mL), kanamycin (50  $\mu$ g/mL), or chloramphenicol (34  $\mu$ g/mL).

#### 4.1.5.2 Storage of *E. coli*

*E. coli* cultures on LB-Agar plates containing the respective antibiotics were stored at 4 °C for several weeks.

For long time storage, *E. coli* cells were stored as glycerol stocks at -80 °C. Glycerol stocks were prepared by dilution of 800 µL of an overnight culture (in LB medium containing the respective selection antibiotics) with 250 µL of 87 % glycerol in a screw-cap tube. The tubes were directly stored at -80 °C without pre-cooling steps.

#### 4.1.6 Devices and equipment

**Table 4.15: Devices and equipment used in this work with the respective manufacturers.**

Devices and equipment	Manufacturer
780 AxioObserver.Z1 laser scanning confocal microscope	Carl Zeiss AG, Oberkochen, Germany
Acquity UPLC H-class coupled to TUV and QDa detectors (ACQUITY UPLC HSS T3 1.8 µm, 2.1 × 100 mm column, and ACQUITY UPLC BEH C8 1.7 µm, 2.1 × 100 mm column)	Waters, Milford, Massachusetts, USA
Äkta Purifier	GE Healthcare Bio-Sciences AB, Uppsala, Sweden
Axio Vert.A1	Carl Zeiss AG, Oberkochen, Germany
Beckmann Ultrazentrifuge Optima LE-80K – Rotor 55.2 Ti	Beckman Coulter GmbH, Krefeld, Germany
Biovision 1000/26mx	Vilber Lourmat, Marne-la-Vallée, France
Bürker Counting chamber	Paul Marienfeld GmbH & Co.KG, Lauda-Königshofen, Germany
FluoLink	Vilber, Lourmat, Marne-la-Vallée, France
Heraeus Multifuge X3 FR	Thermo Fisher Scientific™, Waltham Massachusetts, USA
HiLoad™ 16/60 Superdex™ 200 pg	GE Healthcare Bio-Sciences AB, Uppsala, Sweden
HisTrap™ HP (1 mL and 5 mL)	GE Healthcare Bio-Sciences AB, Uppsala, Sweden or Cytiva Europe GmbH, Freiburg, Germany
HiTrap™ Desalting	GE Healthcare Bio-Sciences AB, Uppsala, Sweden
iCycler Detection System (MyiQ™)	BIO-RAD, Hercules, California, USA
Microfuge® 22R Centrifuge	Beckman Coulter GmbH, Krefeld, Germany
MIDI 1 Electrophoresis Unit	Carl Roth GmbH & Co. KG, Karlsruhe, Germany

<b>Devices and equipment</b>	<b>Manufacturer</b>
Mini Trans-Blot® Electrophoretic Transfer Cell	BIO-RAD, Hercules, California, USA
Mini-PROTEAN® Tetra Cell Casting Stand	BIO-RAD, Hercules, California, USA
Mini-PROTEAN® Tetra Vertical electrophoresis cell	BIO-RAD, Hercules, California, USA
NanoDrop™ 2000c	Thermo Fisher Scientific™, Waltham Massachusetts, USA
Odyssey® 9120 Infrared Imaging System	LI-COR Biosciences, Lincoln, Nebraska, USA
peqSTAR 96 Universal Gradient	Peqlab Biotechnologie GmbH, Erlangen, Germany
Power PAC 300	BIO-RAD, Hercules, California, USA
PowerPac Basic Power Supply	BIO-RAD, Hercules, California, USA
PURELAB® Ultra	ELGA LabWater by VeoliaWater Solutions & Technologies, Saint-Maurice, France
QuantStudio5	Applied Biosystems, Waltham, MA, USA
Resource™ S	Cytiva Sweden AB, Uppsala, Sweden
Rotilabo® filter papers type 601	Carl Roth®, Karlsruhe, Germany
Rotilabo®-syringe filters 0.22 µm	Carl Roth®, Karlsruhe, Germany
SafeSeal micro tube 2 mL	SARSTEDT AG & Co., Nümbrecht, Germany
Sonifier® W-250 D	Branson Ultrasonics Corporation, Danbury, Connecticut, USA
Sonopuls HD 200	BANDELIN electronic GmbH & Co. KG, Berlin, Germany
Sonopuls microtips MS 72 and KE 76	BANDELIN electronic GmbH & Co. KG, Berlin, Germany
Sorvall LYNX 4000 super speed centrifuge	BIO-RAD, Hercules, California, USA
StepOne™ Real-Time PCR System	Applied Biosystems, Waltham, MA, USA
Supor® 450 Membrane Disc Filters, 0.45 µm – 47 mm	Pall Corporation, Port Washington, New York, USA
Strep-Tactin™ XT 1 mL	ÎBA Lifesciences GmbH, Göttingen, Germany
TC10 Automated Cell Counter	BIO-RAD, Hercules, California, USA
Tecan infinite® M200	Tecan Trading AG, Männedorf, Switzerland
Tecan Spark®	Tecan Trading AG, Männedorf, Switzerland
TurboBlot Device	BIO-RAD, Hercules, California, USA

Devices and equipment	Manufacturer
UCT clean-up® CEC 0811Z	Amchro GmbH, Hattersheim, Germany
UCT clean-up® CEC 1811Z	Amchro GmbH, Hattersheim, Germany
Varifuge 3.0 – RS Rotor #8074	Heraeus Holding GmbH, Hanau, Germany

#### 4.1.7 Software and web tools

Table 4.16: Software that was used to gather and analyze experimental data.

Software	Version	Provider
Geneious R10	10.2.3	Biomatters, Ltd., Auckland, New Zealand
GraphPad Prism 7	7.05	GraphPad Software, Inc., San Diego California, USA
Image Studio Lite	5.2	LI-COR Biosciences, Lincoln, Nebraska, USA
MyiQ	1.0.410	BIO-RAD, Hercules, California, USA
NanoDrop™ 2000c	1.5	Thermo Fisher Scientific™, Waltham Massachusetts, USA
QuantStudio Design & Analysis Software	v1.5.2	Applied Biosystems, Waltham, MA, USA
SPARKCONTROL	3.0	Tecan Trading AG, Männedorf, Switzerland
Stepone Software	V2.1	Thermo Fisher Scientific™, Waltham Massachusetts, USA
Tecan i-control 1.10	3.4.2.0	Tecan Austria GmbH
UNICORN	5.31 (Build 743)	General Electric Company
Zen core	2.6	Carl Zeiss AG, Oberkochen, Germany

Table 4.17: Online tools and web services used.

Web tools	Link	Date of access
NEBcloner®	<a href="https://nebcloner.neb.com/#!/">https://nebcloner.neb.com/#!/</a>	26.07.2022
NEBioCalculator®	<a href="https://nebiocalculator.neb.com/#!/ligation">https://nebiocalculator.neb.com/#!/ligation</a>	26.07.2022
Oligo Calc: The Oligonucleotide Properties Calculator	<a href="http://biotools.nubic.northwestern.edu/OligoCalc.html">http://biotools.nubic.northwestern.edu/OligoCalc.html</a>	26.07.2022
BioRender.com	<a href="https://app.biorender.com/">https://app.biorender.com/</a>	26.08.2022

## 4.2 Cloning work

### 4.2.1 Standard techniques for DNA preparation

#### 4.2.1.1 Polymerase chain reaction

Polymerase chain reactions (PCRs) were either carried out using the Phusion® High-Fidelity DNA Polymerase or the Q5® High-Fidelity DNA Polymerase (Table 4.6). Reaction mixes were prepared according to the protocol of the manufacturer, and samples were run using the protocol shown in Table 4.18.

**Table 4.18: Standard protocol for the amplification of DNA.**

Step	Cycles	Temperature	Time
Initial denaturation	1×	98 °C	30 s
Denaturation		98 °C	10 s
Annealing	30×	61 °C	20 s
Elongation		72 °C	50s/kb
Final elongation	1×	72 °C	2 min (Q5) or 5 min (Phusion)
Storage		4 °C	hold

Primers were designed to have an annealing temperature of approximately 56 °C calculated using the 'Oligo Calc webtool' (see Table 4.17). Purification of the PCR product was either achieved directly using the GeneJET PCR Purification or by agarose gel electrophoresis and the GeneJET Gel Extraction Kit if side products occurred. Purification was performed according to the manufacturers' protocol (Table 4.6), respectively.

#### 4.2.1.2 Restriction digest

Typically, 1 µg of DNA was digested in a 50 µL reaction containing either one or two restriction enzymes as described in the manual of the manufacturer. Most restriction digests were carried out at 37 °C for 1 h except for SfiI digests which were carried out at 50 °C instead. If enzymes were labeled as 'time-safer qualified,' the incubation time was reduced to 15 min.

If possible, restriction enzymes were heat-inactivated following the digest. Depending on the enzyme, the reaction mix was either incubated at 65 °C for 15 min, at 80 °C for 20 min, or kept on ice until further use if inactivate was not possible. In case the restriction digest was used for the linearization of a plasmid, the product was purified directly using a PCR purification kit. If one or more specific fragments of the digested DNA were needed, DNA agarose gel electrophoresis was performed.

#### 4.2.1.3 DNA agarose gel electrophoresis

Agarose concentration was adapted depending on the size of the expected product, as shown in Table 4.19.

**Table 4.19: Concentration of agarose used for the separation of DNA fragments.**

Size of DNA fragment	Concentration of agarose
100-500 bp	1.5 %
>500-8,000 bp	1 %
>8,000 bp	0.8 %

For quantitative purification, the whole sample was taken and mixed with the respective amount of 6× DNA loading dye. If the total volume exceeded 50 µL, the sample was split and run using multiple gel pockets. Analytical gel electrophoresis was performed using a 5 µL aliquot of the respective sample mixed with 1 µL of 6x DNA loading dye. Agarose gel electrophoresis was performed in 1×TAE with 120 V for 25 min if one fragment (>1 kb) or fragments with large size differences (>1 kb) were analyzed. If separation of fragments with similar sizes (<1 kb) was necessary or if the fragment was below 1 kb in size, conditions were adapted to 100 V for 45 min.

To purify DNA fragments, bands were visualized at 312 nm using a UV-transilluminator, cut out, and transferred to 2 mL reaction tubes. Gel pieces were purified using the GeneJET Gel Extraction Kit following the manual of the manufacturer.

#### 4.2.1.4 Ligation of up to 3 DNA fragments

DNA fragments that were digested, as described before, were ligated by T4 DNA ligase. A molar ratio of 1:3 (vector to insert, or 1:3:3 vector to insert to insert) was used in most reactions calculated using the NEBioCalculator online tool (Table 4.17). If the ligation did not work out, the molar ratio was increased to 1:5 (vector to insert, or 1:5:5 vector to insert to insert). Ligation reactions were prepared according to the manufacturers' protocol and incubated for 30 min at room temperature (RT), followed by an inactivation step at 65 °C for 10 min afterward. The inactivated reaction mix was kept on ice until transformation in *E. coli* was performed.

#### 4.2.1.5 Assembly of multiple DNA fragments

For complex cloning projects that could not be accomplished by PCR, restriction digest, and common ligation techniques, the NEBuilder® HiFi DNA Assembly Master Mix (hereafter referred to as NEBuilder, Table 4.6) was used. This allowed the combination of up to five DNA fragments simultaneously. Vector DNA was linearized either by PCR or by restriction digest, while inserts were prepared by PCR so that the respective adjacent fragments shared a complementary region of about 20 bp. DNA Fragments were combined for 30 min at 50 °C following the manual of the manufacturer.

### 4.2.2 Plasmid preparation

Maps of the most promising plasmids prepared in this work as well as lists of the respective primers used, can be found in appendix chapters 9.1 (primers) and 9.2 (plasmid maps). Plasmids that were not prepared in this work are stated as such with their respective origin. Recombinant LPCAT2 expression constructs (*E. coli*) will not be described here since the approach was abandoned due to unsatisfactory results. For the same reason, plasmid maps of transient transfection constructs will not be shown.

Human cDNA clones (Table 4.20) of ‘Homo sapiens acyl-CoA synthetase long-chain family member 4’ (ACSL4) and ‘Homo sapiens lysophosphatidylcholine acyltransferase 2’ (LPCAT2) were purchased from BioCat GmbH, Heidelberg, Germany.

**Table 4.20: Commercially available plasmids.**

Vector	Specifications
<b>pBlueScriptR</b>	human cDNA clone of the ‘Homo sapiens acyl-CoA synthetase long-chain family member 4’
<b>pOTB7</b>	human cDNA clone of the ‘Homo sapiens lysophosphatidylcholine acyltransferase 2’

Plasmids used for recombinant protein expression in *E. coli* are shown in Table 4.21. The pET28a(+)\_PALOX expression plasmid, containing a 15-lipoxygenating enzyme from *Pseudomonas aeruginosa*, was kindly provided by Univ.-Prof. Dr. sc. med. Hartmut Kühn (Charité Berlin).

**Table 4.21: Plasmids for recombinant protein expression in *E. coli*.**

Plasmids	Specifications
<b>pBJ01_ACSL4_StrepII</b>	pET24a(+) backbone with ACSL4 gene (short isoform 42-711 aa) with C-terminal StrepII-tag
<b>pBJ03_ACSL4_His6x</b>	pET24a(+) backbone with ACSL4 gene (short isoform 42-711 aa) with C-terminal His6x-tag
<b>pET28a(+)_PALOX</b>	pET28a(+) backbone with the gene of a 15-lipoxygenating enzyme from <i>Pseudomonas aeruginosa</i>

The ACSL4 gene sequence was amplified by PCR using a commercially available human ACSL4 cDNA clone (Table 4.20) as template. Primer pair BG02/BJ10 was used to insert a NdeI and a HindIII restriction site at the 5'- or 3'-end, respectively. The PCR product, as well as a pET24a(+) vector, were digested using both restriction enzymes, and, following a purification step, the fragments were ligated using T4 DNA ligase. The resulting plasmid (**pBJ01\_ACSL4\_StrepII**) was used as template for the preparation of pBJ03\_ACSL4\_His6x. A PCR was run around the vector using the phosphorylated primer pair BJ13/BJ14, excluding the StrepII-tag sequence. The PCR product was ligated using T4 DNA ligase to obtain the expression plasmid **pBJ03\_ACSL4\_His6x**.

Constructs for transient transfection of HEK293T cells were based on the pcDNA3.1(+) backbone (Table 4.22). pcDNA3.1\_5LO and pSG5-FLAP (only used as template for amplification of FLAP) were kindly provided by Prof. Dr. Olof Rådmark (Karolinska Institute, Stockholm Sweden), whereas pcDNA3.1\_ALOX15B (hereafter referred to as pcDNA3.1\_15LO2) was kindly provided by Univ.-Prof. Dr. sc. med. Hartmut Kühn (Charité Berlin). The plasmids pcDNA3.1\_ALOX15 (hereafter referred to as pcDNA3.1\_15LO1) and pcDNA3.1\_mCh\_ALOX15B (only used as template for amplification of mCherry) were prepared and kindly provided by Dr. Roland Ebert.

### pcDNA3.1\_5LO\_P2A\_mCh

The 5-LO sequence was amplified using pcDNA3.1\_5LO as template and the primer pair BJ91/BJ92. The PCR inserted an EcoRI restriction site at the 5'-end and part of a P2A linker sequence containing an AatII restriction site at the 3'-end. Next, the mCherry sequence was amplified using pcDNA3.1\_mCh\_ALOX15B as template and the primer pair BJ97/BJ98. The resulting PCR product contained an AatII restriction site as well as the second part of the P2A linker sequence at the 5'-end and an XbaI restriction site at the 3'-end. PCR products were digested using the respective restriction enzymes, while the pcDNA3.1\_5LO vector was digested with EcoRI and XbaI. All three fragments were purified and ligated in one step afterward.

### pcDNA3.1\_FLAP

Thus far, transient transfection of FLAP was performed using a pSG5 backbone, while lipoxygenases were transfected using the pcDNA3.1 backbone. To ensure similar transfection efficiencies in co-transfections with 5-LO and FLAP, the backbone was exchanged.

pSG5-FLAP was used as PCR template in combination with primers BJ77 and BJ78. The PCR product contained an EcoRI restriction site at the 5'-end of the FLAP gene as well as an XhoI restriction site at the 3'-end. The PCR product and the pcDNA3.1 vector were digested using EcoRI and XhoI, and the purified fragments were ligated using the T4 DNA ligase.

**pcDNA3.1\_15LO1\_P2A\_mCh** and **pcDNA3.1\_15LO2\_P2A\_mCh** were prepared accordingly, using pcDNA3.1\_15LO1 as template with primer pair BJ93/BJ94 and pcDNA3.1\_15LO2 as template with primer pair BJ95/BJ96, respectively.

### pcDNA3.1\_5LO\_P2A\_FLAP\_T2A\_mCh

The preparation of a construct containing three genes separated either by P2A or T2A linker was achieved in multiple steps. First, FLAP and mCherry were amplified using pcDNA3.1\_FLAP as template with the primer pair BJ99/BJ100 or pcDNA3.1\_mCh\_ALOX15B as template with the primer pair BJ98/BJ102. The PCR product of FLAP contained an AatII restriction site and part of the P2A linker sequence at the 5'-end and part of the T2A linker sequence at the 3'-end, while the PCR product of mCherry contained part of the T2A linker sequence at the 5'-end and an XbaI restriction site at the 3'-end. The remaining part of the T2A linker was ordered as a single-stranded oligo (primer BJ101), and all three parts were combined using the NEBuilder. The ligated sequence was amplified by PCR using the primer pair BJ98/BJ99, followed by restriction digest using AatII and XbaI. The 5-LO sequence, as well as the pcDNA3.1 backbone, were prepared as described for pcDNA3.1\_5LO\_P2A\_mCh, and ligation of all three fragments resulted in the final pcDNA3.1\_5LO\_P2A\_FLAP\_T2A\_mCh plasmid.

**Table 4.22: Plasmids for transient transfection of HEK293T cells.**

Plasmids	Specifications
pcDNA3.1	pcDNA3.1(+) backbone with a non-coding DNA sequence as vector control



Plasmids	Specifications
pcDNA3.1_5LO	pcDNA3.1(+) backbone containing the 5-LO gene
pcDNA3.1_15LO1	pcDNA3.1(+) backbone containing the 15-LO 1 gene
pcDNA3.1_15LO2	pcDNA3.1(+) backbone containing the 15-LO 2 gene
pcDNA3.1_5LO_P2A_FLAP	pcDNA3.1 backbone with 5-LO and FLAP gene separated by a P2A linker sequence
pcDNA3.1_FLAP	pcDNA3.1(+) backbone containing FLAP gene
pcDNA3.1_5LO_P2A_mCh	pcDNA3.1(+) backbone with 5-LO gene, P2A linker sequence and mCherry gene
pcDNA3.1_15LO1_P2A_mCh	pcDNA3.1(+) backbone with 15-LO1 gene, P2A linker sequence and mCherry gene
pcDNA3.1_15LO2_P2A_mCh	pcDNA3.1(+) backbone with 15-LO2 gene, P2A linker sequence and mCherry gene
pcDNA3.1_5LO_P2A_FLAP_T2A_mCh	pcDNA3.1 backbone with 5-LO gene, P2A linker sequence, FLAP gene, T2A linker sequence, and mCherry gene, successively

Stable transfection of HEK293T cells should be achieved using the optimized sleeping beauty (SB) system [279]. Here, an SB vector containing the gene of interest (GOI) is co-transfected with another vector encoding for the SB100X transposase. The SB vectors pSBbiGH (Addgene plasmid #60514) and pSBtetGP (Addgene plasmid #60495) were kindly gifted by Dr. Eric Kowarz (Goethe University Frankfurt), and the pSB100X plasmid was kindly provided by Prof. Dr. Zoltan Ivics (Goethe University Frankfurt). Plasmids derived from the pSBbiGH vector were used for constitutive overexpression of the GOI (Table 4.23), while plasmids derived from pSBtetGP were used for doxycycline-treatment dependent protein expression (Table 4.24).

#### **pSBbiGH\_ACSL4**

The ACSL4 gene was amplified by PCR using pBJ01\_ACSL4\_His6x as template and primer pair BJ17/BJ18. The PCR product contained SfiI restriction sites at both ends that slightly varied in sequence to ensure the correct orientation in the final vector. pSBbiGH vector and PCR product were digested with SfiI, and purified fragments were ligated using T4 DNA ligase.

**pSBbiGH\_LPCAT2** was prepared accordingly, using a commercially available human LPCAT2 cDNA clone (Table 4.20) as template and primer pair BJ19/BJ20.

#### **pSBbiGH\_ACSL4\_P2A\_LPCAT2**

The preparation of a construct carrying both ACSL4 and LPCAT2 sequences separated by a P2A linker sequence was achieved in two steps. First, ACSL4 and LPCAT2 sequences were amplified using pBJ01\_ACSL4\_His6x as template with primer pair BJ17/BJ21 or a human LPCAT2 cDNA clone (Table 4.20) as template with the primer pair BJ20/BJ22, respectively. The resulting PCR product of the ACSL4 gene was designed to carry a SfiI restriction site at

the 5'-end and part of the P2A linker sequence containing an AatII restriction site at the 3'-end. The PCR product of the LPCAT2 gene was designed the other way around and contained an AatII restriction site as well as the second part of the P2A linker sequence at the 5'-end and a SfiI restriction site at the 3'-end. Both PCR products were digested using only AatII, and the purified fragments were ligated by T4 DNA ligase. The ligated insert was used as template for a PCR using the primer pair BJ17/BJ20 to enrich the amount of DNA. The amplified insert was purified, and both insert and pSBbiGH vector were digested using SfiI. Final plasmid formation was achieved by ligation of the purified fragments by T4 DNA ligase.

### **pSBtetmChP**

Preparation of plasmids for the stable integration of already transfected cell lines required the exchange of the enhanced green fluorescent protein (EGFP) to mCherry.

The EGFP sequence of the pSBtetGP plasmid was removed by PCR due to the lack of restriction sites using the primer pair BJ103/BJ104, while the mCherry sequence was amplified from pcDNA3.1\_mCh\_ALOX15B using the primer pair BJ111/BJ112. Since conventional restriction cloning was not possible, the PCR product of mCherry was designed to contain 20 nucleotides at both the 5'- and the 3'-end that were complementary to the respective backbone part of the linearized pSBtetGP fragment (lacking EGFP). The final plasmid was obtained using the NEBuilder.

### **pSBtetmChP\_5LO**

The 5-LO gene sequence was obtained by PCR using pcDNA3.1\_5LO as template and the primer pair BJ109/BJ119. The primer pair added an overhang of 20 bp to each side of the gene complementary to the incorporation sites of the target vector. pSBtetmChP was digested using SfiI, and ligation was achieved using the NEBuilder.

### **pSBtetmChP\_FLAP\_P2A\_5LO**

pcDNA3.1\_FLAP was used as PCR template for the FLAP sequence with primer pair BJ117/BJ118, while pcDNA3.1\_5LO was used as PCR template for the 5-LO sequence with primers BJ119/BJ120. The backbone was obtained by restriction digest of pSBtetmChP with SfiI, and all fragments were combined using the NEBuilder.

### **pSBtetmChP\_15LO1**

The 15-LO1 sequence was obtained by PCR using pcDNA3.1\_15LO1 as template and the primer pair BJ105/BJ106. The primer pair added SfiI restriction sites to both ends of the lipoxygenase sequence. pSBtetmChP and the PCR product were digested using SfiI, and the purified fragments were joined by T4 DNA ligase.

**pSBtetmChP\_15LO2** was prepared analogously to pSBtetmChP\_15LO1 only varying in template (pcDNA3.1\_15LO2) and primer pair (BJ107/108) used.

**Table 4.23: Plasmids used for stable transfection and constitutive protein expression.**

Plasmids	Specifications
pSBbiGH	SB plasmid for stable integration and permanent overexpression. SB-transposon with a constitutive bi-directional promoter, one side: SfiI cloning site for GOI (contains filler DNA), other side: GFP and hygromycin resistance gene.
pSBbiGH_ACSL4	pSBbiGH backbone with ACSL4 gene (short isoform)
pSBbiGH_ACSL4_P2A_LPCAT2	pSBbiGH backbone with ACSL4 gene (short isoform) and LPCAT2 gene separated by P2A linker sequence
pSBbiGH_LPCAT2	pSBbiGH backbone with LPCAT2 gene

**Table 4.24: Plasmids for stable transfection and inducible protein expression.**

Plasmid	Description
pSBtetGP	SB-transposon with inducible SfiI cloning site for GOI (contains firefly luciferase) and constitutive expression of GFP, rtTA, and hygromycin resistance gene
pSBtetmChP	pSBtetGP backbone, but GFP was exchanged with mCherry
pSBtetmChP_5LO	pSBtetmChP backbone with 5-LO gene instead of firefly luciferase
pSBtetmChP_FLAP_P2A_5LO	pSBtetmChP backbone with 5-LO and FLAP gene separated by a P2A linker sequence instead of firefly luciferase
pSBtetmChP_15LO1	pSBtetmChP backbone with 15-LO1 gene instead of firefly luciferase
pSBtetmChP_15LO2	pSBtetmChP backbone with 15-LO2 gene instead of firefly luciferase

### 4.2.3 Transformation in *E. coli*

Plasmids prepared as described above were either transformed into DH5 $\alpha$  competent cells for amplification purposes or into BL21(De3) competent cells for recombinant protein expression. Competent cells were thawed on ice for approx. 10 min. 50  $\mu$ L of the respective cells were transferred into 1.5 mL reaction tubes, and either 1  $\mu$ L of plasmid DNA (50-100 ng) or 2  $\mu$ L of a ligation mix was added. If the plasmid concentration was lower than 10 ng/ $\mu$ L, up to 5  $\mu$ L of DNA was used. The reaction tube was carefully flicked to mix cells and DNA and then incubated on ice for 30 min. Then, a heat shock was performed at 42 °C for either 25 s (BL21(De3)) or 45 s (DH5 $\alpha$ ) in a thermocycler and put on ice for 1 min. 500  $\mu$ L of warm SOC medium was added, and the reaction tube was incubated at 37 °C, 350 rpm for 1 h in a thermocycler.

### 4.2.4 Selection

Transformed cells were centrifuged for 2 min, 1,000 rcf at RT, and the supernatant was discarded so that approx. 50  $\mu$ L remained in the reaction tube. The cell pellet was resuspended, and 20  $\mu$ L were plated on LB-Agar plates containing the respective selection

antibiotic. LB-Agar plates were incubated at 37 °C overnight until colony formation was visible and were then stored at 4 °C for up to one month.

#### 4.2.5 Amplification and isolation of vector DNA

The amplification of vector DNA was either done in a small scale for newly assembled constructs or in a large scale for already verified plasmids. Small-scale amplifications were performed in 8 mL LB medium with the respective selection antibiotic, inoculated with a clone from a selection plate, and incubated at 37 °C, 180 rpm overnight. Large-scale amplifications were performed in 500 mL LB medium with the respective selection antibiotics and inoculated either with a clone from a selection plate or with 500 µL transformation mix. Incubation conditions were the same as described for small-scale amplifications.

Afterward, cells were harvested for either 10 min (small-scale) or 20 min (large-scale) at 4 °C and 4,000 rcf, and the supernatant was discarded. Isolation of the amplified DNA from the cell pellets was achieved using either a MiniPrepKit (Thermo Fisher Scientific™, small scale) or a MaxiPrepKit (MACHEREY-NAGEL GmbH & Co. KG, large scale) according to the manuals of the manufacturers.

DNA concentrations were determined on a NanoDrop™ 2000c.

#### 4.2.6 DNA sequencing

Verification of new plasmids was achieved using sanger sequencing (Microsynth AG, Schweiz), and comparison of sequences was performed with the Geneious R10 software (see Table 4.16).

### 4.3 Protein expression and purification of ACSL4

All buffers used in the purification process of recombinant ACSL4 (Table 4.25) were prepared in ultra-pure water and both filtered and degassed before use.

**Table 4.25: Buffers used for purification of recombinant ACSL4.**

Buffer	Composition
Lysis buffer	20 mM NaPi, pH 7.4, 200 mM NaCl, 10 mM imidazole, 1 mM DTT, 5 % (v/v) glycerol
Wash buffer	20 mM NaPi, pH 7.4, 200 mM NaCl, 20 mM imidazole, 1 mM DTT, 5 % (v/v) glycerol
Elution buffer	20 mM NaPi, pH 7.4, 200 mM NaCl, 300 mM imidazole, 1 mM DTT, 5 % (v/v) glycerol
IEX buffer A	20 mM NaPi, pH 6.5, 1 mM DTT, 5 % (v/v) glycerol
IEX buffer B	20 mM NaPi, pH 6.5, 1 M NaCl, 1 mM DTT, 5 % (v/v) glycerol

#### 4.3.1 Pre-culture

A pre-culture was prepared prior to the expression culture. For this purpose, 20 mL LB medium containing kanamycin as selection antibiotic was inoculated either with a clone of a selection

plate or with a few crystals of a frozen glycerol stock. The pre-culture was incubated at 37 °C, 180 rpm for 16 h.

### **4.3.2 Large-scale expression**

Expression cultures were prepared using 500 mL LB medium containing kanamycin and were inoculated with 10 mL of the pre-culture. Cultures were incubated at 37 °C and 180 rpm until an OD<sub>600</sub> of 0.6 to 0.8 was reached (approx. 1-1.5 h). Then, IPTG was added to a final concentration of 0.25 mM, and the incubation was continued at 20 °C and 180 rpm overnight (16-20 h). Harvest of the cells was achieved by centrifugation for 20 min at 4 °C and 4,000 rcf, and the supernatant was discarded. Cell pellets were either transferred to 50 mL tubes and stored at -20 °C or purified directly.

### **4.3.3 Cell lysis and disruption by sonification**

Cell pellets were resuspended in 20 mL lysis buffer supplemented with 0.4 mM PMSF, 0.1 % Triton X-100, 1 mM EDTA, 60 µg/mL STI and 50 mg lysozyme. The cell suspension was kept on ice for 30 min before cell disruption was performed. Cell disruption was achieved by sonification alternating between 0.5 s pulse and 1 s pause for 15 min. Cell debris was removed by centrifugation for 15 min at 4 °C and 10,000 rcf, and the supernatant was transferred into a clean 50 mL tube.

### **4.3.4 Ultracentrifugation**

Ultracentrifugation of the supernatant was performed for 70 min at 4 °C and 100,000 rcf. The supernatant was transferred to a 50 mL tube, and MgCl<sub>2</sub> solution was added to a final concentration of 1 mM.

### **4.3.5 Ni-affinity chromatography**

Ni-affinity chromatography was performed using either a 1 mL or 5 mL HisTrap™ HP column and an ÄKTA Purifier System. The column was equilibrated with 5 column volumes (CV) of lysis buffer and a flow rate of 5 mL/min. Then, the supernatant of the ultracentrifugation was loaded with a reduced flow rate of 2.5 mL/min. Following the application of the sample, the flow rate was increased again to 5 mL/min, and protein impurities were removed in two washing steps with 7 CV of lysis buffer and 5 CV of wash buffer, successively. Elution was achieved with 6 CV of elution buffer. Elution fractions were combined and concentrated until the total volume was below 5 mL. The full method of the run is shown in appendix chapter 9.3.1.

### **4.3.6 Desalting and buffer exchange**

Buffer exchange of up to 5 mL protein solution was achieved using three consecutive HiTrapDesalting columns (CV = 3×5 mL = 15 mL). Columns were equilibrated with 1.3 CV of IEX buffer A and a flow rate of 3 mL/min. The protein solution was applied with a reduced flow rate of 2 mL/min followed by 5 CV of IEX buffer A. Protein elution was tracked at 280 nm, and successful desalting was verified by conductivity monitoring. Protein fractions were combined and concentrated until the volume was below 5 mL. The full method of the run is shown in appendix chapter 9.3.2.

### 4.3.7 Ion exchange chromatography (IEX)

IEX was performed using a Resource S column (CV = 1 mL). The column was equilibrated with 5 CV of IEX buffer A and a flow rate of 2 mL/min before the protein solution was applied with a reduced flow rate of 0.5 mL/min. Following protein application, the unbound protein was washed off with 2 CV of IEX buffer A. Protein elution was achieved using a gradient ranging from 0-70 % of IEX buffer B over 20 CV. Elution fractions were combined and concentrated if necessary. The full method of the run is shown in appendix chapter 9.3.3.

### 4.3.8 Size exclusion chromatography (SEC)

SEC was performed using a HiLoad™ 16/60 Superdex™ 200 pg column (CV = 120 mL). The column was equilibrated with 1 CV of SEC buffer (20 mM NaP<sub>i</sub>, pH 7.4, 200 mM NaCl, 5 % (v/v) glycerol, and varying concentrations of Triton X-100) at a flow rate of 1.2 mL/min before a maximum of 5 mL protein solution was added with a reduced flow rate of 0.5 mL/min. Elution was achieved with 1.25 CV of SEC buffer with a flow rate of 1.2 mL/min. The full method of the run is shown in appendix chapter 9.3.4.

## 4.4 Protein expression and purification of PALOX

All buffers used in the purification process of recombinant PALOX (Table 4.26) were prepared in ultra-pure water and both filtered and degassed before use.

**Table 4.26: Buffers used for purification of recombinant PALOX.**

Buffer	Composition
Lysis buffer	25 mM HEPES, pH 7.4, 150 mM NaCl, 10 mM imidazole
Wash buffer	25 mM HEPES, pH 7.4, 150 mM NaCl, 30 mM imidazole
Elution buffer	25 mM HEPES, pH 7.4, 150 mM NaCl, 250 mM imidazole
PALOX buffer	25 mM HEPES, pH 7.4, 150 mM NaCl

Protein expression and purification of PALOX were performed as described for ACSL4 in chapter 4.3, excluding the IEX purification step. Apart from this, the purification process only differed in the buffers used (Table 4.26) during Ni-affinity chromatography and the final buffer exchange (PALOX buffer).

## 4.5 Analysis of recombinant proteins

### 4.5.1 Determination of protein concentration

To determine protein concentrations, the absorbance at 280 nm was measured on a NanoDrop™ 2000c against a suited control (buffer without protein). Extinction coefficients and molecular weight (MW) were calculated based on the amino acid sequence of the respective protein using the Geneious R10 software. The quotient of MW and extinction coefficient was used to correct the absorbance value and gain the protein concentration.

#### 4.5.2 Concentration of proteins

To increase the concentration of protein solutions Amicon™ Centrifugal Filter Units (10 kDa cut-off) were used. Filter units containing the protein solution were centrifuged for 10 min at 4 °C and 3,000 rcf. Progress and integrity of the filter column were checked in-between runs by determination of protein concentration in both flowthrough and concentrate. Centrifugation was continued until the desired concentration or volume was reached. After every third run, the protein solution in the upper chamber was pipetted up and down to prevent blockage of the filter membrane.

#### 4.5.3 Storage of purified proteins

Protein solutions were either stored at 4 °C overnight or concentrated (>2 mg/mL) and stored in 500 µL aliquots at -80 °C following a snap freeze in liquid nitrogen.

#### 4.5.4 Sodium dodecylsulfate polyacrylamide gel electrophoresis (SDS-PAGE)

SDS-PAGE, in combination with coomassie brilliant blue staining, was used to check the purification process of recombinant proteins. In addition, SDS-PAGE was also performed in advance of western blotting of recombinant proteins or cell culture samples.

If SDS-PAGE was run to analyze recombinant protein expression, samples were typically taken from ÄTKA fractions of flowthrough, washing, and elution steps. Samples that contained large amounts of protein, like flowthrough or concentrated protein solutions, were diluted 1:10 prior to use. Before the run, samples were mixed with 5× SDS-loading dye and heated to 96 °C for 5 min. SDS samples were chilled on ice for subsequent analysis or stored at -20 °C for later use. 10 µL of each sample was used for analysis together with 2.5 µL of pre-stained protein standards. Separation of proteins was achieved using 1.5 mm hand-cast 10 % gels (with 4 % stacking gel on top). The chamber was filled with running buffer, and SDS-PAGE was performed in two steps. First, samples were focused at 80 V for 10 min before separation was achieved with 130 V for 80 min. Following the run, the electrophoresis cell was disassembled, and the stacking gel part was removed. The running gel was washed three times with 100 mL of ultra-pure water and slow shaking for 5 min each. Subsequently, the water was removed, and coomassie brilliant blue solution was added so that the gel was covered entirely. Shaking was continued for 1 h before the staining solution was removed, and 100 mL of ultra-pure water was added for another hour. Protein bands were visualized using an Odyssey® 9120 Infrared Imaging System. In case of low protein or high background signal, the gel was shaken in 100 mL of fresh ultra-pure water overnight and scanned again. If the protein expression should be verified by Western blotting, two identical SDS-PAGE gels were run, and only one was stained with coomassie brilliant blue, while the second one was used for Western blotting.

If cell lysates should be analyzed by Western blotting, 20 µg total protein determined by Bicinchoninic acid assay (BCA), as described in 4.7.5, were mixed with 5× SDS loading dye and filled up with ultra-pure water to a final volume of either 15 or 20 µL, depending on the concentration. All samples were heated to 96 °C for 5 min and chilled on ice before the run. The whole sample volume was used for analysis, and SDS-PAGE was run as described above.

### 4.5.5 Western blotting

At first, Western blotting was performed using the conventional wet tank blot technique. Later on, the method was changed to the Trans-Blot Turbo Transfer System, which reduced the operation time by over an hour with comparable transfer efficiency.

Proteins were transferred to nitrocellulose membranes (0.2  $\mu\text{m}$ ), and following the transfer, membranes were blocked in EveryBlot blocking buffer for 5-15 min at RT. Membranes were incubated with primary antibodies, as indicated in Table 4.8. Following the incubation, membranes were washed four times with 5 mL TBS-T (TBS with 0.1 % Tween-20) for 5 min each. Then, incubation with the respective secondary antibodies was performed, as shown in Table 4.9. Membranes were washed again, three times with 5 mL TBS-T for 5 min each and one time with 5 mL TBS. Membranes were stored in TBS at 4 °C.

Protein bands were visualized on an Odyssey Infrared Imaging System, and analysis was accomplished using the Image Studio software (Table 4.16).

## 4.6 Human cell culture

### 4.6.1 Cultivation

HEK293T cells (both wild type and stable transfected) were cultured in DMEM supplemented with 10 % FBS, 100  $\mu\text{g}/\text{mL}$  streptomycin, 100 U/mL penicillin, and 1 mM sodium pyruvate. Cultures were split every 3-4 days in a ratio of 1:10 and incubated at 37 °C, 95 % humidity, and 5 %  $\text{CO}_2$ . Periodically, cultures were tested for contaminations by PCR (Mycoplasma) and by cultivation on LB-Agar plates (microbial infection).

### 4.6.2 Cell harvest and cell count

HEK293T cells cultured in flasks were either harvested using trypsin-EDTA (TE) or by tapping the flask. If cells were to be used in an experiment, TE was used to ensure a better distribution, while the tapping technique was only used to split the cells. To harvest the cells, the old medium was discarded, and cells were washed with 5-10 mL PBS depending on the size of the flask. Small (25  $\text{cm}^2$ ), medium (75  $\text{cm}^2$ ), and large flasks (175  $\text{cm}^2$ ) were incubated with 1 mL, 3 mL, or 5 mL of warm TE for 2 min, followed by the addition of 4 mL, 7 mL, or 15 mL DMEM, respectively. Cell suspensions were transferred to 15 mL or 50 mL tubes, and 20  $\mu\text{L}$  samples were taken for cell count. Samples were diluted 1:1 with 0.4 % trypan blue solution and counted on a TC10 automated cell counter. Cell suspensions that were not evenly distributed were counted by hand using a Bürker counting chamber. Here, 20  $\mu\text{L}$  of cell suspension was diluted with 40  $\mu\text{L}$  of 0.4 % trypan blue solution.

Cells that were seeded in 15 cm dishes were scraped using a spatula. The medium was discarded, and the cells were carefully washed with 10 mL of cold PBS. Then, 20 mL PBS was added per dish, cells were scraped, and cell suspensions were transferred to 50 mL tubes on ice. Another 20 mL of PBS was used to rinse the dish and was also transferred to the respective tube. Due to this harsh harvesting technique, cells were, in general, not counted afterward.



Harvested cells were centrifuged (340 rcf, 5 min, RT), and the supernatant was discarded. The further preparation of the cell pellets was highly dependent on the experimental use and is therefore described in the respective chapters.

### **4.6.3 Storage of cells**

For long time storage cells were grown in large culture flasks and harvested at approx. 70 % confluency. Cells were counted, and following a centrifugation step (340 rcf, RT, 5 min), the medium was discarded. Cell pellets were resuspended in cryomedium (cultivation medium containing 5 % DMSO) to a final concentration of  $5 \times 10^6$  cells/mL. Cryo vials were filled with 1 mL of cell suspension each and frozen immediately at  $-80$  °C wrapped in paper balls to slow down the freezing process.

### **4.6.4 Thawing of cells**

One vial of frozen cells (typically 1 mL containing  $5 \times 10^6$  cells) was thawed at RT and diluted in 13 mL of cultivation medium. Following a centrifugation step (340 rcf, RT, 5 min), the supernatant was discarded, and the cell pellet was resuspended in 5 mL of fresh cultivation medium. The cell suspension was transferred into a small cell culture flask, and the medium was supplemented with an additional 10 % of FBS. After 24 h, the medium was exchanged for standard cultivation medium, and cells were treated as described in chapter 4.6.1.

## **4.7 Cell culture experiments**

### **4.7.1 Transient transfection of HEK293T cells**

$5 \times 10^6$  HEK293T cells were seeded in 15 mL DMEM in a 15 cm dish and let adhere for 24 h. A mix of 55 µg polyethylenimine (PEI) and 11 µg of the respective plasmid was prepared in OptiMEM without serum in a total volume of 1.1 mL and incubated at RT for 30 min. Then, 16 µL 25 mM chloroquine solution was added to the medium in the cell culture dish (final concentration after addition of the transfection mix is 25 µM), and 1 mL of the transfection mix was added dropwise (final amounts: 50 µg PEI and 10 µg DNA). The cells were kept in the transfection medium for 16 h before the medium was exchanged with fresh cultivation medium. If the transfection plasmid contained the mCherry gene, successful transfection was monitored by fluorescent microscopy. Cells were incubated for an additional 24 h at 37 °C before experiments were performed.

### **4.7.2 Transfection efficiency**

Transfection efficiencies could only be determined for constructs carrying a fluorescent protein. Here, mCherry was used as a fluorescence marker which allowed the discrimination in mCherry positive and negative cells. Following the transfection procedure as described in 4.7.1, randomly chosen parts of each cell culture dish were analyzed for their average transfection efficiency. For this purpose, both white light and fluorescence images of the respective areas were taken, and the ratio of mCherry-positive cells to total cell number was determined. To ensure that the resulting transfection efficiency was as accurate as possible, the average of at least three areas per plate was taken.

### 4.7.3 Stable transfection of HEK293T cells using the sleeping beauty system

The optimized sleeping beauty system [279] was used to create stable cell lines. Depending on the intended use of these cell lines, overexpression of the GOI was either established in a constitutive or inducible manner.

Permanent overexpression was reached using the pSBbiGH backbone, which contained the respective GOIs (Table 4.23), GFP as a fluorescence marker, and a hygromycin resistance gene for positive selection.  $1 \times 10^5$  HEK293T cells per well were seeded in a 6-well plate and let adhere for 24 h. A transfection mix was prepared and incubated at RT for 30 min before the dropwise addition. The mix (for one well) contained the respective pSBbiGH plasmid (2.25  $\mu$ g), a second plasmid carrying the SB100X transposase gene (0.25  $\mu$ g), and PEI (12.5  $\mu$ g) diluted in OptiMEM without serum in a total volume of 250  $\mu$ L. Plates were incubated for 16 h before the medium was exchanged for cultivation medium for 24 h. Successful transfection was checked by GFP fluorescence. Cells were carefully washed with 1 mL PBS and 2.5 mL of selection medium (cultivation medium containing 400  $\mu$ g/mL Hygromycin B) was added. Cells were kept in selection medium for 6 days in total with medium exchange on days 3 and 5. Successful positive selection was checked by GFP fluorescence. Wells that contained only GFP-positive cells were chosen for further handling. The medium was exchanged for cultivation medium, and once a confluency of 70 % was reached, the cells were transferred to small culture flasks. Protein overexpression was verified by Western blotting, and new cell lines were renamed, as shown in Table 4.27.

**Table 4.27: Stable cell lines with constitutive protein expression.**

Name of new cell line	Transfection plasmid
HEK293T_ACSL4	pSBbiGH_ACSL4
HEK293T_ACSL4+ LPCAT2	pSBbiGH_ACSL4_P2A_LPCAT2
HEK293T_LPCAT2	pSBbiGH_LPCAT2
HEK293T_VC	pSBbiGH

In order to prevent already transfected cell lines from negative effects caused by a second permanent overexpression, pSBbiGH constructs were replaced by pSBtetmChP constructs (Table 4.24). These plasmids contained a reverse tetracycline-controlled transactivator in combination with a tight TRE promoter which resulted in a silenced gene expression until treatment with doxycycline. In addition, these plasmids carried the gene of interest, mCherry, as a fluorescence marker as well as a puromycin resistance gene for positive selection. Transfection was carried out as described above for pSBbiGH plasmids. Incubation in transfection medium for 16 h was followed by a mCherry fluorescence check, and the medium was exchanged for cultivation medium. After 24 h, the medium was discarded, cells were washed with 1 mL PBS and 2.5 mL of fresh selection medium containing 2.5  $\mu$ g/mL puromycin was added. Cells were kept in selection medium for 6 days in total with medium exchange on day 3 and day 5. If cells showed homogeneous mCherry expression, the medium was exchanged for cultivation medium, and upon a confluency of 70 %, cells were transferred to

small culture flasks. The incorporated system was checked for functionality by Western blotting. Therefore,  $1 \times 10^6$  transfected cells were seeded in two separate culture flasks ( $75 \text{ cm}^2$ ) each and incubated for three days. On day 4, cells were treated with doxycycline as described in chapter 4.7.6, and protein overexpression was checked via Western blotting. Verified cell lines were renamed, as shown in Table 4.28.

**Table 4.28: Stable cell lines with inducible lipoxygenase expression.**

<b>Name of new cell line</b>	<b>Transfection plasmid</b>
HEK293T_ACSL4_5LO	pSBtetmChP_5LO
HEK293T_ACSL4_5LO+FLAP	pSBtetmChP_5LO_P2A_FLAP
HEK293T_ACSL4_15LO1	pSBtetmChP_15LO1
HEK293T_ACSL4_15LO2	pSBtetmChP_15LO2
HEK293T_ACSL4+ LPCAT2_5LO	pSBtetmChP_5LO
HEK293T_ACSL4+LPCAT2_5LO+FLAP	pSBtetmChP_5LO_P2A_FLAP
HEK293T_ACSL4+ LPCAT2_15LO1	pSBtetmChP_15LO1
HEK293T_ACSL4+ LPCAT2_15LO2	pSBtetmChP_15LO2
HEK293T_VC_5LO	pSBtetmChP_5LO
HEK293T_VC_5LO+FLAP	pSBtetmChP_5LO_P2A_FLAP
HEK293T_VC_15LO1	pSBtetmChP_15LO1
HEK293T_VC_15LO2	pSBtetmChP_15LO2

#### 4.7.4 Cell lysis

In preparation for Western blotting, cells were lysed by sonication. Harvested cell pellets (see chapter 4.6.2) were resuspended in lysis buffer (20 mM Tris-HCl, pH 7.4, 150 mM NaCl, 2 mM EDTA, 1 % Triton X-100 and 0.5 % NP-40) supplemented with the protease inhibitor mix cOmplete Mini and the phosphatase inhibitor mix PhosSTOP according to the manufacturer's protocol, respectively. Typically,  $5 \times 10^6$  cells were suspended in 100  $\mu\text{L}$  of supplemented lysis buffer, and the cell suspension was vigorously shaken for 10 s. After a 10 min rest on ice, the cell suspension was shaken again, and sonication was performed. The cell suspension was sonicated three times for 10 s each with rests on ice in-between. Sonication was performed using an ultrasonic homogenizer with the Sonopuls microtip MS 72 at 10 % of the maximum amplitude. Homogenized cells were centrifuged for 10 min at  $4 \text{ }^\circ\text{C}$  and 10,000 rcf, and supernatants were transferred to fresh 1.5 mL tubes. Cell lysates contained the soluble protein fraction and were either analyzed directly by BCA or stored at  $-20 \text{ }^\circ\text{C}$ .

#### 4.7.5 Bicinchoninic acid assay (BCA)

Cell lysates were diluted 1:15 in ultra-pure water, and protein concentration was determined in duplicates using the Pierce BCA-Kit following the protocol of the manufacturer. To calculate the amount of total protein in the samples, a concentration curve of bovine serum albumin

(BSA) in ultra-pure water was prepared. Absorption of samples and the dilution series were measured at 562 nm using a Tecan plate reader, and concentrations were determined.

#### **4.7.6 Doxycycline treatment**

Cells were seeded and let adhere for 24 h before doxycycline treatment. An aqueous 2 mg/mL stock solution of doxycycline was pre-diluted 1:100 in DMEM before another 1:100 dilution in the respective cultivation medium. Medium of the cells was exchanged for the doxycycline-containing medium with a final concentration of 0.2 µg/mL, and cells were incubated for 24 h before further experiments were conducted.

#### **4.7.7 Sample preparation for membrane composition analysis**

To determine membrane compositions, samples of wild-type, transiently transfected and/or stably transfected HEK293T cells were used.

For HEK293T wild type and permanently overexpression cell lines,  $8 \times 10^6$  cells were seeded in 15 cm dishes and harvested after 48 h. The cell suspension was centrifuged for 5 min at 340 rcf, and RT, the supernatant was discarded, and the pellet was washed with 5 mL PBS. Following another centrifugation step, the pellet was resuspended in 1 mL PBS and transferred into 2 mL protein low-bind tubes. The tubes were centrifuged at 340 rcf, and 4 °C for 5 min, and the supernatant was discarded carefully using a pipette tip. Dry pellets were stored at -80 °C.

HEK293T cells transfected with the inducible SB system were prepared as follows.  $8\text{-}10 \times 10^6$  cells were seeded in two 15 cm cell culture dishes each and let adhere overnight. The medium of one dish was exchanged for cultivation medium containing 0.2 µg/mL doxycycline for 24 h (see chapter 4.7.6 for more details). For control reasons, the other dish was kept untreated. Following the doxycycline treatment, dry cell pellets were prepared and stored as described before. For RSL3 and/or Ferrostatin treatment, HEK293T\_LPCAT2\_15LO1 cells were seeded as described above. Following doxycycline treatment, 10 µM RSL3, 1 µM Ferrostatin or a combination of both were added for 4 h before dry cell pellets were prepared. HEK293T\_LPCAT2 cells were used as lipoxygenase control and DMSO-treated cells were used as compound controls.

Cell pellets were sent on dry ice to our collaborators of the laboratory of Prof. Dr. Nils Helge Schebb in Wuppertal. Samples were prepared for the analysis by Malwina Mainka, Laura Carpanedo or Susanne Reif. Non-esterified and total oxylipins were prepared and analyzed by LC-MS following solid phase extraction as described [204,209–211].

During the non-esterified and total oxylipin preparations of the RSL3/Ferrostatin sample set in Wuppertal, either 500 µM 15-LO1 Inhibitor BLX3387 were added and dry pellets were reconstituted in PBS (HEK293T\_LPCAT2, HEK293T\_LPCAT2\_5LO and HEK293T\_LPCAT2\_15LO1 cells) or, due to the lack of an effective 15-LO2 inhibitor, HEK293T\_LPCAT2\_15LO2 cells were directly reconstituted in 50 % (v/v) MeOH (HEK293T\_LPCAT2\_15LO2). Analysis was performed as described before [204,209–211].

#### 4.7.8 Cell viability assay

Cell viability was determined using a commercially available WST-1 reagent.  $2.5 \times 10^4$  HEK293T cells were seeded per well in cultivation medium in a 96-well plate and let adhere overnight. The medium was discarded, and cells were washed with white DMEM (cultivation medium without phenol red). 90  $\mu\text{L}$  of white DMEM was added to the cells afterwards, and either 10  $\mu\text{L}$  of compound or DMSO was added to a total volume of 100  $\mu\text{L}$ . Cells were incubated at 37 °C and 5 %  $\text{CO}_2$  for 24 h before 10  $\mu\text{L}$  of the WST-1 reagent was added. Cells were incubated for an additional 2 h before the absorbance at 450 nm and 690 nm was measured using a plate reader. Cell viability was determined in comparison to the DMSO control.

#### 4.7.9 Slide preparation for laser scanning confocal microscopy

$2 \times 10^4$  cells of LO inducible cell lines were seeded per well in 8-well Nunc™ Lab-Tek™ II CC2™ chamber slides and were left to adhere overnight. LO expression was induced by treatment with 200 ng/mL doxycycline for 24 h before cells were fixated or further treated. Additional treatment was performed with 10  $\mu\text{M}$  RSL3 or 3  $\mu\text{M}$  erastin for 4 h or 24 h, respectively. Control cells received DMSO instead. Then, slides were washed with 150  $\mu\text{L}$  cold PBS for 5 min, followed by fixation using 4 % (w/v) PFA in PBS for 15 min at RT. Slides were washed again twice with PBS and permeabilized in 100  $\mu\text{L}$  PBS with 1 % BSA, 0.2 % Triton X-100, and 22.52 mg/mL glycine for 1 h at RT. After another three washing steps with PBS, cells were incubated in 100  $\mu\text{L}$  of the respective antibody solution (Table 4.29, diluted in PBS with 1 % BSA and 0.2 % Triton X-100) for either 3 h at RT or overnight at 4 °C.

**Table 4.29: Primary antibodies and their dilution for confocal staining.**

Antibody	Dilution	Origin
5-LO (10021-1-Ig)	1:50	rabbit
5-LO (66326-1-Ig)	1:50	mouse
15-LO1 (ab119774)	1:50-1:100	mouse
15-LO2 (sc-271290)	1:50-1:100	mouse
ACSL4 (sc-365230)	1:50	mouse
LPCAT2 (PA5-39008)	1:50	rabbit

Cells were washed again three times with PBS before secondary antibody solutions (1:1,000, donkey anti-mouse, donkey anti-rabbit, goat anti-rabbit IgG (H+L) Highly Cross-Adsorbed Secondary Antibody coupled to Alexa Fluor™ Plus 647 and Alexa Fluor™ 532 goat anti-mouse IgG (H+L), Thermo Fisher Scientific™) were added for 1 h at RT. From here on, slides were kept light-protected. Cells were washed three times with PBS before either another target was stained as described above or nuclei were stained using 1  $\mu\text{g}/\text{mL}$  DAPI in PBS for 10 min at RT. After another three washing steps in PBS, slides were mounted with 100-150  $\mu\text{L}$  Mowiol mounting medium and Menzel coverslips according to the manufacturer's manual and kept at RT overnight. Slides were sealed with clear lacquer and stored at 4 °C until analysis.

#### 4.7.10 Laser scanning confocal microscopy

Analysis of prepared slides was performed on a 780 AxioObserver.Z1 laser scanning confocal microscope with Argon and He/Ne 633 nm lasers. A Zeiss Plan-Apochromat 63x/1.4 NA oil lens was used, and excitation was performed with 405, 514, and 633 nm lasers in separated tracks. The pinhole size was kept unchanged during all measurements, and the line average was set to 8 for each channel. The microscope was kindly operated by Tamara Göbel.

### 4.8 Activity assays

#### 4.8.1 ACSL4 activity assay

ACSL4 activity was measured using an indirect activity assay system as described previously with few adaptations [31,280]. In brief, ACSL4 catalyzed formation of CoA thioesters from fatty acids is coupled by an ATP-dependent mechanism and an enzymatic cascade of pyruvate kinase, adenylate kinase, and lactate dehydrogenase to the oxidation of NADH to NAD<sup>+</sup>. The absorbance of NADH is then measured at 334 nm over time, and initial velocities can be determined.

Initial experiments were performed to verify the activity of the ACSL4 protein at different concentrations (1-43 µg/mL ACSL4) and after several days (1-16 days) of storage. The assay was performed in a 96-well format with 200 µL total volume per sample, and its composition is shown in Table 4.30. All components except CoA were premixed and incubated for 1 min at 37 °C using a Tecan infinite® M200 before the assay was started by the addition of CoA to a final concentration of 600 µM. Absorbance at 334 nm was measured over several minutes and compared to a control without ACSL4.

**Table 4.30: Initial setup for the verification of ACSL4 activity.**

<b>Assay component</b>	<b>Final concentrations</b>
Buffer A, pH 8.0	100 mM Tris/HCl, 15 mM MgCl <sub>2</sub> , 150 mM KCl
ATP	10 mM
DTT	5 mM
PEP-K	1 mM
NADH	0.3 mM
ARA	5 µM
Adenylate kinase	22.5 µg/mL
Pyruvate kinase	15 µg/mL
Lactate dehydrogenase	15 µg/mL
ACSL4	1-43 µg/mL
Ultra-pure water	Fill to 140 µL
CoA	600 µM
<b>Total volume</b>	<b>200 µL</b>

The frequency of the repeated absorbance measurements was dependent on the number of samples and thus was adjusted frequently at this point. To verify that the observed decrease in absorbance was due to the formation of ARA-CoA, product formation should be analyzed by UPLC-UV/MS. Furthermore, it had to be ensured that the product formation was catalyzed by ACSL4. For this purpose, additional samples were prepared that only contained the essential components (ATP, ARA, CoA, ACSL4). Since the absence of the unnecessary components prevented the analysis by NADH absorbance, samples were prepared in 1.5 mL tubes and incubated in a preheated thermos shaker. Samples were prepared as described before and, following the addition of CoA, incubated for 5 min at 37 °C. The assay was stopped by placing the tubes on ice. Then, samples were purified by solid phase extraction on C18 columns. Columns were conditioned with 3 mL acetonitrile followed by 3 mL ultra-pure water. Samples (200 µL) were diluted with 2 mL ultra-pure water and applied to the conditioned columns. Columns were washed with 3 mL ultra-pure water before elution was achieved with 500 µL elution buffer (50 mL ultra-pure water, 50 mL acetonitrile, 100 µL 28 % NH<sub>4</sub>OH, 5 µL formic acid) added in two portions. Each portion was incubated for 1 min on the column. Both elution fractions were combined, and 4 µL were applied to an Acquity UPLC H-class coupled to TUV and QDa detectors (operated in positive ESI mode) with an ACQUITY UPLC HSS T3 1.8 µm, 2.1 × 100 mm column. Separation was performed as described by Klett *et al.* [31] using a mixture composed of 1 mL 28 % NH<sub>4</sub>OH, 50 µL formic acid filled up to 1 L with ultra-pure water as mobile phase A and acetonitrile as mobile phase B. The column was equilibrated with 20 % B prior to the sample application. The conditions were held at 20 % B for 0.5 min before the ratio was increased to 40 % B over 3.5 min. The column was held at 40 % B for 2 min before the column was equilibrated again at 20 % B for 3 min. ARA-CoA eluted at 3.7 min and was detected using a single ion recording channel for the m/z value of [M+H]<sup>+</sup>: 1054.42 Da. Acquisition and analysis of product data were performed using the Empower 3 software. Controls without ACSL4 were prepared and treated identically.

**Table 4.31: Stock solutions for ACSL4 activity analysis.**

Stock	Preparation
2× Buffer A: 200 mM Tris/HCl, pH 8.0, 30 mM MgCl <sub>2</sub> , 300 mM KCl	24.23 g/L Tris, 6.1 mg/mL MgCl <sub>2</sub> , 22.37 g/L KCl in ultra-pure water, adjusted with conc. HCl to pH 8.0
400 mM ATP	220 mg/mL ATP in ultra-pure water, neutralized with 10 N NaOH
1 M DTT	150 mg/mL in ultra-pure water
40 mM PEP-K	8.24 mg/mL in ultra-pure water
10 mM NADH	7.1 mg/mL in 100 mM Tris/HCl, pH 8.2
4 mM CoA	3 mg/mL CoA in ultra-pure water, freshly prepared

Following the initial activity tests, the assay setup was adjusted for better comparability and reproducibility. For this purpose, stock solutions were prepared as described in Table 4.31 and stored at -20 °C (except for CoA). While only ARA was used as substrate during the

establishment of the assay, ARA and EPA were used for kinetic studies. Substrates were pre-diluted with 1 % (w/v) Triton X-100 solution to 1 mM before substrate mixes with varying concentrations were prepared according to Table 4.32.

**Table 4.32: Substrate mixes for ACSL4 activity analysis.**

Substrate mix concentration	Final assay concentration
0 $\mu\text{M}$	0 $\mu\text{M}$
35 $\mu\text{M}$	3.5 $\mu\text{M}$
70 $\mu\text{M}$	7 $\mu\text{M}$
100 $\mu\text{M}$	10 $\mu\text{M}$
350 $\mu\text{M}$	35 $\mu\text{M}$
700 $\mu\text{M}$	70 $\mu\text{M}$
1000 $\mu\text{M}$	100 $\mu\text{M}$

The final assay composition is given in Table 4.33. All components except the freshly prepared CoA solution were premixed, and 170  $\mu\text{L}$  per experiment were transferred to a 96-well plate. The plate was incubated at 37  $^{\circ}\text{C}$  for 1 min before 30  $\mu\text{L}$  of a 4 mM CoA solution was added using a Tecan infinite® M200 to start the reaction. The absorbance of NADH was measured at 334 nm in regular intervals of 9 or 10 s over 3-5 min. Initial velocities were determined using data points in the early linear range before saturation was reached.

**Table 4.33: Assay conditions for ACSL4 activity analysis.**

Assay component	Final concentrations
Buffer A, pH 8.0	100 mM Tris/HCl, 15 mM $\text{MgCl}_2$ , 150 mM KCl
ATP	10 mM
DTT	5 mM
PEP-K	1 mM
NADH	0.3 mM
Substrate	20 $\mu\text{L}$ of the respective substrate mix (see Table 4.32)
Adenylate kinase	45 $\mu\text{g}/\text{mL}$
Pyruvate kinase	30 $\mu\text{g}/\text{mL}$
Lactate dehydrogenase	30 $\mu\text{g}/\text{mL}$
ACSL4	0.1 $\mu\text{M}$ (= 7.42 $\mu\text{g}/\text{mL}$ )
Ultra-pure water	Fill to 170 $\mu\text{L}$
CoA	600 $\mu\text{M}$



In order to calculate proper kinetics, an NADH standard curve (0-0.7 mM in 0.1 mM steps) was prepared in buffer A, and absorbance at 334 nm was detected. The decrease in absorbance was correlated to the amount of NADH that underwent oxidation to NAD<sup>+</sup> and thus, the amount of substrate that was converted to its respective CoA thioester could be determined.  $K_m$  and  $V_{max}$  were calculated using the GraphPad Prism 7 software.

#### 4.8.2 LPCAT2 activity assay

HEK293T cells transfected to overexpress the LPCAT2 gene (HEK293T\_LPCAT2) were checked for enzyme activity in an LPCAT2 assay. Initial assay conditions were taken from a publication by Tarui *et al.* [104], but unfortunately, the assay did not yield product. Thus, several parameters were changed, and the protocol that finally led to product formation is described below.

Cells were harvested as described (4.6.2), and cell pellets were resuspended in ice-cold LPCAT2 lysis buffer (Table 4.34) supplemented with the EDTA-free protease inhibitor mix cComplete Mini. Cell suspensions were sonicated as described in 4.7.4, and the total protein amount of the lysates was determined by BCA (4.7.5). To determine the activity, 50 µg of total protein was diluted in 1 mL of LPCAT2 activity buffer (Table 4.34) and mixed with 5 µM of Lyso-PAF and 10 µM acetyl-CoA. Samples were incubated at 37 °C in a water bath for 5 min. Reactions were stopped by addition of 1 mL ice-cold MeOH and kept on ice until further purification. 30 µL of 1 N HCl solution was added to each vial, followed by 500 µL PBS and samples were centrifuged at 944 rcf for 10 min at RT. Supernatants were applied to C18 SPE columns (UCT clean-up® CEC 1811Z). Prior to use, columns were conditioned with 1 mL MeOH followed by 1 mL of ultra-pure water. Then, the supernatants of the assay were added, and the columns were washed with 1 mL of ultra-pure water and 1 mL of 25 % MeOH, successively. Elution was achieved by addition of 300 µL MeOH, and 120 µL of ultra-pure water was added. Eluted samples were centrifuged for 15 min at 18,000 rcf and 4 °C, and 50 µL were transferred into UPLC vials.

10 µL per purified sample were injected, and product analysis was performed on an Acquity UPLC H-class system coupled to TUV and QDa detectors (operated in positive ESI mode) with an ACQUITY UPLC BEH C8 1.7 µm, 2.1 × 100 mm column. Separation was achieved using a flow rate of 0.5 mL/min (column preheated to 40 °C) with linear gradient conditions given in Table 4.35. Products were detected and quantified using selected ion recording channels for the following m/z values: [M+H]<sup>+</sup> 524.0 (16:0-Ac-PAF), 768.6 (16:0-AA-PAF).

In addition, also recombinant LPCAT2 purifications were tested in this assay with varying amounts of protein.

**Table 4.34: HEK293T\_LPCAT2 buffers.**

LPCAT2 buffer	Composition
LPCAT2 lysis buffer	20 mM Tris, pH 7.4
LPCAT2 activity buffer	100 mM Tris, pH 7.4, 1 µM CaCl <sub>2</sub> , 0.015 % (v/v) Tween® 20

**Table 4.35: Separation program for LPCAT2 product analysis. The mobile phase consisted of: A: ultra-pure water, B: acetonitrile, C: methanol, D: 1 % aqueous acetic acid.**

Time [min]	%A	%B	%C	%D
Initial	18	20	57	5
1	14	16	65	5
2	0	0	95	5
7	0	0	95	5
9	18	20	57	5

The assay setup, extraction, and analysis were further improved by Yvonne Kaiser during her master's thesis (Kaiser 2023). For more information on the use of PUFA-CoAs, liquid-liquid extraction, SPE by C8 columns, and final analysis of 18:0-AA-PC, 18:0-EPA-PC, 18:0-15-HETE-PC, and 18:0-DHA-PC, please see her work entitled 'Establishment of a method for the quantification of human lysophosphatidylcholine acyltransferase 2 products via LC-MS'.

#### 4.8.3 Lipoxygenase activity assay

Cells were harvested using TE, washed once with 5 mL PBS and counted. The cell pellet was resuspended in PBS/glucose to a final concentration of  $5 \times 10^6$  cells/mL, and the cell suspension was kept on ice. 1 mL per sample was transferred into glass vials, 2.5  $\mu$ L of a 0.4 M  $\text{CaCl}_2$  solution was added (final concentration 1 mM, see Table 4.36 for all used solutions), and the respective vial was briefly shaken for a few seconds. A compound mix was prepared in advance, containing 2 mM ARA and 0.25 mM calcium ionophore A23187. To start the reaction, 10  $\mu$ L of the compound mix was added per vial (assay concentrations: 20  $\mu$ M ARA and 2.5  $\mu$ M Ionophore). The vial was shaken briefly and then incubated at 37 °C in a water bath. After 10 min, the reaction was stopped by the addition of 1 mL ice-cold MeOH, and the vial was put on ice.

**Table 4.36: Solutions used to determine lipoxygenase activity.**

Solutions	Description
$\text{Ca}^{2+}$ ionophore A23187 stock solution	2 mM in MeOH
AA stock solution	80 mM in EtOH
PBS/glucose	1 mg/mL glucose dissolved in PBS
Compound mix	2 mM AA, 0.25 mM $\text{Ca}^{2+}$ ionophore A23187

In preparation for the analysis by UPLC-MS, samples were purified as described before [281]. 30  $\mu$ L of 1 N HCl solution, 500  $\mu$ L PBS as well as 10  $\mu$ L PGB<sub>1</sub> (200 ng in 10  $\mu$ L) as internal standard were per well. Next, samples were centrifuged at 944 rcf and RT for 10 min, and subsequently, supernatants were transferred onto SPE C18 columns. Columns were conditioned in advance with 1 mL MeOH followed by 1 mL of ultra-pure water. Supernatants were added, and columns were washed with 1 mL of ultra-pure water and 1 mL of 25 % MeOH

successively. Finally, elution was achieved with 300  $\mu\text{L}$  MeOH, and 120  $\mu\text{L}$  of ultra-pure water was added. Prior to application, samples were centrifuged for 15 min at 18,000 rcf and 4 °C. Then, 50  $\mu\text{L}$  were transferred into UPLC vials, and 10  $\mu\text{L}$  were injected for analysis.

**Table 4.37: Separation program for lipoxygenase product analysis. The mobile phase consisted of A: ultra-pure water, B: acetonitrile, C: methanol, D: 1 % aqueous acetic acid.**

Time [min]	%A	%B	%C	%D
Initial	45	34	16	5
5.2	39	38.1	17.9	5
5.21	20	51	24	5
7.4	12.7	56	26.3	5

Product analysis was performed as described recently [282] on an Acquity UPLC H-class coupled to TUV and QDa detectors (operated in negative ESI mode) with an ACQUITY UPLC HSS T3 1.8  $\mu\text{m}$ , 2.1  $\times$  100 mm column. Separation was achieved using a flow rate of 0.5 mL/min (column preheated to 40 °C) with linear gradient conditions given in Table 4.37. PGB<sub>1</sub>, 6-trans-LTB<sub>4</sub>, 6-trans-12-epi-LTB<sub>4</sub>, and LTB<sub>4</sub> were detected at 280 nm and 335.2 Da, while 5-HETE, 12-HETE, and 15-HETE were detected at 235 nm and 319.2 Da, respectively. Acquisition, processing, and analysis of product data were performed using the Empower 3 software. Data were correlated to the number of cells used and presented as amount per  $1 \times 10^6$  or  $5 \times 10^6$  cells. Controls without cells were used to correct the determined data for non-enzymatic oxidation.

#### 4.8.4 PA-LOX activity assay

Purified PA-LOX was diluted to 7 nM in 25 mM HEPES, pH 6.5-7.5, 150 mM NaCl and 1 mL was transferred into a glass vial. Following the addition of 10  $\mu\text{M}$  ARA, the assay was incubated for 10 min at 37 °C in a water bath. Incubation was stopped by addition of 1 mL ice-cold MeOH, and samples were purified and analyzed as described in 4.8.3.

## 4.9 Thermal shift experiments

### 4.9.1 Buffer and salt screen

After the expression and purification of recombinant proteins, a stability screen was performed. Different conditions were tested in a thermal shift assay (TSA), including buffer systems, pH values, salt concentrations, and glycerol amounts in a 96-well format (qPCR plates on an iCycler Detection System or a StepOne™ Real-Time PCR System). For easier and faster handling, deep-well buffer plates (96-well), kindly provided by Dr. Steffen Brunst, were used. These contained a set of common buffers with twice the concentration (200 mM) to be tested. 20  $\mu\text{L}$  per condition per well were transferred to 96-well qPCR plates pre-cooled to 4 °C. Recombinant protein solutions were mixed with SYPRO™ Orange (SO) protein gel stain and diluted with ultra-pure water to a concentration of 10  $\mu\text{M}$  protein and 10 $\times$  SO. The addition of 20  $\mu\text{L}$  protein mix per well resulted in a final buffer concentration of 100 mM, a protein concentration of 5  $\mu\text{M}$ , and 5 $\times$  SO. The final plates contained 40  $\mu\text{L}$  total volume per well and

were sealed with transparent foil. Then, plates were incubated at 20 °C for 2 min before heating up to 89 °C either with 1 °C/min (iCycler) or 1 %/min (Stepone). Excitation was performed at 490 nm, and emission was measured at 570 nm. Samples within a plate were measured in triplicates, and, in general, two plates were measured to determine an accurate unfolding temperature  $T_m$ .

#### 4.9.2 Compound screen

For the investigation of a few organic compounds regarding their protein binding, a slightly changed setup was used. This time, a buffer that showed sufficient protein stability was used for all samples. If possible, the organic compound was also diluted in this buffer to twice the working concentration, and 20  $\mu$ L was transferred into a 96-well plate. The recombinant protein solution was mixed with SO as described in chapter 4.9.1, but buffer instead of ultra-pure water was used. 20  $\mu$ L protein mix was added to the respective compound or DMSO controls containing the same amount of solvent as the samples. Plates were sealed and measured as described above, and  $T_m$  values were analyzed compared to their DMSO controls.

#### 4.9.3 Fatty acid library screen

Screening of multiple organic compounds was performed using an internal fatty acid library (FAL) prepared by many current and former colleagues: Dr. Estel la Buscató, Nathalia Kolakowska-Pilipiak, Dr. René Blöcher, Khang Pau, Dr. Stefano Woltersdorf, Felix Knöll, Beatrice Renelt, Felix Zhu, Dr. Jurema Schmidt, Dr. Julius Pollinger, Dr. Simone Schierle, Dr. Victor Hernandez-Olmos, Ting Liu, Alexander Kaps, Rinusha Rajkumar, Dr. Pascal Heitel and Maximiliane Horz. The FAL contains 160 fatty acid mimetics with a concentration of 50 mM in DMSO. A list of all compounds included in the FAL and their respective Smiles codes can be found in appendix Table 9.8.

Compounds were diluted in DMSO to a concentration of 5 mM, and 0.8  $\mu$ L were transferred per well in a 96-well plate. A mixture of purified protein, SO, and TX-100 was added to a final volume of 40  $\mu$ L (final concentrations: 5  $\mu$ M protein, 10  $\mu$ M compound, 5 $\times$  SO, 0.01 % TX-100). The FAL compounds were measured in two separate plates in single-point experiments. To get appropriate data, the measurement of each plate was repeated, and only compounds that showed effects both times were considered hits.

#### 4.9.4 Prestwick drug fragment library screen

Screening of a large array of small organic compounds was performed using a commercially available drug library from Prestwick Chemical Libraries®. The screen contained 480 small molecules that were obtained through fragmentation of 1500 approved drugs. The term 'small molecules' refers to a molecular weight of less than 300 Da. All compounds included in this screen were obtained with a purity of over 95 % and are soluble in DMSO and PBS with at least 100 mM and 1 mM, respectively. A list with all drug fragments and their respective Smiles codes can be found in the appendix Table 9.9.

Drug fragments were diluted in DMSO to a concentration of 25 mM, and 0.8  $\mu$ L were transferred per well in 96-well plates with control wells containing only DMSO. Then, 39.2  $\mu$ L of a mix containing the purified protein, SO and Triton X-100 were added to a final

concentration of 5  $\mu\text{M}$  purified protein, 5 $\times$  SO, 500  $\mu\text{M}$  compound, and 0.01 % (w/v) TX-100. Since the library design allowed only single-point experiments within a plate, a second plate was measured to verify the outcome. The whole library consists of six 96-well plates, and only drug fragments that showed effects in repeated measurements were considered hits.

#### 4.9.5 Prestwick approved drug library screen

Approved drugs were also screened using a commercially available library from Prestwick Chemical Libraries®. This library contained over 1200 drugs that included a variety of therapeutic classes such as oncology, dermatology, metabolism, and many more. A list of all drugs and their respective Smiles codes can be found in the appendix Table 9.10.

The library was screened in 384-well format with seven plates in total. Plates that already contained the respective compounds were kindly prepared by Dr. Benedict-Tilman Berger and Lewis Elson. Since compounds were aliquoted in a volume of 20 nL, the volume was neglected, and 10  $\mu\text{L}$  of a mixture containing 5  $\mu\text{M}$  purified protein, 5 $\times$  SO, and 0.01 % (w/v) TX-100 were added per well. The final drug concentration was 10  $\mu\text{M}$ , and each compound was measured in duplicates. Plates were measured on a QuantStudio5 device and analyzed with the QuantStudio Design & Analysis Software. Compounds that were chosen for further analysis were measured again in multiple concentrations, as described in chapter 4.9.2.

#### 4.10 Statistics

If not stated otherwise, data are presented as mean + (or  $\pm$ ) standard deviation (SD) of three independent experiments.

Western blot quantifications were correlated to the respective housekeeping gene and normalized on vector control cells. Statistical analysis was then performed using an unpaired t-test with Welch's correction against vector controls. \*  $P < 0.05$ .

Cell viability and oxylipin data were statistically analyzed using 2-way ANOVA with Dunnett's multiple comparisons test. \*  $P < 0.05$ , \*\*  $P < 0.01$ , \*\*\*  $P < 0.001$ .

Significance was determined using the GraphPadPrism7 software (Table 4.16).

## 5 Results

Biosynthesis of esterified lipids is achieved either by *de novo* synthesis, known as the Kennedy pathway, or in the remodeling process referred to as Lands' cycle. The *de novo* synthesis requires a huge variety of enzymes, while the remodeling part is performed by only two enzyme classes: Acyl-CoA synthetases and lysophosphatidylcholine acyltransferases. Although both of these enzyme families consist of multiple members, the enzymes ACSL4 and LPCAT2 were chosen due to their broad substrate acceptance and their prominent expression in leukocytes. In addition, it was investigated whether lipoxygenases are suitable to extend the product spectrum to oxidized lipids, known as oxylipins.

Chapter 5.1 will cover a biosynthetic approach utilizing recombinant enzymes expressed in *E. coli*, while chapters 5.2 and 5.3 will demonstrate an approach using a HEK293T-based overexpression system.

### 5.1 Investigation of a biosynthetic approach for the formation of esterified lipid mediators using recombinant enzymes

#### 5.1.1 Expression and purification of human ACSL4 from *E. coli*

In 2017, Klett *et al.* published the expression and purification of a rat ACSL4 construct in *E. coli* DH5 $\alpha$  utilizing a C-terminal FLAG-tag [31]. They performed activity studies with substrates that differed in chain length and also tested different HETEs and EETs. Thus, they provided evidence that a modification at the C-terminus does not inhibit the enzyme's activity and that the enzyme has a broad substrate spectrum. As the aim of this thesis was the formation of esterified lipid mediators relevant in humans, the human ACSL4 enzyme was used instead of the rat variant. Human ACSL4 is known to occur in two transcripts produced by alternative splicing [56]. ACSL4 version 1 (ACSL4V1) is the main transcript found in most cells, while the second version (ACSL4V2) is located in the brain. The two variants differ in size due to an additional 41 amino acids at the N-terminus of ACSL4V2 [55]. Although there is no protein structure available today, sequence predictions suggest that the additional peptide sequence contains a hydrophobic region that is associated with membrane binding [56]. Therefore, ACSL4V1 was expected to be better soluble than ACSL4V2, which typically goes along with higher yields and an easier purification. Thus, constructs (Table 5.1) based on the shorter isoform ACSL4V1, hereafter only referred to as ACSL4, with approx. 75 kDa in size were prepared as described in chapter 4.2.2.

In the first step, recombinant expression from *E. coli* BL21(De3) cells and subsequent purification were tested. For this purpose, different constructs containing either a StrepII-tag (Trp-Ser-His-Pro-Gln-Phe-Glu-Lys) or His6x-tag (His-His-His-His-His-His) sequence at the C-terminus were prepared. Purification of cell lysates was either tested on a gravity flow column (ATP-Agarose, self-prepared, CV=5 mL, Sigma) or using an automated ÄKTA Purifier System, hereafter referred to as ÄKTA, in combination with StrepTactinXT (CV=1 mL, IBA) or Ni-Sephrose (HisTrap™ HP CV=1 mL or 5 mL, GE or Cytiva) matrices.

Table 5.1: Specifications of recombinant ACSL4 expression constructs.

Plasmids	Specifications
pBJ01_ACSL4_StrepII	Backbone: pET24a(+), bacterial resistance: kanamycin, expression control: lacO, promoter: T7, MCS: ACSL4 gene (short isoform 42-711 aa), N-terminus: untagged (original T7-tag removed), C-terminus: StrepII-tag
pBJ03_ACSL4_His6x	Backbone: pET24a(+), bacterial resistance: kanamycin, expression control: lacO, promoter: T7, MCS: ACSL4 gene (short isoform 42-711 aa), N-terminus: untagged (original T7-tag removed), C-terminus: His6x-tag

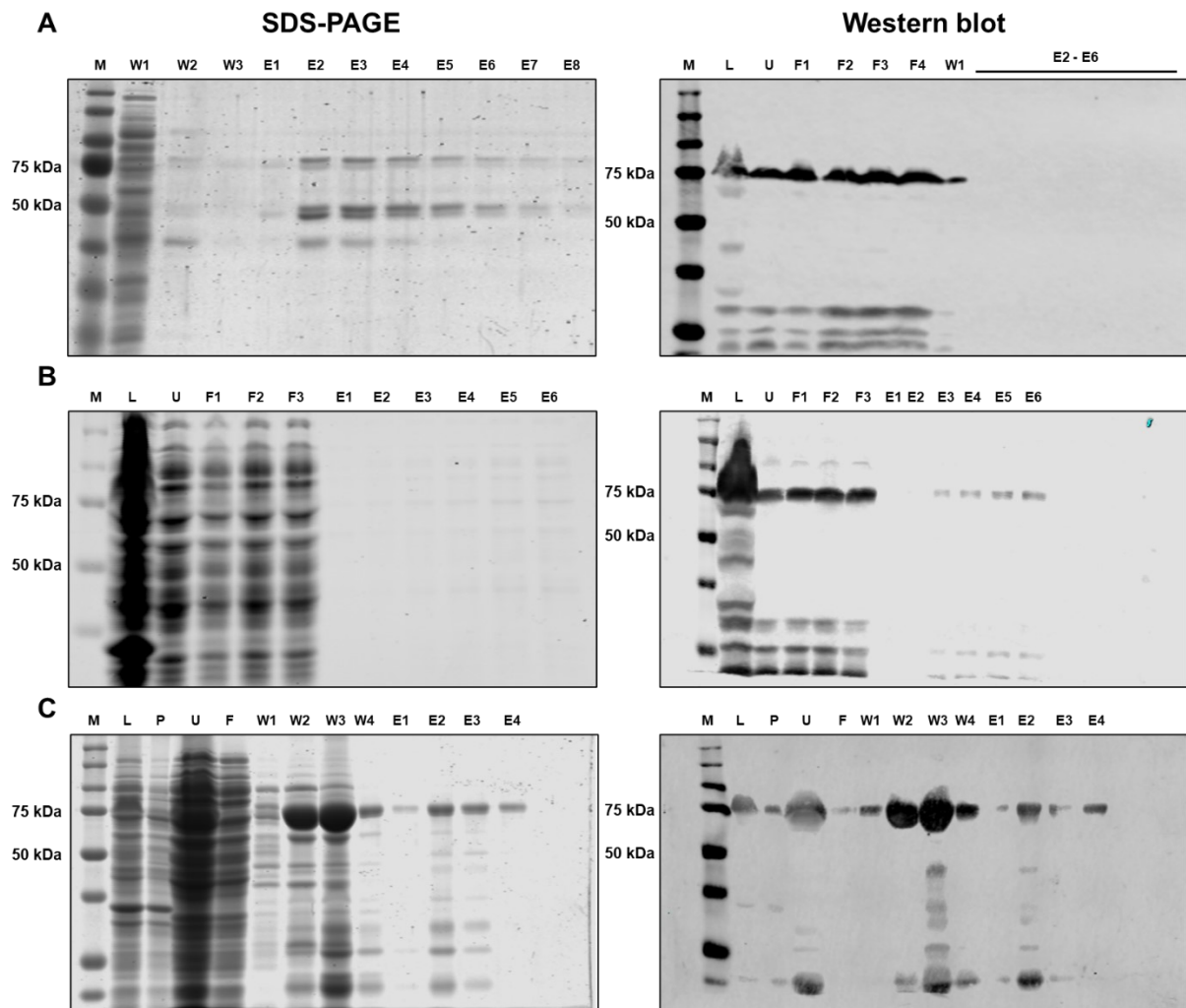


Figure 5.1: Initial expression and purification experiments of different ACSL4 constructs.

Three approaches were tested for purification: ATP-Agarose via the ATP-binding site of ACSL4 (A), C-terminal StrepII-tag with Strep-TactinXT™ column (B), and C-terminal His6x-tag with Ni-Sepharose column (C). Purification fractions were analyzed by SDS-PAGE and coomassie brilliant blue staining (left) or Western blot (right). M: Protein marker, L: Lysate (soluble part of homogenized cells), P: Pellet (insoluble part of homogenized cells), U: Soluble part after 100,000 rcf centrifugation, F: Flow-through, W: Wash fraction, E: Elution fraction. If multiple samples of the same step were collected, the different fractions are indicated with numbers. The same sample volumes were applied per SDS-PAGE or Western blot.

The results of the initial expressions and purifications are shown in Figure 5.1. All constructs were expressed in 500 mL cultures of *E. coli* BL21(De3) cells using 0.25 mM IPTG, which

resulted in protein formation as shown by SDS-PAGE. Once the cell lysates were applied to the respective column, a washing step was performed prior to the elution. The buffer systems used for the wash and elution steps of Figure 5.1 are shown in Table 5.2.

**Table 5.2: Matrices and buffer compositions of initial ACSL4 purification attempts.**

<b>Matrices</b>	<b>Wash buffer</b>	<b>Elution buffer</b>
ATP-Agarose	50 mM PBS, pH 7.4, 1 mM EDTA	50 mM PBS, pH 7.4, 1 mM EDTA, 20 mM ATP
Strep-TactinXT™	20 mM TEA, pH 8.0, 150 mM NaCl, 5 mM EDTA	20 mM TEA, pH 8.0, 150 mM NaCl, 5 mM EDTA, 64 mM biotin
HisTrap™ HP	20 mM NaPi, pH 7.4, 200 mM NaCl, 10 % (v/v) glycerol, 1 % (w/v) Triton X-100, 40 mM imidazole	20 mM NaPi, pH 7.4, 200 mM NaCl, 10 % (v/v) glycerol, 1 % (w/v) Triton X-100, 300 mM imidazole

In addition, the identity of ACSL4 was verified by Western blotting. Purification utilizing the ATP-binding affinity of ACSL4 (Figure 5.1A) showed small bands at the expected protein size of 75 kDa on SDS-PAGE. However, when analyzed with specific antibodies, the protein was found in the flow-through, indicating that the protein either did not bind to the ATP-Agarose matrix or only in vanishingly low amounts. The next attempt included the C-terminal StrepII-tagged ACSL4 construct (ACSL4\_StrepII) and a StrepTactinXT matrix (Figure 5.1B). Purification revealed no bands following elution on SDS-PAGE, and indeed, Western blot analysis verified that the majority of the protein was lost in the flow-through with only minor protein bands in elution fractions E3-E6. Next, expression of the His6x-tagged protein (ACSL4\_His6x) was tested and revealed large amounts of protein on SDS-PAGE, although the majority was found in washing fractions W2 and W3 (Figure 5.1C). Nevertheless, protein that stuck to the column during the washing procedure was successfully eluted afterward and displayed bands visible already on SDS-PAGE. Western blot analysis confirmed that both the eluted protein bands and the large ones of the washing fractions belonged to ACSL4\_His6x. Furthermore, the flow-through showed only a minor protein band, indicating that the interaction of the His6x-tagged protein with the Ni-Sepharose matrix was clearly stronger than the ones tested before. Taken together, the purification attempt using ACSL4\_His6x and the Ni-Sepharose matrix was the only one that showed a decent binding behavior. Although a huge amount of protein was lost during the washing procedure, there was nearly no protein lost during the application, contrary to the ATP-Agarose and StrepTactinXT approaches. Thus, the expression of ACSL4\_His6x purified on Ni-Sepharose was chosen for further optimization.

### 5.1.2 Optimization of ACSL4\_His6x purification and yield

Because the respective SDS-PAGE analysis revealed large ACSL4 bands, the yield was expected to be sufficient for follow-up experiments. However, the majority of the protein was found within the washing fractions, which is why an improved purification procedure had to be established. To improve column binding and reduce protein loss during the washing procedure, several conditions were tested, as listed in Table 5.3.



**Table 5.3: Buffer conditions tested for optimization of ACSL4\_His6x purification.**

For each test, three buffers with varying imidazole concentrations were prepared: One for the application of the protein to the column, one to wash off unspecific bound proteins, and one to elute the pure protein.

Test	Conditions	Application	Washing	Elution
1	20 mM NaPi, pH 7.4, 200 mM NaCl, 10 % (v/v) glycerol, 1 % (w/v) Triton X-100	20 mM imidazole	40 mM imidazole	300 mM imidazole
2	20 mM NaPi, pH 7.4, 200 mM NaCl, 10 % (v/v) glycerol, 0.1 % (w/v) Triton X-100	20 mM imidazole	40 mM imidazole	300 mM imidazole
3	20 mM NaPi, pH 7.4, 200 mM NaCl, 10 % (v/v) glycerol	20 mM imidazole	50 mM imidazole	300 mM imidazole
4	20 mM NaPi, pH 7.4, 200 mM NaCl, 1 mM DTT, 10 % (v/v) glycerol	10 mM imidazole	30 mM imidazole	300 mM imidazole
5	20 mM NaPi, pH 7.4, 200 mM NaCl, 1 mM DTT, 10 % (v/v) glycerol	10 mM imidazole	30 mM imidazole	300 mM imidazole
6	20 mM NaPi, pH 7.4, 200 mM NaCl, 1 mM DTT, 5 % (v/v) glycerol	10 mM imidazole	30 mM imidazole	300 mM imidazole

Protein purification was performed with each set of modified buffers, and the resulting SDS-PAGE analysis is shown in Figure 5.2. The conditions of the initial Ni-affinity chromatography trial (Figure 5.1) were used as starting conditions (Figure 5.2A). Test condition 2 (Figure 5.2B) had a reduced detergent concentration of only 0.1 % Triton X-100 (TX-100), which directly resulted in stronger column binding. Although some smaller bands were visible in the elution fractions E2 and E3, the major bands were derived from ACSL4. In an attempt to increase the protein purity, test condition 3 (Figure 5.2C) had a slightly increased imidazole concentration of 50 mM during the washing step. Moreover, this purification was performed in the absence of TX-100 to further increase the protein binding. Unfortunately, protein binding was heavily weakened, and a protein band was barely visible following the elution. In order to increase the binding again, the imidazole concentrations during protein application and washing were reduced to 10 mM and 30 mM, respectively. In addition, DTT was added to each buffer used. As a result, the amount of ACSL4 lost during the washing procedure was reduced, and protein elution was clearly visible (Figure 5.2 Test D). However, using the recommended purification protocol of the HisTrap™ HP column, elution was achieved over several fractions instead of one sharp peak.

Thus, imidazole concentrations of wash (30 mM) and elution (300 mM) buffers were kept the same, but the amount of wash and elution buffer as well as the volume of the elution fractions, was adjusted. As a result, the first few lanes of Figure 5.2E were similar to the ones of Figure 5.2D, but the modification of the protocol led to protein elution within one defined peak (Figure 5.2E, lane E2). Containing 10 % (v/v) glycerol, the previously mentioned buffer systems were quite viscous, which prevented the use of high flow rates leading to longer purification times. Therefore, the amount of glycerol in Figure 5.2F was cut in half to check whether this would affect protein stability.

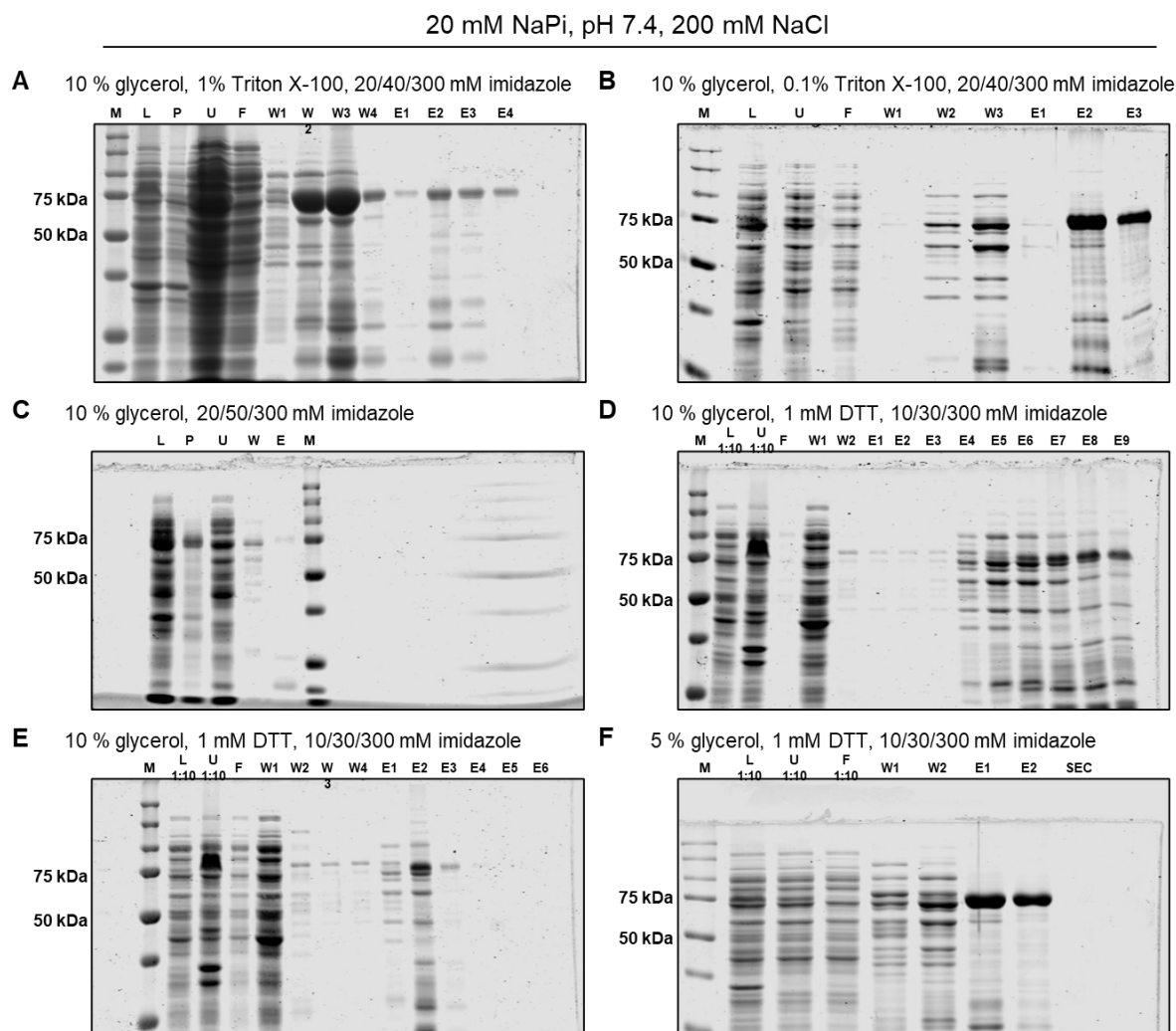


**Figure 5.2: Protein expression and purification of ACSL4\_His6x using different conditions.**

Protein expression was analyzed via SDS-PAGE, stained with coomassie brilliant blue solution. A to F refer to the buffer compositions of Table 5.3. The basic buffer composition is shown on top, and the differences between the buffers are displayed above each gel with imidazole concentrations given as application/wash/elution buffer. M: Protein marker, L: Lysate (soluble part of homogenized cells), P: Pellet (insoluble part of homogenized cells), U: Soluble part after 100,000 rcf centrifugation, F: Flow-through, W: Wash fraction, E: Elution fraction, SEC: Sample after size exclusion chromatography. If multiple samples of the same step were collected, the different fractions are indicated with numbers. The same sample volumes were applied per SDS-PAGE. Samples that were diluted 1:10 are indicated as such.

Fortunately, the reduced amount of glycerol did not affect the run in any way, which enabled increased flow rates and thereby reduced the overall purification duration. Buffer conditions 6 (Table 5.3) were used for all further expression and purification experiments of ACSL4, and the finalized ÄKTA purification method can be found in appendix chapter 9.3.1. Figure 5.3 displays representative chromatograms of the ACSL\_His6x purification via HisTrap™ HP and subsequent HiTrapDesalting columns. Although the purification of His6x-tagged ACSL4 could be optimized in terms of protein binding and elution behavior, the purity was not sufficient. Since the interaction of matrix and protein is mediated through successive histidine residues, other proteins that contain multiple histidine residues might bind as well. To further improve the purity of ACSL4, a second purification step had to be established.

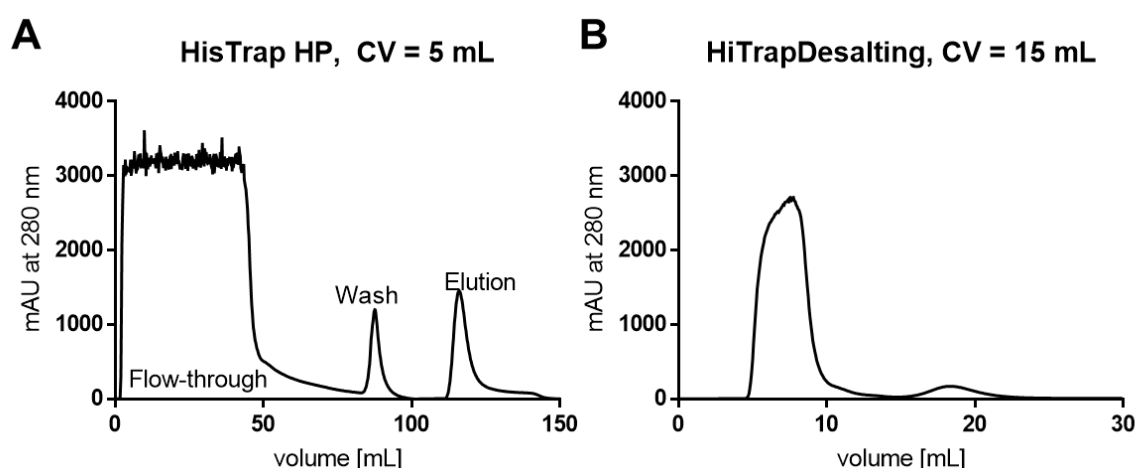


**Figure 5.3: Representative chromatograms of His6x-tagged ACSL4 purification using a 5 mL HisTrap™ HP column (A) and three consecutive 5 mL HiTrapDesalting columns (B).**

The ends of each chromatogram were cut off for better visibility.

Prior to the second purification step, buffer exchange was performed using three consecutive 5 mL HiTrapDesalting columns (Figure 5.3B). Thereby, the total CV was increased to 15 mL, which allowed the application of up to 5 mL of the previously eluted protein solution. Since the purification of one 500 mL expression culture typically resulted in 5 mL of eluted protein solution, the purification process was continued without delay. The small-scale size exclusion chromatography (SEC) removed unwanted low molecular weight components such as imidazole from the purified protein. The obtained protein solution was concentrated using centrifugation filter units until the volume did not exceed 5 mL. Then, the purified protein was used for experiments or another round of purification.

For an initial test run, the elution fractions of the Ni-affinity chromatography of ACSL4\_His6x were combined and used directly for SEC (Figure 5.4). Later on, a buffer exchange, as described before, was performed to obtain the protein solution in SEC buffer (20 mM NaPi, pH 7.4, 200 mM NaCl, 0.1 % (w/v) Triton X-100, 5 % (v/v) glycerol). Figure 5.4A shows the ÄKTA chromatograms of the Ni-affinity chromatography (left) and the SEC run (right). Below, the respective SDS-PAGE analyses of each run are shown (Figure 5.4B). Especially elution fraction 2 (E2) of the HisTrap™ HP column revealed a proper purity. Nevertheless, all fractions of the elution peak were combined, and up to 5 mL were applied to the SEC column.

The chromatogram of the SEC run revealed a small initial peak (A6/7) and a larger protein peak (A9/10). The drop in absorbance at 280 nm right after the large peak was presumably caused by a lack of detergent since the proteins' buffer in this specific test run was not exchanged beforehand. The respective analysis on protein level clearly showed that the ACSL4\_His6x protein was eluted within the larger peak and that the protein bands of the smaller impurities were gone (purity >95 %). Following the SEC, elution fractions A6/7 and A9/10 were concentrated separately. Surprisingly, the filter units used for the concentration step did not lead to an increase in protein concentration. Therefore, the flow-through (F) and the concentrate (C) were analyzed on SDS-PAGE and revealed that, indeed, the majority of

the protein was found within the flow-through. Luckily, the exchange of the 30 kDa MWCO filter units for 10 kDa filters was able to solve the issue.

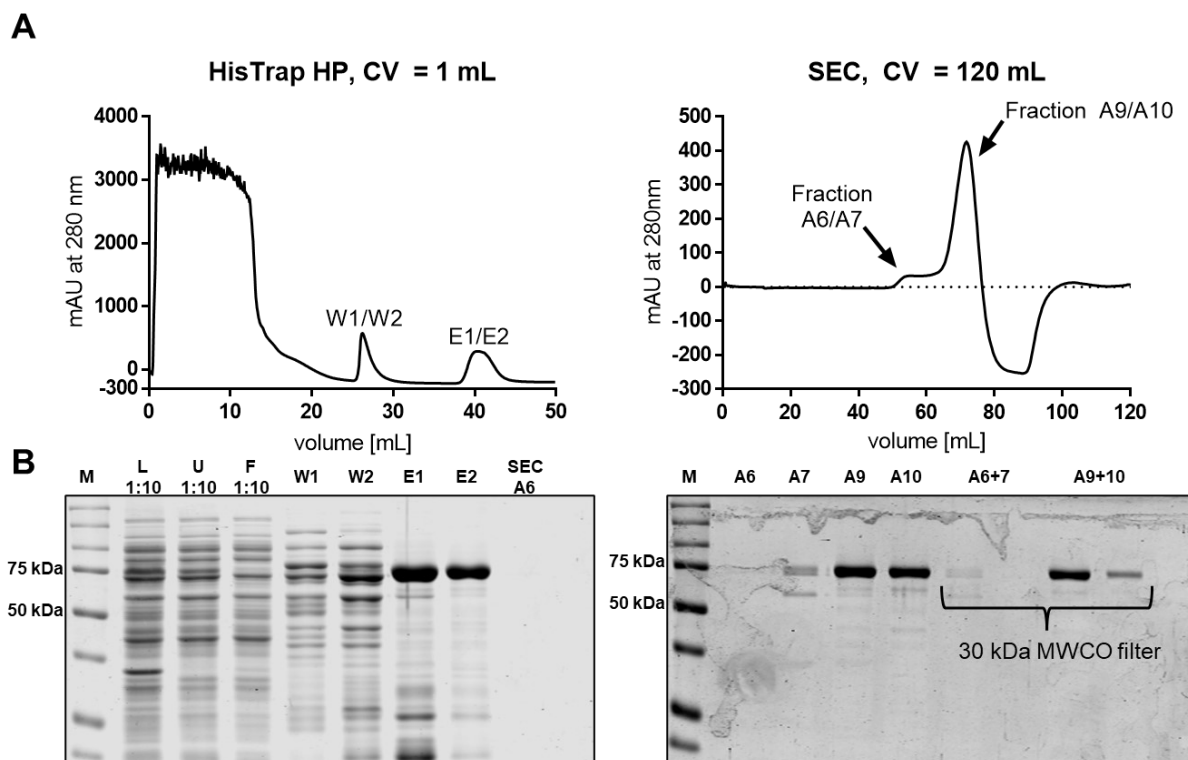


**Figure 5.4: ACSL4\_His6x purification by Ni-affinity chromatography and SEC.**

(A): Chromatograms of the initial purification via HisTrap™ HP column (CV=1 mL) (left) and the subsequent SEC (HiLoad™ 16/60 Superdex™ 200 pg, CV=120 mL) run (right). The ends of each chromatogram were cut off for better visibility. (B): SDS-PAGE analysis of both runs. Specific fractions are indicated within the respective chromatograms. L: Lysate (soluble part of homogenized cells), U: Soluble part after 100,000 rcf centrifugation, F: Flow-through, W: Wash fraction, E: Elution fraction, SEC: Sample after size exclusion chromatography. If multiple samples of the same step were collected, the different fractions are indicated with numbers. The same sample volumes were applied per SDS-PAGE. Samples that were diluted 1:10 are indicated as such.

In addition to the SEC conditions used for the shown run, buffers with lower detergent amounts were tested next (Figure 5.5) to check whether this would affect protein stability. Furthermore, the buffers of all protein solutions were exchanged to the respective SEC buffer before the SEC was performed. Without detergent, the protein eluted in a broad peak after 45 mL (black), indicating protein aggregation. The addition of TX-100 shifted the peak in a concentration-dependent manner to later retention times. While the lowest concentration (0.001 %, blue) only led to a shift of 1 mL, addition of 0.1 % TX-100 (purple) resulted in a shift of around 20 mL. Consequently, the addition of 0.01 % TX-100 resulted in a shift of nearly 10 mL (green). The different retention times indicated the presence of several species, such as protein aggregates (black and blue) but also potentially folded protein (green and purple). Thus, proper folding of the purified ACSL4\_His6x protein was tested by thermal shift experiments, as will be described in chapter 5.1.3.

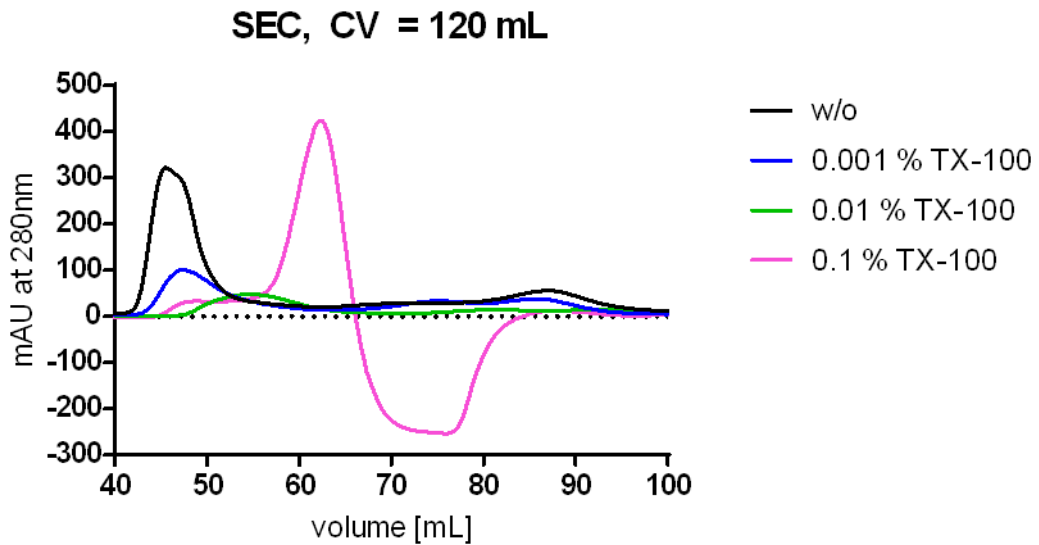


**Figure 5.5: Effect of different Triton X-100 concentrations on the purification of ACSL4\_His6x by SEC.**

SEC was performed in 20 mM NaPi, pH 7.4, 200 mM NaCl, 5 % glycerol, and varying concentrations of Triton X-100 (TX-100) as indicated. Chromatograms were cropped for better visualization of the respective peaks.

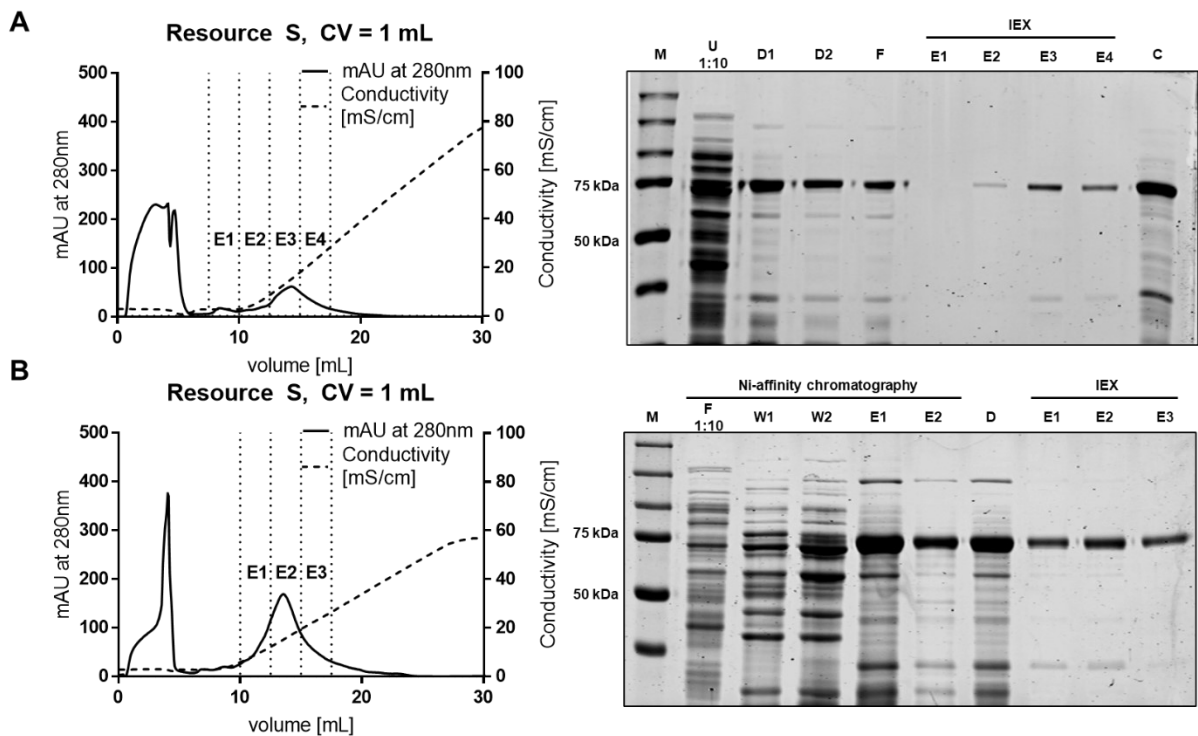


**Figure 5.6: ACSL4\_His6x purification by cation exchange chromatography.**

(A): Cation exchange chromatogram (Resource S, CV=1 mL) of the initial purification run using the recommended settings of the columns' manufacturer (left) and the respective analysis on protein level (right). (B): Cation exchange chromatogram (Resource S, CV=1 mL) of ACSL4\_His6x purification using decreased flow rates (left) and analysis on protein level (right). M: Protein marker, U: Soluble fraction after 100,00 rcf centrifugation, D: Desalted fraction, F: Flow-through, E: Elution fractions, C: Concentrate of final protein solution. Samples diluted 1:10 prior to application are indicated as such. Multiple fractions of the same step are indicated by digits. IEX fractions used for analysis are indicated.

An alternative approach to purify proteins was to utilize the isoelectric point in an ion exchange chromatography. Prediction of the isoelectric point of ACSL4\_His6x based on the amino acid sequence resulted in a value of 8.04 (predicted using the Geneious R10 software, Table 4.16). Thus, cation exchange chromatography, which will be referred to as IEX hereafter, was established. The application of an IEX required the use of low salt buffers since the elution was performed with sodium chloride. Thus, in the first trial run, the elution buffer of the Ni-affinity chromatography was exchanged for IEX buffer A (20 mM NaP<sub>i</sub>, pH 7.4). To elute the protein from the column, IEX buffer B (20 mM NaP<sub>i</sub>, pH 7.4, 1 M NaCl) was prepared. Up to 5 mL of protein solution was applied to the column, and elution was achieved using a linear gradient of both buffers. The increase in NaCl concentration eventually resulted in the elution of the protein in one large peak (Figure 5.6). Elution was achieved when the conductivity reached 15.1 mS/cm at 32 % of IEX buffer B (Figure 5.6A) or 15.2 mS/cm at 28 % of IEX buffer B (Figure 5.6B). Thus, the protein was eluted at a concentration of 280-320 mM NaCl.

The protein content of each fraction indicated below the chromatogram was analyzed by SDS-PAGE. Following buffer exchange to the low salt buffer, a strong ACSL4 band, as well as some smaller bands, were visible (Figure 5.6A, right). The flow-through of the IEX column revealed that a good proportion of the protein did not bind to the column, but the part that did was eluted afterward. IEX elution samples 2-4 (Figure 5.6A, E1-4) showed a good purity with only one visible impurity, slightly below the 37 kDa marker band. The IEX purification technique was shown to yield ACSL4\_His6x with a purity of 91 %, but a large proportion of the protein was lost in the flow-through. Therefore, the flow rate during sample application was lowered from 4 mL/min to 0.5 mL/min to enable a better protein-matrix interaction, and the general flow rate was adjusted to 2 mL/min from 4 mL/min. The respective changes in the flow rate were already visible in the chromatogram (Figure 5.6B, left) since the elution peak-to-flow-through ratio was increased. The following analysis on protein level revealed that the purity was slightly improved from 91 % to 95 % (Figure 5.6B, right). Finally, the pure protein was obtained in a yield of 2.1 mg protein per liter culture.

### 5.1.3 Stability studies on purified recombinant ACSL4\_His6x protein

The stability of the purified protein was tested using thermal shift analysis (TSA). Protein samples purified by Ni-affinity chromatography (Figure 5.7A) or Ni-affinity chromatography with subsequent SEC (Figure 5.7B) were compared. For the first analysis, two buffer systems were chosen: Sodium phosphate (NaP<sub>i</sub>) and Tris. This decision was made based on the already established purification using NaP<sub>i</sub> buffers and a published activity assay in 100 mM Tris that should be performed later on [31,280]. Following Ni-affinity chromatography, ACSL4\_His6x showed increased stability at higher pH values in 100 mM Tris buffers (Figure 5.7A, left). The addition of TX-100 had no effect at the lowest concentration but reduced the stability at higher concentrations. In fact, the addition of detergent caused problems in the analysis of the melting curves and prevented the evaluation of the sample with 0.1 % (w/v) TX-100. The same protein samples were tested in NaP<sub>i</sub> buffers (Figure 5.7A, right). Here, protein stability was nearly unaffected by changes in the pH value, but addition of detergent again led to decreased melting temperatures ( $T_m$ ).

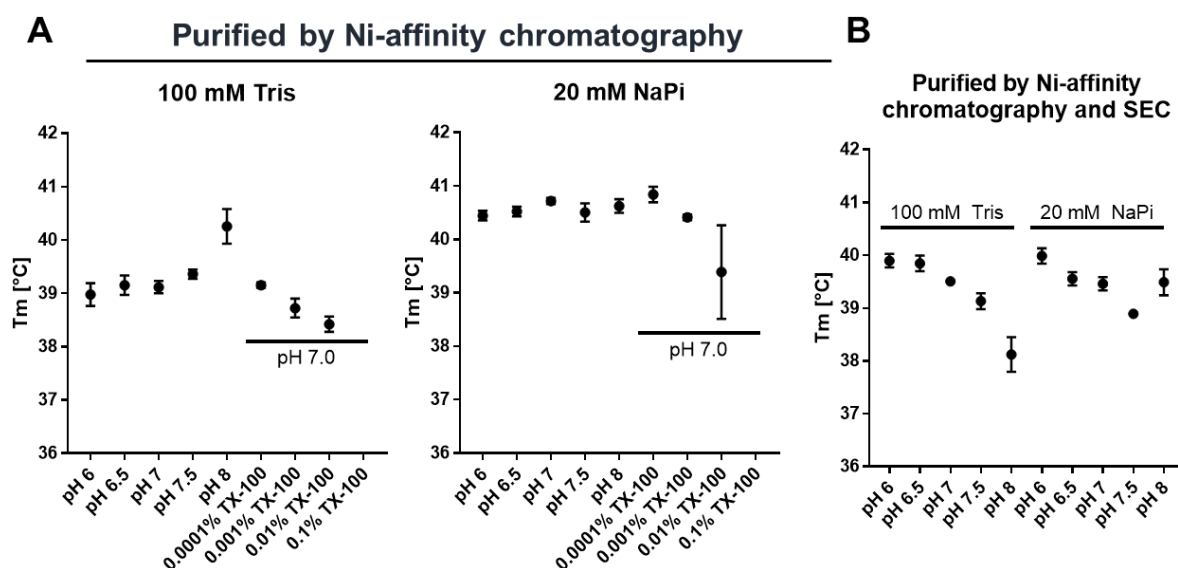


**Figure 5.7: Thermal shift analysis of ACSL4\_His6x protein purified by Ni-affinity chromatography or Ni-affinity chromatography with subsequent SEC.**

Protein stability was tested following Ni-affinity chromatography (A) in 100 mM Tris buffers (left) or sodium phosphate (NaPi) buffers (right). pH values were varied, as well as the Triton X-100 (TX-100) concentration. Samples were measured in triplicates in two independent experiments, and values are displayed as mean  $\pm$  SD. Samples with 0.1 % TX-100 were not evaluable. Stability was also tested following Ni-affinity chromatography and subsequent SEC (B). The same buffer systems as shown in (A) were tested, excluding the TX-100 samples. Values display mean  $\pm$  SD of triplicates.

Next, protein stability following Ni-affinity chromatography and subsequent SEC was tested (Figure 5.7B). Interestingly, the  $T_m$  in both buffer systems was reduced at higher pH values. The clear difference between both protein fractions was the protein purity. Thus, the presence of other proteins might have stabilizing effects on the ACSL4\_His6x protein, probably explaining why the stability of the pure protein was decreased. The addition of detergent was not tested in SEC samples due to the already observed decreases in  $T_m$  in Ni-affinity chromatography samples (Figure 5.7A). Overall, the preparation and analysis of SEC samples were quite troublesome. As shown before (Figure 5.5), SEC of ACSL4\_His6x in the absence of detergent led to a broad peak which eluted early, probably indicating protein aggregation. The addition of TX-100 seemed to favor protein folding, and thus, the protein used for stability experiments was purified using a TX-100 containing SEC buffer. Since the thermal shift data indicated a destabilizing effect of the detergent, this might explain the lower unfolding temperatures following SEC. Repetition of the experiments with freshly purified protein did not lead to further data since the melting curves obtained were not evaluable.

Thus, the purification procedure was shifted from SEC to IEX. Here, expression experiments revealed that the purification did not require any detergent while yielding the protein with a purity of 95 %. Consequently, stability analysis was performed, but this time a larger set of buffer systems was included, as shown in Figure 5.8.

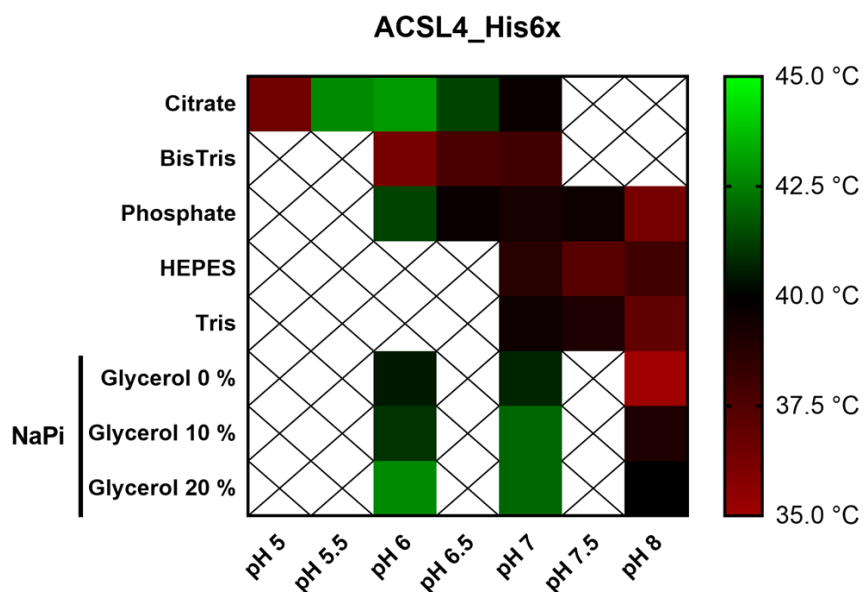


**Figure 5.8: Heatmap of ACSL4\_His6x unfolding temperatures.**

All buffer systems were used at 100 mM. Colors indicate the unfolding temperature ranging from 35 °C (light red) to 45 °C (light green). Crossed-out conditions were not tested. Samples were measured in triplicates. NaPi: Sodium phosphate.

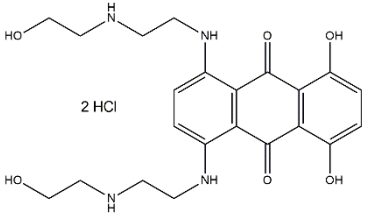
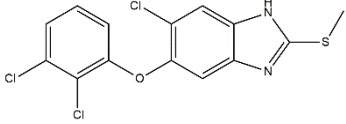
The highest  $T_m$  was found in citrate buffer at pH 6 with 43 °C. In addition, citrate buffer at pH 5.5 and NaPi buffer at pH 6 containing 20 % (v/v) glycerol were only slightly behind at 42.7 °C each. A comparison of all conditions indicated that the protein stability seemed to increase with lower pH until a value of 6 was reached. These findings were in accordance with the previously found results of the stability analysis following SEC purification (Figure 5.7B). Both methods indicate that the pure protein displays enhanced stability at pH 6. The buffer screen also revealed that the addition of glycerol led to a clear improvement in stability. However, with increasing amounts of glycerol, the viscosity also increased, which might cause problems at higher flow rates during the purification procedure. Thus, purification buffers were supplemented with only 5 % (v/v) glycerol in order to enable a fast purification.

### 5.1.3.1 Investigation of the protein-drug interaction of ACSL4\_His6x

Once a proper folding of the ACSL4\_His6x protein was verified by TSA investigations, the same technique was used to screen a Prestwick drug library. ACSL4 is involved in several pathophysiological processes and is even used as a biomarker in some types of cancer. Thus, the identification of a new ACSL4 inhibitor might offer new therapeutic options. The library contained 1280 drugs from multiple therapeutic classes, such as oncology, dermatology, and infectiology, that are, with few exceptions, approved by FDA or EMA. Because of the large number of compounds within the library, the screen was performed in single-point experiments and repeated once. In order to prevent false positive results, only compounds that showed similar effects in both screens were considered hits. 15 drugs were identified that increased the unfolding temperature in one of two experiments, but only 2 compounds had effects in both experiments (Table 5.4).



**Table 5.4:** Approved drug library hits that increased the unfolding temperature of ACSL4 by more than 1 °C compared to DMSO controls. 5 µM protein was incubated with 20 µM compound.

	<b>Mitoxantrone dihydrochloride Prestw-Frag-0674</b>	<b>Triclabendazole Prestw-Frag-1165</b>
<b>ΔT [°C]</b>	<b>1.01 ± 0.30</b>	<b>6.99 ± 0.67</b>
<b>Structure</b>		
<b>Therapeutic class</b>	oncology	infectiology
<b>CAS</b>	70476-82-3	68786-66-3

To verify the effects, both compounds were freshly purchased, and the experiment was repeated. For this purpose, a dilution series ranging from 0.2-200 µM was prepared to check whether the effect was concentration dependent. The experiment was performed in triplicates using freshly purified ACSL4\_His6x protein. As shown in Table 5.5, triclabendazole (Prestw-Frag-1165) was not able to increase the unfolding temperature by more than 0.2 °C, whereas mitoxantrone dihydrochloride (Prestw-Frag-0674) caused a change of up to 0.7 °C. Furthermore, the increase in  $T_m$  with mitoxantrone dihydrochloride was concentration dependent, leading to the highest values in the range of 20-100 µM.

**Table 5.5:** Determined melting temperatures ( $T_m$ ) for the ACSL4\_His6x interaction with mitoxantrone dihydrochloride and triclabendazole.

Experiments were performed with 5 µM of purified ACSL4\_His6x protein and the indicated drug concentrations. DMSO was used as a control. Values shown display mean and SD of triplicates.

<b>Mitoxantrone dihydrochloride Prestw-Frag-0674</b>			<b>Triclabendazole Prestw-Frag-1165</b>		
Concentrations [µM]	$T_m$ [°C]	SD [°C]	Concentrations [µM]	$T_m$ [°C]	SD [°C]
0.2	40.2	0.24	0.2	40.4	0.12
2	40.5	0.01	2	40.4	0.12
10	40.7	0.22	10	40.3	0.01
20	40.9	0.13	20	40.2	0.11
50	40.8	0.13	50	39.8	0.11
100	40.9	0.12	100	39.6	0.32
150	40.7	0.01	150	39.5	0.23

**Mitoxantrone dihydrochloride****Triclabendazole****Prestw-Frag-0674****Prestw-Frag-1165**

Concentrations [ $\mu\text{M}$ ]	T <sub>m</sub> [ $^{\circ}\text{C}$ ]	SD [ $^{\circ}\text{C}$ ]	Concentrations [ $\mu\text{M}$ ]	T <sub>m</sub> [ $^{\circ}\text{C}$ ]	SD [ $^{\circ}\text{C}$ ]
200	40.5	0.22	200	39.3	0.34
DMSO	40.2	0.12	DMSO	40.2	0.12

**5.1.4 Activity investigations of ACSL4\_His6x**

To study the activity of the purified ACSL4\_His6x enzyme, an indirect spectrophotometric assay system was adapted from Hosaka *et al.* [280].

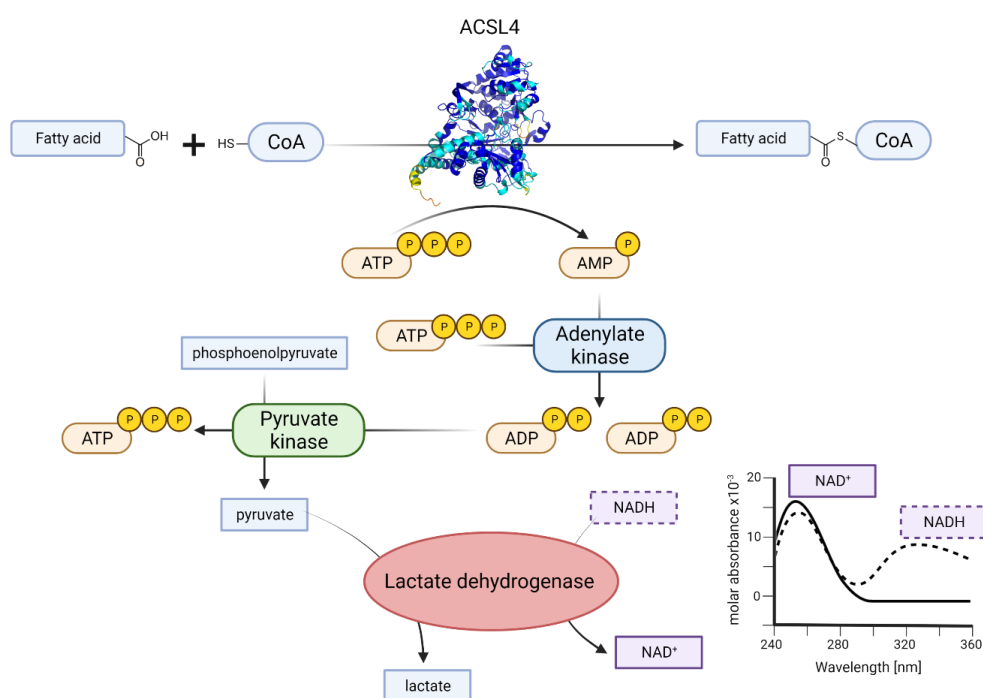


**Figure 5.9: Schematic overview of the ACSL4 activity assay setup.**

As an alternative to isotopic methods, the spectrophotometric assay system coupled the ACSL4-catalyzed acyl-CoA formation to the oxidation of NADH, as shown in Figure 5.9. For this purpose, the ATP consumption of the thioesterification is followed by subsequent reactions of adenylate kinase, pyruvate kinase, and lactate dehydrogenase. Then, the resulting oxidation of NADH was detected at 334 nm, and the decrease over time was used to calculate initial reaction parameters. The original assay set-up was described for the reaction of ACSL1 at 25 °C. Thus, an already adapted system described by Klett *et al.*, suitable also for other ACSLs, was used [31]. Here, ACSL4-catalyzed acyl-CoA formation is performed at 37 °C and tracked over 5 min.

### 5.1.4.1 Initial evaluation of the assay setup

For a first evaluation of the assay system, different amounts of purified protein were applied, and absorbance at 334 nm was tracked. In addition to freshly purified protein, aliquots that were stored at 4 °C or -80 °C for 16 days were tested to check whether the enzymes' activity was affected by the storage conditions (Figure 5.10).

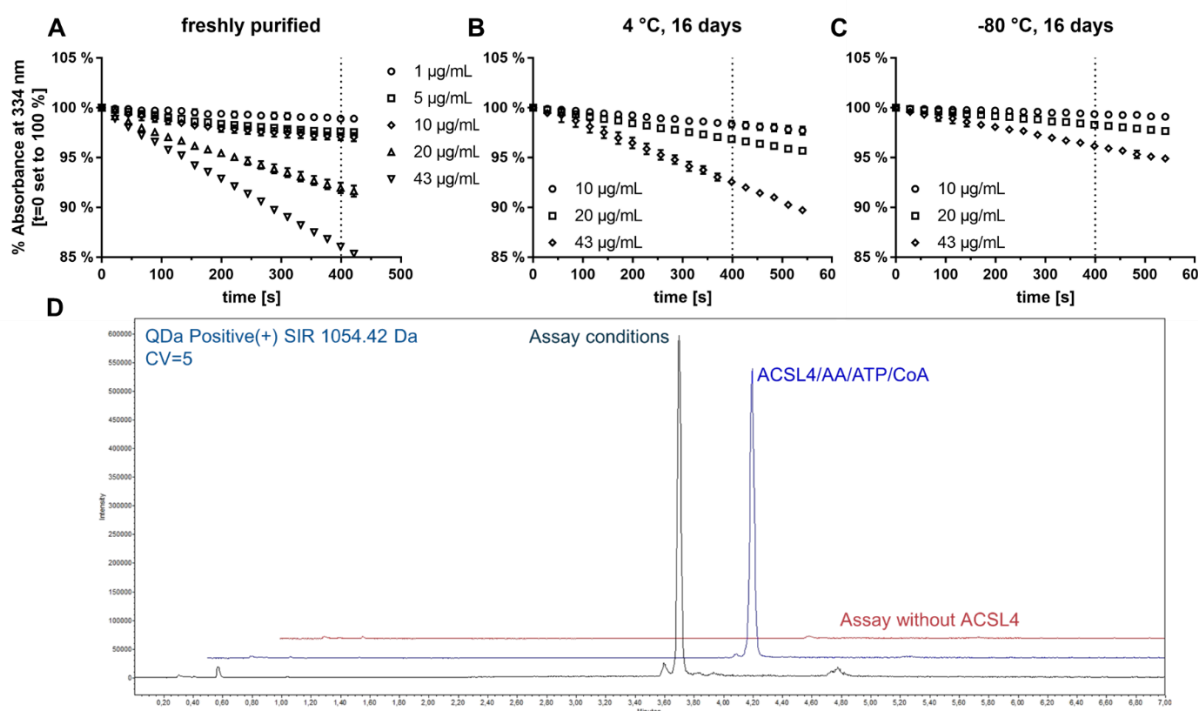


**Figure 5.10: Evaluation of ACSL4\_His6x activity.**

The activity of recombinant ACSL4\_His6x was tested with arachidonic acid (ARA) directly following purification (A) after 16 days of storage at 4 °C (B) and 16 days of storage at -80 °C (C). Absorbance at 334 nm was measured repeatedly using a Tecan plate reader. Samples were corrected using a blank without ACSL4, and the starting absorbance was set to 100 %. For better comparison, the 400 s time point is indicated in each graph. Values display mean  $\pm$  SD of triplicates. Verification of the product formed was achieved by UPLC-MS in positive ESI mode and SIR channel of arachidonoyl-CoA (1054.42 Da) (D). Baselines were shifted for better visibility of the three samples (black: 100 mM Tris/HCl, pH 8.0, 15 mM MgCl<sub>2</sub>, 150 mM KCl, 10 mM ATP, 5 mM DTT, 1 mM PEP-K, 0.3 mM NADH, 5 µM ARA, 22.5 µg/mL adenylate kinase, 15 µg/mL pyruvate kinase, 15 µg/mL lactate dehydrogenase, 43 µg/mL ACSL4\_His6x, 600 µM CoA; blue: 100 mM Tris/HCl, pH 8.0, 15 mM MgCl<sub>2</sub>, 150 mM KCl, 10 mM ATP, 5 µM ARA, 43 µg/mL ACSL4, 600 µM CoA; red: No protein control of blue).

As shown in Figure 5.10A, a decrease in absorbance at 334 nm correlated with the amount of recombinant protein used. Although lower concentrations of 1-10 µg/mL ACSL4 showed very similar results with a decrease of 1-3 % after 400 s, further increase in the ACSL4 concentration to 20 µg/mL and 43 µg/mL led to a decrease of 8 % and 14 %, respectively. The same experiment was repeated with purified ACSL4 that was stored for 16 days either at 4 °C (Figure 5.10B) or -80 °C (Figure 5.10C). Because protein concentrations below 10 µg/mL had only minor effects, the stored samples were directly used in higher concentrations. As shown for the 4 °C samples, the absorbance after 400 s of the 10 µg/mL protein sample was slightly lower than before, with around 2 %. The same was true for the samples containing 20 µg/mL and 43 µg/mL protein leading to a 3 % and 7 % decrease, respectively. In accordance with the lowest concentration, these values were again lower than those of the freshly purified samples.

Repetition of the experiment with samples stored at  $-80\text{ }^{\circ}\text{C}$  revealed a similar pattern. However, these samples showed even less activity than the samples stored at  $4\text{ }^{\circ}\text{C}$ . In order to verify that the product was indeed the expected arachidonoyl-CoA (ARA-CoA), the assay mix was also analyzed by UPLC-MS (Figure 5.10D). For this purpose, another sample was prepared with identical composition containing  $43\text{ }\mu\text{g/mL}$  ACSL4\_His6x, but this time the assay was performed in a volume of  $1\text{ mL}$  in a glass vial and was incubated in a water bath instead. Following the incubation, solid phase extraction was performed, and the extracted sample was analyzed using the selected ion recording (SIR) channel of ARA-CoA ( $m/z\ 1054.42\text{ Da}$ ). The peak clearly indicated the formation of ARA-CoA under standard assay conditions (black line:  $100\text{ mM}$  Tris/HCl,  $\text{pH } 8.0$ ,  $15\text{ mM}$   $\text{MgCl}_2$ ,  $150\text{ mM}$  KCl,  $10\text{ mM}$  ATP,  $5\text{ mM}$  DTT,  $1\text{ mM}$  PEP-K,  $0.3\text{ mM}$  NADH,  $5\text{ }\mu\text{M}$  ARA,  $22.5\text{ }\mu\text{g/mL}$  adenylate kinase,  $15\text{ }\mu\text{g/mL}$  pyruvate kinase,  $15\text{ }\mu\text{g/mL}$  lactate dehydrogenase,  $43\text{ }\mu\text{g/mL}$  ACSL4\_His6x,  $600\text{ }\mu\text{M}$  CoA). To verify that the formation was not caused by another enzyme of the assay mix, a second sample only containing the essential components of the reaction was prepared (blue line:  $100\text{ mM}$  Tris/HCl,  $\text{pH } 8.0$ ,  $15\text{ mM}$   $\text{MgCl}_2$ ,  $150\text{ mM}$  KCl,  $10\text{ mM}$  ATP,  $5\text{ }\mu\text{M}$  ARA,  $43\text{ }\mu\text{g/mL}$  ACSL4,  $600\text{ }\mu\text{M}$  CoA) together with a control lacking the ACSL4\_His6x protein (red line). The UPLC-MS analysis revealed a product peak for the essential components sample, while the control did not show any product formation. Thus, the assay system seemed to be suitable for the formation of ACSL4 products.

#### 5.1.4.2 Setup optimization and evaluation of ACSL4 kinetics

Next, the assay setup was adapted for optimal enzyme kinetic measurements. To ensure that the repeating measures of the absorbance were as comparable as possible, one well was prepared and measured at a time (Figure 5.11).

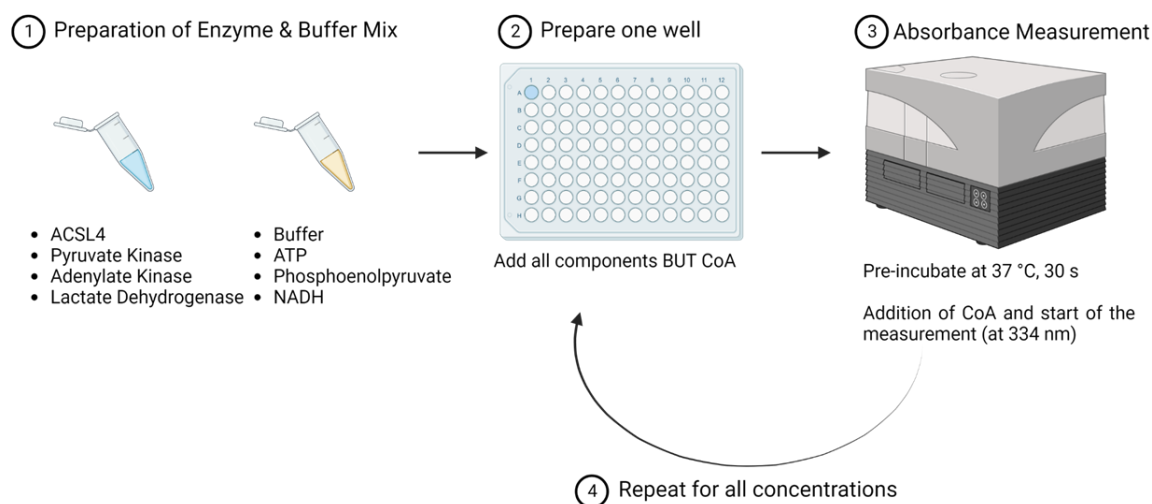


**Figure 5.11: Adaptation of ACSL4 assay setup for the determination of enzyme kinetics.**

ARA and EPA were chosen as substrates for kinetic analyses. Several protein concentrations were tested until a substrate concentration of  $100\text{ }\mu\text{M}$  led to saturation. Experiments were then performed with  $0.1\text{ }\mu\text{M}$  ( $7.42\text{ }\mu\text{g/mL}$ ) of purified ACSL4\_His6x protein. Results of experimental setups using ARA as substrate varied strongly and, thus, prevented the determination of  $K_M$  and  $V_{MAX}$  values. In contrast, investigations using EPA as substrate were reproducible and allowed the calculation of kinetic values, as shown in Figure 5.12.

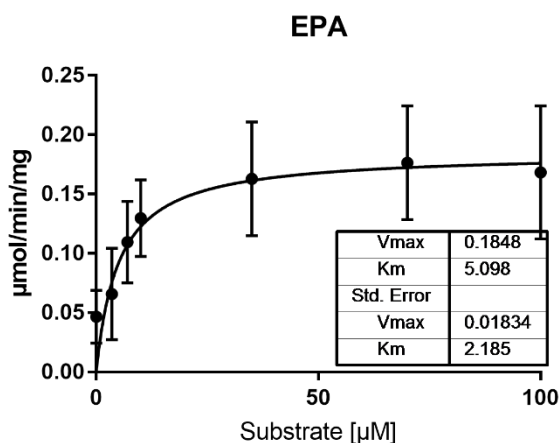


**Figure 5.12: Turnover kinetics of EPA by purified ACSL4\_His6x protein.**

Activity studies were performed with 0.1  $\mu\text{M}$  of purified ACSL4\_His6x protein and the following EPA concentrations: 0  $\mu\text{M}$ , 3.5  $\mu\text{M}$ , 7  $\mu\text{M}$ , 10  $\mu\text{M}$ , 35  $\mu\text{M}$ , 70  $\mu\text{M}$ , and 100  $\mu\text{M}$ . Data display mean  $\pm$  SD of three independent experiments.  $V_{\text{MAX}}$  and  $K_{\text{M}}$  values were determined using the GraphPad Prism 7.05 software.

### 5.1.5 A recombinant 15S-lipoxygenating enzyme from *pseudomonas aeruginosa* (PA-LOX)

As demonstrated above, ACSL4\_His6x stability and activity were analyzed, and product formation of ARA-CoA was verified via UPLC-MS. In order to produce a variety of esterified oxylipins, the use of a 15S-lipoxygenating enzyme from *pseudomonas aeruginosa* (PA-LOX) was investigated next. PA-LOX is a bacterial member of the lipoxygenase family, and the respective expression plasmid was kindly gifted by Univ.-Prof. Dr. sc. med. Hartmut Kühn (Charité Berlin). Expression and purification were performed according to Kalms *et al.* with slight adaptations as described in chapter 4.4 [283]. The major differences were the upscaling from 50 mL expression cultures to 500 mL and the use of an automated ÄKTA purification system in combination with a prepacked HisTrap™ HP column.

The result of a first expression test as well as the analysis of a further upscaled purification, are shown in Figure 5.13. Initial purification of His6x-tagged PA-LOX led to a protein yield of 3.8 mg with a purity of >95 % (Figure 5.13A). However, the sample taken from the insoluble part following cell homogenization (P) showed a clear PA-LOX band, even though this sample was diluted 1:40 prior to application. Determination of the protein intensities and comparison with the eluted fractions (E1 and E2) revealed that 47 % of the total PA-LOX protein was still present in the insoluble fraction, indicating that the protein yield of 3.8 mg represented only 53 % of the total yield. Because a problem during the cell lysis step of the purification procedure was assumed, all buffers were freshly prepared, and suspension of the cell pellets, as well as cell lysis, was prepared with particular caution. Furthermore, four expression cultures (4×500 mL) were prepared in parallel to ensure sufficient protein yield for subsequent experiments. Cell homogenates were combined, and the purification was analyzed by SDS-PAGE (Figure 5.13B). Although the expression led to large amounts of the PA-LOX protein, a not insignificant proportion of the protein was lost during the washing step. Furthermore, a small proportion of the protein seemed to be present in the flow-through, slightly below the 75 kDa marker, indicating that the binding capacity of the purification column was reached.

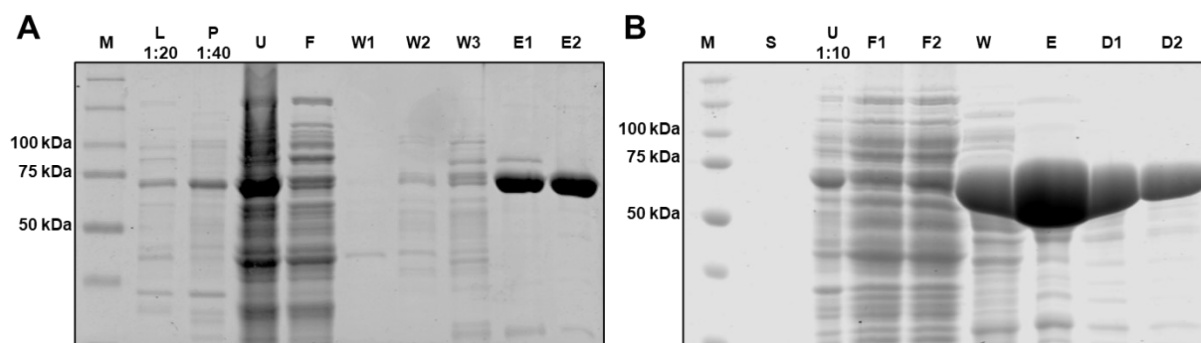


**Figure 5.13: SDS-PAGE analysis of the purification of PA-LOX.**

PA-LOX was expressed in *E. coli* BL21(De3) cells, and the pellet of a 500 mL culture (A) and 4 pooled 500 mL cultures (B) was purified by Ni-affinity chromatography. M: Protein marker, L: Soluble part after cell lysis, P: Pellet (insoluble part after cell lysis), U: Soluble part after 100,000 rcf centrifugation, F: Flow-through, W: Wash fraction, E: Elution fraction, S: Supernatant following cell harvest, D: Desalted fraction. Diluted samples are indicated as such with the respective dilution factor. If multiple fractions per step were analyzed, fractions are marked with digits.

Nevertheless, the protein yield of the eluted proportion was determined, resulting in 33 mg PA-LOX protein with a purity of >90 %. In order to prevent column overload in later expression attempts, two consecutive 1 mL HisTrap™ HP columns were used to double the column volume. Subsequent purification resulted in a yield of 14.9 mg protein from 1 L expression culture. Protein yields of all purifications are shown and compared in Table 5.6. On average, the yield was  $13.0 \pm 4.7$  mg protein per liter culture and might even be higher, taking into account that approx. 50 % of the PA-LOX protein was insoluble during one attempt.

**Table 5.6: Comparison of recombinantly expressed PA-LOX yields.**

Protein yield [mg]	Expression volume [L]	Protein yield [mg/L]
3.8	0.5	7.6
33.0	2 (4×500 mL cultures)	16.5
14.9	1	14.9

### 5.1.6 Stability and activity investigations of purified PA-LOX

After the successful purification of the PA-LOX protein, stability analysis was performed using a thermal shift approach. Several buffer conditions, as well as the effect of salt addition, were analyzed, and the results are shown in Figure 5.14.

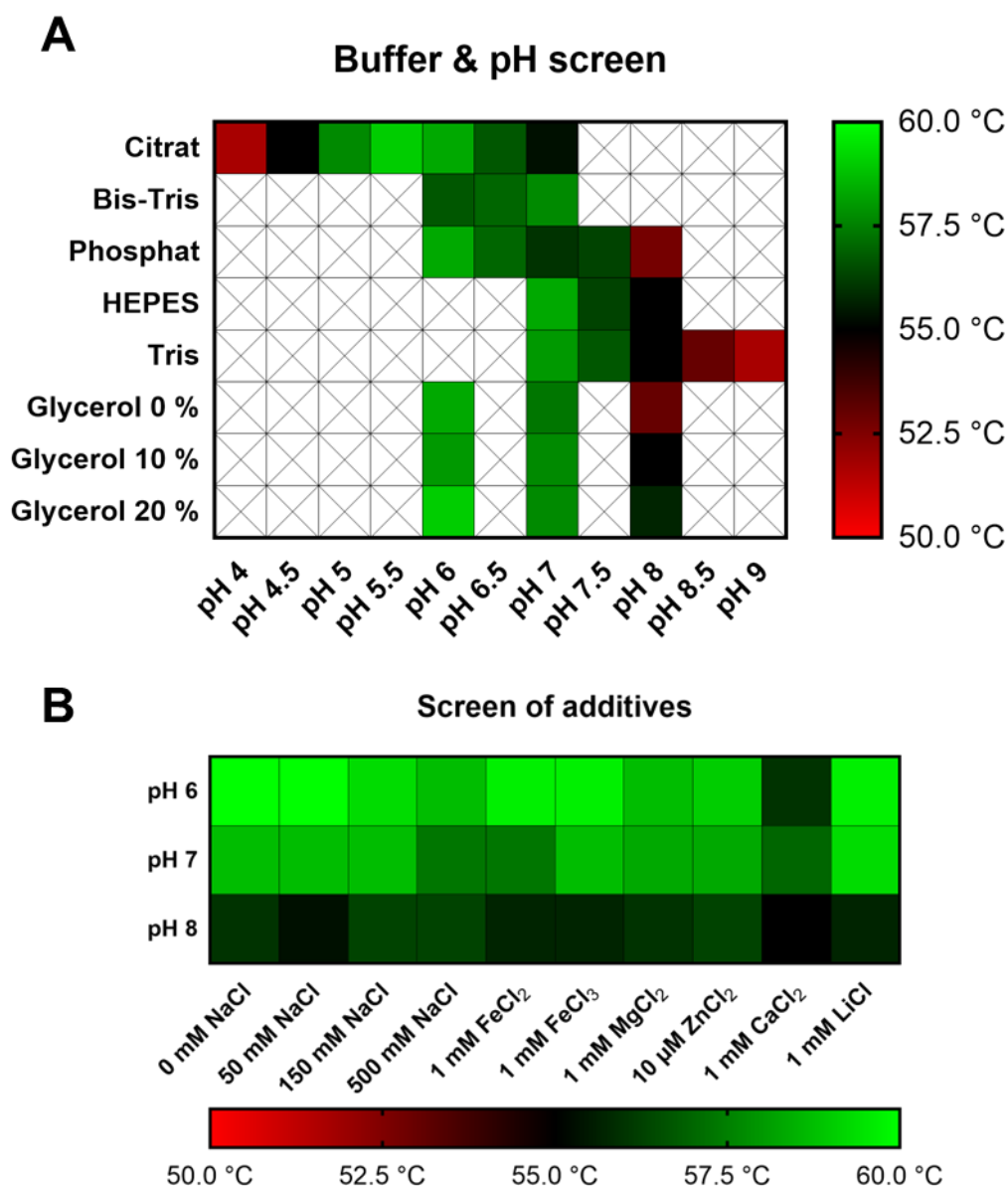


**Figure 5.14: Stability analysis of the recombinant PA-LOX protein.**

Heatmap of several buffer conditions (A), as well as the addition of different salts (B), were tested. 5  $\mu$ M of purified PA-LOX were used for the investigation in 100 mM buffer systems. All salt conditions (B), as well as the glycerol samples of (A), were prepared in 100 mM sodium phosphate buffer. Displayed colors correspond to the mean of triplicate measurements, and the unfolding temperatures are given in the legends shown beside or below the graphic. Crossed-out conditions were not tested.

The thermal shift analysis revealed that the protein was extremely stable up to 50 °C. The lowest unfolding temperature was found in 100 mM citrate buffer at pH 4 with  $51.7 \pm 0.6$  °C, while the highest unfolding temperature ( $60 \pm 0$  °C) was found in 100 mM NaPi at pH 6.0 with up to 50 mM NaCl. The HEPES buffer system used during the purification process of the recombinant protein revealed unfolding temperatures between 55.0 °C and 58.3 °C depending on the pH value. Furthermore, the addition of glycerol increased the stability by up to 20 %. Next, the effect of several salts on the stability of PA-LOX was tested. As shown in Figure 5.14B, supplementation with various salts either did not affect the stability or led to a decrease

of 2 °C to 5 °C. Due to the high stability of the PA-LOX protein in the HEPES buffer system, a buffer exchange prior to activity experiments was not performed.

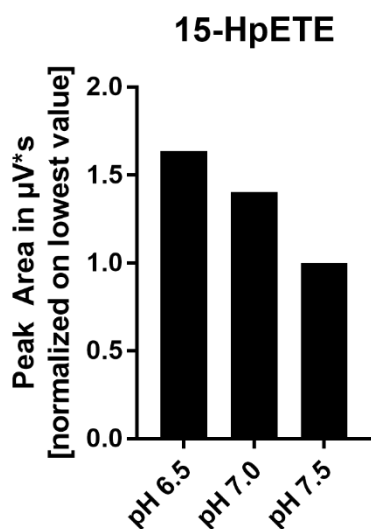


**Figure 5.15: Activity verification of purified PA-LOX.**

The activity of 7 nM purified PA-LOX protein was tested using 10 μM ARA as substrate. Samples were incubated at 37 °C for 10 min, purified by SPE, and analyzed by UPLC-UV/MS. Product formation was checked in selective ion recording mode (335.2 Da), and peak areas were determined and normalized on the lowest sample.

For activity studies, the purified protein was incubated with 10 μM ARA at different pH values, as described in chapter 4.8.4, and product formation was analyzed by UPLC-UV/MS (Figure 5.15). 15-HpETE was identified as the main product, with product levels inversely correlated to the pH value. Consequently, the highest product formation was determined at pH 6.5. Since the activity of the PA-LOX construct used was already studied in detail by the group Univ.-Prof. Dr. sc. med. Hartmut Kühn, no further experiments regarding the activity were performed [283,284].

#### 5.1.6.1 Screen of PA-LOX interaction with an inhouse fatty acid library

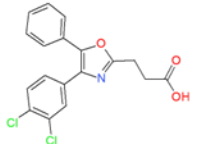
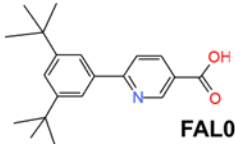
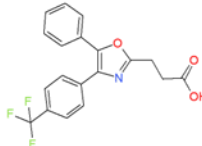
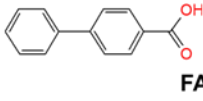
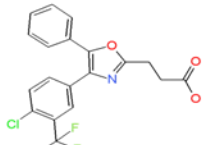
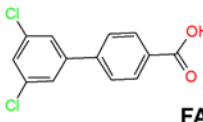
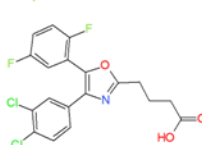
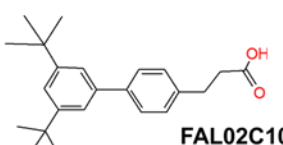
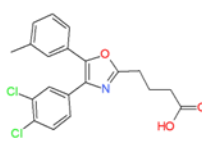
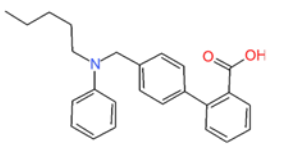
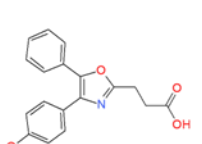
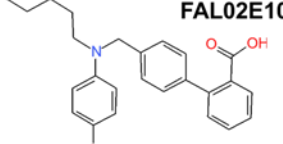
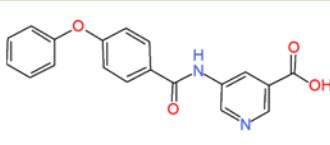
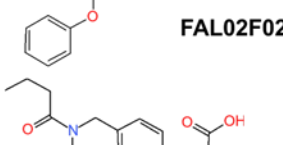
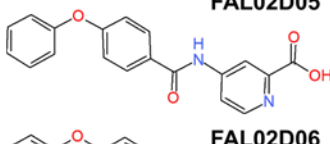
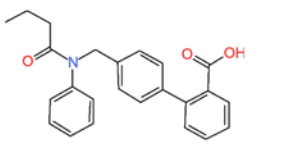
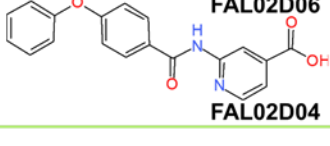
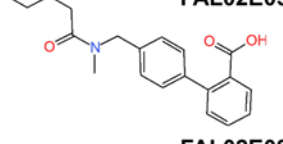
After verification of the protein's functionality, a fatty acid library (FAL) was screened for protein interaction. The FAL contained 160 fatty acid mimetics that were prepared by several current and former colleagues (see chapter 4.9.3).

The interaction was tested by thermal shift experiments, but stabilizing effects were not observed. Since a decrease in the unfolding temperature might also indicate an interaction, compounds with large negative shifts are shown in Table 5.7. 17 compounds led to a decrease of more than 1 °C. Interestingly, the molecules that affected the stability were divided into three groups based on their core structure. However, since stabilizing effects were not observed, no further experiments were performed yet.



**Table 5.7: Results of the FAL screen with the PA-LOX protein.**

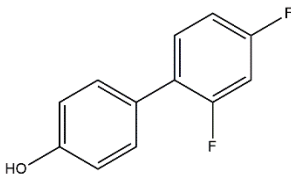
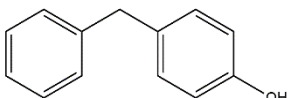
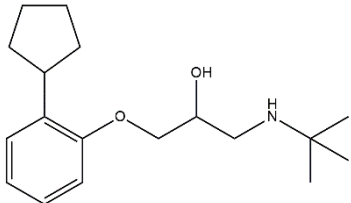
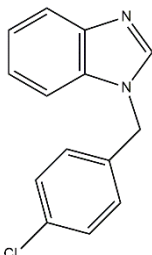
The shown compounds decreased the stability of PA-LOX by more than 1 °C. Values display mean  $\pm$  SD of two single-point determinations. The structures can be subdivided into 4,5-diphenyloxazoles (blue), benzanilides (green), and biphenyls (red). Smiles codes of each compound can be found in appendix Table 9.8 using the respective FAL number.

Compound	$\Delta T$ [°C]	Compound	$\Delta T$ [°C]
 <b>FAL01G06</b>	$-2,3 \pm 0$	 <b>FAL02C11</b>	$-3,3 \pm 0$
 <b>FAL01G05</b>	$-2,3 \pm 0,7$	 <b>FAL02C07</b>	$-1,8 \pm 0,7$
 <b>FAL01G08</b>	$-1,8 \pm 0,7$	 <b>FAL02C08</b>	$-1,3 \pm 0$
 <b>FAL01H08</b>	$-1,8 \pm 0,7$	 <b>FAL02C10</b>	$-1,3 \pm 0$
 <b>FAL01H10</b>	$-1,3 \pm 0$	 <b>FAL02E10</b>	$-2,3 \pm 0$
 <b>FAL01G07</b>	$-1,3 \pm 1,4$	 <b>FAL02E10</b>	$-2,3 \pm 0$
 <b>FAL02D05</b>	$-2,8 \pm 0,7$	 <b>FAL02F02</b>	$-2,8 \pm 0,7$
 <b>FAL02D06</b>	$-1,3 \pm 0$	 <b>FAL02E05</b>	$-1,3 \pm 0$
 <b>FAL02D04</b>	$-1,3 \pm 1,4$	 <b>FAL02E08</b>	$-1,8 \pm 0,7$

### 5.1.6.2 Screen of PA-LOX interaction using a drug fragment library

Next, a Prestwick drug fragment library containing 480 small organic molecules was screened via TSA for PA-LOX interaction. The assay was performed twice, and only compounds that showed results in both runs were considered hits. As already seen for the FAL screen, only destabilizing effects were observed. Nevertheless, the compounds with the strongest negative effects were identified and are shown in Table 5.8. However, due to the large standard deviations and the fact that these compounds are often considered false positives, no further investigations were performed.

**Table 5.8: Drug fragment library hits with the strongest effects on  $\Delta T$ . Values display mean  $\pm$  SD of duplicates.**

Fragment	Prestw-Frag-1237	Prestw-Frag-3455
$\Delta T$ [°C]	$-4.6 \pm 2.8$	$-4.5 \pm 4.2$
Structure		
CAS	59089-68-8	101-53-1
Fragment	Prestw-Frag-0674	Prestw-Frag-1165
$\Delta T$ [°C]	$-3.5 \pm 2.8$	$-3.5 \pm 2.8$
Structure		
CAS	70476-82-3	68786-66-3

### 5.1.7 Expression and purification of human LPCAT2

Once the activation step of the Lands' cycle catalyzed by ACSL4 was established together with the PA-LOX enzyme for a wider product spectrum, the next step was the investigation of the transfer process. For this purpose, a member of the lysophosphatidylcholine acyltransferase family had to be expressed and purified. In order to produce esterified lipid mediators, the activation step by ACSL4 is followed by subsequent transfer of acyl-CoAs into so-called lysophospholipids, which lack one acyl chain typically at the sn-2 position. Since LPCAT2 was reported to accept a variety of activated fatty acids, the enzyme was chosen for experiments, and several expression constructs were prepared. In a first attempt, a construct with an N-terminal His<sub>6</sub>x-tag (His<sub>6</sub>x\_LPCAT2) under the control of a lac operon was tested.

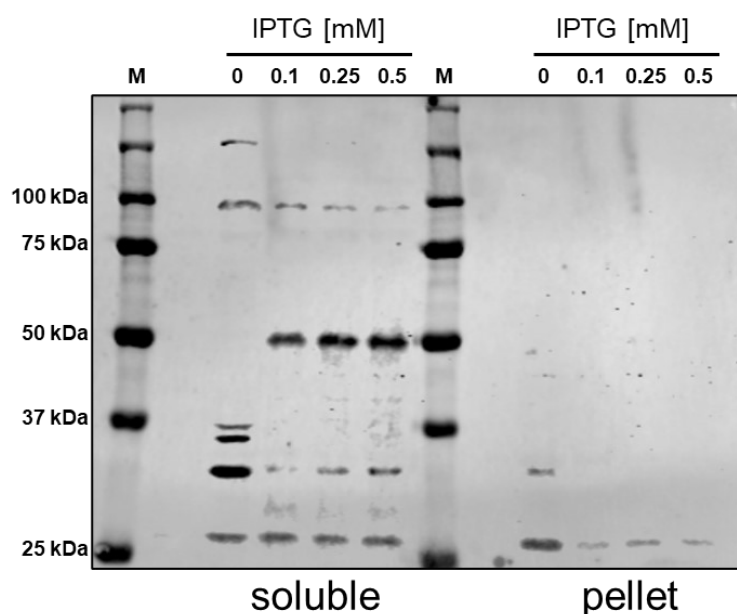


**Figure 5.16: Expression test of His6x-tagged LPCAT2 in *E. coli* BL21(De3) cells.**

Western blot analysis of the recombinant expression of an LPCAT2 construct with N-terminal His6x-tag. Expression cultures were prepared as described for ACSL4 (see chapters 4.3.1 and 4.3.2), but varying IPTG concentrations, as indicated, were used to induce protein expression. After harvesting, cells were homogenized, and the soluble fraction (left), as well as the pellet (right), were analyzed.

As shown in Figure 5.16, the LPCAT2 protein was found exclusively in soluble fractions. Moreover, variation in the IPTG concentrations did not affect the protein yield. Surprisingly, the strongest protein bands were visualized at the 50 kDa marker, although the protein size was expected to be 60,208 Da (UniProt entry: Q7L5N7-1). Since the LPCAT2 antibody used here also displayed bands with approx. 50 kDa in other cell lines, according to the manufacturer, it was uncertain whether the protein was expressed at full length. Thus, another construct containing a C-terminal His6x-tag was prepared. The expression experiment was repeated, and protein bands were visualized using the same LPCAT2 antibody as well as an antibody for the detection of the respective His6x-tag (Figure 5.17).

The respective analysis revealed that the antibody directed against the His6x-tag only bound to the construct with a C-terminal tag (Figure 5.17A), while the antibody targeting the LPCAT2 gene showed bands for both constructs (Figure 5.17B). Therefore, the protein seemed to lack part of the N-terminus. Furthermore, the protein bands of the N-terminal construct were stronger than the ones of the C-terminal construct, indicating that modification at the N-terminus might be beneficial or that modification at the C-terminal end destabilized the enzyme. However, since the experiment was only performed once, this might also be an effect of unequal bacterial growth unrelated to the construct.

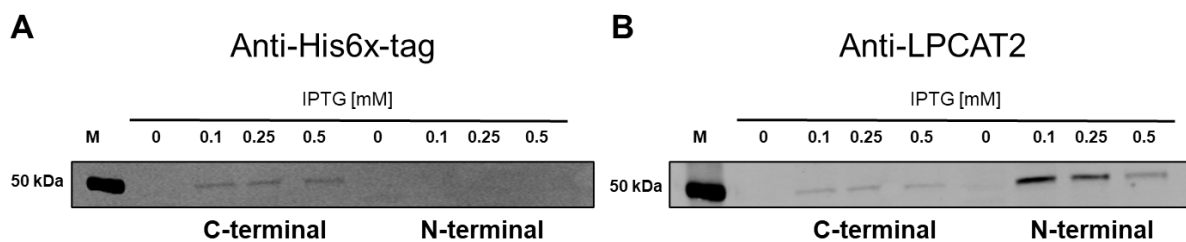


**Figure 5.17: Western blot analysis of His6x-tagged LPCAT2 to determine protein integrity.**

Protein expression of two constructs (C-terminal or N-terminal His6x-tag) was analyzed using an antibody directed against the His6x-tag (A) or an unknown epitope of LPCAT2 (B).

A shortened protein could explain the size difference of 10 kDa on Western blot level. Thus, the N-terminal sequence was analyzed, and potential cleavage regions were predicted (Figure 5.18, dark green areas). Lacking the N-terminal part up to region 1 would reduce the size of the protein by 7-8 kDa, while the sequence up to region 2 would decrease the size by 11-12 kDa. In order to improve protein yields, a shortened LPCAT2 construct was prepared. The sequence was cut between the two regions (sLPCAT2) so that the remaining protein was 50 kDa in size. Expression and purification were performed as described for ACSL4\_His6x (see chapters 4.3.1- 4.3.5), and SDS-PAGE analysis is shown in Figure 5.19.

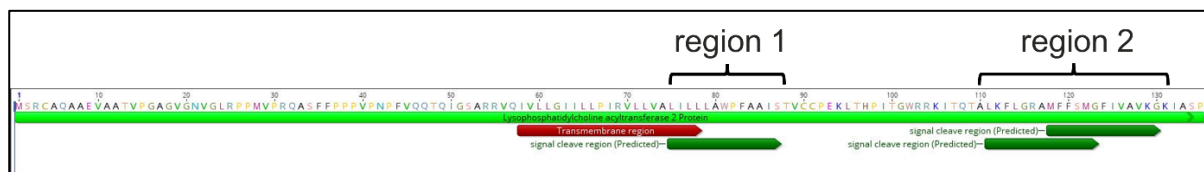


**Figure 5.18: N-terminal amino acid sequence of human LPCAT2.**

Shown are the first 135 amino acids, including a transmembrane region (red) and three predicted cleavage regions (dark green). Due to their overlap, cleavage regions 2 and 3 are indicated as one region (region 2). Sequence prediction was performed using the Geneious R10 software.

SDS-PAGE revealed that the shortened protein version was not purified, and also, wash fractions did not show protein bands at the expected size of 50 kDa. In addition, even the soluble part of the homogenized cells did not show a significant protein overexpression, indicating that the missing N-terminal part probably prevented proper folding of the enzyme and thus might have caused premature digestion. In order to overcome the low expression rates, new constructs using an optimized LPCAT2 sequence were prepared. Moreover, the removed sequence was changed so that the constructs were either cut in predicted cleavage region 1 (s1LPCAT2) or region 2 (s2LPCAT2). The constructs again carried His6x-tags at N- or C-terminus, but this time also, constructs with N-terminal MBP-tags were prepared to enhance solubility. The MBP-tag sequence was separated from the respective LPCAT2 version by a linker region that contained a tobacco etch virus (TEV) cleavage region. This should allow the separation of the tag to obtain the pure LPCAT2 protein.

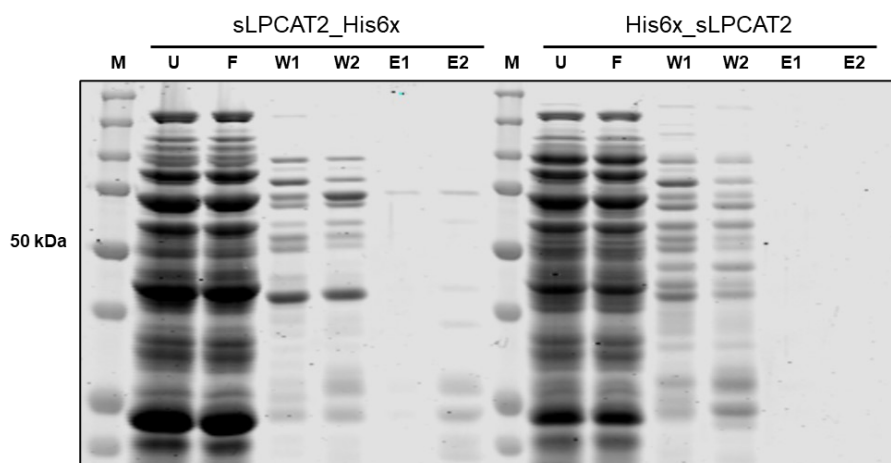


**Figure 5.19: Purification analysis of two shortened LPCAT2 constructs.**

An expression construct with C-terminal His6x-tag is shown on the left side of the gel, while the construct carrying an N-terminal His6x-tag is shown on the right. Both constructs have a size of 50 kDa. M: Protein marker, U: Soluble fraction after 100,000 rcf centrifugation, F: Flow-through, W: Wash fractions, E: Elution fractions. Multiple fractions of the same step are indicated by digits.

At least expression of the MBP-tagged construct led to strongly increased protein amounts. Following Ni-affinity chromatography, elution fractions (Figure 5.20, lanes E1 and E2) were combined, and an excess of MBP-tagged TEV (MBP-TEV), kindly provided by Dr. Whitney Kilu, was added. Cleavage of the fusion protein MBP-s1LPCAT2 was performed for 16 h at 4 °C to remove the MBP-tag. Simultaneously, the protein solution was dialyzed in buffer D (25 mM Tris, pH 7.4, 200 mM KCl, 0.1 % (w/v) Triton X-100, 1 mM DTT, 10 % (v/v) glycerol). Afterward, the protein solution was applied to an MBP-binding column (amylose resin, self-packed, gravity flow, 5 mL, sigma) to separate the cleaved s1LPCAT2 protein. Unfortunately, successfully cleaved s1LPCAT2 protein was not observed (Figure 5.20 lane LPCAT2). Instead, the full-length fusion protein (MBP-s1LPCAT2), the MBP-TEV, and unbound MBP, presumably originated from truncation during translation, was found in the elution fraction (eluted with 25 mM Tris, pH 7.4, 200 mM KCl, 0.1 % (w/v) Triton X-100, 1 mM DTT, 10 % (v/v) glycerol, 10 mM maltose, Figure 5.20 lane MBP). Cleavage of the construct was repeated with freshly purified as well as different aliquots of stored TEV. Furthermore, the incubation duration was elongated to 24 h at 4 °C, and TEV amounts were increased. Unfortunately, the fusion construct was not cleaved under any condition, indicating that the respective cleavage site was not accessible.

Nevertheless, the tagged protein was tested for activity using an adapted version of the assay system described by Tarui *et al.* (0.5 µg microsomal protein fractions, 1 mM acetyl-CoA, 5 µM lyso-PAF in 100 mM Tris, pH 7.4, 1 µM CaCl<sub>2</sub>, 0.015 % (w/v) Tween-20, 5 min at 37 °C) [104]. Although the assay was performed with much higher protein concentrations (>5 µM), product formation could not be determined in any attempt.

Due to problems at each stage of expression, purification, and activity study, the recombinant LPCAT2 approach was not continued.

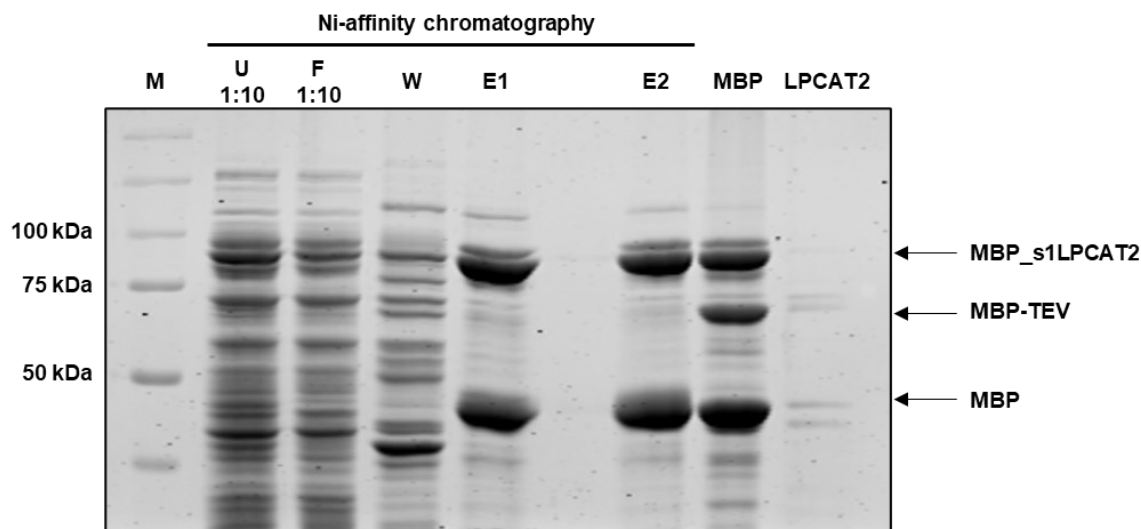


**Figure 5.20: Purification of the MBP\_s1LPCAT2 construct.**

The construct was expressed in *E. coli* BL21(De3) cells and purified by Ni-affinity chromatography (HisTrap™ HP, CV=3 mL). Elution fractions E1 and E2 were combined, incubated with an excess of MBP-TEV, and simultaneously dialyzed in buffer D (25 mM Tris, pH 7.4, 200 mM KCl, 0.1 % (w/v) Triton X-100, 1 mM DTT, 10 % (v/v) glycerol) for 16 h at 4 °C. M: Protein marker, U: Soluble fraction after 100,000 rcf centrifugation, F: Flow-through, W: Wash fractions, E: Elution fractions, MBP: Elution fraction of amylose column (5 mL, self-prepared, gravity flow, sigma), LPCAT2: Flow-through fraction of amylose column. Multiple fractions of the same step are indicated by digits. Diluted samples are indicated as such.

## 5.2 Cell-based overexpression system for the formation of esterified lipid mediators

Another approach for the synthesis of esterified lipid mediators was the expression of key enzymes of the lipid remodeling pathway known as Lands' cycle in a cellular system. Once the overexpression was established, oxidized lipids, hereafter referred to as oxylipins, were analyzed by LC-MS in collaboration with the laboratory of Prof. Dr. Nils Helge Schebb (University of Wuppertal). Further manipulation of the observed oxylipin pattern in the cells was then tested by expressing different human lipoxygenases.

### 5.2.1 Stably transfected HEK293T cells express ACSL4 and/or LPCAT2

HEK293T cells were stably transfected with plasmids carrying the shorter human ACSL4 isoform (UniProt entry: O60488-2) [56] and/or the human LPCAT2 gene (UniProt entry: Q7L5N7-1). In addition, a vector control (VC) cell line was prepared using a vector with an empty MCS. The 'Sleeping Beauty System', as described by Kowarz *et al.*, was selected as the transfection method of choice, and PEI was used as transfection reagent (see chapter 4.7) [279]. New cell lines were termed HEK293T\_VC, HEK293T\_ACSL4, and HEK293T\_LPCAT2 according to the respective transfection vector. An additional cell line was prepared by co-transfection of ACSL4 and LPCAT2 and consequently termed HEK293T\_ACSL4+LPCAT2, hereafter only referred to as HEK293T\_A+L. ACSL4 and LPCAT2 expression was analyzed in each cell line, as shown in Figure 5.21.

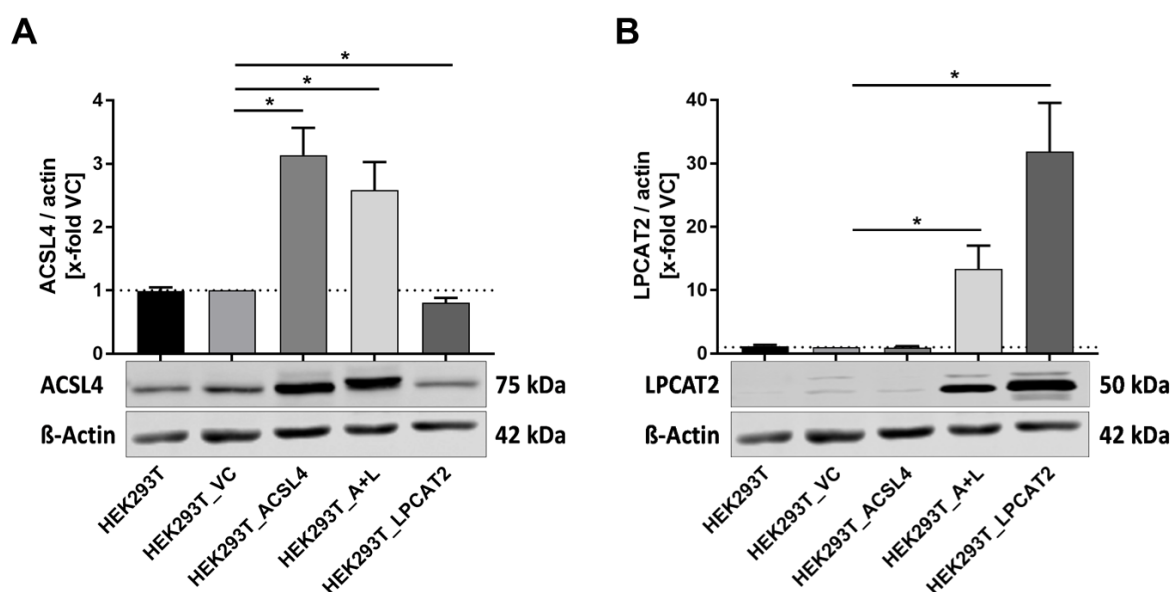


**Figure 5.21: Western blot analysis of stably transfected HEK293T cells.**

Densitometric analysis of the protein expression of ACSL4 (A) and LPCAT2 (B) in HEK293T wild type, vector control cells (HEK293T\_VC) and HEK293T stably overexpressing ACSL4 (HEK293T\_ACSL4), LPCAT2 (HEK293T\_LPCAT2) or ACSL4/LPCAT2 (HEK293T\_A+L) by quantitative Western blot, using  $\beta$ -actin as loading control. A representative blot is shown per experiment. Values display mean + SD of n=3 experiments. Intensities were correlated to the housekeeping gene ( $\beta$ -actin) and normalized on the vector control cells. Statistical analysis: Unpaired t-test with Welch's correction against vector control. \* P<0.05.

Protein expression in empty vector control cells was not altered compared to HEK293T wild-type cells, and thus, the HEK293T\_VC cell line was used for the comparison with ACSL4 and/or LPCAT2 overexpression cell lines. As shown in Figure 5.21A, expression levels of ACSL4 were significantly increased in HEK293T\_ACSL4 and HEK293T\_A+L cells by about 3-fold and 2.5-fold, respectively. Interestingly, ACSL4 expression was slightly downregulated in HEK293T\_LPCAT2 cells. Analysis of the LPCAT2 expression levels (Figure 5.21B) revealed strong and significant upregulation of about 13-fold in HEK293T\_A+L cells and about 30-fold in HEK293T\_LPCAT2 cells. Furthermore, LPCAT2 expression was not affected by ACSL4 overexpression in HEK293T\_ACSL4 cells. Important to note is that a protein size of 60 kDa was expected based on the amino acid sequence of LPCAT2 (UniProt entry: Q7L5N7-1), but protein bands were observed at the 50 kDa marker band. However, example blots of the manufacturer (PA539008, Thermo Fisher Scientific) revealed a similar size in K562 and HT29 cells. Nevertheless, the identity of the protein was confirmed with another antibody obtained from SantaCruz (sc-514354).

### 5.2.2 ACSL4 and LPCAT2 overexpression effects on the oxylipin composition

To verify that the overexpression of ACSL4 and LPCAT2 indeed affected the oxylipin composition of the HEK293T system, initial experiments were performed using HEK293T\_VC, HEK293T\_ACSL4, HEK293T\_LPCAT2, HEK293T\_A+L cells and HEK293T wild-type controls (Figure 5.22 and Figure 5.23). Free and total (sum of free and esterified) oxylipins were determined as described previously, and the results were normalized on the total protein content of each sample to ensure optimal comparability [204,209–211].

Figure 5.22 displays the oxylipin analysis of selected metabolites of oleic acid (black bars), linoleic acid (grey bars), dihomo-gamma-linolenic acid (DGLA; yellow), arachidonic acid (brown), eicosapentaenoic acid (EPA; green) and docosahexaenoic acid (DHA; blue). The initial oxylipin screening revealed that HEK293T\_LPCAT2 and HEK293T\_A+L cells contained elevated total levels throughout the oxylipin spectrum. Interestingly, ACSL4 overexpression alone (HEK293T\_ACSL4) led to increased oxylipin levels of PUFAs derived from oleic acid and linoleic acid, while other oxylipins were only slightly increased. HEK293T\_VC cells showed similar or slightly decreased total oxylipin amounts compared to HEK293T wild-type cells.

Although the initial total oxylipin determination shown here was performed using one biological experiment, a clear trend was observed indicating that HEK293T\_A+L and HEK293T\_LPCAT2 cells had the strongest effects on the oxylipin levels within the HEK293T overexpression system. These initial results were later confirmed in repetition experiments, as will be shown in more detail in chapter 5.3.

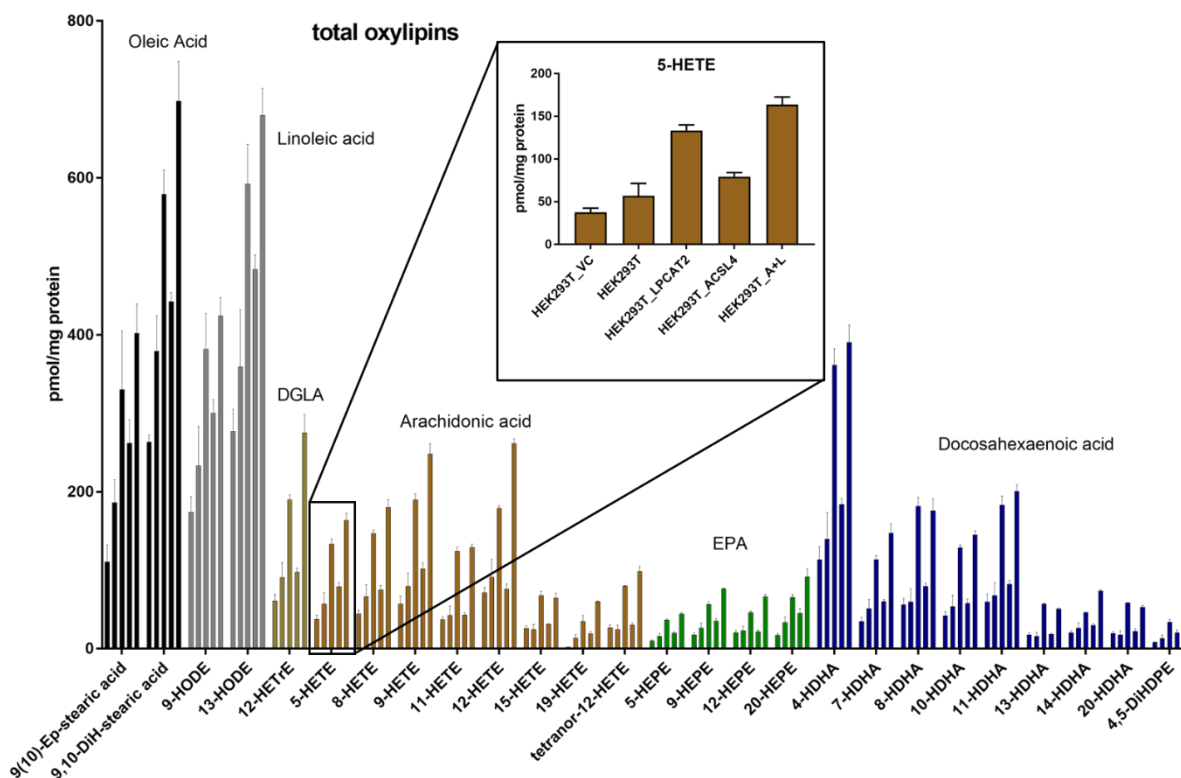


**Figure 5.22: Overview of the total oxylipin formation in different stably transfected HEK293T cell lines.**

$10 \times 10^6$  HEK293T\_VC, HEK293T wild type cells, HEK293T\_LPCAT2, HEK293T\_ACSL4, and HEK293T\_A+L cells (left to right as shown exemplarily for 5-HETE) were carefully harvested, and total oxylipins were determined by LC-MS. Colors indicate products derived from oleic acid (black), linoleic acid (grey), dihomo-gamma-linolenic acid (DGLA; yellow), arachidonic acid (brown), eicosapentaenoic acid (EPA; green) and docosahexaenoic acid (DHA; blue). Values were correlated to the total protein content of each sample and are displayed as mean + SD of triplicates from  $n=1$  experiment.



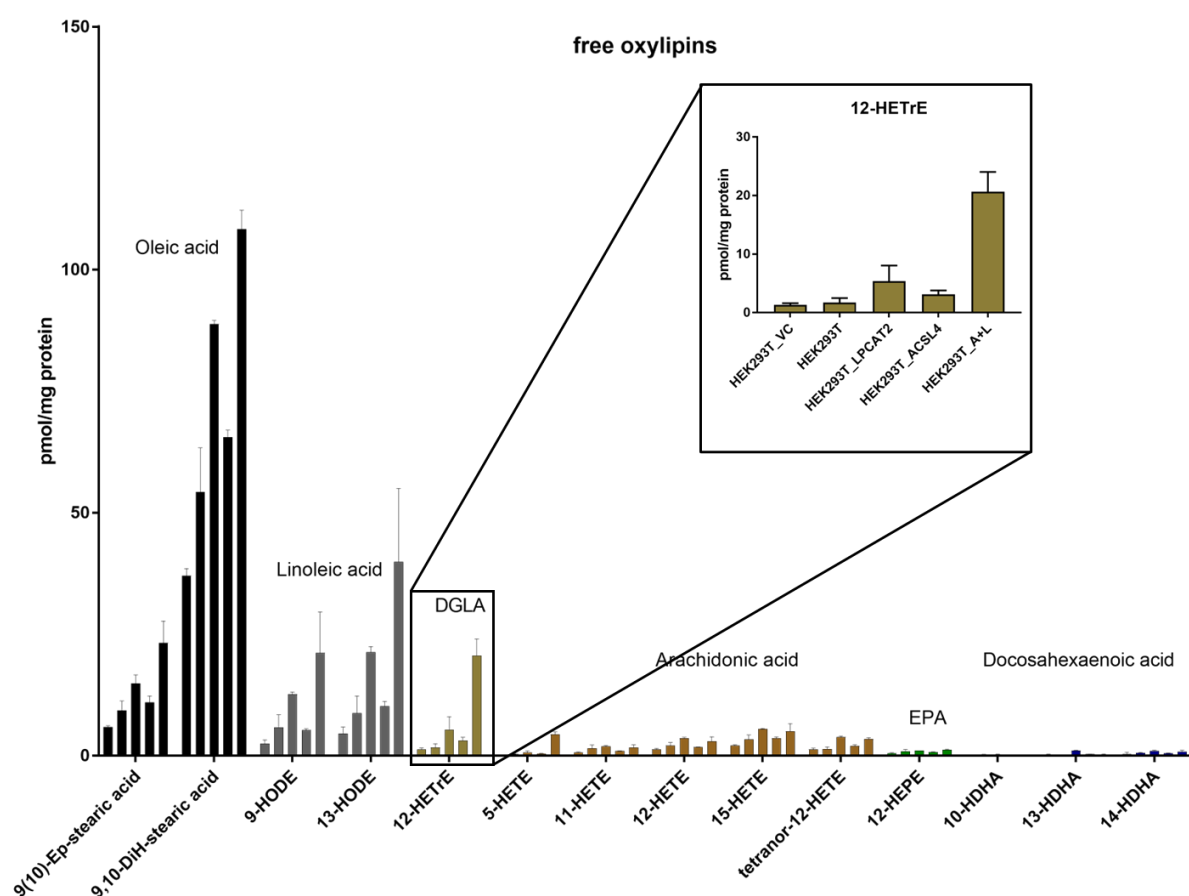


**Figure 5.23: Overview of the free oxylipin formation in different stably transfected HEK293T cell lines.**

$10 \times 10^6$  HEK293T\_VC, HEK293T wild type cells, HEK293T\_LPCAT2, HEK293T\_ACSL4, and HEK293T\_A+L cells (left to right as shown exemplarily for 12-HETE) were carefully harvested, and free oxylipins were determined by LC-MS. Colors indicate products derived from oleic acid (black), linoleic acid (grey), dihomo- $\gamma$ -linolenic acid (DGLA; yellow), arachidonic acid (brown), eicosapentaenoic acid (EPA; green) and docosahexaenoic acid (DHA; blue). Values were correlated to the total protein content of each sample and are displayed as mean + SD of triplicates from  $n=1$  experiment.

In addition to the total oxylipin investigation, free oxylipins were determined. For this purpose, another identical sample was analyzed per cell line. As shown in Figure 5.23, the free oxylipin amounts were clearly lower than the respective total levels, indicating that the majority of these oxylipins existed in an esterified form. Interestingly, the free oxylipin content varied strongly with the type of oxylipin. While 9,10-DiH-stearic acid and 13-HODE were equally represented in the total oxylipin analysis (Figure 5.22), free levels of 13-HODE were approx. 2.5-fold lower than those of 9,10-DiH-stearic acid (Figure 5.23). Nevertheless, a similar tendency of increased oxylipin levels regarding the cell lines HEK293T\_LPCAT2 and HEK293T\_A+L was observed. As already explained above, for the total oxylipin analysis, the initial investigation of these free oxylipins was performed in one biological experiment. Thus, the repetition and follow-up experiments will be shown in chapter 5.3.

Based on these initial findings, follow-up experiments were focused on the cell lines HEK293T\_A+L, HEK293T\_LPCAT2, and HEK293T\_VC. The reduction of cell lines managed in parallel was necessary to ensure comparable experimental conditions, especially with regard to the preparation of additional lipoxygenase-containing cell lines.

### 5.2.3 Transient transfection of 5-LO, 15-LO1 and 15-LO2

In order to further manipulate the oxylipin formation in these cell lines, transient transfection experiments using PEI as transfection reagent and plasmids encoding for 5-LO, 15-LO1, and 15-LO2 were tested. In an initial experiment, a time series was performed to determine the highest 15-LO1 expression. In addition, it was tested whether the presence of chloroquine was able to improve protein formation in general.

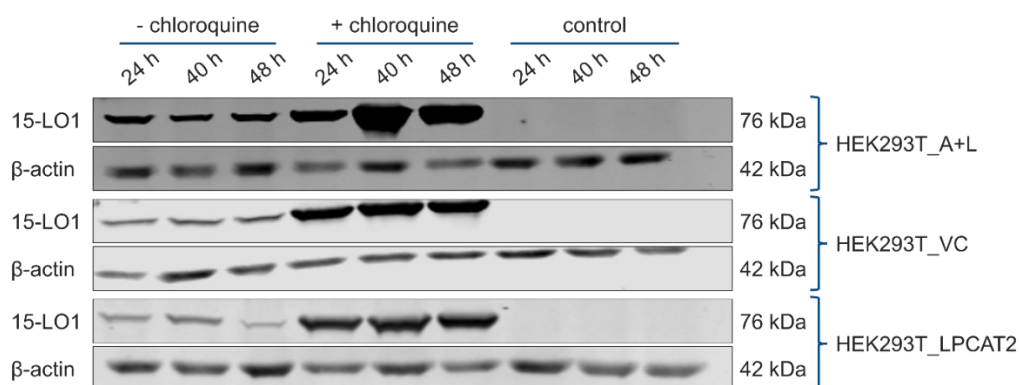


**Figure 5.24: Time series of 15-LO1 expression.**

HEK293T\_A+L, HEK293T\_VC, and HEK293T\_LPCAT2 cells were harvested 24 h, 40 h, or 48 h following transient transfection using a 15-LO1 encoding plasmid. Cell lines were treated with the transfection plasmid and 25  $\mu$ M chloroquine (+chloroquine), solely with the transfection plasmid (-chloroquine) or not at all (control).

As shown in Figure 5.24, the cell lines did not express 15-LO1 under standard conditions (controls). Following transfection, a noticeable protein expression was observed that was further increased in the presence of 25  $\mu$ M chloroquine. In HEK293T\_A+L cells, 15-LO1 expression was strongly increased after 40 h, while HEK293T\_VC and HEK293T\_LPCAT2 showed only slightly elevated protein amounts.

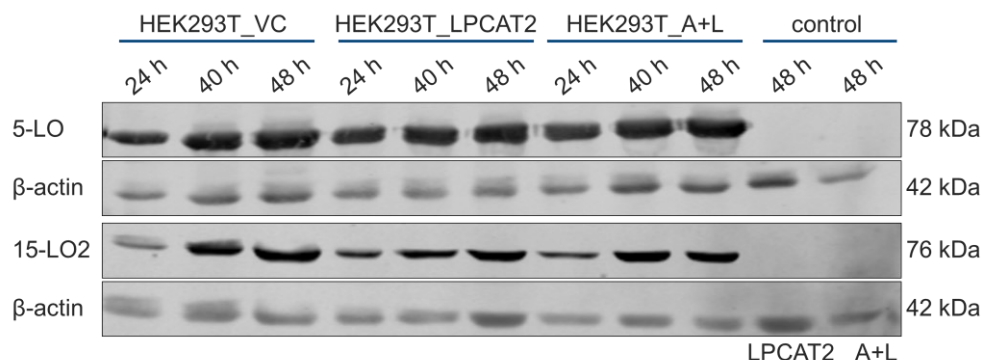


**Figure 5.25: Time series of 5-LO and 15-LO2 expression after transient transfection.**

HEK293T\_VC, HEK293T\_LPCAT2, and HEK293T\_A+L cell lines were harvested 24 h, 40 h, or 48 h after transient transfection with the respective plasmids. All cell lines were additionally treated with 25  $\mu$ M chloroquine for the time of transfection. HEK293T\_LPCAT2 and HEK293T\_A+L cells that did not receive the plasmid were used as controls, as indicated below the Western blot.

Next, a time series of the remaining LOs was prepared to investigate the optimal duration for each protein expression individually (Figure 5.25). Due to the increased 15-LO1 levels, the expression experiments with 5-LO and 15-LO2 were directly performed in the presence of

chloroquine. As shown in Figure 5.25, transient transfection of 5-LO and 15-LO2 led to a clear protein expression. While 5-LO expression was not visibly affected at different time points, 15-LO2 levels were elevated after 40 h and 48 h. Based on these findings, experiments using these transiently transfected cells were performed either 40 h (5-LO and 15-LO1) or 48 h (15-LO2) after the transfection.

#### 5.2.4 Determination of transient transfection efficiencies

Since the initial time series revealed varying protein amounts depending on the construct and cell line used, transfection efficiency of these experiments had to be determined. This was necessary to ensure optimal comparability of oxylipin levels determined in different cell lines. For this purpose, transfection constructs were extended by the red fluorescent protein mCherry. The mCherry sequence was attached to the C-terminal end of each LO, separated by a P2A linker sequence which allowed the formation of two separate proteins using the same promoter without the need for posttranslational cleavage.

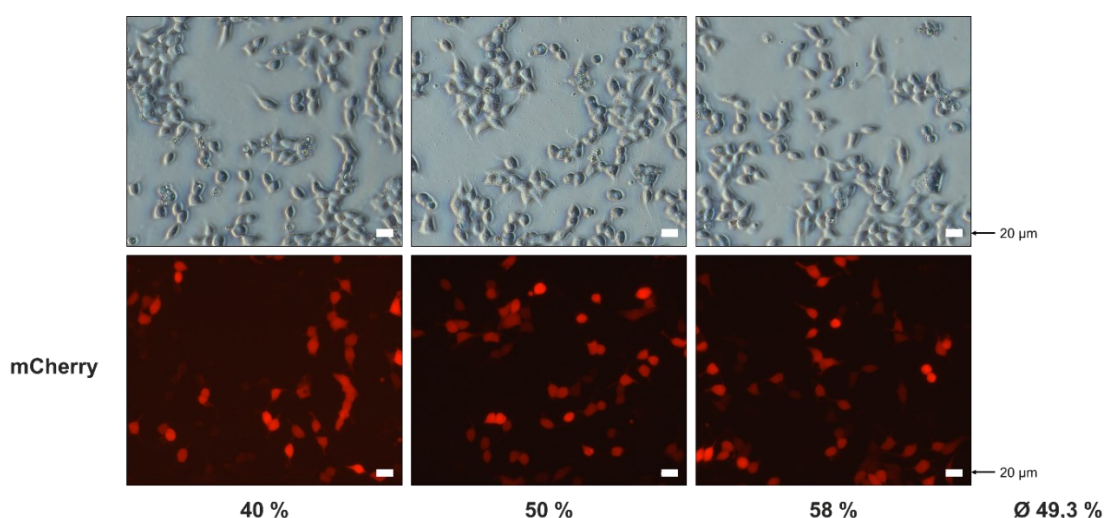


**Figure 5.26: Transfection efficiency determination.**

HEK293T cells were imaged 16 h after transfection using a 5-LO encoding plasmid and 25 µM chloroquine. Three randomly selected areas of the cell culture dish were used for imaging. The fluorescent image of each area is shown below the respective white light image. Transfection efficiencies were calculated by division of fluorescent cell numbers by the total cell number, and the respective values are shown below the images. White bars indicate 20 µm.

To determine accurate transfection efficiencies, three randomly selected areas were imaged per cell culture dish (Figure 5.26). Both white light and fluorescent images were taken of each area, and the respective transfection efficiencies were calculated as the ratio of mCherry positive to total cell number. On average, the transfection efficiency of the 5-LO construct was 49.3 %. As the procedure of calculating the transfection efficiency of only one cell line was already quite time-consuming, the suitability of the technique was questioned with regard to the enormous number of samples that would be required to analyze all cell lines. To ensure that the effort was justified, activity studies with the LO/mCherry constructs were performed in advance.

### 5.2.4.1 LO product formation following transient transfection of LO/mCherry constructs

Analysis of the LO product formation was performed as described by Kreiß *et al.* [282]. For this purpose, transiently transfected cells were counted and assayed, as described in chapter 4.8.3. LO constructs without fluorescent protein-tag were used as positive controls. Surprisingly, LO product formation could not be detected for any mCherry construct, while positive controls gave strong signals.

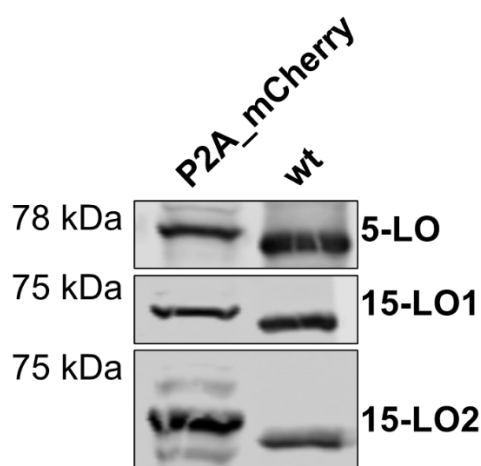


**Figure 5.27: Western blot analysis of 5-LO, 15-LO1, and 15-LO2 expression in transiently transfected HEK293T\_LPCAT2 cells.**

$5 \times 10^6$  HEK293T\_LPCAT2 cells were transiently transfected with 5-LO, 15-LO1, or 15-LO2 containing plasmids either alone or in combination with mCherry as fluorescent protein-tag. Cells were cultivated for 24 h post transfection before protein expression was analyzed. The type of LO is given on the right side, while the construct type is indicated on the top (P2A\_mCherry: Combined construct with fluorescent protein-tag, wt: Wild-type LO construct).

Thus, Western blot analysis was performed to investigate potential issues with the P2A linker that was used for protein separation of LO and mCherry (Figure 5.27). A comparison of LO sizes revealed that the P2A\_mCherry constructs were slightly larger in size, indicating that part of the P2A linker was attached to the C-terminus of each LO. As the C-terminus of LOs is responsible for their catalytic activity, the remaining part of the linker seemed to prevent proper folding leading to inactive enzymes.

The fact that the enzymes were not able to form products together with low transfection efficiencies and a time-consuming procedure raised the need for an alternative approach. Thus, the transient transfection approach was not continued.

### 5.2.5 Doxycycline-dependent expression of 5-LO, 15-LO1 and 15-LO2

Because the transient transfection approach was not successful, stable transfection was considered as an alternative. As the stable transfection using the ‘Sleeping Beauty’ method worked out very well for the constitutive overexpression of ACSL4 and LPCAT2, the same technique should be utilized here. However, to prevent the new cell lines from an unwanted early cell death caused by permanent overexpression of multiple enzymes, the LO expression had to be controlled by a Tet-On system. Ideally, this would allow the precise activation of LO expression only during an experimental setup. HEK293T\_VC, HEK293T\_LPCAT2, and

HEK293T\_A+L cell lines were transfected with constructs carrying either the 5-LO, 15-LO1, or 15-LO2 genes. As a result, three new cell lines were generated per initial cell line, as shown in Table 5.9.

**Table 5.9: Overview of LO containing HEK293T cell lines.**

	HEK293T_VC	HEK293T_LPCAT2	HEK293T_A+L
<b>5-LO</b>	HEK293T_VC_5LO	HEK293T_LPCAT2_5LO	HEK293T_A+L_5LO
<b>15-LO1</b>	HEK293T_VC_15LO1	HEK293T_LPCAT2_15LO1	HEK293T_A+L_15LO1
<b>15-LO2</b>	HEK293T_VC_15LO2	HEK293T_LPCAT2_15LO2	HEK293T_A+L_15LO2

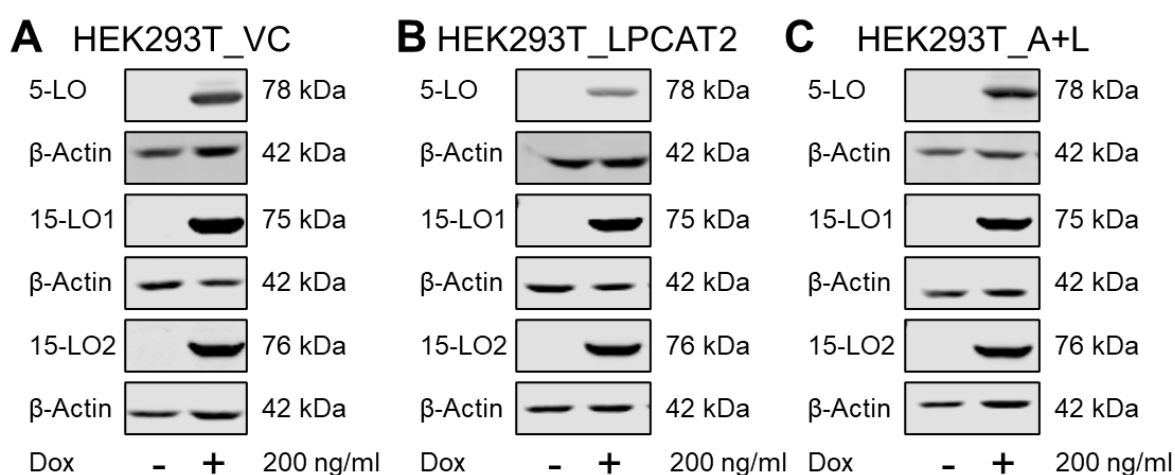


**Figure 5.28: Doxycycline-dependent expression of 5-LO, 15-LO1 and 15-LO2.**

Inducible protein expression of 5-LO, 15-LO1, and 15-LO2 following doxycycline treatment (Dox, 200 ng/mL, 24 h) analyzed by Western blot. Each blot displays one different stable cell line derived from either HEK293T\_VC (A), HEK293T\_LPCAT2 (B), or HEK293T\_A+L (C). A representative blot is shown per experiment.

The respective new cell lines were treated with 200 ng/mL doxycycline for 24 h to induce LO expression, and the results were analyzed on protein level, as shown in Figure 5.28. The Western blot analysis revealed that there was no LO expression under standard cultivation conditions. In contrast, when treated with doxycycline, strong protein bands were visible. This was observed throughout all cell lines, independent of the respective LOs. Although the inducible protein expression was highly reproducible, activity studies had to be performed in advance of further oxylipin investigations.

#### 5.2.5.1 LO product formation using a doxycycline-dependent expression system

Following verification of the inducible LO expression after doxycycline treatment, the activity of each LO had to be investigated. For this purpose, the expression of each LO was induced by treatment with 200 ng/mL doxycycline for 24 h, and the activity was determined as described by Kreiß *et al.* [282]. Untreated cells were used as controls, and the results are shown in Figure 5.29.

Following doxycycline treatment, 5-LO expression led to the formation of 5-HETE and LTs (6-*trans*-LTB<sub>4</sub>, 6-*trans*-12-*epi*-LTB<sub>4</sub>, and LTB<sub>4</sub>) in HEK293T\_VC\_5LO, HEK293T\_A+L\_5LO, and HEK293T\_LPCAT2\_5LO cells, while untreated cells showed no product formation at all. This was also true for 15-LO1 and 15-LO2 expressing cell lines following doxycycline treatment. While 15-LO1 expression led to the formation of mainly 15-HETE with fewer 12-HETE, 15-LO2 expressing cell lines led exclusively to 15-HETE formation. As already seen for 5-LO-containing cell lines, no relevant product formation was observed in untreated cells.

The results of the activity study were in accordance with the analysis on protein level, and thus, further characterization studies were continued using these cell lines.

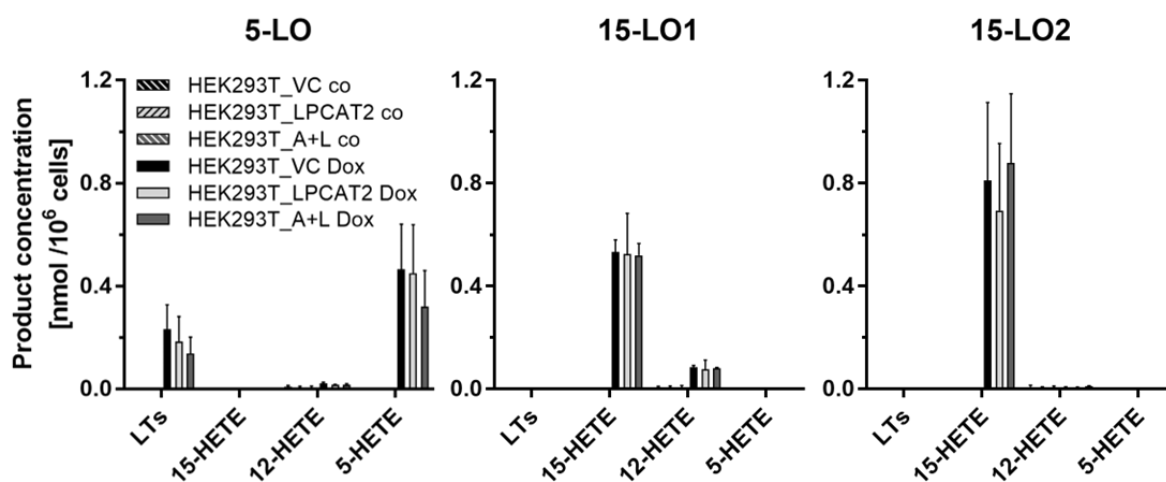


**Figure 5.29: LO product formation in transfected HEK293T cells.**

LO product formation was analyzed in cells with (HEK293T\_LPCAT2\_LO, HEK293T\_A+L\_LO) or without (HEK293T\_VC\_LO) stable overexpression of LPCAT2 and LPCAT2/ACSL4 and inducible expression of either 5-LO, 15-LO1 or 15-LO2. For LO expression, cells were treated with (plain bars) or without (hatched bars) 200 ng/mL doxycycline for 24 h. Afterward,  $5 \times 10^6$  cells were stimulated by 20  $\mu$ M AA, 2.5  $\mu$ M calcium ionophore A23187, and 1 mM CaCl<sub>2</sub> for 10 min at 37 °C and products were analyzed by LC-UV. Data were normalized on  $10^6$  cells (mean + SD, n=3). Leukotrienes (LTs): 6-*trans*-LTB<sub>4</sub>, 6-*trans*-12-*epi*-LTB<sub>4</sub> and LTB<sub>4</sub>.

### 5.2.6 Laser scanning confocal microscopy investigation of ACSL4 and LPCAT2 localization

The short ACSL4 isoform that was used in this work is reported to have a mainly cytosolic localization but is also found at the plasma membrane. In contrast, the long isoform is found in the ER and LDs [45]. Similarly, LPCAT2 is also found in the ER [22] and LDs [77,78]. Since none of these studies were performed in HEK293T cells, laser scanning confocal microscopy studies were conducted next to further characterize the cell lines. Confocal images were kindly taken by Tamara Göbel.

The first analysis included the localization of ACSL4 and LPCAT2 in HEK293T\_VC\_LO and HEK293T\_LPCAT2\_LO (LO: 5-LO, 15-LO1 or 15-LO2) cells (Figure 5.30). Cells were treated with 200 ng/mL doxycycline for 24 h before the fixation and staining procedure was performed. ACSL4 was clearly expressed in both cell lines and was present exclusively in the cytosol. This finding was in accordance with the earlier Western blot analysis of the stably transfected cell

lines, which indicated a visible protein expression in all cells (see chapter 5.2.1). While LPCAT2 was also found exclusively within the cytosol in both cell lines, HEK293T\_VC\_LO cells revealed the formation of small circular spots with increased LPCAT2 concentrations. LPCAT2 is known to occur in lipid droplets, which might be an explanation for the observed behavior. In contrast, there were no circular spots observed in cells that overexpress LPCAT2 (HEK293T\_LPCAT2\_LO).

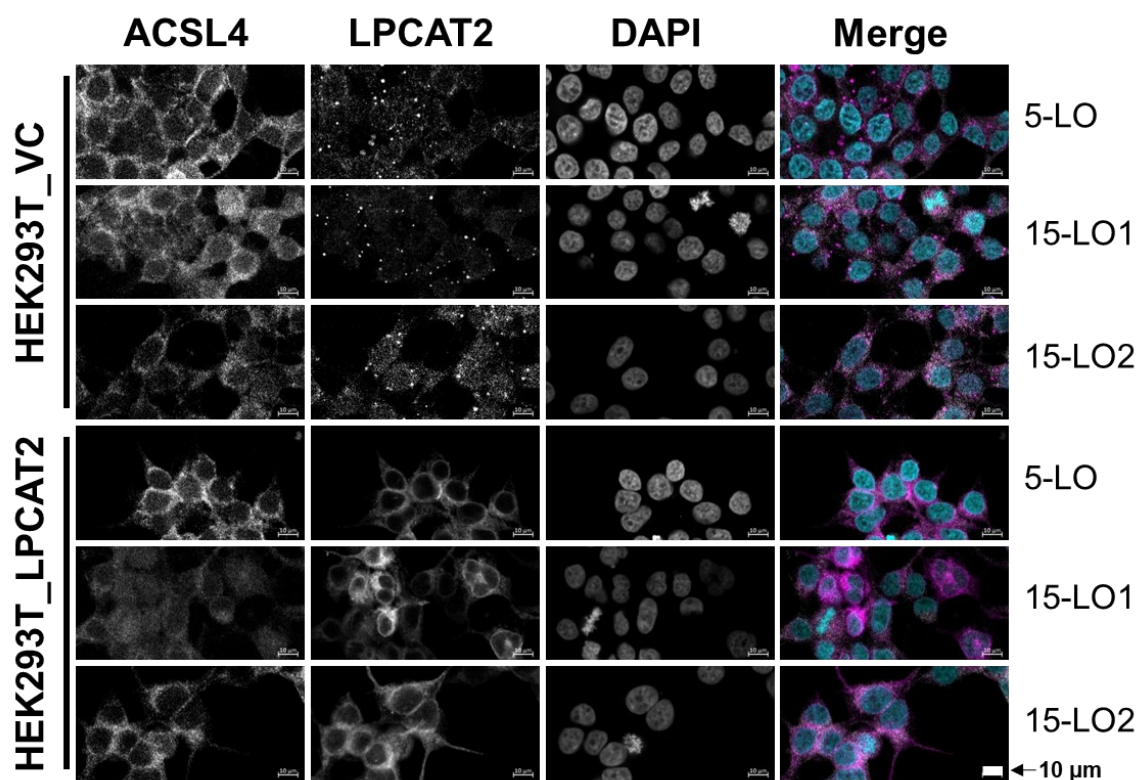


**Figure 5.30: Localization of ACSL4 and LPCAT2 in HEK293T\_VC and HEK293T\_LPCAT2 cells.**

HEK293T\_VC\_LO and HEK293T\_LPCAT2\_LO (LO: 5-LO, 15-LO1 or 15-LO2), induced with 200 ng/mL doxycycline for 24 h, were stained with fluorophore-conjugated secondary antibodies against specific primary antibodies. Nuclei were counterstained using DAPI. Cells were imaged and analyzed on a Zeiss 780 AxioObserver.Z1 laser scanning confocal microscope (Carl Zeiss AG). Images display a representative part of the acquired total image. The fluorescence of single channels is shown in black and white for better contrast, with the overlaid image shown in color (ACSL4: white; LPCAT2: purple, DAPI: turquoise). 10 µm scale bars are given in each image. Brightness and contrast were adjusted in a linear fashion. Images display one of 3 independent experiments.

Next, HEK293T\_A+L\_LO (LO: 5-LO, 15-LO1, or 15-LO2) cells were analyzed regarding the localization of ACSL4 and LPCAT2 (Figure 5.31). In accordance with HEK293T\_VC\_LO and HEK293T\_LPCAT2\_LO cells, ACSL4 was found within the cytosol, indicating that the stable overexpression had no effect on the localization. LPCAT2 expression was also found within the cytosol, as it was seen before in HEK293T\_LPCAT2\_LO cells. Interestingly, a few circular LPCAT2 expression spots were observed this time. As HEK293T\_VC\_LO cells showed plenty of spots, HEK293T\_A+L\_LO cells contained only a few, and HEK293T\_LPCAT2\_LO cells had none, this behavior seemed to be caused by different LPCAT2 amounts. As already seen on Western blot level (see chapter 5.2.1), LPCAT2 expression is increased by 13- and 30-fold in HEK293T\_A+L and HEK293T\_LPCAT2 cells, respectively.



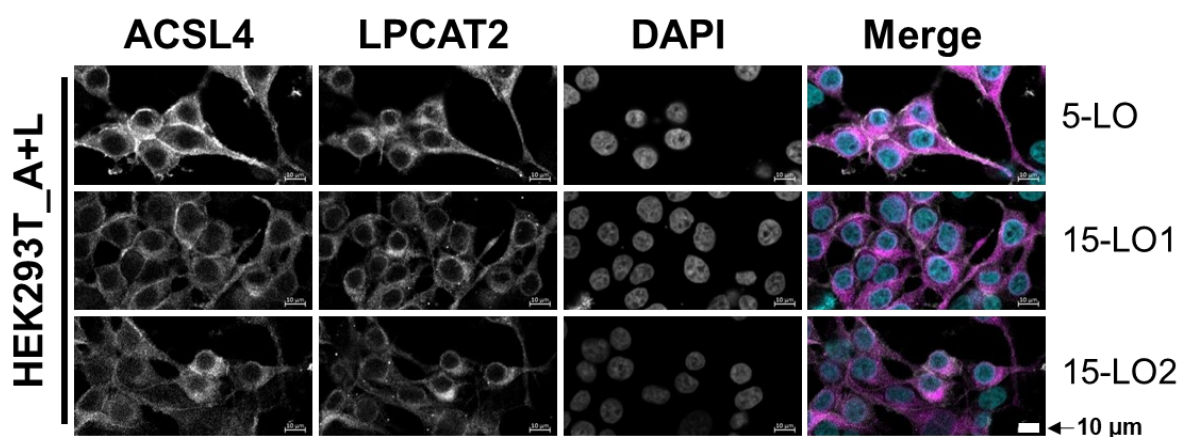


**Figure 5.31: Localization of ACSL4 and LPCAT2 in stably transfected HEK293T\_A+L cells.**

HEK293T\_A+L\_LO cells (LO: 5-LO, 15-LO1 or 15-LO2), induced with 200 ng/ml doxycycline for 24 h, were stained with fluorophore-conjugated secondary antibodies against specific primary antibodies (ACSL4: white; LPCAT2: purple). Nuclei were counterstained using DAPI (turquoise). Cells were imaged and analyzed on a Zeiss 780 AxioObserver.Z1 laser scanning confocal microscope (Carl Zeiss AG). Images display a representative part of the acquired total image. The fluorescence of single channels is shown in black and white for better contrast, with the overlaid image shown in color. 10 µm scale bars are given in each image. Brightness and contrast were adjusted in a linear fashion. Images display one of 3 independent experiments.

### 5.3 Biological characterization of esterified lipid mediators formed in stably transfected HEK293T cells

Once the stable HEK293T overexpression system was established and verified, as described in chapter 5.2, the formation of esterified oxylipins had to be studied in more detail. For this purpose, the initial oxylipin analysis (see chapter 5.2.2) was repeated, and the sample set was expanded by the cell lines HEK293T\_A+L\_LO, HEK293T\_LPCAT2\_LO and HEK293T\_VC\_LO (LO: 5-LO, 15-LO1 or 15-LO2).

#### 5.3.1 Investigation of free and total oxylipins in stably transfected HEK293T cells

A comprehensive set of oxylipins derived from LO-mediated conversion of endogenous ARA, EPA, and DHA was analyzed in collaboration with Laura Carpanedo and Susanne Reif of the Schebb laboratory in Wuppertal. Samples were prepared as described before (see chapter 4.7.7). In short, LO expression was induced by treatment with 200 ng/mL doxycycline for 24 h prior to sample collection. Oxylipin analysis was performed by LC-MS as described previously [204,209–211], and the complete oxylipin analysis, including all metabolites, can be found in appendix chapter 9.5. To get an impression of the oxylipin pattern in these cells without being overwhelmed by the amount of data, Figure 5.32 displays the six most prominent oxylipins in each cell line. Product formation in HEK293T\_VC\_5-LO, HEK293T\_LPCAT2\_5-LO, and HEK293T\_A+L\_5-LO cell lines was comparably low with values between 1.44 nmol/g total protein and 5.48 nmol/g total protein (Figure 5.32A).



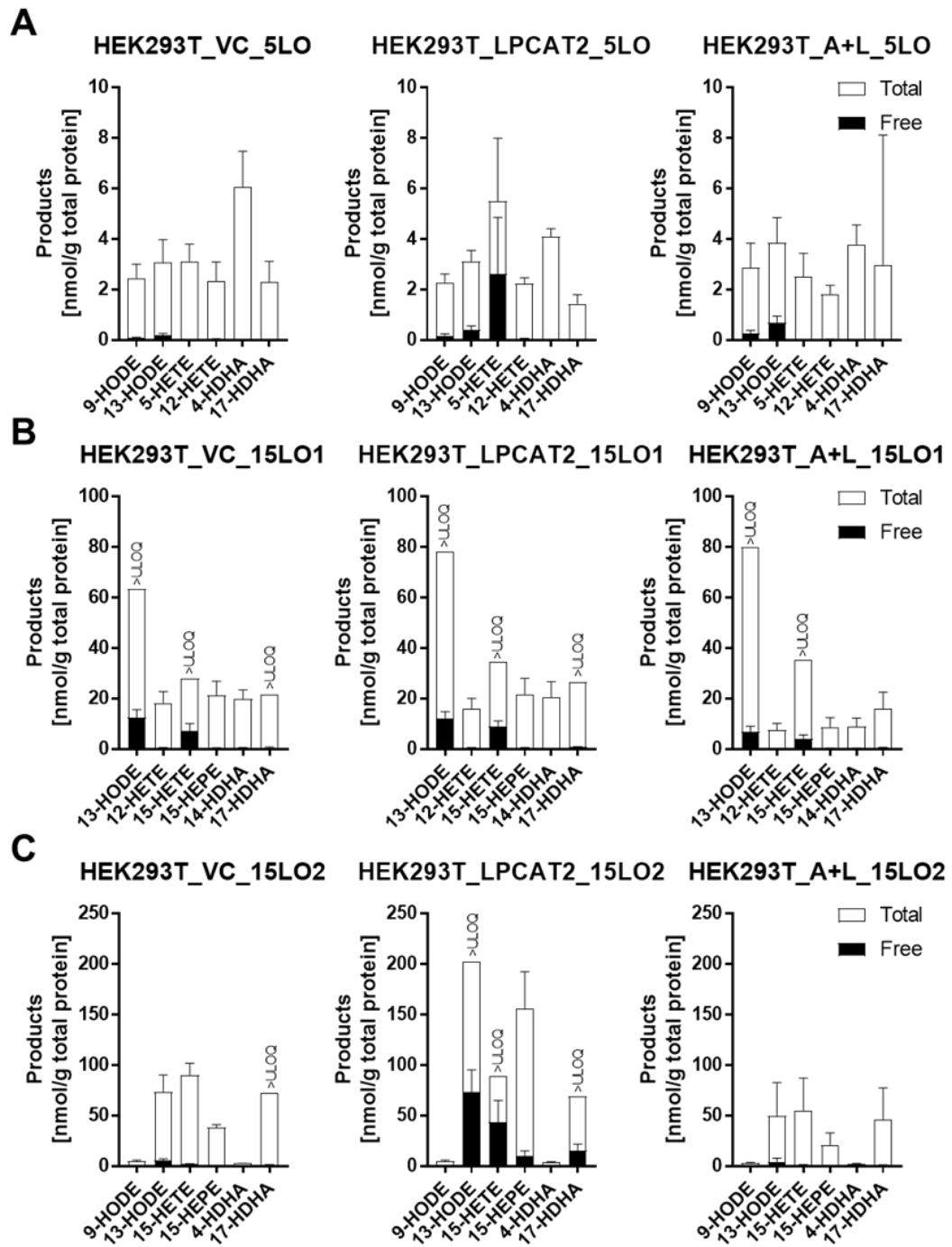


**Figure 5.32: Oxylipin formation in HEK293T\_VC\_LO, HEK293T\_LPCAT2\_LO, and HEK293T\_A+L\_LO cells.**

LO expression was induced with 200 ng/mL doxycycline for 24 h. Pellets of at least  $10^7$  cells were prepared and analyzed by LC-MS. Free and total oxylipin levels were determined and correlated to the total protein content of each sample. Shown are the six most prominent oxylipins of 5-LO containing (A), 15-LO containing (B), and 15-LO2 containing (C) cell lines (see appendix chapter 9.5 for the complete analysis of all metabolites). Total oxylipin levels are displayed as white bars, while the respective free oxylipin levels are shown as black bars within. Samples that reached the upper limit of quantification (UOQ) are indicated as such. Values are displayed as mean + SD of  $n=3$  experiments.

Aside from 5-HETE formation in HEK293T\_LPCAT2\_5-LO cells, which reached 46 % of the total amount, the remaining free oxylipin levels did not exceed 27 % of the respective total amounts. Especially 12-HETE, 4-HDHA, and 17-HDHA were almost completely esterified in

all 5-LO-expressing cell lines. In 15-LO1 expression cell lines (Figure 5.32B), oxylipin levels were clearly elevated compared to 5-LO-containing cells. The main products of 15-LO1, 13-HODE, and 15-HETE reached the upper limit of quantification (ULOQ) in all three cell lines. In addition, 17-HDHA was found in the ULOQ in HEK293T\_VC\_15LO1 and HEK293T\_LPCAT2\_15LO1 cells. Among the different oxylipins, 13-HODE formation was the strongest with >63, >78, and >79 nmol/g total protein in HEK293T\_VC\_15LO1, HEK293T\_LPCAT2\_15LO1 and HEK293T\_A+L\_15LO1, respectively. 15-HETE levels were the second strongest, followed by 17-HDHA. Even higher oxylipin levels were found in 15-LO2-containing cell lines (Figure 5.32C). Interestingly, oxylipin levels were especially enhanced in HEK293T\_LPCAT2\_15LO2 cells. Here, 13-HODE, 15-HETE, and 17-HDHA reached the ULOQ with >202, >89, and >68 nmol/g total protein, respectively. In addition, 15-HEPE was formed with 155.8 nmol/g total protein, indicating that the 15-LO2 enzyme was highly active and did not distinguish between LA, ARA, EPA, and DHA as substrate. Although oxylipin levels were lower in HEK293T\_VC\_15LO2 and HEK293T\_A+L\_15LO2 cells, 13-HODE, 15-HETE, 15-HEPE, and 17-HDHA were again the mainly formed oxylipins. As already seen for the 5-LO-containing cell lines, oxylipins derived from 15-LO1 and 15-LO2 were mainly present in their esterified form. Interestingly, 13-HODE and 15-HETE were also the most prominent free oxylipins found, while 15-HEPE and 17-HDHA were only found in their free form in relevant amounts in HEK293T\_LPCAT2\_15LO2 cells.

### 5.3.2 Cell viability investigation using ferroptosis-inducing agents

As described in 2012 by Dixon *et al.*, an increase in ACSL4 expression as well as enhanced lipid peroxidation, are associated with the cell death mechanism known as ferroptosis [59]. An insertional mutagenesis study also indicated a connection of LPCAT3 with ferroptosis, which raised the question of whether LPCAT2 might also be involved [126].

In order to investigate a potential connection with ferroptosis, HEK293T\_VC, HEK293T\_LPCAT2, and HEK293T\_A+L cells were treated with RSL3 or erastin, small molecules known to be ferroptosis-inducing agents. In order to analyze the behavior of the stable overexpression system, cell viability was determined by WST-1 assay. For this purpose, the ferroptosis-inducing agents erastin and RSL3 were used in varying concentrations, and the results are shown in Figure 5.33. Cell viability of treated cells was compared to DMSO controls. Treatment with 1  $\mu$ M erastin led to a decrease in cell viability in HEK293T\_LPCAT2 and HEK293T\_A+L cells but did not affect HEK293T\_VC cells. At higher concentrations, erastin also affected HEK293T\_VC cells and led to overall reduced cell viability. Although most effects were not significant, cell lines seemed to be affected with ascending order from HEK293T\_VC over HEK293T\_LPCAT2 to HEK293T\_A+L cells. When treated with RSL3, HEK293T\_VC cells were not affected up to a concentration of 3  $\mu$ M. In contrast, HEK293T\_LPCAT2 and HEK293T\_A+L cells were already affected at 0.1  $\mu$ M RSL3. Especially the cell viability of HEK293T\_A+L cells was significantly decreased at several concentrations (0.1  $\mu$ M, 3  $\mu$ M, and 10  $\mu$ M). Overall, RSL3 and erastin treatment had the strongest effects on HEK293T\_A+L cells, except for 1  $\mu$ M RSL3, where HEK293T\_LPCAT2 cells were similarly affected.

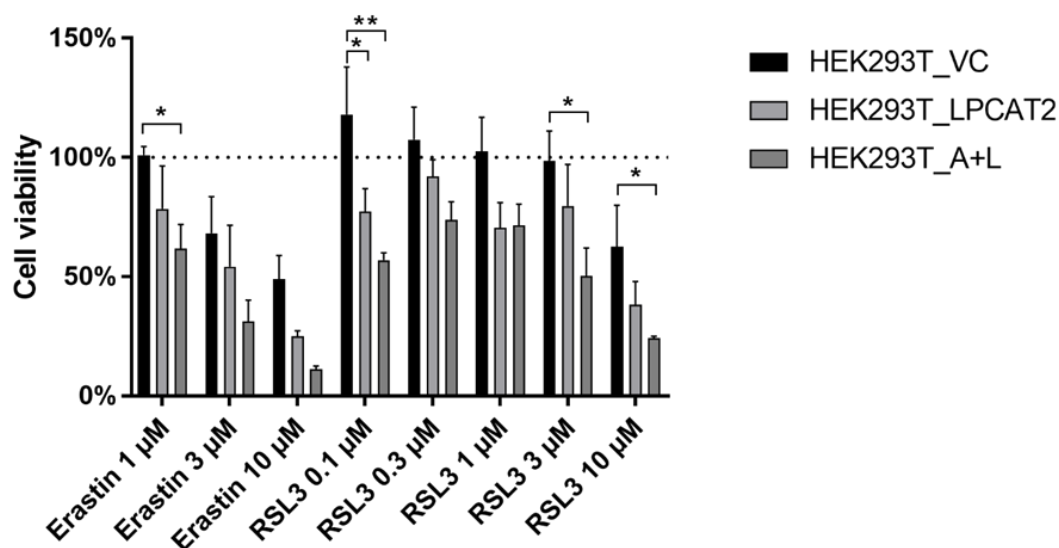


**Figure 5.33: Effects of RSL3 and erastin treatment on the cell viability of stably transfected HEK293T cells.**

$2.5 \times 10^4$  HEK293T\_VC, HEK293T\_LPCAT2, and HEK293T\_A+L cells were treated with varying concentrations of RSL3 or erastin for 24 h followed by treatment with 10  $\mu$ L WST-1 reagent for 2 h at 37 °C. DMSO-treated cells were used as controls and set to 100 %. Absorbance at 450 nm and 690 nm was determined using a Tecan infinite® M200 plate reader. Statistical analysis was performed against DMSO controls using 2-way ANOVA with Dunnet's multiple comparisons test (mean + SD, n=3). \*  $P < 0.05$ , \*\*  $P < 0.01$ .

### 5.3.3 Investigation of LO and LPCAT2 localization following treatment with ferroptosis-inducing agents

Since treatment with the ferroptosis-inducing agents erastin and RSL3 affected the cell viability, especially in LPCAT2-containing cells, laser scanning confocal microscopy investigations were repeated with respective treatments. For this purpose, LO expression was induced in HEK293T\_VC\_LO, HEK293T\_LPCAT2\_LO, and HEK293T\_A+L\_LO cells with 200 ng/mL doxycycline for 24 h before treatment with 3  $\mu$ M erastin or 10  $\mu$ M RSL3 for 24 h or 4 h, respectively. Initially, a duration of 24 h was planned for both compounds according to the cell viability data. However, treatment with 10  $\mu$ M RSL3 for 24 h caused detachment of the cells and thereby prevented confocal analysis. Thus, the incubation duration of the RSL3 treatment had to be shortened to 4 h instead. For a better comparison, the merged confocal images of HEK293T\_A+L\_LO cells are shown in Figure 5.34, and HEK293T\_VC\_LO and the images of HEK293T\_LPCAT2 cells are shown in Figure 5.35. The respective single channels can be found in appendix chapter 9.4.

5-LO was found in the cytosol, and its localization was not affected by treatment with erastin or RSL3 (Figure 5.34). The same behavior was observed for 15-LO2 in treated and control cells (co). Interestingly, 15-LO1 was localized around the nucleus in control cells. Furthermore, when treated with RSL3 or erastin, part of the 15-LO1 protein seemed to move inside the nucleus.

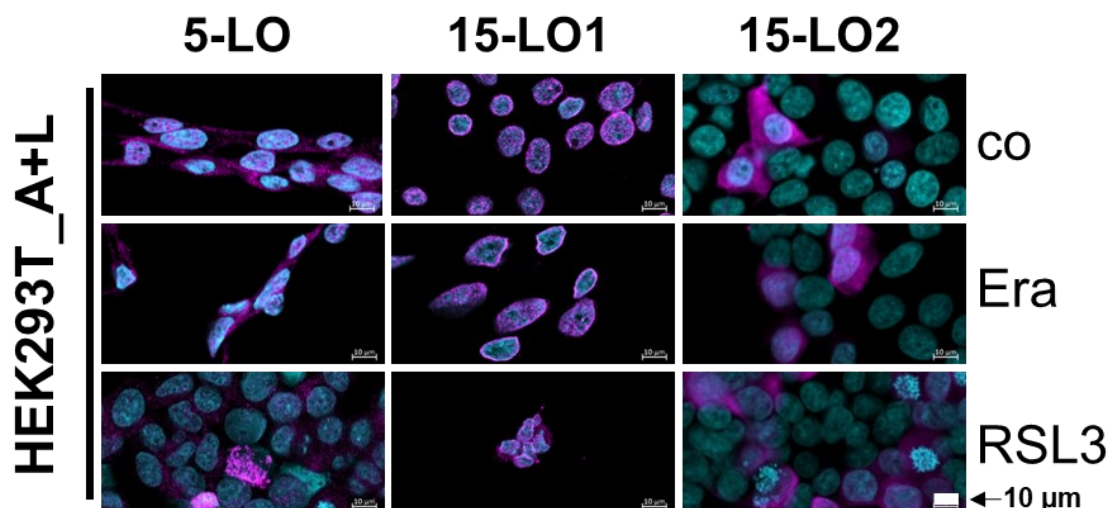


**Figure 5.34: Effect of ferroptosis inducers on the localization of lipoygenases in stably transfected HEK293T cells.**

HEK293T\_A+L\_LO (left: 5-LO, center: 15-LO1, right: 15-LO2) cells were treated with 200 ng/ml doxycycline for 24 h before treatment with 10  $\mu$ M RSL3 or 3  $\mu$ M erastin (Era) for 4 h or 24 h, respectively. Controls (co) received DMSO. Cells were stained with fluorophore-conjugated secondary antibodies against specific primary antibodies (LOs: purple). Nuclei were counterstained using DAPI (turquoise). Cells were imaged and analyzed on a Zeiss 780 AxioObserver.Z1 laser scanning confocal microscope (Carl Zeiss AG). Images display a representative part of the acquired total image. Overlaid images are shown, and 10  $\mu$ m scale bars are given in each image. Brightness and contrast were adjusted in a linear fashion. Images display one of 3 independent experiments (except HEK293T\_A+L\_15LO2, RSL3, n=2).

Figure 5.35 displays the localization of 5-LO, 15-LO1, and 15-LO2 in HEK293T\_VC\_LO and HEK293T\_LPCAT2\_LO cells. Under control (co) conditions, each LO was present within the cytosol of HEK293T\_VC\_LO cells. When treated with erastin (Era), 5-LO translocated to or into the nucleus, while 15-LO1 and 15-LO2 localization was not affected. On the contrary, RSL3 treatment did not affect 5-LO or 15-LO2 localization but led to 15-LO1 localization at the nuclear envelope. In contrast, HEK293T\_LPCAT2\_LO cells revealed a 5-LO and 15-LO2 localization all over the cell. Interestingly, 15-LO1 was found at the nuclear envelope in HEK293T\_LPCAT2\_LO cells even without treatment of RSL3 or erastin. Treatment with either one of the ferroptosis-inducing agents had no further effect on the localization.

Since overexpression of LPCAT2 had an effect, especially on the localization of 15-LO1, further investigations were performed focusing on the cell lines HEK293T\_LPCAT2\_5LO, HEK293T\_LPCAT2\_15LO1, and HEK293T\_LPCAT2\_15LO2. For this purpose, 5-LO, 15-LO1, or 15-LO2 were co-stained with LPCAT2 in combination with RSL3 or erastin treatment (Figure 5.36A). All cell lines displayed a cytosolic localization for LPCAT2 independent of the respective LO and the treatment with RSL3 or erastin. 5-LO and 15-LO2 were located all over the cells without being affected by RSL3 or erastin treatment. As seen before, 15-LO1 was found at the nuclear envelope even without treatment of RSL3 or erastin. Once the cells were treated, 15-LO1 was partially observed within the soluble part of the nucleus.

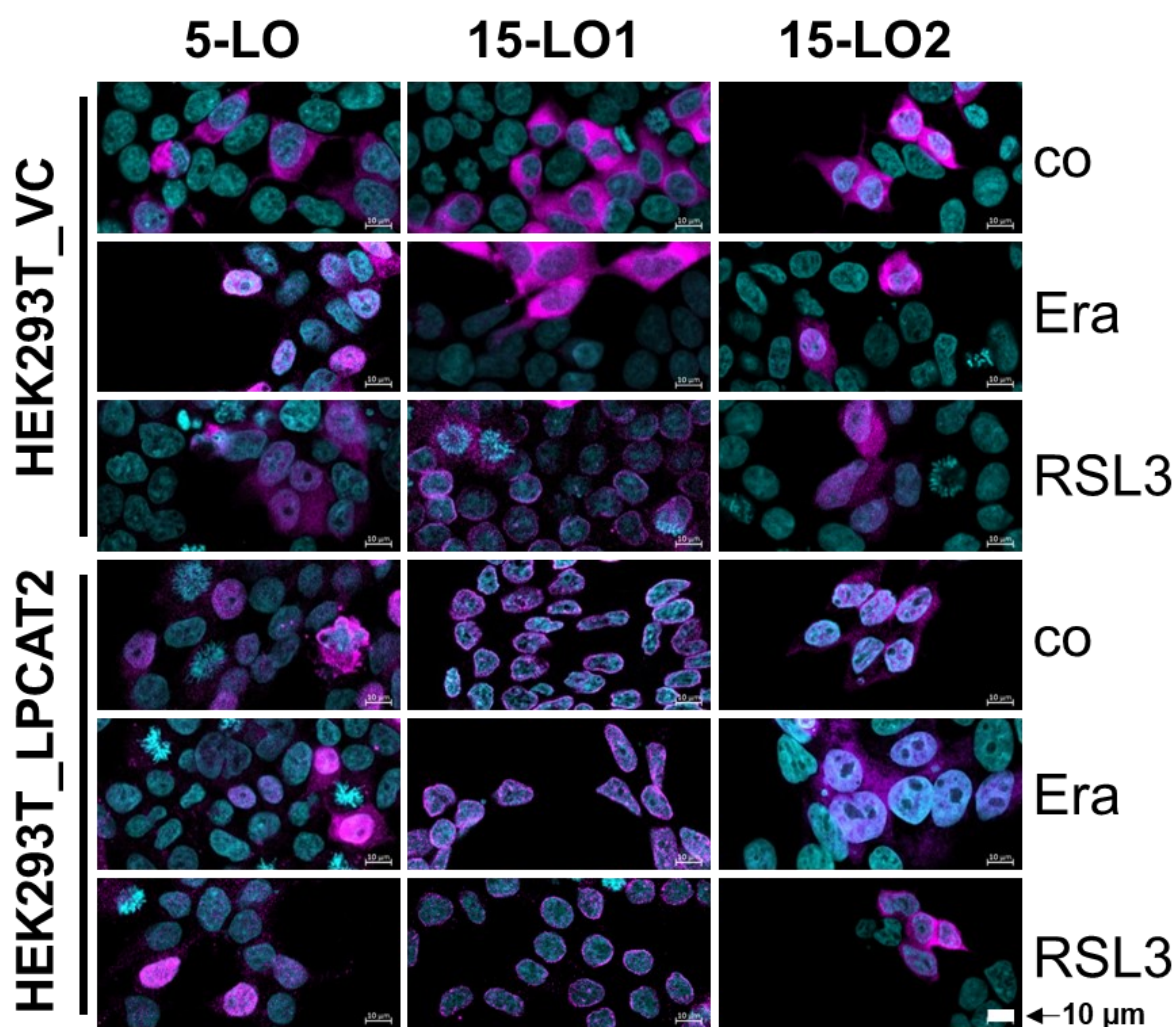


**Figure 5.35: Effect of ferroptosis inducers on the localization of lipoxygenases in stably transfected HEK293T cells.**

HEK293T\_VC\_LO and HEK293T\_LPCAT2\_LO (left: 5-LO, center: 15-LO1, right: 15-LO2) cells were treated with 200 ng/mL doxycycline for 24 h before treatment with 10  $\mu$ M RSL3 or 3  $\mu$ M erastin (Era) for 4 h or 24 h, respectively. Controls (co) received DMSO. Cells were stained with fluorophore-conjugated secondary antibodies against specific primary antibodies (LOs: purple). Nuclei were counterstained using DAPI (turquoise). Cells were imaged and analyzed on a Zeiss 780 AxioObserver.Z1 laser scanning confocal microscope (Carl Zeiss AG). Images display a representative part of the acquired total image. Overlaid images are shown with 10  $\mu$ m scale bars. Brightness and contrast were adjusted in a linear fashion. Images display one of 3 independent experiments.

The new images confirmed the initial findings that 15-LO1 was located at the nuclear envelope in the presence of LPCAT2. Thus, the intensities of the respective markers were analyzed in correlation to their cellular localization (Figure 5.36B). The DAPI signal (turquoise) represented the nuclear compartment, and the histogram indicated that there was basically no LPCAT2 or 15-LO1 inside the nucleus. Interestingly, both 15-LO1 and LPCAT2 displayed a peak at the nuclear membrane, indicating a co-localization.



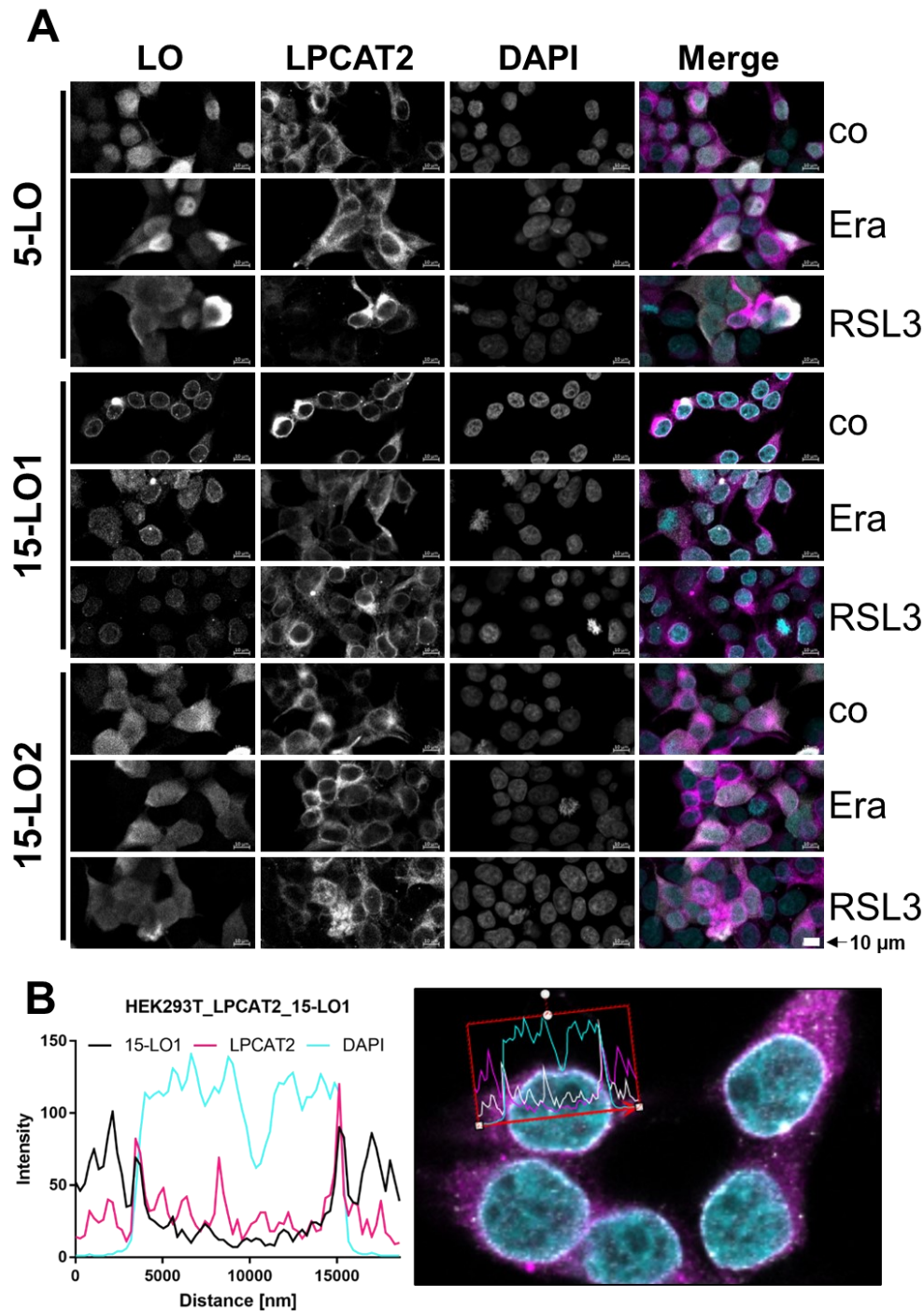


**Figure 5.36: Localization of LOs in stably transfected HEK293T\_LPCAT2 cells.**

HEK293T\_LPCAT2\_LO (LO: 5-LO, 15-LO1 or 15-LO2) cells were treated with 200 ng/mL doxycycline for 24 h before treatment with 10  $\mu$ M RSL3 or 3  $\mu$ M erastin (Era) for 4 h or 24 h, respectively. Controls (co) received DMSO. Cells were stained with fluorophore-conjugated secondary antibodies against specific primary antibodies. Nuclei were counterstained using DAPI. Cells were imaged and analyzed on a Zeiss 780 AxioObserver.Z1 laser scanning confocal microscope (Carl Zeiss AG). (A) Images display a representative part of the acquired total image. The fluorescence of single channels is shown in black and white for better contrast, with the overlaid image shown in color (LOs: white; LPCAT2: purple, DAPI: turquoise). 10  $\mu$ m scale bars are given in each image. Images display one of 3 independent experiments. (B) Histogram of fluorescence intensities (15-LO1: black, LPCAT2: purple, DAPI: turquoise) vs. distance (left) of a cellular profile (right, 15-LO1: white, LPCAT2: purple, DAPI: turquoise) of HEK293T\_LPCAT2\_15LO1 cells. Brightness and contrast were adjusted in a linear fashion.

### 5.3.4 Investigation of the influence of ferroptosis-inducing agent RSL3 on the oxylipin composition of HEK293T\_LPCAT2\_15LO1 cells

Based on the previous results, HEK293T\_LPCAT2 and HEK293T\_LPCAT2\_LO (LO: 5-LO, 15-LO1 or 15-LO2) cells were chosen for further oxylipin analysis. For this purpose, cells were treated with 10  $\mu$ M RSL3 and/or 1  $\mu$ M Ferrostatin for 4 h (Figure 5.37). As initial findings of our collaborators of the Schebb laboratory indicated that part of the previously observed oxylipin amounts might be derived from 15-LO1 and/or 15-LO2 activity during sample preparation for the LC-MS analysis, 500  $\mu$ M 15-LO1 Inhibitor BLX3387 were added.

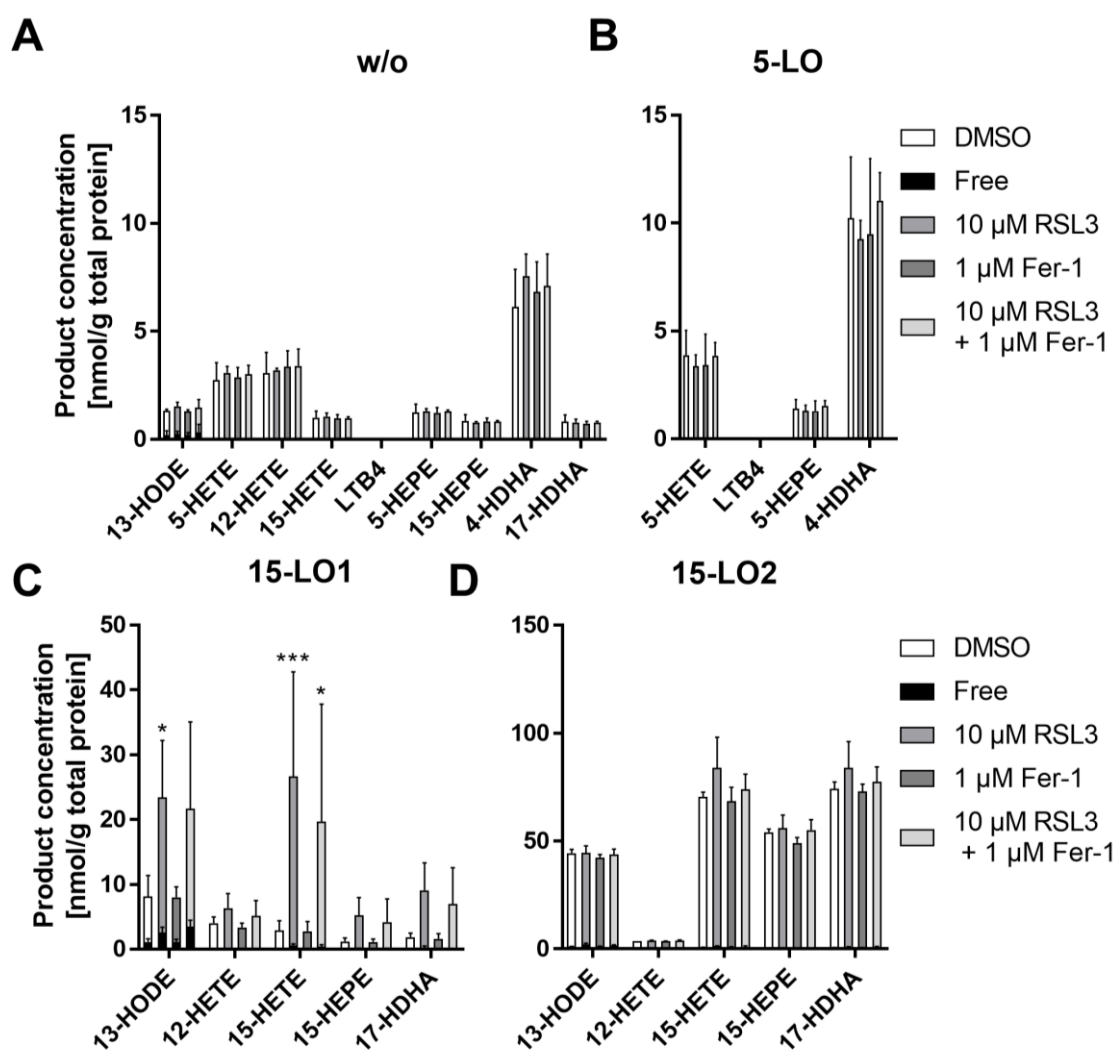


**Figure 5.37: RSL3 treatment increases the oxylipin formation after 4 h in HEK293T\_LPCAT2\_15LO1 cells.**

Levels of esterified and non-esterified oxylipins were determined in  $1 \times 10^7$  HEK293\_LPCAT2 (A) HEK293T\_LPCAT2\_5LO (B), HEK293T\_LPCAT2\_15LO1 (C) or HEK293T\_LPCAT2\_15LO2 (D) cells. (B-D) were treated with 200 ng/mL doxycycline for 24 h prior to treatment with 10  $\mu$ M RSL3, 1  $\mu$ M Fer-1 or a combination of both for 4 h. HEK293T\_LPCAT2 cells (A) served as LO control and DMSO-treated cells served as compound controls. Free and total (free + esterified) oxylipin levels were determined via LC-MS as described and normalized on the total protein content of each sample. The inner black part of each bar represents the non-esterified proportion of the respective oxylipin. Data display mean + SD of 3 independent experiments. Statistical analysis was performed against DMSO controls and significance was tested using 2-way ANOVA with Dunnett's multiple comparisons test. Total oxylipins: \*  $P < 0.05$ , \*\*  $P < 0.01$ , \*\*\*  $P < 0.001$ .

In addition, HEK293T\_LPCAT2\_15LO2 samples were reconstituted directly in 50 % MeOH since the use of commercially available 15-LO2 inhibitors yielded insufficient results. As seen before, oxylipin levels were increased in 15-LO1 expressing cells (Figure 5.37C) and even higher in HEK293T\_LPCAT2\_15LO2 cells (Figure 5.37D) compared to HEK293T\_LPCAT2 controls (Figure 5.37A). RSL3 treatment resulted in an increased formation of 13-HODE, 12-HETE, 15-HETE, 15-HEPE and 17-HDHA in HEK293T\_LPCAT2\_15LO1 cells, whereas an effect on the other cell lines was not observed. The combination treatment of 1  $\mu$ M Ferrostatin and 10  $\mu$ M RSL3 also resulted in increased oxylipin levels in HEK293T\_LPCAT2\_15LO1, whereas 1  $\mu$ M Ferrostatin treatment alone had no effect. Again, the other cell lines were not affected. In addition, the analysis of free and total oxylipins revealed, that all LO products were predominantly esterified.



## 6 Discussion

Eicosanoids are lipid mediators involved in a variety of biological functions, including pro- and anti-inflammatory effects. Derived from PUFAs such as ARA, EPA, and DHA, lipid mediators are typically oxidized lipids, also known as oxylipins. Commonly believed to mediate their effects as free molecules, their esterified counterparts were assumed to have a storage function. However, more recent studies revealed that esterified oxylipins are biologically active and might be a class of lipid mediators on their own. To get an impression of the effects of these new lipid mediators, the present thesis focused on their formation using the enzymes ACSL4, LPCAT2, and several LOs. Two approaches were investigated: Recombinant expression in *E. coli* and stable overexpression in a human cell culture environment.

### 6.1 A recombinant approach for the formation of esterified lipid mediators utilizing PA-LOX, human ACSL4, and human LPCAT2

The first step in the formation of esterified lipid mediators was the activation of PUFAs by human ACSL4 (short isoform, UniProt entry: O60488-2). When this thesis started back in 2017, no reports on the recombinant expression of human ACSL4 were available. Instead, Klett *et al.* had just published the recombinant expression and purification of several rat ACSLs carrying C-terminal FLAG-tags [31]. As the C-terminal FLAG-tag was retained throughout their study, including activity investigations, C-terminal modifications do not seem to inhibit the activity. Based on these data, affinity chromatography using tagged ACSL4 was chosen as the method of choice for the purification of ACSL4 constructs. Expression constructs carrying either a His6x-tag or a StrepII-tag at the C-terminus were prepared as their purification setup is typically more cost-efficient than FLAG-tag purifications [285,286]. In addition, purification via the affinity to ATP was tested. Unfortunately, purification via the ATP-binding site of ACSL4 on an ATP-agarose matrix was not successful (Figure 5.1A), and the use of a StrepII-tag at the C-terminus in combination with a modified streptavidin column (Strep-Tactin™ XT) did not lead to sufficient protein binding (Figure 5.1B). Application of a C-terminal His6x-tag sequence in combination with a HisTrap™ HP column (Ni-affinity chromatography), however, was promising (Figure 5.1C). Although the majority of the protein was eluted during the washing procedure with a 40 mM imidazole-containing buffer (Table 5.2), optimization of the buffer systems and adaptation of the purification method solved the issue (Figure 5.2F). As the purity of the protein was not sufficient following Ni-affinity chromatography alone, SEC and IEX purifications were performed. Both purification techniques led to a final purity of at least 95 % (Figure 5.4B and Figure 5.6B). Utilizing the IEX technique, the protein was eluted in one sharp peak, while the elution behavior of the SEC was highly dependent on the amount of TX-100 (Figure 5.5). In absence of the nonionic detergent, the protein eluted early, indicating the formation of protein aggregates. The same behavior was observed at 0.001 % (w/v) TX-100, but higher concentrations (0.01-0.1 % (w/v)) shifted the elution to later retention times in a concentration-dependent manner. At a concentration of 0.1 % TX-100, a large peak was observed, which might be caused by the formation of micelles as the critical micelle concentration of TX-100 is 0.22 mM or about 0.02 % (w/v) depending on the approximate molecular weight [287]. As the SEC purification revealed that the ACSL4\_His6x protein eluted at different retention times, indicating a variety of protein species, proper folding was

investigated by thermal shift experiments. Although not pure yet, protein fractions purified by Ni-affinity chromatography were tested first. The stability of the protein increased with higher pH in 100 mM Tris buffer from 39.0 °C at pH 6.0 to 40.3 °C at pH 8.0, while the stability in sodium phosphate buffer was overall higher but nearly unaffected by changes in pH (40.4 °C at pH 6.0 to 40.6 °C at pH 8.0) (Figure 5.7A). However, the stability was decreased in both buffer systems in the presence of TX-100. 0.01 % (w/v) TX-100 was the highest concentration that was still evaluable and led to a  $T_m$  of 38.4 °C in Tris and a  $T_m$  of 39.4 °C in NaP<sub>i</sub> buffer. When protein fractions purified by Ni-affinity chromatography and subsequent SEC were analyzed, they revealed that the stability was decreased above pH 6.0 from 39.9 °C to 38.1 °C (pH 8.0) in Tris and 40.0 °C to 38.9 °C (pH 7.5) in NaP<sub>i</sub> buffer (Figure 5.7B). As the previous samples were not as pure as the SEC samples, the stabilizing effects might be caused through protein impurities by protein-protein interactions. Nevertheless, the use of TX-100 led to a destabilization indicating that SEC was not the optimal purification procedure. Thus, protein fractions purified by IEX were analyzed in more detail. Except for the Bis/Tris buffer system, ACSL4 was most stable at pH 6 in citrate and sodium phosphate buffers with a  $T_m$  of 43.0 °C and 42.7 °C, respectively (Figure 5.8). With increasing pH, the stability decreased and the same effect was observed with decreasing pH. Furthermore, addition of up to 20 % (v/v) glycerol had a stabilizing effect. As an increase in glycerol concentration is accompanied by an increase in viscosity, a concentration of only 5 % (v/v) was used for further purification experiments. These results were able to show that the ACSL4\_His6x protein was still properly folded following the purification procedure and that the initially used sodium phosphate buffer system was well suited for the purification of ACSL4\_His6x. Thus, the expression and purification of ACSL4\_His6x by Ni-affinity chromatography and subsequent IEX was successfully established yielding 2.1 mg of 95 % pure protein per 500 mL BL21(De3) *E. coli* culture. Although Klett *et al.* [31] described the expression and purification procedure of several rat ACSLs, they did not report purities or yields, preventing a comparison here. In 2019, Shimbara-Matsubayashi *et al.* reported the expression and purification of a human ACSL4 protein with C-terminal His-tag from Sf9 insect cells (a clone isolated from *Spodoptera frugiperda* Sf21) [56] which confirms the suitability of the His6x-tag for ACSL4 purification. However, the report also did not include any information on the yield or purity of the protein. Thus, this work presents the first successful purification of a human ACSL4 (short isoform, UniProt entry: O60488-2) protein from *E. coli* with reproducible yields and high purity (>95 %) that is well suited for future investigations.

Next, the activity of the purified protein was investigated using an indirect spectrophotometric assay system [31]. The suitability of the assay was evaluated with varying protein amounts and by UPLC-MS analysis (Figure 5.10). Variations of the protein amount revealed concentration-dependent decreases in absorbance that was strongest with freshly purified protein (Figure 5.10A). When the protein was stored for 16 days at 4 °C prior to the assay, the activity was decreased (Figure 5.10B), and this effect was even stronger when the protein was stored at -80 °C (Figure 5.10C). As this was an indirect assay setup, UPLC-MS analysis was performed to verify that the signal was related to the respective product formation. Indeed, the formation of ARA-CoA was detected in positive ionization mode and confirmed by retention time and m/z value (Figure 5.10D). In order to couple the product formation to a detectable

signal, the assay system contained additional enzymes: an adenylate kinase, a pyruvate kinase, and a lactate dehydrogenase. To ensure that the product formation was not caused by one of the other enzymes, the assay was also performed using only the essential components ARA, ACSL4\_His6x, CoA, and ATP. Product formation was detected by UPLC-MS and proved the activity of the purified ACSL4\_His6x protein (Figure 5.10D). Once the general setup was evaluated, enzyme kinetics had to be determined for ARA and EPA. The measurements of ARA varied strongly, and thus kinetics were not evaluable. In contrast, samples that received EPA were reproducible and revealed a  $K_M$  of  $5.1 \pm 2.2 \mu\text{M}$  (Figure 5.12). In 1997, Kang *et al.* [27] already investigated the purified rat ACSL4 protein based on the same spectrophotometric assay system [288] and reported a  $K_M$  of  $12 \mu\text{M}$  for EPA. More recently, Shimbara-Matsubayashi *et al.* [56] investigated the kinetics of both human ACSL4 variants and reported a  $K_M$  of  $5.3 \pm 2.6 \mu\text{M}$  for EPA using the more abundant transcript that was also used during this thesis. Compared to the rat enzyme, the human enzymes bound the substrate, EPA, with at least 2-fold higher affinity. Even more interestingly, the human enzymes displayed a very similar substrate affinity, although the enzyme from the literature was expressed in Sf9 insect cells, while *E. coli* BL21(De3) cells were used during this thesis. Furthermore, the results presented here were obtained from a spectrophotometric assay setup, while Shimbara-Matsubayashi *et al.* utilized a novel LC-MS/MS approach [56]. Given that the spectrophotometric assay system requires several components, including three other enzymes and their respective substrates, it is potentially prone to errors and, therefore, it might be worth considering an analysis by LC-MS/MS in future studies.

Next, a 15-lipoxygenating enzyme from *pseudomonas aeruginosa* (PA-LOX) was investigated. Ideally, this would allow the formation of several products from membrane-bound lipids as the enzyme is able to bind both free and esterified lipids [289,290]. The expression construct was kindly provided by Prof. Dr. Harmut Kühn (Charité Berlin), and the expression and purification procedures were performed as described before [283] with slight adaptations. Thermal shift experiments with the purified protein revealed that PA-LOX was stable up to  $50 \text{ }^\circ\text{C}$  under any buffer condition tested (Figure 5.14). Stability was the highest in 100 mM sodium phosphate buffer at pH 6.0 (Figure 5.14A). In general, the stability was enhanced with an increase in pH up to 6.0 and decreased again at higher pH values. The HEPES buffer system used during the purification procedure was located in between, ranging from  $55.0 \text{ }^\circ\text{C}$  to  $58.3 \text{ }^\circ\text{C}$  depending on the pH. The addition of up to 20 % (v/v) glycerol further increased the stability (Figure 5.14A), while supplementation with several salts had no effect or even decreased the stability (Figure 5.14B). Activity of the purified protein was verified as described before [283], and PA-LOX product formation was analyzed by UPLC-UV/MS as described recently [282]. The analysis revealed the highest product formation at pH 6.5 and decreasing amounts at higher pH values of 7 and 7.5 (Figure 5.15). This is in accordance with current literature, which describes the highest product formation of 15-HEPE at pH 6.8 in bacterial cultures [291] and also correlates with the stability data presented before.

Once the expression and purification of ACSL4 and PA-LOX were established and their activity was evaluated, the LPCAT2 protein responsible for the incorporation of activated PUFAs into the membrane was investigated. Recombinant expression and purification of human LPCAT2 in *E. coli* was not reported when the project started and, to the best of my knowledge, has still

not been described today. Surprisingly, first expression attempts revealed that the protein was observed in Western blot investigations at the 50 kDa marker band, which was around 10 kDa less than expected based on the amino acid sequence (Figure 5.16). As it was unsure whether the smaller size was caused by degradation, truncation, or unusual behavior on SDS-PAGE, expression constructs with N- or C-terminal His6x-tags were prepared. The respective analysis revealed that the N-terminal part was indeed missing while the C-terminus, including the His6x-tag, was still present (Figure 5.17). Therefore, the decrease in size was not caused by an early translational termination but rather by degradation or cleavage of the N-terminal protein part. Sequence analysis revealed two predicted cleavage regions, one after the initial 7-8 kDa and the second after 11-12 kDa of the protein (Figure 5.18). Because the N-terminal part also contained a transmembrane region, several shortened constructs were prepared, lacking different sections of the N-terminal region. In addition, an MBP-tagged construct was prepared to further enhance the solubility of the protein. Only the MBP-tagged protein showed increased yields. However, it was not possible to remove the tag by TEV cleavage. Apparently, the designed cleavage region was not accessible, and also elongated incubation durations and increased TEV concentrations were not able to overcome the issue (Figure 5.20). Based on these findings, the protein did not seem to be properly folded. Nevertheless, the most important parameter of the protein was its activity. Thus, activity studies were performed as described before for microsomal protein fractions of transfected CHO and RAW264.7 cells [104]. Although several LPCAT2 constructs and fractions of each step in the purification procedure were tested, product formation was not observed. The issue was not overcome even though a variety of approaches, such as protein denaturation, refolding, and change of the bacterial expression cell line, were tested. For this reason, the recombinant approach for the formation of esterified lipid mediators was not continued.

## **6.2 Establishing a cell-based model system for the formation of esterified lipid mediators**

An alternative approach to produce esterified lipid mediators was the overexpression of human ACSL4 (short isoform, UniProt entry: O60488-2) and human LPCAT2 (UniProt entry: Q7L5N7-1) in a cellular system to activate and incorporate PUFAs, respectively. Transfection of cell cultures is either achieved by viral or non-viral vectors, which both have their advantages and disadvantages [292]. Typically, viral transfection systems lead to higher transfection effectiveness over non-viral systems but also tend to cause inflammatory responses and gene mutations [293]. In contrast, non-viral transfection systems display a more controlled and defined environment. As the handling of viral systems is also more time-consuming and requires a laboratory with safety level 2, transfection was carried out using a non-viral setup. To address the lower effectiveness of non-viral systems, HEK293T cells were selected as the cell line of choice due to their great transfectability [294,295]. Furthermore, a stable transfection approach using the 'sleeping beauty transposon system' was chosen to enable subsequent antibiotic selection [279]. PEI was applied as transfection reagent as it is the most commonly used reagent in gene therapy and helps to prevent insufficient transfection efficiencies [292]. As a result, the cell lines HEK293T\_ACSL4, HEK293T\_LPCAT2, HEK293T\_ACSL4+LPCAT2 (referred to as HEK293T\_A+L) and the vector control cell line HEK293T\_VC were successfully prepared and analyzed on protein level (Figure 5.21). LPCAT2 expression was strongly

enhanced in HEK293T\_LPCAT2 cells by 30-fold and about 13-fold in HEK293T\_A+L cells, while ACSL4 expression was increased by 3-fold in HEK293T\_ACSL4 cells and 2.5-fold in HEK293T\_A+L cells. Transfection of ACSL4 was repeated to ensure that the lower protein induction was not caused by an experimental error, but the results were confirmed. In 2014, Kan *et al.* reported the ARA-mediated posttranslational degradation of ACSL4 via the ubiquitin-proteasomal pathway [296]. Furthermore, they were able to show that the ACSL4 promoter activity as well as the mRNA stability were not affected. Although the experiments were performed in HepG2 and Huh76 cells, a control mechanism also seems reasonable in HEK293T cells as they are modified human embryonal kidney cells, and an increased ACSL4 expression is correlated with kidney cancer [62].

The functionality of ACSL4 and LPCAT2 was verified by an initial LC-MS analysis of both total (Figure 5.22) and free (Figure 5.23) oxylipins. Overexpression of LPCAT2 (HEK293T\_LPCAT2) led to clearly elevated total oxylipin levels of oxylipins derived from PUFAs such as oleic acid, linoleic acid, ARA or DHA. Overexpression of ACSL4 (HEK293T\_ACSL4) also increased total oxylipin levels but to a lesser extent. Consequently, the highest oxylipin formation of most PUFAs was observed when ACSL4 and LPCAT2 were co-expressed in HEK293T\_A+L cells. A similar pattern was observed for free oxylipins with elevated oxylipin levels in HEK293T\_LPCAT2 and HEK293T\_A+L cells. The amount of free oxylipins was at least five times lower compared to the respective total values indicating that the majority of these oxylipins is esterified, presumably within membranes. Based on these findings, a comprehensive oxylipin analysis was performed and will be discussed in chapter 6.5.

In order to produce specific oxylipins such as 5-HETE, 12-HETE, or 15-HETE, the previously described system was extended by one of the following LOs: 5-LO, 15-LO1 or 15-LO2. Because extensive genomic modification of cell lines tends to cause premature cell death, the first approach was to use a transient expression system. In order to enable the comparison between all cell lines, transfection efficiencies had to be determined. For this purpose, expression constructs containing the respective LO as well as mCherry as fluorescent protein marker were prepared. To ensure that mCherry expression levels were correlated with the LO expression, both proteins were linked by a P2A linker [297,298]. This design leads to the formation of two separate proteins through ribosome skipping [299,300]. Unfortunately, the small part of the linker sequence that remained at the C-terminal end of the LOs (Figure 5.27) inhibited their activity. Therefore, the strategy was revamped, and stable genomic integration was performed. To prevent premature cell death due to enhanced cellular stress by constitutive overexpression of several proteins, an inducible system was implemented [279]. This allowed the precise LO induction through treatment with 200 ng/mL doxycycline for 24 h. Although inducible expression systems are often described as leaky, no protein expression was observed in absence of doxycycline (Figure 5.28). To confirm the activity of the induced LOs, product formation of leukotrienes, 5-HETE, 12-HETE, and 15-HETE was determined by UPLC-UV/MS as described by Kreiß *et al.* [282]. All LOs were active following induction by doxycycline, while product formation was not observed in non-induced controls (Figure 5.29). In accordance with current literature [139,158,176,177], 5-LO expression led to the formation

of 5-HETE and leukotrienes, 15-LO1 expression caused 12- and 15-HETE formation, and 15-LO2 expression yielded solely 15-HETE.

### **6.3 Cell viability of LPCAT2 overexpressing cell lines is reduced following ferroptosis induction**

Increased lipid peroxidation and ACSL4 overexpression are typically signs of a cell death mechanism known as ferroptosis [60,61]. Furthermore, LPCAT3, an isoenzyme of LPCAT2, has also been linked to ferroptosis [101,126]. However, a correlation between LPCAT2 and ferroptosis has not been investigated so far. Thus, cell viability of cell lines HEK293T\_VC, HEK293T\_A+L, and HEK293T\_LPCAT2 was determined by WST-1 assay following ferroptosis induction with erastin (inhibitor of cystine/glutamate antiporter system Xc-) or RSL3 (GPX4 inhibitor) (Figure 5.33). A concentration range of 0.1-10  $\mu$ M RSL3 and 1-10  $\mu$ M erastin was analyzed, and a predominant pattern was observed. Cell viability of HEK293T\_LPCAT2 cells was reduced compared to HEK293T\_VC cells, and the reduction was even stronger in HEK293T\_A+L cells. These findings correlate with the results of the initial oxylipin analysis, which revealed increased oxylipin formation in HEK293T\_LPCAT2 cells, which was further enhanced in HEK293T\_A+L cells (Figure 5.22). As already mentioned above, increased lipid peroxidation is a key marker for ferroptosis [60,61], and thus, overexpression of LPCAT2 seems to promote ferroptotic cell death. The fact that overexpression of ACSL4, a known biomarker, and promoter of ferroptosis [60], further enhances the effect underlines this assumption. Taken together, these results indicate that LPCAT3 might not be the only member of the LPCAT family that plays a role in the cell death mechanism known as ferroptosis.

### **6.4 LPCAT2 overexpression alters 15-LO1 localization in stably transfected HEK293T cells**

The short isoform of ACSL4, which was used in this work, is described to have a cytosolic localization but is also found at the plasma membrane, while the longer isoform, expressed exclusively in neurons, is found in the ER and LDs [45]. LPCAT2 is also described as having an ER-like expression pattern [22] and also has the ability to translocate to LDs [77,78]. However, it is important to note that these findings were determined in different cell lines, such as COS-7 and HuH-7 (ACSL4) or CHO and HeLa cells (LPCAT2), using a mix of transient and stable transfection techniques as well as GFP-tagged and untagged constructs. Therefore, it was of interest whether ACSL4 and LPCAT2 were localized similarly in the HEK293T-based overexpression system. For this purpose, laser scanning confocal microscopy analysis was performed. In accordance with the initial Western blot analysis (Figure 5.21), ACSL4 was found throughout all cell lines within the cytosol (Figure 5.30 and Figure 5.31). LPCAT2 was also found within the cytosol, but the localization was altered depending on the level of LPCAT2 expression. While several small circular spots were observed in HEK293T\_VC\_LO cells, none were found in HEK293T\_LPCAT2\_LO cells (Figure 5.30). In HEK293T\_A+L\_LO cells, where LPCAT2 expression is only upregulated by 13-fold compared to the 30-fold induction in HEK293T\_LPCAT2 cells, fewer spots were observed (Figure 5.31). As mentioned above, LPCAT2 is reported to translocate to LDs which typically consist of neutral lipids and phospholipids but may also contain proteins [77,78]. Furthermore, knock-out experiments have

shown that the absence of LPCAT2 and LPCAT1 increases the size of LDs [79]. Thus, it seems reasonable to assume that overexpression causes smaller LDs which might explain why LDs were not observed in HEK293T\_LPCAT2\_LO cells. As the setup used for the laser scanning confocal microscopy analysis restricted the simultaneous investigation to three targets, an ER marker was not included in the investigation. Although the expression pattern of LPCAT2 in HEK293T\_LPCAT2 cells seems to be very similar to the ones reported by Agarwal and Garg in CHO and HeLa cells [22], verification of an ER-like expression pattern should be included in future investigations.

Once the cellular localizations of ACSL4 and LPCAT2 were determined, 5-LO, 15-LO1, and 15-LO2 were analyzed next. It has been shown that 5-LO is able to shuttle between cytosol and nucleus depending on its phosphorylation state [161,162]. Upon stimulation, 5-LO also translocates to the nuclear membrane, where it interacts with FLAP to form its products, such as 5-HETE and leukotrienes [164,165]. Despite its ability to move between cytosol and nucleus, previous studies described a nuclear localization in HEK293 cells overexpressing 5-LO [168,301,302]. Interestingly, laser scanning confocal microscopy investigations of HEK293T\_VC\_5LO, HEK293T\_LPCAT2\_5LO, and HEK293T\_A+L\_5LO cells revealed a predominantly cytosolic localization under control conditions (co) (Figure 5.34 and Figure 5.35). A comparison of the experimental setup of this work with setups of current literature indicates that there might be several reasons for the deviant behavior. On the one hand, previous studies often used constitutive expression systems, which tend to increase cellular stress by increased oxylipin formation [168,301,302]. In contrast, an inducible LO expression system was used in this work. Here, 5-LO is exclusively expressed during the last 24 h prior to fixation of the cells, which may result in less oxidative stress and thereby lower activation of p38, consequently leading to less phosphorylation at Ser271 [303,304]. Due to the influence of Ser271 phosphorylation on the localization of 5-LO, which has been proven with a Ser271Ala mutation as well as inhibitors of p38 and CaMKII, phosphorylation as a result of enhanced oxidative stress by RSL3 treatment might also explain the partial shift in 5-LO localization into the nucleus (Figure 5.34 and Figure 5.35). On the other hand, some studies used fluorescent protein tags such as GFP or mCherry to visualize the 5-LO localization [149,305], which results in increased molecular weight and thus may have altered its properties. In this thesis, visualization of the cellular localization was exclusively determined by fluorophore-labeled antibodies to prevent an artificial behavior. Taken together, it is reasonable that the localization of 5-LO is different from previous reports, presumably due to milder conditions in terms of oxidative stress.

In contrast to 5-LO, 15-LO1 has been described to occur solely within the cytosol translocating to the nuclear envelope when intracellular calcium levels are increased [179,306,307]. The same behavior was originally described for 15-LO2 back in 2002. However, one year later, the same group reported that the enzyme was also found within the nucleus and at the cell-cell border [196,197]. In the present thesis, 15-LO2 was found within the cytosol, which is in accordance with the 15-LO2 overexpression in HEK293 cells of Bender *et al.* [308]. When the localization of 15-LO1 was analyzed, HEK293T\_VC\_15LO1 cells displayed a cytosolic presence (Figure 5.35) which was expected from the literature [179]. In HEK293T\_LPCAT2\_15LO1 (Figure 5.35) and HEK293T\_A+L\_15LO1 (Figure 5.34) cells,

however, 15-LO1 was found at the nuclear envelope. Moreover, when the cells were treated with RSL3, a common ferroptosis inducer, 15-LO1 of the VC cells translocated to the nuclear envelope as well (Figure 5.35). This was highly unexpected as the cells were not stimulated with calcium ionophore or exogenous calcium. However, in 2018 Maher *et al.* summarized the role of  $\text{Ca}^{2+}$  in oxidative glutamate toxicity in a review article [309]. The term oxidative glutamate toxicity refers to the inhibition of the cystine/glutamate antiporter Xc- by glutamate, which results in the depletion of GSH and, thus, promotes the formation of ROS. Accumulation of ROS then leads to an increased formation of inositol-1,4,5-trisphosphate which subsequently results in the release of  $\text{Ca}^{2+}$  from the ER. Similarly, treatment with the ferroptosis inducer RSL3, which inhibits GPX4 directly and thereby promotes ROS formation [116,310], might have caused  $\text{Ca}^{2+}$  release from the ER in this work. As a result, 15-LO1 is activated and translocates to the nuclear envelope. In fact, oxidative glutamate toxicity is considered to be very similar, if not identical, to ferroptosis [309], which altogether explains the localization of 15-LO1 in HEK293T\_VC\_15LO1 cells. In contrast, in HEK293T\_LPCAT2\_15LO1 and HEK293T\_A+L\_15LO1 cells, 15-LO1 was already present at the nuclear envelope under control conditions. As overexpression of LPCAT2 increased the oxylipin formation compared to HEK293T\_VC cells (Figure 5.22 and Figure 5.23) and promoted ferroptotic conditions in cell viability investigations (as discussed in chapter 6.3), it is very likely that ferroptosis is already initiated in these cells even under standard conditions. As a result, ROS formation is increased, leading to  $\text{Ca}^{2+}$  release from the ER and, consequently, activation and translocation of 15-LO1 to the nuclear envelope.

Surprisingly, treatment with erastin, another common inducer of ferroptosis, did not alter 15-LO1 localization similarly in HEK293T\_VC\_15LO1 cells (Figure 5.35). Erastin inhibits the cystine/glutamate antiporter Xc- and therefore induces ferroptosis by depletion of GSH [117], whereas RSL3 targets GPX4 directly [116,310]. As inhibition of the cystine/glutamate antiporter Xc- by glutamate results in the release of  $\text{Ca}^{2+}$  from the ER [309], this should also be the case for inhibition by erastin treatment indicating that increased cytosolic calcium levels might not be the only trigger for 15-LO1 translocation. However, whether the translocation of 15-LO1 might partially be caused by an interaction of the enzyme with RSL3 and/or GPX4 remains highly elusive and needs to be investigated in future studies. Nevertheless, a general connection between LOs and ferroptosis has been shown in *GPx4<sup>-/-</sup>* cells treated with inhibitors such as zileuton, PD146176, NDGA, and others [114,310]. Although lipid peroxidation is considered one of the main drivers of ferroptosis, increased oxylipin formation alone is not able to induce ferroptotic cell death. Indeed, ferroptosis was only triggered when oxylipins were found to be esterified [121,311]. Evidence has been provided that 15-LO1/2 may translocate to the nuclear membrane to form a complex with PEBP1 which shifts the substrate preference of 15-LO1 and 15-LO2 to AA-PE [121]. As a result, 15-HpETE-PE is directly formed within the membrane and facilitates ferroptotic cell death under GPX4-impaired conditions [121,311]. Based on these findings, it may be reasonable to assume that the translocation of 15-LO1 to the nuclear envelope is triggered during ferroptosis induction by RSL3, as was seen in this thesis. However, it is unclear why 15-LO2 was not affected in a similar way or why erastin did not lead to similar translocation effects. As discussed before, LPCAT2 expression seems to promote ferroptotic cell death (Figure 5.33) and also causes translocation of 15-LO1 to the



nuclear membrane (Figure 5.34 and Figure 5.35). Although, to the best of my knowledge, there is no literature on an interaction of LPCAT2 and 15-LO1 or LPCAT2 and ferroptosis, in general, available today, the data presented in this thesis suggest a connection. Even though this does not prove any interaction, analysis of the fluorescence histograms of 15-LO1, LPCAT2, and DAPI revealed that the enzymes are located in close proximity around the nucleus (Figure 5.36B). Therefore, an interesting target for future investigations might be whether a PEBP1-like interaction between 15-LO1 and LPCAT2 takes place.

## 6.5 Investigation of the cellular oxylipin profile

The initial oxylipin analysis not only revealed interesting differences between the cell lines but also revealed elevated levels of nearly all measured oxylipins. Thus, a comprehensive LC-MS analysis was performed in collaboration with Laura Carpanedo and Susanne Reif from the laboratory of Prof. Dr. Nils Helge Schebb (University of Wuppertal). Since RSL3 treatment was correlated with a change in 15-LO1 localization in HEK293T\_VC\_15LO1 cells (as discussed in chapter 6.4), oxylipin investigations were extended. The analysis included total and free oxylipins derived from several substrates such as ARA, EPA, and DHA but also oleic acid, LA, and others [204,209–211] (see appendix Table 9.4 and Table 9.5 for the complete analysis).

Surprisingly, total oxylipin levels in 5-LO-containing cell lines were below 7 nmol/g total protein (Figure 5.32A), while some of the main products of 15-LO1 and 15-LO2 exceeded the upper limit of quantification (ULOQ, Figure 5.32). In accordance with the initial oxylipin screen, 13-HODE was one of the major oxylipins formed in 15-LO1-containing cells accompanied by 15-HETE and 17-HDHA, while 12-HETE, 15-HEPE, and 14-HDHA were formed to a lesser extent (Figure 5.32B). In 15-LO2 expressing cells, 13-HODE, 15-HETE, 15-HEPE, and 17-HDHA were the predominantly formed products in all cell lines (Figure 5.32C). This is in accordance with current literature on mammalian 15-LOs, which described a dual activity of 15-LO1 producing 15-HETE and 12-HETE from ARA while 15-LO2 exclusively forms 15-HETE [177]. Furthermore, it has been shown that the enzymes accept a variety of substrates, including omega-3 (n-3) and omega-6 (n-6) polyenoic fatty acids such as LA, ARA or EPA, and DHA, respectively. Interestingly, the presented data revealed similar levels of ARA and DHA-derived products, while EPA products were found to a lesser extent. This is in contrast with reports on the substrate specificity of human 15-LOs that describe a preference for substrates with a higher degree of unsaturation [177]. However, these observations were made in experiments supplemented with exogenous substrates, which does not reflect the setup used in this work. Here, oxylipin levels were determined without supplementation of exogenous substrates so that the product formation is dependent on endogenous substrate levels. While n-3 fatty acids such as EPA and DHA are commonly present in low amounts, n-6 fatty acids such as ARA are more abundant [312,313], and consequently, ARA-derived products are formed in similar amounts as oxylipins derived from preferred substrates. While overexpression of 15-LO1 and 15-LO2 resulted in a high product formation exceeding the ULOQ for some oxylipins, 5-LO overexpression caused only a minor oxylipin formation. This was unexpected as the initial activity analysis indicated a comparable overall activity of each LO (Figure 5.29). However, the initial analysis was performed upon stimulation with exogenous 20  $\mu$ M ARA, 2.5  $\mu$ M calcium ionophore A23187, and 1 mM  $\text{CaCl}_2$ , whereas total oxylipin formation was determined in

unstimulated cells. 5-LO product formation has been shown to be stimulated by elevated intracellular calcium levels and phosphorylation, which causes translocation to the nuclear membrane. Here, 5-LO co-localizes with cPLA<sub>2</sub>, which releases ARA from the membrane, and FLAP, which transfers ARA into the active site of 5-LO [166,167]. In the absence of exogenous ARA, however, 5-LO lacks activity in intact HEK293 cells [168]. Furthermore, the authors reported that even co-expression of 5-LO and FLAP in HEK293 cells and treatment with calcium ionophore A23187 did not result in a relevant 5-LO product formation. Although these findings indicated a potential problem with the cPLA<sub>2</sub>-mediated release of ARA, 12-LO expression in HEK293 cells led to 12-HpETE formation under the same conditions questioning an issue with the substrate availability [168]. In contrast, incubations with exogenous ARA resulted in a substantial 5-LO product formation [168] and thus, stimulation with exogenous substrates and calcium ionophore A23187 should be included in future experiments to trigger 5-LO product formation.

To determine whether the esterified oxylipins were formed directly or via incorporation, another sample set, which included treatment with RSL3 and/or Ferrostatin, an inhibitor of membrane oxygenation, was prepared (see appendix Table 9.6 and Table 9.7). The respective oxylipin analysis revealed, that RSL3 treatment led to an increased formation of 13-HODE, 12-HETE, 15-HETE, 15-HEPE and 17-HDHA in HEK293T\_LPCAT2\_15LO1 cells that was also observed when the cells were treated with a combination of RSL3 and Ferrostatin (Figure 5.37C). This is in accordance with current literature as RSL3 is described to inhibit GPX4 and thereby prevents the reduction of lipid hydroperoxides leading to ferroptosis eventually [314]. In addition, the observed oxylipins were predominantly esterified while the ratio of free to total oxylipins was not affected by the Ferrostatin treatment. As Ferrostatin inhibits lipid ROS formation [59], the increased amounts of esterified oxylipins in 15-LO1 expressing cells seem to be formed mainly by oxygenation of free PUFAs and subsequent incorporation. Interestingly, HEK293T\_LPCAT2\_15LO2 cells were not affected by treatment with RSL3 or RSL3/Ferrostatin. Although there is currently no explanation for the difference in 15-LO1 and 15-LO2 behavior, these results underline the special role for 15-LO1 that was already seen in the cellular localization experiments as discussed in chapter 6.4.

With regard to the laser scanning confocal microscopy study discussed in chapter 6.4, it was of interest to what extent HEK293T\_LPCAT2\_15LO1 cells differed in their oxylipin composition from 5-LO or 15-LO2 containing cells given that only 15-LO1 was located at the nuclear envelope (Figure 5.34 and Figure 5.35). As already mentioned before, the main difference compared to 5-LO expressing HEK293T\_LPCAT2\_5LO cells was the strongly increased oxylipin formation in HEK293T\_LPCAT2\_15LO1 cells. However, oxylipin formation was also strongly increased in 15-LO2 expressing cells, but 15-LO2 did not translocate to the nuclear membrane. Thus, HEK293T\_LPCAT2\_15LO1 and HEK293T\_LPCAT2\_15LO2 cells were compared. The major difference between these cell lines was the formation of 12-HETE. As already seen during the initial activity study (Figure 5.29), 15-LO1 expression led to 12-HETE formation, whereas 15-LO2 expression resulted solely in 15-HETE formation. The observed difference in 15-LO1 and 15-LO2 activity is in accordance with the current literature [177]. Thus, the question arises whether the localization around the nuclear membrane of 15-LO1 is related to 12-HETE formation. Although this might explain the difference in cellular localization

of 15-LO1 (nuclear envelope) and 15-LO2 (cytosol) in HEK293T\_LPCAT2\_LO cells under control conditions, it does not explain the different localization of 15-LO1 in HEK293T\_VC\_15LO1 compared to HEK293T\_LPCAT2\_15LO1 cells (Figure 5.35). Furthermore, the previous oxylipin analysis revealed similar amounts of 12-HETE for HEK293T\_VC\_15LO1 and HEK293T\_LPCAT2\_15LO1 cells (Figure 5.32). Thus, it seems quite unlikely that the formation of 12-HETE is responsible for the translocation of 15-LO1 to the nuclear membrane indicating another mechanism. As already discussed in chapter 6.4, RSL3-mediated  $\text{Ca}^{2+}$  release and/or a potential PEBP1-like interaction of LPCAT2 and 15-LO1 might be interesting targets for future investigations.

## 6.6 Conclusion and perspective

The present thesis focused on the formation of esterified lipid mediators. An approach utilizing recombinantly expressed enzymes in *E. coli* was not successful, so that a HEK293T-based overexpression system was established instead. The system contained human ACSL4 and LPCAT2, two enzymes responsible for the activation and incorporation of PUFAs into membranes, respectively. Stable overexpression resulted in elevated oxylipin levels that were predominantly esterified. Additional overexpression of 5-LO, 15-LO1, or 15-LO2 then allowed the formation of specific oxylipins. Characterization of these cell lines by laser scanning confocal microscopy revealed that the overexpression of LPCAT2 caused 15-LO1 translocation to the nuclear membrane. Interestingly, treatment with RSL3, a ferroptosis-inducing agent, had a similar effect. Although a link between LPCAT2 and the cell death mechanism ferroptosis has not been shown today, the presented data indicate a possible connection. A cell viability study supported this assumption as increased sensitivity to RSL3 and erastin, another ferroptosis inducer, was observed in LPCAT2-expressing cell lines compared to control cells. Subsequent analysis of the oxylipin content of the stably transfected HEK293T cells expressing LPCAT2 revealed elevated oxylipin levels. As lipid peroxidation is one of the key features of ferroptotic cell death, this also suggests a connection between LPCAT2 expression and ferroptosis.

Taken together, this work presents the formation of esterified lipid mediators using a HEK293T-based overexpression system and, in addition to it, highly indicates a connection between LPCAT2 and the cell death mechanisms ferroptosis which has not been reported so far. As ferroptosis is involved in several pathologies, including neurodegeneration, autoimmune diseases, and tumorigenesis [125], LPCAT2 might be an interesting new target for therapeutic applications.

However, there are several questions that remain unanswered and need to be targeted in future investigations, including the following:

- What causes the translocation of 15-LO1 to the nuclear membrane in HEK293T\_LPCAT2\_15LO1 cells?
- Is it the same mechanism responsible for RSL3-mediated translocation of 15-LO1?
- Does LPCAT2 interact directly with 15-LO1, in a PEBP1-like manner or otherwise?
- Why does 15-LO2 not translocate to the membrane under these conditions?

## 7 Zusammenfassung

Lipidmediatoren spielen eine wichtige Rolle bei der Regulation verschiedener biologischer Funktionen wie z.B. der Entstehung oder Auflösung von Entzündungsreaktionen. Typischerweise handelt es sich dabei um oxidierte Lipide, auch Oxylipine genannt, die sowohl durch Autoxidation als auch enzymkatalysiert entstehen können. Dabei kann die Oxidation der Lipide durch mehr als 50 verschiedene Enzyme katalysiert werden, die sich je nach Zelltyp unterscheiden. Interessanterweise kann die Bildung solcher Oxylipine in den meisten Fällen auf den Lipoxygenase-, Cyclooxygenase- oder Cytochrom P450-Metabolismus zurückgeführt werden. Ursprünglich ging man davon aus, dass nur ungebundene Oxylipine eine Wirkung vermitteln, während ihre veresterten Gegenstücke als Speicher für nicht benötigte Oxylipine dienen. Erst neuere Untersuchungen brachten ans Licht, dass auch diese veresterten Lipidmediatoren eine eigene Wirkung vermitteln können. Dabei konnte bereits gezeigt werden, dass die vermittelte Wirkung in einigen Fällen sogar gegenläufig zu der der freien Mediatoren ist. Daher geht man inzwischen davon aus, dass veresterte Oxylipine eine eigene Klasse von Lipidmediatoren darstellen. Da diese Sichtweise zu Beginn der vorliegenden Doktorarbeit noch relativ neu war, war der Zugang zu solchen veresterten Lipiden nicht uneingeschränkt möglich. Viele Lipide waren nicht erhältlich oder recht teuer. Daher konzentriert sich diese Arbeit auf die Etablierung der Biosynthese von veresterten Lipidmediatoren, um diese anschließend hinsichtlich ihrer Wirkung charakterisieren zu können.

Typischerweise werden veresterte Lipidmediatoren im Körper in einer zweistufigen Reaktion ausgehend aus mehrfach ungesättigten Fettsäuren gebildet. Der erste Schritt ist die Aktivierung einer Fettsäure durch einen Vertreter der Acyl-CoA-Synthetase-Familie, während im zweiten Schritt die aktivierte Fettsäure durch einen Vertreter der Lysophosphatidylcholin Acyltransferase Familie auf ein Lyso-Phospholipid übertragen wird. Als Lyso-Phospholipid werden Phospholipide bezeichnet, denen eine der beiden Fettsäureketten fehlt. Diese werden typischerweise durch das Enzym Phospholipase A<sub>2</sub> abgespalten und bilden in Kombination mit den oben genannten Enzymen einen Remodellierungszyklus. Dieser Mechanismus wurde bereits im Jahre 1958 von William E. Lands beschrieben und ist seitdem als „Lands' Zyklus“ bekannt. Um möglichst viele Lipidmediatoren herstellen zu können, wurden aus jeder Familie Enzyme mit hoher Substrattoleranz ausgewählt: „*Acyl-CoA Synthetase long-chain family member 4*“ (ACSL4) und „*Lysophosphatidylcholine acyltransferase 2*“ (LPCAT2). Zur Herstellung der veresterten Oxylipine wurden zwei Ansätze verfolgt.

Zunächst wurde die rekombinante Expression und Aufreinigung der beiden humanen Enzyme in *E. coli* BL21(De3) untersucht. Das humane ACSL4-Gen wird in zwei Isoformen mit unterschiedlicher Größe exprimiert. Da die längere Isoform zusätzliche Aminosäuren am N-terminalen Ende enthält, die für einen Membrananker kodieren, wurde in dieser Arbeit die kürzere Isoform gewählt, um ein vermeintlich besser lösliches Protein zu erhalten. Zusätzlich wurde am C-terminalen Ende des Proteins ein His<sub>6</sub>x-Tag eingefügt um eine Aufreinigung mittels Ni-Affinitätschromatographie durchführen zu können. Zuvor hatte bereits eine Publikation über die Aktivität von ACSL4 (aus der Ratte) gezeigt, dass ein C-terminaler Peptid-Tag selbst Kinetikuntersuchungen nicht negativ beeinflusst. Die anschließende Aufreinigung mittels Ni-Affinitätschromatographie lieferte bereits ein aktives und gefaltetes Protein,

allerdings waren noch viele Verunreinigungen vorhanden. Daher sollte in einem zweiten Aufreinigungsschritt die Reinheit weiter verbessert werden. Dazu wurden Größenausschluss- und Ionenaustauschchromatographie (IEX) miteinander verglichen. Beide Methoden lieferten eine vergleichbare Reinheit von >95 %, jedoch zeigte sich, dass das Protein nur nach der Aufreinigung mittels IEX noch aktiv war. Im Zuge der Aktivitätsuntersuchungen konnte hier ein mit der Literatur vergleichbarer  $K_m$  für Eicosapentaensäure bestimmt werden. Da es sich bei dem verwendeten Assay um ein indirektes System handelt, welches die Aktivierung der Fettsäure durch ACSL4 über drei weitere Enzyme mit der Oxidation von NADH koppelt, ist das Setup potentiell fehleranfällig. Daher sollte für eine weitere Analyse der Aktivität ein direkter LC-MS-Ansatz in Betracht gezogen werden. Neben der Aktivität wurde auch die Stabilität des Proteins in Form der Schmelztemperatur ( $T_m$ ) bestimmt. Es zeigte sich, dass das Protein bei pH 6 die höchste Stabilität aufwies ( $T_m = 43\text{ °C}$ ), welche durch Zugabe von Glycerin noch gesteigert werden konnte. Insgesamt konnte somit eine neue Expressions- und Aufreinigungsstrategie für die humane ACSL4 etabliert werden, welche zu einem reinen, aktiven und gefalteten Protein führt. Um möglichst viele Oxylipine gezielt herstellen zu können, wurde anschließend die Expression und Aufreinigung einer Lipoxygenase aus *Pseudomonas aeruginosa* (PA-LOX) etabliert. Das Expressionsplasmid wurde freundlicherweise von Univ.-Prof. Dr. sc. med. Hartmut Kühn (Charité Berlin) zur Verfügung gestellt und die Aufreinigung erfolgte unter leichter Abwandlung einer bereits publizierten Methode. Anschließende Stabilitäts- und Aktivitätsuntersuchungen bestätigten die Funktionsfähigkeit des Enzyms.

Der nächste Schritt zur Synthese von veresterten Lipidmediatoren war die Übertragung der aktivierten Fettsäuren auf ein Lyso-Phospholipid. Da es keine Literatur zur rekombinanten Expression der humanen LPCAT2 in *E. coli* gab, wurde ein Ansatz mit His6x-Tag und Ni-Affinitätschromatographie als Startpunkt gewählt. Es zeigte sich, dass das Protein zwar exprimiert wurde, jedoch nur in sehr geringen Mengen. Außerdem zeigte eine Western-Blot-Analyse, dass das Protein etwa 10 kDa kleiner war als erwartet. Durch Anbringen von His6x-Tags am N- bzw. C-Terminus und Inkubation mit einem Anti-His6x-Tag Antikörper konnte festgestellt werden, dass der N-terminale Teil des Proteins fehlte. Eine genauere Analyse der Aminosäuresequenz ergab drei potentielle N-terminale Spaltstellen, die zu einer Verkürzung des Proteins um 7-12 kDa führen könnten. Anhand der Aminosäuresequenz konnte auch eine vermutete Transmembranregion identifiziert werden, weshalb weitere Expressionskonstrukte mit verkürzten N-terminalen Enden erstellt wurden. Um die Löslichkeit des Proteins trotz potentieller Transmembranbereiche zu verbessern, wurde zusätzlich ein Konstrukt mit N-terminalem MBP-Tag erstellt. Leider führte keine dieser Modifikationen zu einer Verbesserung und auch weitere Optimierungen der Expressions- und Pufferbedingungen sowie eine Denaturierung und Rückfaltung des Proteins waren nicht erfolgreich. Da letztendlich kein aktives Protein erhalten werden konnte, wurde der Ansatz der Synthese veresteter Lipidmediatoren mittels rekombinanter Proteine aus *E. coli* nicht weiter verfolgt.

Um dennoch veresterte Lipidmediatoren synthetisieren und untersuchen zu können, war ein neuer Ansatz erforderlich. Die Wahl fiel auf die Etablierung stabiler Zelllinien, die die Enzyme ACSL4 und/oder LPCAT2 überexprimieren. Wie beim rekombinanten Ansatz in *E. coli* sollte anschließend eine Co-Expression verschiedener Lipoxygenasen (LOs) erfolgen, um gezielt bestimmte Oxylipine herstellen zu können. Da das Projekt somit auf eine mehrfach genetische

Modifikation der Zellen abzielte, wurde als Ausgangszelllinie die humane embryonale Nierenzelllinie 293T (HEK293T) gewählt. Diese lässt sich vergleichsweise einfach, d.h. ohne Verwendung viraler Partikel, transfizieren und benötigt zudem keine teuren Transfektionsreagenzien. Um zunächst das ACSL4- und LPCAT2-Gen stabil in das Genom der HEK293T Zellen zu integrieren, wurde die sogenannte „*Sleeping Beauty*“-Technologie eingesetzt. Durch Co-Expression einer Transposase konnten die entsprechenden Sequenzen in das Genom der Zellen integriert werden. Zusätzlich wurde ein Antibiotikaresistenzgen integriert, das anschließend die Selektion mit Hygromycin B ermöglichte. Die erfolgreiche Überexpression wurde auf Proteinebene verifiziert und das Oxylinprofil der Zellen wurde mittels LC-MS in Zusammenarbeit mit der Arbeitsgruppe von Prof. Dr. Nils Helge Schebb (Bergische Universität Wuppertal) bestimmt. Dabei wurden sowohl die freien Oxyline wie auch die Gesamtoxylinbildung ermittelt. Die anschließende Analyse ergab, dass die Überexpression von ACSL4 und/oder LPCAT2 nicht wie erwartet zu einem erhöhten Anteil an veresterten Oxylinen führte. Stattdessen wurde insgesamt eine erhöhte Oxylinproduktion beobachtet. Während die Überexpression von ACSL4 nur zu einer leichten Erhöhung führte, zeigte die Expression von LPCAT2 einen deutlichen Anstieg. Die stärkste Oxylinproduktion wurde jedoch durch Co-Expression von ACSL4 und LPCAT2 erreicht.

Um zu untersuchen, ob das Oxylinprofil der Zellen gezielt beeinflusst werden kann, sollten im Anschluss auch 5-LO, 15-LO1 oder 15-LO2 exprimiert werden. Hierzu wurde zunächst ein transients Ansatz gewählt, um die bereits stabil transfizierten Zelllinien nicht unnötig zu stressen. Da die Effizienz transients Transfektionen jedoch stark schwanken kann, wurden Konstrukte mit mCherry, einem rot fluoreszierenden Protein, erzeugt. Mit Hilfe eines Fluoreszenzmikroskops sollte es so möglich sein, die Anzahl der transfizierten Zellen zu bestimmen. Leider zeigte die Untersuchung der LO-Aktivität keine Produktbildung. Mittels Western-Blot-Analyse konnte die Inaktivität der LOs schließlich auf einen kleinen Teil des Linkers zurückgeführt werden, der zur Trennung der jeweiligen LOs vom mCherry-Gen verwendet wurde. Um dieses Problem zu umgehen, wurde erneut ein Ansatz zur stabilen Integration mit Hilfe der „*Sleeping Beauty*“-Technologie verfolgt. Da die permanente Expression von LOs jedoch mit einem erhöhten oxidativen Stress in den Zellen einhergeht, wurde ein induzierbarer Promotor verwendet. Dieser verhindert unter Standardbedingungen die Expression des nachfolgenden Gens, kann aber durch Inkubation mit Doxycyclin-haltigem Medium (200 ng/mL, 24 h) aktiviert werden. Um sicherzustellen, dass die neuen doppelt transfizierten Zellen sowohl die ursprünglich transfizierten Gene ACSL4 und/oder LPCAT2 wie auch die neuen LOs enthalten, wurden die neuen Konstrukte mit einem weiteren Antibiotikaresistenzgen ausgestattet. Nach Selektion mit Hygromycin B und Puromycin konnten so erfolgreich transfizierte Zelllinien erhalten werden. Das induzierbare Expressionssystem wurde anschließend mittels Western-Blot-Analyse untersucht und zeigte, dass eine LO-Expression nur nach Behandlung mit Doxycyclin nachweisbar war. Dies konnte ebenfalls durch die Untersuchung der LO-Produktbildung bestätigt werden. Auch hier war eine Aktivität der jeweiligen LO nur nach vorheriger Behandlung mit Doxycyclin nachweisbar. Zur weiteren Charakterisierung der Zelllinien wurden Konfokalmikroskopiebilder aufgenommen, um zunächst die Lokalisation von ACSL4 und LPCAT2 zu untersuchen. Wie erwartet befand sich ACSL4 im Zytosol der Zellen. Die Lokalisation von LPCAT2 hingegen variierte je nach

Expressionslevel. In Kontrollzelllinien, die nur geringe Mengen an LPCAT2 exprimieren, wurde das Protein vermehrt in kleinen zirkulären Bereichen gefunden, während die Überexpression von LPCAT2 zu einer Verteilung im Zytosol führte.

Da die Zelllinien nun auch verschiedene LOs exprimierten, wurde das Oxylinprofil der Zellen erneut bestimmt. Überraschenderweise zeigte sich, dass die Expression von 5-LO nur einen minimalen Einfluss auf die Oxylinbildung hatte. Dagegen wurden in Zelllinien, die 15-LO1 oder 15-LO2 exprimierten, deutlich erhöhte Werte vor allem an 13-Hydroxy-9Z,11E-octadecadiensäure (13-HODE), 15-Hydroxy-5Z,8Z,11Z,13E-eicosatetraensäure (15-HETE) und 17-Hydroxy-4Z,7Z,10Z,13Z,15E,19Z-docosahexaensäure (17-HDHA) detektiert. Dies war unerwartet, da alle drei LOs in der vorangegangenen Aktivitätsuntersuchung mit exogener Arachidonsäure und Calciumionophor zu einer vergleichbaren Produktbildung geführt hatten.

Die Untersuchung des Oxylinprofils umfasste dabei sowohl die Bestimmung der freien Oxyline wie auch der Gesamtoxyline. Der Vergleich der beiden Spezies zeigte, dass die Mehrzahl der Oxyline überwiegend verestert vorlag. Trotz der stark erhöhten Oxylinbildung nach Expression von 15-LO1 bzw. 15-LO2 waren auch hier die entsprechenden Produkte überwiegend verestert. Da die vermehrte Bildung oxidierter Lipide eine Schlüsselkomponente bei Zelltod-mechanismen wie der Ferroptose darstellt, wurde die Zellviabilität der verschiedenen HEK293T-Derivate getestet. Dazu wurden die Zellen mit den Ferroptose-induzierenden Substanzen Erastin oder RSL3 behandelt, und ihr Verhalten im Vergleich zu Leervektorkontrollen analysiert. Da ACSL4 bereits als Biomarker für Ferroptose bekannt ist, war es nicht überraschend, dass die Expression von ACSL4 zu einem vermehrten Zelltod führte. Interessanterweise war dies jedoch auch in LPCAT2-überexprimierenden Zellen der Fall. Obwohl für LPCAT3, einem mit LPCAT2 verwandten Enzym, bereits eine Rolle bei der Entstehung von Ferroptose beschrieben wurde, ist meines Wissens bisher kein Zusammenhang zwischen Ferroptose und LPCAT2 publiziert worden. Um die Reaktion der Zelllinien auf Erastin und RSL3 weiter zu untersuchen, wurden weitere Konfokalmikroskopieuntersuchungen mit und ohne Behandlung durchgeführt. Dabei fiel vor allem die Lokalisation der 15-LO1 auf. Diese befand sich in den Kontrollzellen überwiegend im Zytosol der Zellen und wanderte durch Behandlung mit Erastin teilweise in den Zellkern. RSL3 hingegen führte dazu, dass sich das Protein vollständig an die Kernmembran anlagerte. Überraschenderweise lag 15-LO1 in LPCAT2-überexprimierenden Zellen bereits in unbehandelten Proben an der Kernmembran vor. Die Tatsache, dass die Lokalisation nach Überexpression von LPCAT2 und nach Behandlung mit RSL3 nahezu identisch war, könnte darauf hindeuten, dass tatsächlich ein Zusammenhang zwischen LPCAT2 und Ferroptose besteht. Darüber hinaus zeigte die Abstandsuntersuchung von LPCAT2 und 15-LO1, dass sich die beiden Enzyme nicht nur an der Kernmembran, sondern auch in räumlicher Nähe zueinander befanden.

Da sowohl die Untersuchung der Zellviabilität wie auch die Lokalisation der 15-LO1 darauf hindeuteten, dass die Expression der LPCAT2 zumindest eine unterstützende Rolle bei der Entwicklung von Ferroptose spielen könnte, wurde eine weitere Oxylinanalyse durchgeführt. Diesmal wurden die HEK293T\_LPCAT2\_15LO1 Zelllinie für 4 h mit RSL3 und/oder Ferrostatin behandelt, um das Oxylinprofil in ferroptotischen Zellen zu untersuchen. Da Ferrostatin die

Oxidation innerhalb von Membranen inhibiert, sollte dies eine Aussage über die Herkunft der veresterten Oxylipine erlauben. Wie erwartet waren die Oxylipinspiegel nach Inkubation mit RSL3 teilweise deutlich erhöht. Zudem zeigte auch die Kombinationsbehandlung mit RSL3 und Ferrostatin eine vergleichbare Erhöhung. Da sowohl die freien wie auch die Gesamtoxylipine bestimmt wurden, konnte festgestellt werden, dass die Oxylipine auch unter diesen Bedingungen überwiegend verestert vorlagen. Da die Behandlung mit Ferrostatin hier zu keiner nennenswerten Änderung führte, scheinen die beobachteten Oxylipine nicht durch eine direkte Oxidation veresteter Substrate zu entstehen. Stattdessen ist es wahrscheinlicher, dass zunächst freie Fettsäuren oxidiert werden und diese dann im Anschluss in die entsprechenden Phospholipide eingebaut werden.

Insgesamt konnte im Rahmen dieser Arbeit ein HEK293T-basiertes Überexpressionssystem entwickelt werden, welches die Bildung von veresterten Lipidmediatoren ermöglicht. Dabei erlaubt die gezielte Induktion der LO-Expression eine Modifikation des Oxylipinprofils der Zellen. Darüber hinaus konnte in mehreren Untersuchungen gezeigt werden, dass die verwendete Acyltransferase „LPCAT2“ vermutlich mit dem Zelltodmechanismus Ferroptose in Verbindung steht. Da dieser Zusammenhang bisher nicht publiziert ist, stellt er einen vielversprechenden neuen Ansatzpunkt für zukünftige Therapien dar. Ferroptose spielt unter anderem bei neurodegenerativen Erkrankungen, aber auch bei Autoimmun- und Tumorerkrankungen eine wichtige Rolle, weshalb neue Behandlungsansätze sehr gefragt sind.



## 8 References

- [1] S.J. Singer, G.L. Nicolson, The fluid mosaic model of the structure of cell membranes, *Science*. 175 (1972) 720–731.
- [2] J. Lenard, S.J. Singer, Protein conformation in cell membrane preparations as studied by optical rotatory dispersion and circular dichroism., *Proc. Natl. Acad. Sci. U. S. A.* 56 (1966) 1828–35.
- [3] S. Shukla, T. Baumgart, Enzymatic trans-bilayer lipid transport: Mechanisms, efficiencies, slippage, and membrane curvature., *Biochim. Biophys. acta. Biomembr.* 1863 (2021) 183534.
- [4] A. Chakrabarti, Phospholipid asymmetry in biological membranes: Is the role of phosphatidylethanolamine underappreciated?, *J. Membr. Biol.* 254 (2021) 127–132.
- [5] K. Simons, J.L. Sampaio, Membrane organization and lipid rafts., *Cold Spring Harb. Perspect. Biol.* 3 (2011) a004697.
- [6] J. Huang, G.W. Feigenson, A microscopic interaction model of maximum solubility of cholesterol in lipid bilayers, *Biophys. J.* 76 (1999) 2142–2157.
- [7] G. van Meer, D.R. Voelker, G.W. Feigenson, Membrane lipids: Where they are and how they behave., *Nat. Rev. Mol. Cell Biol.* 9 (2008) 112–24.
- [8] A. Yamashita, Y. Hayashi, Y. Nemoto-Sasaki, M. Ito, S. Oka, T. Tanikawa, K. Waku, T. Sugiura, Acyltransferases and transacylases that determine the fatty acid composition of glycerolipids and the metabolism of bioactive lipid mediators in mammalian cells and model organisms., *Prog. Lipid Res.* 53 (2014) 18–81.
- [9] E.P. Kennedy, S.B. Weiss, The function of cytidine coenzymes in the biosynthesis of phospholipides., *J. Biol. Chem.* 222 (1956) 193–214.
- [10] W.E. Lands, Metabolism of glycerolipides; a comparison of lecithin and triglyceride synthesis., *J. Biol. Chem.* 231 (1958) 883–8.
- [11] P.J. Brophy, P.C. Choy, J.R. Toone, D.E. Vance, Choline kinase and ethanolamine kinase are separate, soluble enzymes in rat liver., *Eur. J. Biochem.* 78 (1977) 491–5.
- [12] R. Sundler, B. Akesson, Regulation of phospholipid biosynthesis in isolated rat hepatocytes. Effect of different substrates, *J. Biol. Chem.* 250 (1975) 3359–3367.
- [13] F. Gibellini, T.K. Smith, The Kennedy pathway-de novo synthesis of phosphatidylethanolamine and phosphatidylcholine, *IUBMB Life.* 62 (2010) 414–428.
- [14] K. Athenstaedt, Phosphatidic acid biosynthesis in the model organism yeast *Saccharomyces cerevisiae* - a survey, *Biochim. Biophys. Acta - Mol. Cell Biol. Lipids.* 1866 (2021) 158907.
- [15] N.J. Blunsom, S. Cockcroft, Phosphatidylinositol synthesis at the endoplasmic reticulum., *Biochim. Biophys. acta. Mol. cell Biol. lipids.* 1865 (2020) 158471.
- [16] A.K. Kimura, T. Kimura, Phosphatidylserine biosynthesis pathways in lipid homeostasis: Toward resolution of the pending central issue for decades, *FASEB J.* 35 (2021) 1–15.
- [17] H. Shindou, D. Hishikawa, T. Harayama, M. Eto, T. Shimizu, Generation of membrane diversity by lysophospholipid acyltransferases, *J. Biochem.* 154 (2013) 21–28.
- [18] I. Kudo, M. Murakami, Phospholipase A2 enzymes., *Prostaglandins Other Lipid Mediat.* 68–69 (2002) 3–58.
- [19] W.E.M. Lands, I. Merkl, Metabolism of Glycerolipids, *J. Biol. Chem.* 238 (1963) 898–

904.

- [20] W.E.M. Lands, Metabolism of Glycerolipids, *J. Biol. Chem.* 235 (1960) 2233–2237.
- [21] E. Soupene, H. Fyrst, F.A. Kuypers, Mammalian acyl-CoA:lysophosphatidylcholine acyltransferase enzymes, *Proc. Natl. Acad. Sci. U.S.A.* 105 (2008) 88–93.
- [22] A.K. Agarwal, A. Garg, Enzymatic activity of the human 1-acylglycerol-3-phosphate-O-acyltransferase isoform 11: upregulated in breast and cervical cancers, *J. Lipid Res.* 51 (2010) 2143–2152.
- [23] H. Shindou, D. Hishikawa, H. Nakanishi, T. Harayama, S. Ishii, R. Taguchi, T. Shimizu, A single enzyme catalyzes both platelet-activating factor production and membrane biogenesis of inflammatory cells, *J. Biol. Chem.* 282 (2007) 6532–6539.
- [24] A. Yamashita, Y. Hayashi, N. Matsumoto, Y. Nemoto-Sasaki, S. Oka, T. Tanikawa, T. Sugiura, Glycerophosphate/Acylglycerophosphate acyltransferases, *Biology (Basel)*. 3 (2014) 801–830.
- [25] H. Shindou, T. Shimizu, Acyl-CoA:lysophospholipid acyltransferases, *J. Biol. Chem.* 284 (2009) 1–5.
- [26] M. Rossi Sebastiano, G. Konstantinidou, M.R. Sebastiano, G. Konstantinidou, Targeting long chain acyl-coa synthetases for cancer therapy, *Int. J. Mol. Sci.* 20 (2019) 1–16.
- [27] M.-J. Kang, T. Fujino, H. Sasano, H. Minekura, N. Yabuki, H. Nagura, H. Iijima, T.T. Yamamoto, A novel arachidonate-preferring acyl-CoA synthetase is present in steroidogenic cells of the rat adrenal, ovary, and testis, *Proc. Natl. Acad. Sci. U.S.A.* 94 (1997) 2880–2884.
- [28] E. Oikawa, H. Iijima, T. Suzuki, H. Sasano, H. Sato, A. Kamataki, H. Nagura, M.J. Kang, T. Fujino, H. Suzuki, T.T. Yamamoto, A novel acyl-CoA synthetase, ACS5, expressed in intestinal epithelial cells and proliferating preadipocytes., *J. Biochem.* 124 (1998) 679–85.
- [29] T. Fujino, M.J. Kang, H. Suzuki, H. Iijima, T. Yamamoto, Molecular characterization and expression of rat acyl-CoA synthetase 3., *J. Biol. Chem.* 271 (1996) 16748–52.
- [30] J.E. Kanter, C. Tang, J.F. Oram, K.E. Bornfeldt, Acyl-CoA synthetase 1 is required for oleate and linoleate mediated inhibition of cholesterol efflux through ATP-binding cassette transporter A1 in macrophages., *Biochim. Biophys. Acta.* 1821 (2012) 358–64.
- [31] E.L. Klett, S. Chen, A. Yechoor, F.B. Lih, R.A. Coleman, Long-chain acyl-CoA synthetase isoforms differ in preferences for eicosanoid species and long-chain fatty acids, *J. Lipid Res.* 58 (2017) 884–894.
- [32] M. Lopes-Marques, I. Cunha, M.A. Reis-Henriques, M.M. Santos, L.F.C. Castro, Diversity and history of the long-chain acyl-CoA synthetase (Acsl) gene family in vertebrates., *BMC Evol. Biol.* 13 (2013) 271.
- [33] D.G. Mashek, K.E. Bornfeldt, R.A. Coleman, J. Berger, D.A. Bernlohr, P. Black, C.C. DiRusso, S.A. Farber, W. Guo, N. Hashimoto, V. Khodiyar, F.A. Kuypers, L.J. Maltais, D.W. Nebert, A. Renieri, J.E. Schaffer, A. Stahl, P.A. Watkins, V. Vasiliou, T.T. Yamamoto, Revised nomenclature for the mammalian long-chain acyl-CoA synthetase gene family, *J. Lipid Res.* 45 (2004) 1958–1961.
- [34] D.J. Durgan, J.K. Smith, M.A. Hotze, O. Egbejimi, K.D. Cuthbert, V.G. Zaha, J.R.B. Dyck, E.D. Abel, M.E. Young, Distinct transcriptional regulation of long-chain acyl-CoA synthetase isoforms and cytosolic thioesterase 1 in the rodent heart by fatty acids and insulin., *Am. J. Physiol. Heart Circ. Physiol.* 290 (2006) H2480-97.

- [35] L.O. Li, J.M. Ellis, H.A. Paich, S. Wang, N. Gong, G. Altshuler, R.J. Thresher, T.R. Koves, S.M. Watkins, D.M. Muoio, G.W. Cline, G.I. Shulman, R.A. Coleman, Liver-specific loss of long chain acyl-CoA synthetase-1 decreases triacylglycerol synthesis and beta-oxidation and alters phospholipid fatty acid composition., *J. Biol. Chem.* 284 (2009) 27816–27826.
- [36] J.M. Ellis, S.M. Mentock, M.A. Depetrillo, T.R. Koves, S. Sen, S.M. Watkins, D.M. Muoio, G.W. Cline, H. Taegtmeyer, G.I. Shulman, M.S. Willis, R.A. Coleman, Mouse cardiac acyl coenzyme a synthetase 1 deficiency impairs fatty acid oxidation and induces cardiac hypertrophy., *Mol. Cell. Biol.* 31 (2011) 1252–62.
- [37] J.M. Ellis, L.O. Li, P.-C. Wu, T.R. Koves, O. Ilkayeva, R.D. Stevens, S.M. Watkins, D.M. Muoio, R.A. Coleman, Adipose acyl-CoA synthetase-1 directs fatty acids toward beta-oxidation and is required for cold thermogenesis., *Cell Metab.* 12 (2010) 53–64.
- [38] D.L. Brasaemle, G. Dolios, L. Shapiro, R. Wang, Proteomic analysis of proteins associated with lipid droplets of basal and lipolytically stimulated 3T3-L1 adipocytes., *J. Biol. Chem.* 279 (2004) 46835–42.
- [39] E. Umlauf, E. Csaszar, M. Moertelmaier, G.J. Schuetz, R.G. Parton, R. Prohaska, Association of stomatin with lipid bodies., *J. Biol. Chem.* 279 (2004) 23699–709.
- [40] Y. Fujimoto, H. Itabe, T. Kinoshita, K.J. Homma, J. Onoduka, M. Mori, S. Yamaguchi, M. Makita, Y. Higashi, A. Yamashita, T. Takano, Involvement of ACSL in local synthesis of neutral lipids in cytoplasmic lipid droplets in human hepatocyte HuH7., *J. Lipid Res.* 48 (2007) 1280–92.
- [41] M. Poppelreuther, B. Rudolph, C. Du, R. Großmann, M. Becker, C. Thiele, R. Eehalt, J. Füllekrug, The N-terminal region of acyl-CoA synthetase 3 is essential for both the localization on lipid droplets and the function in fatty acid uptake, *J. Lipid Res.* 53 (2012) 888–900.
- [42] S.Y. Bu, M.T. Mashek, D.G. Mashek, Suppression of long chain acyl-CoA synthetase 3 decreases hepatic de novo fatty acid synthesis through decreased transcriptional activity., *J. Biol. Chem.* 284 (2009) 30474–83.
- [43] Z. Liu, Y. Huang, W. Hu, S. Huang, Q. Wang, J. Han, Y.Q. Zhang, DAcsl, the drosophila ortholog of Acyl-CoA synthetase long-chain family Member 3 and 4, inhibits synapse growth by attenuating bone morphogenetic protein signaling via endocytic recycling, *J. Neurosci.* 34 (2014) 2785–2796.
- [44] T.M. Lewin, J.-H. Kim, D.A. Granger, J.E. Vance, R.A. Coleman, Acyl-CoA synthetase isoforms 1, 4, and 5 are present in different subcellular membranes in rat liver and can be inhibited independently, *J. Biol. Chem.* 276 (2001) 24674–24679.
- [45] E.-M. Küch, R. Vellaramkalayil, I. Zhang, D. Lehnen, B. Brügger, W. Stremmel, R. Eehalt, M. Poppelreuther, J. Füllekrug, Differentially localized acyl-CoA synthetase 4 isoenzymes mediate the metabolic channeling of fatty acids towards phosphatidylinositol, *Biochim. Biophys. Acta - Mol. Cell Biol. Lipids.* 1841 (2014) 227–239.
- [46] I.H. Ansari, M.J. Longacre, S.W. Stoker, M.A. Kendrick, L.M. O'Neill, L.J. Zitour, L.A. Fernandez, J.M. Ntambi, M.J. MacDonald, Characterization of Acyl-CoA synthetase isoforms in pancreatic beta cells: Gene silencing shows participation of ACSL3 and ACSL4 in insulin secretion, *Arch. Biochem. Biophys.* 618 (2017) 32–43.
- [47] D.L. Golej, B. Askari, F. Kramer, S. Barnhart, A. Vivekanandan-Giri, S. Pennathur, K.E. Bornfeldt, Long-chain acyl-CoA synthetase 4 modulates prostaglandin E2 release from human arterial smooth muscle cells, *J. Lipid Res.* 52 (2011) 782–793.

- [48] N. Meller, M.E. Morgan, W.P. Wong, J.B. Altemus, E. Sehayek, Targeting of Acyl-CoA synthetase 5 decreases jejunal fatty acid activation with no effect on dietary long-chain fatty acid absorption., *Lipids Health Dis.* 12 (2013) 88.
- [49] Y. Achouri, B.D. Hegarty, D. Allanic, D. Bécard, I. Hainault, P. Ferré, F. Fougère, Long chain fatty acyl-CoA synthetase 5 expression is induced by insulin and glucose: involvement of sterol regulatory element-binding protein-1c., *Biochimie.* 87 (2005) 1149–55.
- [50] J.D. Horton, N.A. Shah, J.A. Warrington, N.N. Anderson, S.W. Park, M.S. Brown, J.L. Goldstein, Combined analysis of oligonucleotide microarray data from transgenic and knockout mice identifies direct SREBP target genes., *Proc. Natl. Acad. Sci. U. S. A.* 100 (2003) 12027–32.
- [51] S.Y. Bu, D.G. Mashek, Hepatic long-chain acyl-CoA synthetase 5 mediates fatty acid channeling between anabolic and catabolic pathways., *J. Lipid Res.* 51 (2010) 3270–80.
- [52] T. Fujino, T. Yamamoto, Cloning and functional expression of a novel long-chain acyl-CoA synthetase expressed in brain., *J. Biochem.* 111 (1992) 197–203.
- [53] R.F. Fernandez, A.S. Pereyra, V. Diaz, E.S. Wilson, K.A. Litwa, J. Martínez-Gardeazabal, S.N. Jackson, J.T. Brenna, B.P. Hermann, J.B. Eells, J.M. Ellis, Acyl-CoA synthetase 6 is required for brain docosahexaenoic acid retention and neuroprotection during aging, *JCI Insight.* 6 (2021).
- [54] Y. Cao, E. Traer, G.A. Zimmerman, T.M. McIntyre, S.M. Prescott, Cloning, expression, and chromosomal localization of human long-chain fatty acid-CoA ligase 4 (FACL4)., *Genomics.* 49 (1998) 327–30.
- [55] M. Piccini, F. Vitelli, M. Bruttini, B.R. Pober, J.J. Jonsson, M. Villanova, M. Zollo, G. Borsani, A. Ballabio, A. Renieri, FACL4, a new gene encoding long-chain acyl-CoA synthetase 4, is deleted in a family with Alport syndrome, elliptocytosis, and mental retardation, *Genomics.* 47 (1998) 350–358.
- [56] S. Shimbara-Matsubayashi, H. Kuwata, N. Tanaka, M. Kato, S. Hara, Analysis on the substrate specificity of recombinant human Acyl-CoA Synthetase ACSL4 variants, *Biol. Pharm. Bull.* 42 (2019) 850–855.
- [57] P. Liao, W. Wang, W. Wang, I. Kryczek, X. Li, Y. Bian, A. Sell, S. Wei, S. Grove, J.K. Johnson, P.D. Kennedy, M. Gijón, Y.M. Shah, W. Zou, CD8+ T cells and fatty acids orchestrate tumor ferroptosis and immunity via ACSL4., *Cancer Cell.* 40 (2022) 365–378.e6.
- [58] J.M. Drijvers, J.E. Gillis, T. Muijllwijk, T.H. Nguyen, E.F. Gaudiano, I.S. Harris, M.W. LaFleur, A.E. Ringel, C.-H. Yao, K. Kurmi, V.R. Juneja, J.D. Trombley, M.C. Haigis, A.H. Sharpe, Pharmacologic screening identifies metabolic vulnerabilities of CD8+ T cells., *Cancer Immunol. Res.* 9 (2021) 184–199.
- [59] S.J. Dixon, K.M. Lemberg, M.R. Lamprecht, R. Skouta, E.M. Zaitsev, C.E. Gleason, D.N. Patel, A.J. Bauer, A.M. Cantley, W.S. Yang, B. Morrison, B.R. Stockwell, Ferroptosis: An iron-dependent form of nonapoptotic cell death, *Cell.* 149 (2012) 1060–1072.
- [60] H. Yuan, X. Li, X. Zhang, R. Kang, D. Tang, Identification of ACSL4 as a biomarker and contributor of ferroptosis, *Biochem. Biophys. Res. Commun.* 478 (2016) 1338–1343.
- [61] S. Doll, B. Proneth, Y.Y. Tyurina, E. Panzilius, S. Kobayashi, I. Ingold, M. Irmeler, J. Beckers, M. Aichler, A. Walch, H. Prokisch, D. Trümbach, G. Mao, F. Qu, H. Bayir, J. Füllekrug, C.H. Scheel, W. Wurst, J.A. Schick, V.E. Kagan, J.P.F. Angeli, M. Conrad,

- ACSL4 dictates ferroptosis sensitivity by shaping cellular lipid composition, *Nat. Chem. Biol.* 13 (2017) 91–98.
- [62] W.-C. Chen, C.-Y. Wang, Y.-H. Hung, T.-Y. Weng, M.-C. Yen, M.-D. Lai, Systematic analysis of gene expression alterations and clinical outcomes for Long-chain Acyl-Coenzyme A synthetase family in cancer., *PLoS One.* 11 (2016) e0155660.
- [63] G. Lei, Y. Zhang, P. Koppula, X. Liu, J. Zhang, S.H. Lin, J.A. Ajani, Q. Xiao, Z. Liao, H. Wang, B. Gan, The role of ferroptosis in ionizing radiation-induced cell death and tumor suppression., *Cell Res.* 30 (2020) 146–162.
- [64] C. Eberhardt, P.W. Gray, L.W. Tjoelker, Human lysophosphatidic acid acyltransferase: cDNA cloning, expression, and localization to chromosome 9q34.3, *J. Biol. Chem.* 272 (1997) 20299–20305.
- [65] H. Nakanishi, H. Shindou, D. Hishikawa, T. Harayama, R. Ogasawara, A. Suwabe, R. Taguchi, T. Shimizu, Cloning and characterization of mouse lung-type acyl-CoA: lysophosphatidylcholine acyltransferase 1 (LPCAT1): Expression in alveolar type II cells and possible involvement in surfactant production, *J. Biol. Chem.* 281 (2006) 20140–20147.
- [66] X. Chen, B.A. Hyatt, M.L. Mucenski, R.J. Mason, J.M. Shannon, Identification and characterization of a lysophosphatidylcholine acyltransferase in alveolar type II cells., *Proc. Natl. Acad. Sci. U. S. A.* 103 (2006) 11724–9.
- [67] D. Hishikawa, H. Shindou, S. Kobayashi, H. Nakanishi, R. Taguchi, T. Shimizu, Discovery of a lysophospholipid acyltransferase family essential for membrane asymmetry and diversity, *Proc. Natl. Acad. Sci. U. S. A.* 105 (2008) 2830–2835.
- [68] Y. Zhao, Y.-Q. Chen, T.M. Bonacci, D.S. Bredt, S. Li, W.R. Bensch, D.E. Moller, M. Kowala, R.J. Konrad, G. Cao, Identification and characterization of a major liver lysophosphatidylcholine acyltransferase., *J. Biol. Chem.* 283 (2008) 8258–65.
- [69] S. Matsuda, T. Inoue, H.C. Lee, N. Kono, F. Tanaka, K. Gengyo-Ando, S. Mitani, H. Arai, Member of the membrane-bound O-acyltransferase (MBOAT) family encodes a lysophospholipid acyltransferase with broad substrate specificity, *Genes to Cells.* 13 (2008) 879–888.
- [70] T.M. Lewin, P. Wang, R.A. Coleman, Analysis of amino acid motifs diagnostic for the sn-glycerol-3-phosphate acyltransferase reaction., *Biochemistry.* 38 (1999) 5764–71.
- [71] S. Shikano, M. Li, Membrane receptor trafficking: evidence of proximal and distal zones conferred by two independent endoplasmic reticulum localization signals., *Proc. Natl. Acad. Sci. U. S. A.* 100 (2003) 5783–8.
- [72] H. Shindou, M. Eto, R. Morimoto, T. Shimizu, Identification of membrane O-acyltransferase family motifs., *Biochem. Biophys. Res. Commun.* 383 (2009) 320–5.
- [73] X. Rong, C.J. Albert, C. Hong, M.A. Duerr, B.T. Chamberlain, E.J. Tarling, A. Ito, J. Gao, B. Wang, P.A. Edwards, M.E. Jung, D.A. Ford, P. Tontonoz, LXRs Regulate ER Stress and Inflammation through Dynamic Modulation of Membrane Phospholipid Composition, *Cell Metab.* 18 (2013) 685–697.
- [74] T. Harayama, H. Shindou, R. Ogasawara, A. Suwabe, T. Shimizu, Identification of a novel noninflammatory biosynthetic pathway of platelet-activating factor., *J. Biol. Chem.* 283 (2008) 11097–106.
- [75] M.A. Welte, Expanding roles for lipid droplets., *Curr. Biol.* 25 (2015) R470-81.
- [76] K. Tauchi-Sato, S. Ozeki, T. Houjou, R. Taguchi, T. Fujimoto, The surface of lipid

- droplets is a phospholipid monolayer with a unique fatty acid composition., *J. Biol. Chem.* 277 (2002) 44507–12.
- [77] J. Bouchoux, F. Beilstein, T. Pauquai, I.C. Guerrero, D. Chateau, N. Ly, M. Alqub, C. Klein, J. Chambaz, M. Rousset, J.-M. Lacorte, E. Morel, S. Demignot, The proteome of cytosolic lipid droplets isolated from differentiated Caco-2/TC7 enterocytes reveals cell-specific characteristics, *Biol. Cell.* 103 (2011) 499–517.
- [78] C. Moessinger, L. Kuerschner, J. Spandl, A. Shevchenko, C. Thiele, Human lysophosphatidylcholine acyltransferases 1 and 2 are located in lipid droplets where they catalyze the formation of phosphatidylcholine, *J. Biol. Chem.* 286 (2011) 21330–21339.
- [79] C. Moessinger, K. Klizaite, A. Steinhagen, J. Philippou-Massier, A. Shevchenko, M. Hoch, C.S. Ejsing, C. Thiele, Two different pathways of phosphatidylcholine synthesis, the Kennedy Pathway and the Lands Cycle, differentially regulate cellular triacylglycerol storage., *BMC Cell Biol.* 15 (2014) 43.
- [80] N. Dupont, S. Chauhan, J. Arko-Mensah, E.F. Castillo, A. Masedunskas, R. Weigert, H. Robenek, T. Proikas-Cezanne, V. Deretic, Neutral lipid stores and lipase PNPLA5 contribute to autophagosome biogenesis., *Curr. Biol.* 24 (2014) 609–20.
- [81] A.K. Cotte, V. Aires, M. Fredon, E. Limagne, V. Derangère, M. Thibaudin, E. Humblin, A. Scagliarini, J.-P.P.P.P. De Barros, P. Hillon, F. Ghiringhelli, D. Delmas, Lysophosphatidylcholine acyltransferase 2-mediated lipid droplet production supports colorectal cancer chemoresistance, *Nat. Commun.* 9 (2018) 322.
- [82] A. Filipe, J. McLauchlan, Hepatitis C virus and lipid droplets: finding a niche, *Trends Mol. Med.* 21 (2015) 34–42.
- [83] F. Beilstein, M. Lemasson, V. Pène, D. Rainteau, S. Demignot, A.R. Rosenberg, Lysophosphatidylcholine acyltransferase 1 is downregulated by hepatitis C virus: impact on production of lipo-viro-particles., *Gut.* 66 (2017) 2160–2169.
- [84] B. Wang, P. Tontonoz, Phospholipid Remodeling in Physiology and Disease, *Annu. Rev. Physiol.* 81 (2019) 165–188.
- [85] R.J. Mason, J. Nellenbogen, Synthesis of saturated phosphatidylcholine and phosphatidylglycerol by freshly isolated rat alveolar type II cells., *Biochim. Biophys. Acta.* 794 (1984) 392–402.
- [86] T.J. Gregory, W.J. Longmore, M.A. Moxley, J.A. Whitsett, C.R. Reed, A.A. Fowler, L.D. Hudson, R.J. Maunder, C. Crim, T.M. Hyers, Surfactant chemical composition and biophysical activity in acute respiratory distress syndrome., *J. Clin. Invest.* 88 (1991) 1976–81.
- [87] O. Demeure, F. Lecerf, C. Duby, C. Desert, S. Ducheix, H. Guillou, S. Lagarrigue, Regulation of LPCAT3 by LXR., *Gene.* 470 (2011) 7–11.
- [88] A.B. Singh, J. Liu, Identification of hepatic lysophosphatidylcholine acyltransferase 3 as a novel target gene regulated by peroxisome proliferator-activated receptor  $\delta$ ., *J. Biol. Chem.* 292 (2017) 884–897.
- [89] X. Rong, B. Wang, E.N.D. Palladino, T.Q. de Aguiar Vallim, D.A. Ford, P. Tontonoz, ER phospholipid composition modulates lipogenesis during feeding and in obesity, *J. Clin. Invest.* 127 (2017) 3640–3651.
- [90] X. Rong, B. Wang, M.M. Dunham, P.N. Hedde, J.S. Wong, E. Gratton, S.G. Young, D.A. Ford, P. Tontonoz, Lpcat3-dependent production of arachidonoyl phospholipids is a key determinant of triglyceride secretion, *Elife.* 2015 (2015) 1–23.

- [91] T. Hashidate-Yoshida, T. Harayama, D. Hishikawa, R. Morimoto, F. Hamano, S.M. Tokuoka, M. Eto, M. Tamura-Nakano, R. Yanobu-Takanashi, Y. Mukumoto, H. Kiyonari, T. Okamura, Y. Kita, H. Shindou, T. Shimizu, Fatty acid remodeling by LPCAT3 enriches arachidonate in phospholipid membranes and regulates triglyceride transport., *Elife*. 4 (2015).
- [92] K. Taniguchi, H. Hikiji, T. Okinaga, T. Hashidate-Yoshida, H. Shindou, W. Ariyoshi, T. Shimizu, K. Tominaga, T. Nishihara, Essential role of lysophosphatidylcholine acyltransferase 3 in the induction of macrophage polarization in PMA-treated U937 cells., *J. Cell. Biochem*. 116 (2015) 2840–8.
- [93] H. Tanaka, N. Zaima, T. Sasaki, N. Yamamoto, K. Inuzuka, T. Yata, T. Iwaki, K. Umemura, H. Sano, Y. Suzuki, T. Urano, M. Setou, N. Unno, Lysophosphatidylcholine acyltransferase-3 expression is associated with atherosclerosis progression., *J. Vasc. Res*. 54 (2017) 200–208.
- [94] N. Kurabe, T. Hayasaka, M. Ogawa, N. Masaki, Y. Ide, M. Waki, T. Nakamura, K. Kurachi, T. Kahyo, K. Shinmura, Y. Midorikawa, Y. Sugiyama, M. Setou, H. Sugimura, Accumulated phosphatidylcholine (16:0/16:1) in human colorectal cancer; possible involvement of LPCAT4, *Cancer Sci*. 104 (2013) 1295–1302.
- [95] Y. Du, Q. Wang, X. Zhang, X. Wang, C. Qin, Z. Sheng, H. Yin, C. Jiang, J. Li, T. Xu, Lysophosphatidylcholine acyltransferase 1 upregulation and concomitant phospholipid alterations in clear cell renal cell carcinoma., *J. Exp. Clin. Cancer Res*. 36 (2017) 66.
- [96] T. Uehara, H. Kikuchi, S. Miyazaki, I. Iino, T. Setoguchi, Y. Hiramatsu, M. Ohta, K. Kamiya, Y. Morita, H. Tanaka, S. Baba, T. Hayasaka, M. Setou, H. Konno, Overexpression of lysophosphatidylcholine acyltransferase 1 and concomitant lipid alterations in gastric cancer., *Ann. Surg. Oncol*. 23 Suppl 2 (2016) S206-13.
- [97] E. Abdelzaher, M.F. Mostafa, Lysophosphatidylcholine acyltransferase 1 (LPCAT1) upregulation in breast carcinoma contributes to tumor progression and predicts early tumor recurrence., *Tumour Biol*. 36 (2015) 5473–83.
- [98] F. Mansilla, K.-A. da Costa, S. Wang, M. Kruhøffer, T.M. Lewin, T.F. Orntoft, R.A. Coleman, K. Birkenkamp-Demtröder, Lysophosphatidylcholine acyltransferase 1 (LPCAT1) overexpression in human colorectal cancer., *J. Mol. Med. (Berl)*. 87 (2009) 85–97.
- [99] X. Zhou, T.J. Lawrence, Z. He, C.R. Pound, J. Mao, S.A. Bigler, The expression level of lysophosphatidylcholine acyltransferase 1 (LPCAT1) correlates to the progression of prostate cancer., *Exp. Mol. Pathol*. 92 (2012) 105–10.
- [100] K. Grupp, S. Sanader, H. Sirma, R. Simon, C. Koop, K. Prien, C. Hube-Magg, G. Salomon, M. Graefen, H. Heinzer, S. Minner, J.R. Izbicki, G. Sauter, T. Schlomm, M.C. Tsourlakis, High lysophosphatidylcholine acyltransferase 1 expression independently predicts high risk for biochemical recurrence in prostate cancers, *Mol. Oncol*. 7 (2013) 1001–1011.
- [101] P. Ke, X. Bao, C. Liu, B. Zhou, M. Huo, Y. Chen, X. Wang, D. Wu, X. Ma, D. Liu, S. Chen, LPCAT3 is a potential prognostic biomarker and may be correlated with immune infiltration and ferroptosis in acute myeloid leukemia: a pan-cancer analysis, *Transl. Cancer Res*. 11 (2022) 3491–3505.
- [102] J.E.M. Upton, E. Grunebaum, G. Sussman, P. Vadas, Platelet activating factor (PAF): A mediator of inflammation, *BioFactors*. 48 (2022) 1189–1202.
- [103] R. Morimoto, H. Shindou, Y. Oda, T. Shimizu, Phosphorylation of lysophosphatidylcholine acyltransferase 2 at Ser 34 enhances platelet-activating factor

- production in endotoxin-stimulated macrophages, *J. Biol. Chem.* 285 (2010) 29857–29862.
- [104] M. Tarui, H. Shindou, K. Kumagai, R. Morimoto, T. Harayama, T. Hashidate, H. Kojima, T. Okabe, T. Nagano, T. Nagase, T. Shimizu, Selective inhibitors of a PAF biosynthetic enzyme lysophosphatidylcholine acyltransferase 2, *J. Lipid Res.* 55 (2014) 1386–1396.
- [105] J.F.R. Kerr, A.H. Wyllie, A.R. Currie, Apoptosis: A basic biological phenomenon with wide-ranging implications in tissue kinetics, *Br. J. Cancer.* 26 (1972) 239–257.
- [106] S. Elmore, Apoptosis: A review of programmed cell death, *Toxicol. Pathol.* 35 (2007) 495–516.
- [107] M.S. D'Arcy, Cell death: a review of the major forms of apoptosis, necrosis and autophagy., *Cell Biol. Int.* 43 (2019) 582–592.
- [108] N. Mizushima, B. Levine, A.M. Cuervo, D.J. Klionsky, Autophagy fights disease through cellular self-digestion., *Nature.* 451 (2008) 1069–75.
- [109] A. Degterev, Z. Huang, M. Boyce, Y. Li, P. Jagtap, N. Mizushima, G.D. Cuny, T.J. Mitchison, M.A. Moskowitz, J. Yuan, Chemical inhibitor of nonapoptotic cell death with therapeutic potential for ischemic brain injury., *Nat. Chem. Biol.* 1 (2005) 112–9.
- [110] Y. Fang, S. Tian, Y. Pan, W. Li, Q. Wang, Y. Tang, T. Yu, X. Wu, Y. Shi, P. Ma, Y. Shu, Pyroptosis: A new frontier in cancer., *Biomed. Pharmacother.* 121 (2020) 109595.
- [111] V. Brinkmann, U. Reichard, C. Goosmann, B. Fauler, Y. Uhlemann, D.S. Weiss, Y. Weinrauch, A. Zychlinsky, Neutrophil extracellular traps kill bacteria., *Science.* 303 (2004) 1532–5.
- [112] S. Dolma, S.L. Lessnick, W.C. Hahn, B.R. Stockwell, Identification of genotype-selective antitumor agents using synthetic lethal chemical screening in engineered human tumor cells., *Cancer Cell.* 3 (2003) 285–96.
- [113] W.S. Yang, B.R. Stockwell, Synthetic lethal screening identifies compounds activating iron-dependent, nonapoptotic cell death in oncogenic-RAS-harboring cancer cells., *Chem. Biol.* 15 (2008) 234–45.
- [114] A. Seiler, M. Schneider, H. Förster, S. Roth, E.K. Wirth, C. Culmsee, N. Plesnila, E. Kremmer, O. Rådmark, W. Wurst, G.W. Bornkamm, U. Schweizer, M. Conrad, Glutathione peroxidase 4 senses and translates oxidative stress into 12/15-lipoxygenase dependent- and AIF-mediated cell death., *Cell Metab.* 8 (2008) 237–48.
- [115] A. Banjac, T. Perisic, H. Sato, A. Seiler, S. Bannai, N. Weiss, P. Kölle, K. Tschoep, R.D. Issels, P.T. Daniel, M. Conrad, G.W. Bornkamm, The cystine/cysteine cycle: a redox cycle regulating susceptibility versus resistance to cell death., *Oncogene.* 27 (2008) 1618–28.
- [116] W.S. Yang, R. Sriramaratnam, M.E. Welsch, K. Shimada, R. Skouta, V.S. Viswanathan, J.H. Cheah, P.A. Clemons, A.F. Shamji, C.B. Clish, L.M. Brown, A.W. Girotti, V.W. Cornish, S.L. Schreiber, B.R. Stockwell, Regulation of ferroptotic cancer cell death by GPX4, *Cell.* 156 (2014) 317–331.
- [117] S.J. Dixon, D. Patel, M. Welsch, R. Skouta, E. Lee, M. Hayano, A.G. Thomas, C. Gleason, N. Tatonetti, B.S. Slusher, B.R. Stockwell, Pharmacological inhibition of cystine-glutamate exchange induces endoplasmic reticulum stress and ferroptosis, *Elife.* 2014 (2014) 1–25.
- [118] X. Chen, C. Yu, R. Kang, D. Tang, Iron metabolism in ferroptosis, *Front. Cell Dev. Biol.* 8 (2020) 1089.



- [119] F. Kuang, J. Liu, Y. Xie, D. Tang, R. Kang, MGST1 is a redox-sensitive repressor of ferroptosis in pancreatic cancer cells, *Cell Chem. Biol.* 28 (2021) 765-775.e5.
- [120] C. Li, Y. Zhang, J. Liu, R. Kang, D.J. Klionsky, D. Tang, Mitochondrial DNA stress triggers autophagy-dependent ferroptotic death, *Autophagy.* 17 (2021) 948–960.
- [121] S.E. Wenzel, Y.Y. Tyurina, J. Zhao, C.M. St. Croix, H.H. Dar, G. Mao, V.A. Tyurin, T.S. Anthony-muthu, A.A. Kapralov, A.A. Amoscato, K. Mikulska-Ruminska, I.H. Shrivastava, E.M. Kenny, Q. Yang, J.C. Rosenbaum, L.J. Sparvero, D.R. Emler, X. Wen, Y. Minami, F. Qu, S.C. Watkins, T.R. Holman, A.P. VanDemark, J.A. Kellum, I. Bahar, H. Bayir, V.E. Kagan, PEBP1 warden ferroptosis by enabling lipoxygenase generation of lipid death signals, *Cell.* 171 (2017) 628-641.e26.
- [122] W.S. Yang, K.J. Kim, M.M. Gaschler, M. Patel, M.S. Shchepinov, B.R. Stockwell, Peroxidation of polyunsaturated fatty acids by lipoxygenases drives ferroptosis, *Proc. Natl. Acad. Sci. U.S.A.* 113 (2016) E4966–E4975.
- [123] B. Yan, Y. Ai, Q. Sun, Y. Ma, Y. Cao, J. Wang, Z. Zhang, X. Wang, Membrane damage during ferroptosis is caused by oxidation of phospholipids catalyzed by the oxidoreductases POR and CYB5R1, *Mol. Cell.* 81 (2021) 355-369.e10.
- [124] Y. Zou, H. Li, E.T. Graham, A.A. Deik, J.K. Eaton, W. Wang, G. Sandoval-Gomez, C.B. Clish, J.G. Doench, S.L. Schreiber, Cytochrome P450 oxidoreductase contributes to phospholipid peroxidation in ferroptosis, *Nat. Chem. Biol.* 16 (2020) 302–309.
- [125] B.R. Stockwell, Ferroptosis turns 10: Emerging mechanisms, physiological functions, and therapeutic applications, *Cell.* 185 (2022) 2401–2421.
- [126] S.J. Dixon, G.E. Winter, L.S. Musavi, E.D. Lee, B. Snijder, M. Rebsamen, G. Superti-Furga, B.R. Stockwell, Human haploid cell genetics reveals roles for lipid metabolism genes in nonapoptotic cell death, *ACS Chem. Biol.* 10 (2015) 1604–1609.
- [127] P.M. Maloberti, A.B. Duarte, U.D. Orlando, M.E. Pasqualini, A.R. Solano, C. López-Otín, E.J. Podestá, Functional interaction between acyl-CoA synthetase 4, lipoxygenases and cyclooxygenase-2 in the aggressive phenotype of breast cancer cells., *PLoS One.* 5 (2010) e15540.
- [128] L. Jiang, N. Kon, T. Li, S.-J. Wang, T. Su, H. Hibshoosh, R. Baer, W. Gu, Ferroptosis as a p53-mediated activity during tumour suppression, *Nature.* 520 (2015) 57–62.
- [129] B. Chu, N. Kon, D. Chen, T. Li, T. Liu, L. Jiang, S. Song, O. Tavana, W. Gu, ALOX12 is required for p53-mediated tumour suppression through a distinct ferroptosis pathway, *Nat. Cell Biol.* 21 (2019) 579–591.
- [130] M. Jennis, C.-P. Kung, S. Basu, A. Budina-Kolomets, J.I.J. Leu, S. Khaku, J.P. Scott, K.Q. Cai, M.R. Campbell, D.K. Porter, X. Wang, D.A. Bell, X. Li, D.S. Garlick, Q. Liu, M. Hollstein, D.L. George, M.E. Murphy, An African-specific polymorphism in the TP53 gene impairs p53 tumor suppressor function in a mouse model., *Genes Dev.* 30 (2016) 918–30.
- [131] K.S. Singh, J.I.J. Leu, T. Barnoud, P. Vonteddu, K. Gnanapradeepan, C. Lin, Q. Liu, J.C. Barton, A. V. Kossenkov, D.L. George, M.E. Murphy, F. Dotiwala, African-centric TP53 variant increases iron accumulation and bacterial pathogenesis but improves response to malaria toxin., *Nat. Commun.* 11 (2020) 473.
- [132] H. Zheng, L. Jiang, T. Tsuduki, M. Conrad, S. Toyokuni, Embryonal erythropoiesis and aging exploit ferroptosis., *Redox Biol.* 48 (2021) 102175.
- [133] N.L. Jenkins, S.A. James, A. Salim, F. Sumardy, T.P. Speed, M. Conrad, D.R. Richardson, A.I. Bush, G. McColl, Changes in ferrous iron and glutathione promote

- ferroptosis and frailty in aging *Caenorhabditis elegans*, *Elife*. 9 (2020) 1–28.
- [134] H. Wang, P. An, E. Xie, Q. Wu, X. Fang, H. Gao, Z. Zhang, Y. Li, X. Wang, J. Zhang, G. Li, L. Yang, W. Liu, J. Min, F. Wang, Characterization of ferroptosis in murine models of hemochromatosis, *Hepatology*. 66 (2017) 449–465.
- [135] E.P. Amaral, D.L. Costa, S. Namasivayam, N. Riteau, O. Kamenyeva, L. Mittereder, K.D. Mayer-Barber, B.B. Andrade, A. Sher, A major role for ferroptosis in *Mycobacterium tuberculosis*-induced cell death and tissue necrosis, *J. Exp. Med.* 216 (2019) 556–570.
- [136] H.H. Dar, Y.Y. Tyurina, K. Mikulska-Ruminska, I. Shrivastava, H.-C. Ting, V.A. Tyurin, J. Krieger, C.M. St Croix, S. Watkins, E. Bayir, G. Mao, C.R. Armbruster, A. Kapralov, H. Wang, M.R. Parsek, T.S. Anthonymuthu, A.F. Ogunsola, B.A. Flitter, C.J. Freedman, J.R. Gaston, T.R. Holman, J.M. Pilewski, J.S. Greenberger, R.K. Mallampalli, Y. Doi, J.S. Lee, I. Bahar, J.M. Bomberger, H. Bayir, V.E. Kagan, C.M. St. Croix, S. Watkins, E. Bayir, G. Mao, C.R. Armbruster, A. Kapralov, H. Wang, M.R. Parsek, T.S. Anthonymuthu, A.F. Ogunsola, B.A. Flitter, C.J. Freedman, J.R. Gaston, T.R. Holman, J.M. Pilewski, J.S. Greenberger, R.K. Mallampalli, Y. Doi, J.S. Lee, I. Bahar, J.M. Bomberger, H. Bayir, V.E. Kagan, *Pseudomonas aeruginosa* utilizes host polyunsaturated phosphatidylethanolamines to trigger theft-ferroptosis in bronchial epithelium, *J. Clin. Invest.* 128 (2018) 4639–4653.
- [137] T. Nagasaki, A.J. Schuyler, J. Zhao, S.N. Samovich, K. Yamada, Y. Deng, S.P. Ginebaugh, S.A. Christenson, P.G. Woodruff, J. V. Fahy, J.B. Trudeau, D. Stoyanovsky, A. Ray, Y.Y. Tyurina, V.E. Kagan, S.E. Wenzel, 15LO1 dictates glutathione redox changes in asthmatic airway epithelium to worsen type 2 inflammation, *J. Clin. Invest.* 132 (2022).
- [138] C.D. Funk, X.S. Chen, E.N. Johnson, L. Zhao, Lipoxygenase genes and their targeted disruption, *Prostaglandins Other Lipid Mediat.* 68–69 (2002) 303–312.
- [139] J.Z. Haeggström, C.D. Funk, Lipoxygenase and leukotriene pathways: biochemistry, biology, and roles in disease, *Chem. Rev.* 111 (2011) 5866–5898.
- [140] H. Kuhn, S. Banthiya, K. van Leyen, Mammalian lipoxygenases and their biological relevance., *Biochim. Biophys. Acta.* 1851 (2015) 308–30.
- [141] I. Ivanov, D. Heydeck, K. Hofheinz, J. Roffeis, V.B. O'Donnell, H. Kuhn, M. Walther, Molecular enzymology of lipoxygenases, *Arch. Biochem. Biophys.* 503 (2010) 161–174.
- [142] M. Hamberg, B. Samuelsson, On the specificity of the oxygenation of unsaturated fatty acids catalyzed by soybean lipoxygenase., *J. Biol. Chem.* 242 (1967) 5329–5335.
- [143] E.N. Segraves, T.R. Holman, Kinetic investigations of the rate-limiting step in human 12- and 15-lipoxygenase, *Biochemistry*. 42 (2003) 5236–5243.
- [144] M. Hamberg, B. Samuelsson, Prostaglandin Endoperoxides. Novel Transformations of Arachidonic Acid in Human Platelets\*, *Proc. Natl. Acad. Sci.* 71 (1974) 3400–3404.
- [145] J. Virmani, E.N. Johnson, A.J.P. Klein-Szanto, C.D. Funk, Role of “platelet-type” 12-lipoxygenase in skin carcinogenesis., *Cancer Lett.* 162 (2001) 161–5.
- [146] Y. Zheng, H. Yin, W.E. Boeglin, P.M. Elias, D. Crumrine, D.R. Beier, A.R. Brash, Lipoxygenases mediate the effect of essential fatty acid in skin barrier formation: a proposed role in releasing omega-hydroxyceramide for construction of the corneocyte lipid envelope., *J. Biol. Chem.* 286 (2011) 24046–56.
- [147] P. Krieg, G. Fürstenberger, The role of lipoxygenases in epidermis., *Biochim. Biophys. Acta.* 1841 (2014) 390–400.

- [148] T. Matsumoto, C.D. Funk, O. Rådmark, J.O. Höög, H. Jörnvall, B. Samuelsson, Molecular cloning and amino acid sequence of human 5-lipoxygenase., *Proc. Natl. Acad. Sci. U. S. A.* 85 (1988) 26–30.
- [149] A.-K. Ball, K. Beilstein, S. Wittmann, D. Sürün, M.J. Saul, F. Schnütgen, N. Flamand, R. Capelo, A.S. Kahnt, H. Frey, L. Schaefer, R. Marschalek, A.-K. Häfner, D. Steinhilber, Characterization and cellular localization of human 5-lipoxygenase and its protein isoforms 5-LO $\Delta$ 13, 5-LO $\Delta$ 4 and 5-LOp12, *Biochim. Biophys. Acta - Mol. Cell Biol. Lipids.* 1862 (2017) 561–571.
- [150] A.-K. Häfner, K. Beilstein, P. Graab, A.-K. Ball, M.J. Saul, B. Hofmann, D. Steinhilber, Identification and characterization of a new protein isoform of human 5-Lipoxygenase., *PLoS One.* 11 (2016) e0166591.
- [151] L.H. Boudreau, J. Bertin, P.P. Robichaud, M. Laflamme, R.J. Ouellette, N. Flamand, M.E. Surette, Novel 5-lipoxygenase isoforms affect the biosynthesis of 5-lipoxygenase products., *FASEB J.* 25 (2011) 1097–105.
- [152] J. Esser, M. Rakonjac, B. Hofmann, L. Fischer, P. Provost, G. Schneider, D. Steinhilber, B. Samuelsson, O. Rådmark, Coactosin-like protein functions as a stabilizing chaperone for 5-lipoxygenase: role of tryptophan 102, *Biochem. J.* 425 (2010) 265–274.
- [153] P. Provost, J. Doucet, T. Hammarberg, G. Gerisch, B. Samuelsson, O. Radmark, 5-Lipoxygenase interacts with coactosin-like protein., *J. Biol. Chem.* 276 (2001) 16520–7.
- [154] V. Dincbas-Renqvist, G. Pépin, M. Rakonjac, I. Plante, D.L. Ouellet, A. Hermansson, I. Goulet, J. Doucet, B. Samuelsson, O. Rådmark, P. Provost, Human Dicer C-terminus functions as a 5-lipoxygenase binding domain., *Biochim. Biophys. Acta.* 1789 (2009) 99–108.
- [155] X.S. Chen, C.D. Funk, The N-terminal “beta-barrel” domain of 5-lipoxygenase is essential for nuclear membrane translocation., *J. Biol. Chem.* 276 (2001) 811–8.
- [156] N.C. Gilbert, S.G. Bartlett, M.T. Waight, D.B. Neau, W.E. Boeglin, A.R. Brash, M.E. Newcomer, The structure of human 5-lipoxygenase., *Science.* 331 (2011) 217–9.
- [157] M.D. Percival, Human 5-lipoxygenase contains an essential iron, *J. Biol. Chem.* 266 (1991) 10058–10061.
- [158] O. Rådmark, B. Samuelsson, Regulation of 5-lipoxygenase enzyme activity., *Biochem. Biophys. Res. Commun.* 338 (2005) 102–10.
- [159] M. Noguchi, M. Miyano, T. Matsumoto, Physicochemical characterization of ATP binding to human 5-lipoxygenase., *Lipids.* 31 (1996) 367–71.
- [160] O. Rådmark, O. Werz, D. Steinhilber, B. Samuelsson, 5-Lipoxygenase: regulation of expression and enzyme activity., *Trends Biochem. Sci.* 32 (2007) 332–41.
- [161] M. Luo, S.M. Jones, S.M. Phare, M.J. Coffey, M. Peters-Golden, T.G. Brock, Protein kinase A inhibits leukotriene synthesis by phosphorylation of 5-lipoxygenase on serine 523., *J. Biol. Chem.* 279 (2004) 41512–20.
- [162] O. Werz, D. Szellas, D. Steinhilber, O. Rådmark, Arachidonic acid promotes phosphorylation of 5-lipoxygenase at Ser-271 by MAPK-activated protein kinase 2 (MK2)., *J. Biol. Chem.* 277 (2002) 14793–800.
- [163] S. Markoutsas, D. Sürün, M. Karas, B. Hofmann, D. Steinhilber, B.L. Sorg, Analysis of 5-lipoxygenase phosphorylation on molecular level by MALDI-MS., *FEBS J.* 281 (2014) 1931–47.
- [164] M. Abramovitz, E. Wong, M.E. Cox, C.D. Richardson, C. Li, P.J. Vickers, 5-

- lipoxygenase-activating protein stimulates the utilization of arachidonic acid by 5-lipoxygenase., *Eur. J. Biochem.* 215 (1993) 105–11.
- [165] J.W. Woods, J.F. Evans, D. Ethier, S. Scott, P.J. Vickers, L. Hearn, J.A. Heibin, S. Charleson, I.I. Singer, 5-lipoxygenase and 5-lipoxygenase-activating protein are localized in the nuclear envelope of activated human leukocytes., *J. Exp. Med.* 178 (1993) 1935–46.
- [166] M. Peters-Golden, T.G. Brock, Intracellular compartmentalization of leukotriene synthesis: unexpected nuclear secrets., *FEBS Lett.* 487 (2001) 323–6.
- [167] J. Evans, A. Ferguson, R. Mosley, J. Hutchinson, What's all the FLAP about?: 5-lipoxygenase-activating protein inhibitors for inflammatory diseases, *Trends Pharmacol. Sci.* 29 (2008) 72–78.
- [168] J. Gerstmeier, C. Weinigel, D. Barz, O. Werz, U. Garscha, An experimental cell-based model for studying the cell biology and molecular pharmacology of 5-lipoxygenase-activating protein in leukotriene biosynthesis, *Biochim. Biophys. Acta - Gen. Subj.* 1840 (2014) 2961–2969.
- [169] P.P. McDonald, S.R. McColl, P.H. Naccache, P. Borgeat, Studies on the activation of human neutrophil 5-lipoxygenase induced by natural agonists and Ca<sup>2+</sup> ionophore A23187., *Biochem. J.* 280 ( Pt 2 (1991) 379–85.
- [170] J. Fettel, B. Kühn, N.A. Guillen, D. Sürün, M. Peters, R. Bauer, C. Angioni, G. Geisslinger, F. Schnütgen, D.M. Heringdorf, O. Werz, P. Meybohm, K. Zacharowski, D. Steinhilber, J. Roos, T.J. Maier, Sphingosine-1-phosphate (S1P) induces potent anti-inflammatory effects in vitro and in vivo by S1P receptor 4-mediated suppression of 5-lipoxygenase activity, *FASEB J.* 33 (2019) 1711–1726.
- [171] O. Rådmark, O. Werz, D. Steinhilber, B. Samuelsson, 5-Lipoxygenase, a key enzyme for leukotriene biosynthesis in health and disease, *Biochim. Biophys. Acta.* 1851 (2015) 331–339.
- [172] M. Luo, S.M. Jones, M. Peters-Golden, T.G. Brock, Nuclear localization of 5-lipoxygenase as a determinant of leukotriene B<sub>4</sub> synthetic capacity., *Proc. Natl. Acad. Sci. U. S. A.* 100 (2003) 12165–70.
- [173] P. Christmas, B.M. Weber, M. McKee, D. Brown, R.J. Soberman, Membrane localization and topology of leukotriene C<sub>4</sub> synthase., *J. Biol. Chem.* 277 (2002) 28902–8.
- [174] M.E. Newcomer, N.C. Gilbert, Location, location, location: compartmentalization of early events in leukotriene biosynthesis., *J. Biol. Chem.* 285 (2010) 25109–14.
- [175] T.G. Brock, Y.-J. Lee, E. Maydanski, T.L. Marburger, M. Luo, R. Paine, M. Peters-Golden, Nuclear localization of leukotriene A<sub>4</sub> hydrolase in type II alveolar epithelial cells in normal and fibrotic lung., *Am. J. Physiol. Lung Cell. Mol. Physiol.* 289 (2005) L224-32.
- [176] S. Adel, F. Karst, À. González-Lafont, M. Pekárová, P. Saura, L. Masgrau, J.M. Lluch, S. Stehling, T. Horn, H. Kuhn, D. Heydeck, Evolutionary alteration of ALOX15 specificity optimizes the biosynthesis of antiinflammatory and proresolving lipoxins, *Proc. Natl. Acad. Sci. U. S. A.* 113 (2016) E4266–E4275.
- [177] L. Kutzner, K. Goloshchapova, D. Heydeck, S. Stehling, H. Kuhn, N.H. Schebb, Mammalian ALOX15 orthologs exhibit pronounced dual positional specificity with docosahexaenoic acid, *Biochim. Biophys. Acta - Mol. Cell Biol. Lipids.* 1862 (2017) 666–675.
- [178] T. Schewe, W. Halangk, C. Hiesch, S.M. Rapoport, A lipoxygenase in rabbit

- reticulocytes which attacks phospholipids and intact mitochondria, *FEBS Lett.* 60 (1975) 149–152.
- [179] R. Brinckmann, K. Schnurr, D. Heydeck, T. Rosenbach, G. Kolde, H. Kühn, Membrane translocation of 15-lipoxygenase in hematopoietic cells is calcium-dependent and activates the oxygenase activity of the enzyme., *Blood.* 91 (1998) 64–74.
- [180] J. Zhao, V.B. O'Donnell, S. Balzar, C.M. St. Croix, J.B. Trudeau, S.E. Wenzel, 15-Lipoxygenase 1 interacts with phosphatidylethanolamine-binding protein to regulate MAPK signaling in human airway epithelial cells, *Proc. Natl. Acad. Sci. U. S. A.* 108 (2011) 14246–14251.
- [181] S.A. Gillmor, A. Villaseñor, R. Fletterick, E. Sigal, M.F. Browner, The structure of mammalian 15-lipoxygenase reveals similarity to the lipases and the determinants of substrate specificity., *Nat. Struct. Biol.* 4 (1997) 1003–9.
- [182] I. Ivanov, H. Kuhn, D. Heydeck, Structural and functional biology of arachidonic acid 15-lipoxygenase-1 (ALOX15), *Gene.* 573 (2015) 1–32.
- [183] R.G. Snodgrass, B. Brüne, Regulation and functions of 15-lipoxygenases in human macrophages, *Front. Pharmacol.* 10 (2019) 719.
- [184] J.A. Nadel, D.J. Conrad, I.F. Ueki, A. Schuster, E. Sigal, Immunocytochemical localization of arachidonate 15-lipoxygenase in erythrocytes, leukocytes, and airway cells., *J. Clin. Invest.* 87 (1991) 1139–45.
- [185] S.J.A. Wuest, M. Crucet, C. Gemperle, C. Loretz, M. Hersberger, Expression and regulation of 12/15-lipoxygenases in human primary macrophages., *Atherosclerosis.* 225 (2012) 121–7.
- [186] R.G. Snodgrass, E. Zezina, D. Namgaladze, S. Gupta, C. Angioni, G. Geisslinger, D. Lütjohann, B. Brüne, A novel function for 15-Lipoxygenases in cholesterol homeostasis and CCL17 production in human macrophages., *Front. Immunol.* 9 (2018) 1906.
- [187] S. Uderhardt, J.A. Ackermann, T. Fillep, V.J. Hammond, J. Willeit, P. Santer, M. Mayr, M. Biburger, M. Miller, K.R. Zellner, K. Stark, A. Zarbock, J. Rossaint, I. Schubert, D. Mielenz, B. Dietel, D. Raaz-Schrauder, C. Ay, T. Gremmel, J. Thaler, C. Heim, M. Herrmann, P.W. Collins, G. Schabbauer, N. Mackman, D. Voehringer, J.L. Nadler, J.J. Lee, S. Massberg, M. Rauh, S. Kiechl, G. Schett, V.B. O'Donnell, G. Krönke, Enzymatic lipid oxidation by eosinophils propagates coagulation, hemostasis, and thrombotic disease., *J. Exp. Med.* 214 (2017) 2121–2138.
- [188] G. Bannenberg, C.N. Serhan, Specialized pro-resolving lipid mediators in the inflammatory response: An update., *Biochim. Biophys. Acta.* 1801 (2010) 1260–73.
- [189] J.T. Huang, J.S. Welch, M. Ricote, C.J. Binder, T.M. Willson, C. Kelly, J.L. Witztum, C.D. Funk, D. Conrad, C.K. Glass, Interleukin-4-dependent production of PPAR-gamma ligands in macrophages by 12/15-lipoxygenase., *Nature.* 400 (1999) 378–82.
- [190] V.B. O'Donnell, M. Aldrovandi, R.C. Murphy, G. Krönke, Enzymatically oxidized phospholipids assume center stage as essential regulators of innate immunity and cell death., *Sci. Signal.* 12 (2019) 2293.
- [191] T. Rothe, F. Gruber, S. Uderhardt, N. Ipseiz, S. Rössner, O. Oskolkova, S. Blüml, N. Leitinger, W. Bicker, V.N. Bochkov, M. Yamamoto, A. Steinkasserer, G. Schett, E. Zinser, G. Krönke, 12/15-Lipoxygenase-mediated enzymatic lipid oxidation regulates DC maturation and function., *J. Clin. Invest.* 125 (2015) 1944–54.
- [192] B.H. Maskrey, A. Bermúdez-Fajardo, A.H. Morgan, E. Stewart-Jones, V. Dioszeghy, G.W. Taylor, P.R.S.S. Baker, B. Coles, M.J. Coffey, H. Kühn, V.B. O'Donnell, Activated

- platelets and monocytes generate four hydroxyphosphatidylethanolamines via lipoxygenase, *J. Biol. Chem.* 282 (2007) 20151–20163.
- [193] A.H. Morgan, V. Dioszeghy, B.H. Maskrey, C.P. Thomas, S.R. Clark, S.A. Mathie, C.M. Lloyd, H. Kühn, N. Topley, B.C. Coles, P.R. Taylor, S.A. Jones, V.B. O'Donnell, Phosphatidylethanolamine-esterified eicosanoids in the mouse: tissue localization and inflammation-dependent formation in Th-2 disease., *J. Biol. Chem.* 284 (2009) 21185–91.
- [194] A.R. Brash, W.E. Boeglin, M.S. Chang, Discovery of a second 15S-lipoxygenase in humans., *Proc. Natl. Acad. Sci. U. S. A.* 94 (1997) 6148–52.
- [195] C. Abrial, S. Grassin-Delyle, H. Salvator, M. Brollo, E. Naline, P. Devillier, 15-Lipoxygenases regulate the production of chemokines in human lung macrophages., *Br. J. Pharmacol.* 172 (2015) 4319–30.
- [196] B. Bhatia, C.J. Maldonado, S. Tang, D. Chandra, R.D. Klein, D. Chopra, S.B. Shappell, P. Yang, R.A. Newman, D.G. Tang, Subcellular localization and tumor-suppressive functions of 15-lipoxygenase 2 (15-LOX2) and its splice variants., *J. Biol. Chem.* 278 (2003) 25091–100.
- [197] S. Tang, B. Bhatia, C.J. Maldonado, P. Yang, R.A. Newman, J. Liu, D. Chandra, J. Traag, R.D. Klein, S.M. Fischer, D. Chopra, J. Shen, H.E. Zhau, L.W.K. Chung, D.G. Tang, Evidence that arachidonate 15-lipoxygenase 2 is a negative cell cycle regulator in normal prostate epithelial cells., *J. Biol. Chem.* 277 (2002) 16189–201.
- [198] D. Schweiger, G. Fürstenberger, P. Krieg, Inducible expression of 15-lipoxygenase-2 and 8-lipoxygenase inhibits cell growth via common signaling pathways., *J. Lipid Res.* 48 (2007) 553–64.
- [199] P.M. Hutchins, R.C. Murphy, Cholesteryl ester acyl oxidation and remodeling in murine macrophages: formation of oxidized phosphatidylcholine., *J. Lipid Res.* 53 (2012) 1588–97.
- [200] R. Ganesan, K.M. Henkels, L.E. Wrenshall, Y. Kanaho, G. Di Paolo, M.A. Frohman, J. Gomez-Cambronero, Oxidized LDL phagocytosis during foam cell formation in atherosclerotic plaques relies on a PLD2-CD36 functional interdependence., *J. Leukoc. Biol.* 103 (2018) 867–883.
- [201] L.M. Hultén, F.J. Olson, H. Aberg, J. Carlsson, L. Karlström, J. Borén, B. Fagerberg, O. Wiklund, 15-Lipoxygenase-2 is expressed in macrophages in human carotid plaques and regulated by hypoxia-inducible factor-1alpha., *Eur. J. Clin. Invest.* 40 (2010) 11–7.
- [202] M.W. Buczynski, D.S. Dumlao, E.A. Dennis, Thematic review series: Proteomics. An integrated omics analysis of eicosanoid biology., *J. Lipid Res.* 50 (2009) 1015–38.
- [203] C. Gladine, A.I. Ostermann, J.W. Newman, N.H. Schebb, MS-based targeted metabolomics of eicosanoids and other oxylipins: Analytical and inter-individual variabilities, *Free Radic. Biol. Med.* 144 (2019) 72–89.
- [204] A.I. Ostermann, E. Koch, K.M. Rund, L. Kutzner, M. Mainka, N.H. Schebb, Targeting esterified oxylipins by LC-MS - Effect of sample preparation on oxylipin pattern., *Prostaglandins Other Lipid Mediat.* 146 (2020) 106384.
- [205] V.J. Hammond, V.B. O'Donnell, Esterified eicosanoids: generation, characterization and function, *Biochim. Biophys. Acta.* 1818 (2012) 2403–2412.
- [206] J.A. Gordon, P.H. Figard, G.E. Quinby, A.A. Spector, 5-HETE: uptake, distribution, and metabolism in MDCK cells, *Am. J. Physiol. Physiol.* 256 (1989) C1–C10.

- [207] M.E. Brezinski, C.N. Serhan, Selective incorporation of (15S)-hydroxyeicosatetraenoic acid in phosphatidylinositol of human neutrophils: agonist-induced deacylation and transformation of stored hydroxyeicosanoids., *Proc. Natl. Acad. Sci.* 87 (1990) 6248–6252.
- [208] I. Willenberg, A.I. Ostermann, N.H. Schebb, Targeted metabolomics of the arachidonic acid cascade: current state and challenges of LC-MS analysis of oxylipins, *Anal. Bioanal. Chem.* 407 (2015) 2675–2683.
- [209] N.M. Hartung, M. Mainka, R. Pfaff, M. Kuhn, S. Biernacki, L. Zinnert, N.H. Schebb, Development of a quantitative proteomics approach for cyclooxygenases and lipoxygenases in parallel to quantitative oxylipin analysis allowing the comprehensive investigation of the arachidonic acid cascade, *Anal. Bioanal. Chem.* 415 (2023) 913–933.
- [210] K.M. Rund, A.I. Ostermann, L. Kutzner, J.-M. Galano, C. Oger, C. Vigor, S. Wecklein, N. Seiwert, T. Durand, N.H. Schebb, Development of an LC-ESI(-)-MS/MS method for the simultaneous quantification of 35 isoprostanes and isofurans derived from the major n3- and n6-PUFAs, *Anal. Chim. Acta.* 1037 (2018) 63–74.
- [211] L. Kutzner, K.M. Rund, A.I. Ostermann, N.M. Hartung, J.-M. Galano, L. Balas, T. Durand, M.S. Balzer, S. David, N.H. Schebb, Development of an optimized LC-MS method for the detection of specialized pro-resolving mediators in biological samples, *Front. Pharmacol.* 10 (2019) 169.
- [212] N.H. Schebb, H. Kühn, A.S. Kahnt, K.M. Rund, V.B. O'Donnell, N. Flamand, M. Peters-Golden, P.J. Jakobsson, K.H. Weylandt, N. Rohwer, R.C. Murphy, G. Geisslinger, G.A. FitzGerald, J. Hanson, C. Dahlgren, M.W. Alnouri, S. Offermanns, D. Steinhilber, Formation, signaling and occurrence of specialized pro-resolving lipid mediators—What is the evidence so far?, *Front. Pharmacol.* 13 (2022) 1–22.
- [213] C.P. Thomas, L.T. Morgan, B.H. Maskrey, R.C. Murphy, H. Kühn, S.L. Hazen, A.H. Goodall, H.A. Hamali, P.W. Collins, V.B. O'Donnell, Phospholipid-esterified eicosanoids are generated in agonist-activated human platelets and enhance tissue factor-dependent thrombin generation, *J. Biol. Chem.* 285 (2010) 6891–6903.
- [214] S.R. Clark, C.J. Guy, M.J. Scurr, P.R. Taylor, A.P. Kift-Morgan, V.J. Hammond, C.P. Thomas, B. Coles, G.W. Roberts, M. Eberl, S.A. Jones, N. Topley, S. Kotecha, V.B. O'Donnell, Esterified eicosanoids are acutely generated by 5-lipoxygenase in primary human neutrophils and in human and murine infection, *Blood.* 117 (2011) 2033–2043.
- [215] J. Zhao, B. Maskrey, S. Balzar, K. Chibana, A. Mustovich, H. Hu, J.B. Trudeau, V. O'Donnell, S.E. Wenzel, Interleukin-13–induced MUC5AC Is Regulated by 15-Lipoxygenase 1 Pathway in Human Bronchial Epithelial Cells, *Am. J. Respir. Crit. Care Med.* 179 (2009) 782–790.
- [216] X. Luo, H.-B. Gong, H.-Y. Gao, Y.-P. Wu, W.-Y. Sun, Z.-Q. Li, G. Wang, B. Liu, L. Liang, H. Kurihara, W.-J. Duan, Y.-F. Li, R.-R. He, Oxygenated phosphatidylethanolamine navigates phagocytosis of ferroptotic cells by interacting with TLR2, *Cell Death Differ.* 28 (2021) 1971–1989.
- [217] P.C. Calder, Eicosanoids., *Essays Biochem.* 64 (2020) 423–441.
- [218] A. Yamaguchi, E. Botta, M. Holinstat, Eicosanoids in inflammation in the blood and the vessel, *Front. Pharmacol.* 13 (2022) 3973.
- [219] N. Chiang, C.N. Serhan, Structural elucidation and physiologic functions of specialized pro-resolving mediators and their receptors, *Mol. Aspects Med.* 58 (2017) 114–129.
- [220] C.N. Serhan, N. Chiang, T.E. Van Dyke, Resolving inflammation: dual anti-inflammatory

- and pro-resolution lipid mediators., *Nat. Rev. Immunol.* 8 (2008) 349–61.
- [221] A.S. Kahnt, N.H. Schebb, D. Steinhilber, Formation of lipoxins and resolvins in human leukocytes, *Prostaglandins Other Lipid Mediat.* 166 (2023) 106726.
- [222] C.A. Dinarello, Anti-inflammatory agents: Present and future., *Cell.* 140 (2010) 935–50.
- [223] R. Medzhitov, Origin and physiological roles of inflammation., *Nature.* 454 (2008) 428–35.
- [224] C. Nathan, Neutrophils and immunity: Challenges and opportunities, *Nat. Rev. Immunol.* 6 (2006) 173–182.
- [225] C.N. Serhan, J. Savill, Resolution of inflammation: the beginning programs the end., *Nat. Immunol.* 6 (2005) 1191–7.
- [226] C.N. Serhan, Resolution phase of inflammation: novel endogenous anti-inflammatory and proresolving lipid mediators and pathways., *Annu. Rev. Immunol.* 25 (2007) 101–37.
- [227] M. Peters-Golden, W.R. Henderson, Leukotrienes., *N. Engl. J. Med.* 357 (2007) 1841–54.
- [228] C.D. Funk, Prostaglandins and leukotrienes: advances in eicosanoid biology., *Science.* 294 (2001) 1871–5.
- [229] M. Peters-Golden, T.G. Brock, 5-lipoxygenase and FLAP., *Prostaglandins. Leukot. Essent. Fatty Acids.* 69 (2003) 99–109.
- [230] B. Samuelsson, Leukotrienes: mediators of immediate hypersensitivity reactions and inflammation., *Science.* 220 (1983) 568–75.
- [231] J.F. Penrose, K.F. Austen, The biochemical, molecular, and genomic aspects of leukotriene C4 synthase., *Proc. Assoc. Am. Physicians.* 111 (1999) 537–46.
- [232] T. Yokomizo, T. Izumi, K. Chang, Y. Takuwa, T. Shimizu, A G-protein-coupled receptor for leukotriene B4 that mediates chemotaxis., *Nature.* 387 (1997) 620–4.
- [233] T. Yokomizo, K. Kato, K. Terawaki, T. Izumi, T. Shimizu, A second leukotriene B(4) receptor, BLT2. A new therapeutic target in inflammation and immunological disorders., *J. Exp. Med.* 192 (2000) 421–32.
- [234] T. Yokomizo, M. Nakamura, T. Shimizu, Leukotriene receptors as potential therapeutic targets., *J. Clin. Invest.* 128 (2018) 2691–2701.
- [235] T. Okuno, Y. Iizuka, H. Okazaki, T. Yokomizo, R. Taguchi, T. Shimizu, 12(S)-Hydroxyheptadeca-5Z, 8E, 10E-trienoic acid is a natural ligand for leukotriene B4 receptor 2., *J. Exp. Med.* 205 (2008) 759–66.
- [236] K.R. Lynch, G.P. O'Neill, Q. Liu, D.S. Im, N. Sawyer, K.M. Metters, N. Coulombe, M. Abramovitz, D.J. Figueroa, Z. Zeng, B.M. Connolly, C. Bai, C.P. Austin, A. Chateauneuf, R. Stocco, G.M. Greig, S. Kargman, S.B. Hooks, E. Hosfield, D.L. Williams, A.W. Ford-Hutchinson, C.T. Caskey, J.F. Evans, Characterization of the human cysteinyl leukotriene CysLT1 receptor., *Nature.* 399 (1999) 789–93.
- [237] C.E. Heise, B.F. O'Dowd, D.J. Figueroa, N. Sawyer, T. Nguyen, D.S. Im, R. Stocco, J.N. Bellefeuille, M. Abramovitz, R. Cheng, D.L. Williams, Z. Zeng, Q. Liu, L. Ma, M.K. Clements, N. Coulombe, Y. Liu, C.P. Austin, S.R. George, G.P. O'Neill, K.M. Metters, K.R. Lynch, J.F. Evans, Characterization of the human cysteinyl leukotriene 2 receptor., *J. Biol. Chem.* 275 (2000) 30531–6.



- [238] C. Corrigan, K. Mallett, S. Ying, D. Roberts, A. Parikh, G. Scadding, T. Lee, Expression of the cysteinyl leukotriene receptors cysLT1 and cysLT2 in aspirin-sensitive and aspirin-tolerant chronic rhinosinusitis, *J. Allergy Clin. Immunol.* 115 (2005) 316–322.
- [239] Y. Hui, Y. Cheng, I. Smalera, W. Jian, L. Goldhahn, G.A. Fitzgerald, C.D. Funk, Directed vascular expression of human cysteinyl leukotriene 2 receptor modulates endothelial permeability and systemic blood pressure., *Circulation.* 110 (2004) 3360–6.
- [240] A. Rossi, C. Pergola, A. Koeberle, M. Hoffmann, F. Dehm, P. Bramanti, S. Cuzzocrea, O. Werz, L. Sautebin, The 5-lipoxygenase inhibitor, zileuton, suppresses prostaglandin biosynthesis by inhibition of arachidonic acid release in macrophages, *Br. J. Pharmacol.* 161 (2010) 555–570.
- [241] W.W. Busse, K.A. McGill, R.J. Horwitz, Leukotriene pathway inhibitors in asthma and chronic obstructive pulmonary disease., *Clin. Exp. Allergy.* 29 Suppl 2 (1999) 110–5.
- [242] V. Capra, G.E. Rovati, P. Mangano, C. Buccellati, R.C. Murphy, A. Sala, Transcellular biosynthesis of eicosanoid lipid mediators, *Biochim. Biophys. Acta - Mol. Cell Biol. Lipids.* 1851 (2015) 377–382.
- [243] C.N. Serhan, M. Hamberg, B. Samuelsson, Trihydroxytetraenes: a novel series of compounds formed from arachidonic acid in human leukocytes., *Biochem. Biophys. Res. Commun.* 118 (1984) 943–9.
- [244] C.N. Serhan, Lipoxins and aspirin-triggered 15-epi-lipoxins are the first lipid mediators of endogenous anti-inflammation and resolution, *Prostaglandins Leukot. Essent. Fat. Acids.* 73 (2005) 141–162.
- [245] J.A. Giménez-Bastida, W.E. Boeglin, O. Boutaud, M.G. Malkowski, C. Schneider, Residual cyclooxygenase activity of aspirin-acetylated COX-2 forms 15 R - prostaglandins that inhibit platelet aggregation, *FASEB J.* 33 (2019) 1033–1041.
- [246] C.N. Serhan, B.D. Levy, Resolvins in inflammation: emergence of the pro-resolving superfamily of mediators., *J. Clin. Invest.* 128 (2018) 2657–2669.
- [247] S. Libreros, A.E. Shay, R. Nshimiyimana, D. Fichtner, M.J. Martin, N. Wourms, C.N. Serhan, A New E-Series Resolvin: RvE4 Stereochemistry and Function in Efferocytosis of Inflammation-Resolution., *Front. Immunol.* 11 (2020) 631319.
- [248] C.N. Serhan, Lipoxin biosynthesis and its impact in inflammatory and vascular events, *Biochim. Biophys. Acta (BBA)/Lipids Lipid Metab.* 1212 (1994) 1–25.
- [249] C.N. Serhan, K.A. Sheppard, Lipoxin formation during human neutrophil-platelet interactions. Evidence for the transformation of leukotriene A4 by platelet 12-lipoxygenase in vitro., *J. Clin. Invest.* 85 (1990) 772–80.
- [250] P.C. Norris, S. Libreros, C.N. Serhan, Resolution metabolomes activated by hypoxic environment., *Sci. Adv.* 5 (2019) eaax4895.
- [251] L. Kutzner, K. Goloshchapova, K.M. Rund, M. Jübermann, M. Blum, M. Rothe, S.F. Kirsch, W.-H. Schunck, H. Kühn, N.H. Schebb, Human lipoxygenase isoforms form complex patterns of double and triple oxygenated compounds from eicosapentaenoic acid., *Biochim. Biophys. acta. Mol. cell Biol. lipids.* 1865 (2020) 158806.
- [252] Y. Isobe, M. Itagaki, Y. Ito, S. Naoe, K. Kojima, M. Ikeguchi, M. Arita, Comprehensive analysis of the mouse cytochrome P450 family responsible for omega-3 epoxidation of eicosapentaenoic acid, *Sci. Rep.* 8 (2018) 7954.
- [253] C.N. Serhan, C.B. Clish, J. Brannon, S.P. Colgan, N. Chiang, K. Gronert, Novel Functional Sets of Lipid-Derived Mediators with Antiinflammatory Actions Generated

- from Omega-3 Fatty Acids via Cyclooxygenase 2–Nonsteroidal Antiinflammatory Drugs and Transcellular Processing, *J. Exp. Med.* 192 (2000) 1197–1204.
- [254] S.F. Oh, P.S. Pillai, A. Recchiuti, R. Yang, C.N. Serhan, Pro-resolving actions and stereoselective biosynthesis of 18S E-series resolvins in human leukocytes and murine inflammation, *J. Clin. Invest.* 121 (2011) 569–581.
- [255] C.N. Serhan, N.A. Petasis, Resolvins and protectins in inflammation resolution., *Chem. Rev.* 111 (2011) 5922–43.
- [256] Y. Isobe, M. Arita, S. Matsueda, R. Iwamoto, T. Fujihara, H. Nakanishi, R. Taguchi, K. Masuda, K. Sasaki, D. Urabe, M. Inoue, H. Arai, Identification and structure determination of novel anti-inflammatory mediator resolvin E3, 17,18-dihydroxyeicosapentaenoic acid., *J. Biol. Chem.* 287 (2012) 10525–10534.
- [257] C.N. Serhan, S. Hong, K. Gronert, S.P. Colgan, P.R. Devchand, G. Mirick, R.-L. Moussignac, Resolvins: a family of bioactive products of omega-3 fatty acid transformation circuits initiated by aspirin treatment that counter proinflammation signals., *J. Exp. Med.* 196 (2002) 1025–37.
- [258] K. Petrich, P. Ludwig, H. Kühn, T. Schewe, The suppression of 5-lipoxygenation of arachidonic acid in human polymorphonuclear leucocytes by the 15-lipoxygenase product (15S)-hydroxy-(5Z,8Z,11Z,13E)-eicosatetraenoic acid: structure-activity relationship and mechanism of action., *Biochem. J.* 314 ( Pt 3 (1996) 911–6.
- [259] T. Schewe, K. Petrich, P. Ludwig, H. Kühn, S. Nigam, Effect of 15-HETE on the 5-lipoxygenase pathway in neutrophils. Genuine inhibitor or alternative substrate?, *Adv. Exp. Med. Biol.* 447 (1999) 95–105.
- [260] P.C. Calder, Eicosapentaenoic and docosahexaenoic acid derived specialised pro-resolving mediators: Concentrations in humans and the effects of age, sex, disease and increased omega-3 fatty acid intake., *Biochimie.* 178 (2020) 105–123.
- [261] S.F. Oh, M. Dona, G. Fredman, S. Krishnamoorthy, D. Irimia, C.N. Serhan, Resolvin E2 formation and impact in inflammation resolution., *J. Immunol.* 188 (2012) 4527–34.
- [262] A.E. Barden, M. Moghaddami, E. Mas, M. Phillips, L.G. Cleland, T.A. Mori, Specialised pro-resolving mediators of inflammation in inflammatory arthritis., *Prostaglandins. Leukot. Essent. Fatty Acids.* 107 (2016) 24–9.
- [263] R. Ebert, R. Cumbana, C. Lehmann, L. Kutzner, A. Toewe, N. Ferreirós, M.J. Parnham, N.H. Schebb, D. Steinhilber, A.S. Kahnt, Long-term stimulation of toll-like receptor-2 and -4 upregulates 5-LO and 15-LO-2 expression thereby inducing a lipid mediator shift in human monocyte-derived macrophages, *Biochim. Biophys. Acta - Mol. Cell Biol. Lipids.* 1865 (2020) 158702.
- [264] N. Chiang, G. Fredman, F. Bäckhed, S.F. Oh, T. Vickery, B.A. Schmidt, C.N. Serhan, Infection regulates pro-resolving mediators that lower antibiotic requirements., *Nature.* 484 (2012) 524–8.
- [265] O. Werz, J. Gerstmeier, S. Libreros, X. De la Rosa, M. Werner, P.C. Norris, N. Chiang, C.N. Serhan, Human macrophages differentially produce specific resolvin or leukotriene signals that depend on bacterial pathogenicity, *Nat. Commun.* 9 (2018) 59.
- [266] N. Chiang, C.N. Serhan, S.-E. Dahlén, J.M. Drazen, D.W.P. Hay, G.E. Rovati, T. Shimizu, T. Yokomizo, C. Brink, The lipoxin receptor ALX: potent ligand-specific and stereoselective actions in vivo., *Pharmacol. Rev.* 58 (2006) 463–87.
- [267] T. Takano, S. Fiore, J.F. Maddox, H.R. Brady, N.A. Petasis, C.N. Serhan, Aspirin-triggered 15-epi-lipoxin A4 (LXA4) and LXA4 stable analogues are potent inhibitors of

- acute inflammation: evidence for anti-inflammatory receptors., *J. Exp. Med.* 185 (1997) 1693–704.
- [268] S. Fiore, S.W. Ryeom, P.F. Weller, C.N. Serhan, Lipoxin recognition sites. Specific binding of labeled lipoxin A4 with human neutrophils., *J. Biol. Chem.* 267 (1992) 16168–76.
- [269] S. Fiore, J.F. Maddox, H.D. Perez, C.N. Serhan, Identification of a human cDNA encoding a functional high affinity lipoxin A4 receptor., *J. Exp. Med.* 180 (1994) 253–260.
- [270] T. Christophe, A. Karlsson, M.-J. Rabiet, F. Boulay, C. Dahlgren, Phagocyte Activation by Trp-Lys-Tyr-Met-Val-Met, Acting through FPRL1/LXA 4 R, is not Affected by Lipoxin A 4, *Scand. J. Immunol.* 56 (2002) 470–476.
- [271] A. Planagumà, T. Domenech, I. Jover, I. Ramos, S. Sentellas, R. Malhotra, M. Miralpeix, Lack of activity of 15-epi-lipoxin A4 on FPR2/ALX and CysLT1 receptors in interleukin-8-driven human neutrophil function, *Clin. Exp. Immunol.* 173 (2013) 298–309.
- [272] N. Chiang, J. Dalli, R.A. Colas, C.N. Serhan, Identification of resolvin D2 receptor mediating resolution of infections and organ protection., *J. Exp. Med.* 212 (2015) 1203–17.
- [273] C.T. Schoeder, A.B. Mahardhika, A. Drabczyńska, K. Kieć-Kononowicz, C.E. Müller, Discovery of Tricyclic Xanthines as Agonists of the Cannabinoid-Activated Orphan G-Protein-Coupled Receptor GPR18., *ACS Med. Chem. Lett.* 11 (2020) 2024–2031.
- [274] S. Krishnamoorthy, A. Recchiuti, N. Chiang, S. Yacoubian, C.-H. Lee, R. Yang, N.A. Petasis, C.N. Serhan, Resolvin D1 binds human phagocytes with evidence for proresolving receptors., *Proc. Natl. Acad. Sci. U. S. A.* 107 (2010) 1660–5.
- [275] S. Krishnamoorthy, A. Recchiuti, N. Chiang, G. Fredman, C.N. Serhan, Resolvin D1 receptor stereoselectivity and regulation of inflammation and proresolving microRNAs., *Am. J. Pathol.* 180 (2012) 2018–27.
- [276] J. Dalli, J.W. Winkler, R.A. Colas, H. Arnardottir, C.-Y.C. Cheng, N. Chiang, N.A. Petasis, C.N. Serhan, Resolvin D3 and aspirin-triggered resolvin D3 are potent immunoresolvents., *Chem. Biol.* 20 (2013) 188–201.
- [277] S.R. Foster, A.S. Hauser, L. Vedel, R.T. Strachan, X.-P. Huang, A.C. Gavin, S.D. Shah, A.P. Nayak, L.M. Haugaard-Kedström, R.B. Penn, B.L. Roth, H. Bräuner-Osborne, D.E. Gloriam, Discovery of Human Signaling Systems: Pairing Peptides to G Protein-Coupled Receptors., *Cell.* 179 (2019) 895-908.e21.
- [278] C. Southern, J.M. Cook, Z. Neetoo-Isseljee, D.L. Taylor, C.A. Kettleborough, A. Merritt, D.L. Bassoni, W.J. Raab, E. Quinn, T.S. Wehrman, A.P. Davenport, A.J. Brown, A. Green, M.J. Wigglesworth, S. Rees, Screening  $\beta$ -arrestin recruitment for the identification of natural ligands for orphan G-protein-coupled receptors., *J. Biomol. Screen.* 18 (2013) 599–609.
- [279] E. Kowarz, D. Löscher, R. Marschalek, Optimized sleeping beauty transposons rapidly generate stable transgenic cell lines, *Biotechnol. J.* 10 (2015) 647–653.
- [280] K. Hosaka, M. Mishina, T. Tanaka, T. Kamiryo, S. Numa, Acyl-coenzyme-A synthetase I from *Candida lipolytica*. Purification, properties and immunochemical studies., *Eur. J. Biochem.* 93 (1979) 197–203.
- [281] O. Werz, D. Steinhilber, Selenium-dependent peroxidases suppress 5-lipoxygenase activity in B-lymphocytes and immature myeloid cells. The presence of peroxidase-insensitive 5-lipoxygenase activity in differentiated myeloid cells, *Eur. J. Biochem.* 242

- (1996) 90–97.
- [282] M. Kreiß, J.H. Oberlis, S. Seuter, I. Bischoff-Kont, D. Sürün, D. Thomas, T. Göbel, T. Schmid, O. Rådmark, R.P. Brandes, R. Fürst, A.-K. Häfner, D. Steinhilber, Human 5-lipoxygenase regulates transcription by association to euchromatin, *Biochem. Pharmacol.* 203 (2022) 115187.
- [283] S. Banthiya, J. Kalms, E. Galemou Yoga, I. Ivanov, X. Carpena, M. Hamberg, H. Kuhn, P. Scheerer, Structural and functional basis of phospholipid oxygenase activity of bacterial lipoxygenase from *Pseudomonas aeruginosa*, *Biochim. biophys. acta.* 1861 (2016) 1681–1692.
- [284] J. Kalms, S. Banthiya, E. Galemou Yoga, M. Hamberg, H.-G. Holzhutter, H. Kuhn, P. Scheerer, The crystal structure of *Pseudomonas aeruginosa* lipoxygenase Ala420Gly mutant explains the improved oxygen affinity and the altered reaction specificity, *Biochim. Biophys. acta. Mol. cell Biol. lipids.* 1862 (2017) 463–473.
- [285] X. Zhao, G. Li, S. Liang, Several affinity tags commonly used in chromatographic purification, *J. Anal. Methods Chem.* 2013 (2013) 1–8.
- [286] A. Einhauer, A. Jungbauer, The FLAG<sup>TM</sup> peptide, a versatile fusion tag for the purification of recombinant proteins, *J. Biochem. Biophys. Methods.* 49 (2001) 455–465.
- [287] G.E. Tiller, T.J. Mueller, M.E. Dockter, W.G. Struve, Hydrogenation of Triton X-100 eliminates its fluorescence and ultraviolet light absorption while preserving its detergent properties, *Anal. Biochem.* 141 (1984) 262–266.
- [288] T. Tanaka, K. Hosaka, M. Hoshimaru, S. Numa, Purification and properties of long-chain acyl-coenzyme-A synthetase from rat liver., *Eur. J. Biochem.* 98 (1979) 165–72.
- [289] A. Garreta, S.P. Val-Moraes, Q. García-Fernández, M. Busquets, C. Juan, A. Oliver, A. Ortiz, B.J. Gaffney, I. Fita, À. Manresa, X. Carpena, Structure and interaction with phospholipids of a prokaryotic lipoxygenase from *Pseudomonas aeruginosa*, *FASEB J.* 27 (2013) 4811–4821.
- [290] S. Banthiya, M. Pekárová, H. Kuhn, D. Heydeck, Secreted lipoxygenase from *Pseudomonas aeruginosa* exhibits biomembrane oxygenase activity and induces hemolysis in human red blood cells, *Arch. Biochem. Biophys.* 584 (2015) 116–124.
- [291] R.E. Vance, S. Hong, K. Gronert, C.N. Serhan, J.J. Mekalanos, The opportunistic pathogen *Pseudomonas aeruginosa* carries a secretable arachidonate 15-lipoxygenase, *Proc. Natl. Acad. Sci. U. S. A.* 101 (2004) 2135–2139.
- [292] X. Cai, R. Dou, C. Guo, J. Tang, X. Li, J. Chen, J. Zhang, Cationic polymers as transfection reagents for nucleic acid delivery, *Pharmaceutics.* 15 (2023) 1502.
- [293] N. Bessis, F.J. GarciaCozar, M.-C. Boissier, Immune responses to gene therapy vectors: influence on vector function and effector mechanisms, *Gene Ther.* 11 (2004) S10–S17.
- [294] R.B. DuBridge, P. Tang, H.C. Hsia, P.-M. Leong, J.H. Miller, M.P. Calos, Analysis of mutation in human cells by using an Epstein-Barr virus shuttle system, *Mol. Cell. Biol.* 7 (1987) 379–387.
- [295] W.S. Pear, G.P. Nolan, M.L. Scott, D. Baltimore, Production of high-titer helper-free retroviruses by transient transfection., *Proc. Natl. Acad. Sci. U. S. A.* 90 (1993) 8392–6.
- [296] C.F.K. Kan, A.B. Singh, D.M. Stafforini, S. Azhar, J. Liu, Arachidonic acid downregulates acyl-CoA synthetase 4 expression by promoting its ubiquitination and proteasomal degradation, *J. Lipid Res.* 55 (2014) 1657–1667.

- [297] Z. Liu, O. Chen, J.B.J. Wall, M. Zheng, Y. Zhou, L. Wang, H. Ruth Vaseghi, L. Qian, J. Liu, Systematic comparison of 2A peptides for cloning multi-genes in a polycistronic vector, *Sci. Rep.* 7 (2017).
- [298] A.L. Szymczak, D.A. Vignali, Development of 2A peptide-based strategies in the design of multicistronic vectors, *Expert Opin. Biol. Ther.* 5 (2005) 627–638.
- [299] M.L.L. Donnelly, G. Luke, A. Mehrotra, X. Li, L.E. Hughes, D. Gani, M.D. Ryan, Analysis of the aphthovirus 2A/2B polyprotein “cleavage” mechanism indicates not a proteolytic reaction, but a novel translational effect: a putative ribosomal “skip”., *J. Gen. Virol.* 82 (2001) 1013–1025.
- [300] M.L.L. Donnelly, L.E. Hughes, G. Luke, H. Mendoza, E. Ten Dam, D. Gani, M.D. Ryan, The “cleavage” activities of foot-and-mouth disease virus 2A site-directed mutants and naturally occurring “2A-like” sequences., *J. Gen. Virol.* 82 (2001) 1027–1041.
- [301] A.-K. Häfner, J. Gerstmeier, M. Hörnig, S. George, A.-K. Ball, M. Schröder, U. Garscha, O. Werz, D. Steinhilber, Characterization of the interaction of human 5-lipoxygenase with its activating protein FLAP, *Biochim. Biophys. Acta - Mol. Cell Biol. Lipids.* 1851 (2015) 1465–1472.
- [302] N.C. Gilbert, J. Gerstmeier, E.E. Schexnaydre, F. Börner, U. Garscha, D.B. Neau, O. Werz, M.E. Newcomer, Structural and mechanistic insights into 5-lipoxygenase inhibition by natural products, *Nat. Chem. Biol.* 16 (2020) 783–790.
- [303] K.A. Harrison, R.C. Murphy, Isoleukotrienes are biologically active free radical products of lipid peroxidation, *J. Biol. Chem.* 270 (1995) 17273–17278.
- [304] K.-J. Cho, J.-M. Seo, J.-H. Kim, Bioactive lipoxygenase metabolites stimulation of NADPH oxidases and reactive oxygen species, *Mol. Cells.* 32 (2011) 1–5.
- [305] J. Svartz, E. Hallin, Y. Shi, M. Söderström, S. Hammarström, Identification of regions of leukotriene C4 synthase which direct the enzyme to its nuclear envelope localization., *J. Cell. Biochem.* 98 (2006) 1517–27.
- [306] M. Walther, R. Wiesner, H. Kuhn, Investigations into calcium-dependent membrane association of 15-lipoxygenase-1. Mechanistic roles of surface-exposed hydrophobic amino acids and calcium., *J. Biol. Chem.* 279 (2004) 3717–25.
- [307] T. Hammarberg, P. Provost, B. Persson, O. Rådmark, The N-terminal domain of 5-Lipoxygenase binds calcium and mediates calcium stimulation of enzyme activity, *J. Biol. Chem.* 275 (2000) 38787–38793.
- [308] G. Bender, E.E. Schexnaydre, R.C. Murphy, C. Uhlsøn, M.E. Newcomer, Membrane-dependent activities of human 15-LOX-2 and its murine counterpart: Implications for murine models of atherosclerosis., *J. Biol. Chem.* 291 (2016) 19413–24.
- [309] P. Maher, K. van Leyen, P.N. Dey, B. Honrath, A. Dolga, A. Methner, The role of Ca<sup>2+</sup> in cell death caused by oxidative glutamate toxicity and ferroptosis, *Cell Calcium.* 70 (2018) 47–55.
- [310] J.P. Friedmann Angeli, M. Schneider, B. Proneth, Y.Y. Tyurina, V.A. Tyurin, V.J. Hammond, N. Herbach, M. Aichler, A. Walch, E. Eggenhofer, D. Basavarajappa, O. Rådmark, S. Kobayashi, T. Seibt, H. Beck, F. Neff, I. Esposito, R. Wanke, H. Förster, O. Yefremova, M. Heinrichmeyer, G.W. Bornkamm, E.K. Geissler, S.B. Thomas, B.R. Stockwell, V.B. O'Donnell, V.E. Kagan, J.A. Schick, M. Conrad, Inactivation of the ferroptosis regulator Gpx4 triggers acute renal failure in mice., *Nat. Cell Biol.* 16 (2014) 1180–91.
- [311] V.E. Kagan, G. Mao, F. Qu, J.P.F. Angeli, S. Doll, C.S. Croix, H.H. Dar, B. Liu, V.A.

Tyurin, V.B. Ritov, A.A. Kapralov, A.A. Amoscato, J. Jiang, T. Anthony Muthu, D. Mohammadyani, Q. Yang, B. Proneth, J. Klein-Seetharaman, S. Watkins, I. Bahar, J. Greenberger, R.K. Mallampalli, B.R. Stockwell, Y.Y. Tyurina, M. Conrad, H. Bayir, Oxidized arachidonic and adrenic PEs navigate cells to ferroptosis, *Nat. Chem. Biol.* 13 (2017) 81–90.

- [312] L. Hodson, C.M. Skeaff, B.A. Fielding, Fatty acid composition of adipose tissue and blood in humans and its use as a biomarker of dietary intake, *Prog. Lipid Res.* 47 (2008) 348–380.
- [313] T. Manzoni Jacintho, H. Gotho, M. Gidlund, C. Garcia Marques, R. Torrinhas, M. Mirtes Sales, D. Linetzky Waitzberg, Anti-inflammatory effect of parenteral fish oil lipid emulsion on human activated mononuclear leukocytes, *Nutr. Hosp.* 24 (2009) 288–296.
- [314] Y. Xie, W. Hou, X. Song, Y. Yu, J. Huang, X. Sun, R. Kang, D. Tang, Ferroptosis: Process and function, *Cell Death Differ.* 23 (2016) 369–379.

## 9 Appendix

### 9.1 Primer

Table 9.1: Cloning primer.

Primer (rec. ACSL4 expression)	Sequence
BG02_ACSL4_StepII_TGA_HindIII_rev	CATTGAACGGAATGTATGGGGCCAAAGCCGGCCGAAGCGCTTGAGCCAC CCGCAGTTGAAAAATGAAAAGCTTTAAGCC
BJ10_NdeI_ACSL4_for	GCAGCACATATGGCAAAAGAGAATAAAAAGCTAAGCCC
BJ13_P_ACSL4_for	TTTCCCCCATACATTGTTCAATG
BJ14_P_pET24a+_rev	GCGGCCGCACTCGAGC
<b>Primer (stable transfection)</b>	<b>Sequence</b>
BJ17_SfiI_ACSL4_for	GCCGCAGGCCTCTGAGGCCACCATGGCAAAAGAGAATAAAAGCTAAGCCC
BJ18_ACSL4_SfiI'_rev	CTCGAGGGCCTGACAGGCCCTTATTTGCCCCCATACATTGTTCAATG
BJ20_LPCAT2_SfiI'_rev	CTCGAGGGCCTGACAGGCCCTCAGTCATCTTTTTGTCTGAGGTAATC
BJ21_ACSL4_GSGP2A(Teil1)_rev	CTCGAGGACGTCACCAGCCTGCTTCAGCAGGCTGAAGTTAGTCCAC TGCCITTTGCCCCCATACATTGTTCAATG
BJ22_GSGP2A(Teil2)_LPCAT2_for	GCCGCAGACGTCGAGGAGAATCCTGGCCCATGAGCCGGTGCCCCAG
BJ104_EGFPdel_for	GGCAGTGGAGCTAACTTCAG
BJ105_SfiI_15LO1_for	GCAAAAGGCCCTCTGAGGCCATGGGTCTCTACCGCATCCG

Table 9.2: Primers for preparation of plasmids for transient transfection in HEK293T cells.

Primer	Sequence
BJ77_EcoRI_FLAP_for	GCAGCAGAATTCATGGATCAAGAAACTGTAGGC
BJ78_FLAP_XhoI_rev	CCCCCTACTTCTCATTCCCTAAGTCTGAGGACAGCA
BJ91_EcoRI_5LO_for	GTGGTGGAATTCACCATGC
BJ92_Cterm_5LO_P2A(1)_rev	CTCCTCGACGTCACCAGCCTGCTTCAGCAGGCTGAAGTTAGCTCCACTGCCGATGG CCACACTGTTCCGGAATC
BJ93_EcoRI_15LO1_for	GTGGTGGAATTCACCATGGGTCTCTACCGCATCCG
BJ94_Cterm_15LO1_P2A(1)_rev	CTCCTCGACGTCACCAGCCTGCTTCAGCAGGCTGAAGTTAGCTCCACTGCCGATGG CCACACTGTTTCACCC
BJ95_EcoRI_15LO2_for	GTGGTGGAATTCACCATGGCCGAGTTCAAGGCTCAG
BJ96_Cterm_15LO2_P2A(1)_rev	CTCCTCGACGTCACCAGCCTGCTTCAGCAGGCTGAAGTTAGCTCCACTGCCGATGG AGACGCTGTTCTCGATG
BJ97_P2A(2)_mCh_for	GCTGGTGACGTCGAGGAGAATCCTGGCCCCATGGTGAGCAAGGGCGAGG
BJ98_mCh_XbaI_rev	GGATGTTCTAGACTCGACTCAGAGTCCGGACTTGTACAGCTC
BJ99_P2A(2)_FLAP_for	GCTGGTGACGTCGAGGAGAATCCTGGCCCCATGGATCAAGAAACTGTAGGCAATGTTG
BJ100_FLAP_T2A_rev	CCCCTGCCCTCTCCACTGCCCGGGAATGAGAAGTAGAGGGGAG
BJ101_GSG_T2A_for	GGCAGTGAGAGGGCCAGGGGAAGTCTTCTAACATGCCGGGACCGTGAGGAAAATCCCG GCCCA
BJ102_T2A_mCh_for	GTGGAGGAAAATCCCGGCCCAATGGTGAGCAAGGGCGAGG



Table 9.3: Primers for preparation of plasmids for stable transfection of HEK293T cells.

Primer	Sequence
BJ106_15LO1_Sfil'_rev	CTTTGGCGCCTGACAGGCCCTCAGATGGCCACACTGTTTCCACC
BJ107_Sfil'_15LO2_for	GCAAAGGGCCTCTGAGGCCATGGCCGAGTTTCCAGGGTTCAG
BJ108_15LO2_Sfil'_rev	CTTTGGCGCCTGACAGGCCCTCAGATGGAGACCGCTGTTCTCGATG
BJ109_NEB_5LO_for	CTTCCTACCCCTCGAAAGGCCCTCTGAGGCCATGCCCTCCTACACGGTCCAC
BJ110_FLAP_NEB_rev	CTATCGATGGAAGCTTGGCCTGACACAGGCCCTCAGGGAATGAGAAGTAGAGGGGAG
BJ111_NEB_mCh_for	CCTCTGCACCTGAGGCCACCATGGTGAGCAAGGGCGGAGG
BJ112_mCh_NEB_rev	GAAGTTAGTAGCTCCACTGCCGAGTCCGGACTTGTACAGCTC
BJ119_5LO_Sfil'_rev	CGATGGAAGCTTGGCCTGACAGGCCCTCAGATGGCCACACTGTTCCGG

## 9.2 Plasmid maps

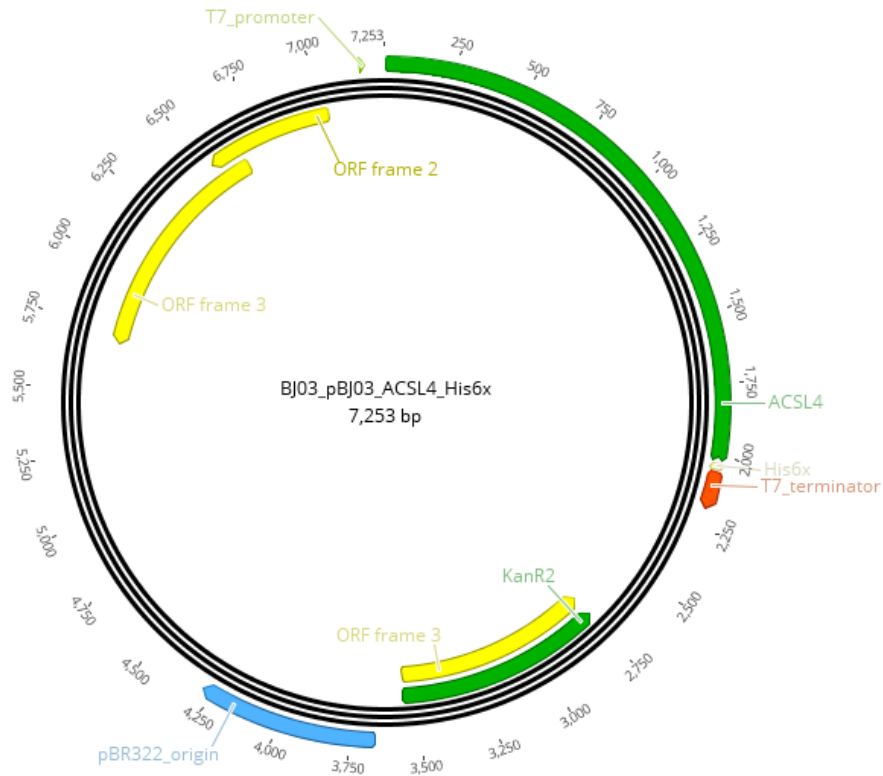


Figure 9.1: Recombinant expression plasmid of ACSL4 with C-terminal His6x-tag.

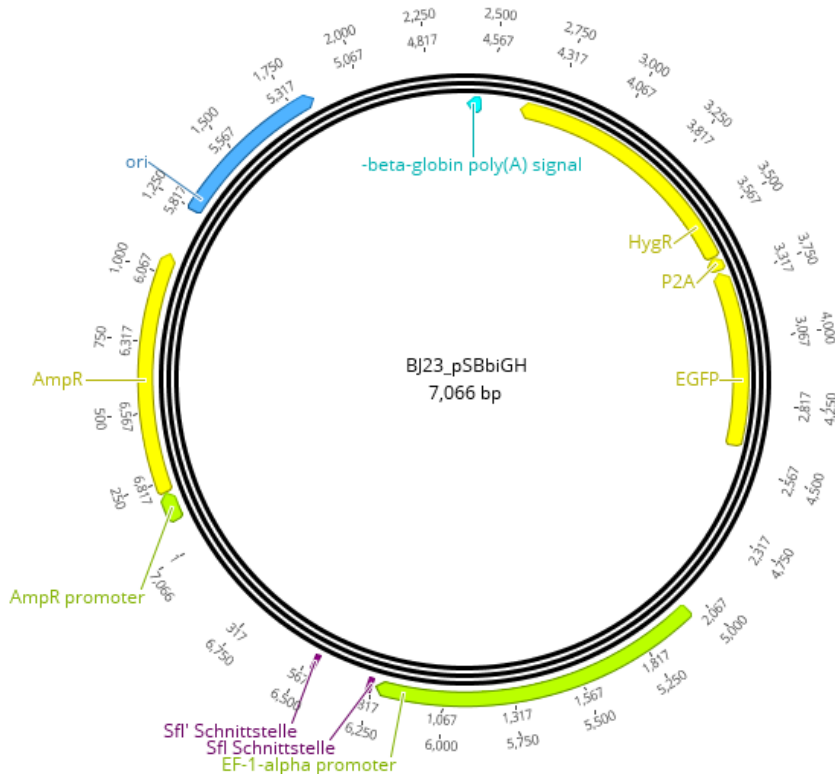
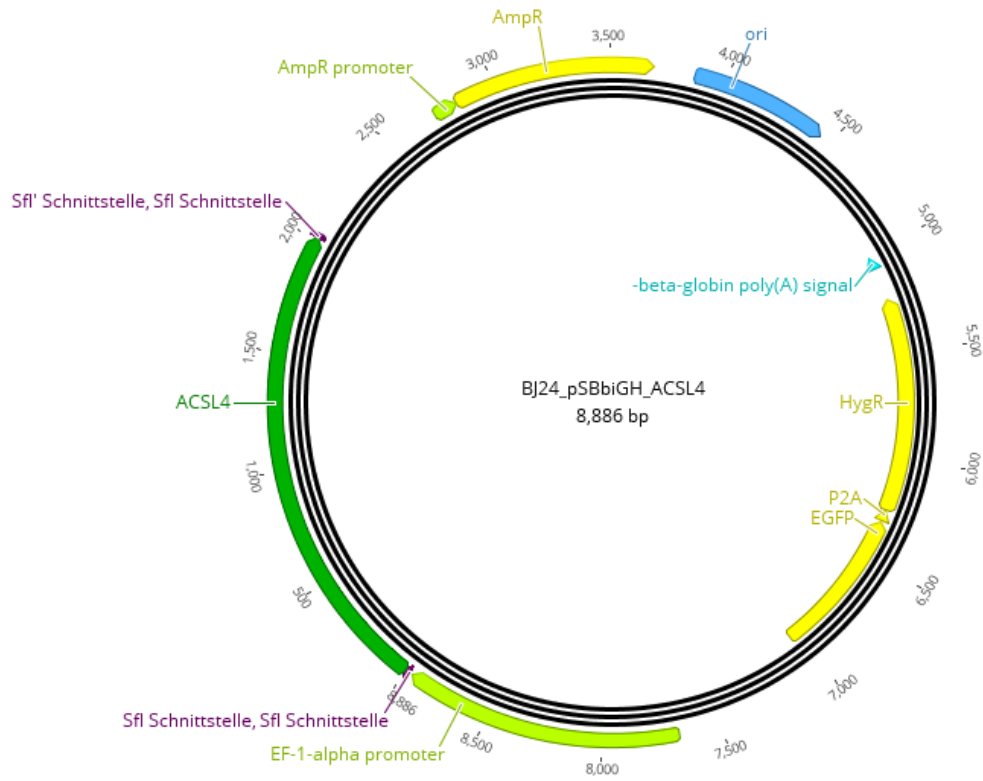
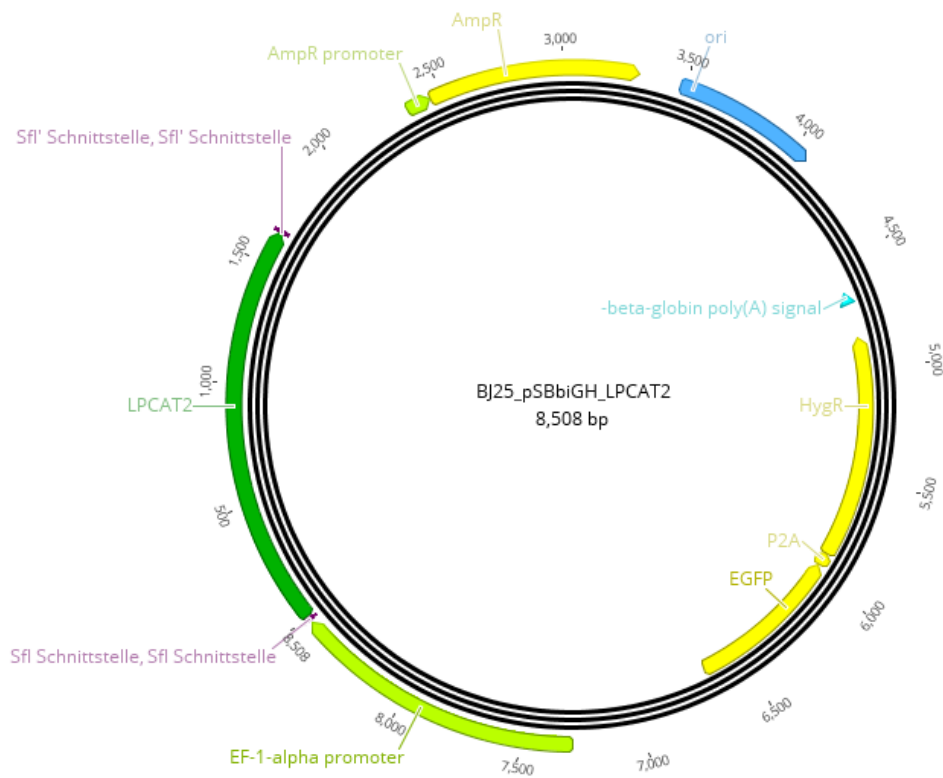


Figure 9.2: Sleeping beauty transfection plasmid with empty MCS.



**Figure 9.3: Sleeping beauty transfection plasmid for constitutive expression of ACSL4.**



**Figure 9.4: Sleeping beauty transfection plasmid for constitutive expression of LPCAT2.**

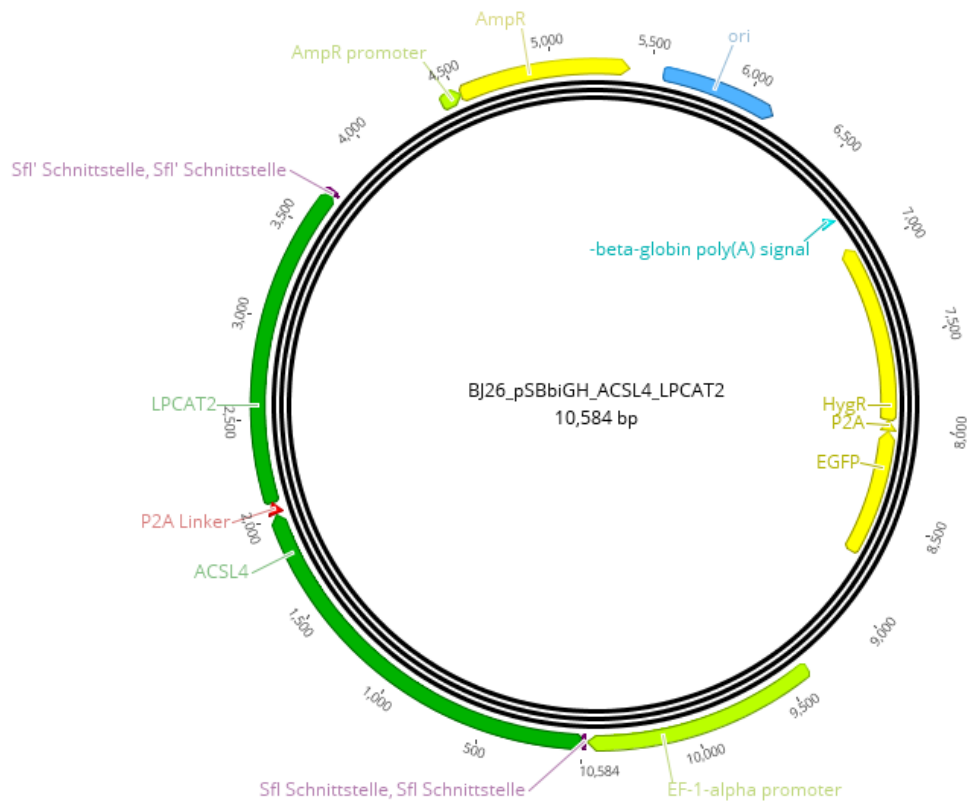


**Figure 9.5: Sleeping beauty transfection plasmid for constitutive expression of the genes ACSL4 and LPCAT2 separated by a P2A linker sequence.**

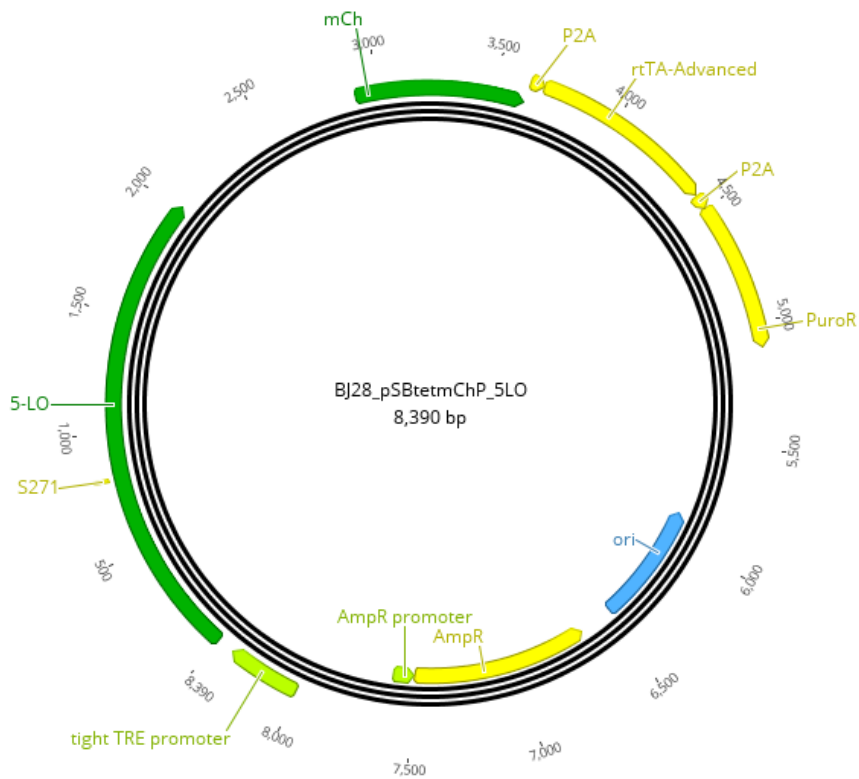


**Figure 9.6: Sleeping beauty transfection plasmid for inducible expression of 5-LO.**

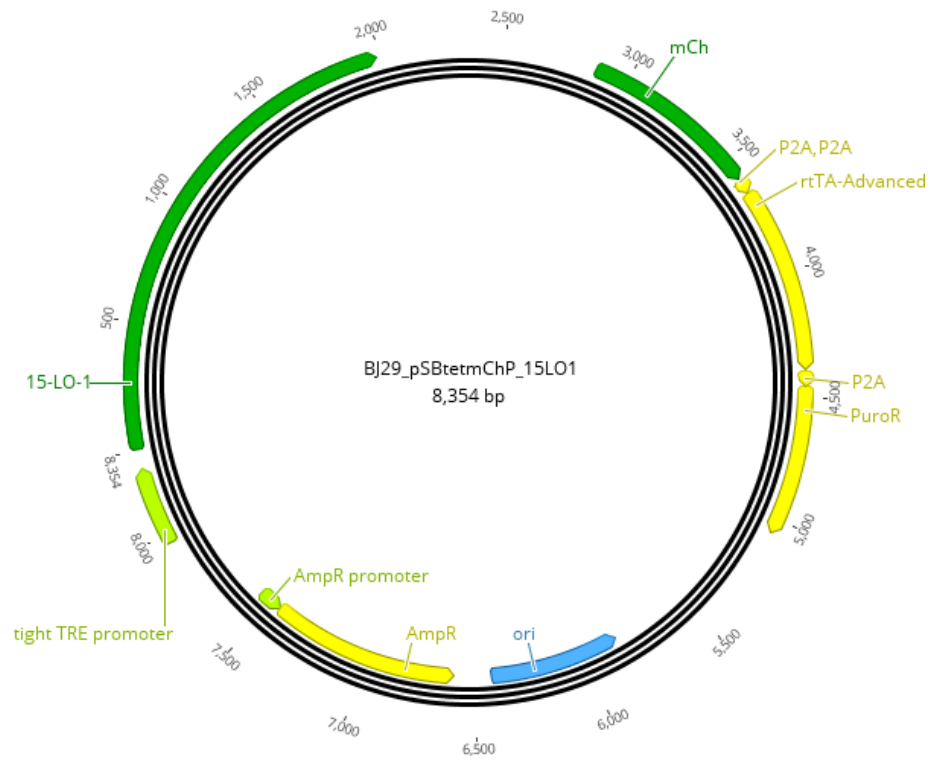


Figure 9.7: Sleeping beauty transfection plasmid for inducible expression of 15-LO1.

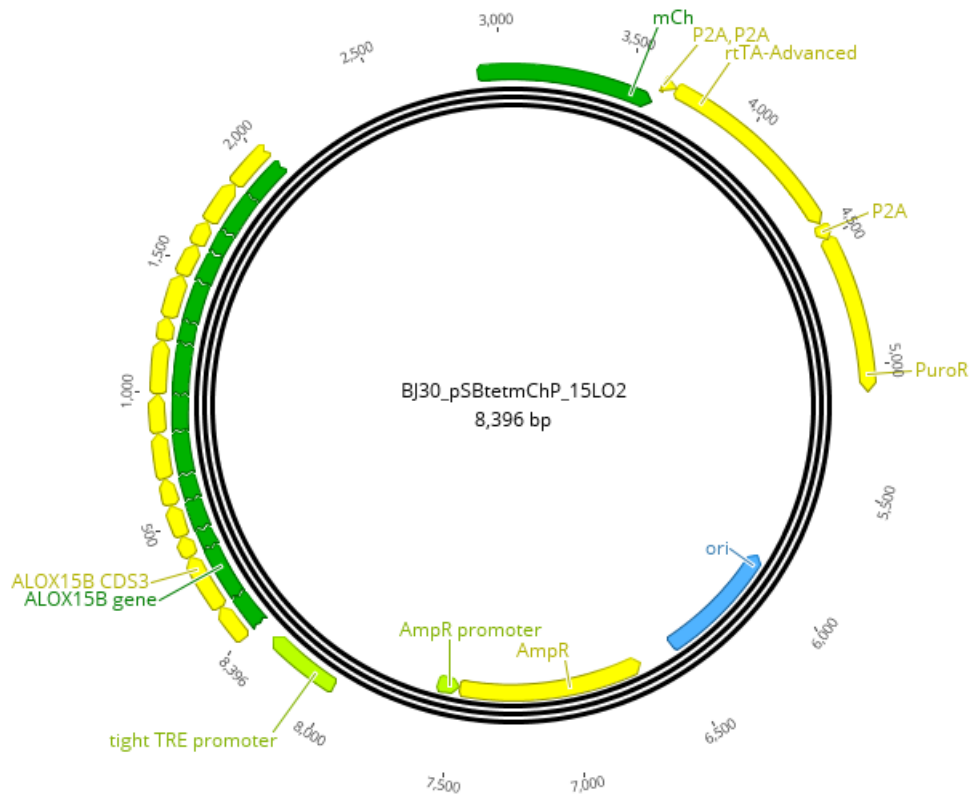


Figure 9.8: Sleeping beauty transfection plasmid for inducible expression of 15-LO2.

## 9.3 ÄKTA methods for protein purification

### 9.3.1 Ni-affinity chromatography – HisTrap™ HP, CV = 5 mL

```

Main method:
┌ (Main)
  0.00 Base Volume 5.027 {ml} HisTrap_HP_5_ml
  0.00 Flow 5.00 {ml/min}
  0.00 Alarm_Pressure Enabled 0.48 {MPa} 0.00 {MPa}
  0.00 SystemPumpControlMode Normal 0.27 {MPa} 0.10 {ml/min}
  0.00 Wavelength 280 {nm} 254 {nm} 210 {nm}
┌ 0.00 Block Washing_1
  (Washing_1)
  0.00 Base SameAsMain
  0.00 PumpInlet (A2)#MilliQ
  10.00 End_Block
┌ 0.00 Block Equilibration
  (Equilibration)
  0.00 Base SameAsMain
  0.00 PumpInlet (A1)#Washing_buffer
  0.00 Gradient 0.0 {%B} 0.00 {base}
  0.00 OutletValve F2
  25 AutoZeroUV
  25.00 End_Block
┌ 0.00 Block Sample
  (Sample)
  0.00 Base SameAsMain
  0.00 Flow 2.50 {ml/min}
  0.00 InjectionValve Inject
  0.00 Fractionation 18mm 10 {ml} TubeNumber[A.1] Volume 0 A
  45 InjectionValve Load
  45 FractionationStop
  45 End_Block
┌ 0.00 Block Washing_3
  (Washing_3)
  0.00 Base SameAsMain
  0.00 InjectionValve Load
  0.00 Flow 5.00 {ml/min}
  35.00 End_Block
┌ 0.00 Block W5
  (W5)
  0.00 Base SameAsMain
  0.00 Fractionation 18mm 9 {ml} NextTube Volume 0 0 0
  0.00 InjectionValve Load
  0.00 PumpInlet B2
  0.00 Gradient 100 {%B} 0.00 {base}
  0.00 Flow 5.00 {ml/min}
  25.00 End_Block
┌ 0.00 Block Elution_1
  (Elution_1)
  0.00 Base SameAsMain
  0.00 PumpInlet B1
  0.00 Fractionation 18mm 2.500 {ml} NextTube Volume 0 0 0
  0.00 Gradient 100.0 {%B} 0.00 {base}
  30.00 End_Block
┌ 0.00 Block Elution_2
  (Elution_2)
  0.00 Base SameAsMain
  0.00 Gradient 100.0 {%B} 0.00 {base}
  1 FractionationStop
  1 End_Block
┌ 0.00 Block Washing_4
  (Washing_4)
  0.00 Base SameAsMain
  0.00 Gradient 0.0 {%B} 0.00 {base}
  0.00 PumpInlet A1
  25.00 End_Block
┌ 0.00 Block MilliQ_A2
  (MilliQ_A2)
  0.00 Base SameAsMain
  0.00 PumpInlet A2
  25.00 End_Block

```

Figure 9.9: Method: Result\Bjarne\220913HisTrap5mlACSL4His6x001.res

### 9.3.2 Buffer exchange – HiTrapDesalting, CV = 15 mL (3x5 mL)

Main method:

```

▣ (Main)
  0.00 Base CV 5.027 {ml} HiTrap_Desalting
  0.00 Wavelength 280 {nm} 211 {nm} 254 {nm}
  0.00 SystemPumpControlMode PressFlowControl 0.27 {MPa} 0.10 {ml/min}
  0.00 Flow 3.00 {ml/min}
  0.00 InjectionValve Load
  0.00 PumpInlet A1
  0.00 Alarm_Pressure Enabled 0.30 {MPa} 0.00 {MPa}
▣ 0.00 Block Equilibrierung
  (Equilibrierung)
  0.00 Base SameAsMain
  2.5 OutletValve F2
  4 AutoZeroUV
  4 End_Block
▣ 0.00 Block AuftragundElution
  (AuftragundElution)
  0.00 Base SameAsMain
  0.00 Flow 2.00 {ml/min}
  0.00 Fractionation 18mm 2 {ml} TubeNumber[C.1] Volume
  0.00 InjectionValve Inject
  3.00 FractionationStop
  6.00 End_Block
▣ 0.00 Block Waschen
  (Waschen)
  0.00 Base SameAsMain
  0.00 Flow 3.00 {ml/min}
  0.00 PumpInlet A2
  0.00 Gradient 0 {%B} 0.00 {base}
  0.00 FractionationStop
  6.00 InjectionValve Load
  6.00 End_Block

```

Figure 9.10 Method: Result\Bjarne\220913HitrapACSL4His6x(3x5ml)001.res

### 9.3.3 Cation exchange chromatography – Resource S, CV = 1 mL

Main method:

```

▣ (Main)
  0.00 Base CV 0.965 {ml} (RESOURCE_S_1_ml)#Column
▣ 0.00 Block Start_with_PumpWash_Purifier
  (Start_with_PumpWash_Purifier)
  0.00 Base SameAsMain
  0.00 PumpWashPurifier (OFF)#Wash_Inlet_A1_(OFF)#Wash_Inlet_A2_(OFF)#Wash_Inlet_B1_(OFF)#Wash_Inlet_B2_
  0.00 End_Block
▣ 0.00 Block Flow_Rate
  (Flow_Rate)
  0.00 Base SameAsMain
  0.00 Flow (2)#Flow_Rate {ml/min}
  0.00 End_block
▣ 0.00 Block Column_Pressure_Limit
  (Column_Pressure_Limit)
  0.00 Base SameAsMain
  0.00 Alarm_Pressure Enabled (1.50)#Column_PressureLimit {MPa} 0.00 {MPa}
  0.00 End_Block
▣ 0.00 Block Start_Instructions
  (Start_Instructions)
  0.00 Base SameAsMain
  0.00 Wavelength (280)#Wavelength_1 {nm} (254)#Wavelength_2 {nm} (211)#Wavelength_3 {nm}
  0.00 AveragingTimeUV (1.28)#Averaging_Time_UV {sec}
  0.00 End_block

```

```

❏ 0.00 Block Eluent_A_Inlet
  (Eluent_A_Inlet)
  0.00 Base SameAsMain
  0.00 PumpAInlet (A1)#Pump_A_Inlet
  0.00 End_block
❏ 0.00 Block Eluent_B_Inlet
  (Eluent_B_Inlet)
  0.00 Base SameAsMain
  0.00 PumpBInlet (B1)#Pump_B_Inlet
  0.00 End_block
❏ 0.00 Block Start_Conc_B
  (Start_Conc_B)
  0.00 Base SameAsMain
  0.00 Gradient (0)#Start_ConcB {%B} 0.00 {base}
  0.00 End_block
❏ 0.00 Block System_Volume_Compensation
  (System_Volume_Compensation)
  0.00 Base Volume
  (8)#Compensation_Volume_End_Block
❏ 0.00 Block Column_Equilibration
  (Column_Equilibration)
  0.00 Base SameAsMain
  (5)#Equilibrate_with_End_Block
❏ 0.00 Block AutoZero_UV
  (AutoZero_UV)
  0.00 Base SameAsMain
  0.00 Watch_Off UV1
  0.00 AutoZeroUV
  0.00 End_Block
❏ 0.00 Block Aut_PressureFlow_Regulation
  (Aut_PressureFlow_Regulation)
  0.00 Base Time
  0.00 SystemPumpControlMode (Normal)#System_Pump (0)#System_PressLevel {MPa} (0)#System_MinFlow {ml/min}
  0.00 End_Block
❏ 0.00 Block Outlet_Valve_F2
  (Outlet_Valve_F2)
  0.00 Base SameAsMain
  0.00 OutletValve F2
  0.00 End_Block
❏ 0.00 Block Flowthrough_Fractionation
  (Flowthrough_Fractionation)
  0.00 Base SameAsMain
  0.00 Fractionation (18mm)#Flowthrough_TubeType (5)#Flowthrough_FracSize {ml} (TubeNumber[F.1])#Flowthrough_StartAt Volume
  0.00 End_block
❏ 0.00 Block Sample_Injection_
  (Sample_Injection_)
  0.00 Base SameAsMain
  0.00 InjectionValve Inject
❏ 0.00 Block Sample_Injection
  (Sample_Injection)
  0.00 Base Volume
  0.00 Flow 0.5 {ml/min}
  (3.5)#Empty_loop_with_End_Block
  0.00 InjectionValve Load
  0.00 End_block
❏ 0.00 Block Aut_PressureFlow_Regulation
  (Aut_PressureFlow_Regulation)
  0.00 Base Time
  0.00 SystemPumpControlMode (Normal)#System_Pump (0)#System_PressLevel {MPa} (0)#System_MinFlow {ml/min}
  0.00 End_Block
❏ 0.00 Block Flow_Rate

```



```

(Flow_Rate)
0.00 Base SameAsMain
0.00 Flow (2)#Flow_Rate {ml/min}
0.00 End_block
▣ 0.00 Block Wash_Out_Unbound_Sample
(Wash_Out_Unbound_Sample)
0.00 Base SameAsMain
▣ 0.00 Block Aut_PressureFlow_Regulation
(Aut_PressureFlow_Regulation)
0.00 Base Time
0.00 SystemPumpControlMode (Normal)#System_Pump (0)#System_PressLevel {MPa} (0)#System_MinFlow {ml/min}
0.00 End_Block
(2)#Wash_column_with End_block
▣ 0.00 Block Stop_Flowthrough_Fractionation
(Stop_Flowthrough_Fractionation)
0.00 Base SameAsMain
0.00 FractionationStop
▣ 0.00 Block Delay0p02min
(Delay0p02min)
0.00 Base Time
0.02 End_Block
0.00 End_Block
▣ 0.00 Block Outlet_Valve_Reset
(Outlet_Valve_Reset)
0.00 Base SameAsMain
0.00 OutletValve WasteF1
0.00 End_Block
▣ 0.00 Block Aut_PressureFlow_Reset
(Aut_PressureFlow_Reset)
0.00 Base Time
0.00 SystemPumpControlMode Normal 0.00 {MPa} 0.10 {ml/min}
▣ 0.00 Block Delay0p02min
(Delay0p02min)
0.00 Base Time
0.02 End_Block
0.00 End_Block
▣ 0.00 Block Outlet_Valve_F2
(Outlet_Valve_F2)
0.00 Base SameAsMain
0.00 OutletValve F2
0.00 End_Block
▣ 0.00 Block Fractionation
(Fractionation)
0.00 Base SameAsMain
0.00 Fractionation (18mm)#TubeType_EluateFrac (2.5)#Eluate_Frac_Size {ml} (NextTube)#EluateFrac_StartAt Volume
0.00 Peak_Fractionation (18mm)#TubeType_PeakFrac (0)#Peak_Frac_Size {ml} (FirstTube)#PeakFrac_StartAt Volume
0.00 End_block
▣ 0.00 Block Flow_Rate
(Flow_Rate)
0.00 Base SameAsMain
0.00 Flow (2)#Flow_Rate {ml/min}
0.00 End_block
▣ 0.00 Block Linear_Gradient
(Linear_Gradient)
0.00 Base SameAsMain
0.00 Gradient (70)#Target_ConcB {%B} (20.00)#Length_of_Gradient {base}
20.00 End_Block
▣ 0.00 Block Gradient_Delay
(Gradient_Delay)
0.00 Base Volume
(8)#Gradient_Delay End_Block

```

```
▣ 0.00 Block Fractionation_Stop
  (Fractionation_Stop)
  0.00 Base SameAsMain
  0.00 FractionationStop
  0.00 Peak_FracStop
  0.00 End_Block
▣ 0.00 Block Outlet_Valve_Reset
  (Outlet_Valve_Reset)
  0.00 Base SameAsMain
  0.00 OutletValve WasteF1
  0.00 End_Block
▣ 0.00 Block Clean_after_Elution
  (Clean_after_Elution)
  0.00 Base SameAsMain
  0.00 Gradient 100 {%B} 0.00 {base}
  (5)#Clean_with End_Block
▣ 0.00 Block Eluent_A_Inlet
  (Eluent_A_Inlet)
  0.00 Base SameAsMain
  0.00 PumpAInlet (A1)#Pump_A_Inlet
  0.00 End_block
▣ 0.00 Block Eluent_B_Inlet
  (Eluent_B_Inlet)
  0.00 Base SameAsMain
  0.00 PumpBInlet (B1)#Pump_B_Inlet
  0.00 End_block
▣ 0.00 Block Start_Conc_B
  (Start_Conc_B)
  0.00 Base SameAsMain
  0.00 Gradient (0)#Start_ConcB {%B} 0.00 {base}
  0.00 End_block
▣ 0.00 Block Length_of_Reequilibration
  (Length_of_Reequilibration)
  0.00 Base SameAsMain
▣ 0.00 Block System_Volume_Compensation
  (System_Volume_Compensation)
  0.00 Base Volume
  (8)#Compensation_Volume End_Block
  (5.00)#Reequilibrate_with End_Block
```

**Figure 9.11: Method: Result\Bjarne\190724 CationIEX 1mL ACSL4001.res**

### 9.3.4 Size exclusion chromatography – HiLoad™ 16/60 Superdex™ 200 pg, CV = 120 mL

Main method:

```
▣ (Main)
0.00 Base CV 120.637 {ml} HiLoad_16/60_Superdex_200_prep_grade
0.00 Wavelength 280 {nm} 254 {nm} 211 {nm}
0.00 Alarm_Pressure Enabled 0.35 {MPa} 0.00 {MPa}
0.00 SystemPumpControlMode PressFlowControl 0.30 {MPa} 0.10 {ml/m}
▣ 0.00 Block Waschen1_MQ
(Waschen1_MQ)
0.00 Base SameAsMain
0.00 PumpAInlet A2
0.00 Flow 1.60 {ml/min}
0.00 Gradient 0 {%B} 0.00 {base}
1.00 End_Block
▣ 0.00 Block Equilibrierung
(Equilibrierung)
0.00 Base SameAsMain
0.00 PumpAInlet A1
0.00 Flow 1.2 {ml/min}
0.99 AutoZeroUV
1.00 End_Block
▣ 0.00 Block Auftrag
(Auftrag)
0.00 Base Volume
0.00 Flow 0.5 {ml/min}
0.00 InjectionValve Inject
5 End_Block
▣ 0.00 Block Elution
(Elution)
0.00 Base SameAsMain
0.0 Flow 1.20 {ml/min}
0.1 InjectionValve Load
0.1 OutletValve F2
0.10 Fractionation 18mm 5 {ml} FirstTube Volume
1.25 FractionationStop
1.25 End_Block
▣ 0.00 Block Waschen2
(Waschen2)
0.00 Base SameAsMain
0.00 PumpAInlet A2
0.00 OutletValve WasteF1
0.00 Flow 1.20 {ml/min}
0.00 Gradient 0 {%B} 0.00 {base}
0.80 OutletValve F2
1.00 End_Block
```

Figure 9.12: Method: Result\Bjarne\211206BJACSL4SE001.res

## 9.4 Laser scanning confocal microscopy images

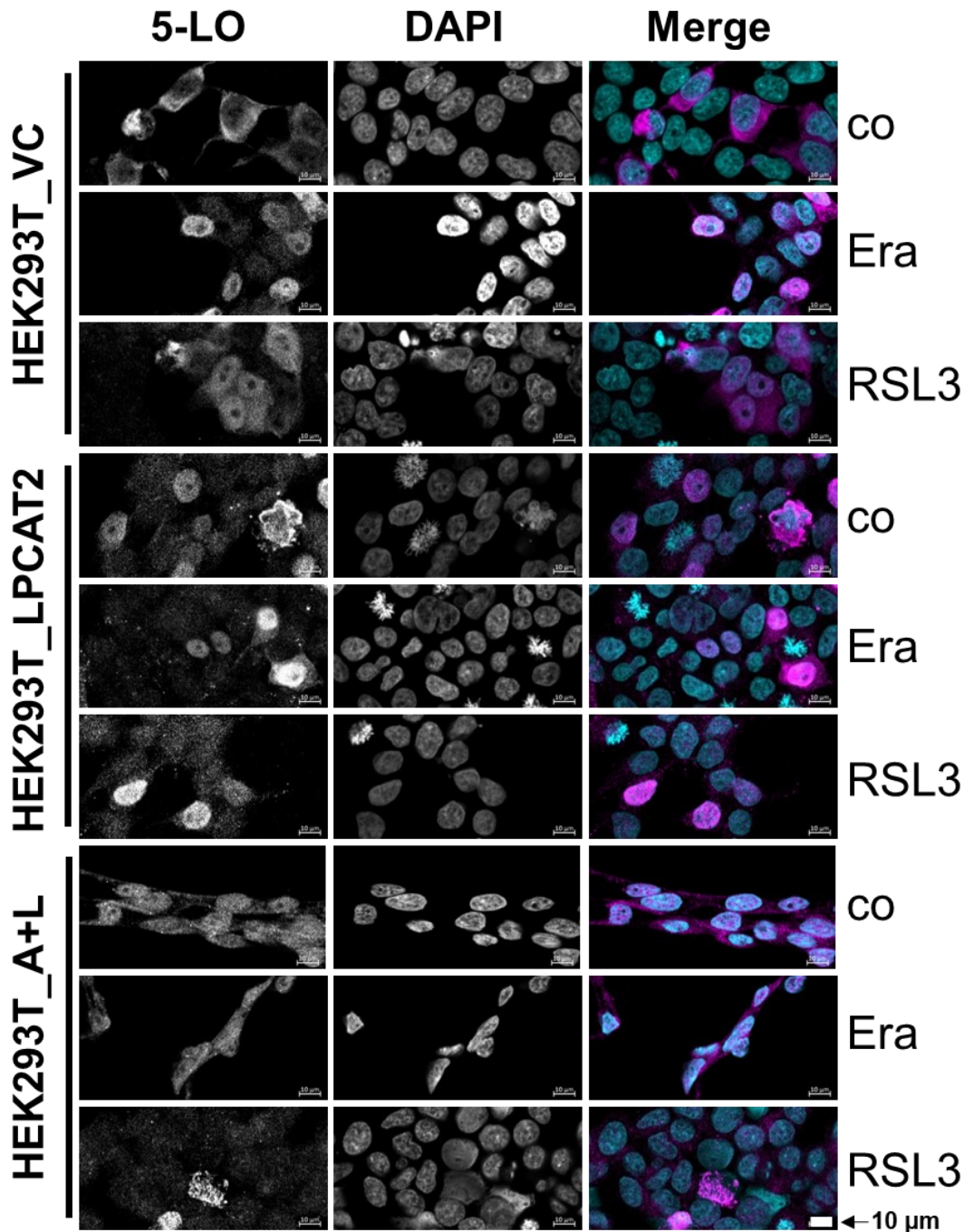


**Figure 9.13: Effect of ferroptosis inducers on the localization of 5-lipoxygenase in stably transfected HEK293T cells.**

HEK293T\_VC\_5LO, HEK293T\_LPCAT2\_5LO, and HEK293T\_A+L\_5LO cells were treated with 200 ng/ml doxycycline for 24 h before treatment with 10 µM RSL3 or 3 µM erastin for 4 h or 24 h, respectively. Controls (co) received DMSO. Cells were stained with fluorophore-conjugated antibodies against 5-LO (purple). Nuclei were counterstained using DAPI (turquoise). Cells were imaged and analyzed on a Zeiss 780 AxioObserver.Z1 laser scanning confocal microscope (Carl Zeiss AG). Images display a representative part of the acquired total image. The fluorescence of single channels is shown in black and white for better contrast, with the overlaid image shown in color. 10 µm scale bars are given in each image. Brightness and contrast were adjusted in a linear fashion. Images display one of 3 independent experiments.

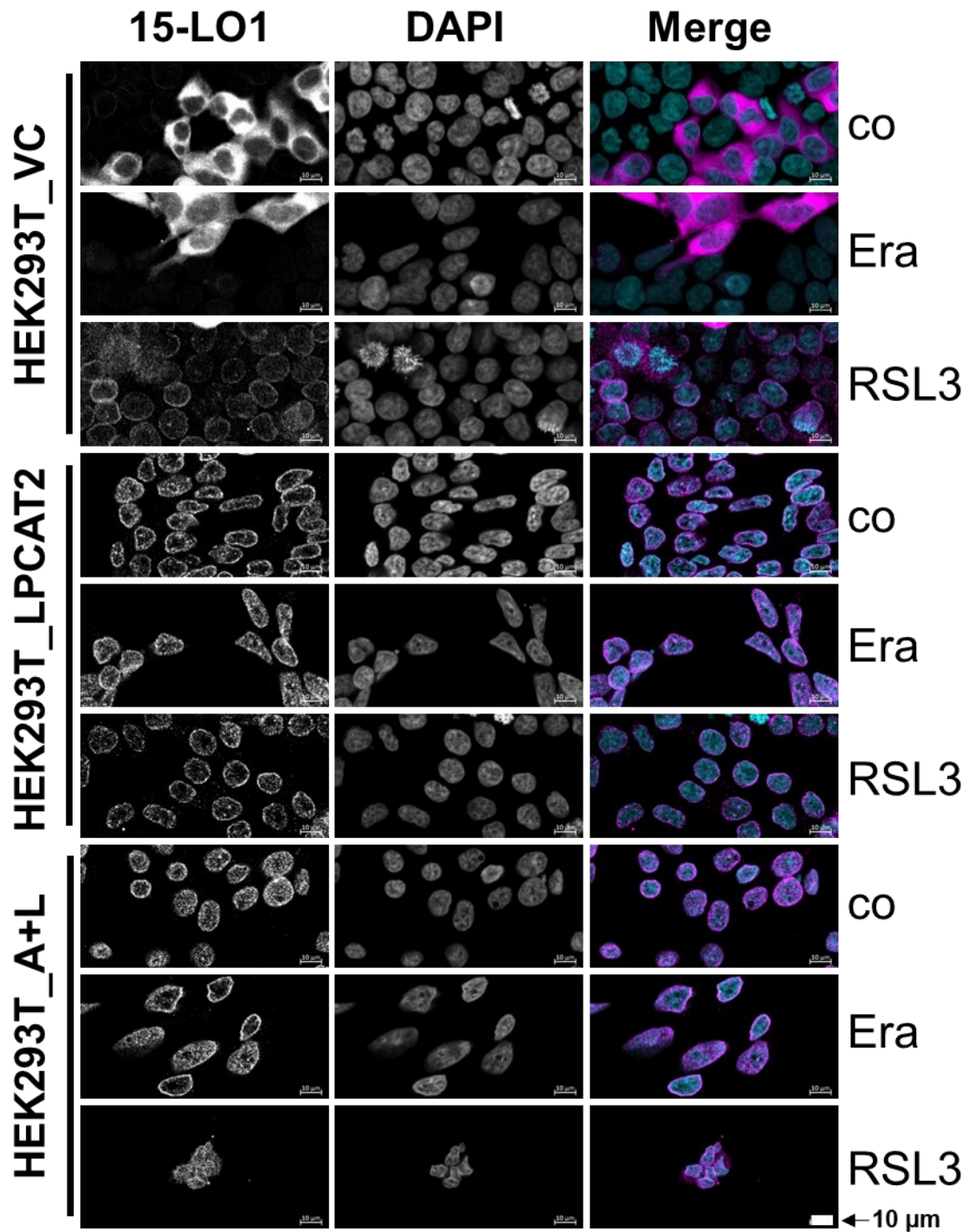


**Figure 9.14: Effect of ferroptosis inducers on the localization of 15-lipoxygenase 1 in stably transfected HEK293T cells.**

HEK293T\_VC\_15LO1, HEK293T\_LPCAT2\_15LO1, and HEK293T\_A+L\_15LO1 cells were treated with 200 ng/ml doxycycline for 24 h before treatment with 10 μM RSL3 or 3 μM erastin for 4 h or 24 h, respectively. Controls (co) received DMSO. Cells were stained with fluorophore-conjugated antibodies against 15-LO1 (purple). Nuclei were counterstained using DAPI (turquoise). Cells were imaged and analyzed on a Zeiss 780 AxioObserver.Z1 laser scanning confocal microscope (Carl Zeiss AG). Images display a representative part of the acquired total image. The fluorescence of single channels is shown in black and white for better contrast, with the overlaid image shown in color. 10 μm scale bars are given in each image. Brightness and contrast were adjusted in a linear fashion. Images display one of 3 independent experiments.

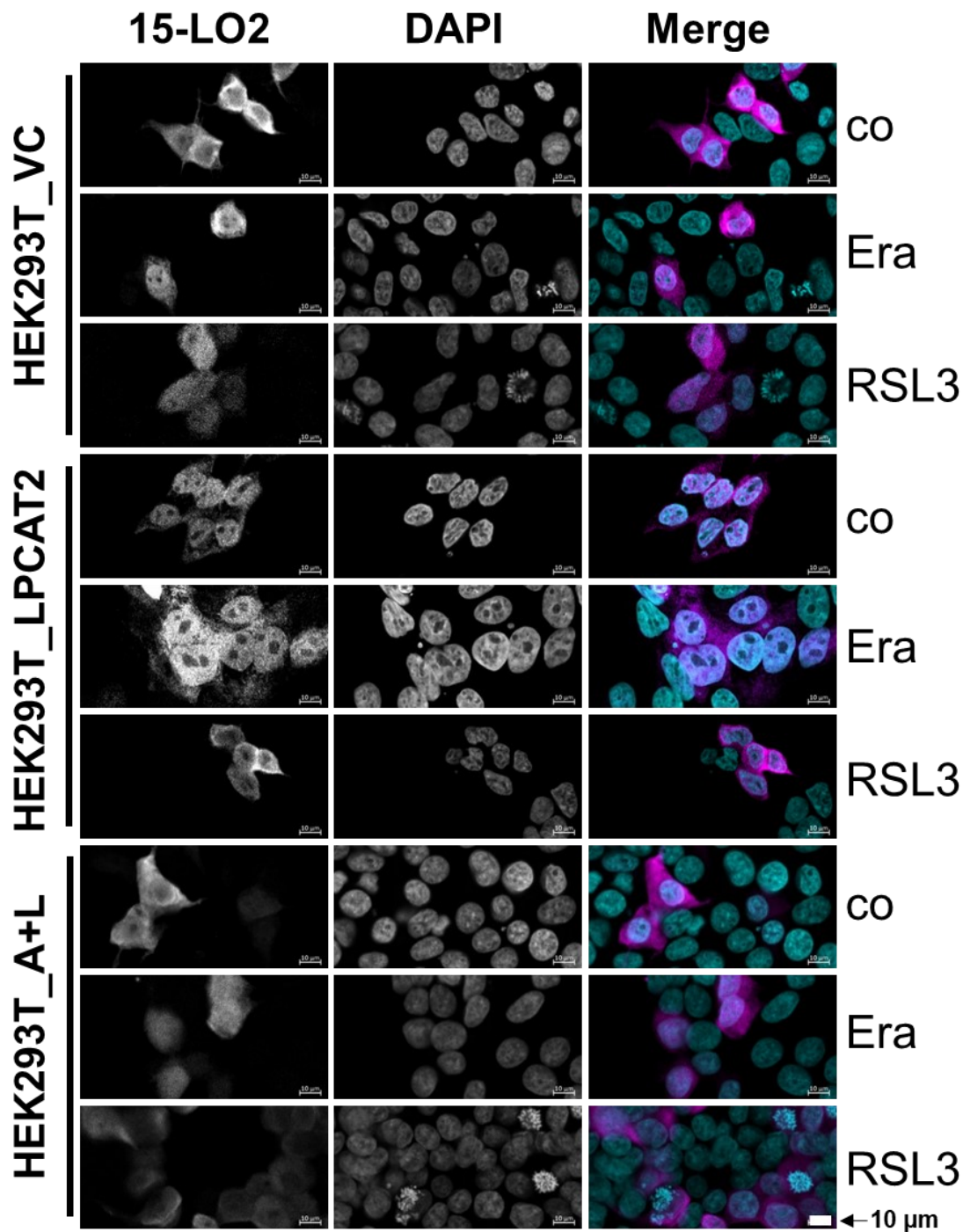


**Figure 9.15: Effect of ferroptosis inducers on the localization of 15-lipoxygenase 2 in stably transfected HEK293T cells.**

HEK293T\_VC\_15LO2, HEK293T\_LPCAT2\_15LO2, and HEK293T\_A+L\_15LO2 cells were treated with 200 ng/ml doxycycline for 24 h before treatment with 10 μM RSL3 or 3 μM erastin for 4 h or 24 h, respectively. Controls (co) received DMSO. Cells were stained with fluorophore-conjugated antibodies against 15-LO2 (purple). Nuclei were counterstained using DAPI (turquoise). Cells were imaged and analyzed on a Zeiss 780 AxioObserver.Z1 laser scanning confocal microscope (Carl Zeiss AG). Images display a representative part of the acquired total image. The fluorescence of single channels is shown in black and white for better contrast, with the overlaid image shown in color. 10 μm scale bars are given in each image. Brightness and contrast were adjusted in a linear fashion. Images display one of 3 independent experiments (except HEK293T\_A+L\_15LO2, RSL3, n=2).

## 9.5 Complete oxylipin analysis

**Table 9.4: Complete total oxylipin analysis in 1x10<sup>7</sup> HEK293T cells.**

HEK293T\_VC\_LO, HEK293T\_LPCAT2\_LO, and HEK293T\_A+L\_LO (5-LO, 15-LO1, 15-LO2) were treated with 200 ng/mL doxycycline for 24 h (+DOXY). Controls received fresh medium without doxycycline for 24 h (-DOXY). HEK293T\_LPCAT2\_LO (5-LO, 15-LO1, 15-LO2) were treated with doxycycline before treatment with 10 µM RSL3 for 4 or 24 h (+DOXY,+RSL3 4 h; +DOXY,+RSL3 24 h). Controls received DMSO (+DOXY,+DMSO). Total oxylipins were prepared and analyzed by LC-MS/MS following solid phase extraction as described [204,209–211]. Total oxylipin concentrations were normalized on the protein content. The lower limit of quantification (LLOQ) and the upper limit of quantification (ULOQ) differ depending on the number of cells, i.e., the protein used for the analysis. For ULOQ, the exact value for each sample is shown, while the highest LLOQ is indicated. Shown is the mean ± SD, n=3.

cell line	treatment	Arachidonic acid (AA; 20:4 n6)			
		5,12-DiHETE	5,15-DiHETE	8,15-DiHETE	6-trans-LTB4
HEK293T_VC	-DOXY	<2.55	<5.11	<64.5	<5.11
HEK293T_VC_5-LO	-DOXY	<2.55	<5.11	<64.5	<5.11
HEK293T_VC_15-LO1	-DOXY	<2.55	<5.11	<64.5	<5.11
HEK293T_VC_15-LO2	-DOXY	<2.55	<5.11	<64.5	<5.11
HEK293T_LPCAT2	-DOXY	<2.55	<5.11	<64.5	<5.11
HEK293T_LPCAT2_5-LO	-DOXY	<2.55	<5.11	<64.5	<5.11
HEK293T_LPCAT2_15-LO1	-DOXY	<2.55	<5.11	<64.5	<5.11
HEK293T_LPCAT2_15-LO2	-DOXY	<2.55	<5.11	<64.5	<5.11
HEK293T_A+L	-DOXY	<2.55	<5.11	<64.5	<5.11
HEK293T_A+L_5-LO	-DOXY	<2.55	<5.11	<64.5	<5.11
HEK293T_A+L_15-LO1	-DOXY	<2.55	<5.11	<64.5	<5.11
HEK293T_A+L_15-LO2	-DOXY	<2.55	<5.11	<64.5	<5.11
HEK293T_VC	+DOXY	<2.11	<4.22	<53.3	<4.22
HEK293T_VC_5-LO	+DOXY	<2.11	<4.22	<53.3	<4.22
HEK293T_VC_15-LO1	+DOXY	<2.11	1994 ± 616	2844 ± 607	<4.22
HEK293T_VC_15-LO2	+DOXY	<2.11	<4.22	<53.3	<4.22
HEK293T_LPCAT2	+DOXY	<2.11	<4.22	<53.3	<4.22
HEK293T_LPCAT2_5-LO	+DOXY	<2.11	<4.22	<53.3	<4.22
HEK293T_LPCAT2_15-LO1	+DOXY	<2.11	1996 ± 670	2308 ± 1068	<4.22
HEK293T_LPCAT2_15-LO2	+DOXY	130 ± 18,1	2383 ± 711	<53.3	<4.22
HEK293T_A+L	+DOXY	<2.11	<4.22	<53.3	<4.22
HEK293T_A+L_5-LO	+DOXY	<2.11	<4.22	<53.3	<4.22
HEK293T_A+L_15-LO1	+DOXY	<2.11	766 ± 393	725 ± 231	<4.22
HEK293T_A+L_15-LO2	+DOXY	<2.11	<4.22	<53.3	<4.22
HEK293T_LPCAT2	+DOXY,+DMSO	<6.28	<12.6	<158	<12.6
HEK293T_LPCAT2_5-LO	+DOXY,+DMSO	<6.28	<12.6	<158	1164 ± 380
HEK293T_LPCAT2_15-LO1	+DOXY,+DMSO	<6.28	9241 ± 1951	9731 ± 1502	<12.6
HEK293T_LPCAT2_15-LO2	+DOXY,+DMSO	<6.28	3669 ± 1708	<158	<12.6
HEK293T_LPCAT2	+DOXY,+RSL3 4h	<6.28	<12.6	<158	<12.6
HEK293T_LPCAT2_5-LO	+DOXY,+RSL3 4h	<6.28	<12.6	<158	484 ± 84,5
HEK293T_LPCAT2_15-LO1	+DOXY,+RSL3 4h	<6.28	5848 ± 989	6521 ± 907	<12.6
HEK293T_LPCAT2_15-LO2	+DOXY,+RSL3 4h	<6.28	1113 ± 1005	<158	<12.6
HEK293T_LPCAT2	+DOXY,+RSL3 24h	<6.28	<12.6	<158	<12.6
HEK293T_LPCAT2_5-LO	+DOXY,+RSL3 24h	<6.28	<12.6	<158	733 ± 228
HEK293T_LPCAT2_15-LO1	+DOXY,+RSL3 24h	<6.28	11057 ± 814	9399 ± 6499	<12.6
HEK293T_LPCAT2_15-LO2	+DOXY,+RSL3 24h	<6.28	3039 ± 1106	<158	<12.6



cell line	treatment	Eicosapentaenoic Acid (EPA; 20:5 n3)					Docosahexaenoic Acid (DHA; 22:6 n3)				
		5-HEPE	12-HEPE	15-HEPE	4-HDHA	7-HDHA	14-HDHA	17-HDHA			
HEK293T_VC	-DOXY	272 ± 26,9	200 ± 42,4	<5.11	2242 ± 76,9	378 ± 334	174 ± 39,7	<43,4			
HEK239T_VC_5-LO	-DOXY	489 ± 107	520 ± 89,0	377 ± 68,8	3709 ± 744	975 ± 449	496 ± 31,7	<43,4			
HEK239T_VC_15-LO1	-DOXY	508 ± 95,0	524 ± 78,2	370 ± 39,5	3801 ± 418	870 ± 265	527 ± 92,1	<43,4			
HEK293T_VC_15-LO2	-DOXY	290 ± 42,6	228 ± 102	<5.11	2340 ± 402	623 ± 37,5	208 ± 73,9	<43,4			
HEK293T_LPCAT2	-DOXY	314 ± 11,2	243 ± 71,1	273 ± 31,6	2986 ± 279	854 ± 142	282 ± 99,2	<43,4			
HEK239T_LPCAT2_5-LO	-DOXY	370 ± 21,4	300 ± 87,6	355 ± 73,0	2961 ± 249	881 ± 93,8	315 ± 112	<43,4			
HEK239T_LPCAT2_15-LO1	-DOXY	447 ± 61,0	501 ± 28,1	462 ± 57,9	3638 ± 749	1143 ± 522	547 ± 43,0	<43,4			
HEK239T_LPCAT2_15-LO2	-DOXY	325 ± 8,08	301 ± 46,6	213 ± 183	2763 ± 153	909 ± 67,4	305 ± 99,6	<43,4			
HEK293T_A+L	-DOXY	315 ± 71,8	217 ± 9,02	<5.11	2328 ± 213	644 ± 152	242 ± 59,2	<43,4			
HEK239T_A+L_5-LO	-DOXY	277 ± 32,6	186 ± 24,8	<5.11	2095 ± 142	608 ± 5,14	213 ± 62,8	<43,4			
HEK239T_A+L_15-LO1	-DOXY	425 ± 68,2	504 ± 42,8	371 ± 63,2	3351 ± 636	638 ± 133	575 ± 149	<43,4			
HEK239T_A+L_15-LO2	-DOXY	335 ± 16,8	254 ± 8,56	<5.11	2476 ± 371	783 ± 104	251 ± 53,8	<43,4			
HEK293T_VC	+DOXY	340 ± 49,5	408 ± 45,9	299 ± 30,4	3215 ± 293	858 ± 147	515 ± 7,84	<35,9			
HEK239T_VC_5-LO	+DOXY	708 ± 238	504 ± 198	697 ± 410	6063 ± 1401	998 ± 231	630 ± 152	2287 ± 819			
HEK239T_VC_15-LO1	+DOXY	496 ± 133	2959 ± 755	21235 ± 5540	5289 ± 527	903 ± 388	19796 ± 3574	>21511			
HEK239T_VC_15-LO2	+DOXY	275 ± 38,9	503 ± 27,3	38299 ± 2586	2590 ± 140	466 ± 402	878 ± 83,8	>72573			
HEK293T_LPCAT2	+DOXY	428 ± 27,8	472 ± 51,8	392 ± 43,0	3888 ± 162	1039 ± 17,6	645 ± 17,7	332 ± 58,8			
HEK239T_LPCAT2_5-LO	+DOXY	1248 ± 525	571 ± 19,1	609 ± 72,6	4076 ± 323	1245 ± 210	652 ± 35,7	1440 ± 352			
HEK239T_LPCAT2_15-LO1	+DOXY	594 ± 28,4	3059 ± 746	21553 ± 6370	5936 ± 707	993 ± 245	20319 ± 6317	>26585			
HEK239T_LPCAT2_15-LO2	+DOXY	342 ± 68,5	781 ± 153	155801 ± 36428	4222 ± 73,2	1123 ± 117	2045 ± 400	>68931			
HEK293T_A+L	+DOXY	309 ± 11,6	354 ± 74,1	169 ± 148	3163 ± 260	797 ± 99,5	555 ± 19,5	<35,9			
HEK239T_A+L_5-LO	+DOXY	396 ± 113	365 ± 61,2	605 ± 511	3775 ± 772	845 ± 136	590 ± 200	2977 ± 5131			
HEK239T_A+L_15-LO1	+DOXY	500 ± 43,4	1532 ± 523	8732 ± 3703	5907 ± 799	1109 ± 275	8918 ± 3312	15838 ± 6663			
HEK239T_A+L_15-LO2	+DOXY	240 ± 21,0	383 ± 58,0	20817 ± 12015	2403 ± 311	714 ± 108	948 ± 133	45984 ± 31270			
HEK293T_LPCAT2	+DOXY,+DMSO	462 ± 26,4	322 ± 62,2	410 ± 37,9	3380 ± 174	935 ± 102	290 ± 36,8	<107			
HEK239T_LPCAT2_5-LO	+DOXY,+DMSO	2739 ± 689	463 ± 124	814 ± 253	3845 ± 324	1378 ± 119	363 ± 57,5	<107			
HEK239T_LPCAT2_15-LO1	+DOXY,+DMSO	787 ± 255	23022 ± 8985	121704 ± 51213	14622 ± 13951	3501 ± 3399	71763 ± 11036	122128 ± 53043			
HEK239T_LPCAT2_15-LO2	+DOXY,+DMSO	179 ± 153	830 ± 237	304811 ± 81758	6333 ± 1910	1135 ± 1001	1814 ± 468	363830 ± 126061			
HEK293T_LPCAT2	+DOXY,+RSL3 4h	325 ± 26,6	339 ± 57,0	338 ± 23,8	2738 ± 391	681 ± 113	469 ± 35,4	<107			
HEK239T_LPCAT2_5-LO	+DOXY,+RSL3 4h	1263 ± 177	375 ± 38,9	361 ± 59,1	2557 ± 135	875 ± 108	438 ± 0,81	<107			
HEK239T_LPCAT2_15-LO1	+DOXY,+RSL3 4h	423 ± 86,6	10954 ± 2365	64966 ± 13970	5159 ± 2095	1351 ± 422	49700 ± 8899	63195 ± 17458			
HEK239T_LPCAT2_15-LO2	+DOXY,+RSL3 4h	279 ± 20,5	621 ± 57,3	134064 ± 22499	3077 ± 131	724 ± 207	1308 ± 216	210591 ± 47492			
HEK293T_LPCAT2	+DOXY,+RSL3 24h	469 ± 19,1	377 ± 61,6	416 ± 86,1	3563 ± 535	870 ± 77,0	295 ± 29,1	<107			
HEK239T_LPCAT2_5-LO	+DOXY,+RSL3 24h	1653 ± 342	510 ± 132	687 ± 159	4166 ± 568	1489 ± 253	444 ± 149	<107			
HEK239T_LPCAT2_15-LO1	+DOXY,+RSL3 24h	604 ± 93,1	15192 ± 7254	81372 ± 38888	13390 ± 7885	3211 ± 1684	59905 ± 26615	85881 ± 43340			
HEK239T_LPCAT2_15-LO2	+DOXY,+RSL3 24h	301 ± 59,0	843 ± 307	287251 ± 92917	3498 ± 1419	<12,6	2014 ± 765	>241207			



cell line	treatment	Linoleic Acid (LA; 18:2 n6)			Arachidonic acid (AA; 20:4 n6)		
		9-HODE	13-HODE	5-HETE	12-HETE	15-HETE	tetranor- 12-HETE
HEK293T_VC	-DOXY	1325 ± 227	1768 ± 443	1120 ± 31,4	767 ± 277	378 ± 62,7	234 ± 33,0
HEK239T_VC_5-LO	-DOXY	1365 ± 244	1815 ± 285	1724 ± 663	2212 ± 235	899 ± 125	1157 ± 229
HEK239T_VC_15-LO1	-DOXY	1441 ± 323	2038 ± 653	1525 ± 296	2132 ± 254	1024 ± 89,5	1019 ± 108
HEK293T_VC_15-LO2	-DOXY	1308 ± 413	1622 ± 555	1216 ± 198	928 ± 461	458 ± 184	291 ± 131
HEK293T_LPCAT2	-DOXY	2315 ± 750	3859 ± 1331	1759 ± 181	988 ± 203	695 ± 206	388 ± 91,4
HEK239T_LPCAT2_5-LO	-DOXY	3445 ± 856	5827 ± 1262	1885 ± 212	1233 ± 484	750 ± 132	538 ± 149
HEK239T_LPCAT2_15-LO1	-DOXY	1399 ± 90,0	1918 ± 111	1769 ± 633	2019 ± 219	944 ± 84,5	1125 ± 196
HEK293T_LPCAT2_15-LO2	-DOXY	2136 ± 247	3540 ± 334	1735 ± 46,2	1176 ± 538	716 ± 82,3	506 ± 96,7
HEK293T_A+L	-DOXY	1396 ± 11,5	2205 ± 349	1224 ± 82,7	970 ± 195	509 ± 67,1	376 ± 35,3
HEK239T_A+L_5-LO	-DOXY	1232 ± 263	1861 ± 385	1155 ± 51,1	874 ± 248	465 ± 81,5	237 ± 66,3
HEK239T_A+L_15-LO1	-DOXY	1441 ± 292	1873 ± 395	1241 ± 293	2234 ± 345	1028 ± 174	789 ± 190
HEK293T_A+L_15-LO2	-DOXY	1450 ± 116	2204 ± 250	1357 ± 247	1010 ± 339	502 ± 116	369 ± 129
HEK293T_VC	+DOXY	2362 ± 242	3777 ± 469	1638 ± 178	1716 ± 133	1028 ± 125	565 ± 78,7
HEK239T_VC_5-LO	+DOXY	2450 ± 540	3057 ± 907	3113 ± 683	2321 ± 763	1636 ± 471	984 ± 263
HEK239T_VC_15-LO1	+DOXY	2654 ± 448	>63269	1918 ± 536	18186 ± 4485	>27838	903 ± 202
HEK293T_VC_15-LO2	+DOXY	4923 ± 818	73192 ± 16781	1382 ± 70,4	1778 ± 201	90109 ± 11676	545 ± 88,1
HEK293T_LPCAT2	+DOXY	1767 ± 337	2551 ± 604	2075 ± 110	2163 ± 61,2	999 ± 163	684 ± 24,7
HEK239T_LPCAT2_5-LO	+DOXY	2263 ± 349	3099 ± 441	5480 ± 2503	2229 ± 228	1296 ± 119	797 ± 72,5
HEK239T_LPCAT2_15-LO1	+DOXY	3360 ± 729	>78193	2184 ± 354	16036 ± 4012	>34405	1130 ± 80,6
HEK293T_LPCAT2_15-LO2	+DOXY	4947 ± 759	>202737	2843 ± 218	2752 ± 434	>89204	901 ± 130
HEK293T_A+L	+DOXY	2169 ± 270	3350 ± 477	1550 ± 137	1591 ± 338	845 ± 163	538 ± 31,6
HEK239T_A+L_5-LO	+DOXY	2867 ± 966	3840 ± 1005	2500 ± 926	1817 ± 340	1430 ± 626	350 ± 20,1
HEK293T_A+L_15-LO1	+DOXY	2744 ± 324	>79685	2320 ± 790	7560 ± 2574	>35061	803 ± 104
HEK239T_A+L_15-LO2	+DOXY	2789 ± 832	49512 ± 33028	1340 ± 44,1	1624 ± 223	55134 ± 31819	360 ± 34,0
HEK293T_VC	+DOXY,+DMSO	2375 ± 1060	3955 ± 1770	1861 ± 96,2	1184 ± 162	903 ± 155	515 ± 78,6
HEK239T_LPCAT2_5-LO	+DOXY,+DMSO	2366 ± 193	3736 ± 386	12261 ± 3999	1641 ± 204	1376 ± 385	779 ± 66,7
HEK239T_LPCAT2_15-LO1	+DOXY,+DMSO	10877 ± 2605	>327309	11045 ± 10792	148066 ± 34906	>144016	518 ± 97,1
HEK293T_LPCAT2_15-LO2	+DOXY,+DMSO	5930 ± 743	>336568	5218 ± 1861	2169 ± 465	>148090	736 ± 163
HEK293T_LPCAT2	+DOXY,+RSL3 4h	2304 ± 284	4514 ± 271	1466 ± 244	1514 ± 127	934 ± 125	475 ± 71,7
HEK239T_LPCAT2_5-LO	+DOXY,+RSL3 4h	2680 ± 799	4558 ± 1176	5540 ± 305	1512 ± 193	813 ± 50,7	569 ± 80,4
HEK239T_LPCAT2_15-LO1	+DOXY,+RSL3 4h	5354 ± 1524	>293457	3836 ± 1616	62785 ± 8803	>129121	473 ± 67,3
HEK293T_LPCAT2_15-LO2	+DOXY,+RSL3 4h	4338 ± 795	>332313	2117 ± 147	1933 ± 138	>146218	623 ± 38,6
HEK293T_LPCAT2	+DOXY,+RSL3 24h	1450 ± 168	2380 ± 110	1865 ± 228	1259 ± 259	949 ± 280	495 ± 85,5
HEK239T_LPCAT2_5-LO	+DOXY,+RSL3 24h	2325 ± 611	3305 ± 809	7869 ± 2112	1920 ± 485	1126 ± 232	791 ± 159
HEK239T_LPCAT2_15-LO1	+DOXY,+RSL3 24h	12242 ± 7575	>415537	9588 ± 5569	105256 ± 51898	>182836	541 ± 123
HEK293T_LPCAT2_15-LO2	+DOXY,+RSL3 24h	5281 ± 1190	>429998	3005 ± 1325	2122 ± 509	>189199	713 ± 152

**Table 9.5: Complete non-esterified oxylipin analysis in 1x10<sup>7</sup> HEK293T cells.**

HEK293T\_VC\_LO, HEK293T\_LPCAT2\_LO, and HEK293T\_A+L\_LO (5-LO, 15-LO1, 15-LO2) were treated with 200 ng/mL doxycycline for 24 h (+DOXY). Controls received fresh medium without doxycycline for 24 h (-DOXY). HEK293T\_LPCAT2\_LO (5-LO, 15-LO1, 15-LO2) were treated with doxycycline before treatment with 10 μM RSL3 for 4 or 24 h (+DOXY,+RSL3 4 h; +DOXY,+RSL3 24 h). Controls received DMSO (+DOXY,+DMSO). Non-esterified oxylipins were prepared and analyzed by LC-MS/MS following solid phase extraction as described [204,209–211]. Non-esterified oxylipin concentrations were normalized on the protein content. The lower limit of quantification (LLOQ) and the upper limit of quantification (ULOQ) differ depending on the number of cells, i.e., the protein used for the analysis. For ULOQ, the exact value for each sample is shown, while the highest LLOQ is indicated. Shown is the mean ± SD, n=3.

cell line	treatment	Arachidonic acid (AA; 20:4 n6)					
		5,12-DIHEETE	5,15-DIHEETE	8,15-DIHEETE	LTB4	6-trans-LTB4	
HEK293T_VC	-DOXY	<0.94	<1.89	<23.8	<1.89	<4.72	
HEK293T_VC_5-LO	-DOXY	<0.94	<1.89	<23.8	<1.89	<4.72	
HEK293T_VC_15-LO1	-DOXY	<0.94	<1.89	<23.8	<1.89	<4.72	
HEK293T_VC_15-LO2	-DOXY	<0.94	<1.89	<23.8	<1.89	<4.72	
HEK293T_LPCAT2	-DOXY	<0.94	<1.89	<23.8	<1.89	<4.72	
HEK293T_LPCAT2_5-LO	-DOXY	<0.94	<1.89	<23.8	<1.89	<4.72	
HEK293T_LPCAT2_15-LO1	-DOXY	<0.94	<1.89	<23.8	<1.89	<4.72	
HEK293T_LPCAT2_15-LO2	-DOXY	<0.94	<1.89	<23.8	<1.89	<4.72	
HEK293T_A+L	-DOXY	<0.94	<1.89	<23.8	<1.89	<4.72	
HEK293T_A+L_5-LO	-DOXY	<0.94	<1.89	<23.8	<1.89	<4.72	
HEK293T_A+L_15-LO1	-DOXY	<0.94	<1.89	<23.8	<1.89	<4.72	
HEK293T_A+L_15-LO2	-DOXY	<0.94	<1.89	<23.8	<1.89	<4.72	
HEK293T_VC	+DOXY	<1.02	<2.03	<25.6	<2.03	<5.07	
HEK293T_VC_5-LO	+DOXY	<1.02	<2.03	<25.6	30,4 ± 7,98	<5.07	
HEK293T_VC_15-LO1	+DOXY	<1.02	198 ± 87,6	72,4 ± 53,8	<2.03	<5.07	
HEK293T_VC_15-LO2	+DOXY	<1.02	<2.03	<25.6	<2.03	<5.07	
HEK293T_LPCAT2	+DOXY	<1.02	<2.03	<25.6	<2.03	<5.07	
HEK293T_LPCAT2_5-LO	+DOXY	<1.02	<2.03	<25.6	<2.03	<5.07	
HEK293T_LPCAT2_15-LO1	+DOXY	<1.02	171 ± 70,0	65,8 ± 63,1	284 ± 270	98,5 ± 86,8	
HEK293T_LPCAT2_15-LO2	+DOXY	<1.02	309 ± 113	<25.6	<2.03	<5.07	
HEK293T_A+L	+DOXY	<1.02	<2.03	<25.6	<2.03	<5.07	
HEK293T_A+L_5-LO	+DOXY	<1.02	<2.03	<25.6	<2.03	<5.07	
HEK293T_A+L_15-LO1	+DOXY	<1.02	65,7 ± 35,0	<25.6	<2.03	<5.07	
HEK293T_A+L_15-LO2	+DOXY	<1.02	<2.03	<25.6	<2.03	<5.07	
HEK293T_LPCAT2	+DOXY,+DMSO	<0.67	<1.33	<16.79	<1.33	<3.32	
HEK293T_LPCAT2_5-LO	+DOXY,+DMSO	<0.67	27,1 ± 23,2	<16.79	1230 ± 501	356 ± 104	
HEK293T_LPCAT2_15-LO1	+DOXY,+DMSO	770 ± 298	7218 ± 3513	6793 ± 793	<1.33	<3.32	
HEK293T_LPCAT2_15-LO2	+DOXY,+DMSO	<0.67	591 ± 240	<16.79	<1.33	<3.32	
HEK293T_LPCAT2	+DOXY,+RSL3 4h	<0.67	<1.33	<16.79	<1.33	<3.32	
HEK293T_LPCAT2_5-LO	+DOXY,+RSL3 4h	<0.67	21,3 ± 18,8	<16.79	581 ± 163	190 ± 34,1	
HEK293T_LPCAT2_15-LO1	+DOXY,+RSL3 4h	436 ± 111	6127 ± 1116	4149 ± 494	<1.33	<3.32	
HEK293T_LPCAT2_15-LO2	+DOXY,+RSL3 4h	<0.67	229 ± 10,2	<16.79	<1.33	<3.32	
HEK293T_LPCAT2	+DOXY,+RSL3 24h	<0.67	<1.33	<16.79	<1.33	<3.32	
HEK293T_LPCAT2_5-LO	+DOXY,+RSL3 24h	<0.67	34,2 ± 30,7	<16.79	774 ± 162	189 ± 42,2	
HEK293T_LPCAT2_15-LO1	+DOXY,+RSL3 24h	719 ± 516	12287 ± 3653	8391 ± 3390	<1.33	<3.32	
HEK293T_LPCAT2_15-LO2	+DOXY,+RSL3 24h	<0.67	500 ± 171	<50.1	<1.33	<3.32	

cell line	treatment	Eicosapentaenoic Acid (EPA; 20:5 n3)					Docosahexaenoic Acid (DHA; 22:6 n3)					
		5-HEPE	12-HEPE	15-HEPE	4-HDHA	7-HDHA	14-HDHA	17-HDHA				
HEK293T_VC	-DOXY	<1.11	<1.89	<1.89	<1.89	<1.89	<1.89	<1.89	<1.89	<1.89	<1.89	<16.0
HEK239T_VC_5-LO	-DOXY	<1.11	<1.89	<1.89	<1.89	<1.89	<1.89	<1.89	<1.89	<1.89	<1.89	<16.0
HEK239T_VC_15-LO1	-DOXY	<1.11	<1.89	<1.89	<1.89	<1.89	<1.89	<1.89	<1.89	<1.89	<1.89	<16.0
HEK239T_VC_15-LO2	-DOXY	<1.11	<1.89	<1.89	<1.89	<1.89	<1.89	<1.89	<1.89	<1.89	<1.89	<16.0
HEK239T_LPCAT2	-DOXY	<1.11	<1.89	<1.89	<1.89	<1.89	<1.89	<1.89	<1.89	<1.89	<1.89	<16.0
HEK239T_LPCAT2_5-LO	-DOXY	<1.11	<1.89	<1.89	<1.89	<1.89	<1.89	<1.89	<1.89	<1.89	<1.89	<16.0
HEK239T_LPCAT2_15-LO1	-DOXY	<1.11	<1.89	<1.89	<1.89	<1.89	<1.89	<1.89	<1.89	<1.89	<1.89	<16.0
HEK239T_LPCAT2_15-LO2	-DOXY	<1.11	<1.89	<1.89	<1.89	<1.89	<1.89	<1.89	<1.89	<1.89	<1.89	<16.0
HEK293T_A+L	-DOXY	<1.11	<1.89	<1.89	<1.89	<1.89	<1.89	<1.89	<1.89	<1.89	<1.89	<16.0
HEK239T_A+L_5-LO	-DOXY	<1.11	<1.89	<1.89	<1.89	<1.89	<1.89	<1.89	<1.89	<1.89	<1.89	<16.0
HEK239T_A+L_15-LO1	-DOXY	<1.11	<1.89	<1.89	<1.89	<1.89	<1.89	<1.89	<1.89	<1.89	<1.89	<16.0
HEK239T_A+L_15-LO2	-DOXY	<1.11	<1.89	<1.89	<1.89	<1.89	<1.89	<1.89	<1.89	<1.89	<1.89	<16.0
HEK293T_VC	+DOXY	<1.20	<2.03	<2.03	<2.03	<2.03	<2.03	<2.03	<2.03	<2.03	<2.03	<17.2
HEK239T_VC_5-LO	+DOXY	<1.20	<2.03	<2.03	<2.03	<2.03	<2.03	<2.03	<2.03	<2.03	<2.03	<17.2
HEK239T_VC_15-LO1	+DOXY	<1.20	57.3 ± 17.8	371 ± 125	21.8 ± 18.2	633 ± 186	460 ± 66.5	1155 ± 162	21.8 ± 18.2	460 ± 66.5	633 ± 186	1155 ± 162
HEK239T_VC_15-LO2	+DOXY	<1.20	<2.03	655 ± 74.2	<2.03	<2.03	<2.03	<2.03	<2.03	<2.03	<2.03	<17.2
HEK293T_LPCAT2	+DOXY	<1.20	<2.03	<2.03	11.8 ± 9.32	<2.03	11.8 ± 9.32	<2.03	<2.03	<2.03	<2.03	<17.2
HEK239T_LPCAT2_5-LO	+DOXY	657 ± 520	9.98 ± 7.77	<2.03	24.4 ± 7.93	<2.03	119 ± 89.5	<2.03	119 ± 89.5	<2.03	<2.03	<17.2
HEK239T_LPCAT2_15-LO1	+DOXY	<1.20	51.7 ± 3.83	453 ± 62.2	<2.03	16.3 ± 13.0	16.3 ± 13.0	712 ± 122	16.3 ± 13.0	449 ± 32.2	712 ± 122	14990 ± 6462
HEK239T_LPCAT2_15-LO2	+DOXY	<1.20	33.9 ± 14.5	10166 ± 4874	<2.03	<2.03	<2.03	<2.03	<2.03	166 ± 63.4	14990 ± 6462	<17.2
HEK293T_A+L	+DOXY	<1.20	<2.03	<2.03	<2.03	<2.03	<2.03	<2.03	<2.03	<2.79	<17.2	<17.2
HEK239T_A+L_5-LO	+DOXY	<1.20	<2.03	<2.03	<2.03	<2.03	<2.03	<2.03	<2.03	<2.79	<17.2	<17.2
HEK239T_A+L_15-LO1	+DOXY	<1.20	40.3 ± 6.46	287 ± 88.1	<2.03	<2.03	<2.03	<2.03	<2.03	285 ± 59.5	474 ± 136	<17.2
HEK239T_A+L_15-LO2	+DOXY	<1.20	<2.03	298 ± 204	<2.03	<2.03	<2.03	<2.03	<2.03	<2.79	500 ± 550	<17.2
HEK293T_LPCAT2	+DOXY,+DMSO	<0.78	13.1 ± 10.8	33.2 ± 13.8	16.0 ± 12.5	<1.33	16.0 ± 12.5	<1.33	<1.33	<1.83	<11.3	<11.3
HEK239T_LPCAT2_5-LO	+DOXY,+DMSO	2105 ± 626	<1.33	33.8 ± 12.7	39.6 ± 6.42	<1.33	248 ± 85.2	<1.33	248 ± 85.2	14.3 ± 10.7	<11.3	<11.3
HEK239T_LPCAT2_15-LO1	+DOXY,+DMSO	<0.78	2633 ± 1468	367 ± 328	<1.33	<1.33	<1.33	<1.33	<1.33	304 ± 236	<11.3	<11.3
HEK239T_LPCAT2_15-LO2	+DOXY,+DMSO	<0.78	<1.33	20196 ± 5238	<1.33	<1.33	<1.33	<1.33	<1.33	167 ± 5.47	20777 ± 5498	<11.3
HEK293T_LPCAT2	+DOXY,+RSL3 4h	<0.78	<1.33	<1.33	13.6 ± 3.43	<1.33	13.6 ± 3.43	<1.33	<1.33	21.2 ± 6.67	<11.3	<11.3
HEK239T_LPCAT2_5-LO	+DOXY,+RSL3 4h	758 ± 249	8.73 ± 7.10	<1.33	24.4 ± 3.12	<1.33	125 ± 21.8	<1.33	125 ± 21.8	13.9 ± 10.7	<11.3	<11.3
HEK239T_LPCAT2_15-LO1	+DOXY,+RSL3 4h	<0.78	791 ± 58.0	486 ± 170	<1.33	<1.33	<1.33	<1.33	<1.33	417 ± 121	<11.3	<11.3
HEK239T_LPCAT2_15-LO2	+DOXY,+RSL3 4h	<0.78	<1.33	9287 ± 1072	<1.33	<1.33	<1.33	<1.33	<1.33	112 ± 103	13818 ± 2157	<11.3
HEK293T_LPCAT2	+DOXY,+RSL3 24h	<0.78	16.6 ± 6.57	30.8 ± 25.2	22.6 ± 4.34	<1.33	<1.33	<1.33	<1.33	<1.83	<11.3	<11.3
HEK239T_LPCAT2_5-LO	+DOXY,+RSL3 24h	794 ± 223	26.1 ± 7.58	20.5 ± 16.7	48.9 ± 14.2	<1.33	281 ± 90.4	<1.33	281 ± 90.4	<1.83	<11.3	<11.3
HEK239T_LPCAT2_15-LO1	+DOXY,+RSL3 24h	<0.78	1749 ± 662	1344 ± 1138	<1.33	<1.33	<1.33	<1.33	<1.33	1030 ± 1013	<11.3	<11.3
HEK239T_LPCAT2_15-LO2	+DOXY,+RSL3 24h	<0.78	41.2 ± 39.3	23152 ± 6377	<1.33	<1.33	<1.33	<1.33	<1.33	217 ± 104	27005 ± 9137	<11.3

cell line	treatment	Linoleic Acid (LA; 18:2 n6)			Arachidonic acid (AA; 20:4 n6)		
		9-HODE	13-HODE	5-HETE	12-HETE	15-HETE	tetranor-12-HETE
HEK293T_VC	-DOXY	167 ± 60.9	315 ± 71.3	<0.66	59.7 ± 8.25	<4.15	12.3 ± 0.92
HEK239T_VC_5-LO	-DOXY	74.6 ± 24.7	138 ± 41.9	<0.66	21.8 ± 1.18	<4.15	43.3 ± 6.54
HEK239T_VC_15-LO1	-DOXY	85.7 ± 29.8	168 ± 53.4	<0.66	28.0 ± 1.20	<4.15	45.4 ± 6.88
HEK293T_VC_15-LO2	-DOXY	3118 ± 5067	5724 ± 9329	<0.66	62.9 ± 3.23	<4.15	16.2 ± 5.34
HEK293T_LPCAT2	-DOXY	325 ± 155	948 ± 767	<0.66	68.5 ± 19.4	<4.15	25.4 ± 8.60
HEK239T_LPCAT2_5-LO	-DOXY	291 ± 109	752 ± 463	<0.66	67.9 ± 15.7	<4.15	33.2 ± 6.04
HEK239T_LPCAT2_15-LO1	-DOXY	65.0 ± 17.0	111 ± 36.9	<0.66	23.4 ± 1.38	<4.15	42.5 ± 2.51
HEK239T_LPCAT2_15-LO2	-DOXY	298 ± 87.1	682 ± 361	<0.66	58.5 ± 7.50	<4.15	29.2 ± 9.35
HEK293T_A+L	-DOXY	139 ± 18.2	528 ± 312	<0.66	67.0 ± 8.12	<4.15	22.9 ± 4.81
HEK239T_A+L_5-LO	-DOXY	129 ± 23.4	317 ± 91.8	<0.66	65.4 ± 17.0	<4.15	14.7 ± 3.67
HEK239T_A+L_15-LO1	-DOXY	65.6 ± 11.3	117 ± 19.5	<0.66	24.7 ± 1.85	<4.15	32.4 ± 5.84
HEK239T_A+L_15-LO2	-DOXY	208 ± 128	557 ± 370	<0.66	68.1 ± 2.04	<4.15	24.5 ± 9.43
HEK293T_VC	+DOXY	133 ± 54.1	397 ± 199	<0.71	17.1 ± 13.1	<4.46	23.6 ± 5.88
HEK239T_VC_5-LO	+DOXY	94.9 ± 18.7	186 ± 77.6	11.1 ± 9.70	34.0 ± 13.7	17.6 ± 14.5	38.8 ± 10.7
HEK239T_VC_15-LO1	+DOXY	95.3 ± 16.0	12558 ± 3035	<0.71	439 ± 142	7099 ± 2921	38.9 ± 9.52
HEK239T_VC_15-LO2	+DOXY	120 ± 24.5	5877 ± 1215	<0.71	<5.07	2079 ± 87.6	18.0 ± 0.51
HEK293T_LPCAT2	+DOXY	116 ± 8.27	327 ± 55.8	11.2 ± 9.55	53.6 ± 9.19	71.0 ± 37.2	43.9 ± 5.27
HEK239T_LPCAT2_5-LO	+DOXY	162 ± 74.1	385 ± 170	2601 ± 2247	56.7 ± 2.21	50.8 ± 12.7	50.9 ± 8.93
HEK239T_LPCAT2_15-LO1	+DOXY	90.4 ± 8.92	12214 ± 2543	<0.71	463 ± 67.6	8978 ± 2176	44.9 ± 3.89
HEK239T_LPCAT2_15-LO2	+DOXY	313 ± 99.0	73079 ± 21951	<0.71	79.6 ± 26.0	43495 ± 21366	48.2 ± 6.02
HEK293T_A+L	+DOXY	153 ± 17.9	351 ± 56.5	<0.71	<5.07	<4.46	21.9 ± 4.15
HEK239T_A+L_5-LO	+DOXY	254 ± 125	687 ± 255	<0.71	33.7 ± 7.81	<4.46	16.5 ± 4.63
HEK239T_A+L_15-LO1	+DOXY	130 ± 22.8	6858 ± 2095	<0.71	247 ± 71.9	4061 ± 1512	35.8 ± 0.63
HEK239T_A+L_15-LO2	+DOXY	142 ± 46.9	4358 ± 3380	<0.71	<5.07	831 ± 608	19.1 ± 0.82
HEK293T_LPCAT2	+DOXY,+DMSO	177 ± 65.2	430 ± 92.5	32.8 ± 4.22	48.8 ± 14.4	61.0 ± 54.5	29.7 ± 6.63
HEK239T_LPCAT2_5-LO	+DOXY,+DMSO	229 ± 82.1	450 ± 119	9284 ± 3746	66.0 ± 10.3	46.8 ± 37.0	39.7 ± 5.00
HEK239T_LPCAT2_15-LO1	+DOXY,+DMSO	562 ± 220	124502 ± 4529	<0.47	4228 ± 709	5311 ± 878	38.4 ± 6.95
HEK239T_LPCAT2_15-LO2	+DOXY,+DMSO	388 ± 111	98685 ± 30713	<0.47	95.3 ± 7.83	71948 ± 23307	36.4 ± 8.94
HEK293T_LPCAT2	+DOXY,+RSL3 4h	635 ± 81.1	2328 ± 73.6	15.2 ± 4.25	54.5 ± 11.3	87.1 ± 14.6	29.5 ± 3.73
HEK239T_LPCAT2_5-LO	+DOXY,+RSL3 4h	534 ± 248	1527 ± 709	3264 ± 1100	52.1 ± 11.6	52.9 ± 4.96	28.2 ± 8.10
HEK239T_LPCAT2_15-LO1	+DOXY,+RSL3 4h	459 ± 82.7	97571 ± 12945	<0.47	2431 ± 205	3018 ± 1060	42.3 ± 7.90
HEK239T_LPCAT2_15-LO2	+DOXY,+RSL3 4h	886 ± 290	67599 ± 11078	<0.47	78.0 ± 22.2	39823 ± 3661	27.0 ± 5.94
HEK293T_LPCAT2	+DOXY,+RSL3 24h	115 ± 2.42	352 ± 80.3	28.0 ± 2.67	50.9 ± 12.8	109 ± 70.3	32.2 ± 5.91
HEK239T_LPCAT2_5-LO	+DOXY,+RSL3 24h	148 ± 11.5	352 ± 93.4	3491 ± 801	83.4 ± 30.0	69.8 ± 28.7	32.3 ± 3.55
HEK239T_LPCAT2_15-LO1	+DOXY,+RSL3 24h	571 ± 429	123222 ± 20682	60.9 ± 52.6	5470 ± 640	9006 ± 6729	31.0 ± 8.67
HEK239T_LPCAT2_15-LO2	+DOXY,+RSL3 24h	413 ± 174	108990 ± 27533	<0.47	95.1 ± 39.0	82887 ± 23265	30.0 ± 3.83

## 9.6 Oxylipin analysis of RSL3/Ferrostatin samples

**Table 9.6: Total oxylipins in 1x10<sup>7</sup> HEK293T cells.**

HEK293T\_LPCAT2\_LO (5-LO, 15-LO1, 15-LO2) were treated with doxycycline before treatment with 10  $\mu$ M RSL3 for 4 or 24 h (+DOXY,+RSL3 4h; +DOXY,+RSL3 24h). Controls received DMSO (+DOXY,+DMSO). Total oxylipins were prepared and analyzed by LC-MS/MS following solid phase extraction as described [204,209–211]. Total oxylipins concentration were normalized on the protein content. The lower limit of quantification (LLOQ) and the upper limit of quantification (ULOQ) differ depending on the amount of cells i.e. the protein used for the analysis. For ULOQ the exact value for each sample is shown, while the highest LLOQ is indicated. Shown is the mean  $\pm$  SD, n=3.

cell line	treatment	concentration of total oxylipins [pmol/g]			
		Linoleic Acid (LA; 18:2 n6)	Arachidonic acid (AA; 20:4 n6)	15-HETE	LTB4
HEK293T_LPCAT2	+DOXY,+DMSO	1315 $\pm$ 65.6	3065 $\pm$ 963	1000 $\pm$ 296	<9.15
HEK239T_LPCAT2_5-LO	+DOXY,+DMSO	1824 $\pm$ 191	3878 $\pm$ 1148	1652 $\pm$ 450	<9.15
HEK239T_LPCAT2_15-LO1	+DOXY,+DMSO	8106 $\pm$ 3231	4013 $\pm$ 952	2873 $\pm$ 1510	<9.15
HEK239T_LPCAT2_15-LO2	+DOXY,+DMSO	44475 $\pm$ 1645	3701 $\pm$ 23.1	70581 $\pm$ 2103	<1.98
HEK293T_LPCAT2	+DOXY,+RSL3 4h	1515 $\pm$ 198	3201 $\pm$ 90.8	1054 $\pm$ 161	<9.15
HEK239T_LPCAT2_5-LO	+DOXY,+RSL3 4h	1701 $\pm$ 421	3374 $\pm$ 522	4010 $\pm$ 586	<9.15
HEK239T_LPCAT2_15-LO1	+DOXY,+RSL3 4h	23424 $\pm$ 8773	6339 $\pm$ 2261	26624 $\pm$ 16151	<9.15
HEK239T_LPCAT2_15-LO2	+DOXY,+RSL3 4h	44503 $\pm$ 3315	3872 $\pm$ 175	84076 $\pm$ 14083	<1.98
HEK293T_LPCAT2	+DOXY,+RSL3/+Fer-1 4h	1470 $\pm$ 377	3005 $\pm$ 412	968 $\pm$ 66.6	<9.15
HEK239T_LPCAT2_5-LO	+DOXY,+RSL3/+Fer-1 4h	1819 $\pm$ 92.3	3861 $\pm$ 609	1473 $\pm$ 250	<9.15
HEK239T_LPCAT2_15-LO1	+DOXY,+RSL3/+Fer-1 4h	21652 $\pm$ 13417	2556 $\pm$ 871	19685 $\pm$ 18107	<9.15
HEK239T_LPCAT2_15-LO2	+DOXY,+RSL3/+Fer-1 4h	43794 $\pm$ 2498	2131 $\pm$ 246	73971 $\pm$ 7105	<1.98
HEK293T_LPCAT2	+DOXY,+Fer-1 4h	1292 $\pm$ 70.0	3365 $\pm$ 723	977 $\pm$ 160	<9.15
HEK239T_LPCAT2_5-LO	+DOXY,+Fer-1 4h	2049 $\pm$ 76.5	3422 $\pm$ 1433	1315 $\pm$ 459	<9.15
HEK239T_LPCAT2_15-LO1	+DOXY,+Fer-1 4h	8000 $\pm$ 1604	3333 $\pm$ 670	2742 $\pm$ 1531	<9.15
HEK239T_LPCAT2_15-LO2	+DOXY,+Fer-1 4h	42458 $\pm$ 1329	3595 $\pm$ 81.5	68574 $\pm$ 6356	<1.98
		Eicosapentaenoic Acid (EPA; 20:5 n3)		Docosahexaenoic Acid (DHA; 22:6 n3)	
		5-HEPE	15-HEPE	4-HDHA	17-HDHA
HEK293T_LPCAT2	+DOXY,+DMSO	1235 $\pm$ 387	849 $\pm$ 289	6139 $\pm$ 1725	812 $\pm$ 312
HEK239T_LPCAT2_5-LO	+DOXY,+DMSO	1400 $\pm$ 422	1180 $\pm$ 353	10229 $\pm$ 2833	1220 $\pm$ 441
HEK239T_LPCAT2_15-LO1	+DOXY,+DMSO	1074 $\pm$ 270	1181 $\pm$ 562	10221 $\pm$ 2546	1848 $\pm$ 614
HEK239T_LPCAT2_15-LO2	+DOXY,+DMSO	590 $\pm$ 29.1	54145 $\pm$ 1501	3193 $\pm$ 215	74272 $\pm$ 3111
HEK293T_LPCAT2	+DOXY,+RSL3 4h	1284 $\pm$ 129	775 $\pm$ 40.5	7555 $\pm$ 1026	782 $\pm$ 144
HEK239T_LPCAT2_5-LO	+DOXY,+RSL3 4h	1295 $\pm$ 270	1035 $\pm$ 226	9262 $\pm$ 861	1009 $\pm$ 231
HEK239T_LPCAT2_15-LO1	+DOXY,+RSL3 4h	1028 $\pm$ 219	5210 $\pm$ 2726	9363 $\pm$ 2518	9078 $\pm$ 4236
HEK239T_LPCAT2_15-LO2	+DOXY,+RSL3 4h	593 $\pm$ 26.1	56137 $\pm$ 6019	3405 $\pm$ 265	83891 $\pm$ 12204
HEK293T_LPCAT2	+DOXY,+RSL3/+Fer-1 4h	1285 $\pm$ 61.0	811 $\pm$ 57.8	7108 $\pm$ 1463	773 $\pm$ 52.0
HEK239T_LPCAT2_5-LO	+DOXY,+RSL3/+Fer-1 4h	1534 $\pm$ 236	1232 $\pm$ 233	11037 $\pm$ 1309	1108 $\pm$ 192
HEK239T_LPCAT2_15-LO1	+DOXY,+RSL3/+Fer-1 4h	911 $\pm$ 316	4178 $\pm$ 3579	8531 $\pm$ 3442	6942 $\pm$ 5599
HEK239T_LPCAT2_15-LO2	+DOXY,+RSL3/+Fer-1 4h	602 $\pm$ 53.4	55154 $\pm$ 4777	3347 $\pm$ 293	77586 $\pm$ 6778
HEK293T_LPCAT2	+DOXY,+Fer-1 4h	1230 $\pm$ 239	829 $\pm$ 146	6839 $\pm$ 1373	735 $\pm$ 96.3
HEK239T_LPCAT2_5-LO	+DOXY,+Fer-1 4h	1289 $\pm$ 475	1088 $\pm$ 410	9484 $\pm$ 3499	999 $\pm$ 335
HEK239T_LPCAT2_15-LO1	+DOXY,+Fer-1 4h	967 $\pm$ 188	1101 $\pm$ 448	9344 $\pm$ 2809	1585 $\pm$ 783
HEK239T_LPCAT2_15-LO2	+DOXY,+Fer-1 4h	537 $\pm$ 22.3	49207 $\pm$ 2446	2961 $\pm$ 361	73050 $\pm$ 3428

**Table 9.7: Non-esterified oxylipins in 1x10<sup>7</sup> HEK293T cells.**

HEK293T\_LPCAT2\_LO (5-LO, 15-LO1, 15-LO2) were treated with doxycycline before treatment with 10  $\mu$ M RSL3 for 4 or 24 h (+DOXY,+RSL3 4 h; +DOXY,+RSL3 24 h). Controls received DMSO (+DOXY,+DMSO). Non-esterified oxylipins were prepared and analyzed by LC-MS/MS following solid phase extraction as described [204,209–211]. Non-esterified oxylipins concentration were normalized on the protein content. The lower limit of quantification (LLOQ) and the upper limit of quantification (ULOQ) differ depending on the amount of cells i.e. the protein used for the analysis. For ULOQ the exact value for each sample is shown, while the highest LLOQ is indicated. Shown is the mean  $\pm$  SD, n=3.

concentration of non-esterified oxylipins [pmol/g]			Arachidonic acid (AA; 20:4 n6)			
cell line	treatment	13-HODE	5-HETE	12-HETE	15-HETE	LTB4
Linoleic Acid (LA; 18:2 n6)						
HEK293T_LPCAT2	+DOXY,+DMSO	199 $\pm$ 190	<0.43	24.1 $\pm$ 8.1	7.4 $\pm$ 4.5	<1.22
HEK239T_LPCAT2_5-LO	+DOXY,+DMSO	94.2 $\pm$ 38.1	<0.43	25.9 $\pm$ 8.6	16.2 $\pm$ 4.3	8.9 $\pm$ 4.3
HEK239T_LPCAT2_15-LO1	+DOXY,+DMSO	108.4 $\pm$ 50.1	<0.43	38.3 $\pm$ 3.4	67.1 $\pm$ 37.7	<1.22
HEK293T_LPCAT2_15-LO2	+DOXY,+DMSO	110.6 $\pm$ 84.1	<0.43	19.8 $\pm$ 1.8	72.0 $\pm$ 80.2	19.2 $\pm$ 13.9
HEK293T_LPCAT2	+DOXY,+RSL3 4h	244 $\pm$ 121	<0.43	29.4 $\pm$ 4.4	10.8 $\pm$ 2.5	<1.22
HEK239T_LPCAT2_5-LO	+DOXY,+RSL3 4h	164 $\pm$ 161	<0.43	28.6 $\pm$ 4.8	12.7 $\pm$ 4.4	5.9 $\pm$ 4.3
HEK239T_LPCAT2_15-LO1	+DOXY,+RSL3 4h	255.8 $\pm$ 81.3	<0.43	97.8 $\pm$ 24.3	57.4 $\pm$ 23.2	<1.22
HEK293T_LPCAT2_15-LO2	+DOXY,+RSL3 4h	210.3 $\pm$ 57.5	<0.43	21.1 $\pm$ 2.1	12.99 $\pm$ 89.7	12.9 $\pm$ 0.51
HEK293T_LPCAT2	+DOXY,+RSL3/+Fer-1 4h	330 $\pm$ 355	<0.43	32.2 $\pm$ 8.0	27.9 $\pm$ 31.0	<1.22
HEK239T_LPCAT2_5-LO	+DOXY,+RSL3/+Fer-1 4h	105 $\pm$ 18.9	<0.43	30.9 $\pm$ 5.3	11.2 $\pm$ 4.7	3.9 $\pm$ 4.6
HEK239T_LPCAT2_15-LO1	+DOXY,+RSL3/+Fer-1 4h	347.2 $\pm$ 99.9	<0.43	75.8 $\pm$ 14.7	398 $\pm$ 273	<1.22
HEK293T_LPCAT2_15-LO2	+DOXY,+RSL3/+Fer-1 4h	1540 $\pm$ 332	<0.43	24.4 $\pm$ 3.3	998 $\pm$ 419	17.7 $\pm$ 21.5
HEK293T_LPCAT2	+DOXY,+Fer-1 4h	207 $\pm$ 97.0	<0.43	27.9 $\pm$ 8.1	17.7 $\pm$ 15.9	<1.22
HEK239T_LPCAT2_5-LO	+DOXY,+Fer-1 4h	311 $\pm$ 433	<0.43	27.5 $\pm$ 7.6	12.5 $\pm$ 9.9	2.4 $\pm$ 2.0
HEK239T_LPCAT2_15-LO1	+DOXY,+Fer-1 4h	1103 $\pm$ 424	<0.43	33.6 $\pm$ 4.4	70.3 $\pm$ 28.2	<1.22
HEK293T_LPCAT2_15-LO2	+DOXY,+Fer-1 4h	1181 $\pm$ 149	<0.43	16.2 $\pm$ 0.62	717 $\pm$ 333	10.0 $\pm$ 1.6
concentration of non-esterified oxylipins [pmol/g]			Docosahexaenoic Acid (DHA; 22:6 n3)			
cell line	treatment	5-HEPE	15-HEPE	4-HDHA	17-HDHA	
Eicosapentaenoic Acid (EPA; 20:5 n3)						
HEK293T_LPCAT2	+DOXY,+DMSO	<0.72	<1.22	<1.22	<8.29	<8.29
HEK239T_LPCAT2_5-LO	+DOXY,+DMSO	<0.72	5.4 $\pm$ 7.2	<1.22	<8.29	<8.29
HEK239T_LPCAT2_15-LO1	+DOXY,+DMSO	<0.72	10.3 $\pm$ 15.7	<1.22	<8.29	<8.29
HEK293T_LPCAT2_15-LO2	+DOXY,+DMSO	<0.39	25.3 $\pm$ 12.3	8.2 $\pm$ 0.52	630 $\pm$ 25.3	630 $\pm$ 25.3
HEK293T_LPCAT2	+DOXY,+RSL3 4h	<0.72	3.4 $\pm$ 3.8	<1.22	<8.29	<8.29
HEK239T_LPCAT2_5-LO	+DOXY,+RSL3 4h	<0.72	<1.22	<1.22	<8.29	<8.29
HEK239T_LPCAT2_15-LO1	+DOXY,+RSL3 4h	<0.72	113 $\pm$ 38.3	<1.22	24.5 $\pm$ 24.1	24.5 $\pm$ 24.1
HEK293T_LPCAT2_15-LO2	+DOXY,+RSL3 4h	<0.39	366 $\pm$ 36.9	<1.22	986 $\pm$ 72.6	986 $\pm$ 72.6
HEK293T_LPCAT2	+DOXY,+RSL3/+Fer-1 4h	<0.72	13.9 $\pm$ 22.0	<1.22	<8.29	<8.29
HEK239T_LPCAT2_5-LO	+DOXY,+RSL3/+Fer-1 4h	<0.72	<1.22	<1.22	<8.29	<8.29
HEK239T_LPCAT2_15-LO1	+DOXY,+RSL3/+Fer-1 4h	<0.72	67.8 $\pm$ 68.2	<1.22	<8.29	<8.29
HEK293T_LPCAT2_15-LO2	+DOXY,+RSL3/+Fer-1 4h	<0.39	364 $\pm$ 66.4	8.9 $\pm$ 1.0	953 $\pm$ 175	953 $\pm$ 175
HEK293T_LPCAT2	+DOXY,+Fer-1 4h	<0.72	9.0 $\pm$ 13.4	<1.22	<8.29	<8.29
HEK239T_LPCAT2_5-LO	+DOXY,+Fer-1 4h	<0.72	<1.22	<1.22	<8.29	<8.29
HEK239T_LPCAT2_15-LO1	+DOXY,+Fer-1 4h	<0.72	<1.22	<1.22	<8.29	<8.29
HEK293T_LPCAT2_15-LO2	+DOXY,+Fer-1 4h	<0.39	229 $\pm$ 31.9	8.1 $\pm$ 1.3	585 $\pm$ 81.7	585 $\pm$ 81.7

## 9.7 Compound libraries

Table 9.8: Fatty acid library.

Compound Nr.	Smiles code
FAL01A02	<chem>FC(F)(F)C1=CC=C(COC2=CC=CC=C2CC(O)=O)C=C1</chem>
FAL01A03	<chem>OC(C1=CC=CC/C=C/C(C2=CC=C(F)C=C2)=O)=C1)=O</chem>
FAL01A04	<chem>O=C(N[C@@H](CCCNC(OC(C)(C)C)=O)C(O)=O)C1=CC=CC=C1</chem>
FAL01A05	<chem>FC(F)(F)C1=NN(C2=CC=C(S(=O)(N)=O)C=C2)C(C3=CC(C)=CC=C3C)=C1</chem>
FAL01A06	<chem>FC(F)(F)C1=NN(C2=CC=C(S(=O)(N)=O)C=C2)C(C3=CC=C(C)C=C3)=C1</chem>
FAL01A07	<chem>CC1=CC=C(C)C(C2=CC(CO)=NN2C3=CC=C(S(N)(=O)=O)C=C3)=C1</chem>
FAL01A08	<chem>BrC1=CC=CC(C2(CCOCC2)C(N)=O)=C1</chem>
FAL01A09	<chem>O=C(CCCC)N(CC1=CC=C(C2=CC=CC=C2C(O)=O)C=C1F)C3=CC=CC=C3</chem>
FAL01A10	<chem>O=C(N(CCCC)CC1=CC=C(C2=CC=CC=C2C(O)=O)C=C1)C3=CC=CC=C3</chem>
FAL01A11	<chem>O=C(CCCC)N(C1=CC=CC=C1)CC2=CC=C(C3=CC=CC=C3C(O)=O)C=C2</chem>
FAL01B02	<chem>O=C(CCCC)N(CC1=CC=C(C2=CC=CC=C2C(O)=O)C=C1)C3=CC=C(Cl)C=C3</chem>
FAL01B03	<chem>O=C(CCCC)N(CC1=CC=C(C2=CC=C(Cl)C=C2C(O)=O)C=C1)C3=CC=CC=C3</chem>
FAL01B04	<chem>FC(F)(F)C1=C(CNC(CCCNC2=CC(Cl)=NC(SC(CCCCC)C(O)=O)=N2)=O)C=CC=C1</chem>
FAL01B05	<chem>FC(F)(F)C1=C(CNC(C2CCN(C3=CC(Cl)=NC(SC(CCCCC)C(O)=O)=N3)CC2)=O)C=CC=C1</chem>
FAL01B06	<chem>FC(F)(F)C1=C(CNC(C2=CC=C(CC(C(O)=O)CC)C=C2)=O)C=CC=C1</chem>
FAL01B07	<chem>FC(F)(F)C1=C(CNC(C2CCN(C3=CC=C(/C=C(CC)/C(O)=O)C=C3)CC2)=O)C=CC=C1</chem>
FAL01B08	<chem>FC(F)(F)C1=C(CNC(C2=CC=C(/C=C3C(NC(S/3)=O)=O)C=C2)=O)C=CC=C1</chem>
FAL01B09	<chem>FC(F)(F)C1=CC=C(CNC(C2=CC=C(/C=C(CC)/C(O)=O)C=C2)=O)C=C1</chem>
FAL01B10	<chem>FC(F)(F)OC1=CC=C(CNC(C2=CC=C(/C=C(C(O)=O)\CC)C=C2)=O)C=C1</chem>
FAL01B11	<chem>OC1=CC=C(CNC(C2=CC=C(/C=C(C(O)=O)\CC)C=C2)=O)C=C1</chem>
FAL01C02	<chem>FC1=CC=C(CNC(C2=CC=C(/C=C(C(O)=O)\CC)C=C2)=O)C(C(F)(F)F)=C1</chem>
FAL01C03	<chem>COC1=CC=C(CNC(C2=CC=C(/C=C(C(O)=O)\CC)C=C2)=O)C(C(F)(F)F)=C1</chem>
FAL01C04	<chem>O=C(C1=CC=C(/C=C(CC)/C(O)=O)C=C1)NCC(C=C2)=CC=C2OC3=CC=CC=C3</chem>
FAL01C05	<chem>O=C(C1=CC=C(CC(CC)C(O)=O)C=C1)NCC2=CC=C(C(F)(F)F)C=C2</chem>
FAL01C06	<chem>O=C(C1=CC=C(CC(CC)C(O)=O)C=C1)NCC2=CC=CC=C2</chem>
FAL01C07	<chem>OC1=CC=C(CNC(C2=CC=C(CC(CC)C(O)=O)C=C2)=O)C=C1</chem>
FAL01C08	<chem>FC(F)(F)C1=C(CNC(C2=CC=C(CC(CC)C(O)=O)C=C2)=O)C=CC(OC)=C1</chem>
FAL01C09	<chem>BrC1=C(CNC(C2=CC=C(/C=C(CC)/C(O)=O)C=C2)=O)C=CC=C1</chem>
FAL01C10	<chem>COC1=CC=C(CNC(C2=CC=C(/C=C(CC)/C(O)=O)C=C2)=O)C=C1</chem>
FAL01C11	<chem>FC(F)(F)C1=C(CNC(C2=CC=CC(/C=C(C(O)=O)\CC)C=C2)=O)C=CC=C1</chem>
FAL01D02	<chem>O=C(C1=CC=C(/C=C(CC)/C(O)=O)C=C1)NCC2=C(OC(F)(F)F)C=CC=C2</chem>
FAL01D03	<chem>CIC1=CC=C(CNC(C2=CC=C(/C=C(CC)/C(O)=O)C=C2)=O)C=C1</chem>
FAL01D04	<chem>COC1=CC=C(CNC(C2=CC=C(CC(CC)C(O)=O)C=C2)=O)C=C1</chem>
FAL01D05	<chem>FC(F)(F)C1=C(CNC(C2=CC=CC(CC(CC)C(O)=O)C=C2)=O)C=CC=C1</chem>
FAL01D06	<chem>CIC1=CC=C(COC(C2=CC=C(CC(CC)C(O)=O)C=C2)=O)C=C1</chem>
FAL01D07	<chem>FC(F)(F)C1=C(CNC(C2=CC=C(C3=CC=C(C(O)=O)C=C3)C=C2)=O)C=CC=C1</chem>
FAL01D08	<chem>FC(F)(F)C1=C(CNC(C2=CC=C(CC(C3=CC=CC=C3)C(O)=O)C=C2)=O)C=CC=C1</chem>
FAL01D09	<chem>FC(F)(F)C1=C(CNC(C2=CC=C(CC(CCC)C(O)=O)C=C2)=O)C=CC=C1</chem>
FAL01D10	<chem>FC(F)(F)C1=C(CNC(C2=CC=C(CCC(O)=O)C=C2)=O)C=CC=C1</chem>
FAL01D11	<chem>FC(F)(F)C1=C(CNC(C2=CC=C(C3=CC=CC(C(O)=O)C=C3)C=C2)=O)C=CC=C1</chem>
FAL01E02	<chem>OC(/C(CCCC)=C/C1=C(OCC2=CC=C(C(F)(F)F)C=C2)C=CC(OCC3=CC(C(OC)=CC(C(F)(F)F)=N4)=C4C=C3)=C1)=O</chem>

Compound Nr.	Smiles code
FAL01E03	<chem>OC(/C(CC1CC1)=C/C2=C(OCC3=CC=C(F)C=C3)C=CC(OCC4=CC(C(OC)=CC(C(F)(F)F)=N5)=C5C=C4)=C2)=O</chem>
FAL01E04	<chem>OC(/C(CCC)=C/C1=C(OC)C=CC(OCC2=CC(C(OC)=CC(C(F)(F)F)=N3)=C3C=C2)=C1)=O</chem>
FAL01E05	<chem>FC1=CC=C(COC2=CC=C(OCC3=CC(C=CC=C4)=C4C=C3)C=C2/C=C(CCC)/C(O)=O)C=C1</chem>
FAL01E06	<chem>FC1=CC=C(COC2=CC=C(COC3=CC(C=CC=N4)=C4C=C3)C=C2/C=C(CCC)/C(O)=O)C=C1</chem>
FAL01E07	<chem>OC(/C(CCCC)=C/C1=C(OCC2=CC=C(F)C=C2)C=CC(OCC3=CC(C(OC)=CC(C(F)(F)F)=N4)=C4C=C3)=C1)=O</chem>
FAL01E08	<chem>OC(/C(CCCC)=C/C1=C(OCC2=CC=C(OC(F)(F)F)C=C2)C=CC(OCC3=CC(C(OC)=CC(C(F)(F)F)=N4)=C4C=C3)=C1)=O</chem>
FAL01E09	<chem>OC(/C(CCC)=C/C1=C(OCC2=CC=C(F)C=C2)C=CC(OCC3=CC(C(OC)=CC(C(F)(F)F)=N4)=C4C=C3)=C1)=O</chem>
FAL01E10	<chem>OC(/C(CC)=C/C1=C(OCC2=CC=C(F)C=C2)C=CC(OCC3=CC(C(OC)=CC(C(F)(F)F)=N4)=C4C=C3)=C1)=O</chem>
FAL01E11	<chem>OC(/C=C/C1=C(OCC2=CC=C(F)C=C2)C=CC(OCC3=CC(C(OC)=CC(C(F)(F)F)=N4)=C4C=C3)=C1)=O</chem>
FAL01F02	<chem>OC(/C(C)=C/C1=C(OCC2=CC=C(F)C=C2)C=CC(OCC3=CC(C(OC)=CC(C(F)(F)F)=N4)=C4C=C3)=C1)=O</chem>
FAL01F03	<chem>OC(/C(CCC)=C/C1=C(OCC2=CC=C(F)C=C2)C=CC(OCC3=CC(C=CN4)=C4C=C3)=C1)=O</chem>
FAL01F04	<chem>OC(/C(CCC)=C/C1=C(OCC2=CC(F)=CC=C2)C=CC(OCC3=CC(C(OC)=CC(C(F)(F)F)=N4)=C4C=C3)=C1)=O</chem>
FAL01F05	<chem>OC(/C(CCC)=C/C1=C(OCC2=C(F)C=CC=C2)C=CC(OCC3=CC(C(OC)=CC(C(F)(F)F)=N4)=C4C=C3)=C1)=O</chem>
FAL01F06	<chem>OC(CCc(cc1-c2cccc2)nn1-c1cccc(Cl)c1)=O</chem>
FAL01F07	<chem>Cc1cccc(-n2nc(CCC(O)=O)cc2-c2cccc2)c1</chem>
FAL01F08	<chem>OC(CCc(cc1-c2cccc2)nn1-c1cccc(C(F)(F)F)c1)=O</chem>
FAL01F09	<chem>COc1cccc(-n2nc(CCC(O)=O)cc2-c2cccc2)c1</chem>
FAL01F10	<chem>CS(c(cc1)ccc1-n1nc(CCC(O)=O)cc1-c1cccc1)(=O)=O</chem>
FAL01F11	<chem>NS(c(cc1)ccc1-n1nc(CCC(O)=O)cc1-c1cccc1)(=O)=O</chem>
FAL01G02	<chem>OC(CCc1nc(-c2cccc2)c(-c(cc2)ccc2F)o1)=O</chem>
FAL01G03	<chem>OC(CCc1nc(-c(cc2)ccc2F)c(-c2cccc2)o1)=O</chem>
FAL01G04	<chem>OC(CCc1nc(-c2cccc(F)c2)c(-c2cccc2)o1)=O</chem>
FAL01G05	<chem>OC(CCc1nc(-c2ccc(C(F)(F)F)cc2)c(-c2cccc2)o1)=O</chem>
FAL01G06	<chem>OC(CCc1nc(-c(cc2)cc(Cl)c2Cl)c(-c2cccc2)o1)=O</chem>
FAL01G07	<chem>COc(cc1)ccc1-c1c(-c2cccc2)oc(CCC(O)=O)n1</chem>
FAL01G08	<chem>OC(CCc1nc(-c(cc2)cc(C(F)(F)F)c2Cl)c(-c2cccc2)o1)=O</chem>
FAL01G09	<chem>CC(C(O)=O)Sc1nc(-c2cccc2)c(-c2cccc2)[nH]1</chem>
FAL01G10	<chem>OC(CCc(cc1-c2cccc(Cl)c2)nn1-c1cccc1)=O</chem>
FAL01G11	<chem>OC(CCc(cc1-c2cccc(OC(F)(F)F)c2)nn1-c1cccc1)=O</chem>
FAL01H02	<chem>OC(CCc(cc1-c2cccc(C(F)(F)F)c2)nn1-c1cccc1)=O</chem>
FAL01H03	<chem>CS(c(cc1)ccc1-c1cc(CCC(O)=O)nn1-c1cc(OC(F)(F)F)ccc1)(=O)=O</chem>
FAL01H04	<chem>CC(C)Oc1cccc(-c2cc(CCC(O)=O)nn2-c2cccc2)c1</chem>
FAL01H05	<chem>CS(c(cc1)ccc1-n1nc(CCC(O)=O)cc1-c1cc(OC(F)(F)F)ccc1)(=O)=O</chem>
FAL01H06	<chem>Cc1cccc(-c2cc(CCC(O)=O)nn2-c2cccc2)c1</chem>
FAL01H07	<chem>COc1cccc(-c2cc(CCC(O)=O)nn2-c2cccc2)c1</chem>
FAL01H08	<chem>OC(CCCc1nc(-c(cc2)cc(Cl)c2Cl)c(-c(cc2)F)c2F)o1)=O</chem>
FAL01H09	<chem>Cc1noc(C)c1-c1c(-c(cc2)cc(Cl)c2Cl)nc(CCCC(O)=O)o1</chem>
FAL01H10	<chem>Cc1cccc(-c2c(-c(cc3)cc(Cl)c3Cl)nc(CCCC(O)=O)o2)c1</chem>
FAL01H11	<chem>OC(CCCc1nc(-c(cc2)cc(Cl)c2Cl)co1)=O</chem>
FAL02A02	<chem>OC(Cc(cccc1)c1Nc(c(Cl)ccc1)c1Cl)=O</chem>
FAL02A03	<chem>NS(c(cc(C(O)=O)c(NCc1ccc1)c1)c1Cl)(=O)=O</chem>
FAL02A04	<chem>CC(C)Cc1ccc(C(C)C(O)=O)cc1</chem>



Compound Nr.	Smiles code
FAL02A05	<chem>Cc1c(CC(O)=O)c(cc(cc2)OC)c2n1C(c(cc1)ccc1Cl)=O</chem>
FAL02A06	<chem>OC(c(cccc1)c1O)=O</chem>
FAL02A07	<chem>CCCc1nc(c(C)cc(-c2nc(cccc3)c3n2C)c2)c2n1Cc(cc1)ccc1-c(cccc1)c1C(O)=O</chem>
FAL02A08	<chem>CC(C)(C(O)=O)Oc1ccc(CCNC(c(cc2)ccc2Cl)=O)cc1</chem>
FAL02A09	<chem>OC(c1cccc(-c2nc(-c(cc3)cc(Cl)c3Cl)c(-c3ccccc3)o2)c1)=O</chem>
FAL02A10	<chem>OC(c(cc1)ccc1-c1nc(-c(cc2)cc(Cl)c2Cl)c(-c2ccccc2)o1)=O</chem>
FAL02A11	<chem>OC(Cc(onc1-c2ccccc2)c1-c1ccccc1)=O</chem>
FAL02B02	<chem>NS(c(cc1)ccc1-n1nc(CCC(O)=O)cc1-c1ccccc1)(=O)=O</chem>
FAL02B03	<chem>OC(Cc(cc1-c2ccccc2)nn1-c(cc1)ccc1OC(F)(F)F)=O</chem>
FAL02B04	<chem>NS(c(cc1)ccc1-c1cc(CCC(O)=O)nn1-c1ccccc1)(=O)=O</chem>
FAL02B05	<chem>OC(c(cccc1)c1Nc1ccccc1)=O</chem>
FAL02B06	<chem>OC(c(cccc1)c1Nc1nc2ccccc2cc1)=O</chem>
FAL02B07	<chem>CN(c1cccc(Cl)c1)c(cccc1)c1C(O)=O</chem>
FAL02B08	<chem>COc1ccc(Nc(cccc2)c2C(O)=O)c1</chem>
FAL02B09	<chem>OC(c(cccc1)c1Nc(cc1)ccc1OC(F)(F)F)=O</chem>
FAL02B10	<chem>OC(c(cccc1)c1Nc(cc1)ccc1Oc1ccccc1)=O</chem>
FAL02B11	<chem>COc(cc1)cc(Nc2ccccc(Cl)c2)c1C(O)=O</chem>
FAL02C02	<chem>OC(c(ccc(F)c1)c1Nc1cccc(Cl)c1)=O</chem>
FAL02C03	<chem>Cc(ccc(Nc(ccc(C(F)(F)F)c1)c1C(O)=O)c1)c1Cl</chem>
FAL02C04	<chem>Cc1cccc(Nc2cc(Cl)nc(SCC(O)=O)n2)c1C</chem>
FAL02C05	<chem>OC(CSc1nc(Nc2c(CCC3)c3ccc2)cc(Cl)n1)=O</chem>
FAL02C06	<chem>CCC(C(O)=O)Sc1nc(Nc2c(C)c(C)ccc2)cc(Cl)n1</chem>
FAL02C07	<chem>OC(c(cc1)ccc1-c1ccccc1)=O</chem>
FAL02C08	<chem>OC(c(cc1)ccc1-c1cc(Cl)cc(Cl)c1)=O</chem>
FAL02C09	<chem>CC(C)(C)c1cc(-c2ccc(CC(O)=O)cc2)cc(C(C)(C)C)c1</chem>
FAL02C10	<chem>CC(C)(C)c1cc(-c2ccc(CCC(O)=O)cc2)cc(C(C)(C)C)c1</chem>
FAL02C11	<chem>CC(C)(C)c1cc(-c(cc2)nc2C(O)=O)cc(C(C)(C)C)c1</chem>
FAL02D02	<chem>OC(c1cc(NC(c(cc2)ccc2OCCCCc2ccccc2)=O)ccc1)=O</chem>
FAL02D03	<chem>OC(c1cc(NC(c(cc2)ccc2Oc2ccccc2)=O)nc1)=O</chem>
FAL02D04	<chem>OC(c1cncc(NC(c(cc2)ccc2Oc2ccccc2)=O)c1)=O</chem>
FAL02D05	<chem>OC(c1nc(NC(c(cc2)ccc2Oc2ccccc2)=O)ccc1)=O</chem>
FAL02D06	<chem>OC(c1nccc(NC(c(cc2)ccc2Oc2ccccc2)=O)c1)=O</chem>
FAL02D07	<chem>COc1c(cc(COc(cc2)cc(/C=C(\CC3CC3)/C(O)=O)c2OCc(cc2)ccc2F)cc2)c2nc(C(F)(F)F)c1</chem>
FAL02D08	<chem>CCC/C(/C(O)=O)=C\c(cc(cc1)OCc(ccc2nc(C(F)(F)F)c3)cc2c3OC)c1NC(c(cc1)ccc1F)=O</chem>
FAL02D09	<chem>CCC/C(/C(O)=O)=C\c(cc(cc1)OCc(cc23)ccc3nc(C(F)(F)F)cc2OC)c1OCc1ccncc1</chem>
FAL02D10	<chem>Cc(cc1)cc2c1OC(c(cc1)ccc1-c(cccc1)c1C(O)=O)N(c1ccccc1)C2=O</chem>
FAL02D11	<chem>CCCC1=C(C)OC(c(cc2)ccc2-c(cccc2)c2C(O)=O)N(c2ccccc2)C1=O</chem>
FAL02E02	<chem>CCC/C(/C(O)=O)=C\c(cc(cc1)OCc2cc3ccncc3cc2)c1OCC1CC[NH+](C)CC1.[O-]C=O</chem>
FAL02E03	<chem>CCC(N(Cc(cc1)ccc1-c(cccc1)c1C(O)=O)c1ccccc1)=O</chem>
FAL02E04	<chem>CCCC(N(Cc(cc1)ccc1-c(cccc1)c1C(O)=O)C(C)C)=O</chem>
FAL02E05	<chem>CCCC(N(Cc(cc1)ccc1-c(cccc1)c1C(O)=O)c1ccccc1)=O</chem>
FAL02E06	<chem>CCCC(NCc(cc1)ccc1-c(cccc1)c1C(O)=O)=O</chem>
FAL02E07	<chem>CCCC(N(Cc(cc1)ccc1-c(cccc1)c1C(O)=O)Cc(cc1)ccc1-c(cccc1)c1C(O)=O)=O</chem>

Compound Nr.	Smiles code
FAL02E08	<chem>CCCC(N(C)Cc(cc1)ccc1-c(cccc1)c1C(O)=O)=O</chem>
FAL02E09	<chem>CCCC(N(Cc(cc1)ccc1-c(cccc1)c1C(O)=O)C1CCCC1)=O</chem>
FAL02E10	<chem>CCCCCN(Cc(cc1)ccc1-c(cccc1)c1C(O)=O)c1cccc1</chem>
FAL02E11	<chem>CCCC(N(Cc(cc1)ccc1N(CCC1)C1C(O)=O)c1cccc1)=O</chem>
FAL02F02	<chem>CCCCCN(Cc(cc1)ccc1-c(cccc1)c1C(O)=O)c(cc1)ccc1Oc1cccc1</chem>
FAL02F03	<chem>CCCC(N1Cc(cc2)ccc2-c(cccc2)c2-c2nnn[nH]2)=NC(C)(C(C)C)C1=O</chem>
FAL02F04	<chem>CCCC(N(Cc(cc1)ccc1-c(cccc1)c1C(O)=O)c1cccc1)=O</chem>
FAL02F05	<chem>OC(c(cccc1)c1-c1ccc(CN2C(c3cccc3)=NC3(CCCC3)C2=O)cc1)=O</chem>
FAL02F06	<chem>OC(c(cccc1)c1-c1ccc(CN(C(Cc2cccc2)=NC23CCCC3)C2=O)cc1)=O</chem>
FAL02F07	<chem>CCCC(N1Cc(cc2)ccc2-c(cccc2)c2C(O)=O)=NC2(CCCC2)C1=O</chem>
FAL02F08	<chem>CCCC(N1)N(Cc(cc2)ccc2-c(cccc2)c2C(O)=O)C2(CCCC2)C1=O</chem>
FAL02F09	<chem>CCCC(N1)N(Cc(cc2)ccc2-c(cccc2)c2C(O)=O)C2(CC2)C1=O</chem>
FAL02F10	<chem>OC(c(cccc1)c1-c1ccc(CN(C(Cc2cccc2)=NC23CCCC3)C2=O)cc1)=O</chem>
FAL02F11	<chem>OC(c(cccc1)c1-c1ccc(CN(C(Cc2cccc2)=O)c2cccc2)cc1)=O</chem>
FAL02G02	<chem>CC(C)C(N(Cc(cc1)ccc1-c(cccc1)c1C(O)=O)c1cccc1)=O</chem>
FAL02G03	<chem>CC(C)CC(N(Cc(cc1)ccc1-c(cccc1)c1C(O)=O)c1cccc1)=O</chem>
FAL02G04	<chem>CCCC(N(Cc(cc1)ccc1-c(cccc1)c1-c1nnn[nH]1)C1=O)=NC1(C)c1cccc1</chem>
FAL02G05	<chem>CCCC(C)(c(cccc1)c1N1Cc(cc2)ccc2-c(cccc2)c2C(O)=O)C1=O</chem>
FAL02G06	<chem>CCCC(NC1(C)C)N(Cc(cc2)ccc2-c(cccc2)c2-c2nnn[nH]2)C1=O</chem>
FAL02G07	<chem>CCCC(N1Cc(cc2)ccc2-c(cccc2)c2-c2nnn[nH]2)=NC(C)(C)C1=O</chem>
FAL02G08	<chem>OC(c(cccc1)c1-c1ccc(CN(C(c2cccc2)=O)c2cccc2)cc1)=O</chem>
FAL02G09	<chem>CCCC(N(C1)Cc2c1ccc(-c(cccc1)c1C(O)=O)c2)=O</chem>
FAL02G10	<chem>CCCCN(c(ccc(-c(cccc1)c1C(O)=O)c1)c1N1Cc2cccc2)C1=O</chem>
FAL02G11	<chem>CCCC(n1c(ccc(-c(cccc2)c2-c2nnn[nH]2)c2)c2c(Cc2cccc2)c1)=O</chem>
FAL02H02	<chem>OC(Cc1ccc(COc2cc(CCC3)c3cc2)cc1)=O</chem>
FAL02H03	<chem>OC(CCc1ccc(COc2cc(CCC3)c3cc2)cc1)=O</chem>
FAL02H04	<chem>OC(c1ccc(CNc2cc(CCC3)c3cc2)cc1)=O</chem>
FAL02H05	<chem>CN(Cc(cc1)ccc1C(O)=O)c1cc(CCC2)c2cc1</chem>
FAL02H06	<chem>OC(c(cc1)ccc1OCc1cc(CCC2)c2cc1)=O</chem>
FAL02H07	<chem>OC(c1ccc(COc(cccc2)c2OC(F)(F)F)cc1)=O</chem>
FAL02H08	<chem>OC(c1ccc(COc2cccc(Cl)c2)cc1)=O</chem>
FAL02H09	<chem>OC(c(cc1)ccc1OCc1cccc(Cl)c1)=O</chem>
FAL02H10	<chem>OC(c1ccc(COc2c(C(F)(F)F)cc(C(F)(F)F)cc2)cc1)=O</chem>
FAL02H11	<chem>CC(C)(C)c(cc1)ccc1C(Nc1cc(n(Cc(cc2)ccc2C(O)=O)cc2)c2cc1)=O</chem>

Table 9.9: Prestwick drug fragment library.

Prestw Frag Number	CAS number	Smiles code
Prestw-Frag-0608	120-29-6	<chem>CN1C2CCC1CC(O)C2</chem>
Prestw-Frag-1001	1635-31-0	<chem>NC1=Cc2cccc2OC1=O</chem>
Prestw-Frag-1003	81819-90-1	<chem>Cc1cc(nnc1N)c2cccc2</chem>
Prestw-Frag-1006	35207-08-0	<chem>NC(=O)NS(=O)(=O)c1cccc1</chem>
Prestw-Frag-1008	5393-55-5	<chem>CC(=O)Nc1nncs1</chem>
Prestw-Frag-1013	3469-00-9	<chem>COC(=O)C(c1cccc1)c2cccc2</chem>
Prestw-Frag-1014	16502-01-5	<chem>C1Cc2c(CN1)[nH]c3cccc23</chem>

Prestw Frag Number	CAS number	Smiles code
Prestw-Frag-1016	2219-84-3	<chem>Cc1cc(ccc1O)C(C)(C)CC(C)(C)C</chem>
Prestw-Frag-1017	7221-40-1	<chem>C[N+](C)(CCO)Cc1cccc1</chem>
Prestw-Frag-1019	4461-29-4	<chem>NC(=O)Cc1cccc1</chem>
Prestw-Frag-1033	726-18-1	<chem>COc1ccc(Cc2ccc(OC)cc2)cc1</chem>
Prestw-Frag-1039	144721-50-6	<chem>NCc1c(N)ccc(Cl)c1Cl</chem>
Prestw-Frag-1047	37385-05-0	<chem>CCC(=O)Nc1ncnc2[nH]cnc12</chem>
Prestw-Frag-1050	83783-69-1	<chem>Nc1nc2cccc2n1Cc3ccc(F)cc3</chem>
Prestw-Frag-1053	943-45-3	<chem>CC(C)(Oc1cccc1)C(=O)O</chem>
Prestw-Frag-1060	59315-44-5	<chem>NC1=CC=CNC1=O</chem>
Prestw-Frag-1071	619-73-8	<chem>OCc1ccc(cc1)[N+](=O)[O-]</chem>
Prestw-Frag-1076	35303-76-5	<chem>NCCc1ccc(cc1)S(=O)(=O)N</chem>
Prestw-Frag-1086	24469-51-0	<chem>CCN(CC)CCNC(=O)c1cccc1O</chem>
Prestw-Frag-1087	59-49-4	<chem>O=C1Nc2cccc2O1</chem>
Prestw-Frag-1094	189763-57-3	<chem>CC(=O)c1ccc(N2CCNCC2)c(F)c1</chem>
Prestw-Frag-1128	1097817-28-1	<chem>Cc1oncc1C(=O)N</chem>
Prestw-Frag-1164	2948-92-7	<chem>C(N1CCCC1)c2nc3cccc3[nH]2</chem>
Prestw-Frag-1165	107456-42-8	<chem>Clc1ccc(Cn2cnc3cccc23)cc1</chem>
Prestw-Frag-1193	3540-95-2	<chem>C(CN1CCCC1)C(c2cccc2)c3cccc3</chem>
Prestw-Frag-1200	13532-52-0	<chem>CC(Oc1cccc1)C(=O)N</chem>
Prestw-Frag-1228	no CAS	<chem>CCCCOc1cc(C(=O)NC)c2cccc2n1</chem>
Prestw-Frag-1239	22510-33-4	<chem>OC(=O)c1cc(ccc1O)c2ccc(F)cc2</chem>
Prestw-Frag-1273	5852-92-6	<chem>COc1cc2CCN(C)C(C)c2cc1OC</chem>
Prestw-Frag-1275	13485-59-1	<chem>COc1cc2CCN(C)Cc2cc1OC</chem>
Prestw-Frag-1303	1615-14-1	<chem>OCCn1ccnc1</chem>
Prestw-Frag-1320	16524-22-4	<chem>Cc1cccc(Nc2cccc2C(=O)O)c1</chem>
Prestw-Frag-1323	27469-60-9	<chem>Fc1ccc(cc1)C(N2CCNCC2)c3ccc(F)cc3</chem>
Prestw-Frag-1335	136167-44-7	<chem>COc1cccc1OCCCO</chem>
Prestw-Frag-1338	18181-71-0	<chem>COc1cccc1OCCO</chem>
Prestw-Frag-1343	14007-64-8	<chem>CCC(C(=O)OCCN(CC)CC)c1cccc1</chem>
Prestw-Frag-1345	855839-32-6	<chem>CCN(CC)CCOc1cccc1O</chem>
Prestw-Frag-1350	7132-15-2	<chem>CNC(=O)c1cnc(C)cn1</chem>
Prestw-Frag-1356	61-49-4	<chem>CNCCc1c[nH]c2cccc12</chem>
Prestw-Frag-1358	859065-14-8	<chem>COc1ccc(CNc2ncccn2)cc1</chem>
Prestw-Frag-1362	15832-09-4	<chem>COc1ccc2C(=O)COc2c1</chem>
Prestw-Frag-1382	25485-88-5	<chem>Oc1cccc1C(=O)OC2CCCC2</chem>
Prestw-Frag-1389	62618-09-1	<chem>NCC(O)COc1cccc2cccc12</chem>
Prestw-Frag-1398	20980-22-7	<chem>C1CN(CCN1)c2ncccn2</chem>
Prestw-Frag-1406	3967-53-1	<chem>COC(=O)C(CO)c1cccc1</chem>
Prestw-Frag-1441	147330-32-3	<chem>c1ccc(cc1)c2cccc2c3nnn[nH]3</chem>
Prestw-Frag-1445	51012-67-0	<chem>COc1ccc(CCN(C)C)cc1OC</chem>
Prestw-Frag-1446	13078-76-7	<chem>CNCCc1ccc(OC)c(OC)c1</chem>
Prestw-Frag-1453	957-51-7	<chem>CN(C)C(=O)C(c1cccc1)c2cccc2</chem>
Prestw-Frag-1471	52329-60-9	<chem>Nc1nc2cc(ccc2[nH]1)C(=O)c3cccc3</chem>
Prestw-Frag-1480	608-07-1	<chem>COc1ccc2[nH]cc(CCN)c2c1</chem>
Prestw-Frag-1494	5521-55-1	<chem>Cc1cnc(cn1)C(=O)O</chem>
Prestw-Frag-1517	1615-15-2	<chem>Cc1nccn1CCO</chem>
Prestw-Frag-1523	93413-90-2	<chem>CNCC(c1ccc(OC)cc1)C2(O)CCCC2</chem>
Prestw-Frag-1545	1697-18-3	<chem>Oc1cccc1C(=O)Nc2cccc2Cl</chem>
Prestw-Frag-1553	no CAS	<chem>CN1CCc2cccc(N)c2C1</chem>
Prestw-Frag-1559	53242-88-9	<chem>Clc1ccc(CC2=NNC(=O)c3cccc23)cc1</chem>
Prestw-Frag-1566	84484-78-6	<chem>CC(C)CC(N)C1(CCC1)c2ccc(Cl)cc2</chem>

Prestw Frag Number	CAS number	Smiles code
Prestw-Frag-1595	1208935-09-4	<chem>OCCOc1cccc2[nH]ccc12</chem>
Prestw-Frag-1654	115-46-8	<chem>OC(C1CCNCC1)(c2ccccc2)c3ccccc3</chem>
Prestw-Frag-1691	1519-94-4	<chem>CC(N)COc1cccc1</chem>
Prestw-Frag-1694	28783-41-7	<chem>C1Cc2sccc2CN1</chem>
Prestw-Frag-1700	23145-92-8	<chem>Clc1cccc(CN2CCNCC2)c1</chem>
Prestw-Frag-1704	82525-17-5	<chem>Clc1ccc(cc1)c2cncnc2</chem>
Prestw-Frag-1717	96604-75-0	<chem>CCCC(=O)Nc1cccc(c1)C(=O)C</chem>
Prestw-Frag-1722	449-55-8	<chem>C1Nc2ccccc2Cc3ccccc13</chem>
Prestw-Frag-1735	2618-38-4	<chem>CCN(CC)CCOC(=O)c1cccc1</chem>
Prestw-Frag-1745	37140-70-8	<chem>CC(=O)NCc1ccnc1</chem>
Prestw-Frag-1747	471254-13-4	<chem>Oc1ccc(cc1)C(=O)NCc2ccnc2</chem>
Prestw-Frag-1750	140-40-9	<chem>CC(=O)Nc1ncc(s1)[N+](=O)[O-]</chem>
Prestw-Frag-1806	2025339-64-2	<chem>Fc1cccc(F)c1N2CCNCC2</chem>
Prestw-Frag-1812	30893-64-2	<chem>COc1ccc(OCC(=O)N)cc1</chem>
Prestw-Frag-1817	30486-56-7	<chem>C1CNCCN(C1)C(c2ccccc2)c3ccccc3</chem>
Prestw-Frag-1833	05/10/3598	<chem>NC(=O)COc1ccc(Cl)cc1</chem>
Prestw-Frag-1856	35891-74-8	<chem>CC(N)C(=O)Nc1cccc1C</chem>
Prestw-Frag-1861	51765-51-6	<chem>CS(=O)(=O)Nc1cccc1Oc2ccccc2</chem>
Prestw-Frag-1867	10399-13-0	<chem>COC(=O)C(O)(C1CCCC1)c2ccccc2</chem>
Prestw-Frag-1904	5814-41-5	<chem>O=C1Nc2ccccc2Nc3ccccc13</chem>
Prestw-Frag-1910	57075-84-0	<chem>CCCOc1cccc1C(=N)N</chem>
Prestw-Frag-1925	50376-82-4	<chem>NCCOC(c1ccc(F)cc1)c2ccc(F)cc2</chem>
Prestw-Frag-1929	18366-40-0	<chem>CC(C)(C)NCC(O)c1cccc1</chem>
Prestw-Frag-1944	67514-07-2	<chem>OCCCN1CCN(CC1)c2ccccc2</chem>
Prestw-Frag-1945	36245-26-8	<chem>OCCN1CCN(CC1)c2ccccc2</chem>
Prestw-Frag-1946	70849-59-1	<chem>CN1CCN(CC1)c2ccccc2</chem>
Prestw-Frag-1953	886-06-6	<chem>O=C(CCN1CCCC1)c2ccccc2</chem>
Prestw-Frag-1977	98-64-6	<chem>NS(=O)(=O)c1ccc(Cl)cc1</chem>
Prestw-Frag-2005	52047-55-9	<chem>CCN(CC)CCOc1ccc(cc1)C(=O)C</chem>
Prestw-Frag-2049	77-55-4	<chem>OC(=O)C1(CCCC1)c2ccccc2</chem>
Prestw-Frag-2123	138-41-0	<chem>NS(=O)(=O)c1ccc(cc1)C(=O)O</chem>
Prestw-Frag-2168	4164-21-0	<chem>CC(C)NCC(O)c1cccc1</chem>
Prestw-Frag-2208	41038-40-8	<chem>COc1ccc(OC)c(c1)C(C)O</chem>
Prestw-Frag-2212	21867-69-6	<chem>COc1ccc(CN2CCNCC2)cc1</chem>
Prestw-Frag-2234	22821-77-8	<chem>CS(=O)(=O)c1ccc(CO)cc1</chem>
Prestw-Frag-2237	19490-92-7	<chem>CC(O)(c1cccc1)c2ccccc2</chem>
Prestw-Frag-2238	31796-72-2	<chem>OC(c1cccc1)c2ccccc2</chem>
Prestw-Frag-2253	1096863-52-3	<chem>CCCCOc1cc(ccc1N)C(=O)OC</chem>
Prestw-Frag-2256	4570-41-6	<chem>Nc1oc2ccccc2n1</chem>
Prestw-Frag-2268	360-97-4	<chem>NC(=O)c1nc[nH]c1N</chem>
Prestw-Frag-2303	586-95-8	<chem>OCc1ccncc1</chem>
Prestw-Frag-2348	10378-69-5	<chem>NC(=N)CSCc1cccc1</chem>
Prestw-Frag-2356	22881-33-0	<chem>Clc1ccc(CNc2ccccc2)cc1</chem>
Prestw-Frag-2360	5388-42-1	<chem>O=C1N(Cc2ccccc12)c3ccccc3</chem>
Prestw-Frag-2362	99855-37-5	<chem>CCC(=O)Nc1ccc(CC(=O)O)cc1</chem>
Prestw-Frag-2366	4695-13-0	<chem>NC(=O)C(c1cccc1)c2ccccc2</chem>
Prestw-Frag-2383	102-14-7	<chem>OC(=O)CCC(=O)Nc1cccc1</chem>
Prestw-Frag-2453	68599-71-3	<chem>COCCOC(=O)c1ccc(N)cc1</chem>
Prestw-Frag-2487	99855-42-2	<chem>CC(=O)N(CCC(=O)O)c1cccc1</chem>
Prestw-Frag-2537	771-99-3	<chem>C1CC(CCN1)c2ccccc2</chem>
Prestw-Frag-2541	59-67-6	<chem>OC(=O)c1cccc1</chem>

Prestw Frag Number	CAS number	Smiles code
Prestw-Frag-2569	129010-86-2	COc1cccc1N2CCN(CCCN)CC2
Prestw-Frag-2645	102993-98-6	c1ccc(cc1)C(c2cccc2)n3cncn3
Prestw-Frag-2724	342044-71-7	CCCOc1ccc(cc1N)C(=O)OCC
Prestw-Frag-2774	125-85-9	CCN(CC)CCOC(=O)C1(CCCC1)c2cccc2
Prestw-Frag-2806	17782-05-7	Cc1cccc1Nc2ncccc2C(=O)O
Prestw-Frag-2808	87766-25-4	NCCCOc1cccc(CN2CCCC2)c1
Prestw-Frag-2868	7189-67-5	c1ccc(cc1)C(c2cccc2)n3ccnc3
Prestw-Frag-3120	891-60-1	CCN(CC)CCNC(=O)c1ccc(N)c(Cl)c1
Prestw-Frag-3257	21598-26-5	C1CN(CCN1c2cccc2)c3cccc3
Prestw-Frag-3334	419543-02-5	FC(F)(F)c1ccc(cc1)C(=O)C2CCCC2
Prestw-Frag-3336	1670-87-7	NC(=O)c1ccc2[nH]ccc2c1
Prestw-Frag-3342	3706-26-1	COc1ccc(CC(C)N)cc1
Prestw-Frag-3360	117761-02-1	C1CC1Nc2ncnc3[nH]cnc23
Prestw-Frag-3368	95339-74-5	CNS(=O)(=O)CCc1cccc1
Prestw-Frag-3371	n.a.	COC(=O)CN1CCc2scccc2C1
Prestw-Frag-3426	89027-27-0	Fc1ccc(cc1)C(=O)CCCN2CCNCC2
Prestw-Frag-3452	no CAS	CNCCN(C)C(c1cccc1)c2cccc2
Prestw-Frag-3454	635-85-8	COc1ccc(CCN)cc1OC
Prestw-Frag-3455	101-53-1	Oc1ccc(Cc2cccc2)cc1
Prestw-Frag-3459	13754-41-1	O=C1CN(Cc2cccc2)CCN1
Prestw-Frag-3460	109384-27-2	CN1CCNCC1=O
Prestw-Frag-3461	1912-48-7	Cn1cc(CC(=O)O)c2cccc12
Prestw-Frag-3692	98897-36-0	CN1CCN(CCCC(=O)c2ccc(F)cc2)CC1
Prestw-Frag-3693	148942-00-1	CN(C)CCCC(=O)c1ccc(F)cc1
Prestw-Frag-3703	6272-26-0	Oc1ccc2C(=O)COc2c1
Prestw-Frag-3704	no CAS	CNC(=O)c1c(OC)ccc(Br)c1OC
Prestw-Frag-0674	36507-48-9	CC(C)(C)NCC(O)COc1cccc1C2CCCC2
Prestw-Frag-1000	91-64-5	O=C1Oc2cccc2C=C1
Prestw-Frag-1009	4005-51-0	Nc1nncs1
Prestw-Frag-1028	89-25-8	CC1=CC(=O)N(N1)c2cccc2
Prestw-Frag-1031	13214-66-9	NCCCCc1cccc1
Prestw-Frag-1032	13183-79-4	Cn1nnnc1S
Prestw-Frag-1045	69-72-7	OC(=O)c1cccc1O
Prestw-Frag-1051	85098-70-0	COc1ccc(CCN2CCC(N)CC2)cc1
Prestw-Frag-1063	881-26-5	COc1cc2[C@H](C)NCCc2cc1O
Prestw-Frag-1064	645-33-0	COc1ccc(CCN)cc1O
Prestw-Frag-1075	247098-18-6	CCC=C(C)CN(C(=O)NCCc2cccc2)C1=O
Prestw-Frag-1083	1450-74-4	CC(=O)c1cc(Cl)ccc1O
Prestw-Frag-1098	137-00-8	Cc1ncsc1CCO
Prestw-Frag-1099	6485-67-2	N[C@@H](C(=O)N)c1cccc1
Prestw-Frag-1101	32943-25-2	Clc1ccc2CCc3cccc3Nc2c1
Prestw-Frag-1106	119-56-2	OC(c1cccc1)c2ccc(Cl)cc2
Prestw-Frag-1110	34803-66-2	C1CN(CCN1)c2ccccn2
Prestw-Frag-1111	85006-31-1	COC(=O)c1scc(C)c1N
Prestw-Frag-1121	92-59-1	CCN(Cc1cccc1)c2cccc2
Prestw-Frag-1122	91-01-0	OC(c1cccc1)c2cccc2
Prestw-Frag-1125	3060-41-1	NCC(CC(=O)O)c1cccc1
Prestw-Frag-1126	2019-34-3	OC(=O)CCc1ccc(Cl)cc1
Prestw-Frag-1130	15074-17-6	CC1=C(O)c2cccc2OC1=O
Prestw-Frag-1131	1076-38-6	OC1=CC(=O)Oc2cccc12
Prestw-Frag-1133	39989-39-4	COc1ccc2ccncc2c1

Prestw Frag Number	CAS number	Smiles code
Prestw-Frag-1138	6136-37-4	CN1C(=O)Nc2nc[nH]c2C1=O
Prestw-Frag-1141	3978-34-5	CNC(C)(C)Cc1cccc1
Prestw-Frag-1154	696-45-7	COc1cc(N)ncn1
Prestw-Frag-1156	529-35-1	Oc1cccc2CCCCc12
Prestw-Frag-1161	108-33-8	Cc1nnc(N)s1
Prestw-Frag-1162	841-77-0	C1CN(CCN1)C(c2cccc2)c3cccc3
Prestw-Frag-1163	87179-40-6	C(\C=C\c1cccc1)N2CCNCC2
Prestw-Frag-1167	7252-84-8	COc1ccc(N)nn1
Prestw-Frag-1182	24155-42-8	OC(Cn1ccnc1)c2ccc(Cl)cc2Cl
Prestw-Frag-1183	15248-39-2	COc1cc2ccncc2cc1OC
Prestw-Frag-1184	5469-69-2	Nc1ccc(Cl)nn1
Prestw-Frag-1187	54-11-5	CN1CCC[C@H]1c2ccnc2
Prestw-Frag-1188	696-23-1	Cc1ncc([nH]1)[N+](=O)[O-]
Prestw-Frag-1189	54396-44-0	Cc1c(N)cccc1C(F)(F)F
Prestw-Frag-1191	16344-24-4	OC(=O)c1ccnc1Nc2cccc2
Prestw-Frag-1204	57005-71-7	CN1CCN(CC1)c2nccc(N)n2
Prestw-Frag-1214	5470-49-5	CS(=O)(=O)c1ccc(N)cc1
Prestw-Frag-3759	1126-00-7	c1ccc(cc1)n2cccn2
Prestw-Frag-1236	33892-75-0	COc1cccc2C(=O)CCCc12
Prestw-Frag-1237	59089-68-8	Oc1ccc(cc1)c2ccc(F)cc2F
Prestw-Frag-1238	656304-77-7	OC(=O)c1cccc(c1)c2ccc(F)cc2F
Prestw-Frag-1240	323-87-5	OC(=O)c1cc(ccc1O)c2cccc2
Prestw-Frag-1264	6650-04-0	CC(C)C1NCCc2c1[nH]c3cccc23
Prestw-Frag-1268	65767-07-9	NC1=NCCN1
Prestw-Frag-1276	03/12/2328	COc1cc2CCNCCc2cc1OC
Prestw-Frag-1297	24621-70-3	OCc1cc2cccc2[nH]1
Prestw-Frag-1299	41340-36-7	CCc1cccc2c(CCO)c[nH]c12
Prestw-Frag-1311	55147-68-7	N1C(N[C@@H](C1=O)C)=O
Prestw-Frag-1313	219636-76-7	COc1ccc(cc1N2CCCC2)C(=O)O
Prestw-Frag-1319	13278-36-9	OC(=O)c1cccc1Nc2cccc(Cl)c2
Prestw-Frag-1322	2646-97-1	Nc1cccc(c1)C(F)(F)F
Prestw-Frag-1325	82-92-8	CN1CCN(CC1)C(c2cccc2)c3cccc3
Prestw-Frag-1337	538-43-2	OCC(O)COc1cccc1
Prestw-Frag-1346	27652-89-7	OC(c1ccc(Cl)cc1)c2cccn2
Prestw-Frag-1348	08/03/7401	CCOC(=O)C1c2cccc2Oc3cccc13
Prestw-Frag-1361	7169-34-8	O=C1COc2cccc12
Prestw-Frag-1365	39512-49-7	OC1(CCNCC1)c2ccc(Cl)cc2
Prestw-Frag-1368	582-83-2	CCCC(=O)c1ccc(F)cc1
Prestw-Frag-1372	3189-13-7	COc1ccc2cc[nH]c2c1
Prestw-Frag-1374	2380-86-1	c12[nH]ccc1ccc(c2)O
Prestw-Frag-1394	1869-24-5	NS(=O)(=O)c1cccc1C(F)(F)F
Prestw-Frag-1397	32231-06-4	C(N1CCNCC1)c2ccc3OCOc3c2
Prestw-Frag-1408	2820-37-3	Cc1c[nH]nc1C
Prestw-Frag-1419	54-85-3	NNC(=O)c1ccncc1
Prestw-Frag-1420	613-94-5	NNC(=O)c1cccc1
Prestw-Frag-1428	271-73-8	c1cnc2[nH]ncc2c1
Prestw-Frag-1439	65-45-2	NC(=O)c1cccc1O
Prestw-Frag-1444	155413-72-2	C(C1NCCc2cccc12)c3cccc3
Prestw-Frag-1462	6297-14-9	CCN(CC)Cc1cc(N)ccc1O
Prestw-Frag-1475	6935-27-9	C(Nc1cccc1)c2cccc2
Prestw-Frag-1476	103-55-9	CN(C)CCNCC1cccc1

Prestw Frag Number	CAS number	Smiles code
Prestw-Frag-1478	1016-47-3	<chem>CC(=O)NCCc1c[nH]c2ccccc12</chem>
Prestw-Frag-1492	30536-19-7	<chem>Nc1c(Cl)ccc2nsnc12</chem>
Prestw-Frag-1495	98-97-5	<chem>OC(=O)c1cnccn1</chem>
Prestw-Frag-1499	6094-36-6	<chem>OC(=O)CC[C@H](NC(=O)c1ccccc1)C(=O)O</chem>
Prestw-Frag-1506	20469-61-8	<chem>COc1cc(C)cc(C)c1C</chem>
Prestw-Frag-1540	6969-90-0	<chem>CN(C)C(=O)Oc1ccccc1</chem>
Prestw-Frag-1543	121-87-9	<chem>Nc1ccc(cc1Cl)[N+](=O)[O-]</chem>
Prestw-Frag-1547	17438-14-1	<chem>COC(=O)C1=C(C)NC(=C(C1)C(=O)OC)C</chem>
Prestw-Frag-1552	n.a.	<chem>CN1CC(c2ccccc2)c3cccc(N)c3C1</chem>
Prestw-Frag-1557	74852-62-3	<chem>COc1ccc(cc1)N2CCN(CC2)c3cccc(N)cc3</chem>
Prestw-Frag-1560	119-39-1	<chem>O=C1NN=Cc2ccccc12</chem>
Prestw-Frag-1561	32003-14-8	<chem>O=C1NN=C(Cc2ccccc2)c3ccccc13</chem>
Prestw-Frag-1575	1218-35-5	<chem>Cc1cc(cc(C)c1)CC2=NCCN2C(C)(C)C</chem>
Prestw-Frag-1587	20662-53-7	<chem>O=C1Nc2ccccc2N1C3CCNCC3</chem>
Prestw-Frag-1632	1587546-91-5	<chem>CCN1CCCC1CNC(=O)c2ccc(N)cc2</chem>
Prestw-Frag-1643	153-98-0	<chem>NCCc1c[nH]c2ccc(O)cc12</chem>
Prestw-Frag-1645	1953-54-4	<chem>Oc1ccc2[nH]ccc2c1</chem>
Prestw-Frag-1647	1072-67-9	<chem>Cc1onc(N)c1</chem>
Prestw-Frag-1648	826-85-7	<chem>Nc1ccnn1c2ccccc2</chem>
Prestw-Frag-1661	4935-96-0	<chem>NC(=O)CN1C(=O)c2ccccc2C1=O</chem>
Prestw-Frag-1667	1694-06-0	<chem>Cc1ccc(cc1)S(=O)(=O)NC(=O)N</chem>
Prestw-Frag-1673	6969-71-7	<chem>O=C1NN=C2C=CC=CN12</chem>
Prestw-Frag-1686	529-64-6	<chem>OCC(C(=O)O)c1ccccc1</chem>
Prestw-Frag-1716	40188-45-2	<chem>CCCC(=O)Nc1ccc(O)c(c1)C(=O)C</chem>
Prestw-Frag-1731	3086-62-2	<chem>COc1cc(cc(OC)c1OC)C(=O)N</chem>
Prestw-Frag-1739	6515-36-2	<chem>Oc1ccc2C(=O)CC(Oc2c1)c3ccccc3</chem>
Prestw-Frag-1740	491-37-2	<chem>O=C1CCOc2ccccc12</chem>
Prestw-Frag-1741	303-26-4	<chem>Clc1ccc(cc1)C(N2CCNCC2)c3ccccc3</chem>
Prestw-Frag-1767	6057-60-9	<chem>OC(=O)CCCc1ccc(cc1)c2ccccc2</chem>
Prestw-Frag-1768	2051-95-8	<chem>OC(=O)CCC(=O)c1ccccc1</chem>
Prestw-Frag-1772	28075-29-8	<chem>CNCCC(c1ccccc1)c2ccccc2</chem>
Prestw-Frag-1775	23068-80-6	<chem>COc1ccc(Cl)cc1C(=O)N</chem>
Prestw-Frag-1782	5231-96-9	<chem>CC(=O)Nc1cccn1</chem>
Prestw-Frag-1791	108-39-4	<chem>Cc1cccc(O)c1</chem>
Prestw-Frag-1807	83-07-8	<chem>CN1N(C(=O)C(=C1)N)c2ccccc2</chem>
Prestw-Frag-1818	5470-36-0	<chem>NNCCc1ccccc1</chem>
Prestw-Frag-1824	1912-43-2	<chem>Cc1[nH]c2ccccc2c1CC(=O)O</chem>
Prestw-Frag-1826	126541-78-4	<chem>CC(C)(C)NCCc1ccccc1</chem>
Prestw-Frag-1832	143999-83-1	<chem>Clc1ccc(OCC(=O)N2CCNCC2)cc1</chem>
Prestw-Frag-1859	492-37-5	<chem>CC(C(=O)O)c1ccccc1</chem>
Prestw-Frag-1860	119-61-9	<chem>O=C(c1ccccc1)c2ccccc2</chem>
Prestw-Frag-1868	31252-42-3	<chem>C(C1CCNCC1)c2ccccc2</chem>
Prestw-Frag-1869	1021-25-6	<chem>O=C1NCN(c2ccccc2)C13CCNCC3</chem>
Prestw-Frag-1878	578-68-7	<chem>Nc1ccnc2ccccc12</chem>
Prestw-Frag-1884	118-93-4	<chem>CC(=O)c1ccccc1O</chem>
Prestw-Frag-1887	65875-39-0	<chem>N(CCNCc1ccc(cc1)OC)(C)C</chem>
Prestw-Frag-1889	66356-53-4	<chem>CN(C)Cc1oc(CSCCN)cc1</chem>
Prestw-Frag-1894	70-55-3	<chem>Cc1ccc(cc1)S(=O)(=O)N</chem>
Prestw-Frag-1895	98-10-2	<chem>NS(=O)(=O)c1ccccc1</chem>
Prestw-Frag-1898	1747-60-0	<chem>COc1ccc2nc(N)sc2c1</chem>
Prestw-Frag-1902	07/07/5755	<chem>O=C1CCNc2ccccc2N1</chem>

Prestw Frag Number	CAS number	Smiles code
Prestw-Frag-1923	7111-76-4	<chem>Cc1ccccc1C(O)c2ccccc2</chem>
Prestw-Frag-1924	365-24-2	<chem>OC(c1ccc(F)cc1)c2ccc(F)cc2</chem>
Prestw-Frag-1935	29654-55-5	<chem>OCc1cc(O)cc(O)c1</chem>
Prestw-Frag-1941	16735-19-6	<chem>CC(N)C(=O)c1ccccc1</chem>
Prestw-Frag-1952	03/10/2603	<chem>COC(=O)Nc1ccccc1</chem>
Prestw-Frag-1961	5330-97-2	<chem>ONC(=O)Cc1ccccc1</chem>
Prestw-Frag-1968	2215-77-2	<chem>OC(=O)c1ccc(Oc2ccccc2)cc1</chem>
Prestw-Frag-1971	5451-39-8	<chem>NC(=O)Cc1ccccc1</chem>
Prestw-Frag-1993	1665-59-4	<chem>CCN(CC)CCNc1ccccc1</chem>
Prestw-Frag-1996	5294-61-1	<chem>Cc1cccc(C)c1NC(=O)CN2CCNCC2</chem>
Prestw-Frag-1999	51-45-6	<chem>NCCc1c[nH]cn1</chem>
Prestw-Frag-2017	65-71-4	<chem>CC1=CNC(=O)NC1=O</chem>
Prestw-Frag-2018	6873-44-5	<chem>CNC(=O)c1ccc(Cl)cc1</chem>
Prestw-Frag-2021	19947-75-2	<chem>Cc1noc(N)c1C</chem>
Prestw-Frag-2023	5183-78-8	<chem>CNS(=O)(=O)c1ccccc1</chem>
Prestw-Frag-2031	188758-93-2	<chem>CN(C)CCNC(=O)c1ccc(N)cc1</chem>
Prestw-Frag-2047	67914-60-7	<chem>CC(=O)N1CCN(CC1)c2ccc(O)cc2</chem>
Prestw-Frag-2051	1205-30-7	<chem>NS(=O)(=O)c1cc(ccc1Cl)C(=O)O</chem>
Prestw-Frag-2052	501661-50-3	<chem>OC(=O)c1ccccc1NCc2occc2</chem>
Prestw-Frag-2058	No CAS	<chem>COc1cc(N)c(Cl)cc1C(=O)NC2CCNCC2</chem>
Prestw-Frag-2060	1205-72-7	<chem>NC1CCN(Cc2ccccc2)CC1</chem>
Prestw-Frag-2070	51-67-2	<chem>NCCc1ccc(O)cc1</chem>
Prestw-Frag-2072	5469-70-5	<chem>Nc1ccccc1</chem>
Prestw-Frag-2092	29342-05-0	<chem>CC1=CC(=O)N(O)C(=C1)C2CCCCC2</chem>
Prestw-Frag-2100	6343-32-4	<chem>CN(C)C(c1ccccc1)c2ccccc2</chem>
Prestw-Frag-2108	402-52-8	<chem>COc1ccc(cc1)C(F)(F)F</chem>
Prestw-Frag-2111	80663-95-2	<chem>NC(=N)NCc1cccc(l)c1</chem>
Prestw-Frag-2118	91168-31-9	<chem>COc1ccc2[nH]c(SC)nc2c1</chem>
Prestw-Frag-2124	0	<chem>CCN(CC)S(=O)(=O)c1ccccc1</chem>
Prestw-Frag-2127	56-04-2	<chem>CC1=CC(=O)NC(=S)N1</chem>
Prestw-Frag-2131	1452-77-3	<chem>NC(=O)c1ccccc1</chem>
Prestw-Frag-2136	615-15-6	<chem>Cc1nc2ccccc2[nH]1</chem>
Prestw-Frag-2140	1918-77-0	<chem>OC(=O)Cc1cccs1</chem>
Prestw-Frag-2144	87-41-2	<chem>O=C1OCc2ccccc12</chem>
Prestw-Frag-2152	3516-95-8	<chem>Oc1ccccc1C(=O)CCc2ccccc2</chem>
Prestw-Frag-2176	948007-59-8	<chem>OC1=CNS(=O)(=O)c2ccsc12</chem>
Prestw-Frag-2181	328-90-5	<chem>OC(=O)c1ccc(cc1)C(F)(F)F</chem>
Prestw-Frag-2183	670-95-1	<chem>c1ccc(cc1)c2c[nH]cn2</chem>
Prestw-Frag-2185	950-99-2	<chem>Cc1c(C)c2OC(C)(C)CCc2c(C)c1O</chem>
Prestw-Frag-2193	63283-42-1	<chem>COc1cc2CCNC(C)c2cc1OC</chem>
Prestw-Frag-2201	156-43-4	<chem>CCOc1ccc(N)cc1</chem>
Prestw-Frag-2210	No CAS	<chem>CC(CCCN(C)C)Nc1ccccc1</chem>
Prestw-Frag-2215	110475-31-5	<chem>C(N1CCNCC1)c2ccccc2</chem>
Prestw-Frag-2219	451-40-1	<chem>O=C(Cc1ccccc1)c2ccccc2</chem>
Prestw-Frag-2229	104-29-0	<chem>OCC(O)COc1ccc(Cl)cc1</chem>
Prestw-Frag-2235	599-67-7	<chem>CC(O)(c1ccccc1)c2ccccc2</chem>
Prestw-Frag-2239	6631-94-3	<chem>CC(=O)c1ccc2Sc3ccccc3Nc2c1</chem>
Prestw-Frag-2299	274-09-9	<chem>C1Oc2ccccc2O1</chem>
Prestw-Frag-2304	100-55-0	<chem>OCc1ccccc1</chem>
Prestw-Frag-2313	87-62-7	<chem>Cc1cccc(C)c1N</chem>
Prestw-Frag-2337	1220-83-3	<chem>COc1cc(NS(=O)(=O)c2ccc(N)cc2)ncn1</chem>



Prestw Frag Number	CAS number	Smiles code
Prestw-Frag-2346	619-45-4	<chem>COC(=O)c1ccc(N)cc1</chem>
Prestw-Frag-2352	4940-39-0	<chem>OC(=O)C1=CC(=O)c2ccccc2O1</chem>
Prestw-Frag-2373	872-35-5	<chem>Sc1ncc[nH]1</chem>
Prestw-Frag-2389	70918-74-0	<chem>O=C(C1COc2ccccc2O1)N3CCNCC3</chem>
Prestw-Frag-2397	101125-32-0	<chem>Fc1ccc(cc1)c2c[nH]c3ccccc23</chem>
Prestw-Frag-2408	20577-27-9	<chem>O=C1NC=CC=C1C#N</chem>
Prestw-Frag-2410	694-85-9	<chem>CN1C=CC=CC1=O</chem>
Prestw-Frag-2423	4358-87-6	<chem>COC(=O)C(O)c1ccccc1</chem>
Prestw-Frag-2440	14367-47-6	<chem>CCN(CCCCO)C(C)Cc1ccc(OC)cc1</chem>
Prestw-Frag-2443	504-29-0	<chem>Nc1cccn1</chem>
Prestw-Frag-2464	553-03-7	<chem>O=C1CCc2ccccc2N1</chem>
Prestw-Frag-2473	3306-62-5	<chem>Nc1ccccc1S(=O)(=O)N</chem>
Prestw-Frag-2477	14529-53-4	<chem>CCOc1cccn1</chem>
Prestw-Frag-2484	19833-96-6	<chem>COC(=O)C(O)(C1CCCC1)c2ccccc2</chem>
Prestw-Frag-2493	119-65-3	<chem>c1ccc2cnccc2c1</chem>
Prestw-Frag-2499	6100-60-3	<chem>COc1ccc(O)cc1O</chem>
Prestw-Frag-2501	290-37-9	<chem>c1cnccn1</chem>
Prestw-Frag-2506	89-84-9	<chem>CC(=O)c1ccc(O)cc1O</chem>
Prestw-Frag-2532	623-05-2	<chem>OCc1ccc(O)cc1</chem>
Prestw-Frag-2539	583-39-1	<chem>Sc1nc2ccccc2[nH]1</chem>
Prestw-Frag-2562	30165-97-0	<chem>Oc1nscn1N2CCOCC2</chem>
Prestw-Frag-2566	2415-80-7	<chem>ClC1(Cl)CC1c2ccccc2</chem>
Prestw-Frag-2576	495-69-2	<chem>OC(=O)CNC(=O)c1ccccc1</chem>
Prestw-Frag-2577	122-59-8	<chem>OC(=O)COc1ccccc1</chem>
Prestw-Frag-2578	621-88-5	<chem>NC(=O)COc1ccccc1</chem>
Prestw-Frag-2579	103-82-2	<chem>OC(=O)Cc1ccccc1</chem>
Prestw-Frag-2580	103-81-1	<chem>NC(=O)Cc1ccccc1</chem>
Prestw-Frag-2587	1453-82-3	<chem>NC(=O)c1ccncc1</chem>
Prestw-Frag-2592	148-24-3	<chem>Oc1cccc2ccncc12</chem>
Prestw-Frag-2593	635-27-8	<chem>Clc1cccc2ncccc12</chem>
Prestw-Frag-2600	1210-34-0	<chem>OC1c2ccccc2CCc3ccccc13</chem>
Prestw-Frag-2608	49823-14-5	<chem>C(Cn1ccnc1)c2ccccc2</chem>
Prestw-Frag-2620	4238-71-5	<chem>C(c1ccccc1)n2ccnc2</chem>
Prestw-Frag-2647	71486-43-6	<chem>Fc1ccc(cc1)C2(CCCCC2)C#N</chem>
Prestw-Frag-2652	6843-49-8	<chem>CC1(NC(=O)NC1=O)c2ccccc2</chem>
Prestw-Frag-2669	4241-27-4	<chem>CC1=CC=C(C#N)C(=O)N1</chem>
Prestw-Frag-2675	13754-86-4	<chem>O=C1CCc2[nH]ccc12</chem>
Prestw-Frag-2693	23485-68-9	<chem>OC(=O)CCc1oc(cn1)c2ccccc2</chem>
Prestw-Frag-2695	14224-99-8	<chem>Cc1oc(c2ccccc2)c(n1)c3ccccc3</chem>
Prestw-Frag-2701	552-41-0	<chem>COc1ccc(C(=O)C)c(O)c1</chem>
Prestw-Frag-2706	1518-84-9	<chem>Oc1ccccc1C2CCCC2</chem>
Prestw-Frag-2713	1121-07-9	<chem>CN1C(=O)CCC1=O</chem>
Prestw-Frag-2722	4022-81-5	<chem>NC(=N)NC(=N)Nc1ccc(Cl)cc1</chem>
Prestw-Frag-2755	1197-22-4	<chem>CS(=O)(=O)Nc1ccccc1</chem>
Prestw-Frag-2769	951-78-0	<chem>OC[C@H]1O[C@@H](C[C@H]1O)N2C=CC(=O)NC2=O</chem>
Prestw-Frag-2780	942-01-8	<chem>C1CCc2c(C1)[nH]c3ccccc23</chem>
Prestw-Frag-2789	No CAS	<chem>C(Oc1ccc2OCOc2c1)[C@H]3CCCCN3</chem>
Prestw-Frag-2794	4314-66-3	<chem>CCNC(=O)c1ccncc1</chem>
Prestw-Frag-2799	942-24-5	<chem>COC(=O)c1c[nH]c2ccccc12</chem>
Prestw-Frag-2803	119836-08-7	<chem>OC1CCN(CC1)c2ccccc2F</chem>
Prestw-Frag-2807	57978-41-3	<chem>OC(=O)c1ccncc1Nc2cccc(Cl)c2</chem>

Prestw Frag Number	CAS number	Smiles code
Prestw-Frag-2809	73279-04-6	Oc1cccc(CN2CCCC2)c1
Prestw-Frag-2818	26930-17-6	CCNC(=O)c1ccc(Cl)cc1
Prestw-Frag-2826	591-27-5	Nc1cccc(O)c1
Prestw-Frag-2849	127852-28-2	C[C@@H](O)c1cc(cc(c1)C(F)(F)F)C(F)(F)F
Prestw-Frag-2853	119532-26-2	Clc1cccc(N2CCNCC2)c1Cl
Prestw-Frag-2854	22246-18-0	Oc1ccc2CCC(=O)Nc2c1
Prestw-Frag-2887	18039-42-4	c1ccc(cc1)c2nnn[nH]2
Prestw-Frag-2898	95-95-4	Oc1cc(Cl)c(Cl)cc1Cl
Prestw-Frag-2912	90-90-4	Brc1ccc(cc1)C(=O)c2ccccc2
Prestw-Frag-2921	1357388-52-3	NCCCCN1CCN(CC1)c2ncccn2
Prestw-Frag-2935	1016519-99-5	Nc1cccc(Nc2ncccn2)c1
Prestw-Frag-2947	7042-36-6	CC(C)(C)OC(=O)C=Cc1ccccc1
Prestw-Frag-2958	23972-41-0	C1COC(CN1)c2ccccc2
Prestw-Frag-2960	104-01-8	COc1ccc(CC(=O)O)cc1
Prestw-Frag-2968	03/06/5223	CCc1ccc(CCO)nc1
Prestw-Frag-2972	2933-29-1	Nc1nc2CCCCc2s1
Prestw-Frag-2992	35604-67-2	CCOc1ccccc1OCC2CNCCO2
Prestw-Frag-2995	94-71-3	CCOc1ccccc1O
Prestw-Frag-3011	16096-33-6	c1ccc(cc1)n2ccc3ccccc23
Prestw-Frag-3012	0	CN1CCN(CC1)S(=O)(=O)c2ccccc2
Prestw-Frag-3017	88919-22-6	CNS(=O)(=O)Cc1ccc2[nH]cc(CCN)c2c1
Prestw-Frag-3033	91-19-0	c1ccc2nccnc2c1
Prestw-Frag-3046	43200-81-3	OC1N(C(=O)c2nccnc12)c3ccc(Cl)cn3
Prestw-Frag-3060	5925-93-9	Cc1ccc(N)c(c1)C#N
Prestw-Frag-3062	1875-88-3	OCCc1ccc(Cl)cc1
Prestw-Frag-3073	31251-41-9	Clc1ccc2C(=O)c3ncccc3CCc2c1
Prestw-Frag-3088	27829-46-5	CCN(CC)C(=O)C=Cc1ccccc1
Prestw-Frag-3090	3465-72-3	OC(=O)C=Cc1cnc[nH]1
Prestw-Frag-3100	56456-47-4	OCC1ccc(F)cc1F
Prestw-Frag-3101	3273-14-1	OCCn1cncn1
Prestw-Frag-3114	79047-41-9	CCCCc1nc(Cl)c(CO)[nH]1
Prestw-Frag-3137	635-46-1	C1CNc2ccccc2C1
Prestw-Frag-3150	1133115-40-8	Fc1ccnc1N2CCCC2
Prestw-Frag-3188	1730-48-9	COc1ccc2CCCCc2c1
Prestw-Frag-3190	91-76-9	Nc1nc(N)nc(n1)c2ccccc2
Prestw-Frag-3198	150322-73-9	Fc1ccccc1CC(=O)C2CC2
Prestw-Frag-3202	7055-03-0	Cc1ccccc1C(=O)Nc2ccccc2
Prestw-Frag-3221	277299-70-4	CC1=CC(=O)N(N1)c2ccc(C)c(C)c2
Prestw-Frag-3225	160968-99-0	Oc1ccccc1OCC(F)(F)F
Prestw-Frag-3241	641571-11-1	Cc1cn(cn1)c2cc(N)cc(c2)C(F)(F)F
Prestw-Frag-3247	108-79-2	Cc1cc(C)nc(O)n1
Prestw-Frag-3250	606-83-7	OC(=O)CC(c1ccccc1)c2ccccc2
Prestw-Frag-3253	762240-92-6	FC(F)(F)c1nnc2CNCCn12
Prestw-Frag-3262	96225-96-6	CN1CCN(CC1)c2cc(N)ncn2
Prestw-Frag-3264	951-77-9	NC1=NC(=O)N(C=C1)[C@H]2C[C@H](O)[C@@H](CO)O2
Prestw-Frag-3302	320-67-2	NC1=NC(=O)N(C=N1)[C@H]2O[C@H](CO)[C@@H](O)[C@H]2O
Prestw-Frag-3313	121751-67-5	COc1ccc(cc1)S(=O)(=O)N2CCNCC2
Prestw-Frag-3314	18637-00-8	CCOc1ccccc1C(=N)N
Prestw-Frag-3324	121-66-4	Nc1ncc(s1)[N+](=O)[O-]
Prestw-Frag-3329	707-99-3	Nc1ncnc2c1ncn2CCO
Prestw-Frag-3341	334981-10-1	Nc1ccc(CS(=O)(=O)N2CCCC2)cc1

Prestw Frag Number	CAS number	Smiles code
Prestw-Frag-3362	29268-15-3	CS(=O)(=O)NC(Cc1ccccc1)C(=O)O
Prestw-Frag-3382	614-18-6	CCOC(=O)c1cccnc1
Prestw-Frag-3458	5625-67-2	O=C1CNCCN1
Prestw-Frag-3462	70146-15-5	NC1CCc2ccccc12
Prestw-Frag-3463	109-11-5	O=C1COCCN1
Prestw-Frag-3664	52867-35-3	CN1NC(=O)C=C1
Prestw-Frag-3665	39742-60-4	O=C1CCN(CCc2ccccc2)CC1
Prestw-Frag-3667	56341-41-4	Fc1ccc2NC(=O)Cc2c1
Prestw-Frag-3668	5292-21-7	OC(=O)CC1CCCC1
Prestw-Frag-3669	54060-30-9 No CAS in reaxys for HCl salt	Nc1cccc(c1)C#C
Prestw-Frag-3670	16153-81-4	CN1CCN(CC1)c2ccc(N)cc2
Prestw-Frag-3671	26116-12-1	CCN1CCCC1CN
Prestw-Frag-3673	70931-28-1	Fc1ccc(CN2CCNCC2)cc1
Prestw-Frag-3677	13754-38-6	O=C(N1CCNCC1)c2ccccc2
Prestw-Frag-3678	4887-80-3	COc1ccc2[nH]cnc2c1
Prestw-Frag-3679	05/05/5424	Nc1cnc2ccccc2n1
Prestw-Frag-3680	1075-89-4	O=C1CC2(CCC2)CC(=O)N1
Prestw-Frag-3682	2217-43-8	Nc1ccc2CCCCc2c1
Prestw-Frag-3683	7552-07-0	Nc1ncns1
Prestw-Frag-3686	3162-29-6	CC(=O)c1ccc2OCOc2c1
Prestw-Frag-3689	22600-77-7	NCc1ncc[nH]1
Prestw-Frag-3690	60986-88-1	CNC(=O)c1c(C)onc1c2ccccc2
Prestw-Frag-3696	2380-94-1	Oc1ccc2[nH]cnc2
Prestw-Frag-3698	20295-64-8	COc1cc2CCNC(=O)Cc2cc1OC
Prestw-Frag-3705	138713-44-7	C1COCC(N1)c2ccccc2
Prestw-Frag-3706	65487-32-3	CC(C(=O)O)c1cccc(F)c1
Prestw-Frag-3709	61894-99-3	NC1CCc2[nH]c3ccccc3c2C1
Prestw-Frag-3711	117-34-0	OC(=O)C(c1ccccc1)c2ccccc2
Prestw-Frag-3712	7500-40-5	C1CNCCC(C1)c2ccccc2
Prestw-Frag-3713	1470-94-6	Oc1ccc2CCc2c1
Prestw-Frag-3716	24666-56-6	NC1CCC(=O)NC1=O
Prestw-Frag-3717	515-30-0	CC(O)(C(=O)O)c1cccc1
Prestw-Frag-3718	1373253-20-3	O=C1CNCCN1
Prestw-Frag-3722	39244-80-9	C(N1CCNCC1)c2ccccc2
Prestw-Frag-3723	474711-89-2	NC(=O)N1CCNCC1
Prestw-Frag-3724	5272-86-6	Cc1n[nH]c(C)c1N
Prestw-Frag-3726	20154-03-4	FC(F)(F)c1cc[nH]n1
Prestw-Frag-3727	6457-49-4	OCC1CCNCC1
Prestw-Frag-3728	4606-65-9	OCC1CCCNCC1
Prestw-Frag-3729	51047-52-0	C1CN(CCN1)c2ccccc2
Prestw-Frag-3730	15029-30-8	O=C(CC#N)N1CCCC1
Prestw-Frag-3731	26391-06-0	CCN(CC)C(=O)CC#N
Prestw-Frag-3732	98491-38-4	C1COc2ccccc2N1
Prestw-Frag-3733	21404-94-4	CC(C)(CN)c1ccccc1
Prestw-Frag-3734	22433-69-8	O=C1NC=NC=C1c2ccccc2
Prestw-Frag-3735	1196-38-9	O=C1NCCc2ccccc12
Prestw-Frag-3738	1011-17-2	Oc1cccc1N2CCNCC2
Prestw-Frag-3739	2471-69-4	COc1ccc2CC(CCc2c1)C(=O)O
Prestw-Frag-3740	1622-57-7	Cn1c(N)nc2ccccc12
Prestw-Frag-3741	495-76-1	OCc1ccc2OCOc2c1
Prestw-Frag-3742	89-25-8	CC1=CC(=O)N(N1)c2ccccc2

Prestw Frag Number	CAS number	Smiles code
Prestw-Frag-3743	1826-16-0	Cc1nc(cs1)c2ccccc2
Prestw-Frag-3744	7164-98-9	c1ccc(cc1)n2ccnc2
Prestw-Frag-3745	1355248-06-4	Cc1nc(cs1)c2ccccc2F
Prestw-Frag-3746	885066-15-9	NCCc1ccc(F)cc1F
Prestw-Frag-3747	1357352-51-2	NCc1cscn1
Prestw-Frag-3749	10578-75-3	NCCOCc1ccccc1
Prestw-Frag-3750	17379-01-0	C1Cc2ccccc2CCN1
Prestw-Frag-3751	935-43-3	NCC1(CC1)c2ccccc2
Prestw-Frag-3752	38585-62-5	Cc1[nH]cnc1CO
Prestw-Frag-3753	106243-23-6	C1CC(CCN1)c2c[nH]cn2
Prestw-Frag-3754	100206-86-8	CNC(=O)c1cc(Cl)c(N)cc1OC
Prestw-Frag-3755	625442-71-9	CC(CO)Nc1ccccc1
Prestw-Frag-3756	89895-06-7	CC(=O)C1CCNCC1
Prestw-Frag-3757	108-29-2	CC1CCC(=O)O1

Table 9.10: Prestwick approved drug library.

Prestwick Nr.	CAS number	Smiles code
Prestw-1	134-58-7	c12/N=C(\NC(c1nn[nH]2)=O)/N
Prestw-2	97-59-6	N1C(NC(C1=O)NC(=O)N)=O
Prestw-3	59-66-5	c1(S(=O)(=O)N)sc(nn1)NC(=O)C
Prestw-4	1115-70-4	C(NC(=N)N)(=N)N(C)C
Prestw-5	64228-81-5	[N+](C(c2c(cc(c2)OC)OC)CC1)Cc1cc(c(cc1)OC)OC)(CCC(=O)OCCCOCC(C[N+](C(c2c(cc(c2)OC)OC)CC1)Cc1cc(c(cc1)OC)OC)C)=O)C
Prestw-6	338-98-7	[C@]12([C@@](C(COC(=O)C)=O)(CC[C@]1([C@]1([C@@]([C@@]3(\C=C/C(\C=C3)=O)\C C1)C)([C@H](C2)O)F)[H])[H])O)C
Prestw-7	17440-83-4	c1(nc(c(nc1N)N)Cl)C(NC(=N)N)=O
Prestw-8	137-88-2	[n+](Cc2c(nc(nc2)CCC)N)c(C)cccc1
Prestw-9	58-93-5	S1(c2cc(S(=O)(=O)N)c(cc2NCN1)Cl)(=O)=O
Prestw-10	57-67-0	S(NC(=N)N)(c1ccc(N)cc1)(=O)=O
Prestw-11	1084-65-7	S1(c2cc(S(=O)(=O)N)c(cc2CCC1)C)(=O)=O
Prestw-12	104-31-4	c1c(ccc(c1)C(OCCOC)=O)NCCCC
Prestw-13	135-09-1	S1(c2cc(S(=O)(=O)N)c(C(F)(F)F)cc2NCN1)(=O)=O
Prestw-14	6209-17-2	S(N(C(=O)C)[Na])(c1ccc(N)cc1)(=O)=O
Prestw-15	543-15-7	C(O)(CCCC(N)C)(C)C
Prestw-16	72-14-0	S(Nc1nccs1)(c1ccc(N)cc1)(=O)=O
Prestw-17	59-92-7	C([C@H](Cc1cc(c(cc1)O)O)N)(=O)O
Prestw-18	54-42-2	N1(C(NC(/C=C1)/I)=O)=O)[C@@H]1O[C@@H]([C@H](C1)O)CO
Prestw-19	62571-86-2	N1(C([C@@H](CS)C)=O)[C@H](C(=O)O)CCC1
Prestw-20	38304-91-5	N=1/C(N(/C(=C1)N1CCCC1)/N)O=N
Prestw-21	526-08-9	S(Nc1n(ccc1)c1ccccc1)(c1ccc(N)cc1)(=O)=O
Prestw-22	81-13-0	C([C@@H](C(CO)(C)C)O)(=O)NCCCCO
Prestw-23	68-35-9	S(Nc1ncccc1)(c1ccc(N)cc1)(=O)=O
Prestw-24	68-23-5	C=1/2/[C@@]3([C@]([C@]4([C@@]([C@](C#C)(CC4)O)(CC3)C)[H])(CC\C1\CC(=O)CC2)[H])[H]
Prestw-25	15318-45-3	S(c1ccc([C@H]([C@H](NC(C(Cl)Cl)=O)CO)O)cc1)(=O)(=O)C
Prestw-26	51481-61-9	c1(nc[nH]c1C)CSCC/N=C(\NC#N)/NC
Prestw-27	562-10-7	C(c1ncccc1)(c1ccccc1)(OCCN(C)C)C
Prestw-28	1070-11-7	N([C@@H](CO)CC)CCN[C@@H](CO)CC
Prestw-29	60-80-0	C\1(N(N(\C=C1)C)C)c1ccccc1)=O
Prestw-30	1672-63-5	C1(\C=C(/N1c1ccccc1)C)C)O=O
Prestw-31	56-75-7	[N+](c1ccc([C@H]([C@H](NC(C(Cl)Cl)=O)CO)O)cc1)([O-])=O
Prestw-32	18694-40-1	n1(c2nc(cc(n2)C)OC)c(cc(n1)C)OC

Prestwick Nr.	CAS number	Smiles code
Prestw-33	479-18-5	<chem>c12c(C(N(C(N1C)=O)C)=O)n(cn2)CC(O)CO</chem>
Prestw-34	396-01-0	<chem>c12c(nc(c(n1)N)c1cccc1)c(nc(n2)N)N</chem>
Prestw-35	80-08-0	<chem>S(c1ccc(N)cc1)(c1ccc(N)cc1)(=O)=O</chem>
Prestw-36	2751-09-9	<chem>[C@@]12(C([C@@H]([C@H]([C@H]([C@H](OC([C@@H]([C@H]([C@@H]([C@@H](O[C@@H]3[C@@H]([C@H](C[C@H](O3)C)N(C)C)OC(=O)C)[C@H](C1)C)C)O[C@@H]1O[C@H]([C@H]([C@H](C1)OC)OC(=O)C)C)=O)C)C)OC(=O)C)C)=O)OC2</chem>
Prestw-37	58-14-0	<chem>n1c(c(c(nc1N)CC)c1ccc(cc1)Cl)N</chem>
Prestw-38	55-97-0	<chem>[N+](CCCCC[N+](C)(C)C)(C)C</chem>
Prestw-39	22494-42-4	<chem>c1(cc(c2c(cc(cc2)F)F)ccc1O)C(=O)O</chem>
Prestw-40	50-65-7	<chem>[N+](c1cc(c(NC(c2c(ccc(c2)Cl)O)=O)cc1)Cl)([O-])=O</chem>
Prestw-41	51-05-8	<chem>C(c1ccc(N)cc1)(=O)OCCN(CC)CC</chem>
Prestw-42	964-52-3	<chem>c1(cc(c(cc1OCCN(C)C)C)OC(=O)C)C(C)C</chem>
Prestw-43	138-92-1	<chem>n1[nH]ccc1CCN</chem>
Prestw-44	34552-84-6	<chem>S1(N(/C(=C(\c2c1cccc2)/O)/C(Nc1noc(c1)C)=O)C)(=O)=O</chem>
Prestw-45	22204-53-1	<chem>COc1ccc2cc(ccc2c1)[C@H](C)C(=O)O</chem>
Prestw-46	550-99-2	<chem>C/1(=N/CCN1)\Cc1c2c(ccc1)cccc2</chem>
Prestw-47	53885-35-1	<chem>c12c(scc1)CCN(C2)Cc1c(Cl)cccc1</chem>
Prestw-48	67-92-5	<chem>C1(C(=O)OCCN(CC)CC)(C2CCCC2)CCCC1</chem>
Prestw-49	532-59-2	<chem>C(OC(CN(C)C)(CC)C)(=O)c1cccc1</chem>
Prestw-50	73-78-9	<chem>c1(NC(=O)CN(CC)CC)c(ccc1)C</chem>
Prestw-1795	12650-69-0	<chem>CC(=CC(=O)O)CCCCCCCC(=O)O)CC1OCC(C(C1O)O)CC1C(C(C(C)O)C)O1</chem>
Prestw-52	298-46-4	<chem>N1(C(=O)N)c2c(\C=C/c3c1cccc3)cccc2</chem>
Prestw-53	1098-60-8	<chem>N1(c2c(Sc3c1cccc3)ccc(C(F)(F)F)c2)CCN(C)C</chem>
Prestw-54	61-68-7	<chem>c1(c(Nc2c(c(ccc2)C)C)cccc1)C(=O)O</chem>
Prestw-55	968-81-0	<chem>S(NC(NC1CCCC1)=O)(c1ccc(C(=O)C)cc1)(=O)=O</chem>
Prestw-56	15676-16-1	<chem>S(c1cc(C(NCC2N(CCC2)CC)=O)c(cc1)OC)(=O)(=O)N</chem>
Prestw-57	5987-82-6	<chem>C(c1cc(c(cc1)N)OCCCC)(=O)OCCN(CC)CC</chem>
Prestw-58	126-27-2	<chem>C(N(C(Cc1cccc1)(C)C)C)(CN(CC(N(C(Cc1cccc1)(C)C)C)=O)CCO)=O</chem>
Prestw-59	132-20-7	<chem>C(CCN(C)C)(c1ncccc1)c1cccc1</chem>
Prestw-60	59-97-2	<chem>C/1(=N/CCN1)\Cc1cccc1</chem>
Prestw-61	26155-31-7	<chem>C=1(/N(CCC\N1)C)\C=C\c1c(ccs1)C</chem>
Prestw-62	51-56-9	<chem>N1([C@]2(C[C@H](OC(C(c3cccc3)O)=O)C[C@@]1(CC2)[H])[H])C</chem>
Prestw-63	21829-25-4	<chem>C=1(\C(\C(=C(/N/C1)C)\C)C(=O)OC)c1c([N+](O)=O)cccc1)/C(=O)OC</chem>
Prestw-64	69-09-0	<chem>N1(c2c(Sc3c1cccc3)ccc(c2)Cl)CCN(C)C</chem>
Prestw-65	147-24-0	<chem>C(c1cccc1)(c1cccc1)OCCN(C)C</chem>
Prestw-66	25953-17-7	<chem>n1nc(cc(c1NCCN1CCOCC1)C)c1cccc1</chem>
Prestw-67	22916-47-8	<chem>c1(c(cc(cc1)Cl)Cl)C(Cn1ncc1)OCc1c(cc(cc1)Cl)Cl</chem>
Prestw-68	579-56-6	<chem>N(C(C(c1ccc(cc1)O)O)C)C(COc1cccc1)C</chem>
Prestw-69	34381-68-5	<chem>c1(c(OCC(CNC(C)C)O)ccc(NC(=O)CCC)c1)C(=O)C</chem>
Prestw-70	2398-96-1	<chem>C(N(c1cc(ccc1)C)C)(Oc1cc2c(cc1)cccc2)=S</chem>
Prestw-71	3778-76-5	<chem>c1(nncc2c1cccc2)NNC(=O)OCC</chem>
Prestw-72	113-52-0	<chem>N1(c2c(CCc3c1cccc3)cccc2)CCN(C)C</chem>
Prestw-73	38194-50-2	<chem>C/1(\C(=C(/c2c1ccc(c2)F)\CC(=O)O)\C)=C/c1ccc(S(=O)C)cc1</chem>
Prestw-74	549-18-8	<chem>C/1(\c2c(CCc3c1cccc3)cccc2)=C/CCN(C)C</chem>
Prestw-75	50-42-0	<chem>C(C(c1cccc1)c1cccc1)(=O)OCCN(CC)CC</chem>
Prestw-76	85-79-0	<chem>c1(C(=O)NCCN(CC)CC)c2c(nc(c1)OCCCC)cccc2</chem>
Prestw-77	53-03-2	<chem>[C@]12([C@@](C(=O)CO)(CC[C@]1([C@]1([C@@]([C@@]3(\C(=C/C(\C=C3)=O)\CC1)C)(C(C2)=O)[H])[H])[H])O)C</chem>
Prestw-78	130-61-0	<chem>N1(c2c(Sc3c1cccc3)ccc(c2)SC)CCC1N(C)CCCC1</chem>
Prestw-79	62-97-5	<chem>[N+]1(CC/C(=C(/c2cccc2)\c2cccc2)/CC1)(C)C</chem>
Prestw-80	554-92-7	<chem>c1(c(cc(C(NC2ccc(cc2)OCCN(C)C)=O)cc1OC)OC)OC</chem>
Prestw-81	443-48-1	<chem>c1(n(c(nc1)C)CCO)[N+](O)=O</chem>

Prestwick Nr.	CAS number	Smiles code
Prestw-1424	129453-61-8	[C@]12([C@](C[C@]3([C@]1([C@@H](Cc1c3ccc(c1)O)CCCCCCCCS(=O)CCCC(F)(F)F)(F)F)[H])[H])([C@H](CC2O)C)[H]
Prestw-83	116-38-1	[N+](c1cc(O)ccc1)(CC)(C)C
Prestw-84	3160-91-6	C(NC(=N)N)(N1CCOCC1)=N
Prestw-85	1134-47-0	C(CC(c1ccc(cc1)Cl)CN)(=O)O
Prestw-86	59277-89-3	c1/2c(ncn1COCCO)C(N/C(=N2)/N)=O
Prestw-87	364-98-7	S1(N/C(=N)c2c1cc(cc2)Cl)/C(=O)=O
Prestw-88	58-15-1	C1(\C=C(/N(N1c1cccc1)C)C)\N(C)C)=O
Prestw-1179	55-98-1	S(=O)(=O)(OCCCCOS(=O)(=O)C)C
Prestw-90	13523-86-9	c12c([nH]cc1)cccc2OCC(CNC(C)C)O
Prestw-91	82-02-0	c12c(c(c3c(c1OC)ccc3)OC)O\C(=C/C2=O)\C
Prestw-92	61129-30-4	C(=C\N(C)C)(\c1ccc(cc1)Br)/c1cnccc1
Prestw-93	115-46-8	C(c1cccc1)(c1cccc1)(C1CCNCC1)O
Prestw-94	446-86-6	c1(c(Sc2c3c([nH]cn3)ncn2)n(cn1)C)[N+](O-)=O
Prestw-95	52-76-6	[C@]12([C@]([C@]3([C@@]([C@@]4(\C(\CC3)=C/CCC4)[H])(CC1)[H])[H])(CC[C@]2(C#C)O)[H])C
Prestw-96	23256-50-0	c1(c(Cl)cccc1Cl)/C=N/NC(=N)N
Prestw-97	97-77-8	C(SSC(=S)N(CC)CC)(=S)N(CC)CC
Prestw-98	530-75-6	C(c1c(OC(=O)C)cccc1)(Oc1c(C(=O)O)cccc1)=O
Prestw-99	21535-47-7	N12C(c3c(Cc4c1cccc4)cccc3)CN(CC2)C
Prestw-100	31430-18-9	c1(nc2c([nH]1)ccc(Cc1sccc1)=O)c2)NC(=O)OC
Prestw-101	41372-20-7	[C@@]12(c3c(c4c(C1)ccc(c4O)O)cccc3CCN2C)[H].[C@@]12(c3c(c4c(C1)ccc(c4O)O)cccc3CCN2C)[H]
Prestw-102	14028-44-5	C1(=Nlc2c(Oc3c1cc(cc3)Cl)cccc2)/N1CCNCC1
Prestw-103	969-33-5	C1(/c2c(\C=C/c3c1cccc3)cccc2)=C1/CCN(CC1)C
Prestw-104	76824-35-6	S(NC(=N)CCSCc1nc(\N=C(/N)N)sc1)(=O)(=O)N
Prestw-105	17230-88-5	[C@]12(\C=C/c3c(C1)cn3)CC[C@]1([C@@]2(CC[C@]2([C@]1(CC[C@]2(C#C)O)[H])C)[H])[H]C
Prestw-106	65141-46-0	[N+](O-)(=O)OCCNC(c1cnccc1)=O
Prestw-1314	111025-46-8	N1C(SC(C1=O)Cc1ccc(cc1)OCCc1ncc(cc1)CC)=O
Prestw-108	32795-47-4	c12c(C(CN(C1)C)c1cccc1)cccc2N
Prestw-1810	173334-57-1	CC(C)[C@@H](Cc1ccc(c(c1)OCCOC)OC)C[C@@H]([C@H](C[C@@H](C(C)C)C(=O)NCC(C)C(=O)N)O)N
Prestw-1192	53-39-4	[C@]12([C@@]3([C@]([C@]4([C@@]([C@](CC4)O)C)(CC3)C)[H])(CC[C@]1(CC(OC2)=O)[H])[H])[H]C
Prestw-111	357-08-4	[C@]123[C@@]4([C@H](N(CC1)CC=C)Cc1c2c(O[C@H]3C(CC4)=O)c(cc1)O)O
Prestw-112	17560-51-9	N1(C(c2c(NC1)C)cc(c(S(=O)(=O)N)c2)Cl)=O)c1c(C)cccc1
Prestw-113	93107-08-5	C=1(/C(c2c(N\C1)C1CC1)cc(c(c2)F)N1CCNCC1)=O)\C(=O)O
Prestw-114	7177-48-2	N12[C@@H]([C@@H](C1=O)NC([C@@H](c1cccc1)N)=O)SC([C@@H]2C(=O)O)(C)C
Prestw-115	52-86-8	C1(CCN(CC1)CCCC(c1ccc(cc1)F)=O)(c1ccc(cc1)Cl)O
Prestw-116	16676-29-2	[C@]123[C@@]4([C@H](N(CC5CC5)CC1)Cc1c2c(O[C@H]3C(CC4)=O)c(cc1)O)O
Prestw-117	113-92-8	C(CCN(C)C)(c1ccc(cc1)Cl)c1ncccc1
Prestw-118	23277-43-2	[C@]123[C@@]4([C@H](N(CC1)CC1CCC1)Cc1c2c(O[C@H]3[C@H](CC4)O)c(cc1)O)O
Prestw-119	80530-63-8	c1(C(NCc2cnccc2)=O)cc(C(NCc2cnccc2)=O)ccc1OC
Prestw-120	124-94-7	[C@]12([C@]([C@@H](C[C@]1([C@]1([C@@]([C@@]3(\C=C/C(\C=C3)=O)\CC1)C)([C@H](C2)O)F)[H])[H])O)(C(=O)CO)O
Prestw-121	22260-51-1	N12[C@@]([O[C@](C1=O)(NC([C@@H]1\C=C/3\c4c5c(c([nH]c5ccc4)Br)C[C@]3(N(C1)C)[H])=O)C(C)C)([C@]1(N(C([C@@H]2CC(C)C)=O)CCC1)[H])O
Prestw-1471	90-84-6	C(C(N(CC)CC)C)(=O)c1cccc1
Prestw-123	81-23-2	[C@]12([C@]([C@]3([C@@]([C@@]4([C@](CC3=O)(CC(=O)CC4)[H])C)(CC1=O)[H])[H])(CC[C@@H]2[C@@H](CCC(=O)O)C)[H]C
Prestw-1184	65899-73-2	c1(c(scc1)Cl)COC(c1c(cc(cc1)Cl)Cl)Cn1cncc1
Prestw-125	58-39-9	N1(c2c(Sc3c1cccc3)ccc(c2)Cl)CCCN1CCN(CC1)CCO
Prestw-126	51773-92-3	c12nc(C(F)F)F)cc(c1cccc2C(F)F)C(C1NCCCC1)O



Prestwick Nr.	CAS number	Smiles code
Prestw-166	138-37-4	<chem>S(c1ccc(cc1)CN)(=O)(=O)N</chem>
Prestw-167	not available	<chem>c1(nc2c(s1)cc(OC(F)(F)F)cc2)N</chem>
Prestw-168	67-20-9	<chem>C1(NC(CN1/N=C/c1oc([N+][O-])=O)cc1)=O</chem>
Prestw-169	304-20-1	<chem>C/1(N=N/C=C/2\1C1\C=C/C=C2)=N\N</chem>
Prestw-170	156-51-4	<chem>N(N)CCc1ccccc1</chem>
Prestw-171	1197-18-8	<chem>C([C@H]1CC[C@@H](CC1)CN)(=O)O</chem>
Prestw-172	519-37-9	<chem>c12c(C(N(C(N1C)=O)C)=O)n(cn2)CCO</chem>
Prestw-173	1986-47-6	<chem>[C@H]1(C[C@@H]1N)c1ccccc1</chem>
Prestw-174	5560-59-8	<chem>N(CCCc1ccccc1)(CCc1ccccc1)CC</chem>
Prestw-175	89796-99-6	<chem>N(c1c(Cl)cccc1Cl)c1c(CC(=O)OCC(=O)O)cccc1</chem>
Prestw-176	305-33-9	<chem>C(NNC(C)C)(=O)c1ccncc1</chem>
Prestw-177	723-46-6	<chem>S(Nc1noc(c1)C)(c1ccc(N)cc1)(=O)=O</chem>
Prestw-178	59-47-2	<chem>O(c1c(C)cccc1)CC(O)CO</chem>
Prestw-179	834-28-6	<chem>N(C(=N)NCCc1ccccc1)C(=N)N</chem>
Prestw-180	13311-84-7	<chem>c1(C(F)(F)F)c([N+][O-])=O)ccc(NC(=O)C(C)C)c1</chem>
Prestw-181	83-07-8	<chem>C1(\C=C/N(N1c1ccccc1)C)\C)\N)=O</chem>
Prestw-182	16595-80-5	<chem>C/1\2=N/[C@H](CN1CCS2)c1ccccc1</chem>
Prestw-183	306-07-0	<chem>C(#C)CN(Cc1ccccc1)C</chem>
Prestw-184	532-03-6	<chem>C(=O)(OCC(COc1c(OC)cccc1)O)N</chem>
Prestw-185	78110-38-0	<chem>N1(C([C@H]([C@@H]1C)NC(/C(/c1nc(sc1)N)=N)OC(C(=O)O)(C)C)=O)S(=O)(=O)O</chem>
Prestw-186	642-78-4	<chem>N12[C@@]([C@H](C1=O)NC(c1c(noc1C)c1c(Cl)cccc1)=O)(SC([C@H]2C([O-])=O)(C)C)[H]</chem>
Prestw-1812	175481-36-4	<chem>CC(=O)N[C@H](COC)C(=O)NCc1ccccc1</chem>
Prestw-188	52-62-0	<chem>[N+]1(CCCCC[N+]2(C)CCCC2)(C)CCCC1</chem>
Prestw-189	1214-39-7	<chem>c12c(nc[nH]1)ncnc2NCc1ccccc1</chem>
Prestw-190	64-77-7	<chem>S(NC(=O)NCCCC)(c1ccc(cc1)C)(=O)=O</chem>
Prestw-191	3092-17-9	<chem>c1(c(ccc(c1)OC)OC)C(CNC(=O)CN)O</chem>
Prestw-192	50-35-1	<chem>N1(C(c2c(C1=O)cccc2)=O)C1C(NC(=O)CC1)=O</chem>
Prestw-193	14698-29-4	<chem>C=1(/C(c2c(N(\1C)CC)cc1c(c2)OCO1)=O)\C(=O)O</chem>
Prestw-194	51803-78-2	<chem>S(Nc1c(cc([N+][O-])=O)cc1)Oc1ccccc1)(=O)(=O)C</chem>
Prestw-1231	85650-56-2	<chem>[C@]12([C@](c3c(Oc4c1cc(cc4)Cl)cccc3)(CN(C2)C)[H])[H]</chem>
Prestw-196	6493-05-6	<chem>c12c(C(N(C(N1C)=O)CCCC(=O)C)=O)n(cn2)C</chem>
Prestw-197	33402-03-8	<chem>c1([C@H]([C@@H](N)C)O)cc(O)ccc1</chem>
Prestw-198	18559-94-9	<chem>c1(cc(ccc1O)C(CNC(C)C)C)O)CO</chem>
Prestw-199	1786-81-8	<chem>C(Nc1c(C)cccc1)(=O)C(NCCC)C</chem>
Prestw-200	7689-03-4	<chem>N12C(\c3c(C1)cc1c(n3)cccc1)=C/C/1=C(\C2=O)/COC([C@]1(O)CC)=O</chem>
Prestw-201	66357-59-3	<chem>[N+]/(C=C(/NC)NCCSCc1oc(cc1)CN(C)C)/([O-])=O</chem>
Prestw-202	51-24-1	<chem>c1(c(cc(cc1)CC(=O)O)O)c1cc(c(cc1)O)I</chem>
Prestw-203	530-78-9	<chem>C(c1cc(Nc2c(C(=O)O)cccc2)ccc1)(F)(F)F</chem>
Prestw-204	42835-25-6	<chem>C1(=C\N2c3c(C1=O)cc(cc3CCC2C)F)/C(=O)O</chem>
Prestw-205	13710-19-5	<chem>c1(c(Nc2c(c(Cl)ccc2)C)cccc1)C(=O)O</chem>
Prestw-206	6385-02-0	<chem>c1(Nc2c(C([O-])=O)cccc2)c(c(ccc1Cl)C)Cl</chem>
Prestw-1181	5630-53-5	<chem>C/1\2=C/C[C@H]([C@]3([C@]4([C@@]([C@](C#C)(CC4)O)(CC[C@]13[H])C)[H])C)\CC(=O)CC2</chem>
Prestw-208	738-70-5	<chem>n1c(c(Cc2cc(c(c2)OC)OC)OC)cnc1N)N</chem>
Prestw-209	7232-21-5	<chem>c1(c(cc(c(c1)Cl)N)OC)C(=O)NCCN(CC)CC</chem>
Prestw-210	43210-67-9	<chem>c1(nc2c([nH]1)ccc(c2)Sc1ccccc1)NC(=O)OC</chem>
Prestw-211	36322-90-4	<chem>S1(N(\C(=C(/c2c1cccc2)\O)\C(Nc1ncccc1)=O)C)(=O)=O</chem>
Prestw-212	33401-94-4	<chem>C=1(\N(CCC/N1)C)/C=C/c1sccc1</chem>
Prestw-213	5053-08-7	<chem>C1(OC2(CCN(CC2)CCc2cccc2)CN1)=O</chem>
Prestw-214	25812-30-0	<chem>C(C(CCCO)c1c(ccc(c1)C)C)(C)C(=O)O</chem>



Prestwick Nr.	CAS number	Smiles code
Prestw-215	3413-64-7	<chem>C(=O)(NCCN(CC)CC)COc1ccc(cc1)OC</chem>
Prestw-216	51012-33-0	<chem>S(c1cc(C(=O)NCCN(CC)CC)c(cc1)OC)(=O)(=O)C</chem>
Prestw-217	31431-39-7	<chem>c1(nc2c([nH]1)ccc(C(=O)c1ccccc1)c2)NC(=O)OC</chem>
Prestw-218	36330-85-5	<chem>C(c1ccc(cc1)c1ccccc1)(=O)CCC(=O)O</chem>
Prestw-219	22071-15-4	<chem>C(c1cc(C(C(=O)O)C)ccc1)(=O)c1ccccc1</chem>
Prestw-220	26807-65-8	<chem>S(c1cc(C(NN2c3c(CC2C)cccc3)=O)ccc1Cl)(=O)(=O)N</chem>
Prestw-221	70458-96-7	<chem>C=1(\C(c2c(N(/C1)CC)cc(c2)F)N1CCNCC1)=O)/C(=O)O</chem>
Prestw-222	1397-94-0	<chem>C1(C(O[C@H]([C@@H]([C@H](C(O[C@@H]1C)=O)CCCCC)OC(=O)CC(C)C)=O)NC(c1c(c(NC(=O)[H])ccc1)O)=O</chem>
Prestw-223	1218-35-5	<chem>c1(c(cc(cc1C)C(C)(C)C)C)C\1=N\CCN1</chem>
Prestw-224	2315-02-8	<chem>c1(c(c(c(c1)C)C/C/1=N/CCN1)C)O)C(C)C</chem>
Prestw-225	2139-47-1	<chem>C=1(/C(N(N(\C1)C)C)c1ccccc1)=O)\NC(c1cnccc1)=O</chem>
Prestw-226	126-07-8	<chem>[C@]12(C(c3c(O1)c(c(cc3OC)OC)Cl)=O)/C=C\C(C[C@H]2C)=O)/OC</chem>
Prestw-227	1163-36-6	<chem>c1(n(c2c(n1)cccc2)Cc1ccc(Cl)cc1)CN1CCCC1</chem>
Prestw-228	1508-75-4	<chem>C(C(c1ccccc1)CO)(N(Cc1cnccc1)CC)=O</chem>
Prestw-229	23327-57-3	<chem>c12C(OCCN(Cc1cccc2)C)c1ccccc1</chem>
Prestw-230	73-05-2	<chem>N(c1cc(O)ccc1)(C\C1=N\CCN1)c1ccc(cc1)C</chem>
Prestw-231	41340-25-4	<chem>c12[nH]c3c(c1CCOC2(CC(=O)O)CC)cccc3CC</chem>
Prestw-232	6106-81-6	<chem>[C@]12([C@]([O1]([C@]1([N+][C@@]2(C[C@H](C1)OC([C@@H](c1ccccc1)CO)=O)[H])([O-])C)[H])[H])N1([C@@]2(C[C@@H](OC([C@H](c3ccccc3)CO)=O)C[C@]1(CC2)[H])[H])C</chem>
Prestw-233	101-31-5	<chem>N1([C@@]2(C[C@@H](OC([C@H](c3ccccc3)CO)=O)C[C@]1(CC2)[H])[H])C</chem>
Prestw-234	886-74-8	<chem>C(=O)(OCC(COc1ccc(Cl)cc1)O)N</chem>
Prestw-1771	61422-45-5	<chem>N/1(C(NC(/C=C1)/F)=O)=O)C(=O)NCCCCC</chem>
Prestw-236	20153-98-4	<chem>c1(c(cc(C(=O)OCCCN2CCN(CCC2)CCOC(c2cc(c(c2)OC)OC)OC)=O)cc1OC)OC)OC</chem>
Prestw-237	82419-36-1	<chem>N\12c3c(c(c(cc3C(\C=C1)\C(=O)O)=O)F)N1CCN(CC1)C)OCC2C</chem>
Prestw-238	98079-52-8	<chem>C=1(/C(c2c(N(\C1)CC)c(c(N1CC(NCC1)C)c(c2)F)F)=O)\C(=O)O</chem>
Prestw-239	341-69-5	<chem>c1(C(c2ccccc2)OCCN(C)C)c(C)cccc1</chem>
Prestw-240	6620-60-6	<chem>C(C(NC(=O)c1ccccc1)CCC(=O)O)(N(CCC)CCC)=O</chem>
Prestw-241	5370-01-4	<chem>c1(OCC(N)C)c(ccc1C)C</chem>
Prestw-242	3717-88-2	<chem>c12O\C=C(/C(c1ccc2C(=O)OCCN1CCCC1)=O)\C)c1ccccc1</chem>
Prestw-243	2438-72-4	<chem>C(=O)(NO)Cc1ccc(cc1)OCCCC</chem>
Prestw-244	125-84-8	<chem>C1(NC(=O)CCC1(c1ccc(N)cc1)CC)=O</chem>
Prestw-245	17692-31-8	<chem>N1(CCN(CC(O)CO)CC1)c1ccccc1</chem>
Prestw-246	85371-64-8	<chem>C(=N\C#N)/\NC(C(C)(C)C)\Nc1cnccc1</chem>
Prestw-247	54965-21-8	<chem>c1(nc2c([nH]1)ccc(c2)SCCC)NC(=O)OC</chem>
Prestw-248	4205-91-8	<chem>C/1(\Nc2c(Cl)cccc2Cl)=N/CCN1</chem>
Prestw-249	31677-93-7	<chem>C(c1cc(Cl)ccc1)(C(NC(C)(C)C)C)=O</chem>
Prestw-250	13707-88-5	<chem>O(c1c(CC=C)ccc1)CC(CNC(C)C)O</chem>
Prestw-251	58-94-6	<chem>S1(c2cc(S(=O)(=O)N)c(cc2\N=C/N1)Cl)(=O)=O</chem>
Prestw-252	3254-89-5	<chem>C(c1ccccc1)(c1ccccc1)(O)CCCN1CCCC1</chem>
Prestw-253	68-22-4	<chem>[C@]12([C@]([C@]3([C@@]([C@@]4(\C=C/C(=O)CC4)\CC3)[H])(CC1)[H])[H])(CC[C@]2(C#C)O)[H])C</chem>
Prestw-254	894-71-3	<chem>C/1(\c2c(CCc3c1cccc3)cccc2)=C\CCNC</chem>
Prestw-255	4394-00-7	<chem>c1(c(C(=O)O)occn1)Nc1cc(C(F)F)ccc1</chem>
Prestw-256	4759-48-2	<chem>C\1(/C=C/C=C/C=C/C=C\C(=O)O)/C)/C=C(\CCCC1(C)C)/C</chem>
Prestw-257	302-79-4	<chem>C\1(/C=C/C=C/C=C/C=C/C=C\C(=O)O)/C)/C=C(\CCCC1(C)C)/C</chem>
Prestw-258	2508-72-7	<chem>N(C/C/1=N/CCN1)(Cc1ccccc1)c1ccccc1</chem>
Prestw-259	58-54-8	<chem>c1(c(c(c(OCC(=O)O)cc1)Cl)Cl)C(C=C)CC=O</chem>
Prestw-260	55268-74-1	<chem>N1(C(=O)C2CCCC2)CC2N(C(C1)=O)CCc1c2cccc1</chem>
Prestw-261	434-03-7	<chem>[C@]12(\C=C/C(=O)CC1)\CC[C@@]1([C@@]2(CC[C@]2([C@]1(CC[C@]2(C#C)O)[H])C)[H])C</chem>
Prestw-262	550-70-9	<chem>C=C/CN1CCCC1)/(c1ccc(cc1)C)\c1ncccc1</chem>
Prestw-263	1229-29-4	<chem>C\1(/c2c(OCC3c1cccc3)cccc2)=C\CCN(C)C</chem>

Prestwick Nr.	CAS number	Smiles code
Prestw-264	536-43-6	<chem>N1(CCC(c2ccc(cc2)OCCCC)=O)CCCCC1</chem>
Prestw-265	523-87-5	<chem>C(c1ccccc1)(c1ccccc1)OCCN(C)C</chem>
Prestw-266	3737-09-5	<chem>C(C(=O)N)(CCN(C(C)C)C(C)C)(c1ncccc1)c1ccccc1</chem>
Prestw-267	23593-75-1	<chem>C(n1cncc1)(c1c(Cl)cccc1)(c1ccccc1)c1ccccc1</chem>
Prestw-268	42971-09-5	<chem>n1/2c3c(c4c1cccc4)CCN1[C@]3([C@])(/C=C2/C(=O)OCC)(CCC1)CC[H]</chem>
Prestw-269	17321-77-6	<chem>N1(c2cc(ccc2CCc2c1cccc2)Cl)CCCN(C)C</chem>
Prestw-270	13636-18-5	<chem>C(c1ccccc1)(c1ccccc1)CCNC(c1ccccc1)C</chem>
Prestw-271	1617-90-9	<chem>n12[C@](C[C@]3([C@]4(c1c(c1c2cccc1)CCN4CCC3)[H])CC)(C(=O)OC)O</chem>
Prestw-272	53-86-1	<chem>n1(c(c2c1ccc(c2)OC)CC(=O)O)C(c1ccc(cc1)Cl)=O</chem>
Prestw-273	53-06-5	<chem>[C@]12([C@@](C(=O)CO)(CC[C@]1([C@]1([C@@]([C@@]3(\C=C/C(=O)CC3)\CC1)C)(C(C2)=O)[H])[H])[H])O)C</chem>
Prestw-274	50-24-8	<chem>[C@]12([C@@](C(=O)CO)(CC[C@]1([C@]1([C@@]([C@@]3(\C=C/C(\C=C3)=O)\CC1)C)([C@H](C2)O)[H])[H])[H])O)C</chem>
Prestw-275	49562-28-9	<chem>C(C(Oc1ccc(C(c2ccc(cc2)Cl)=O)cc1)(C)C)(OC(C)C)=O</chem>
Prestw-276	28395-03-1	<chem>S(c1c(c(cc1)C(=O)O)NCCCC)Oc1ccccc1(=O)(=O)N</chem>
Prestw-277	32780-64-6	<chem>c1(cc(ccc1O)C(CNC(CCc1ccccc1)C)O)C(=O)N</chem>
Prestw-278	298-57-7	<chem>N1(C(c2ccccc2)c2ccccc2)CCN(CC1)C/C=C/c1ccccc1</chem>
Prestw-279	83-43-2	<chem>[C@]12(\C=C/C(\C=C1)=O)[C@H](C[C@@]1([C@@]2([C@H](C[C@@]2([C@@](C(=O)CO)(CC[C@]21[H])O)C)O)[H])[H])C</chem>
Prestw-280	6151-40-2	<chem>N12[C@@]([C@H](c3c4c(ncc3)ccc(c4)OC)O)(C[C@@]([C@H](C1)C=C)(CC2)[H])[H]</chem>
Prestw-281	514-36-3	<chem>[C@]12([C@@](C(COC(=O)C)=O)(CC[C@]1([C@]1(C([C@@]3(\C=C/C(=O)CC3)\CC1)C)([C@H](C2)O)F)[H])[H])O)C</chem>
Prestw-282	1944-12-3	<chem>c1(cc(cc1)O)O)C(CNC(Cc1ccc(cc1)O)C)O</chem>
Prestw-283	1982-36-1	<chem>N1(C(c2ccc(cc2)Cl)c2ccccc2)CCN(CCC1)C</chem>
Prestw-284	1642-54-2	<chem>C(N1CCN(CC1)C)(N(CC)CC)=O</chem>
Prestw-285	474-25-9	<chem>[C@]12([C@]([C@]3([C@@]([C@@]4([C@]([C@H]3O)(C[C@@H](CC4)O)[H])C)(CC1)[H])[H])(CC[C@@H]2[C@@H](CCC(=O)O)C)[H])C</chem>
Prestw-286	6724-53-4	<chem>C(CC1NCCCC1)(C1CCCCC1)C1CCCCC1</chem>
Prestw-287	1508-65-2	<chem>C(C(=O)OCC#CCN(CC)CC)(c1ccccc1)(C1CCCCC1)O</chem>
Prestw-288	749-02-0	<chem>C12(N(CNC1=O)c1ccccc1)CCN(CC2)CCCC(c1ccc(cc1)F)=O</chem>
Prestw-289	59-33-6	<chem>N(c1ncccc1)(Cc1ccc(cc1)OC)CCN(C)C</chem>
Prestw-290	57-96-5	<chem>N1(N(C(C1=O)CCS(=O)c1ccccc1)=O)c1ccccc1c1ccccc1</chem>
Prestw-291	14663-23-1	<chem>N1=C(N(CC1=O)/N=C/c1oc(cc1)c1ccc([N+][O-])=O)cc1)[O-]</chem>
Prestw-292	25332-39-2	<chem>N1/2C(N(\N=C1\C=C/C=C2)CCCN1CCN(c2cc(Cl)ccc2)CC1)=O</chem>
Prestw-293	65513-72-6	<chem>c1(C(OCC(O)CO)=O)c(Nc2c3c(cc(cc3)Cl)ncc2)cccc1</chem>
Prestw-294	13187-06-9	<chem>C1(/c2c(Sc3c1cccc3)cccc2)=C1/CCN(CC1)C</chem>
Prestw-295	66104-23-2	<chem>c12c3c([C@@]4([C@](N(C[C@@H](C4)CSC)CCC)(C1)[H])[H])cccc3[nH]c2</chem>
Prestw-296	53164-05-9	<chem>n1(c(c2c1ccc(c2)OC)CC(=O)OCC(=O)O)C(c1ccc(cc1)Cl)=O</chem>
Prestw-297	132-69-4	<chem>n1(nc2c1cccc2)OCCCN(C)C)Cc1ccccc1</chem>
Prestw-298	34161-23-4	<chem>N1(C(OCc2ccc(Cl)cc2)=O)CCN(Cc2cc3c(OCO3)cc2)CC1</chem>
Prestw-299	84371-65-3	<chem>C1\2=C\3/C(=C\C(=O)CC3)/CC[C@]1([C@]1([C@](C[C@@]2(c2ccc(N(C)C)cc2)[H])([C@](C#CC)(CC1)O)C)[H])[H]</chem>
Prestw-300	537-12-2	<chem>C(Nc1ccccc1)(OC(CN1CCCC1)COC(Nc1ccccc1)=O)=O</chem>
Prestw-301	83915-83-7	<chem>N1(C([C@@H](N[C@H](C(=O)O)CCc2ccccc2)CCCCN)=O)[C@H](C(=O)O)CCC1</chem>
Prestw-302	859-18-7	<chem>[C@@H]1(O[C@@H]([C@@H]([C@H]([C@H]1O)O)SC)[C@H](NC([C@H]1N(C[C@@H](C1)CCC)C)=O)[C@H](O)C</chem>
Prestw-303	147416-96-4	<chem>N1(c2c(C(Nc3c1cccc3)=O)csc2C)C(CN1CCN(CC1)C)=O</chem>
Prestw-304	24169-02-6	<chem>c1(c(cc(cc1)Cl)Cl)C(Cn1cncc1)OCc1ccc(Cl)cc1</chem>
Prestw-305	18010-40-7	<chem>C(Nc1c(cccc1C)C)(C1N(CCCC)CCCC1)=O</chem>
Prestw-306	14976-57-9	<chem>[C@@]([c1ccc(cc1)Cl)(c1ccccc1)(OCC[C@@H]1N(CCC1)C)C</chem>
Prestw-307	6153-64-6	<chem>[C@@]1\2([C@]([C@@H](\C=C/C(=O)N)O)N(C)C)([C@H]([C@]1(\C=C2\O)\C(c2c([C@]1(O)C)cccc2)=O)[H])O)[H]O</chem>
Prestw-308	2062-78-4	<chem>C1(N(c2c(N1)cccc2)C1CCN(CC1)CCCC(c1ccc(cc1)F)c1ccc(cc1)F)=O</chem>
Prestw-309	6398-98-7	<chem>c12c(Nc3cc(c(cc3)O)CN(CC)CC)ccnc1cc(cc2)Cl</chem>
Prestw-310	2753-45-9	<chem>C(c1cc(c(cc1)OC)OC)(=O)OCCCN(C(Cc1ccc(cc1)OC)C)CC</chem>

Prestwick Nr.	CAS number	Smiles code
Prestw-311	23210-58-4	<chem>N1(C(C(c2ccc(cc2)O)O)C)CCC(Cc2cccc2)CC1</chem>
Prestw-312	30484-77-6	<chem>N1(C(c2ccc(cc2)F)c2ccc(cc2)F)CCN(CC1)C/C=C/c1cccc1</chem>
Prestw-313	440-17-5	<chem>N1(c2c(Sc3c1cccc3)ccc(C(F)(F)F)c2)CCCN1CCN(CC1)C</chem>
Prestw-314	76095-16-4	<chem>N1(C([C@@H](N[C@H](C(=O)OCC)CCc2cccc2)C)=O)[C@H](C(=O)O)CCC1</chem>
Prestw-315	13614-98-7	<chem>[C@]12(/C=C\3/C(c4c(c(ccc4O)N(C)C)CC3CC1[C@H](/C=C(\C2=O)/C(=O)N)/O)N(C)C=O/O)O</chem>
Prestw-316	10238-21-8	<chem>S(NC(NC1CCCC1)=O)(c1ccc(cc1)CCNC(c1ccc(c1)Cl)OC)=O)(=O)=O</chem>
Prestw-317	60-02-6	<chem>C(=N)(NCCN1CCCCC1)N.C(=N)(NCCN1CCCCC1)N</chem>
Prestw-318	69-05-6	<chem>c1(c2c(nc3c1ccc(c3)Cl)ccc(c2)OC)NC(CCCN(CC)CC)C</chem>
Prestw-319	92953-10-1	<chem>[N+](CC)(CC)(CCCCC)CCCCc1ccc(Cl)cc1</chem>
Prestw-320	146-56-5	<chem>N1(c2c(Sc3c1cccc3)ccc(C(F)(F)F)c2)CCCN1CCN(CC1)CCO</chem>
Prestw-321	3810-74-0	<chem>N(C1C(OC(C(C1O)O)CO)OC2C(OC(C2(O)C=O)C)OC3C(C(C(C(C3O)O)NC(=N)N)O)NC(=N)N)C</chem>
Prestw-322	81403-68-1	<chem>n1c(nc2c(c1N)cc(c(c2)OC)OC)N(CCCNC(C1OCCC1)=O)C</chem>
Prestw-323	94-20-2	<chem>S(NC(=O)NCCC)(c1ccc(cc1)Cl)(=O)=O</chem>
Prestw-324	154-41-6	<chem>[C@H](c1cccc1)([C@H](N)C)O</chem>
Prestw-325	50-81-7	<chem>C\1(=C([C@H](OC1=O)[C@@H](O)CO)/O)/O</chem>
Prestw-326	555-30-6	<chem>[C@](C(=O)O)(Cc1cc(c(cc1)O)O)(N)C</chem>
Prestw-327	not available	<chem>N1\2C([C@]([C@]1(SC\C(=C2\C(=O)O)\CSc1n(nnn1)C)[H])(NC([C@H](NC(N1C(C(N(CC1)CC)=O)=O)=O)c1ccc(cc1)O)=O)[H])=O</chem>
Prestw-328	61-80-3	<chem>n1c(oc2c1cc(cc2)Cl)N</chem>
Prestw-329	1684-40-8	<chem>c1(c2c(nc3c1cccc3)CCCC2)N</chem>
Prestw-330	104344-23-2	<chem>N(CC(COc1ccc(cc1)COCCOC(C)C)O)C(C)C.N(CC(COc1ccc(cc1)COCCOC(C)C)O)C(C)C</chem>
Prestw-1813	192725-17-0	<chem>Cc1cccc(c1OCC(=O)N[C@@H](Cc2cccc2)[C@H](C[C@H](Cc3cccc3)NC(=O)[C@H](C(C)C)N4CCCCN4=O)O)C</chem>
Prestw-332	6673-35-4	<chem>C(Nc1ccc(OCC(CNC(C)C)O)cc1)(=O)C</chem>
Prestw-333	30516-87-1	<chem>N/1(C(NC(/C=C1)/C)=O)=O)[C@@H]1O[C@@H]([C@H](C1)N=[N+]=[N-])CO</chem>
Prestw-334	127-69-5	<chem>S(Nc1c(c(no1)C)C)(c1ccc(N)cc1)(=O)=O</chem>
Prestw-335	37762-06-4	<chem>c12c(C(N=C(/N1))c1c(OCCC)cccc1)=O)[nH]nn2</chem>
Prestw-336	80-77-3	<chem>S1(C(N(C(CC1)=O)C)c1ccc(cc1)Cl)(=O)=O</chem>
Prestw-337	614-39-1	<chem>C(c1ccc(N)cc1)(=O)NCCN(CC)CC</chem>
Prestw-338	1867-73-8	<chem>n1([C@H]2[C@@H]([C@@H]([C@H](O2)CO)O)O)c2c(nc1)c(ncn2)NC</chem>
Prestw-339	29110-48-3	<chem>N(C(=N)N)C(Cc1c(Cl)cccc1Cl)=O</chem>
Prestw-340	57808-66-9	<chem>C1(N(c2c(N1)cc(cc2)Cl)C1CCN(CC1)CCCN1C(Nc2c1cccc2)=O)=O</chem>
Prestw-341	54-31-9	<chem>S(c1cc(c(cc1Cl)NCc1occc1)C(=O)O)(=O)(=O)N</chem>
Prestw-342	135-23-9	<chem>N(c1ncccc1)(Cc1sccc1)CCN(C)C</chem>
Prestw-343	58-28-6	<chem>N1(c2c(CCc3c1cccc3)cccc2)CCCN</chem>
Prestw-344	17780-75-5	<chem>C(#C)CN(CCCOc1c(cc(cc1)Cl)Cl)C</chem>
Prestw-345	21898-19-1	<chem>c1(c(cc(cc1Cl)C(CNC(C)(C)O)Cl)N</chem>
Prestw-346	10347-81-6	<chem>[C@@]12(c3c([C@](c4c1cccc4)(CC2)[H])cccc3)CCCN</chem>
Prestw-347	85-31-4	<chem>n1(c2c(nc1)c(nc(n2)N)S)[C@H]1[C@@H]([C@@H]([C@H](O1)CO)O)O</chem>
Prestw-348	6469-93-8	<chem>C\1(/c2c(Sc3c1cccc3)ccc(c2)Cl)=C\CCN(C)C</chem>
Prestw-349	23239-51-2	<chem>[C@@H](c1ccc(cc1)O)([C@@H](NCCc1ccc(cc1)O)C)O</chem>
Prestw-350	5786-21-0	<chem>C\1(=Nc2c(Nc3c1cccc3)ccc(c2)Cl)/N1CCN(CC1)C</chem>
Prestw-351	77-36-1	<chem>C1(NC(c2c1cccc2)=O)(c1cc(S(=O)(=O)N)c(cc1)Cl)O</chem>
Prestw-352	49745-95-1	<chem>c1(c(ccc(c1)CCNC(CCc1ccc(cc1)O)C)O)O</chem>
Prestw-353	71320-77-9	<chem>C(c1ccc(cc1)Cl)(=O)NCCN1CCOCC1</chem>
Prestw-354	636-54-4	<chem>S(c1cc(C(NN2[C@H](CCC[C@H]2C)C)=O)ccc1Cl)(=O)(=O)N</chem>
Prestw-355	3105-97-3	<chem>c12c(Sc3c(C1=O)cccc3)c(ccc2NCCN(CC)CC)CO</chem>
Prestw-356	18422-05-4	<chem>n1([C@H]2[C@@H]([C@@H]([C@H](O2)COP(=O)(O)O)O)O)c2c(nc1)c(ncn2)N</chem>
Prestw-357	26787-78-0	<chem>N12[C@@H]([C@@H](C1=O)NC([C@H](c1ccc(cc1)O)N)=O)SC([C@@H]2C(=O)O)(C)C</chem>
Prestw-1603	100299-08-9	<chem>C=1(\c2[n-]nnn2)/C(N\2/C(=N\1)/C(=C\2)/C)=O</chem>
Prestw-359	6700-34-1	<chem>[C@]123c4c([C@@H]([C@]1(CCCC2)[H])N(CC3)C)ccc(c4)OC</chem>













Prestwick Nr.	CAS number	Smiles code
Prestw-565	5908-99-6	<chem>N1([C@H]2C[C@@H](OC(C(c3ccccc3)CO)=O)C[C@H]1CC2)C.N1([C@H]2C[C@@H](OC(C(c3ccccc3)CO)=O)C[C@H]1CC2)C</chem>
Prestw-566	64-47-1	<chem>[C@]12([C@@](N(c3c1cc(OC(=O)NC)cc3)C)(N(CC2)C)[H])C.[C@]12([C@@](N(c3c1cc(OC(=O)NC)cc3)C)(N(CC2)C)[H])C</chem>
Prestw-1139	84625-61-6	<chem>N1(C(N(N=C1)C(CC)C)=O)c1ccc(N2CCN(c3ccc(OCC4OC(c5c(cc(cc5)Cl)Cl)(Cn5ncnc5)OC4)cc3)CC2)cc1</chem>
Prestw-1174	56180-94-0	<chem>[C@H]1([C@@H]([C@H]([C@H](O[C@@H]2[C@@H]([C@H]([C@H](N[C@@H]3[C@@H]([C@H]([C@@H](\C(=C3)CO)O)O)[C@H](O2)C)O)O)[C@H](O1)CO)O)O)[C@H]1[C@@H]([C@H]([C@@H](O[C@@H]1CO)O)O)O</chem>
Prestw-1403	130929-57-6	<chem>c1([N+]([O-])=O)c(cc(C=C(/C(N(CC)CC)=O)\C#N)c1)O)O</chem>
Prestw-1449	98-92-0	<chem>C(c1cnccc1)(=O)N</chem>
Prestw-571	136-47-0	<chem>C(c1ccc(NCCCC)cc1)(=O)OCCN(C)C</chem>
Prestw-572	83919-23-7	<chem>[C@]12([C@](OC(c3ccc3)=O)([C@@H](C[C@]1([C@]1([C@@]([C@@]3(\C=C/C(\C=C3)=O)\CC1)C)([C@H](C2)O)Cl)[H])[H])C)C(=O)CC)C</chem>
Prestw-1467	97322-87-7	<chem>N1C(SC(C1=O)C)c1ccc(OCC2(Oc3c(c(c(c3C)C)O)C)CC2)C)cc1=O</chem>
Prestw-574	4342-03-4	<chem>c1(c(N=NN(C)C)[nH]cn1)C(=O)N</chem>
Prestw-1351	113712-98-4	<chem>n1c([nH]c2c1nc(cc2)OC)S(Cc1c(c(c(c1)C)OC)C)=O</chem>
Prestw-576	3598-37-6	<chem>N1(c2c(Sc3c1cccc3)ccc(c2)C(=O)C)CCCN(C)C</chem>
Prestw-1271	128196-01-0	<chem>[C@]1(c2c(CO1)cc(C#N)cc2)(c1ccc(cc1)F)CCCN(C)C</chem>
Prestw-1158	91374-20-8	<chem>N1C(Cc2c1cccc2CCN(CCC)CCC)=O</chem>
Prestw-1297	103890-78-4	<chem>C=1(\C(\C(=C(/N/C1)C)\C(=O)OCC)c1c/C=C/C(OC(C)C)C)=O)cccc1/C(=O)OCC</chem>
Prestw-1228	74863-84-6	<chem>S(c1c2NCC(Cc2ccc1)C)(N[C@H](C(N1[C@@H](C(=O)O)C[C@@H](CC1)C)=O)CCNC(=N)N)(=O)=O</chem>
Prestw-1328	98769-81-4	<chem>O([C@H]([C@@]1(OCCNC1)[H])c1cccc1)c1c(OCC)cccc1</chem>
Prestw-1498	54-30-8	<chem>C(c1cccc1)(NCCN(CC)CC)C(OCCC(C)C)=O</chem>
Prestw-583	61-25-6	<chem>c12c(nccc1cc(c(c2)OC)OC)Cc1cc(c(cc1)OC)OC</chem>
Prestw-584	65-19-0	<chem>c12c(c3c([nH]1)cccc3)CCN1[C@]2[C[C@@]2([C@@H](C(=O)OC)[C@H](CC[C@]2(C1)[H])O)[H])[H]</chem>
Prestw-1500	137234-62-9	<chem>[C@](c1c(cc(cc1)F)F)([C@H](c1c(F)cn1)C)(Cn1ncnc1)O</chem>
Prestw-1211	41294-56-8	<chem>[C@]12([C@](\C(=C/C=C\3/C([C@H](C[C@@H](C3)O)O)=C)\CCC1)(CC[C@@H]2[C@@H](CCCC(C)C)C)[H])C</chem>
Prestw-587	73963-72-1	<chem>n1(nnnc1CCCCOc1cc2c(NC(=O)CC2)cc1)C1CCCC1</chem>
Prestw-588	1953-04-4	<chem>[C@]1\23c4c(O[C@H]1C[C@H](\C=C2)O)c(ccc4CN(CC3)C)OC</chem>
Prestw-1130	79307-93-0	<chem>N1(/N=C(\c2c(C1=O)cccc2)/Cc1ccc(Cl)cc1)C1CCN(CCC1)C</chem>
Prestw-1409	54350-48-0	<chem>c1(c(c(c(cc1C)OC)C)C)C=C\C(=C=C\C(=C\C(=O)OCC)\C)C</chem>
Prestw-1274	87233-61-2	<chem>c1(nc2c(n1CCOCC)cccc2)N1CCN(CCC1)C</chem>
Prestw-1407	30544-47-9	<chem>C(c1cc(Nc2c(C(=O)OCCOCCO)cccc2)ccc1)(F)F</chem>
Prestw-1369	151319-34-5	<chem>n12c(c(cn1)C#N)nccc2c1cc(N(C(=O)C)CC)ccc1</chem>
Prestw-594	15307-79-6	<chem>N(c1c(Cl)cccc1Cl)c1c(CC([O-])=O)cccc1</chem>
Prestw-1410	107868-30-4	<chem>[C@@]1\2(\C(\C(C[C@@]3([C@@]1(CC[C@]1([C@]3(CCC1=O)[H])C)[H])=C)=C/C(\C=C2)=O)C</chem>
Prestw-1499	7554-65-6	<chem>n1[nH]cc(c1)C</chem>
Prestw-1183	85622-93-1	<chem>n12c(c(nc1)C(=O)N)\N=N/N(C2=O)C</chem>
Prestw-598	7361-61-7	<chem>C/1(\Nc2c(cccc2)C)=N/CCCS1</chem>
Prestw-1132	57470-78-7	<chem>C(Nc1cc(c(OCC(CNC(C)C)O)cc1)C(=O)C)(N(CC)CC)=O</chem>
Prestw-1367	43200-80-2	<chem>N1(C(c2c(C1=O)nccn2)OC(N1CCN(CC1)C)=O)c1ncc(cc1)Cl</chem>
Prestw-1198	53902-12-8	<chem>c1(c(NC(/C=C/c2cc(c(cc2)OC)OC)=O)cccc1)C(=O)O</chem>



Prestwick Nr.	CAS number	Smiles code
Prestw-1341	106516-24-9	<chem>n1(cc(c2c1ccc(c2)Cl)C1CCN(CCN2C(NCC2)=O)CC1)c1ccc(cc1)F</chem>
Prestw-641	73384-60-8	<chem>c1(nc2c([nH]1)cccn2)c1c(cc(S(=O)C)cc1)OC</chem>
Prestw-1270	184475-35-2	<chem>c12c(ncnc1cc(c2)OCCCN1CCOCC1)OC)Nc1cc(c(cc1)F)Cl</chem>
Prestw-643	3385-03-3	<chem>[C@@]12([C@@]3([C@]([C@]4([C@@]([C@]5(\C(\C@H)(C4)F)=C/C(\C=C5)=O)C)([C@H](C3)O)[H])[H])(C[C@H]1OC(O2)(C)C)[H])C(=O)CO</chem>
Prestw-644	1195-16-0	<chem>C1(C(NC(=O)C)CCS1)=O</chem>
Prestw-645	1524-88-5	<chem>[C@@]12([C@@]3([C@]([C@]4([C@@]([C@]5(\C(\C@H)(C4)F)=C/C(=O)CC5)C)([C@H](C3)O)[H])[H])(C[C@H]1OC(O2)(C)C)[H])C(=O)CO</chem>
Prestw-1125	64211-46-7	<chem>C(\c1c(cc(cc1)Cl)Cl)/Cn1cnc1)=N/OCc1c(cc(cc1)Cl)Cl</chem>
Prestw-1166	90098-04-7	<chem>C\1(=C\C(Nc2c1cccc2)=O)/CC(NC(c1ccc(cc1)Cl)=O)C(=O)O</chem>
Prestw-1154	75530-68-6	<chem>C=1(\C(\C(=C(/N/C1/C)\C#N)\C(=O)OC)c1cc([N+][O-])=O)ccc1)/C(OC(C)C)=O</chem>
Prestw-649	22668-01-5	<chem>n1(ccnc1[N+][O-])=O)CC(=O)NCCO</chem>
Prestw-1601	53251-94-8	<chem>C1([C@]2(C[C@@]1(CCC2CCOCC[N+]1(Cc2c(cc(c2)OC)OC)Br)CCOCC1)[H])[H])(C)C</chem>
Prestw-651	93479-97-1	<chem>N1(C(\C(=C(/C1)\C)\CC)=O)C(=O)NCCc1ccc(S(NC(N[C@@H]2CC[C@H](CC2)C)=O)(=O)=O)cc1</chem>
Prestw-652	17617-45-7	<chem>[C@]123[C@]4([C@]([C5C(O[C@@H]([C@]4(OC1=O)[H])[C@@H]5C(=C)C)=O)(CC2O3)O)C</chem>
Prestw-653	76-90-4	<chem>C(C(c1cccc1)(c1cccc1)O)(OC1C[N+](CCC1)(C)C)=O</chem>
Prestw-654	22457-89-2	<chem>n1c(c(CN/C=C(\SC(=O)c2cccc2)/CCOP(=O)(O)O)/C)C(=O)cnc1C)N</chem>
Prestw-655	3093-35-4	<chem>[C@@]12([C@@]3([C@]([C@]4([C@@]([C@]5(\C(=C/C(=O)CC5)\CC4)C)([C@H](C3)O)F)[H])(C[C@H]1OC(O2)(C)C)[H])C(=O)CCl</chem>
Prestw-656	17575-22-3	<chem>O1C(C(C(C1CO)O)O)OC2C(OC(CC2OC(=O)C)OC3C(OC(CC3O)OC4C(OC(CC4O)OC9CC8C(C5(C(C6(C(C5)O)(C(CC6)C7=CC(=O)OC7)C)O)(CC8)C)C)(CC9)C)C)C</chem>
Prestw-657	2898-76-2	<chem>c1(nc(c(nc1N)N)Cl)C(\N=C(\NCc1cccc1)/N)=O</chem>
Prestw-658	27470-51-5	<chem>N1(N(C(C1=O)(CCCC)COC(=O)CCC(O)=O)=O)c1cccc1)c1cccc1</chem>
Prestw-659	525-79-1	<chem>c12c(nc[nH]1)ncnc2NCc1occc1</chem>
Prestw-660	71751-41-2	<chem>[C@]1/2([C@]3([C@]([OC/C3=C=C\C[C@@H](C(\C=C\C[C@]3(O[C@]4(O[C@@]([C@H](\C=C4)C)([C@](C)([H])CC)[H])C[C@@H](OC1=O)C3)[H])\C)O[C@@]1(O[C@H](C([C@H](C1)OC)O[C@H]([C@H](C1)OC)O)[H])C)[H])C)([C@@H]/(C=C2)/C)O)[H]</chem>
Prestw-1317	103177-37-3	<chem>c1(/C=2/Oc3c(C(\C2)=O)cccc3NC(c2ccc(cc2)OCCCCc2cccc2)=O)nnn[nH]1</chem>
Prestw-1477	52-66-4	<chem>[C@@H](C(=O)O)(C(S)(C)C)N</chem>
Prestw-1365	111406-87-2	<chem>c1(sc2c(c1)cccc2)C(N(C(=O)N)O)C</chem>
Prestw-1432	79794-75-5	<chem>C\1(/c2c(cc(cc2)Cl)CCc2c1nccc2)=C/1\CCN(C(=O)OCC)CC1</chem>
Prestw-1387	4961-41-5	<chem>N(CCNCCNCCN)CCN</chem>
Prestw-666	63675-72-9	<chem>C=1(\C(\C(=C(/N/C1/C)\C)\C(=O)OC)c1c([N+][O-])=O)ccc1)/C(OCC(C)C)=O</chem>
Prestw-1507	652-37-9	<chem>c12c(N(C(N(C1=O)C)=O)C)ncn2CC(O)=O</chem>
Prestw-1165	55079-83-9	<chem>c1(c(c(c(cc1C)OC)C)C)C=C\C(=C\C=C\C(=C\C(=O)O)\C)\C</chem>
Prestw-1162	68291-97-4	<chem>S(Cc1noc2c1cccc2)(=O)(=O)N</chem>
Prestw-1173	84504-69-8	<chem>c1(nc(nc(n1)N)N)c1c(ccc(c1)Cl)Cl</chem>
Prestw-671	152-62-5	<chem>[C@]12([C@]([C@]3([C@]([C@]4(\C(\C=C3)=C/C(=O)CC4)C)(CC1)[H])[H])(CC[C@@H]2C(=O)C)[H]C</chem>
Prestw-1346	103628-48-4	<chem>S(=O)(=O)(Cc1cc2c(c[nH]c2cc1)CCN(C)C)NC</chem>
Prestw-1456	909-39-7	<chem>N1(c2c(\C=C/c3c1cccc3)cccc2)CCCN1CCN(CC1)CCO</chem>
Prestw-1447	3374-05-8	<chem>C=1(\C(c2c(N(/C1)CC)nc(cc2)C)=O)/C([O-])=O</chem>
Prestw-1475	1173-88-2	<chem>N12[C@@H]([C@@H](C1=O)NC(c1c(noc1C)c1cccc1)=O)SC([C@@H]2C([O-])=O)(C)C</chem>
Prestw-676	11072-93-8	<chem>C(OC1[C@@H](C2([C@@H](C[C@]/3(C4(CCC5[C@@](CO)(C(CCC5(C4C/C=C3/C2CC1(C)C)C)OC1O[C@H]([C@@H](O[C@@H]2O[C@H]([C@H]([C@H]([C@H]2O)O)O)CO)[C@@H]([C@H]1O[C@@H]1O[C@@H](C([C@H]([C@H]1O)O)O)CO)O)C(O)=O)C)C)O)C)OC(C)=O)([H])=C(C)C)O=O</chem>

Prestwick Nr.	CAS number	Smiles code
Prestw-631	67-03-8	[N+] <sub>1</sub> (=CSC(=C1C)CCO)Cc2c(nc(nc2)C)N
Prestw-1349	89786-04-9	S1([C@]([C@H](N2[C@H]1CC2=O)C(=O)O)(Cn1nnc1)C)(=O)=O
Prestw-1285	114084-78-5	C(P(=O)(O)O)(P(=O)(O)O)(CCN(CCCCC)C)O
Prestw-1363	81-81-2	C/1(=C(/c2c(OC1=O)cccc2)\O)\C(CC(=O)C)c1cccc1
Prestw-1318	52549-17-4	O1c2c(Cc3c1ccc(c3)C(C(=O)O)C)cccn2
Prestw-1340	3366-95-8	c1(n(c(nc1)C)CC(O)C)[N+](O)=O
Prestw-1833	171596-29-5	[H][C@]12CC3=C(NC4=CC=CC=C4)[C@H](N1C(=O)CN(C)C2=O)C1=CC2=C(OCO2)C=C1
Prestw-1798	223673-61-8	OC(c1cccc1)CNCCc1ccc(NC(Cc2csc(n2)N)=O)cc1
Prestw-1508	122647-32-9	S(Nc1ccc(cc1)C(O)CCCN(CC)CCCCC)(=O)(=O)C
Prestw-1799	220620-09-7	O=C(CNC(C)C)Nc1c(O)c2C(=O)C=3C(Cc2c(c1)N(C)C)CC1C(O)(C3O)C(=O)C(=C(O)C1N(C)C)C(=O)N
Prestw-1465	27203-92-5	[C@@]1([C@H](CN(C)C)CCCC1)(c1cc(OC)ccc1)O
Prestw-688	7280-37-7	S(Oc1cc2c([C@@]3([C@]([C@]4([C@@](C(CC4=O)(CC3)C)[H])(CC2)[H])[H])cc1)(=O)(=O)O
Prestw-1253	149-64-4	[C@]12([C@@](O1)([C@]1([N+](C@]2(C[C@H](C1)OC([C@H](c1cccc1)CO)=O)[H])(CCC)C)[H])[H])H
Prestw-1494	136572-09-3	N12\C(\c3c(C1)c(c1c(n3)ccc(OC(N3CCC(N4CCCC4)CC3)=O)c1)CC)=C/C/1=C(\C2=O)/COC([C@]1(O)CC)=O
Prestw-1353	1401-69-0	[C@H]1([C@@H]([C@H]([C@@H]([C@H](O1)C)O[C@H]1CC([C@H]([C@@H](O1)C)O)(O)C)N(C)C)O[C@H]1[C@H]([C@H]([C@@H]([C@H]([C@@H]([C@H]([C@H]([C@H]([C@H]([C@H]([C@H]([C@H]1CC=O)C)=O)/C)CO[C@H]1[C@H]([C@H]([C@@H]([C@H]([C@H](O1)C)O)OC)OC)CC)=O)O)C
Prestw-692	59729-32-7	C1(c2c(CO1)cc(C#N)cc2)(c1ccc(cc1)F)CCCN(C)C
Prestw-693	53-60-1	N1(c2c(Sc3c1cccc3)cccc2)CCCN(C)C
Prestw-694	127-79-7	S(Nc1nc(ccn1)C)(c1ccc(N)cc1)(=O)=O
Prestw-1170	93413-69-5	C(C1(O)CCCC1)(c1ccc(cc1)OC)CN(C)C
Prestw-696	86-35-1	N1(C(NC(C1=O)c1cccc1)=O)CC
Prestw-1834	1132935-63-7	COC1=C(C=C(C=C1C1=CC2=CC=C(NS(C)(=O)=O)C=C2C=C1)N1C=CC(=O)NC1=O)C(C)(C)C
Prestw-698	522-48-5	C/1(\C2c3c(CCC2)cccc3)=N/CCN1
Prestw-699	84-16-2	C(C(c1ccc(cc1)O)CC)(c1ccc(cc1)O)CC
Prestw-700	56796-39-5	[C@]1(NC(CSCC#N)=O)(C(N)2[C@@]1(SC\C=C2\C(=O)[O-])\CSc1n(nnn1)C)[H]=O)OC
Prestw-701	58947-95-8	C(CCN1CCCC1)(c1cccc1)(C1CCCC1)O
Prestw-702	116-43-8	c1(ccc(cc1)NC(=O)CCC(O)=O)S(Nc1scn1)(=O)=O
Prestw-703	22881-35-2	C\1(=C(\C(N1C)c1cccc1)=O)/C(C)C/CN(C(Cc1cccc1)C)C
Prestw-704	4093-35-0	c1(c(cc(c(c1)Br)N)OC)C(=O)NCCN(CC)CC
Prestw-705	25155-18-4	C(c1cc(c(cc1)OCCOCC[N+](Cc1cccc1)(C)C)(CC(C)(C)C)(C)C
Prestw-706	1620-21-9	N1(C(c2ccc(cc2)Cl)c2cccc2)CCN(CC1)C
Prestw-707	132-18-3	C(OC1CCN(CC1)C)(c1cccc1)c1cccc1
Prestw-708	121-54-0	C(c1ccc(cc1)OCCOCC[N+](Cc1cccc1)(C)C)(CC(C)(C)C)(C)C
Prestw-709	3902-71-4	c12c(\C(=C/C(O1)=O)\C)cc1c(c2C)oc(c1)C
Prestw-1136	69975-86-6	c12c(C(N(C(N1C)=O)C)=O)n(cn2)CC1OCCO1
Prestw-711	127-71-9	S(NC(=O)c1cccc1)(c1ccc(N)cc1)(=O)=O
Prestw-712	94-09-7	C(c1ccc(N)cc1)(=O)OCC
Prestw-713	5907-38-0	C=1(\C(N(N/C1/C)C)c1cccc1)=O)/N(CS([O-])(=O)=O)C
Prestw-714	87-33-2	[C@]12([C@@H](CO[C@@]1([C@H](CO2)O[N+](O-)=O)[H])O[N+](O-)=O)[H]
Prestw-715	80-32-0	S(Nc1nnc(Cl)cc1)(c1ccc(N)cc1)(=O)=O
Prestw-716	637-58-1	N1(CCCOc2ccc(cc2)OCCCC)CCOCC1
Prestw-717	98319-26-7	[C@]12([C@]([C@]3([C@@]([C@]4(\C=C/C(N[C@@]4(CC3)[H])=O)C)(CC1)[H])[H])(CC[C@H]2C(NC(C)C)=O)[H])C

Prestwick Nr.	CAS number	Smiles code
Prestw-718	426-13-1	<chem>[C@]1\2([C@@]3([C@]([C@]4([C@@]([C@](CC4)(C(=O)C)O)(C[C@@H]3O)C)[H])(C[C@@H](/C1=C/C(\C=C2)=O)C)[H])F)C</chem>
Prestw-719	58-71-9	<chem>N1\2C([C@]([C@]1(SC\C=C2\C([O-])=O)\COC(=O)C)[H])(NC(Cc1sccc1)=O)[H])=O</chem>
Prestw-720	56238-63-2	<chem>N1\2C([C@]([C@]1(SC\C=C2\C([O-])=O)\COC(=O)N)[H])(NC(/C(/c1occcc1)=N)OC(=O)[H])=O</chem>
Prestw-721	5588-16-9	<chem>S1(c2c(NC(N1)CSCC=C)cc(c(S(=O))(=O)N)c2)Cl(=O)=O</chem>
Prestw-722	18342-39-7	<chem>C=1(/C(N(N(\C1\C)C)c1ccccc1)=O)\NC(C)C</chem>
Prestw-723	132-93-4	<chem>N12[C@@]([C@@](C1=O)(NC(C(Oc1ccccc1)C)=O)[H])(SC([C@@H]2C([O-])=O)(C)C)[H]</chem>
Prestw-724	80-35-3	<chem>S(Nc1nnc(cc1)OC)(c1ccc(N)cc1)(=O)=O</chem>
Prestw-725	138-14-7	<chem>C(N(O)CCCCNC(=O)CCC(N(O)CCCCCN)=O)(=O)CCC(=O)NCCCCCN(C(=O)C)O</chem>
Prestw-726	1212-72-2	<chem>C(NC)(Cc1ccccc1)(C)C.C(NC)(Cc1ccccc1)(C)C</chem>
Prestw-1140	88678-31-3	<chem>C(N(c1nc(OC)ccc1)C)(Oc1cc2c(cc1)CCCC2)=S</chem>
Prestw-728	122-11-2	<chem>S(Nc1nc(nc(c1)OC)OC)(c1ccc(N)cc1)(=O)=O</chem>
Prestw-729	63-74-1	<chem>S(c1ccc(N)cc1)(=O)(=O)N</chem>
Prestw-730	80573-04-2	<chem>c1(C([O-])=O)c(ccc(/N=N/c2ccc(C(=O)NCCC([O-])=O)cc2)c1)O</chem>
Prestw-731	967-80-6	<chem>S([N-]c1nc2c(nc1)cccc2)(c1ccc(N)cc1)(=O)=O</chem>
Prestw-732	18883-66-4	<chem>[C@@H]1(NC(N(N=O)C)=O)[C@H]([C@@H]([C@H](O[C@@H]1O)CO)O)O</chem>
Prestw-733	56392-17-7	<chem>N(CC(COc1ccc(cc1)CCOC)O)C(C)C.N(CC(COc1ccc(cc1)CCOC)O)C(C)C</chem>
Prestw-734	2135-17-3	<chem>[C@]1\2([C@@]3([C@]([C@]4([C@@]([C@]([C@@H](C4)C)(C(=O)CO)O)(C[C@@H]3O)C)[H])(C[C@@H](/C1=C/C(\C=C2)=O)F)[H])F)C</chem>
Prestw-735	54143-56-5	<chem>c1(C(NCC2NCCCC2)=O)c(OCC(F)(F)F)ccc(c1)OCC(F)(F)F</chem>
Prestw-736	27164-46-1	<chem>N1\2C([C@]([C@]1(SC\C=C2\C([O-])=O)\CSc1sc(nn1)C)[H])(NC(Cn1nnnc1)=O)[H])=O</chem>
Prestw-1702	635-41-6	<chem>COc1c(OC)cc(C(=O)N2CCOCC2)cc1OC</chem>
Prestw-738	6035-45-6	<chem>C/1\2=C(/N/C(=N/C1=O)/N)\NCC(N2C=O)CNc1ccc(C(N[C@H](C([O-])=O)CCC([O-])=O)cc1</chem>
Prestw-739	829-74-3	<chem>c1(cc(c(cc1)O)O)[C@H]([C@@H](N)C)O</chem>
Prestw-1820	161814-49-9	<chem>CC(C)CN(C[C@H]([C@H](Cc1ccccc1)NC(=O)O[C@H]2CCOC2)O)S(=O)(=O)c3ccc(cc3)N</chem>
Prestw-1821	155206-00-1	<chem>CCNC(=O)CCC/C=C\C[C@H]1[C@H]([C@H]([C@H]([C@H]1/C=C/[C@H](CCc2ccccc2)O)O)O</chem>
Prestw-742	144-82-1	<chem>S(Nc1sc(nn1)C)(c1ccc(N)cc1)(=O)=O</chem>
Prestw-743	2668-66-8	<chem>[C@]12(\C(=C/C(=O)CC1)[C@H](C[C@@]1([C@@]2([C@H](C[C@]2([C@]1(CC[C@@H]2C(=O)C)[H])C)O)[H])[H])C)C</chem>
Prestw-744	42461-84-7	<chem>c1ccc(c(n1)Nc1c(c(ccc1)C(F)(F)F)C)O=O</chem>
Prestw-745	8025-81-8	<chem>C1(C(C(C(O1)C)OC1CC(C(C(O1)C)O)O)C)N(C)C)O[C@H]1[C@H]([C@@H](CC(O[C@@H](C/C=C/C=C/[C@H](OC2OC(C(C2)N(C)C)C)[C@@H](C[C@@H]1CC=O)C)C)=O)O['R'])OC</chem>
Prestw-746	596-51-0	<chem>C(C(c1ccccc1)(C1CCCC1O)(OC1C[N+](CC1)(C)C)=O</chem>
Prestw-1600	170729-80-3	<chem>N/1=C(/NNC1=O)CN1[C@H]([C@@H](O[C@@H](c2cc(C(F)(F)F)cc(C(F)(F)F)c2)OCC1)c1ccc(cc1)F</chem>
Prestw-748	22373-78-0	<chem>[C@]12(O[C@]([C@H]([C@H]([C@H](C([O-])=O)C)OC)C)([C@@H]([C@H](C1)O)C)[H]O[C@]([C@@]1(O[C@]([C@@]3(O[C@@]([C@]4(O[C@@]([C@H](C[C@@H]4C)C)O)CO)[H])(C[C@@H]3C)[H])[H])(CC1)CC)[H])(CC2)C c1(cc(c(cc1)O)O)C(C(NC)C)CC)O</chem>
Prestw-1822	141626-36-0	<chem>CCCCN(CCCC)CCCOc1ccc(cc1)C(=O)c2c(CCCC)oc3ccc(NS(=O)(=O)C)cc23</chem>
Prestw-751	63590-64-7	<chem>c1(nc(c2c(n1)cc(c2)OC)OC)N1CCN(C(C2OCCC2)=O)CC1</chem>
Prestw-752	136-40-3	<chem>n1c(c(/N=N/c2ccccc2)ccc1N)N</chem>
Prestw-753	64-73-3	<chem>[C@@]12(\C(=C/3\C(c4c([C@H]([C@]3(C[C@]1([C@@H](\C(=C(/C2=O)\C(=O)N)O)N(C)C)[H])[H])O)c(ccc4O)Cl)=O)O</chem>
Prestw-754	53746-45-5	<chem>c1(cccc(c1)C(C(=O)[O-])C)Oc1ccccc1.c1(cccc(c1)C(C(=O)[O-])C)Oc1ccccc1</chem>
Prestw-755	59703-84-3	<chem>N12[C@@]([C@@](C1=O)(NC([C@H](NC(N1C(C(N(CC1)CC)=O)=O)=O)c1ccccc1)=O)[H])(SC([C@@H]2C([O-])=O)(C)C)[H]</chem>
Prestw-756	56-53-1	<chem>C(=C(/c1ccc(cc1)O)\CC)(\c1ccc(cc1)O)/CC</chem>
Prestw-757	569-57-3	<chem>C(=C(/c1ccc(cc1)OC)\Cl)(/c1ccc(cc1)OC)c1ccc(cc1)OC</chem>
Prestw-758	53797-35-6	<chem>[C@]1(C(O[C@@]2([C@@H]([C@H]([C@H]([C@H](O2)CN)O)N)[H])[C@H](C[C@H]([C@@H]1O)N)N)O[C@H]1[C@@H]([C@@H]([C@H](O1)CO)O)O)[H]</chem>
Prestw-759	62-51-1	<chem>[N+](CC(OC(=O)C)C)(C)C</chem>
Prestw-760	125-51-9	<chem>C(C(c1ccccc1)(c1ccccc1)O)(OC1C[N+](CCC1)(CC)C)=O</chem>

Prestwick Nr.	CAS number	Smiles code
Prestw-761	94-25-7	<chem>C(c1ccc(N)cc1)(=O)OCCCC</chem>
Prestw-762	144-83-2	<chem>S(Nc1ncccc1)(c1ccc(N)cc1)(=O)=O</chem>
Prestw-763	3685-84-5	<chem>C(=O)(COc1ccc(Cl)cc1)OCCN(C)C</chem>
Prestw-764	3759-92-0	<chem>c1([N+][O-]=O)oc(C=N/N2C(OC(C2)CN2CCOCC2)=O)cc1</chem>
Prestw-765	91-53-2	<chem>C=1(\c2c(NC(/C1)(C)C)ccc(c2)OCC)/C</chem>
Prestw-766	19387-91-8	<chem>n1(c(cnc1C)[N+][O-])CCS(CC)(=O)=O</chem>
Prestw-767	22195-34-2	<chem>C12(OC(CO1)CNC(=N)N)CCCCC2.C12(OC(CO1)CNC(=N)N)CCCCC2</chem>
Prestw-768	5536-17-4	<chem>n1([C@H]2[C@H]([C@@H]([C@H](O2)CO)O)c2c(nc1)c(ncn2)N</chem>
Prestw-769	651-06-9	<chem>S(Nc1ncc(cn1)OC)(c1ccc(N)cc1)(=O)=O</chem>
Prestw-770	71-81-8	<chem>[N+](CCC(C(=O)N)(c1cccc1)c1cccc1)(C(C)C)(C(C)C)C.[I-]</chem>
Prestw-771	66734-13-2	<chem>[C@]12(C([C@@H](C[C@]1([C@]1([C@@]([C@@]3\(\C(=C/C(\C=C3)=O)\C[C@H]1Cl)C)([C@H](C2)O)[H])(H)C)(C(=O)CC)OC(=O)CC)C</chem>
Prestw-772	75706-12-6	<chem>c1(C(Nc2ccc(C(F)(F)F)cc2)=O)c(onc1)C</chem>
Prestw-773	797-63-7	<chem>[C@]12([C@]([C@]3([C@@]([C@@]4(\C(=C/C(=O)CC4)CC3)[H])(CC1)[H])(H)(CC[C@]2(C#C)O)[H])CC</chem>
Prestw-774	356-12-7	<chem>[C@@]12([C@@]3([C@]([C@]4([C@@]([C@@]5(\C([C@H](C4)F)=C/C(\C=C5)=O)C)([C@H](C3)O)F)[H])(C[C@H]1OC(O2)(C)C)[H])C)C(COC(=O)C)=O</chem>
Prestw-775	1981-58-4	<chem>S([N-]c1nc(cc(n1)C)C)(c1ccc(N)cc1)(=O)=O</chem>
Prestw-776	93-14-1	<chem>O(c1c(OC)cccc1)CC(O)CO</chem>
Prestw-777	22573-93-9	<chem>N(C(=N)NCC(CC)CCCC)C(=N)NCCCCCNC(NC(=N)NCC(CC)CCCC)=N</chem>
Prestw-1835	850649-62-6	<chem>CN1C(=O)C=C(C2CCC[C@H](N)C2)N(Cc3cccc3C#N)C1=O.OC(=O)c4cccc4</chem>
Prestw-779	64092-48-4	<chem>c1(n(c(cc1C)CC([O-])=O)C)C(c1ccc(cc1)Cl)=O</chem>
Prestw-780	28657-80-9	<chem>c12c(OCO1)cc1c(c2)C(/C(=N/N1CC)/C(O)=O)=O</chem>
Prestw-781	25122-46-7	<chem>[C@]12([C@]([C@H](C[C@]1([C@]1([C@@]([C@@]3\(\C(=C/C(\C=C3)=O)CC1)C)([C@H](C2)O)F)[H])(H)C)(C(=O)CC)OC(=O)CC)C</chem>
Prestw-782	518-28-5	<chem>[C@@]12([C@@]([C@@H](c3c([C@@H]1O)cc1c(c3)OCO1)c1cc(c(c1)OC)OC)OC)(C(OC2)=O)[H])[H]</chem>
Prestw-783	882-09-7	<chem>c1c(ccc(c1)OC(C)(C)C(O)=O)Cl</chem>
Prestw-784	73-48-3	<chem>S1(c2c(NC(N1)Cc1cccc1)cc(c(S(=O)(=O)N)c2)C(F)(F)F)(=O)=O</chem>
Prestw-785	66-76-2	<chem>C1(=C(\c2c(OC1=O)cccc2)/O)/C/C1=C(/c2c(OC1=O)cccc2)O</chem>
Prestw-786	60-56-0	<chem>c1(n(ccn1)C)S</chem>
Prestw-787	129-16-8	<chem>C12(c3c(c(c(c3)Br)[O-])[Hg]O)Oc3c1cc(c(c3)[O-])Br)OC(c1c2cccc1)=O</chem>
Prestw-788	532-76-3	<chem>C(OC(CNC1CCCC1)C)(=O)c1cccc1</chem>
Prestw-789	548-66-3	<chem>C(C(c1cccc1)C1CCCC1)(=O)OCCN(CC)CC</chem>
Prestw-790	66-81-9	<chem>[C@]1(C([C@H](C[C@@H](C1)C)C)=O)([C@@H](CC1CC(NC(=O)C1)=O)O)[H]</chem>
Prestw-791	23979-41-1	<chem>c1(cc2c(cc(cc2)OC)cc1)[C@H](C([O-])=O)C</chem>
Prestw-792	25535-16-4	<chem>[n+]1(c2c(c3c(c1c1cccc1)cc(cc3)N)ccc(c2)N)CCC[n+](CC)(CC)C</chem>
Prestw-793	14984-68-0	<chem>N1(CCOC(c2ccc(cc2)Cl)c2cccc2)CCCCC1</chem>
Prestw-1823	133040-01-4	<chem>CCCCc1ncc(\C=C(/Cc2cccs2)C(=O)O)n1Cc3ccc(cc3)C(=O)O</chem>
Prestw-795	59-63-2	<chem>c1(noc(c1)C)C(=O)NNCc1cccc1</chem>
Prestw-796	434-13-9	<chem>[C@@]12([H])[C@@]([C@@]3([H])[C@]([C@@]([C@@H](CCC(O)=O)C)(CC3)[H])(C)CC1)([H])CC[C@]1([H])[C@@]2(CC[C@H](C1)O)C</chem>
Prestw-797	7104-38-3	<chem>N1(c2c(Sc3c1cccc3)ccc(c2)OC)C[C@@H](CN(C)C)C</chem>
Prestw-798	84-17-3	<chem>C(\C(\c1ccc(cc1)O)=C\C)/c1ccc(cc1)O)=C/C</chem>
Prestw-799	6856-31-1	<chem>C(CCN1CCCC1)(c1cccc1)(c1cccc1)O</chem>
Prestw-800	60719-84-8	<chem>C=1(\C(N\C=C(/C1)\c1ccncc1)=O)N</chem>
Prestw-801	3505-38-2	<chem>C(c1ccc(cc1)Cl)(c1ncccc1)OCCN(C)C</chem>
Prestw-802	554-57-4	<chem>C=1(/SC(N(\N1)C)=NC(=O)C)\S(=O)(=O)N</chem>
Prestw-803	77-04-3	<chem>C1(C(N\C=C/C1=O)=O)(CC)CC</chem>
Prestw-804	21736-83-4	<chem>[C@@]12([C@](O[C@]3([C@](O1)([C@H]([C@H]([C@H]([C@@H]3O)NC)O)NC)[H])(H)(O[C@@H](CC2=O)C)[H])O</chem>
Prestw-805	19562-30-2	<chem>c1(ncc2c(n1)N(/C=C(\C2=O)/C(O)=O)CC)N1CCCC1</chem>
Prestw-806	521-78-8	<chem>N1(c2c(Cc3c1cccc3)cccc2)CC(CN(C)C)C</chem>
Prestw-807	6170-42-9	<chem>N(c1ncccc1)(Cc1ccc(Cl)cc1)CCN(C)C</chem>

Prestwick Nr.	CAS number	Smiles code
Prestw-808	67-45-8	<chem>c1([N+](O)=O)oc(C=NN2C(OCC2)=O)cc1</chem>
Prestw-809	120-97-8	<chem>c1(S(=O)(=O)N)c(cc(S(=O)(=O)N)c1)Cl</chem>
Prestw-810	61318-91-0	<chem>c1(cc(cc1)Cl)Cl)C(SCc1ccc(Cl)cc1)Cn1nccc1</chem>
Prestw-1233	34031-32-8	<chem>[C@H]1([C@H]([C@@H]([C@H](O[C@H]1S[Au]=P(CC)(CC)CC)COC(=O)C)OC(=O)C)OC(=O)C)OC(=O)C</chem>
Prestw-812	15826-37-6	<chem>C1(c2c(O/C=C1)/C([O-])=O)cccc2OCC(COC1c2C(\C=C/Oc2ccc1)\C([O-])=O)O=O</chem>
Prestw-813	16980-89-5	<chem>n1([C@@H]2O[C@@]3(OP(OC[C@]3([C@H]2OC(=O)CCC)[H])([O-])=O)[H])c2c(nc1)c(NC(=O)CCC)ncn2</chem>
Prestw-814	52152-93-9	<chem>N1\2C([C@]([C@]1(SC\C=C2\C([O-])=O)\C[n+]1ccc(C(=O)N)cc1)[H])(NC([C@H](S([O-])=O)=O)c1cccc1)=O)[H]=O</chem>
Prestw-815	6064-83-1	<chem>P(Oc1c(C(=O)O)cccc1)(=O)(O)O</chem>
Prestw-816	40828-46-4	<chem>c1(ccc(cc1)C(C)C(=O)C(c1sccc1)=O</chem>
Prestw-1509	14484-47-0	<chem>[C@@]1/2([C@@]3([C@]([C@]4([C@@]([C@@]5(\C=C/C(\C=C5)=O)\CC4)C)([C@H](C3)O)[H])[H])(C[C@]1(O/C(=N2)/C)[H])[H])C(COC(=O)C)=O</chem>
Prestw-818	42200-33-9	<chem>c12C[C@@H]([C@@H](Cc1cccc2OCC(CNC(C)(C)C)O)O)O</chem>
Prestw-819	64953-12-4	<chem>[C@@]1(C(N\2[C@@]1)OC\C=C2\C([O-])=O)\CS1n(nnn1)C)[H]=O)(NC([C@H](C([O-])=O)c1ccc(cc1)O)=O)OC</chem>
Prestw-820	317-34-0	<chem>N1(c2c(C(N(C1=O)C)=O)[nH]cn2)C.N1(c2c(C(N(C1=O)C)=O)[nH]cn2)C</chem>
Prestw-821	37091-65-9	<chem>N12[C@@]([C@@](C1=O)(NC([C@H](NC(N1C(NCC1)=O)=O)c1cccc1)=O)[H])(SC([C@@H]2C([O-])=O)(C)C)[H]</chem>
Prestw-822	3485-62-9	<chem>C(C(c1cccc1)(c1cccc1)O)(OC1C[N+](CCC1CC2)C)=O</chem>
Prestw-823	1220-83-3	<chem>S(Nc1ncnc(c1)OC)(c1ccc(N)cc1)(=O)=O</chem>
Prestw-824	91-33-8	<chem>S1(c2c(N=C/N1)\CSCc1cccc1)cc(c(S(=O)(=O)N)c2)Cl(=O)=O</chem>
Prestw-825	133-67-5	<chem>S1(NC(Nc2c1cc(S(=O)(=O)N)c(c2)Cl)C(Cl)Cl(=O)=O</chem>
Prestw-826	1949-20-8	<chem>n1c(noc1CCN(CC)CC)c1cccc1</chem>
Prestw-827	50-34-0	<chem>C1(c2c(Oc3c1cccc3)cccc2)C(=O)OCC[N+](C(C)C)(C(C)C)C</chem>
Prestw-1361	35604-67-2	<chem>N1CC(OCC1)COc1c(OCC)cccc1</chem>
Prestw-829	695-53-4	<chem>N1C(OC(C1=O)(C)C)=O</chem>
Prestw-830	985-13-7	<chem>c12c(nccc1cc(c(c2)OCC)OCC)Cc1cc(c(cc1)OCC)OCC</chem>
Prestw-831	149-16-6	<chem>C(c1ccc(N)cc1)(=O)OCCCN(CCCC)CCCC</chem>
Prestw-832	33564-30-6	<chem>[C@@]1(C(N\2[C@@]1)SC\C=C2\C([O-])=O)\COC(=O)N)[H]=O)(NC(Cc1sccc1)=O)OC</chem>
Prestw-1824	138729-47-2	<chem>CN1CCN(CC1)C(=O)O[C@H]2c3c(ncn3)C(=O)N2c4ccc(cn4)Cl</chem>
Prestw-834	1476-53-5	<chem>C1(=C(\c2c(OC1=O)c(c(O[C@H]1[C@@H]([C@@H]([C@H](C(O1)(C)C)OC(=O)N)O)cc2)C)/O)/NC(c1cc(c([O-])cc1)C)\C=C(/C)\C)=O</chem>
Prestw-1800	139264-17-8	<chem>O=C1NC(Cc2ccc3[nH]cc(CCN(C)C)c3c2)CO1</chem>
Prestw-836	31842-01-0	<chem>N1(C(c2c(C1)cccc2)=O)c1ccc(C(C(=O)O)C)cc1</chem>
Prestw-837	7421-40-1	<chem>C=1/2[C@]([C@]3([C@@]([C@@]4([C@]([C@@H](OC(=O)CCC([O-])=O)CC4)(C)C)(CC3)[H])C)/C1=O)[H])C)(CC[C@@]1([C@]2[C@@]([C@]([O-])=O)(CC1)C)[H])C)C</chem>
Prestw-838	16034-77-8	<chem>c1(N(CC(C(=O)O)C)C(=O)C)c(c(cc1))N </chem>
Prestw-839	82410-32-0	<chem>c1/2c(ncn1COC(CO)(CO)[H])C(N/C(=N2)/N)=O</chem>
Prestw-840	1094-08-2	<chem>N1(c2c(Sc3c1cccc3)cccc2)CC(N(CC)CC)C</chem>
Prestw-1455	132539-06-1	<chem>c12c(Nc3c(\N=C1\N1CCN(CC1)C)cccc3)sc(c2)C</chem>
Prestw-842	4330-99-8	<chem>c12c(cccc1)Sc1c(N2CC(CN(C)C)C)cccc1.c12c(cccc1)Sc1c(N2CC(CN(C)C)C)cccc1</chem>
Prestw-843	7177-50-6	<chem>N12[C@@]([C@@](C1=O)(NC(c1c3c(ccc1OCC)cccc3)=O)[H])(SC([C@@H]2C([O-])=O)(C)C)[H]</chem>
Prestw-844	1508-76-5	<chem>C(CCN1CCCC1)(c1cccc1)(C1CCCC1)O</chem>
Prestw-845	60414-06-4	<chem>[C@@]12([C@](O[C@@]([C@@H]1OCCCN(C)C)([C@H](O)CO)[H])(OC(O2)(C)C)[H])[H]</chem>
Prestw-846	72-33-3	<chem>[C@]12([C@]([C@]3([C@@]([C@@]4(CC3)cc(cc4)OC)(CC1)[H])[H])(CC[C@]2(C#C)O)[H])C</chem>
Prestw-847	27912-14-7	<chem>c12c(c(OC[C@H](CNC(C)(C)C)O)ccc1)CCCC2=O</chem>
Prestw-848	92339-11-2	<chem>c1(c(c(c(c1)C(NCC(O)CO)=O))C(NCC(O)CO)=O)N(C(=O)C)CC(CN(c1c(c(c(c1)C(NCC(O)CO)=O))C(NCC(O)CO)=O))C(=O)O</chem>
Prestw-1379	105956-97-6	<chem>N1(c2c(C/C(=C1)/C(=O)O)=O)cc(c(c2Cl)N1CC(C)N)F)C1CC1</chem>
Prestw-850	474-86-2	<chem>C/1=2[C@]3([C@@](C(CC3)=O)(CC[C@@]1(c1c(C1C2)cc(cc1)O)[H])C)[H]</chem>
Prestw-851	110429-35-1	<chem>c12cc(OC[C@H]3[C@H](c4ccc(cc4)F)CCNC3)ccc1OCO2</chem>

Prestwick Nr.	CAS number	Smiles code
Prestw-1454	447-41-6	<chem>N(C(C(c1ccc(cc1)O)O)C)C(CCc1ccccc1)C</chem>
Prestw-853	6893-02-3	<chem>c1(c(cc(cc1)C[C@@H](C(=O)O)N)I)Oc1cc(c(cc1)O)I</chem>
Prestw-854	80214-83-1	<chem>[C@]1([C@@H]([C@H](C[C@H](O1)C)N(C)C)O)(O[C@@H]1[C@H]([C@@H]([C@H](C(O[C@@H]([C@]([C@@H]([C@H](C(CO)C)C)O)(O)C)CC)=O)C)O[C@H]1C[C@]([C@H]([C@@H](O1)C)O)(OC)C)[H]</chem>
Prestw-855	5534-09-8	<chem>[C@]12([C@]([C@H](C[C@]1([C@]1([C@@]([C@@]3(C=C/C(C=C3)=O)CC1)C)[C@H](C2)O)C)I)[H])[H]C(C(COC(=O)CC)=O)OC(=O)CC)C</chem>
Prestw-856	64490-92-2	<chem>c1(n(c(CC([O-])=O)cc1)C)C(c1ccc(cc1)C)=O</chem>
Prestw-857	47141-41-3	<chem>c12c(c(OC[C@@H](CNC(C)(C)C)O)ccc1)CCCC2=O</chem>
Prestw-858	77883-43-3	<chem>c1(nc(c2c(n1)cc(c(c2)OC)OC)N)N1CCN(C(C2Oc3c(OC2)cccc3)=O)CC1</chem>
Prestw-859	93957-55-2	<chem>c1(n(c2c(c1c1ccc(cc1)F)cccc2)C(C)C)/C=C/[C@@H](C[C@@H](CC([O-])=O)O)O</chem>
Prestw-1836	4789-68-8	<chem>Clc4cc2c(Sc1cccc1CC2N3CCN(C)CC3)cc4</chem>
Prestw-861	60142-96-3	<chem>C1(CCCCC1)(CC(O)=O)CN</chem>
Prestw-862	82640-04-8	<chem>c1(c(sc2c1ccc(c2)O)c1ccc(cc1)O)C(c1ccc(cc1)OCCN1CCCC1)=O</chem>
Prestw-1801	126544-47-6	<chem>OC1CC2(C)C(C3C1C1(C=CC(C=C1CC3)=O)C)CC1C2(OC(C2CCCC2)O1)C(COC(C(C)C)=O)=O</chem>
Prestw-1837	320345-99-1	<chem>OC(C(=O)O[C@H]1C[N+]2(CCCOC3=CC=CC=C3)CCC1CC2)(C1=CC=CS1)C1=CC=CS1</chem>
Prestw-865	79902-63-9	<chem>C=12/[C@]([C@@H](OC(C(C)C)=O)C[C@H](C1)C)([C@@](CC[C@]1(OC(C[C@@H](C1)O)=O)[H])([C@H](C=C2)C)[H])[H]</chem>
Prestw-866	320-67-2	<chem>[N@@]1(C2[C@H]([C@H]([C@H](O2)CO)O)O)C(/N=C(N=C1)/N)=O</chem>
Prestw-867	1263-89-4	<chem>[C@@H]1([C@](OC2[C@H]([C@H]([C@H]([C@H](O2)CO)O)N)([C@H](C[C@H]([C@@H]1O)N)N)[H])O[C@]1([C@@H]([C@H](O[C@@]2([C@@H]([C@H]([C@@H]([C@@H](O2)CN)O)O)N)[H])[C@H](O1)CO)O)[H]</chem>
Prestw-868	103-90-2	<chem>C(Nc1ccc(cc1)O)(=O)C</chem>
Prestw-869	85-73-4	<chem>c1cccc(c1C(O)=O)C(Nc1ccc(cc1)S(Nc1nccs1)(=O)=O)=O</chem>
Prestw-870	491-70-3	<chem>c12c(\C=C(/Oc1cc(cc2O)O)\c1cc(c(cc1)O)O)=O</chem>
Prestw-871	60166-93-0	<chem>c1(c(c(c(c1)NC(=O)[C@@](O)(C)[H])C(NC(CO)CO)=O)I)C(NC(CO)CO)=O</chem>
Prestw-872	73334-07-3	<chem>c1(c(c(c(c1)C(NCC(O)CO)=O)I)NC(=O)COC)I)C(N(CC(O)CO)C)=O</chem>
Prestw-873	5967-84-0	<chem>N1(c2c(C(N(C1=O)C)=O)[nH]cn2)C</chem>
Prestw-874	83-67-0	<chem>c12c(C(NC(N1C)=O)=O)n(cn2)C</chem>
Prestw-875	50-55-5	<chem>c12[nH]c3c(c1CCN1[C@@]2[C@]2([C@@H]([C@H]([C@H](OC(c4cc(c(c4)OC)OC)OC)=O)C[C@@]2(C1)[H])OC)C(=O)OC)[H])[H]ccc(c3)OC</chem>
Prestw-1239	90357-06-5	<chem>S(CC(C(Nc1cc(C(F)F)F)c(C#N)cc1=O)(O)C)(c1ccc(cc1)F)(=O)=O</chem>
Prestw-877	55-16-3	<chem>[C@@H]12[C@@H](O1)[C@H]1N([C@@H]2C[C@H](C1)OC([C@@H](c1ccccc1)CO)=O)C</chem>
Prestw-878	87771-40-2	<chem>c1(c(c(c(c1)C(NCC(O)CO)=O)I)C(NCC(O)CO)=O)I)N(C(=O)CO)CCO</chem>
Prestw-1495	117976-89-3	<chem>c1(nc2c([nH]1)cccc2)S(Cc1c(c(ccn1)OCCOC)C)=O</chem>
Prestw-880	51-83-2	<chem>C(=O)(N)OCC[N+](C)(C)C</chem>
Prestw-881	59-67-6	<chem>C(c1cnccc1)(=O)O</chem>
Prestw-882	64-65-3	<chem>N1C(=O)CC(CC1=O)(CC)C</chem>
Prestw-883	1672-46-4	<chem>[C@]12([C@@]([C@@H](C3=C(CO)C)=O)CC1)([C@@H](C[C@@]1([C@@]3([C@](CC[C@@]21[H])(C[C@H](CC3)O)[H])C)[H])O)C)O</chem>
Prestw-884	6284-40-8	<chem>[C@H]([C@@H]([C@@H](O)CNC)O)([C@H](O)CO)O</chem>
Prestw-1510	115956-13-3	<chem>c1(C(O[C@H]2C[C@@]3(N4[C@](C2)(C[C@@](C(C4)=O)(C3)[H])[H])=O)c[nH]c2c1cccc2</chem>
Prestw-886	130-26-7	<chem>c12c(c(cc(c1ccn2)Cl)I)O</chem>
Prestw-887	131-57-7	<chem>c1(C(=O)c2cccc2)c(cc(cc1)OC)O</chem>
Prestw-888	58-33-3	<chem>N1(c2c(Sc3c1cccc3)cccc2)CC(N(C)C)C</chem>
Prestw-1167	13739-02-1	<chem>c12c(c3c(C(c1cc(C(=O)O)cc2OC(=O)C)=O)cccc3OC(=O)C)=O</chem>
Prestw-1137	81161-17-3	<chem>C(=O)(CCc1ccc(OCC(CNC(C)C)O)cc1)OC</chem>
Prestw-1486	50-03-3	<chem>[C@]12([C@@]([C@@H](C(COC(=O)C)=O)(CC[C@]1([C@]1([C@@]([C@@]3(C=C/C(=O)CC3)\CC1)C)([C@H](C2)O)[H])[H])O)C</chem>
Prestw-1416	31430-15-6	<chem>c1(nc2c([nH]1)ccc(C(c1ccc(cc1)F)=O)c2)NC(=O)OC</chem>
Prestw-893	5728-52-9	<chem>C(=O)(Cc1ccc(c2cccc2)cc1)O</chem>



Prestwick Nr.	CAS number	Smiles code
Prestw-894	94-26-8	<chem>C(c1ccc(cc1)O)(=O)OCCCC</chem>
Prestw-895	61-78-9	<chem>C(NCC(=O)O)(c1ccc(N)cc1)=O</chem>
Prestw-896	1188-21-2	<chem>[C@@](C(=O)O)(NC(=O)C)(CC(C)C)[H]</chem>
Prestw-897	51940-44-4	<chem>C=1(\C(c2c(nc(nc2)N2CCNCC2)N(/C1)CC)=O)/C(=O)O</chem>
Prestw-898	131-53-3	<chem>C(c1c(cc(cc1)OC)O)(c1c(O)cccc1)=O</chem>
Prestw-899	382-45-6	<chem>[C@]12([C@]([C@]3([C@@]([C@@]4(\C=C/C(=O)CC4)\CC3)C)(C(C1)=O)[H])[H])(CCC2=O)[H]C</chem>
Prestw-900	52-88-0	<chem>[N@@+](C1([C@@H]2C[C@@H](OC(Cc3cccc3)CO)=O)CC1CC2)(C)C</chem>
Prestw-901	90-33-5	<chem>c12OC(/C=C(\c1ccc(c2)O)/C)=O</chem>
Prestw-1512	188062-50-2	<chem>c12n(cnc1c(nc(n2)N)NC1CC1)[C@H]1\C=C/[C@H](C1)CO</chem>
Prestw-903	3736-81-0	<chem>C(N(c1ccc(OC(c2occc2)=O)cc1)C)(C(Cl)Cl)=O</chem>
Prestw-904	54-36-4	<chem>C(C(c1cnc1)C)C(c1cnc1)=O</chem>
Prestw-905	64887-14-5	<chem>C1(N(/C(=C\C1N1C)=O)/NCCCN1CCN(c2c(OC)cccc2)CC1)C=O</chem>
Prestw-906	1841-19-6	<chem>C12(N(CNC1=O)c1cccc1)CCN(CC2)CCCC(c1ccc(cc1)F)c1ccc(cc1)F</chem>
Prestw-907	51146-56-6	<chem>C([C@H](c1ccc(cc1)CC(C)C)(=O)O</chem>
Prestw-908	297-76-7	<chem>[C@]12([C@]([C#C](OC(=O)C)CC[C@]1([C@]1([C@@]([C@@]3(\C=C/[C@@H](OC(=O)C)CC3)\CC1)[H])(CC2)[H])[H])[H]C</chem>
Prestw-909	42924-53-8	<chem>c12c(cc(cc1)OC)ccc(c2)CCC(=O)C</chem>
Prestw-910	57754-86-6	<chem>O(c1c(OC)cccc1)C(c1cccc1)CCNC</chem>
Prestw-911	14638-70-1	<chem>c1c(c(ccc1[C@@H](CNC(C)C)O)O)O</chem>
Prestw-912	103-16-2	<chem>O(c1ccc(cc1)O)Cc1cccc1</chem>
Prestw-913	3306-62-5	<chem>S(c1c(N)cccc1)(=O)(=O)N</chem>
Prestw-914	53-16-7	<chem>[C@]12([C@]([C@]3([C@@]([C@@]4(c4c(CC3)cc(cc4)O)(CC1)[H])[H])(CCC2=O)[H])C</chem>
Prestw-915	97964-56-2	<chem>C(NC(C(N(CCCCC)CCCC)=O)CCC([O-])=O)(c1cc(c(cc1)Cl)Cl)=O</chem>
Prestw-916	39562-70-4	<chem>C=1(\C(\C(=C(/N/C1/C)\C)\C(=O)OCC)c1cc([N+][[O-])=O)ccc1)/C(=O)OC</chem>
Prestw-917	5104-49-4	<chem>c1(c(ccc(c1)C(C(=O)O)C)c1cccc1)F</chem>
Prestw-918	66085-59-4	<chem>C=1(\C(\C(=C(/N/C1/C)\C)\C(=O)OCCOC)c1cc([N+][[O-])=O)ccc1)/C(OC(C)C)=O</chem>
Prestw-919	1405-87-4	<chem>N1[C@@H](C(=O)N[C@H](C(=O)NCCCC[C@H](NC([C@@H](NC([C@@H](NC([C@@H](NC(C/2CS/C(=N2)/C(N)C(CC)C)=O)CC(C)C)=O)CCC(=O)O)=O)C(=O)N[C@@H](C(N[C@H](C(=O)N[C@@H](C(N[C@H](C1=O)Cc1[nH]cnc1)=O)Cc1cccc1)[C@@H](C)C)=O)CCCN)CC(=O)N)CC(=O)O</chem>
Prestw-1825	204519-65-3	<chem>CO\N=C\1/CN(CC1CN)c2nc3N(C=C(C(=O)O)C(=O)c3cc2F)C4CC4</chem>
Prestw-921	76963-41-2	<chem>[N+](\C=C(\NC)/NCCSCc1nc(sc1)CN(C)C)([O-])=O</chem>
Prestw-922	106243-16-7	<chem>C(N1CCC(c2nc[nH]c2)CC1)(NC1CCCC1)=S</chem>
Prestw-923	73210-73-8	<chem>C(N1CCOCC1)(=O)NCCNCC(COc1ccc(cc1)O)O.C(N1CCOCC1)(=O)NCCNCC(COc1ccc(cc1)O)O</chem>
Prestw-1826	171228-49-2	<chem>CC[C@@H]([C@H](C)O)N1N=CN(C1=O)C1=CC=C(C=C1)N1CCN(CC1)C1=CC=C(OCC2CO[C@](CN3C=NC=N3)(C2)C2=C(F)C=C(F)C=C2)C=C1</chem>
Prestw-925	553-08-2	<chem>c1(CN(CC[N+](CC)(C)C)c2nccn2)ccc(cc1)OC</chem>
Prestw-926	79944-56-2	<chem>C1(Oc2c(OC1)cccc2)\C1=N\CCN1</chem>
Prestw-927	82586-55-8	<chem>N1(C([C@@H](N[C@H](C(=O)OCC)CCc2cccc2)C)=O)[C@@H](Cc2c(C1)cccc2)C(=O)O</chem>
Prestw-928	63612-50-0	<chem>N1(C(NC(C1=O)(C)C)=O)c1cc(c([N+][[O-])=O)cc1)C(F)(F)F</chem>
Prestw-929	74103-07-4	<chem>n12c(C(C(=O)O)CC1)ccc2C(=O)c1cccc1</chem>
Prestw-930	1225-55-4	<chem>C1(c2c(\C=C/c3c1cccc3)cccc2)CCCN</chem>
Prestw-931	2078-54-8	<chem>c1(c(C)C)cccc1C(C)O</chem>
Prestw-932	97612-24-3	<chem>c1(c(c(cc(c1OC)Cl)CC)O)C(NC[C@H]1N(CCC1)CC)=O</chem>
Prestw-933	125-33-7	<chem>C1(C(NCNC1=O)=O)(c1cccc1)CC</chem>
Prestw-934	2022-85-7	<chem>N\1=C(\C(=C/N1=O)\F)/N</chem>
Prestw-1827	144598-75-4	<chem>Cc1c(c(=O)n2c(n1)C(CCC2)O)CCN3CCC(CC3)c4c5ccc(cc5on4)F</chem>
Prestw-936	3818-50-6	<chem>[N+](Cc1cccc1)(CCOc1cccc1)(C)C</chem>
Prestw-937	853-23-6	<chem>[C@@]12(/C(=C\C[C@@]3([C@@]1(CC[C@]1([C@]3(CCC1=O)[H])C)[H])[H])C[C@@H](OC(=O)C)CC2)C</chem>
Prestw-938	14919-77-8	<chem>c1(c(c(ccc1O)CN)C(N)CO)=O)O</chem>
Prestw-939	606-17-7	<chem>c1(c(c(c(cc1))N)C(=O)CCCC(Nc1c(c(c(cc1))C(=O)O))=O)C(=O)O</chem>

Prestwick Nr.	CAS number	Smiles code
Prestw-1213	315-30-0	c12c(\N=C/NC1=O)[nH]nc2
Prestw-941	67-43-6	N(CCN(CCN(CC(O)=O)CC(O)=O)CC(=O)O)(CC(O)=O)CC(O)=O
Prestw-942	61-75-6	c1(C[N+](CC)(C)C)c(Br)cccc1
Prestw-943	51-15-0	[n+] <sup>1</sup> (c(\C=N\O)cccc1)C
Prestw-944	63-92-3	N(Cc1cccc1)(C(COc1cccc1)C)CCCI
Prestw-945	89365-50-4	c1(cc(ccc1O)C(O)CNCCCCCOCCCCc1cccc1)CO
Prestw-946	645-05-6	n1c(nc(nc1N(C)C)N(C)C)N(C)C
Prestw-947	19237-84-4	c1(nc(c2c(n1)cc(c2)OC)OC)N)N1CCN(C(c2cccc2)=O)CC1
Prestw-948	26921-17-5	c1(c(nsn1)OC[C@H])(CNC(C)(C)C)O)N1CCOCC1
Prestw-949	770-05-8	c1(ccc(cc1)O)C(O)CN
Prestw-1279	3056-17-5	N\1(C(NC(\C=C1)\C)=O)=O)[C@@H]\1O[C@@H](\C=C1)CO
Prestw-951	483-63-6	N(C(/C=C/C)=O)(c1c(C)cccc1)CC
Prestw-1197	89778-26-7	C(=C(/c1cccc1)\CCCI)(/c1ccc(cc1)OCCN(C)C)\c1cccc1
Prestw-536	56715-13-0	C(=O)(Cc1ccc(OC[C@H])(CNC(C)C)O)cc1)N
Prestw-954	25301-02-4	O(COCCOCCO)c1c(Cc2cc(cc(Cc3cc(ccc3OCOCOCOCO)C(CC(C)(C)C)(C)C)c2OCOCOCOC O)C(CC(C)(C)C)(C)C)cc(cc1)C(CC(C)(C)C)(C)C
Prestw-955	73231-34-2	S(c1ccc([C@H])([C@H](NC(C)Cl)=O)CF)O)cc1(=O)(=O)C
Prestw-956	595-33-5	C/1=2\C@@@([C@@]3[C@@](/C=C1/C)([C@]1([C@@]([C@@](CC1)(OC(=O)C)C(=O)C)(C C3)C)[H])[H])[H])(CCC/C2)=O)C
Prestw-957	64-85-7	[C@]12([C@]([C@]3[C@@]([C@@]4(\C=C/C(=O)CC4)CC3)C)(CC1)[H])[H])(CC[C@@H]2C (=O)CO)[H]C
Prestw-958	128-13-2	[C@]12([C@]([C@]3[C@@]([C@@]4([C@](C[C@@H]3O)(C[C@@H](CC4)O)[H])C)(CC1)[H ])[H])(CC[C@@]2([C@@H](CCC(=O)O)C)[H])[H]C
Prestw-959	5875-06-9	C(c1cc(c(cc1)OCCC)N)(=O)OCCN(CC)CC
Prestw-960	60-32-2	C(=O)(O)CCCCCN
Prestw-961	3734-33-6	c1(NC(C[N+](Cc2ccccc2)(CC)CC)=O)c(cccc1)C
Prestw-1259	976-71-6	[C@@]12(\C(\C=C/[C@@]3([C@@]1(CC[C@@]1([C@@]4(OC(=O)CC4)CC[C@]13[H])C)[H] )H])=C/C(=O)CC2)C
Prestw-963	35554-44-0	c1(c(cc(cc1)Cl)Cl)C(Cn1cnc1)OCC=C
Prestw-964	3963-95-9	[C@@]1 <sup>2</sup> ([C@]([C@@H](\C=C(/C1=O)\C(=O)N)O)N(C)C)([C@H]([C@]1(\C=C2\O)\C(c2c( C1=C)cccc2O)=O)[H])O)[H]O
Prestw-1415	50-91-9	N/1(C(NC(/C=C1)/F)=O)=O)[C@@H]1O[C@@H]([C@H](C1)O)CO
Prestw-966	959-24-0	S(Nc1ccc(cc1)C(CNC(C)C)O)(=O)(=O)C
Prestw-1267	16320-04-0	C/1\2=C\3/C(=C\C(=O)CC3)/CC[C@]1([C@]1([C@](\C=C2)([C@](C#C)(CC1)O)CC)[H])[H]
Prestw-968	541-22-0	[N+](CCCCCCCC[N+](C)(C)C)(C)C
Prestw-1514	133099-07-7	C([C@H]1CN(CC1)CCc1cc2c(OCC2)cc1)(C(=O)N)(c1cccc1)c1cccc1
Prestw-1602	86939-10-8	[C@@H]1(c2c([C@H](C1)NC)cccc2)c1cc(c(cc1)Cl)Cl
Prestw-971	73220-03-8	c1(C(NC[C@]2(N(CCC2)CC)[H])=O)c(c(ccc1OC)Br)OC
Prestw-1838	287714-41-4	CC(C)C1=NC(=NC(C2=CC=C(F)C=C2)=C1\C=C\C@@H(O)C[C@@H](O)CC(=O)O)N(C)S( C)(=O)=O
Prestw-973	60762-57-4	n12c3c(c4c1ccc(c4)C)CCCC3NCC2
Prestw-974	51-02-5	c1(cc2c(cc1)cccc2)C(CNC(C)C)O
Prestw-975	57149-08-3	N1(c2c(OC)cccc2)CCN(CC(COc2c3c(ccc2)cccc3)O)CC1
Prestw-976	41094-88-6	c12c(nc(c1NCCCC)C(=O)OCC)C)n(nc2)CC
Prestw-977	101975-10-4	N=1\NC(\C=C/C1/c1cc(c(OC(F)F)cc1)OC)=O
Prestw-978	41100-52-1	C12(CC3(CC(C1)(CC(C2)C3)C)C)N
Prestw-979	78712-43-3	n1cn(cc1)Cc1ccc(\C=C\C(=O)O)cc1
Prestw-980	3605-01-4	c1(N2CCN(Cc3cc4c(OCO4)cc3)CC2)ncccn1
Prestw-981	98636-73-8	[N+](c1ccc(C2(C(=O)OCCN(CC)CC)CCCC2)cc1)([O-])=O
Prestw-982	434-22-0	[C@]12([C@]([C@]3[C@@]([C@@]4(\C=C/C(=O)CC4)CC3)[H])(CC1)[H])[H])(CC[C@@H]2 O)[H]C
Prestw-983	23256-33-9	C(=N)(SCCCN(C)C)N

Prestwick Nr.	CAS number	Smiles code
Prestw-1459	53716-50-0	<chem>c1(nc2cc(S(=O)c3ccccc3)ccc2[nH]1)NC(=O)OC</chem>
Prestw-1268	90-05-1	<chem>c1(c(OC)cccc1)O</chem>
Prestw-1828	154361-50-9	<chem>CCCCOC(=O)Nc1c(cn(c(=O)n1)[C@H]2[C@@H]([C@@H]([C@H](O2)C)O)O)F</chem>
Prestw-1316	104632-25-9	<chem>n1c(sc2c1CC[C@@H](C2)NCCC)N</chem>
Prestw-1452	35189-28-7	<chem>[C@]12([C@@](C#C)(OC(=O)C)CC[C@]1([C@]1([C@@]([C@@]3\(\C=C/C(=NO)CC3)\CC1)[H])(CC2)[H])[H]C</chem>
Prestw-1374	302-22-7	<chem>C/1=2\([C@@]([C@@]3([C@@]([C@@]4\(\C=C1/Cl)([C@]1([C@@]([C@@]([C@@]1(OC(=O)C)C(=O)C)(C3)C)[H])[H])(CCC/C2)=O)C</chem>
Prestw-1310	50-33-9	<chem>N1(N(C(C(C1=O)CCCC)=O)c1cccc1)c1cccc1</chem>
Prestw-991	33342-05-1	<chem>N1(C(C(c2c(C1=O)cc(cc2)OC)(C)C)=O)CCc1ccc(S(NC(NC2CCCC2)=O)(=O)=O)cc1</chem>
Prestw-992	5189-11-7	<chem>C1(/c2c(scc2)CCc2c1cccc2)=C1/CCN(CC1)C</chem>
Prestw-993	36791-04-5	<chem>n1([C@H]2[C@@H]([C@@H]([C@H](O2)CO)O)O)nc(nc1)C(=O)N</chem>
Prestw-994	742-20-1	<chem>S1(c2c(NC(N1)CC1CCCC1)cc(c(S(=O)(=O)N)c2)Cl)(=O)=O</chem>
Prestw-995	61718-82-9	<chem>C(c1ccc(\C(=N)OCCN)\CCCCOC)cc1(F)F</chem>
Prestw-1321	14222-60-7	<chem>C(c1cc(ncc1)CCC)(=S)N</chem>
Prestw-997	80474-14-2	<chem>[C@]1\2([C@@]3([C@]([C@]4([C@]([C@]([C@@H](C4)C)(C(SCF)=O)OC(=O)CC)(C[C@@H]3O)C)[H])(C[C@@H](/C1=C/C(\C=C2)=O)F)[H])F)C</chem>
Prestw-998	633-59-0	<chem>C1(/c2c(Sc3c1cccc3)ccc(c2)Cl)=C/CCN1CCN(CC1)CCO</chem>
Prestw-999	637-32-1	<chem>C(NC(=N)NC(C)C)(Nc1ccc(Cl)cc1)=N</chem>
Prestw-1000	992-21-2	<chem>[C@@]12(/C=C\3/C(c4c([C@]([C@]3[C@]1([C@@H]([C@@]1(C=C(\C2=O)/C(NCNC(C(=O)O)CC)CCN)=O)/O)N(C)C)[H])(O)C)cccc4O)=O)/O)O</chem>
Prestw-1001	23930-37-2	<chem>[C@]12([C@]([C@]3([C@@]([C@@]4([C@@]([C@]([C@@H](CC3)C[C@@H](CC4)O)[H])C)(C(C1)=O)[H])(H)(CC[C@@H]2C(COC(=O)C)=O)[H])C</chem>
Prestw-1002	23930-19-0	<chem>[C@]12([C@]([C@]3([C@@]([C@@]4([C@@]([C@]([C@@H](CC3)C[C@@H](CC4)O)[H])C)(C(C1)=O)[H])(H)(CC[C@@H]2C(=O)C)[H])C</chem>
Prestw-1003	13539-59-8	<chem>N1\2N(C(C(C1=O)CCC)=O)c1c(\N=C2\N(C)C)ccc(c1)C</chem>
Prestw-1004	59263-76-2	<chem>C1(c2cc(O)ccc2)(CN(C)CCCC1)CC</chem>
Prestw-1005	37321-09-8	<chem>C12O[C@H](O[C@]3([C@@H]([C@H]([C@@H]([C@@H]([C@@H]3N)N)O)O)[H])[C@@H](C[C@@]1(OC([C@H]([C@H]2O)NC)O[C@@]1([C@@H]([C@H]([C@@H]([C@H](O1)CO)N)O)O)[H])[H])N</chem>
Prestw-1802	635728-49-3	<chem>O=S(N(CC(C)C)CC(O)C(NC(=O)OC1COC2OCCC12)Cc1cccc1)(c1ccc(N)cc1)=O</chem>
Prestw-1007	2105-43-3	<chem>n1c(c(CN(\C(=C(\SSCC2OCCC2)/CCO)\C)C=O)cnc1)C)N</chem>
Prestw-1008	56974-61-9	<chem>C(=N)(NCCCCC(OC1ccc(C(=O)OCC)cc1)=O)N</chem>
Prestw-1009	33817-20-8	<chem>N12[C@@]([C@@](C1=O)(NC([C@@H](c1cccc1)N)=O)[H])(SC([C@@H]2C(OCOC(C(C)C)C)C)=O)(C)C)[H]</chem>
Prestw-1746	53882-12-5	<chem>c1(c(c(NC(C(=O)O)=O)cc(C#N)c1)Cl)NC(C(=O)O)=O</chem>
Prestw-1011	1847-24-1	<chem>N12[C@@]([C@@](C1=O)(NC(c1c(noc1C)c1c(F)cccc1)Cl)=O)[H])(SC(C2C([O-])=O)(C)C)[H]</chem>
Prestw-1012	15421-84-8	<chem>n12c(ncn1)nc(cc2N(CC)CC)C</chem>
Prestw-1013	2169-75-7	<chem>C1(c2c(CCc3c1cccc3)cccc2)OC1C[C@@H]2N([C@H](C1)CC2)C</chem>
Prestw-1014	79617-96-2	<chem>c12[C@]([c3cc(c(cc3)Cl)Cl)(CC[C@@]([c1cccc2)(NC)[H])[H]</chem>
Prestw-1015	2624-44-4	<chem>S(c1cc(ccc1O)O)(=O)(=O)O</chem>
Prestw-1016	75438-57-2	<chem>c1(c(nc(nc1OC)C)Cl)N/C1=N/CCN1</chem>
Prestw-1017	534-87-2	<chem>c1(cc(O)ccc1)C(O)CNCC</chem>
Prestw-1018	745-65-3	<chem>C1(C[C@H]([C@H](\C=C\1[C@@H](O)CCCC)[C@H]1CCCCCCC(=O)O)O)=O</chem>
Prestw-1019	10310-32-4	<chem>[C@@H]1([C@](OC([C@@H]1O)OCC)([C@H](OCc1cccc1)COCc1cccc1)[H])OCc1cccc1</chem>
Prestw-1020	49697-38-3	<chem>[C@]12([C@]([C@]3([C@@]([C@@]4\(\C=C/C(\C=C4)=O)\CC3)C)([C@H](C1)O)[H])[H])(C[C@@H]([C@@]2(C(=O)CC)C)[H])C</chem>

Prestwick Nr.	CAS number	Smiles code
Prestw-1021	75695-93-1	<chem>C=1/C/C(=C(N\C1\C)/C)/C(=O)OC)c1c2c(non2)ccc1)\C(OC(C)C)=O</chem>
Prestw-1774	130636-43-0	<chem>C1(N/C(=C\C(N1C)=O)/NCCN(CCCc1ccc([N+][O-])=O)cc1)CCO)C)=O</chem>
Prestw-1023	7492-31-1	<chem>C(=C\CCC(NC)C)\(C)/C.C(=C\CCC(NC)C)\(C)/C</chem>
Prestw-1024	23256-30-6	<chem>S1(CC(N(N=Cc2oc([N+][O-])=O)cc2)CC1)C(=O)=O</chem>
Prestw-1025	112809-51-5	<chem>n1(ncnc1)C(c1ccc(C#N)cc1)c1ccc(C#N)cc1</chem>
Prestw-1829	100986-85-4	<chem>C[C@H]1COc2c(N3CCN(C)CC3)c(F)cc4C(=O)C(=CN1c24)C(=O)O</chem>
Prestw-1027	71395-14-7	<chem>N(C(=O)C(N)C)c1c(cccc1C)C</chem>
Prestw-1028	5928-84-7	<chem>N12[C@@]([C@@](C1=O)(NC(=O)COc1ccccc1)[H])(SC(C2C(=O)O)(C)C)[H].N12[C@@]([C@@](C1=O)(NC(=O)COc1ccccc1)[H])(SC(C2C(=O)O)(C)C)[H]</chem>
Prestw-1029	106266-06-2	<chem>C=1\C(N2C(=N/C1/C)CCCC2=O)/CCN1CCC(c2noc3c2ccc(c3)F)CC1</chem>
Prestw-1030	56211-40-6	<chem>S(NC(NC(C)C)=O)(c1c(Nc2cc(ccc2)C)ccnc1)(=O)=O</chem>
Prestw-1031	36167-63-2	<chem>c12c3c(cc(c1ccc(C(F)(F)F)c2)C(CCN(CCCC)CCCC)O)c(cc(c3)Cl)Cl</chem>
Prestw-1032	23964-57-0	<chem>c1(c(NC(=O)C(NCCC)C)c(cs1)C)C(=O)OC</chem>
Prestw-1033	58652-20-3	<chem>[C@]12([C@@](CC[C@]1([C@@]1/C=C\C=3[C@@]([C@]1(CC2)[H])(CCC(/C3)=O)[H])/C)[H])(OC(=O)C)C(=O)C</chem>
Prestw-1034	15500-66-0	<chem>[C@]12([C@]([C@]3([C@@]([C@]4[C@H]([N+](C)CCCC5)[C@H](C[C@@]4(CC3)[H])O C(=O)C)C(C1)[H])[H])(C[C@H]([C@H]2OC(=O)C)[N+](C)CCCC1)[H])C</chem>
Prestw-1035	15622-65-8	<chem>c12c([nH]c(c1CC)C)CCC(C2=O)CN1CCOCC1</chem>
Prestw-1036	15180-03-7	<chem>[C@@]123C4N(\C=C/5/C6[C@@]7([C@]8([N+](C/C/[C@]5(C8)[H])=C\CO)(CC7)CC=C)[H])c5c(N6\C=C4\C[C@@]4(\C1[N@@+][C@]1(C4)[H])(CC2)CC=C=C\CO)[H])cccc5)c1c3ccc c1</chem>
Prestw-1037	7481-89-2	<chem>N1(C/N=C\C=C1)/N=O)[C@@H]1O[C@@H](CC1)CO</chem>
Prestw-1038	2508-79-4	<chem>c1(C[C@](C(OCC)=O)(C)N)cc(c(cc1)O)O</chem>
Prestw-1039	79547-78-7	<chem>[C@]1([C@@H](CN([C@]2(CC[C@](C#N)(c3ccc(cc3)F)CC2)[H])CC1)C)(C(=O)O)c1ccccc1</chem>
Prestw-1040	3546-41-6	<chem>n1(c(cc(c1C)C=Cc1ccc2cc(ccc2[n+](1C)N(C)C)C)c1ccccc1.n1(c(cc(c1C)C=Cc1ccc2cc(ccc2[n+](1C)N(C)C)C)c1ccccc1</chem>
Prestw-1041	33125-97-2	<chem>c1(n(cnc1)[C@H](c1ccccc1)C)C(=O)OCC</chem>
Prestw-1042	4310-35-4	<chem>C(CC[N+](CC)(CC)CC)(c1ccccc1)(C1CCCC1)O</chem>
Prestw-1043	38363-32-5	<chem>c1(c(OCC(CNC(C)(C)C)(O)[H])cccc1)C1CCCC1.c1(c(OCC(CNC(C)(C)C)(O)[H])cccc1)C1CCC C1</chem>
Prestw-1044	73771-04-7	<chem>[C@]12([C@](C(COC(=O)CC)=O)(OC(=O)OCC)CC[C@]1([C@]1([C@@]([C@@]\3(\C=C/C(\C=C3)=O)\CC1)C)[C@H](C2)O)[H])[H])C</chem>
Prestw-1045	99592-39-9	<chem>s1c2c(c(c1)COC(c1c(cc(cc1)Cl)Cl)Cn1cnc1)cccc2Cl</chem>
Prestw-1046	135062-02-1	<chem>c1(C(=O)O)c(cc(CC(N[C@H](c2c(N3CCCCC3)cccc2)CC(C)C)=O)cc1)OCC</chem>
Prestw-1047	55837-27-9	<chem>c1(S(=O)(=O)N)c(c(cc(c1)C(=O)O)N1CCCC1)Oc1ccccc1</chem>
Prestw-1048	3819-00-9	<chem>N1(c2c(Sc3c1cccc3)ccc(c2)C(=O)C)CCCN1CCC(CC1)CCO</chem>
Prestw-1049	129-20-4	<chem>N1(N(C(C(C1=O)CCCC)=O)c1ccccc1)c1ccc(cc1)O</chem>
Prestw-1050	73-49-4	<chem>S(c1cc2C(NC(Nc2cc1Cl)CC)=O)(=O)(=O)N</chem>
Prestw-1051	31883-05-3	<chem>N1(c2c(Sc3c1cccc3)ccc(c2)NC(=O)OCC)C(CCN1CCOCC1)=O</chem>
Prestw-1052	96-83-3	<chem>c1c(c(c(c1l)CC(CC)C(O)=O)l)Nl</chem>
Prestw-1053	32887-03-9	<chem>N12[C@@]([C@@](C1=O)(N=C\N1CCCCC1)[H])(SC([C@@H]2C(OCOC(C)(C)C)=O)(C)C)[H]</chem>
Prestw-1054	5714-90-9	<chem>C(C(CN(C)C)C)(OC(=O)CC)(Cc1ccccc1)c1ccccc1</chem>
Prestw-1055	129-77-1	<chem>C(C(c1ccccc1)c1ccccc1)(OC1CN(CCC1)CC)=O</chem>

Prestwick Nr.	CAS number	Smiles code
Prestw-1056	70-00-8	<chem>N1(C(NC/C=C1)/C(F)(F)F)=O)[C@@H]1O[C@@H]([C@H](C1)O)CO</chem>
Prestw-1057	6452-73-9	<chem>O(c1c(OCC=C)cccc1)CC(CNC(C)C)O</chem>
Prestw-1058	103639-04-9	<chem>c12c(n(c3c1cccc3)C)CCC(C2=O)Cn1c(nc1)C</chem>
Prestw-1059	550-83-4	<chem>c1(c(cc(cc1)N)OCCC)C(=O)OCCN(CC)CC</chem>
Prestw-1060	21256-18-8	<chem>c1(c(oc(n1)CCC(=O)O)c1cccc1)c1cccc1</chem>
Prestw-1061	86-34-0	<chem>N1(C(C(CC1=O)c1cccc1)=O)C</chem>
Prestw-1062	59017-64-0	<chem>c1(c(c(c(c1)C(NCC(Nc1c(c(c(c1)C(=O)O))C(=O)NCCO))=O)=O)C(=O)NC)N(C(=O)C)C</chem>
Prestw-1063	65473-14-5	<chem>c1(c2c(ccc1)cccc2)CN(C/C=C/c1cccc1)C</chem>
Prestw-1064	956-03-6	<chem>C(OCC(NCCC)(C)C)(=O)c1cccc1</chem>
Prestw-1065	78415-72-2	<chem>C1(=C\C=C(/NC1=O)\C)c1ccncc1/C#N</chem>
Prestw-1066	53-46-3	<chem>C1(c2c(Oc3c1cccc3)cccc2)C(=O)OCC[N+](CC)(CC)C</chem>
Prestw-1067	74682-62-5	<chem>N12[C@@]([C@@](C1=O)(NC(C(C([O-])=O)c1csc1)=O)[H])(SC([C@@H]2C([O-])=O)(C)C)[H]</chem>
Prestw-1068	1179-69-7	<chem>N1(c2c(Sc3c1cccc3)ccc(c2)SCC)CCCN1CCN(CC1)C</chem>
Prestw-1069	89-57-6	<chem>c1(C(=O)O)c(ccc(c1)N)O</chem>
Prestw-1362	149647-78-9	<chem>C(Nc1cccc1)(=O)CCCCC(=O)NO</chem>
Prestw-1071	39236-46-9	<chem>N1(C(NC(C1NC(NCNC(NC1N(C(NC1=O)=O)CO)=O)=O)=O)CO</chem>
Prestw-1072	103577-45-3	<chem>c1(nc2c([nH]1)cccc2)S(Cc1c(c(OCC(F)(F)F)ccn1)C)=O</chem>
Prestw-1073	590-63-6	<chem>C(OC[C[N+](C)(C)C)C(=O)N</chem>
Prestw-1074	427-51-0	<chem>[C@@]12(\C(\C(=C/[C@@]3([C@@]1(CC[C@@]1([C@@](CC[C@]13[H])(OC(=O)C)C(=O)C)C)[H])[H])\C)=C/C(C1C2C1)=O)C</chem>
Prestw-1075	13071-11-9	<chem>c12c(OCC(CNC(C)C)(O)[H])cccc1cccc2</chem>
Prestw-1076	52214-84-3	<chem>C1(C(C1)c1ccc(OC(C(=O)O)(C)C)cc1)(Cl)Cl</chem>
Prestw-1420	566-48-3	<chem>[C@]12/C(=C(\C(CC1=O)/O)/CC[C@@]1([C@@]2(CC[C@]2([C@]1(CCC2=O)[H])C)[H])[H])C</chem>
Prestw-1078	69-57-8	<chem>N12[C@@]([C@@](C1=O)(NC(=O)Cc1cccc1)[H])(SC([C@@H]2C([O-])=O)(C)C)[H]</chem>
Prestw-1803	7246-14-2	<chem>OC1C(n2cnc3c(OC)nc(nc23)N)OC(CO)C1O</chem>
Prestw-1080	108579-67-5	<chem>c1(nc2c([nH]1)ccc(c2)SC(C)C)NC(=O)OC</chem>
Prestw-1081	4199-10-4	<chem>c12c(OCC(CNC(C)C)(O)[H])cccc1cccc2</chem>
Prestw-1082	104015-29-4	<chem>[C@]12([C@](N(c3c1cc(cc3)O)C)(N(CC2)C)[H])C</chem>
Prestw-1294	16051-77-7	<chem>[N+](O[C@H]1[C@@]2([C@](OC1)([C@H](CO2)O)[H])[H])([O-])=O</chem>
Prestw-1516	50293-90-8	<chem>c1(cc(ccc1O)[C@H](CNC(C)C)O)CO</chem>
Prestw-1493	97240-79-4	<chem>[C@@]12([C@H]([C@H]3[C@H](OC(O3)(C)C)CO1)OC(O2)(C)C)COS(=O)(=O)N</chem>
Prestw-1086	68-41-7	<chem>C1([C@](CON1)(N)[H])=O</chem>
Prestw-1804	121032-29-9	<chem>COc1c(c(OC)ccc1)C(NC1C2N(C(C([O-])=O)C(C)C)S2)C1=O.[Na+]</chem>
Prestw-1088	94-07-5	<chem>c1(ccc(cc1)O)C(O)CNC</chem>
Prestw-1089	339-72-0	<chem>C1([C@@](CON1)(N)[H])=O</chem>
Prestw-1090	118-56-9	<chem>C(c1c(O)cccc1)(OC1CC(CC(C1)C)C)C(=O)</chem>
Prestw-1091	3106-85-2	<chem>[C@H](CCC(O)=O)(NC(=O)C[C@H](NC(=O)C)C(O)=O)C(O)=O</chem>





Prestwick Nr.	CAS number	Smiles code
Prestw-1830	24584-09-6	<chem>C[C@@H](CN1CC(=O)NC(=O)C1)N2CC(=O)NC(=O)C2</chem>
Prestw-1229	129722-12-9	<chem>N1c2cc(ccc2CCC1=O)OCCCN1CCN(c2c(c(Cl)ccc2)Cl)CC1</chem>
Prestw-1405	57-63-6	<chem>[C@]12([C@]([C@]3([C@@]([C@]4(CC3)cc(cc4)O)(CC1)[H])[H])(CC[C@]2(C#C)O)[H])C</chem>
Prestw-1419	67-73-2	<chem>[C@@]12([C@@]3([C@]([C@]4([C@@]([C@@]5(\C(\C@H)(C4)F)=C/C(\C=C5)=O)C)([C@H](C3)O)F)[H])(C[C@H]1OC(O2)(C)C)[H])C(=O)CO</chem>
Prestw-1343	110871-86-8	<chem>c12c(N(\C=C(/C1=O)\C(=O)O)C1CC1)c(c(c2N)F)N1C[C@H](N[C@H](C1)C)C)F</chem>
Prestw-1390	100643-71-8	<chem>C\1(/c2c(cc(cc2)Cl)CCc2c1nccc2)=C\1/CCNCC1</chem>
Prestw-1378	81103-11-9	<chem>[C@@H]1([C@@H]([C@H](C[C@H](O1)C)N(C)C)O)[C@@H]1[C@H]([C@@H]([C@H](C(O[C@@H]([C@]([C@@H]([C@H](C([C@@H](C[C@]1(OC)C)C)=O)C)O)(O)C)CC)=O)C)O)[C@H]1C[C@]([C@H]([C@@H](O1)C)O)(OC)C)C</chem>
Prestw-1199	154-69-8	<chem>N(c1ncccc1)(Cc1cccc1)CCN(C)C</chem>
Prestw-1352	56776-01-3	<chem>c1(c(Cl)cccc1)C(CNC(C)C)C)O</chem>
Prestw-1196	123948-87-8	<chem>N12\C(\c3c(C1)cc1c(c(ccc1n3)O)CN(C)C)=C/C/1=C(\C2=O)/COC([C@]1(O)CC)=O</chem>
Prestw-1232	134523-00-5	<chem>c1(c(n(c1c1cccc1)c1ccc(cc1)F)CC[C@H](C[C@H](CC(=O)O)O)O)C(C)C(Nc1cccc1)=O</chem>
Prestw-1234	83905-01-5	<chem>[C@@H]1([C@@H]([C@H](C[C@H](O1)C)N(C)C)O)[C@@H]1[C@H]([C@@H]([C@H](C(O[C@@H]([C@]([C@@H]([C@H](C([C@@H](C[C@]1(OC)C)C)=O)C)O)(O)C)CC)=O)C)O)[C@H]1C[C@]([C@H]([C@@H](O1)C)O)(OC)C)C</chem>
Prestw-1286	50847-11-5	<chem>c1(c(nn2c1cccc2)C(C)C)C(=O)C(C)C</chem>
Prestw-1433	114798-26-4	<chem>n1(c(c(nc1CCCC)Cl)CO)Cc1ccc(c2c(c3nn[nH]3)cccc2)cc1</chem>
Prestw-1236	132-17-2	<chem>N1([C@@]2[C[C@H](C[C@]1(CC2)[H])OC(c1cccc1)c1cccc1)[H])C</chem>
Prestw-1359	50700-72-6	<chem>[C@]12([C@]([C@]3([C@@]([C@]4(C[C@@H]([C@H](C[C@@]4(CC3)[H])OC(=O)C)N3CCC(CC3)C)(CC1)[H])[H])(C[C@H]([C@@H]2OC(=O)C)[N+1(C)CCCC1)[H])C</chem>
Prestw-1350	144701-48-4	<chem>c1(nc2c(n1C)cccc2)c1cc2n(c(nc2c(c1)C)CCC)Cc1ccc(c2c(C(=O)O)cccc2)cc1</chem>
Prestw-1490	58895-64-0	<chem>[C@]123[C@@]4([C@](N(CC5CC5)CC1)(Cc1c2c(O[C@]3(C(CC4)=C)[H])c(cc1)O)[H])O</chem>
Prestw-1241	60628-96-8	<chem>n1(cnc1)C(c1ccc(cc1)c1cccc1)c1cccc1</chem>
Prestw-1265	112811-59-3	<chem>N\1(c2c(C(\C=C1)\C(=O)O)=O)cc(c2OC)N1CC(NCC1)C)F)C1CC1</chem>
Prestw-1244	147536-97-8	<chem>S(Nc1c(nc(n1)c1nccn1)OCCO)Oc1c(OC)cccc1)(c1ccc(C(C)C)cc1)(=O)=O</chem>
Prestw-1266	95058-81-4	<chem>N\1([C@H]2C([C@@H]([C@H](O2)CO)O)(F)F)C(/N=C(\C=C1)/N)=O</chem>
Prestw-1190	144689-63-4	<chem>c1(c(nc(n1C)ccc(c2c(c3nn[nH]3)cccc2)cc1)CCC)C(O)(C)C(OC/C=1/OC(O1C1)=O)=O</chem>
Prestw-1480	329-63-5	<chem>c1c(c(ccc1C(O)CNC)O)O</chem>
Prestw-1189	158966-92-8	<chem>n1c2cc(ccc2ccc1/C=C/c1cc([C@H](SCC2(CC2)CC(=O)O)CCc2c(C(O)(C)C)cccc2)ccc1)Cl</chem>
Prestw-1180	114977-28-5	<chem>[C@@]12([C@@]([C@]3([C@@]([C@]4([C@@H]1O)(OC3)[H])OC(=O)C)([C@@H]([C@@]1(C(C/[C@H](C2=O)O)=C(\C@H](C1)OC([C@@H]([C@@H](NC(OC(C)C)C)=O)c1cccc1)O)=O)/C)C)O)OC(=O)c1cccc1)[H])C</chem>
Prestw-1376	132203-70-4	<chem>C=1(/C/C(=C(N\C1/C)/C(=O)OCCOC)c1cc([N+](O)=O)ccc1)\C(=O)OC\C=C\c1cccc1</chem>
Prestw-1291	99011-02-6	<chem>c12ncn(c1c1c(nc2N)cccc1)CC(C)C</chem>
Prestw-1423	98048-97-6	<chem>N1(C(CP(OC(OC(=O)CC)C(C)C)=O)CCCCc2cccc2)=O)[C@@H](C[C@H](C1)C1CCCC1)C(=O)O</chem>
Prestw-1290	152459-95-5	<chem>c1(nc(c2ncccc2)ccn1)Nc1cc(NC(c2ccc(CN3CCN(CC3)C)cc2)=O)ccc1C</chem>
Prestw-1446	151096-09-2	<chem>N\1(c2c(C(\C=C1)\C(=O)O)=O)cc(c2N1C[C@]3([C@@]([C@]1(NCCC3)[H])[H])c2OC)F)C1CC1</chem>
Prestw-1421	43229-80-7	<chem>c1(cc(ccc1O)[C@@H](CN[C@H](Cc1ccc(cc1)OC)C)O)NC=O.c1(cc(ccc1O)[C@@H](CN[C@H](Cc1ccc(cc1)OC)C)O)NC=O</chem>
Prestw-1338	101363-10-4	<chem>C=1(\C(c2c3N(/C1)CCSc3c(c2)F)N1CCN(CC1)C)=O)/C(=O)O</chem>
Prestw-1319	81093-37-0	<chem>C=1\2/[C@]([C@@H](OC(=O)[C@H](CC)C)C[C@@H](\C1)O)([C@@H](CC[C@H](C[C@H](C(=O)O)O)O)[C@H](\C=C2)C)[H]</chem>



Prestwick Nr.	CAS number	Smiles code
Prestw-1337	122320-73-4	<chem>N1C(SC(C1=O)Cc1ccc(cc1)OCCN(c1ncccc1)C)=O</chem>
Prestw-1334	123441-03-2	<chem>C(Oc1cc([C@@H](N(C)C)C)ccc1)(N(CC)C)=O</chem>
Prestw-1342	139755-83-2	<chem>c1/2c(n(nc1CCC)C)C/N/C(=N2)/c1cc(S(N2CCN(CC2)C)(=O)=O)ccc1OCC)=O</chem>
Prestw-1207	50-78-2	<chem>c1(C(=O)O)c(OC(=O)C)cccc1</chem>
Prestw-1472	70-30-4	<chem>c1(Cc2c(c(cc2O)Cl)Cl)Cl)c(cc(c1O)Cl)Cl</chem>
Prestw-1764	159989-65-8	<chem>N1([C@H](C(NC(C)C)C)=O)C[C@]2([C@@](C1)(CCCC2)[H])[H]C[C@H]([C@@H](NC(c1c(O)ccc1)C)=O)CSc1cccc1)O</chem>
Prestw-1749	160970-54-7	<chem>c1(c2c(cc(c1)C[C@H](NCCOc1c(OCC(F)(F)F)cccc1)C)CCN2CCCO)C(=O)N</chem>
Prestw-1777	39133-31-8	<chem>c1(c(cc(C(OCC(N(C)C)(c2cccc2)CC)=O)cc1OC)OC)OC</chem>
Prestw-1739	129618-40-2	<chem>N1(c2c(C(Nc3c1nccc3C)=O)cccc2)C1CC1</chem>
Prestw-1707	113-07-5	<chem>C1(C(C(CN1CC)CCN1CCOCC1)(c1cccc1)c1cccc1)=O</chem>
Prestw-1718	68302-57-8	<chem>c12c(nc(c(c1)C(=O)O)N)Oc1c(C2=O)cc(cc1)C(C)C</chem>
Prestw-1719	78613-38-4	<chem>N1(C[C@H](O[C@H](C1)C)C)CC(Cc1ccc(C(C)C)C)cc1C</chem>
Prestw-1786	93106-60-6	<chem>C=1(/C(c2c(N(\C1)C1CC1)cc(N1CCN(CC1)CC)c(c2)F)=O)C(=O)O</chem>
Prestw-1784	58970-76-6	<chem>C([C@H]([C@@H](Cc1cccc1)N)O)(N[C@H](C(=O)O)CC(C)C)=O</chem>
Prestw-1778	99777-81-8	<chem>C(c1cc(c(c(c1)OC)OC)OC)(NC1CNCCC1)=O</chem>
Prestw-1773	35212-22-7	<chem>C=1(\C(c2c(O/C1)cc(OC(C)C)cc2)=O)/c1cccc1</chem>
Prestw-1762	163222-33-1	<chem>N1(C([C@@H]([C@H]1c1ccc(cc1)O)CC[C@@H](c1ccc(cc1)F)O)=O)c1ccc(cc1)F</chem>
Prestw-1761	145202-66-0	<chem>n1cnn(c1)Cc1cc2c(c[nH]c2cc1)CCN(C)C</chem>
Prestw-1760	189188-57-6	<chem>c1(c2c([nH]c1)ccc(c2)OC)\C=N\NC(=N)NCCCC</chem>
Prestw-1758	138786-67-1	<chem>c1([n-]c2c(n1)cc(OC(F)F)cc2)S(Cc1c(c(ccn1)OC)OC)=O</chem>
Prestw-1753	17902-23-7	<chem>N/1(C(NC(/C(=C1)/F)=O)=O)C1OCCC1</chem>
Prestw-1732	134308-13-7	<chem>c1([N+](O)=O)c(cc(c1)C(c1ccc(cc1)C)=O)O)O</chem>
Prestw-1716	850-52-2	<chem>C/1\2=C\3/C(=C\C(=O)CC3)/CC[C@]1([C@]1([C@](\C=C2)([C@](CC1)(O)CC=C)C)[H])[H]</chem>
Prestw-1711	25451-15-4	<chem>C(OCC(COC(=O)N)c1cccc1)(=O)N</chem>
Prestw-1709	2998-57-4	<chem>[C@]12([C@]([C@]3([C@@](c4c(cc(OC(N(CCC1)CC1)=O)cc4)CC3)(CC1)[H])[H])(CC[C@@H]2O)[H])C</chem>
Prestw-1708	116539-60-7	<chem>c1(sccc1)[C@H](Oc1c2c(ccc1)cccc2)CCNC</chem>
Prestw-1706	120011-70-3	<chem>c12C(C(Cc1cc(c2)OC)OC)CC1CCN(Cc2cccc2)CC1)=O</chem>
Prestw-1703	117-10-2	<chem>C1(c2c(C(c3c1c(O)ccc3)=O)cccc2O)=O</chem>
Prestw-1733	55981-09-4	<chem>c1(sc(NC(c2c(OC(=O)C)cccc2)=O)nc1)[N+](O)=O</chem>
Prestw-1748	105816-04-4	<chem>C(N[C@@H](C(=O)O)Cc1cccc1)([C@H]1CC[C@@H](CC1)C(C)C)=O</chem>
Prestw-1721	70356-09-1	<chem>C(C(c1ccc(C(C)C)cc1)=O)C(c1ccc(cc1)OC)=O</chem>
Prestw-1715	24356-94-3	<chem>[C@@]12([C@@]3([C@]([C@]4([C@@]([C@@]5(\C=C/C(=O)CC5)CC4)C)(CC3)[H])[H])(C[C@H]1OC(O2)(c1cccc1)C)[H])C(=O)C</chem>
Prestw-1763	18699-02-0	<chem>C(Nc1ccc(CC(=O)O)cc1)(=O)C</chem>
Prestw-1710	452-35-7	<chem>c1(S(=O)(=O)N)nc2c(s1)cc(cc2)OCC</chem>
Prestw-1722	3978-86-7	<chem>C/1(\c2ncccc2CCc2c1cccc2)=C/1\CCN(CC1)C</chem>
Prestw-1717	90-45-9	<chem>c1(c2c(nc3c1cccc3)cccc2)N</chem>

Prestwick Nr.	CAS number	Smiles code
Prestw-1792	121808-62-6	<chem>N1(C([C@]2(NC(=O)CC2)[H])=O)[C@](C(=O)O)(CSC1)[H]</chem>
Prestw-1766	91599-74-5	<chem>C=1(\[C@H](\C(=C(/N/C1/C)\C)\C(=O)OC)c1cc([N+](O-))=O)ccc1)/C(O[C@H]1CN(Cc2ccccc2)CCC1)=O</chem>
Prestw-1770	129273-38-7	<chem>N1(C([C@]2([C@](C1=O)(CCCC2)[H])[H])=O)CCCCN1CCN(c2nsc3c2cccc3)CC1</chem>
Prestw-1726	70797-11-4	<chem>N1/2C([C@H]([C@]1(SC/C(=C2/C(=O)O)/CSc1n(nnn1)C)[H])NC([C@H](NC(c1c(cc(nc1)C)O)=O)c1ccc(cc1)O)=O)=O</chem>
Prestw-1713	67227-56-9	<chem>c12c(c(c(c1)O)O)Cl)CCNCC2c1ccc(cc1)O</chem>
Prestw-1714	106685-40-9	<chem>[C@@]12(c3cc(c4cc5c(cc(C(=O)O)cc5)cc4)ccc3OC)C[C@]3(C[C@@](C1)(C[C@@](C2)(C3)[H])[H])[H]</chem>
Prestw-1705	50978-11-5	<chem>c1(c(c(c(c1)NC(=O)C)I)NC(=O)C)I)C(=O)O</chem>
Prestw-1743	115256-11-6	<chem>S(Nc1ccc(cc1)OCCN(CCc1ccc(NS(=O)(=O)C)cc1)C)(=O)(=O)C</chem>
Prestw-1776	673-31-4	<chem>C(=O)(N)OCCc1cccc1</chem>
Prestw-1730	64544-07-6	<chem>N1/2C([C@H]([C@H]1SC\C(=C2\C(OC(OC(=O)C)C)=O)\COC(=O)N)NC(\c1occc1)=N/OC)=O</chem>
Prestw-1720	68475-42-3	<chem>C1=2/NC(CN1Cc1c(/N2)ccc(c1Cl)Cl)=O</chem>
Prestw-1701	113665-84-2	<chem>N1([C@@H](c2c(Cl)cccc2)C(=O)OC)Cc2c(scc2)CC1</chem>
Prestw-1723	86-75-9	<chem>C(Oc1c2ncccc2ccc1)(=O)c1cccc1</chem>
Prestw-1785	92-84-2	<chem>N1c2c(Sc3c1cccc3)cccc2</chem>
Prestw-1769	84680-54-6	<chem>N1(C([C@@H](N[C@H](C(=O)O)CCc2cccc2)C)=O)[C@H](C(=O)O)CCC1</chem>
Prestw-1791	148553-50-8	<chem>C(=O)(C[C@H](CC(C)C)CN)O</chem>
Prestw-1841	1051375-16-6	<chem>C[C@@H]1CCO[C@@H]2N1C(=O)C3=C(C(=O)C(=CN3C2)C(=O)NCC4=C(C=C(C=C4)F)F)O</chem>
Prestw-1731	165800-06-6	<chem>C(P(=O)(O)O)(P(=O)(O)O)(Cn1cncc1)O</chem>
Prestw-1727	87239-81-4	<chem>N1/2C([C@H]([C@]1(SC/C(=C2/C(OC(OC(=O)OC(C)C)C)=O)/COC)[H])NC(/C(/c1nc(sc1)N)=N/OC)=O)=O</chem>
Prestw-1736	138402-11-6	<chem>N1(C(C2\N=C1\CCCC)CCCC2)=O)Cc1ccc(c2c(c3nnn[nH]3)cccc2)cc1</chem>
Prestw-1737	157810-81-6	<chem>[C@@H]1(N(C[C@H](C[C@H](C(N[C@H]2c3c(C[C@H]2O)cccc3)=O)Cc2cccc2)O)CCN(C1)Cc1cnccc1)C(NC(C)C)C)=O</chem>
Prestw-1750	91161-71-6	<chem>C(#CC(C)C)C/C=C/CN(Cc1c2c(ccc1)cccc2)C</chem>
Prestw-1700	56-92-8	<chem>n1c(c[nH]c1)CCN</chem>
Prestw-1734	136236-51-6	<chem>C(#C)CN[C@H]1c2c(CC1)cccc2</chem>
Prestw-1712	2002-29-1	<chem>[C@]1/2([C@]3([C@]([C@]4([C@@]([C@]([C@H](C4)C)(C(COC(C(C)C)C)=O)=O)O)(C[C@@H]3O)C)[H])(C[C@@H](/C1=C/C(\C=C2)=O)F)[H])F)C</chem>
Prestw-1756	23047-25-8	<chem>N1(c2c(Cc3c1cccc3)cccc2)CCCN(CC(c1ccc(cc1)Cl)=O)C</chem>
Prestw-1759	181695-72-7	<chem>S(c1ccc(c2c(noc2C)c2cccc2)cc1)(=O)(=O)N</chem>
Prestw-1740	141388-76-3	<chem>N1(c2c(C(\C=C1)\C(=O)O)=O)cc(c(c2Cl)N1C[C@H](N)CCCC1)F)C1CC1</chem>
Prestw-1782	155213-67-5	<chem>n1c(scc1CN(C(N[C@H](C(N[C@H](C[C@@H]([C@@H](NC(=O)OCc1scnc1)Cc1cccc1)O)Cc1cccc1)=O)C(C)C)=O)C(C)C</chem>
Prestw-1752	56390-09-1	<chem>c12c(C(c3c(C1=O)cccc3OC)=O)c(c1c(c2O)C[C@](C[C@@]1(O[C@H]1O[C@H]([C@@H]([C@H](C1)N)O)C)[H])(C(=O)CO)O</chem>
Prestw-1741	82034-46-6	<chem>[C@]12([C@](C(OC(C)=O)(OC(=O)OCC)CC[C@]1([C@]1([C@@]([C@@]3(\C=C/C(\C=C3)=O)\CC1)C)([C@H](C2)O)[H])[H])C</chem>
Prestw-1744	209747-05-7	<chem>c1([C@H](CCN(C(C)C)C(C)C)c2cccc2)c(ccc(c1)C)O</chem>
Prestw-1775	101477-54-7	<chem>c1(c(c(CN2CCN(C(c3ccc(cc3)F)c3ccc(cc3)F)CC2)ccc1OC)OC)OC</chem>
Prestw-1772	99464-64-9	<chem>S1(N/C(=C(\c2c1cccc2)/OC(OC(=O)OCC)C)/C(Nc1ncccc1)=O)C)(=O)=O</chem>
Prestw-1781	122852-69-1	<chem>c12c(n(c3c1cccc3)C)CCN(C2=O)Cc1nc[nH]c1C</chem>
Prestw-1738	105462-24-6	<chem>C(P(=O)(O)O)(P(=O)(O)O)(Cc1cnccc1)O</chem>

Prestwick Nr.	CAS number	Smiles code
Prestw-1783	135729-62-3	<chem>N1(C(c2c3[C@@](C1)(CCCc3ccc2)[H])=O)[C@@H]1CN2CC[C@@]1(CC2)[H]</chem>
Prestw-1780	434-07-1	<chem>[C@]12([C@@]3([C@]([C@]4([C@@]([C@](CC4)(O)C)(CC3)C)[H])(CC[C@]1(CC(/C(/C2)=C/O)=O)[H])[H])[H])C</chem>
Prestw-1765	130209-82-4	<chem>[C@H]1([C@H]([C@H](C[C@H]1O)O)C\C=C/CCCC(=O)OC(C)C)CC[C@H](CCc1cccc1)O</chem>
Prestw-1745	64228-79-1	<chem>[N@@+]1([C@@H](c2c(cc(c(c2)OC)OC)CC1)Cc1cc(c(cc1)OC)OC)(CCC(=O)OCCCCOC(C)C[N@@+]1([C@@H](c2c(cc(c(c2)OC)OC)CC1)Cc1cc(c(cc1)OC)OC)=O)C</chem>
Prestw-1794	357166-30-4	<chem>c12/N=C(\NC(c1c(c[nH]2)CCc1ccc(C(N[C@H](C([O-])=O)CCC([O-])=O)=O)cc1)=O)/N</chem>
Prestw-1793	112887-68-0	<chem>C1(c2c(/N=C(\N1)/C)ccc(c2)CN(c1sc(C(N[C@H](C(=O)O)CCC(=O)O)=O)cc1)C)=O</chem>
Prestw-1729	97519-39-6	<chem>N1\2C([C@H]([C@H]1SC\C=C2\C(=O)O)NC(\C(\c1nc(sc1)N)=C/CC(=O)O)=O)=O</chem>
Prestw-1735	137862-53-4	<chem>N([C@H](C(=O)O)C(C)C)(C(=O)CCCC)Cc1ccc(c2c(c3nnn[nH]3)cccc2)cc1</chem>
Prestw-1788	101152-94-7	<chem>[C@]1([C@H](C1)CN)(C(N(CC)CC)=O)c1cccc1</chem>
Prestw-1768	68786-66-3	<chem>n1c([nH]c2c1cc(c(c2)Oc1c(c(Cl)ccc1)Cl)Cl)SC</chem>
Prestw-1751	70359-46-5	<chem>c1(c2nccnc2ccc1N\C1=N\CCN1)Br</chem>
Prestw-1704	638-94-8	<chem>[C@@]12([C@@]3([C@]([C@]4([C@@]([C@@]5(\C(=C/C(\C=C5)=O)\CC4)C)([C@H](C3)O)[H])[H])(C[C@]1(OC(O2)(C)C)[H])[H])C(=O)CO</chem>
Prestw-1728	121123-17-9	<chem>N1\2C([C@H]([C@H]1SC\C=C2\C(=O)O)C=C\1)NC([C@H](c1ccc(cc1)O)N)=O)=O</chem>



## Declaration of Contribution

Except where stated otherwise by reference or acknowledgment, the work presented was generated by myself, Bjarne Goebel, under the supervision of my advisors, Prof. Dr. Dieter Steinhilber and Dr. Ann-Kathrin Häfner, during my doctoral studies. All contributions from colleagues are explicitly referenced in the thesis. The material listed below was obtained in the context of collaborative research:

**Figure 5.24: Time series of 15-LO1 expression., Figure 5.25: Time series of 5-LO and 15-LO2 expression after transient transfection., Figure 5.26: Transfection efficiency determination. and Figure 5.27: Western blot analysis of 5-LO, 15-LO1, and 15-LO2 expression in transiently transfected HEK293T\_LPCAT2 cells.** pcDNA3.1\_5LO and pSG5-FLAP (only used as template for amplification of FLAP) were kindly provided by Prof. Dr. Olof Rådmark (Karolinska Institute, Stockholm Sweden). pcDNA3.1\_ALOX15B (referred to as pcDNA3.1\_15LO2) was kindly provided by Univ.-Prof. Dr. sc. med. Hartmut Kühn (Charité Berlin). The plasmids pcDNA3.1\_ALOX15 (referred to as pcDNA3.1\_15LO1) and pcDNA3.1\_mCh\_ALOX15B (only used as template for amplification of mCherry) were prepared and kindly provided by Dr. Roland Ebert (Department of Immunology, Genetics and Pathology, Uppsala University). Preparation of further transfection plasmids as well as transfection experiments and analysis were performed by Bjarne Goebel.

**Figure 5.21: Western blot analysis of stably transfected HEK293T cells. and Figure 5.28: Doxycycline-dependent expression of 5-LO, 15-LO1 and 15-LO2.** The Sleeping beauty vector encoding for the SB100X transposase necessary for the stable integration according to [279] was kindly provided by Prof. Dr. Zoltán Ivics (Research Centre ATMP/Haematology, Paul-Ehrlich-Institute). Sleeping beauty vectors with empty MCS were kindly gifted by Eric Kowarz (Institute of Pharmaceutical Biology, Goethe University Frankfurt). Preparation of final transfection plasmids as well as further experimental procedures were performed by Bjarne Goebel.

**Figure 5.8: Heatmap of ACSL4\_His6x unfolding temperatures.** Deep-well buffer plates (96-well, 200 mM) were kindly provided by Dr. Steffen Brunst (Institute of Pharmaceutical Chemistry, Goethe University Frankfurt). Bjarne Goebel performed protein purifications, measurements, and analysis.

**Table 5.4: Approved drug library hits that increased the unfolding temperature of ACSL4 by more than 1 °C compared to DMSO controls. 5 µM protein was incubated with 20 µM compound.** The approved drug library (Prestwick Chemical Libraries®) was kindly provided by the working groups of Prof. Dr. Eugen Proschak and Prof. Dr. Stefan Knapp (Institute of Pharmaceutical Chemistry, Goethe University Frankfurt). Dr. Benedict-Tilman Berger and Lewis Elson (Institute of Pharmaceutical Chemistry, Goethe University Frankfurt) kindly prepared 384-well plates and assisted with the analysis on the QuantStudio5 device (QuantStudio Design & Analysis Software). Protein expression, purification, measurements, and the analysis were performed by Bjarne Goebel.

**Figure 5.13: SDS-PAGE analysis of the purification of PA-LOX.** The expression plasmid pET28a(+)\_PALOX, containing a 15-lipoxygenating enzyme from *Pseudomonas aeruginosa*,

was kindly provided by Univ.-Prof. Dr. sc. med. Hartmut Kühn (Institute of Biochemistry, Charité Berlin). Expression, purification, and analysis on SDS-PAGE were performed by Bjarne Goebel.

**Figure 5.14: Stability analysis of the recombinant PA-LOX protein.** The expression plasmid pET28a(+)\_PALOX, containing a 15-lipoxygenating enzyme from *Pseudomonas aeruginosa*, was kindly provided by Univ.-Prof. Dr. sc. med. Hartmut Kühn (Institute of Biochemistry, Charité Berlin) and deep-well buffer plates (96-well, 200 mM) were kindly provided by Dr. Steffen Brunst (Institute of Pharmaceutical Chemistry, Goethe University Frankfurt). Protein expression, purification, measurements, and the analysis were performed by Bjarne Goebel.

**Table 5.7: Results of the FAL screen with the PA-LOX protein.** The FAL library was prepared by the following colleagues of the Institute of Pharmaceutical Chemistry at the Goethe University Frankfurt: Dr. Estel la Buscató; Nathalia Kolakowska-Pilipiak; Dr. René Blöcher; Khang Pau; Dr. Stefano Woltersdorf; Felix Knöll; Beatrice Renelt; Felix Zhu; Dr. Jurema Schmidt; Dr. Julius Pollinger; Dr. Simone Schierle; Dr. Victor Hernandez-Olmos, Ting Liu, Alexander Kaps, Rinusha Rajkumar, Dr. Pascal Heitel and Maximiliane Horz. Protein expression, purification, measurements, and the analysis were performed by Bjarne Goebel.

**Table 5.8: Drug fragment library hits with the strongest effects on  $\Delta T$ . Values display mean  $\pm$  SD of duplicates.** The small organic compound library (Prestwick Chemical Libraries®) was kindly provided by Prof. Dr. Eugen Proschak (Institute of Pharmaceutical Chemistry, Goethe University Frankfurt). Protein expression, purification, measurements, and the analysis were performed by Bjarne Goebel.

**Figure 5.22: Overview of the total oxylipin formation in different stably transfected HEK293T cell lines.** and **Figure 5.23: Overview of the free oxylipin formation in different stably transfected HEK293T cell lines.** Dr. Malwina Mainka, under the supervision of Prof. Dr. Nils Helge Schebb (Department of Food Chemistry, Faculty of Mathematics and Natural Sciences, University Wuppertal), performed the lipid mediator extraction and analysis via LC-MS/MS. Bjarne Goebel performed sample incubations, preparations, and analyzed the results.

**Figure 5.30: Localization of ACSL4 and LPCAT2 in HEK293T\_VC and HEK293T\_LPCAT2 cells.** and **Figure 5.31: Localization of ACSL4 and LPCAT2 in stably transfected HEK293T\_A+L cells.** and **Figure 5.36: Localization of LOs in stably transfected HEK293T\_LPCAT2 cells.** Tamara Göbel (Institute of Pharmaceutical Chemistry, Goethe University Frankfurt) kindly performed laser scanning confocal microscopy imaging. Bjarne Goebel prepared the samples and analyzed the images.

**Figure 5.32: Oxylipin formation in HEK293T\_VC\_LO, HEK293T\_LPCAT2\_LO, and HEK293T\_A+L\_LO cells.** Laura Carpanedo and Susanne Reif, under the supervision of Prof. Dr. Nils Helge Schebb (Department of Food Chemistry, Faculty of Mathematics and Natural Sciences, University Wuppertal), performed the lipid mediator extraction and analysis via LC-MS/MS. Bjarne Goebel performed sample incubations, preparations, and analyzed the results.

**Figure 5.34: Effect of ferroptosis inducers on the localization of lipoxygenases in stably transfected HEK293T cells.** and **Figure 5.35: Effect of ferroptosis inducers on the localization of lipoxygenases in stably transfected HEK293T cells.** Tamara Göbel (Institute of Pharmaceutical Chemistry, Goethe University Frankfurt) kindly performed laser scanning confocal microscopy imaging. Bjarne Goebel prepared the samples and analyzed the images.

**Figure 5.37: RSL3 treatment increases the oxylipin formation after 4 h in HEK293T\_LPCAT2\_15LO1 cells.** Laura Carpanedo and Susanne Reif, under the supervision of Prof. Dr. Nils Helge Schebb (Department of Food Chemistry, Faculty of Mathematics and Natural Sciences, University Wuppertal), performed the lipid mediator extraction and analysis via LC-MS/MS. Bjarne Goebel planned the sample incubations, and analyzed the results. Svenja Simoni performed the incubations.

**Figure 9.13: Effect of ferroptosis inducers on the localization of 5-lipoxygenase in stably transfected HEK293T cells., Figure 9.14: Effect of ferroptosis inducers on the localization of 15-lipoxygenase 1 in stably transfected HEK293T cells.** and **Figure 9.15: Effect of ferroptosis inducers on the localization of 15-lipoxygenase 2 in stably transfected HEK293T cells.** Tamara Göbel (Institute of Pharmaceutical Chemistry, Goethe University Frankfurt) kindly performed laser scanning confocal microscopy imaging. Bjarne Goebel prepared the samples and analyzed the images.

Parts of the following data that were presented within this thesis were accepted for publication in the peer-reviewed journal 'Frontiers in Cell Death, section Model Systems in Cell Death' on 23.10.2023.

#### **Development of a cell-based model system for the investigation of ferroptosis**

Goebel B, Carpanedo L, Reif S, Göbel T, Simonyi S, Schebb NH, Steinhilber D, Häfner A-K

Front. Cell Death, Sec. Model Systems in Cell Death. Accepted for publication on 23.10.2023.  
<https://doi.org/10.3389/fceld.2023.1182239>

Figure 5.21, Figure 5.28, Figure 5.29, Figure 5.30, Figure 5.31, Figure 5.33, Figure 5.34, Figure 5.35, Figure 5.36, Figure 5.37, Table 9.6, Table 9.7

Following figures were created using BioRender.com.

Figure 2.1, Figure 2.2, Figure 2.3, Figure 2.4, Figure 2.6, Figure 5.9, Figure 5.11